

MASTER
BNL-NCS-17541
(ENDF-201)
3rd Edition (ENDF/B-V)
UC-80
(General Reactor Technology - TID-4500)

ENDF-201
ENDF/B SUMMARY DOCUMENTATION

Compiled by R. Kinsey
July 1979



NATIONAL NUCLEAR DATA CENTER

BROOKHAVEN NATIONAL LABORATORY
ASSOCIATED UNIVERSITIES, INC.
UPTON, NEW YORK 11973

UNDER CONTRACT NO. DE-AC02-76CH00016 WITH THE

UNITED STATES DEPARTMENT OF ENERGY

DISCLAIMER

This book was prepared as an account of work sponsored by an agency of the United States Government. Neither the United States Government nor any agency thereof, nor any of their employees, makes any warranty, express or implied, or assumes any legal liability or responsibility for the accuracy, completeness, or usefulness of any information, apparatus, product, or process disclosed, or represents that its use would not infringe privately owned rights. Reference herein to any specific commercial product, process, or service by trade name, trademark, manufacturer, or otherwise, does not necessarily constitute or imply its endorsement, recommendation, or favoring by the United States Government or any agency thereof. The views and opinions of authors expressed herein do not necessarily state or reflect those of the United States Government or any agency thereof.

THIS DOCUMENT CONTAINS neither recommendations nor conclusions of the United States Government. It is the property of the United States Government, is not to be distributed outside the United States, and has not been subject to the review and approval procedures required of such documents.

File

INTRODUCTION

The purpose of this publication is to provide a localized source of descriptions for the evaluations contained in the ENDF/B Library.

The summary documentation presented in this volume is intended to be a more detailed description than the (File 1) comments contained in the computer readable data files, but not as detailed as the formal reports describing each ENDF/B evaluation.

The summary documentations were written by the CSEWG (Cross Section Evaluation Working Group) evaluators and compiled by NNDC (National Nuclear Data Center). The loose-leaf independent section format was selected for ease of updating when more documentation and/or evaluations become available.

This edition includes documentation for materials found on ENDF/B Version V tapes 501 to 516 (General Purpose File) excluding tape 504. ENDF/B-V also includes tapes containing partial evaluations for the Special Purpose Actinide (521, 522), Dosimetry (531), Activation (532), Gas Production (533), and Fission Product (541-546) files. The materials found on these tapes are documented elsewhere.

For additional information concerning the evaluated files as well as the corresponding experimental data, contact:

National Nuclear Data Center
Brookhaven National Laboratory
Upton, New York 11973

ACKNOWLEDGMENT

The author wishes to give special thanks to the Brookhaven Graphic Arts Division for production of the final pages.

Table of Contents for ENDF/B-V General Purpose File

Z	El	A	MAT	Laboratory	Date	Author
			No.			
1-H	-	1	1301	LASL	Jan77	L.Stewart, R.J.LaBauve, P.G.Young
1-H	-	2	1302	LASL	Jan77	L.Stewart (LASL) A.Horsley (AWRE)
1-H	-	3	1169	LASL	Oct74	Leona Stewart
2-He-	3	1146	LASL		Jun68	Leona Stewart (LASL)
2-He-	4	1270	LASL		Oct73	Nisley, Hale, Young (LASL)
3-Li-	6	1303	LASL		Sep77	G.Hale, L.Stewart, P.G.Young
3-Li-	7	1272	LASL		Oct72	R.J.LaBauve, L.Stewart, M.Battat
4-Be-	9	1304	LLL		Oct76	Howerton, Perkins
5-B	-	10	1305	LASL	Jan77	G.Hale, L.Stewart, P.Young
5-B	-	11	1160	GE-BNL	Nov74	C.Cowan
6-C		1306	ORNL		Jan77	C.Y.Fu and F.G.Perey
7-N	-	14	1275	LASL	Jun75	P.Young, D.Foster, Jr., G.Hale
7-N	-	15	1307	LASL	Mar77	E.Arthur, P.Young, G.Hale
8-O	-	16	1276	LASL	Jun75	P.Young, D.Foster, Jr., G.Hale
8-O	-	17	1317	BNL	Jan78	B.A.Magurno
9-F	-	19	1309	ORNL	Dec76	C.Y.Fu, D.C.Larson, F.G.Perey
11-Na-	23	1311	ORNL		Dec77	D. C. Larson
12-Mg		1312	ORNL		Feb78	D.C.Larson
13-Al-	27	1313	LASL		Aug77	P.G. Young, D.G. Foster, Jr.
14-Si		1314	ORNL		Dec76	Larson, Perey, Drake, Young
15-P	-	31	1315	LLL	Oct77	Howerton
16-S		1347	BNL		Apr79	Divadeenam
16-S	-	32	1316	LLL	Oct77	Howerton
17-Cl		1149	GGA		Feb67	M.S.Allen and M.K.Drake
19-K		1150	GGA		Feb67	M.K.Drake
20-Ca		1320	ORNL		Oct76	C.Y.Fu and F.G.Perey
22-Ti		1322	BUR, ANL, LLL		Aug77	C.Philis, A.Smith, R.Howerton
23-V		1323	ANL, LLL, HEDL		Jan77	A.Smith+, H.Howerton, F.Mann.
24-Cr		1324	BNL		Dec77	A.Prince and T.W.Burrows
25-Mn	-	55	1325	BNL	Mar77	S.F. Mughabghab
26-Fe		1326	ORNL		Oct77	C.Y.Fu and F.G.Perey
27-Co	-	59	1327	BNL	Jun77	S.Mughabghab
28-Ni		1328	BNL		Mar77	M.Divadeenam
29-Cu		1329	ORNL, SAI		Mar78	Fu, Drake, Fricke
36-Kr	-	78	1330	BNL	Dec78	A.Prince
36-Kr	-	80	1331	BNL	Dec78	A.Prince
36-Kr	-	82	1332	BNL	Dec78	A.Prince
36-Kr	-	83	1333	BNL	Dec78	A.Prince
36-Kr	-	84	1334	BNL	Apr78	A.Prince
36-Kr	-	86	1336	BNL	Jun75	A.Prince
40-Zr		1340	SAI		Apr76	M.Drake, D.Sargis, T.Maung
40-Zr	-	90	1385	SAI	Apr76	M.Drake, D.Sargis, T.Maung
40-Zr	-	91	1386	SAI	Apr76	M.Drake, D.Sargis, T.Maung
40-Zr	-	92	1387	SAI	Apr76	M.Drake, D.Sargis, T.Maung
40-Zr	-	94	1388	SAI	Apr76	M.Drake, D.Sargis, T.Maung
40-Zr	-	96	1389	SAI	Apr76	M.Drake, D.Sargis, T.Maung
41-Nb	-	93	1189	ANL, LLL	May74	R.Howerton(LLL) and A.Smith
42-Mo		1321	LLL, HEDL		Feb79	Howerton, Schmittroth, Schenter
43-Tc	-	99	1308	HEDL, BAW	Nov78	Schenter, Livolsi, Schmittroth, et al.
45-Rh	-	103	1310	HEDL, BAW	Nov78	Schenter, Livolsi, Schmittroth, et al.
47-Ag	-	107	1371	HEDL, BNL	Nov78	Schenter, Bhat, Prince, Johnson, et al.

Table of Contents for ENDF/B-V General Purpose File (continued)

Z El	A	MAT	Laboratory	Date	Author
		No.			
47-Ag-109	1373	HEDL, BNL		Nov78	Schenter, Bhat, Prince, Johnson, et al.
48-Cd	1281	BNL		Nov74	S. PearlStein (Translated from U.K.)
48-Cd-113	1318	BNL, HEDL		Nov78	PearlStein, Mann, Schenter
54-Xe-124	1335	BNL		Mar78	M.R. Bhat and S.F. Mughabghab
54-Xe-126	1339	BNL		Mar78	M.R. Bhat and S.F. Mughabghab
54-Xe-128	1348	BNL		Mar78	M.R. Bhat and S.F. Mughabghab
54-Xe-129	1349	BNL		Mar78	M.R. Bhat and S.F. Mughabghab
54-Xe-130	1350	BNL		Mar78	M.R. Bhat and S.F. Mughabghab
54-Xe-131	1351	BNL		Mar78	M.R. Bhat and S.F. Mughabghab
54-Xe-132	1352	BNL		Mar78	M.R. Bhat and S.F. Mughabghab
54-Xe-134	1354	BNL		Mar78	M.R. Bhat and S.F. Mughabghab
54-Xe-135	1294	BNW		May75	B.R. Leonard, Jr. and K.B. Stewart
54-Xe-136	1356	BNL		Mar78	M.R. Bhat and S.F. Mughabghab
55-Cs-133	1355	HEDL, BNL		Nov78	Schenter, Bhat, Prince, Johnson, et al.
56-Ba-138	1353	LLL		Aug78	Howerton
62-Sm-149	1319	HEDL, BNW		Nov78	Schenter, Leonard, Stewart, et al.
63-Eu-151	1357	BNL		Dec77	S.F. Mughabghab
63-Eu-152	1292	BNL		Jun75	H. Takahashi
63-Eu-153	1359	BNL		Feb78	S. Mughabghab
63-Eu-154	1293	BNL		Jun75	H. Takahashi
64-Gd-152	1362	BNL		Jan77	B.A. Magurno
64-Gd-154	1364	BNL		Jan77	B.A. Magurno
64-Gd-155	1365	BNL		Jan77	B.A. Magurno
64-Gd-156	1366	BNL		Jan77	B.A. Magurno
64-Gd-157	1367	BNL		Jan77	B.A. Magurno
64-Gd-158	1368	BNL		Jan77	B.A. Magurno
64-Gd-160	1370	BNL		Jan77	B.A. Magurno
66-Dy-164	1031	BNW		Jun67	B.R. Leonard, Jr. and K.B. Stewart
71-Lu-175	1032	BNW		Jun67	B.R. Leonard, Jr. and K.B. Stewart
71-Lu-176	1033	BNW		Jun67	B.R. Leonard, Jr. and K.B. Stewart
72-Hf	1372	SAI		Apr76	M. Drake, D. Sargis, T. Maung
72-Hf-174	1374	SAI		Apr76	M. Drake, D. Sargis, T. Maung
72-Hf-176	1376	SAI		Apr76	M. Drake, D. Sargis, T. Maung
72-Hf-177	1377	SAI		Apr76	M. Drake, D. Sargis, T. Maung
72-Hf-178	1378	SAI		Apr76	M. Drake, D. Sargis, T. Maung
72-Hf-179	1383	SAI		Apr76	M. Drake, D. Sargis, T. Maung
72-Hf-180	1384	SAI		Apr76	M. Drake, D. Sargis, T. Maung
73-Ta-181	1285	LLL		Nov74	Howerton, Perkins, MacGregor
73-Ta-182	1127	AI		Apr71	J. Otter, C. Dunford, and E. Ottewitte
74-W-182	1128	AI, LASL		Jun73	Otter, Ottewitte, Rose, Young
74-W-183	1129	AI, LASL		Oct74	Otter, Ottewitte, Rose, Young
74-W-184	1130	AI, LASL		Apr74	Otter, Ottewitte, Rose, Young
74-W-186	1131	AI, LASL		Jun73	Otter, Ottewitte, Rose, Young
75-Re-185	1083	GE(NMPO)		Jan68	W.B. Henderson and J.W. Zwick
75-Re-187	1084	GE(NMPO)		Jan68	W.B. Henderson and J.W. Zwick
79-Au-197	1379	BNL		Feb77	S.F. Mughabghab
82-Pb	1382	ORNL		Aug76	C.Y. Fu and F.G. Perey
90-Th-232	1390	BNL		Dec77	Bhat, Smith, Leonard, DeSaussure, et al.
91-Pa-233	1391	HEDL, INEL		May78	Mann, Schenter, Reich
92-U-233	1393	LASL, ORNL+		Dec78	Stewart et al, Weston, Mann
92-U-234	1394	BNL, HEDL, +		Jul78	Divadeenam, Mann, Drake, Reich, et al.

Table of Contents for ENDF/B-V General Purpose File (continued)

Z	El	A	MAT	Laboratory	Date	Author
			No.			
92-U	-235	1395	BNL		Nov77	M.R.Bhat
92-U	-236	1396	BNL, HEDL, +		Jul78	Divadeenam, Mann, McCrosson, Reich, +
92-U	-238	1398	ANL+		Mar79	E.Pennington, A.Smith, W.Poenitz
93-Np	-237	1337	HEDL, SRL, +		Apr78	Mann, Benjamin, Smith, Stein, Reich, +
94-Pu	-238	1338	HEDL, AI, +		Apr78	Mann, Schenter, Alter, Dunford, +
94-Pu	-239	1399	GE-FBRD		Oct76	E.Kujawski, L.Stewart(LASL)
94-Pu	-240	1380	ORNL		Apr77	L.W. Weston
94-Pu	-241	1381	ORNL		Oct77	L.W. Weston, R.Q. Wright, Howerton
94-Pu	-242	1342	HEDL, SRL, +		Oct78	Mann, Benjamin, Madland, Howerton, +
95-Am	-241	1361	HEDL, ORNL		Apr78	Mann, Schenter, and Weston
95-Am	-242m	1369	HEDL, SRL, LLL		Apr78	Mann, Benjamin, Howerton, et al.
95-Am	-243	1363	HEDL, SRL, LLL		Apr78	Mann, Benjamin, Howerton, et al.
96-Cm	-243	1343	HEDL, SRL, LLL		Apr78	Mann, Benjamin, Howerton, et al.
96-Cm	-244	1344	HEDL, SRL, LLL		Apr78	Mann, Benjamin, Howerton, et al.
96-Cm	-245	1345	SRL		Sep75	Benjamin and McCrosson
96-Cm	-246	1346	BNL, SRL, LLL		Jul76	Kinsey, Benjamin, Howerton

SUMMARY DOCUMENTATION FOR ^1H

by

L. Stewart, R. J. LaBauve, and P. G. Young
Los Alamos Scientific Laboratory
Los Alamos, New Mexico

I. SUMMARY

The ^1H evaluation for ENDF/B-V (MAT 1301) is basically the same as the Version IV evaluation. Changes include the addition of correlated error data in MF=33 and different interpolation rules for MT=1 and 2 in MF=3. The evaluation covers the energy range 10^{-5} eV to 20 MeV, and documentation is provided in LA-4574 (1971) and LA-6518-MS (1976).

II. STANDARDS DATA

The $^1\text{H}(\text{n},\text{n})^1\text{H}$ elastic scattering cross section and angular distribution (MF=3, 4; MT=2) are standards in the energy region 1 keV - 20 MeV.

The extensive theoretical analysis of fast-neutron measurements by Hopkins and Breit¹ was used to generate the scattering cross section and angular distributions of the neutrons for the ENDF/B-V file.² The code and the Yale phase shifts³ were obtained from Hopkins⁴ in order to obtain the data on a fine-energy grid. Pointwise angular distributions were produced to improve the precision over that obtained from the published Legendre coefficients.* The phase shifts were also used to extend the energy range down below 200 keV as represented in the original paper.¹

At 100 eV, the elastic cross section calculated from the phase shifts is 20.449 barns, in excellent agreement with the thermal value of 20.442 derived by Davis and Barschall.⁵ Therefore, for the present evaluation, the free-atom scattering cross section is assumed to be constant below 100 eV and equal to the value calculated from the Yale phase shifts at 100 eV giving a thermal cross section of 20.449 b.

Total cross-section measurements are compared with the evaluation in Fig. 1 for the energy range from 10 eV to 0.5 MeV. Similarly, Figs. 2 and 3 compare the evaluation with measured data from 0.5 to 20 MeV. The agreement with the earlier experiments shown in Fig. 2 is quite good over the entire energy range. The 1969 data of Schwartz⁶ included in Fig. 3, however, lie slightly below the evaluation over most of the energy range even though agreement with the 1972 results of Clement⁷ is quite acceptable.

*For $E_n = 30$ MeV, the difference in the 180° cross section is $\sim 1\%$ as calculated from the Legendre coefficients³ compared to that calculated from the phase shifts.

Unfortunately, few absolute values of the angular dependence of the neutrons (or recoil protons) exist and even the relative measurements are often restricted to less than half of the angular range. The experiment of Oda⁸ at 3.1 MeV is not atypical of the earlier distributions which, as shown in Fig. 4, does not agree with the phase-shift predictions. Near 14 MeV, the T(d,n) neutron source has been employed in many experiments to determine the angular distributions. A composite of these measurements is compared with ENDF/B-V in Fig. 5A. Note that most of the experiments are in reasonable agreement on a relative scale, but 10% discrepancies frequently appear among the data sets. The measurements of Cambou⁹ average more than 5% lower than the predicted curve and differences of 5% or more are occasionally apparent among the data of a single set. Figure 5B shows the measurements of Galonsky¹⁰ at 17.9 MeV compared with the evaluation. Again, the agreement on an absolute basis is quite poor.

Elastic scattering angular distributions at 0.1, 5, 10, 20, and 30 MeV are provided in Ref. 11 as Legendre expansion coefficients. Using the Hopkins-Breit phase-shift program and the Yale phase shifts, additional and intermediate energy points were calculated for the present evaluation.² As shown in Figs. 5-16 of Ref. 2, the angular distributions are neither isotropic below 10 MeV nor symmetric about 90° above 10 MeV as assumed in earlier evaluations. In this evaluation, the angular distribution at 100 keV is assumed to be isotropic since the calculated 180°/0° ratio is very nearly unity, that is, 1.0011. At 500 keV, this ratio approaches 1.005. Therefore, the pointwise normalized probabilities as a function of the center-of-mass scattering angle are provided at the following energies: 10⁻⁵ eV (isotropic), 100 keV (isotropic), 500 keV, and at 1-MeV intervals from 1 to 20 MeV.

Certainly the Hopkins-Breit phase shifts reproduce reasonably well the measured angular distributions near 14 MeV. It is important, however, that experiments be made at two or three energies which would, hopefully, further corroborate this analysis. Near 14 MeV, the energy-dependent total cross section is presently assumed to be known to ~ 1% and the angular distribution to ~ 2-3%. At lower energies where the angular distributions approach isotropy, the error estimate on the angular distribution is less than 1%.

It should be pointed out that errors involved in using hydrogen as a standard depend upon the experimental techniques employed and therefore may be significantly larger than the errors placed on the standard cross section. The elastic angular distribution measurements of neutrons scattered by hydrogen, which are available today, seem to indicate that $\sigma(0)$ is difficult to measure with the precision ascribed to the reference standard. If this is the case, then the magnitude of the errors in the $\sigma(0)$ measurements might be indicative of error assignments which should be made on hydrogen flux monitors. That is, it is difficult to assume that hydrogen scattering can be implemented as a standard with much higher precision than it can be measured. Even though better agreement with many past measurements can be reached by renormalizing the absolute scales, such action may not always be warranted.

At this time, no attempt has been made to estimate the effect of errors on the energy scale in ENDF/B. It is clear, however, that a small energy shift would produce a large change in the cross section, especially at low energies. For example, a 50-keV shift in energy near 1 MeV would produce a change in the standard cross section of approximately 2½%. Therefore, precise determination of the incident neutron energy and the energy spread could be very important in employing hydrogen as a cross-section standard, depending upon the experimental technique.

III. ENDF/B-V FILES

File 1. General Information

MT=451. Descriptive data.

File 2. Resonance Parameters

MT=151. Effective scattering radius = 1.27565×10^{-12} cm.

Resonance parameters not given.

File 3. Neutron Cross Sections

MT=1. Total Cross Sections

The total cross sections are obtained by adding the elastic scattering and radiative capture cross sections at all energies, 1.0E-05 eV to 20 MeV.

MT=2. Elastic Scattering

Standard - see discussion in Sec. II.

MT=102. Radiative Capture

These cross sections are taken from the publication of A. Horsley where a value of 332 mb was adopted for the thermal value. See Ref. 51.

MT=251. Average Value of Cosine of Scattering Angle In Lab System from 1.0E-05 Ev to 20 MeV. (Provided by BNL).

MT=252. Average Logarithmic Energy Change Per Collision, from 1.0E-05 eV to 20 MeV. (Provided by BNL).

MT=253. Gamma, from 1.0E-05 eV to 20 MeV. (Provided by BNL).

File 4. Neutron Angular Distributions

MT=2. Neutron elastic scattering angular distributions in the center of mass system, given as normalized pointwise probabilities. See Sec. II above.

File 7. Thermal Neutron Scattering Law Data

MT=4. 0.00001 to 5 eV free gas sigma = 20.449 barns.

File 12. Gamma Ray Multiplicities

MT=102. Radiative Capture Multiplicities.

Multiplicity is unity at all neutron energies. LP=2 is now implemented; therefore, all gamma energies must be calculated.

File 14. Gamma Ray Angular Distributions

MT=102. Radiative capture angular distribution

Assumed isotropic at all neutron energies.

File 33. Correlated Errors

MT=1. Covariance matrix derived from MT=2, 102.

MT=2. Covariance data added for the elastic scattering by D. G. Foster, Jr. (Jan. 77).

MT=102. Covariance data for radiative capture added by P. G. Young (Nov. 7, 1978).

REFERENCES

1. J. C. Hopkins and G. Breit, "The H(n,n)H Scattering Observables Required for High Precision Fast-Neutron Measurements," Nuclear Data A 9, 137 (1971) and private communication prior to publication (1970).
2. L. Stewart, R. J. LaBauve, and P. G. Young, "Evaluated Nuclear Data for Hydrogen in the ENDF/B-II Format," LA-4574 (1971). Neither the cross sections nor the angular distributions have been changed since Version II except to add one more significant figure to the total cross section.
3. R. E. Seamon, K. A. Friedman, G. Breit, R. D. Haracz, J. M. Holt, and A. Prakash, Phys. Rev. 165, 1579 (1968).
4. J. C. Hopkins, private communication to L. Stewart (1970).
5. J. C. Davis and H. H. Barschall, "Adjustment in the n-p Singlet Effective Range," Phys. Lett. 27B, 636 (1968).
6. R. B. Schwartz, R. A. Schrack, and H. T. Heaton, "A Search for Structure in the n-p Scattering Cross Section," Phys. Lett. 30, 36 (1969).
7. J. M. Clement, P. Stoler, C. A. Goulding, and R. W. Fairchild, "Hydrogen and Deuterium Total Neutron Cross Sections in the MeV Region," Nucl. Phys. a 183, 51 (1972).
8. Y. Oda, J. Sanada, and S. Yamabe, "On the Angular Distribution of 3.1-MeV Neutrons Scattered by Protons," Phys. Rev. 80, 469 (1950).
9. F. Cambou, "Amelioration des Methods de Spectrometrie des Neutrons Rapides," Thesis - U. of Paris, CEA-N-2002 (1961).
10. A. Galonsky and J. P. Judish, "Angular Distribution of n-p Scattering at 17.9 MeV," Phys. Rev. 100, 121 (1955).
11. "ENDF/B Summary Documentation," ENDF-201, Compiled by D. Garber, (October 1975).

12. E. Melkonian, "Slow Neutron Velocity Spectrometer Studies of O₂, N₂, A, H₂, H₂O, and Seven Hydrocarbons," *Phys. Rev.* 76, 1950 (1949).
13. D. H. Frisch, "The Total Cross Sections of Carbon and Hydrogen for Neutrons of Energies from 35 to 490 keV," *Phys. Rev.* 70, 589 (1946).
14. W. D. Allen and A. T. G. Ferguson, "The n-p Cross Section in the Range 60-550 keV," *Proc. Phys. Soc. (London)* 68, 1077 (1955).
15. E. Bretscher and E. B. Martin, "Determination of the Collision Cross-Section of H, Deuterium, C and O for Fast Neutrons," *Helv. Phys. Acta* 23, 15 (1950).
16. C. E. Engleke, R. E. Benenson, E. Melkonian, and J. M. Lebowitz, "Precision Measurements of the n-p Total Cross Section at 0.4926 and 3.205 MeV," *Phys. Rev.* 129, 324 (1963).
17. C. L. Bailey, W. E. Bennett, T. Bergstrahl, R. G. Nuckolls, H. T. Richards, and J. H. Williams, "The Neutron-Proton and Neutron-Carbon Scattering Cross Sections for Fast Neutrons," *Phys. Rev.* 70, 583 (1946).
18. E. E. Lampi, G. Frier, and J. H. Williams, "Total Cross Section of Carbon and Hydrogen for Fast Neutrons," *Phys. Rev.* 76, 188 (1949).
19. W. E. Good and G. Scharff-Goldhaber, "Total Cross Sections for 900-keV Neutrons," *Phys. Rev.* 59, 917 (1941).
20. S. Bashkin, B. Petree, F. P. Mooring, and R. E. Peterson, "Dependence of Neutron Cross Sections on Mass Number," *Phys. Rev.* 77, 748 (1950).
21. R. E. Fields, R. L. Becker, and R. K. Adair, "Measurement of the Neutron-Proton Cross Section at 1.0 and 2.5 MeV," *Phys. Rev.* 94, 389 (1954).
22. C. L. Storrs and D. H. Frisch, "Scattering of 1.32 MeV Neutrons by Protons," *Phys. Rev.* 95, 1252 (1954).
23. D. G. Foster, Jr. and D. W. Glasgow, "Neutron Total Cross Sections, 2.5-15 MeV, Part 1 (Experimental)," *Nucl. Instr. and Methods*, 36, 1 (1967).
24. R. E. Fields, "The Total Neutron-Proton Scattering Cross Section at 2.5 MeV," *Phys. Rev.* 89, 908 (1953).
25. G. Ambrosina and A. Sorriaux, "Total Cross Section Efficiency for Carbon, Gluorine and Vanadium," *Comptes Rendus* 260, 3045 (1965).
26. W. H. Zinn, S. Seely, and V. W. Cohen, "Collision Cross SEctions for D-D Neutrons," *Phys. Rev.* 56, 260 (1939).
27. N. Nereson and S. Darden, "Average Neutron Total Cross Sections in the 3- to 12- MeV Region," *Phys. Rev.* 94, 1678 (1954).
28. E. M. Hafner, W. F. Hornyak, C. E. Falk, G. Snow, and T. Coor, "The Total n-p Scattering Cross Section at 4.75 MeV," *Phys. Rev.* 89, 204 (1953).

29. W. Sleator, Jr., "Collision Cross Sections of Carbon and Hydrogen for Fast Neutrons," *Phys. Rev.* 72, 207 (1947).
30. A. Bratenahl, J. M. Peterson, and J. P. Stoering, "Neutron Total Cross Sections in the 7- to 14-MeV Region," UCRL-4980 (1957).
31. A. H. Lasday, "Total Neutron Cross Sections of Several Nuclei at 14 MeV," *Phys. Rev.* 81, 139 (1951).
32. L. S. Goodman, "Total Cross Sections for 14-MeV Neutrons," *Phys. Rev.* 88, 686 (1952).
33. H. L. Poss, E. O. Salant, and L. C. L. Yuan, "Total Cross Sections of Carbon and Hydrogen for 14-MeV Neutrons," *Phys. Rev.* 85, 703 (1951).
34. M. Tanaka, N. Koori, and S. Shirato, "Differential Cross Sections for Neutron-Proton Scattering at 14.1 MeV," *J. Phys. Soc. (Japan)* 28, 11 (1970).
35. M. E. Battat, R. O. Bondelid, J. H. Coon, L. Cranberg, R. B. Day, F. Edes-kuty, A. H. Frentrop, R. L. Henkel, R. L. Mills, R. A. Nobles, J. E. Perry, D. D. Phillips, T. R. Roberts, and S. G. Sydoriak, "Total Neutron Cross Sections of the Hydrogen and Helium Isotopes," *Nucl. Phys.* 12, 291 (1959).
36. J. C. Allred, A. H. Armstrong, and L. Rosen, "The Interaction of 14-MeV Neutrons with Protons and Deuterons," *Phys. Rev.* 91, 90 (1953).
37. C. F. Cook and T. W. Bonner, "Scattering of Fast Neutrons in Light Nuclei," *Phys. Rev.* 94, 651 (1954).
38. H. L. Poss, E. O. Salant, G. A. Snow, and L. C. L. Yuan, "Total Cross Sections for 14-MeV Neutrons," *Phys. Rev.* 87, 11 (1952).
39. P. H. Bowen, J. P. Scanlon, G. H. Stafford, and J. J. Thresher, "Neutron Total Cross Sections in the Energy Range 15 to 120 MeV," *Nucl. Phys.* 22, 640 (1961).
40. J. M. Peterson, A. Bratenahl, and J. P. Stoering, "Neutron Total Cross Sections in the 17- to 29-MeV Range," *Phys. Rev.* 120, 521 (1960).
41. D. E. Groce and B. D. Sowerby, "Neutron-Proton Total Cross Sections Near 20, 24, and 28 MeV," *Nucl. Phys.* 83, 199 (1966).
42. M. L. West II, C. M. Jones, and H. B. Willard, "Total Neutron Cross Sections of Hydrogen and Carbon in the 20-30 MeV Region," ORNL-3778, 94 (1965).
43. R. B. Day, R. L. Mills, J. E. Perry, Jr., and F. Schreb, "Total Cross Section for n-p Scattering at 20 MeV," *Phys. Rev.* 114, 209 (1959).
44. R. B. Day and R. L. Henkel, "Neutron Total Cross Sections at 20 MeV," *Phys. Rev.* 92, 358 (1953).

45. M. E. Remley, W. K. Jentschke, and P. G. Kruger, "Neutron-Proton Scattering Using Organic Crystal Scintillation Detectors," *Phys. Rev.* 89, 1194 (1953).
46. J. D. Seagrave, "Recoil Deuterons and Disintegration Protons from the n-d Interaction, and n-p Scattering at $E_n = 14.1$ MeV," *Phys. Rev.* 97, 757 (1955).
47. S. Shirato and K. Saitoh, "On The Differential Cross Section for Neutron-Proton Scattering at 14.1 MeV," *J. Phys. Soc. (Japan)* 36, 331 (1974).
48. T. Nakamura, "Angular Distribution of n-p Scattering at 14.1 MeV," *J. Phys. Soc. (Japan)* 15, 1359 (1960).
49. A. Suhami and R. Fox, "Neutron-Proton Small Angle Scattering at 14.1 MeV," *Phys. Lett.* 24, 173 (1967).
50. I. Basar, "Elastic Scattering of 14.4 MeV Neutrons on Hydrogen Isotopes," *Few Body Problems Light Nuclei/Nucl. Interactions, Brela*, 867 (1967).
51. A. Horsley, "Neutron Cross Sections of Hydrogen in the Energy Range 0.0001 eV-20 MeV," *Nucl. Data A2*, 243 (1966).

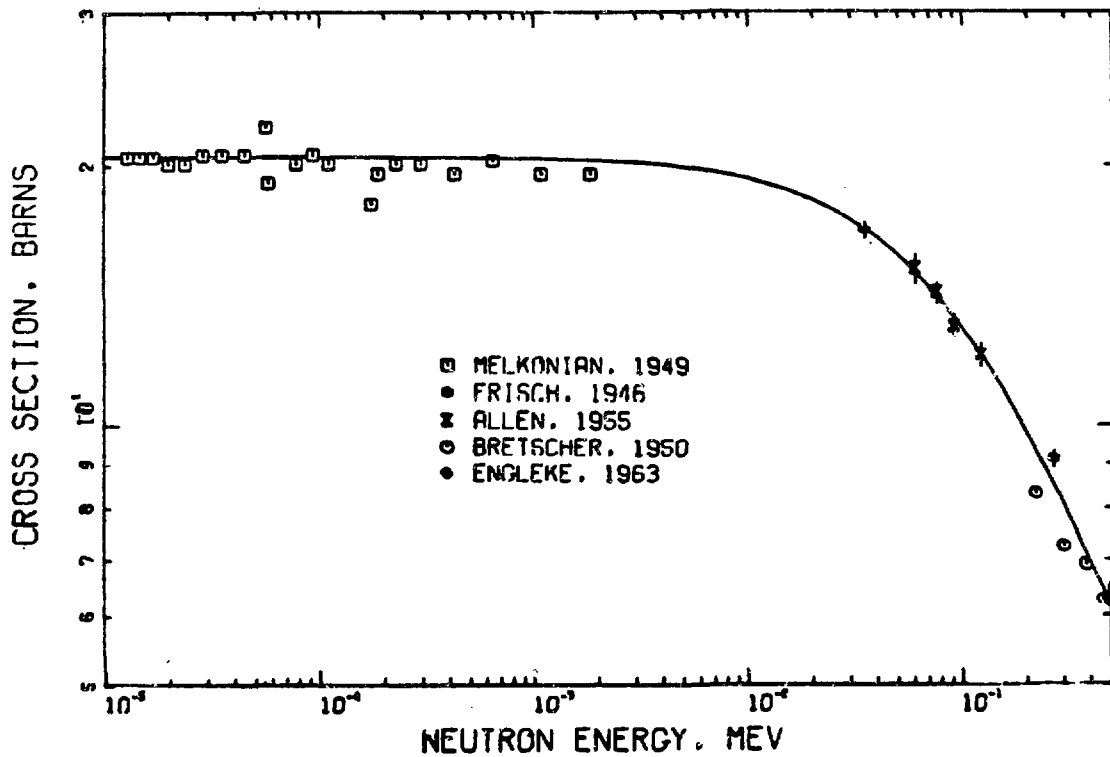


Fig. 1.
Total cross section for hydrogen from 1×10^{-5} eV to 500 keV. The ENDF/B-V evaluation is compared to the measurements of Refs. 12-16.

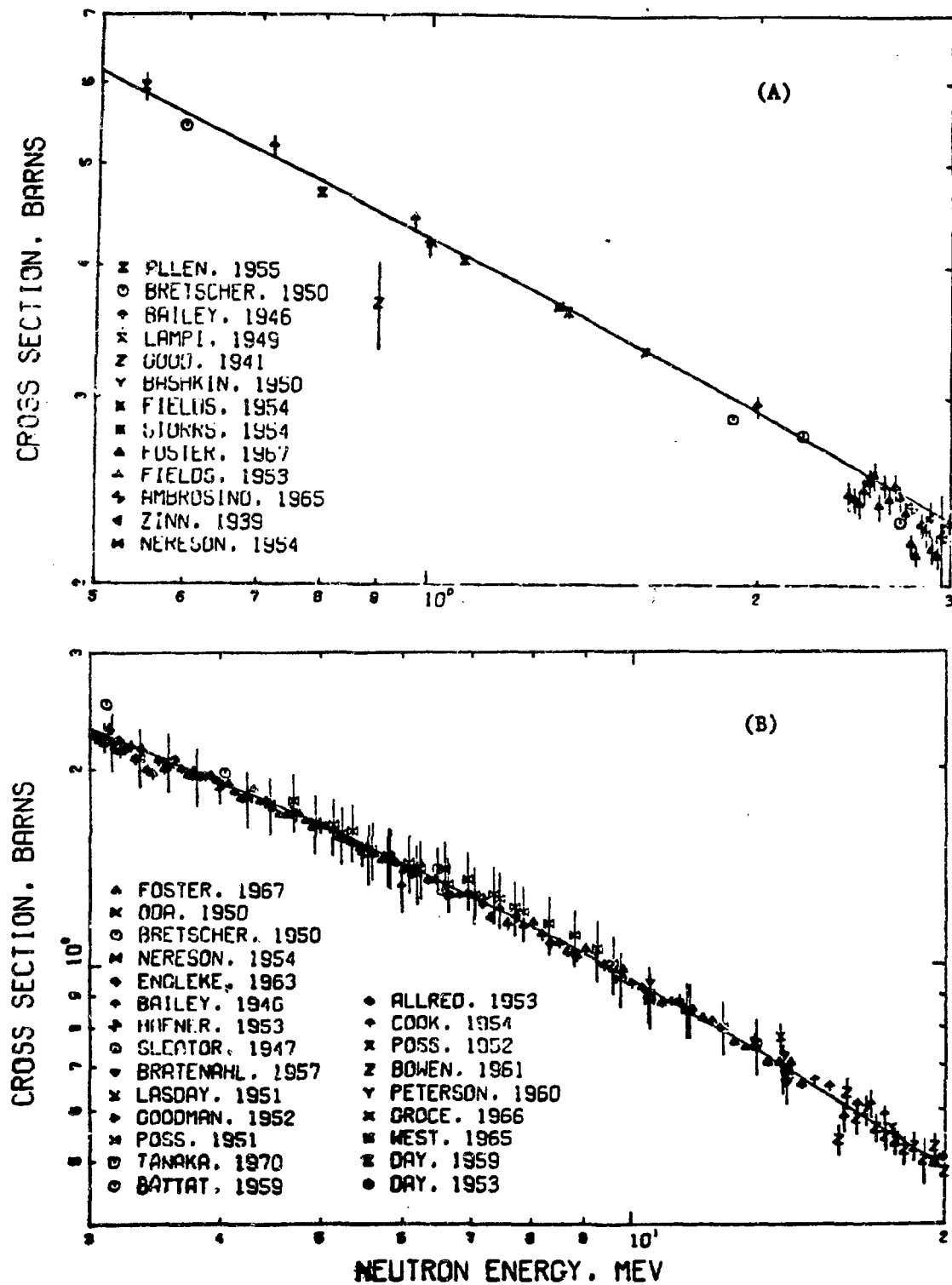


Fig. 2.
Total cross section for hydrogen from 500 keV to 20 MeV. The ENDF/B-V evaluation is compared to measurements reported in Refs. 8, 14-44.

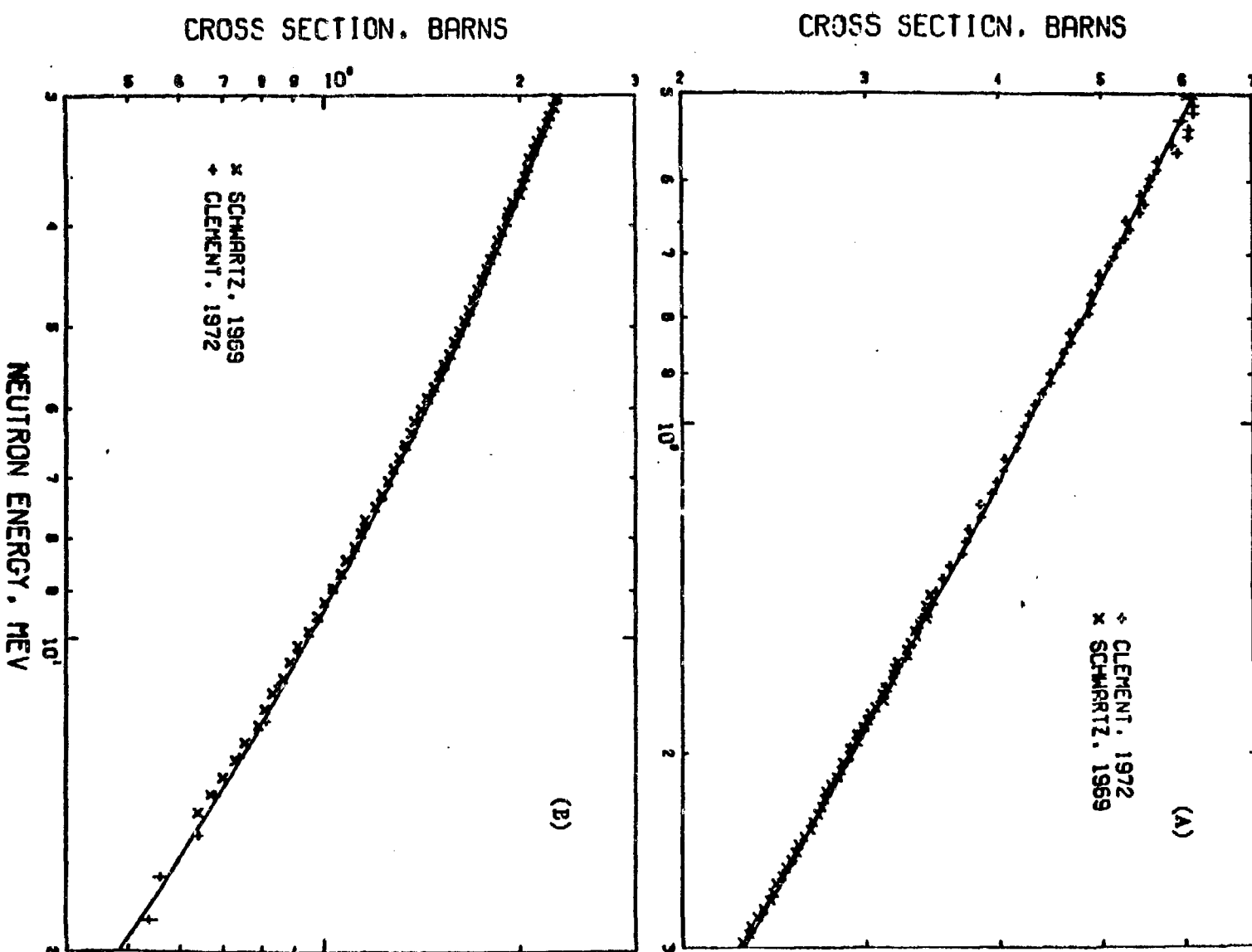


Fig. 3.
Total cross section for hydrogen from 500 keV to 20 MeV. The ENDF/B-V evaluation is compared to measurements reported in Refs. 6 and 7.

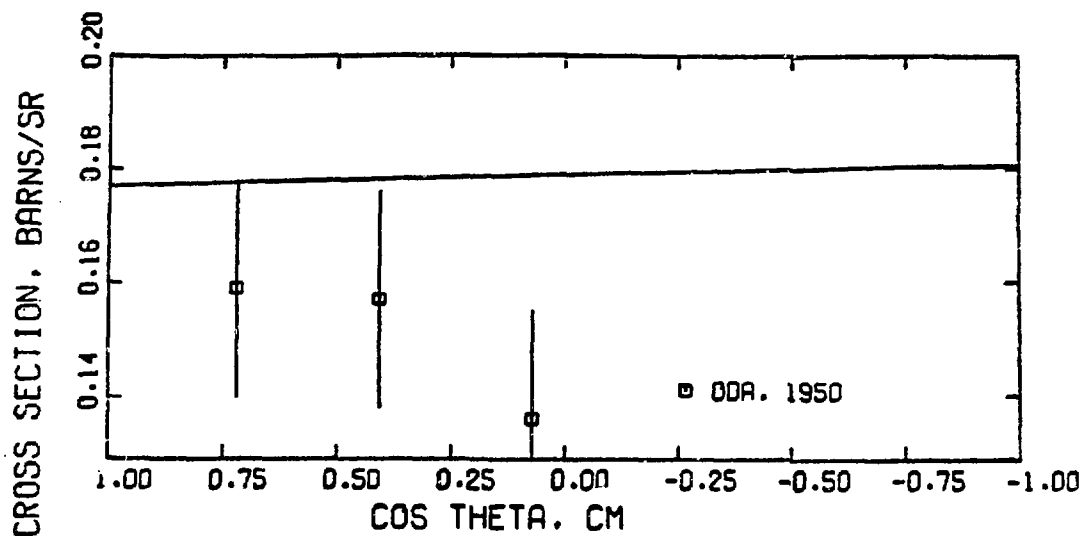


Fig. 4.

Angular distribution of the neutrons elastically scattered from hydrogen at 3.1 MeV. ENDF/B-V is compared with the experimental values of Oda.

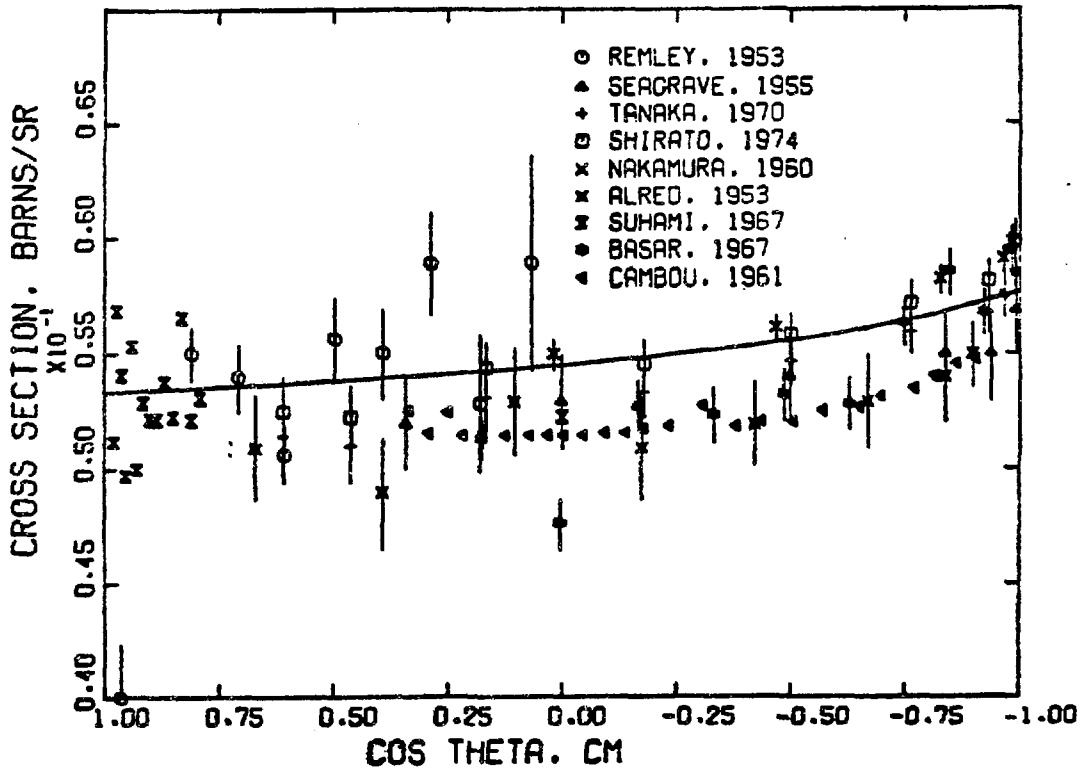


Fig. 5A.

Angular distribution of the neutrons elastically scattered from hydrogen at energies near 14 MeV. The experimental data shown were reported in Refs. 9, 34, 36 and 45-50.

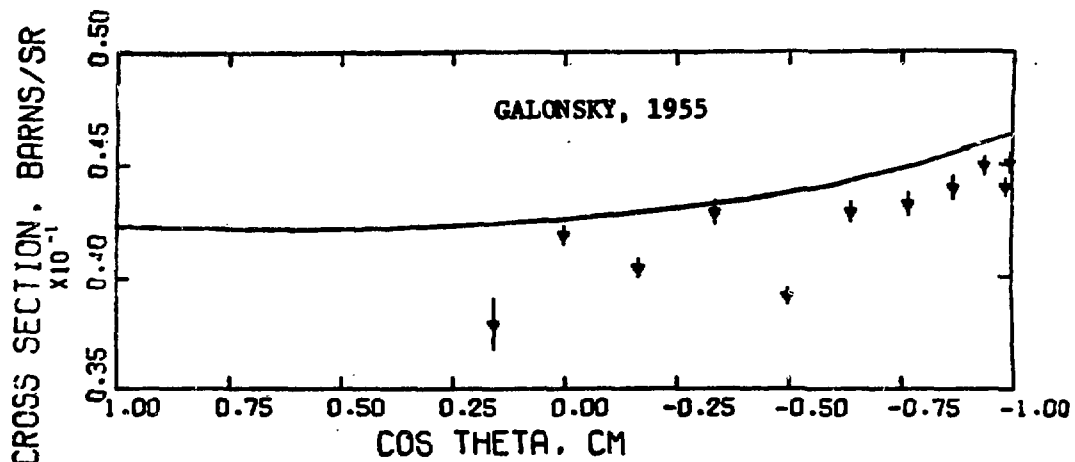


Fig. 5B.

Angular distribution of the neutrons elastically scattered from hydrogen at energies near 17.8 MeV. The experimental data shown were reported in Ref. 10.

SUMMARY DOCUMENTATION FOR ^2H

by

L. Stewart and A. Horsley[†]
Los Alamos Scientific Laboratory
Los Alamos, New Mexico

I. SUMMARY

The ENDF/B-V evaluation (MAT=1302) is entirely different from the Version IV data set and is based upon a revision of an earlier evaluation given in LA-3271 (1968). The main change made to the earlier evaluation was to modify the total and elastic cross sections below 500 keV in order to more closely reflect experimental data from RPI.¹ In addition, Files 8 and 9 have been included to provide tritium production information. The evaluation covers the energy range 10^{-5} eV to 20 MeV.

II. ENDF/B-V FILES

File 1. GENERAL INFORMATION

MT-451. Descriptive data.

File 2. Resonance Parameters

MT=151. Effective scattering radius = 0.51977×10^{-12} cm. Resonance parameters not given.

File 3. Neutron Cross Sections

MT=1. Total Cross Section

All data plotted and compared up to 1967 in LA-3271. Changes incorporated below 1.5 MeV but evaluation does not agree with low-energy experiments at NBS² (which are preliminary) but agrees at higher energies. The Davis data³ show a peculiar drop of a few per cent from 3.5 to 9 MeV but agree above and below these energies.

MT=2. Elastic Cross Sections

Data obtained from integrating n-D and p-D angular distributions. Since the radiative capture is in microbarns, the elastic is

[†]Atomic Weapons Research Establishment, Aldermaston, U.K.

essentially equal to the total cross section below the $n,2n$ threshold and the total minus the $n,2n$ above the threshold. Checks and balances were always made. See LA-3271 for the graphical comparisons.

MT=16. ($n,2n$) Cross Section

Data taken from Holmberg⁴ and from Catron.⁵ See LA-3271. Nothing is known about the cross section above 14 MeV.

MT=102. Radiative Capture Cross Section

The thermal cross section is 506 microbarns which was extrapolated as $1/V$ up to 1 keV. Curve was drawn above this energy to include measurements on the inverse reaction by Bösch.⁶ The 14 MeV value is a factor of 3 lower than Cerineo.⁷ See LA-3271 for graphical results.

File 4. Neutron Angular Distributions

MT=2. Elastic Angular Distributions

Taken from n -D and p -D scattering. Agreement is good with van Oers analysis.⁸ See LA-3271.

MT=16. ($n,2n$) Angular Distributions

Calculated by code of Young⁹ assuming phase space argument, therefore ignoring the observations of the virtual deuteron. See LA-3271 for comparisons with n -D and p -D breakup spectra.

File 5. Neutron Energy Distributions

MT=16. ($n,2n$) Energy Distribution

Discussed under MF=4. Energy distributions calculated assuming pure phase space model.

File 8, 9. Decay Data

MT=102. Decay Information Added For Tritium Production

File 12. Gamma Ray Multiplicities

MT=102. (n,γ) Multiplicity

Assumed a single gamma emitted at all energies. Employed the LP=2 flag to conserve energy.

File 14. Gamma Ray Angular Distributions

MT=102. (n,γ) Angular Distribution

Assumed isotropic.

REFERENCES

1. P. Stoler, N. N. Kaushal, F. Green, E. Harms, and L. Laroze, Phys. Rev. Lett. 29, 1745 (1972).
2. R. B. Schuartz, National Bureau of Standards personal communication (1977).
3. J. C. Davis and H. H. Barschall, Phys. Rev. C3, 1798 (1971).
4. M. Holmberg and J. Hansen, IAEA Conference on Nuclear Data, "Microscopic Cross Sections and Other Data Basis for Nuclear Reactors," Paris, October 17-21, 1966, paper CN-23/18.
5. H. C. Catron, M. D. Goldberg, R. W. Hill, J. M. LeBlanc, J. P. Stoering, C. J. Taylor, and M. A. Williamson, Phys. Rev. 123, 218 (1961).
6. R. Bösch, J. Lang, R. Müller, and Wölfli, Phys. Lett. 8, 120 (1964).
7. M. Cerineo, K. Ilakovac, I. Slaus, and P. Tomas, Phys. Rev. 124, 1947 (1961).
8. W. T. H. van Oers and K. W. Brockman, Jr., Nucl. Phys. 21, 189 (1960).
9. P. G. Young, Los Alamos Scientific Laboratory, personal communication (1977).

SUMMARY DOCUMENTATION FOR ^3H

by

L. Stewart
Los Alamos Scientific Laboratory
Los Alamos, New Mexico

I. SUMMARY

The ENDF/B-V evaluation for ^3H (MAT=1169) is identical to the Version IV evaluation except for the transfer of the decay data from File 1 to File 8. Gamma-ray production data are not included because the radiative capture and (n, n') cross sections are assumed to be negligibly small at all energies. The evaluation covers the energy range 10^{-5} eV to 20 MeV and is documented in LA-3270 (1965).

II. ENDF/B-V FILES

File 1. General Information

MT-451. Descriptive data.

File 2. Resonance Parameters

MT-151. Effective scattering radius = 0.32164×10^{-12} cm. Resonance parameters not given.

File 3. Neutron Cross Sections

MT=1. Total Cross Sections

Total cross sections from 290 keV to 20 MeV from LASL measurements (Ref. 1). Estimated below 290 keV.

MT=2. Elastic Scattering Cross Section

Data taken from measurements (Refs. 2 to 10) up to 1967 on n-T and p-He³ systems. Also, recent measurements on n-T by Seagrave et al. (Ref. 11) and on p-He³ by Morales and Cahill (Ref. 12) and by Hutson et al. (Ref. 13) have been used to update the elastic angular distributions above 15 MeV. (February 1971) (this is the only change made to the evaluation from that described in LA-3270).

MT=16. (n,2n) Cross Section

Only one measurement exists, that of Mather and Pain (Ref. 14) at 14.1 MeV. Estimates of this cross section were therefore made from systematics and the p-He³ reaction studies of Rosen and Leland (Ref. 9) and of Anderson (Ref. 15).

MT=17. (n,3n) Cross Section

No data given since estimates from isospin considerations give essentially zero probabilities. Mather and Pain (Ref. 14) and Cookson (Ref. 16) confirm these estimates.

MT=102. (n, γ) Cross Section (not included)

The measured cross section is less than or equal to 6.7 microbarns at thermal (the sign of the Q-value is uncertain). This cross section is therefore assumed zero at all energies.

MT=251. Average Value of the Scattering Angle in the Laboratory System from 1.0E-05 eV to 20 MeV

MT=252. Average Logarithmic Energy Change Per Collision, From 1.0E-05 eV to 20 MeV

MT=253. Gamma, From 1.0E-05 eV to 20 MeV

File 4. Neutron Angular Distributions

MT=2. Elastic Angular Distributions

These are given in the center-of-mass system as normalized probabilities versus cosine of the scattering angle.

MT=16. (n,2n) Angular Distributions

These are given in the laboratory system as normalized probabilities versus cosine of the scattering angle. See LA-3270 for details on these distribution functions.

File 5. Neutron Energy Distributions

MT=16. (n,2n) Energy Distributions

These are given as normalized probabilities versus energy of the outgoing neutron in the laboratory system. See LA-3270 for details on these distribution functions.

File 8. Decay Data

MT=457. Decay Data Provided by C. Reich (INEL), Based On Chart Of Nuclides, Wapstra's Mass Tables, and Nuclear Data Tables. Placed in ENDF File and Format by BNL and LASL.

Files 12 - 15. Gamma Ray Data (not included)

Only radiative capture produces gamma rays. Since the capture cross section is assumed zero at all energies, these files are purposely left empty.

REFERENCES

1. Los Alamos Physics and Cryogenics Groups, Nucl. Phys. 12, 291 (1959).
2. J. D. Seagrave et al., Phys. Rev. 119, 1981 (1960).
3. J. H. Coon et al., Phys. Rev. 81, 33 (1951).
4. T. B. Clegg et al., Nucl. Phys. 50, 621 (1964).
5. W. Haeberli et al., Phys. Rev. 133, 81178 (1964).
6. J. E. Brolley, Jr., et al., Phys. Rev. 117, 1307 (1960). Data at back angles at which He^3 particles were observed were ignored in this analysis.
7. R. H. Lovberg, Phys. Rev. 103, 1393 (1956).
8. R. A. Vanetsian and E. D. Fedchenko, Sov. J. of Atomic Energy, Trans. 2, 141 (1957), and K. P. Artemov, S. P. Calinin and L. H. Samoilov, JETP 10, 474 (1960). The latter data were not used, since they covered the 5- to 10-MeV energy region and were not available.
9. L. Rosen and W. T. Leland, Wash-1064 (EANDC(US)-79U) (Oct. 1966), p. 99.
10. D. Blanc, F. Cambou, M. Niel, and G. Vedrenne, J. De Physique, Supplement Fasc. 3-4, C1-98 (1966).
11. J. D. Seagrave et al., LA-DC-12954 (1971).
12. J. R. Morales and T. A. Cahill, Bull. Am. Phys. Soc. 14, 554 (1969), and private communication.
13. R. L. Hutson et al., Phys. Rev. 4, C17 (1971).
14. D. S. Mather and L. F. Pain, AWRE 047/69 (1969).
15. John D. Anderson, private communication 1965, and Anderson et al., Phys. Rev. Lett. 15, 66 (1965).

SUMMARY DOCUMENTATION FOR ^3He

by

L. Stewart
Los Alamos Scientific Laboratory
Los Alamos, New Mexico

I. SUMMARY

The ^3He evaluation for ENDF/B-V (MAT=1146) was carried over intact from Version IV. The evaluated data cover the energy range 10^{-5} eV to 20 MeV, and documentation for the standards portion of the data is given in LA-6518-MS (1976).

II. STANDARDS DATA

The $^3\text{He}(\text{n},\text{p})\text{T}$ cross section (MF=3; MT=103) is recognized as a standard in the neutron energy range from thermal to 1 MeV. The present evaluation was performed in 1968 and accepted by the CSEWG Standards Subcommittee for the ENDF/B-III file¹ in 1971. No changes have been recommended for this file; therefore, the present evaluation was carried over from both Versions III and IV of ENDF/B.

The thermal cross section of 5327 b was derived from precise measurements by Als-Nielsen and Dietrich² of the total cross section up to an energy of 11 eV. No experimental measurements on the $^3\text{He}(\text{n},\text{p})$ reaction are available below ~ 5 keV, and the cross section was assumed to follow $1/\nu$ up to 1.7 keV. The evaluation is compared with the available data below 10 keV in Fig. 1. For convenience, the inset includes tabular values of the elastic, (n,p) and total cross sections at a few energies up to 1 keV.

Up to 10 keV, the evaluation is a reasonable representation of the 1966 results of Gibbons and Macklin³ and an average of their cross sections measured in 1963.⁴ These experiments, which extend to 100 keV, are compared with ENDF/B-V in Fig. 2.

From 100 keV to 1 MeV, additional experiments are available. The evaluation is heavily weighted by the data of Refs. 3 and 4 and the cross sections of Perry et al.⁵ as given in Fig. 3. Note that these three measurements are in good agreement among themselves but are higher than the measurements of Batchelor et al.⁶ and of Sayres et al.⁷ On the other hand, Sayres et al. measure an elastic cross section much higher than reported by Seagrave et al.⁸ (noted on the same figure).

In 1970, Costello et al.⁹ measured the (n,p) cross section from 300 keV to 1 MeV and obtained essentially a constant value of 900 mb over this energy range. Agreement of the Costello data with this evaluation above 500 keV is excellent, although from 300 to 400 keV, their measurements are more than 10% lower than ENDF/B-V.

Finally, Lopez et al.¹⁰ measured the relative ratio of the counting rates between ³He and BF₃ proportional counters from 218 eV to 521 keV. To provide a comparison between these two standard cross sections, the Lopez ratios were normalized at 218 eV to the Version IV ratios. Then, by using the present evaluation for the ³He(n,p) cross section to convert the Lopez ratio measurements to ¹⁰B cross sections, reasonable agreement with Version V ¹⁰B(n,α) is obtained. It should be noted, however, that the energy points are too sparse above a few keV to reproduce the structure observed in ¹⁰B.

Although the thermal (n,p) cross section is known to better than 1%, the energy at which this cross section deviates from 1/V is not well established. It should also be emphasized that experiments have not been carried out from 11 eV to a few keV, thereby placing severe restrictions upon the accuracy accompanying the use of the ³He(n,p)T cross-section standard. The 10% error estimates on the ORNL experimental data are directly related to the uncertainties in the analysis of the target samples employed. Certainly, further absolute measurements are needed on this cross-section standard, especially above ~ 100 eV.

III. ENDF/B-V FILES

File 1. General Information

MT=451. Descriptive data.

File 2. Resonance Parameters

MT=151. Scattering length = 0.2821E-12 cm.

File 3. Neutron Cross Sections

MT=1. Total Cross Sections

From 0.00001 eV to 10.8 keV MT1 taken as sum MT2 + MT103. From 10.8 keV to 20.0 MeV MT1 evaluated using experimental data from Ref. 11.

MT=2. Elastic Scattering Cross Sections

From 0.00001 eV to 10.8 keV MT2 taken as constant = 1.0 b. From 10.8 keV to 20.0 MeV MT2=MT1-MT103-MT104 with experimental data from Refs. 7 and 8 as checks. Note that two reactions are missing from the evaluation, namely, (n,n'p) and (n,2n2p). Experimental data at 15 MeV indicate non-zero cross sections for these reactions. In the present evaluation, these reactions are simply absorbed in MT=2.

MT=3. (n,p) Cross Section

Standards reaction - see Sec. II above.

MT=104. (n,d) Cross Sections

Threshold = 4.3614 MeV, Q = -3.2684 MeV. Evaluation from a detailed balance calculation (Ref. 2) and experimental data (Ref. 7).

MT=251. Average Value of Cosine Of Elastic Scattering Angle, Laboratory System.

Obtained from data MF=4, MT=2.

MT=252. Values Of Average Logarithmic Energy Decrement

Obtained from data MF=4, MT=2.

MT=253. Values Of Gamma

Obtained from data MF=4, MT=2.

File 4. Neutron Angular Distributions

MT=2. Angular Distribution Of Secondary Neutrons From Elastic Scattering.

Evaluated from experimental data from Refs. 7, 8, 11-14 covering incident energies as follows:

<u>INCIDENT ENERGY</u>	<u>REFERENCES</u>
1.E-5 eV	(Isotropic)
0.5 MeV	(Isotropic)
1.0 MeV	8
2.0 MeV	8
2.6 MeV	11
3.5 MeV	8
5.0 MeV	11
6.0 MeV	8, 12 (from p+t elastic scattering)
8.0 MeV	7, 12 (from p+t elastic scattering)
14.5 MeV	12, 13 (from p+t elastic scattering)
17.5 MeV	7
20.0 MeV	11 (from p+t elastic scattering)

REFERENCES

1. This evaluation was translated by R. J. LaBauve into the ENDF/B format for Version III.
2. J. Als-Nielsen and O. Dietrich, "Slow Neutron Cross Sections for He³, B, and Au," Phys. Rev. 133, B 925 (1964).
3. J. H. Gibbons and R. L. Macklin, "Total Neutron Yields from Light Elements under Proton and Alpha Bombardment," Phys. Rev. 114, 571 (1959).
4. R. L. Macklin and J. H. Gibbons, Proceedings of the International Conference on the Study of Nuclear Structure with Neutrons, Antwerp, 19-23 July 1965 (North-Holland Publishing Co., 1966), p. 498.
5. J. E. Perry, Jr., E. Haddad, R. L. Henkel, G. A. Jarvis, and R. K. Smith, private communication 1960.

6. R. Batchelor, R. Aves, and T. H. R. Skyrme, "Helium-3 Filled Proportional Counter for Neutron Spectroscopy," *Rev. Sci. Instr.* 26, 1037 (1955).
7. A. R. Sayres, K. W. Jones, and C. S. Wu, "Interaction of Neutrons with He^3 ," *Phys. Rev.* 122, 1853 (1961).
8. J. D. Seagrave, L. Cranberg, and J. E. Simmons, "Elastic Scattering of Fast Neutrons by Tritium and He^3 ," *Phys. Rev.* 119, 1981 (1960).
9. D. G. Costello, S. J. Friesenhahn, and W. M. Lopez, " $^3\text{He}(n,p)\text{T}$ Cross Section from 0.3 to 1.16 MeV," *Nucl. Sci. Eng.* 39, 409 (1970).
10. W. M. Lopez, M. P. Fricke, D. G. Costello, and S. J. Friesenhahn, "Neutron Capture Cross Sections of Tungsten and Rhenium," Gulf General Atomic, Inc. report GA-8835.
11. Los Alamos Physics and Cryogenics Groups, *Nucl. Phys.* 12, 291 (1959).
12. J. E. Brolley, Jr., T. M. Putnam, L. Rosen, and L. Stewart, *Phys. Rev.* 159, 777 (1967).
13. B. Antolkovic, G. Paic, P. Tomas, and R. Rendic, *Phys. Rev.* 159, 777 (1967).
14. L. Rosen and W. Leland, Private communication (1967).

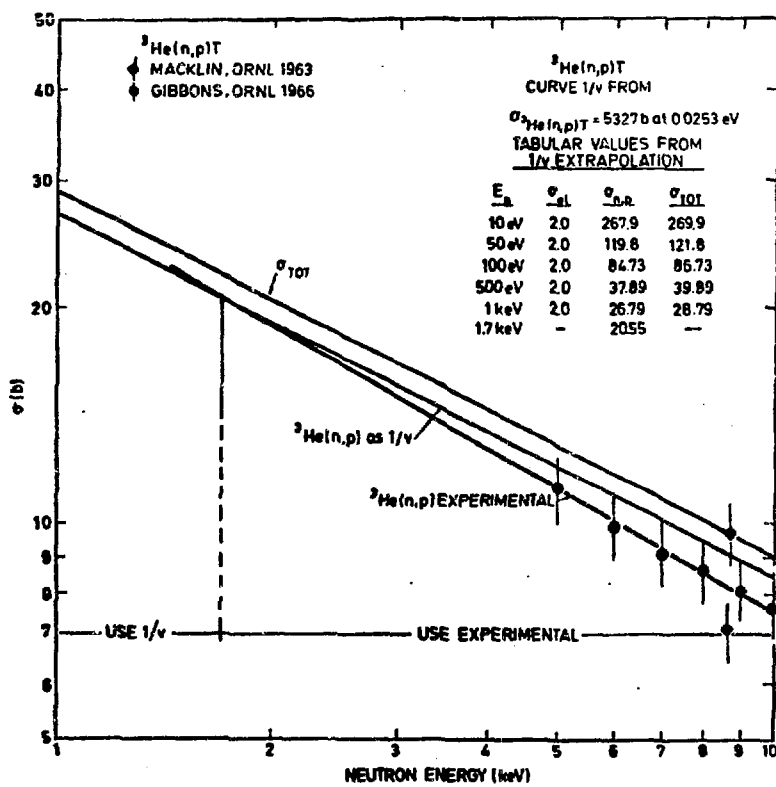


Fig. 1.

The (n,p) and total cross sections for ^3He from 1 to 10 keV. The curve drawn through the experimental points deviates from $1/V$ at 1.7 keV.

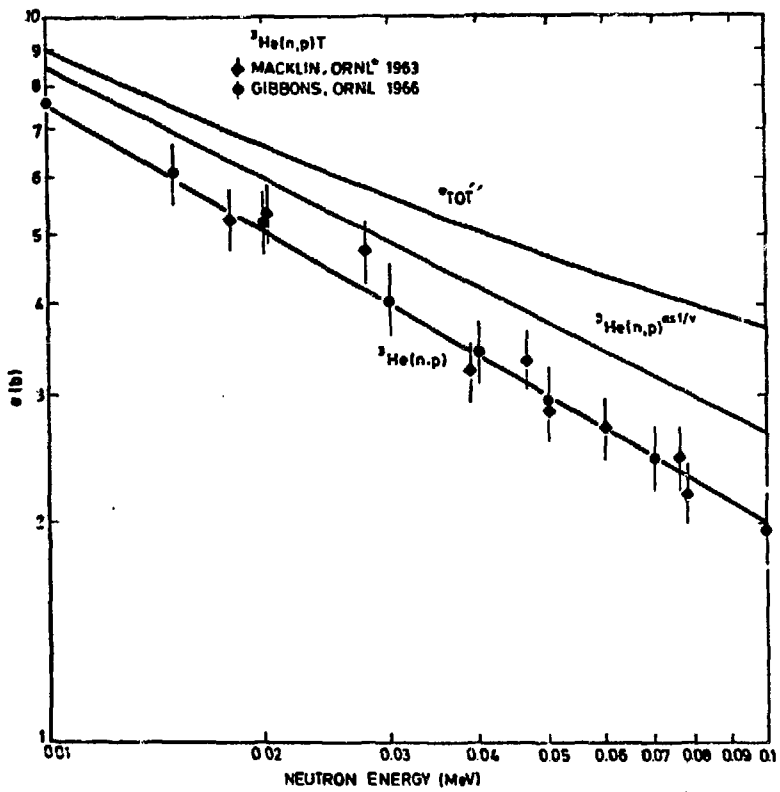


Fig. 2.
The (n,p) and total cross sections for ${}^3\text{He}$ from 10 to 100 keV.

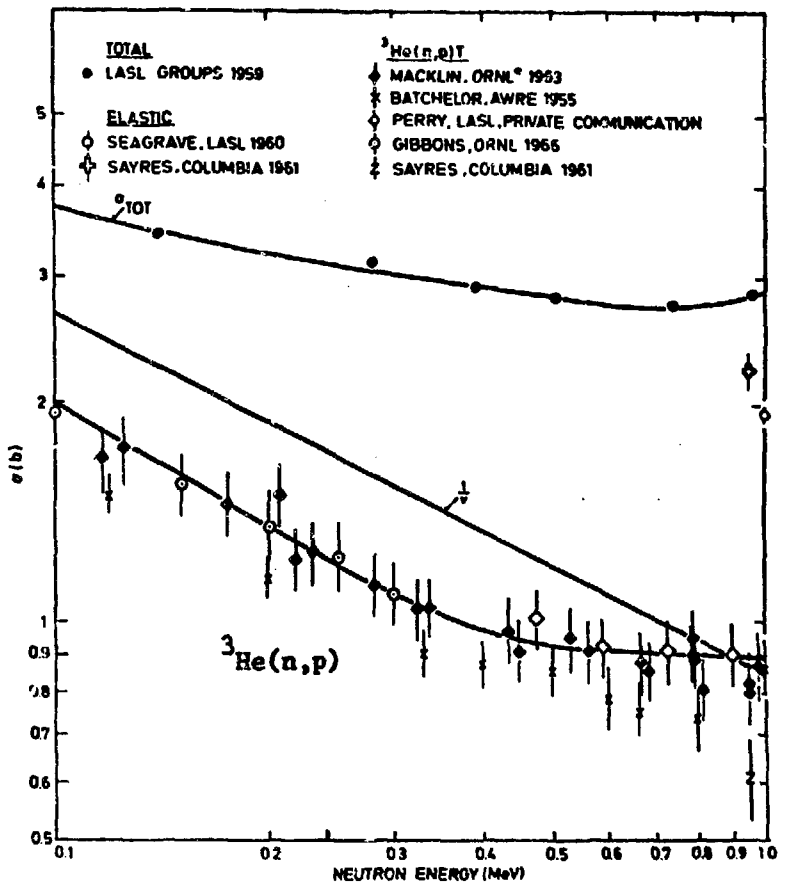


Fig. 3.
The (n,p), elastic, and total cross sections for ${}^3\text{He}$ from 100 keV to 1 MeV. The Costello data⁹ have been omitted for the sake of clarity.

SUMMARY DOCUMENTATION FOR ^4He

by

G. M. Hale, R. A. Nisley, and P. G. Young
Los Alamos Scientific Laboratory
Los Alamos, New Mexico

I. SUMMARY

The ENDF/B-V evaluation for ^4He (MAT 1270) is the same as Version IV except for minor format changes. The evaluation covers the energy range 10^{-5} eV to 20 MeV and is based at all energies on an extensive R-matrix analysis, which is described in NEANDC (J) 38L (reference Do75). By making use of the charge symmetry of nuclear forces, p- ^4He data were included in the analysis along with the available n- ^4He measurements of cross sections, angular distributions, and polarizations. Because of the extent of the data base used and the careful analysis it was given, the cross sections and angular distributions are thought to be accurate to about $\pm 2\%$ at all energies. As all gamma-ray production cross sections are essentially zero for ^4He , gamma ray files (MF=12-16) are deliberately excluded from the evaluation.

II. ENDF/B-V FILES

File 1. General Information

MT=451. Descriptive data.

File 2. Resonance Parameters

MT=151. Effective scattering radius = 0.24579×10^{-12} cm.

Resonance parameters not given.

File 3. Neutron Cross Sections

The 2200 m/s cross sections are as follows:

MT=1 Sigma = 0.75916 b
MT=2 Sigma = 0.75916 b .

MT=1. Total Cross Section

See discussion under MT=2 below.

MT=2. Elastic Scattering Cross Section

Although the only reaction possible for neutrons incident on ${}^4\text{He}$ below 20 MeV is elastic scattering, the majority of the $n-{}^4\text{He}$ data is rather imprecise. In order to overcome this problem, an R-matrix analysis was performed with a data set which included not only the $n-{}^4\text{He}$ data but also very precise $p-{}^4\text{He}$ data. All the available $n-{}^4\text{He}$ and $p-{}^4\text{He}$ data below 20 MeV were considered in the analysis. Since the previous evaluation was completed in 1968, several $n-{}^4\text{He}$ elastic scattering measurements have been done. The most significant of these are the low energy neutron cross sections of Rorer (Ro69), the RPI total cross section measurement (Go73), which cover the range $E_n = 0.7-30$ MeV, and the relative angular distributions of Morgan (Mo68). A complete list of references for the $n-{}^4\text{He}$ data used is given below. The $p-{}^4\text{He}$ data was selected to satisfy very stringent statistical criteria and we believe the possible errors of the predicted values for the $p-{}^4\text{He}$ scattering to be less than 1.0%. A simple model for the charge differences between the $n-{}^4\text{He}$ and $p-{}^4\text{He}$ systems was assumed and the $n-{}^4\text{He}$ and $p-{}^4\text{He}$ data sets were simultaneously analyzed. The values of the cross sections and angular distributions contained in Files 3 and 4 are probably accurate to within 2.0%.

Comparisons of the evaluated and experimental total cross section data are given in Figs. 1-4, and the elastic angular distribution data are included in Figs. 5-11. The neutron polarization measurements that were included in the R-matrix analysis are also shown in Figs. 12 and 13.

File 4. Neutron Angular Distributions

MT=2. Elastic Scattering Angular Distributions.

Obtained from the R-matrix analysis described above under MF=3, MT=2. Legendre polynomial representation used in the cm system. See Figs. 5-11 for data.

REFERENCES

Au62 S. M. Austin et al., Phys. Rev. 126, 1532 (1962).
Br72 W. B. Broste et al., Phys. Rev. C5, 761 (1972).
Bu66 F. W. Busser et al., Nucl. Phys. 88, 593 (1966).
Cr72 D. S. Cramer and L. Cranberg, Nucl. Phys. A180, 273 (1972).
Do75 D. C. Dodder, G. M. Hale, R. A. Nisley, K. Witte, and P. G. Young, Proc. of the EANDC Topical Discussion on "Critique of Nuclear Models and Their Validity in the Evaluation of Nuclear Data," Mar. 1974, p. 1. (Published in NEANDC (J) 38L (1975).
Fa63 U. Fasoli and G. Zago, Nuovo Cimento 30, 1169 (1963).
Go73 C. A. Couplding et al., Nucl. Phys. A215, 253 (1973).
Ho66 B. Hoop, Jr. and H. H. Barschall, Nucl. Phys. 83, 65 (1966).
Je66 R. W. Jewell et al., Phys. Rev. 142 687 (1966).

Ma63 T. H. May et al., Nucl. Phys. 45, 17 (1963) (Rev. Mo68 and Sa68).
Mo68 G. L. Morgan and R. L. Walker, Phys. Rev. 168, 1114 (1968).
Ni71 A. Niiler et al., Phys. Rev. C4, 36 (1971) (Rev. 9-72).
Ro69 D. C. Rorer et al., Nucl. Phys. 133, 410 (1969).
Sa68 J. R. Sawers et al., Phys. Rev. 168, 1102 (1968).
Se53 J. D. Seagrave, Phys. Rev. 92, 1222 (1953).
Sh55 D. F. Shaw, Proc. Phys. Soc. (London) 68, 43 (1955).
Sh64 R. E. Shamp and J. G. Jenkins, Phys. Rev. 135, B99 (1964).
Sm54 J. R. Smith, Phys. Rev. 95, 730 (1954).
St70 T. Stammbach et al., Phys. Rev. C2, 434 (1970).
Wh57 R. E. White and F. J. M. Farley, Nucl. Phys. 3, 476 (1957).
Yo63 P. G. Young et al., Aust. J. Phys. 16, 185 (1963).

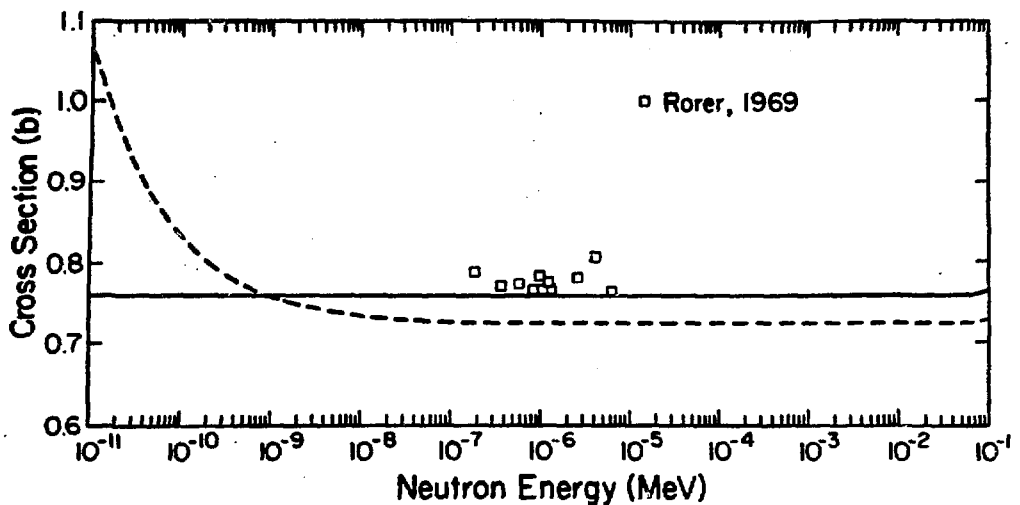


Fig. 1.

Measured and evaluated $n-{}^4\text{He}$ total cross sections between 10^{-5} eV and 100 keV. The solid curve is ENDF/B-V and the dashed curve is ENDF/B-III.

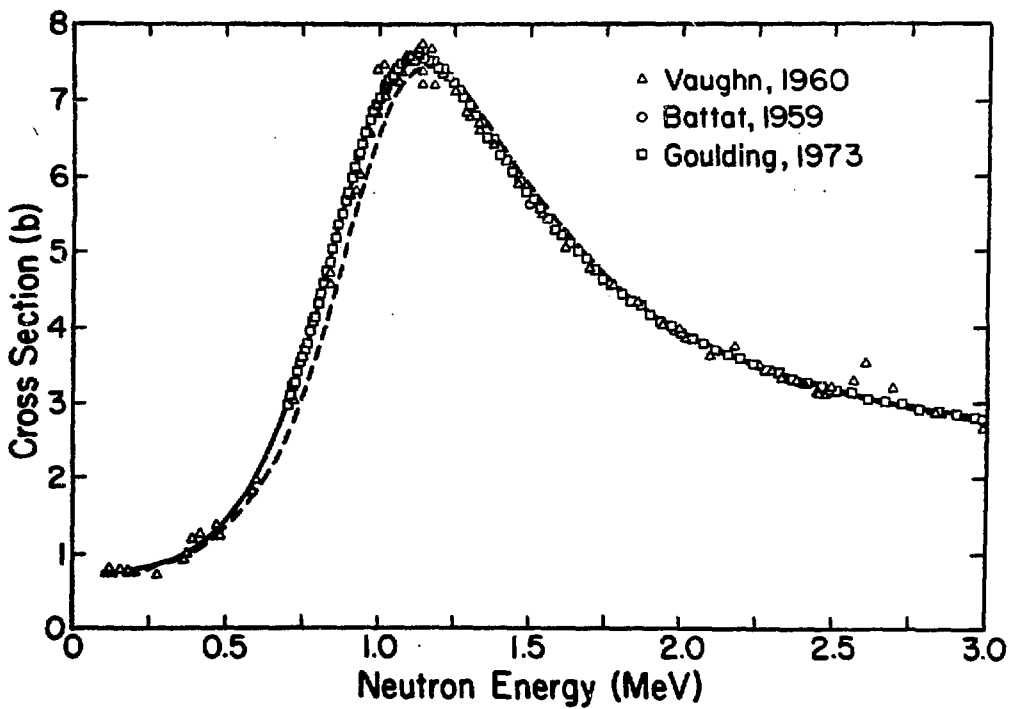


Fig. 2.

Measured and evaluated $n-{}^4\text{He}$ total cross sections between 0 and 3 MeV. The solid curve is ENDF/B-V and the dashed curve is ENDF/B-III.

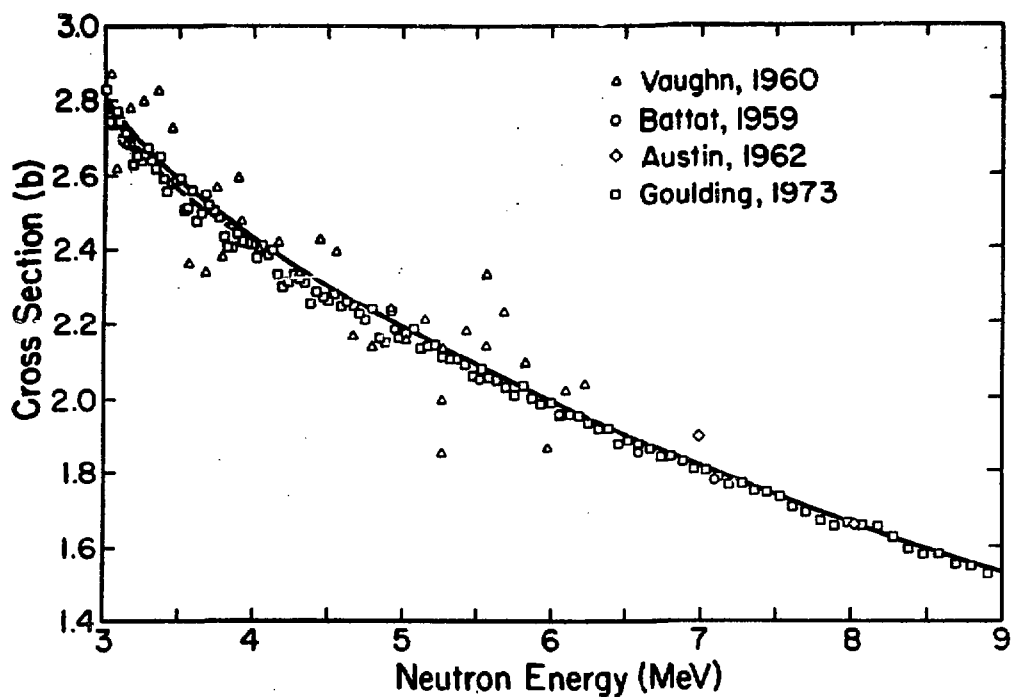


Fig. 3.

Measured and evaluated $n-{}^4He$ total cross sections between 3 and 9 MeV. The solid curve is ENDF/B-V and the dashed curve is ENDF/B-III.

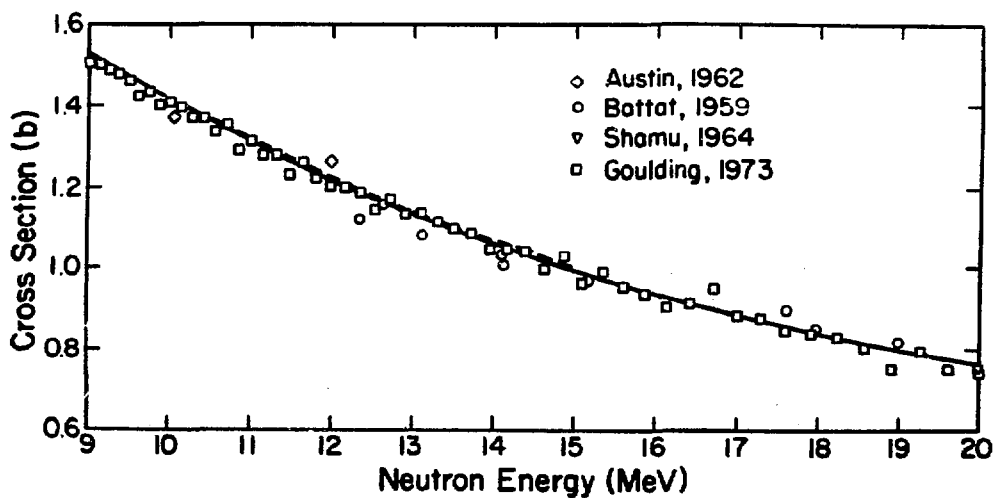


Fig. 4.

Measured and evaluated $n-{}^4He$ total cross sections between 9 and 20 MeV. The solid curve is ENDF/B-V and the dashed curve is ENDF/B-III.

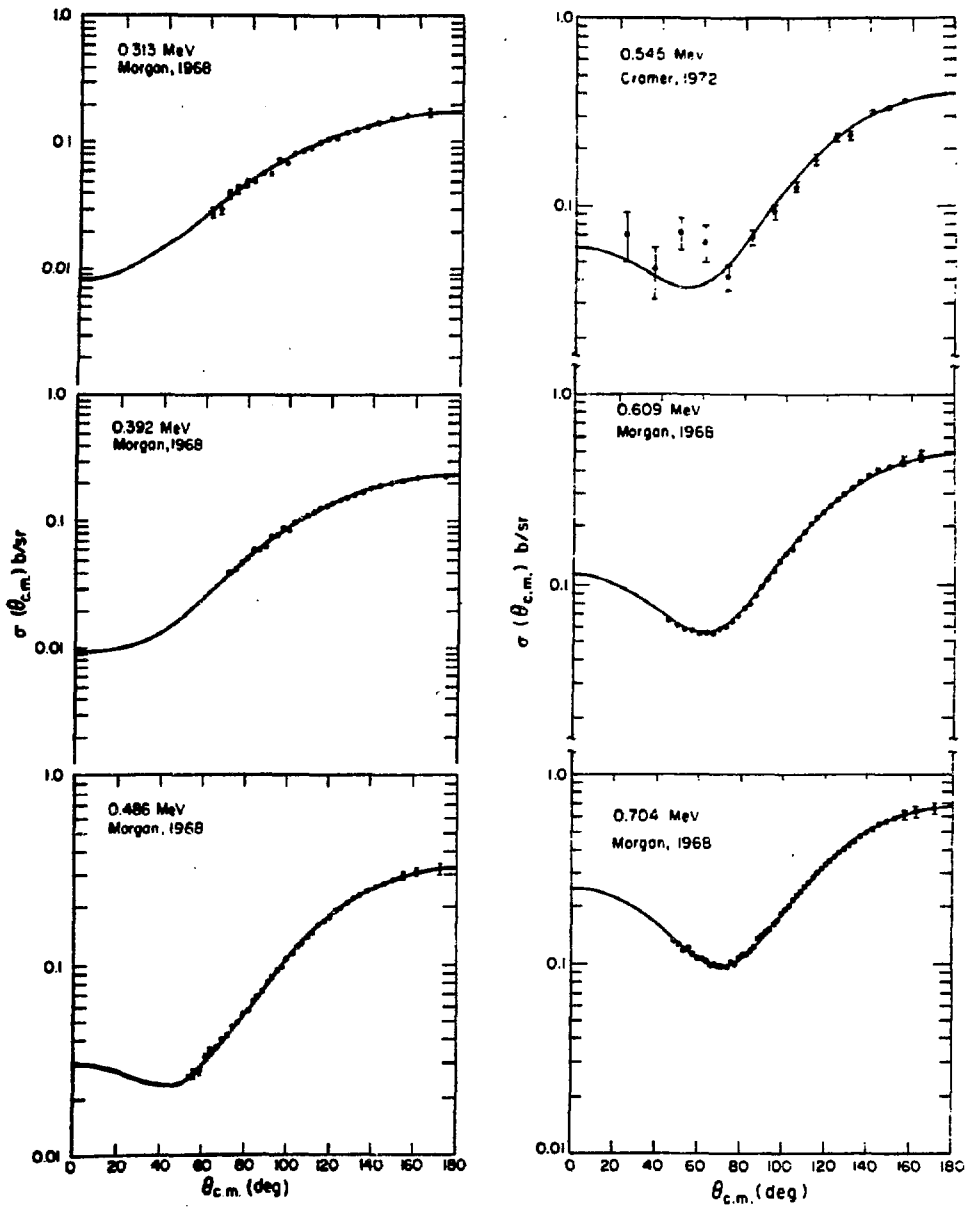


Fig. 5.

Measured and evaluated $n-{}^4He$ differential elastic angular distribution for incident neutron energies between 0.313 and 0.704 MeV.

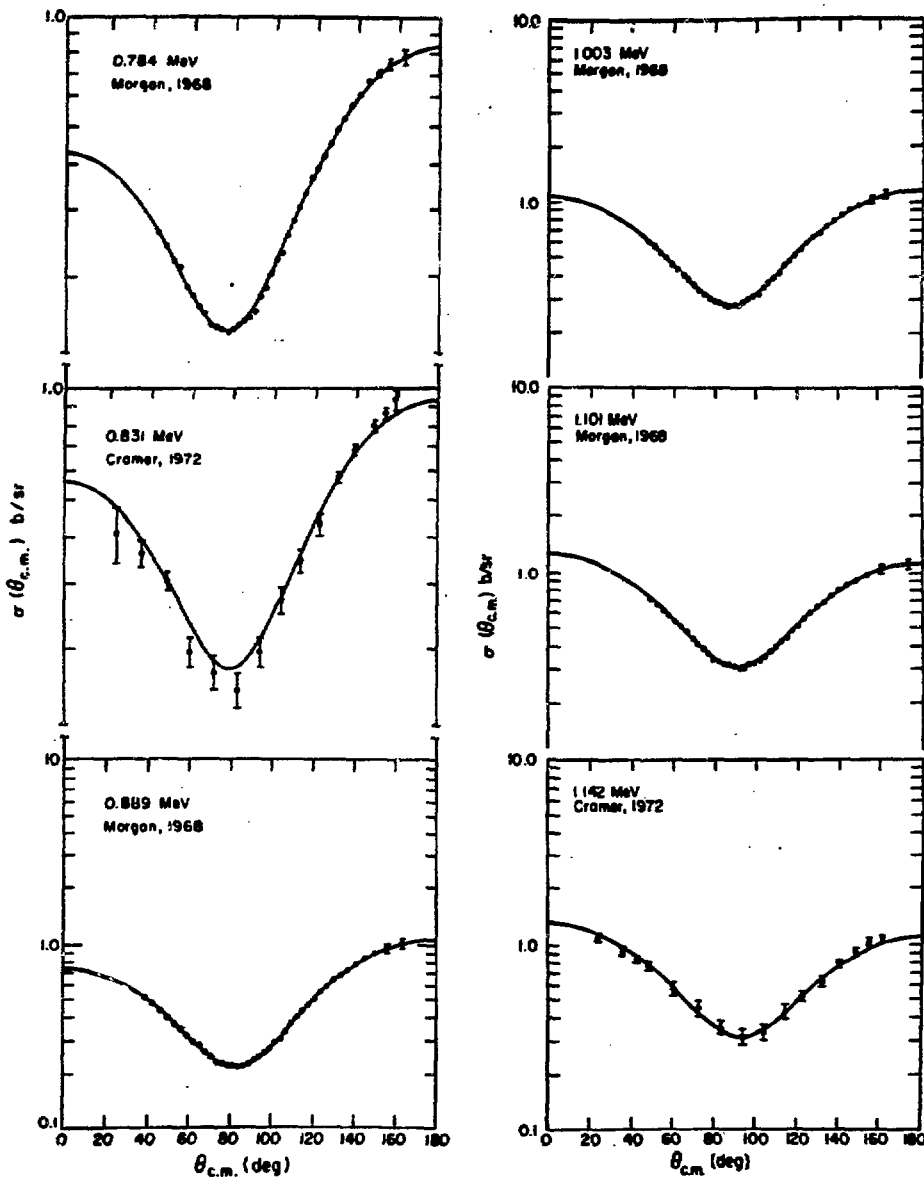


Fig. 6.

Measured and evaluated $n-{}^4He$ differential elastic angular distribution for incident neutron energies between 0.784 and 1.142 MeV.

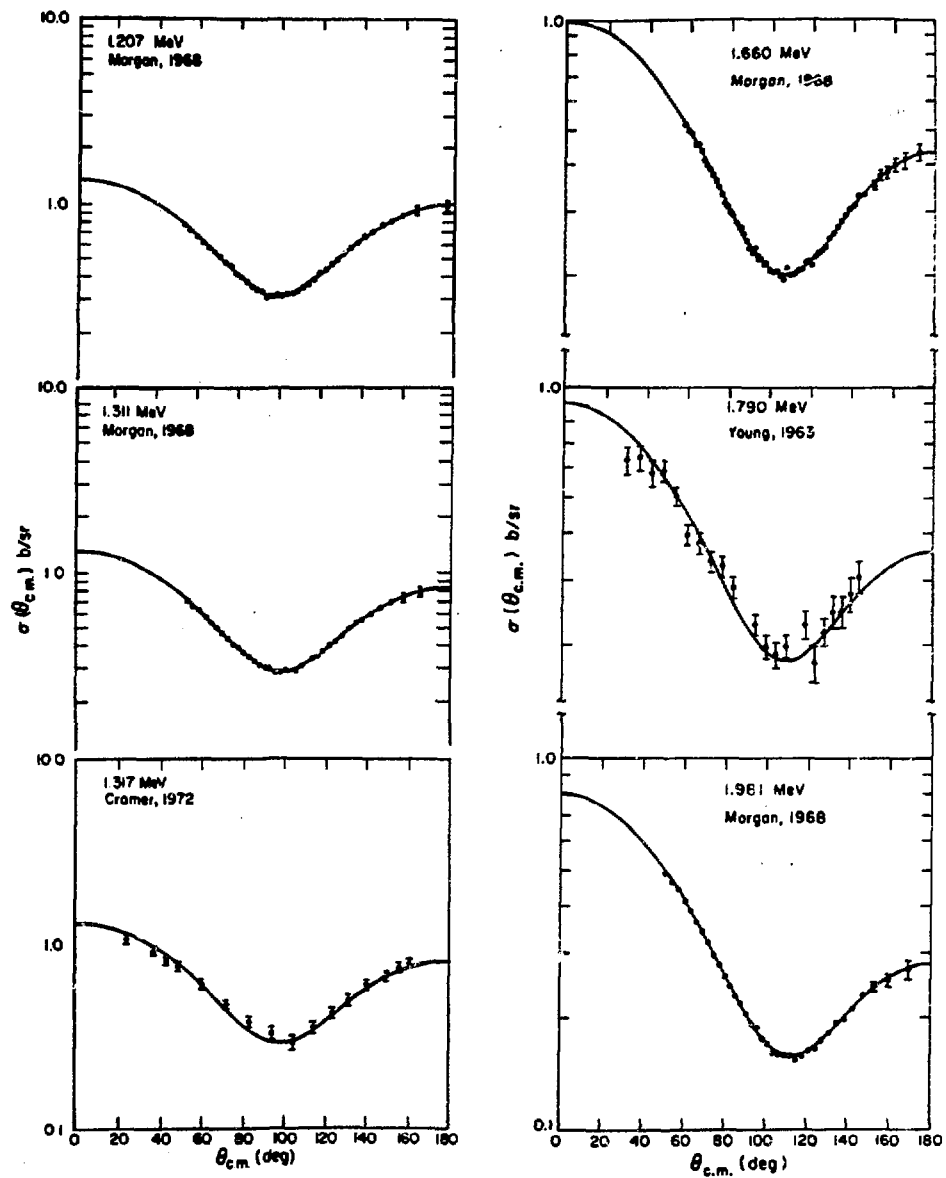


Fig. 7.

Measured and evaluated $n-{}^4\text{He}$ differential elastic angular distribution for incident neutron energies between 1.207 and 1.981 MeV.

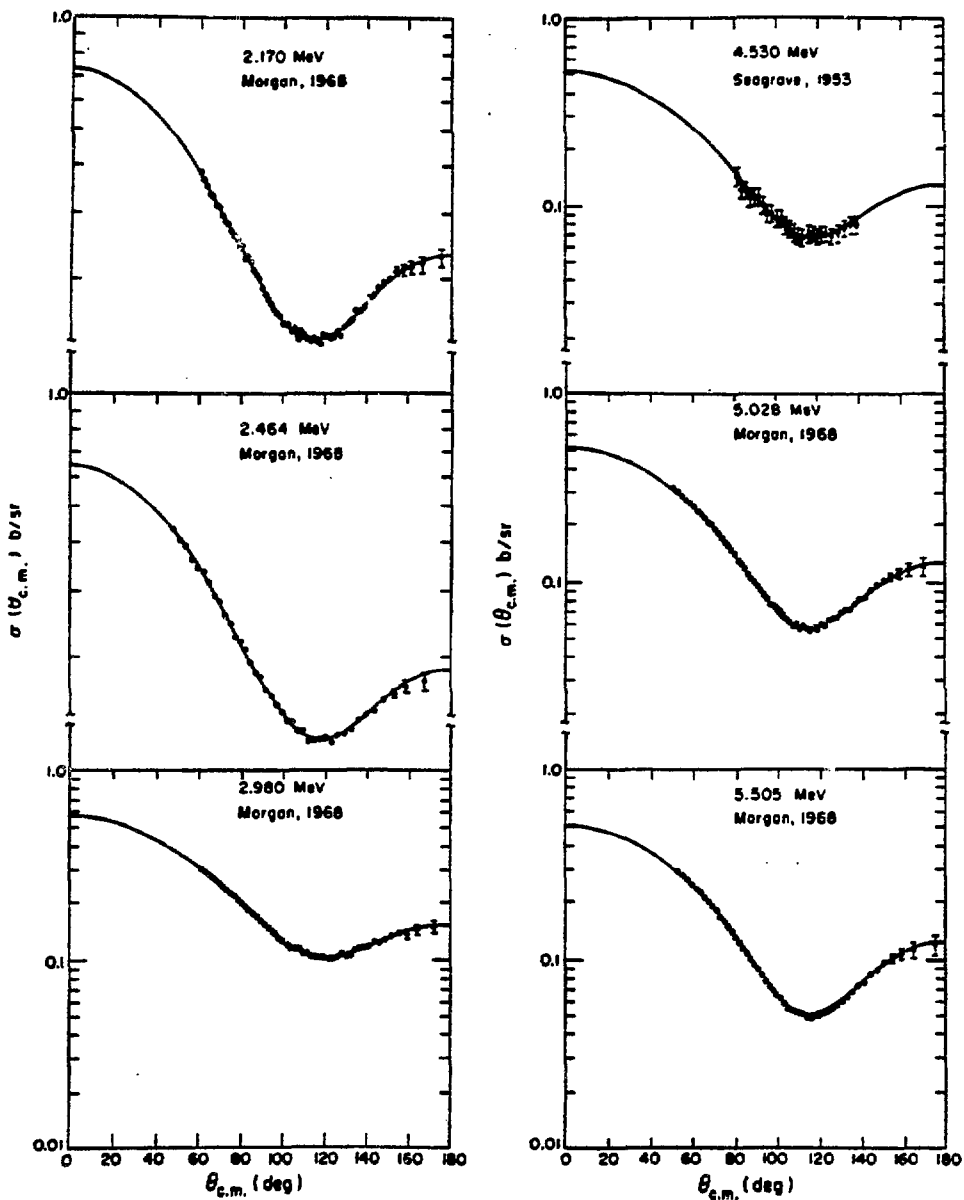


Fig. 8.

Measured and evaluated $n-{}^4\text{He}$ differential elastic angular distribution for incident neutron energies between 2.170 and 5.505 MeV.

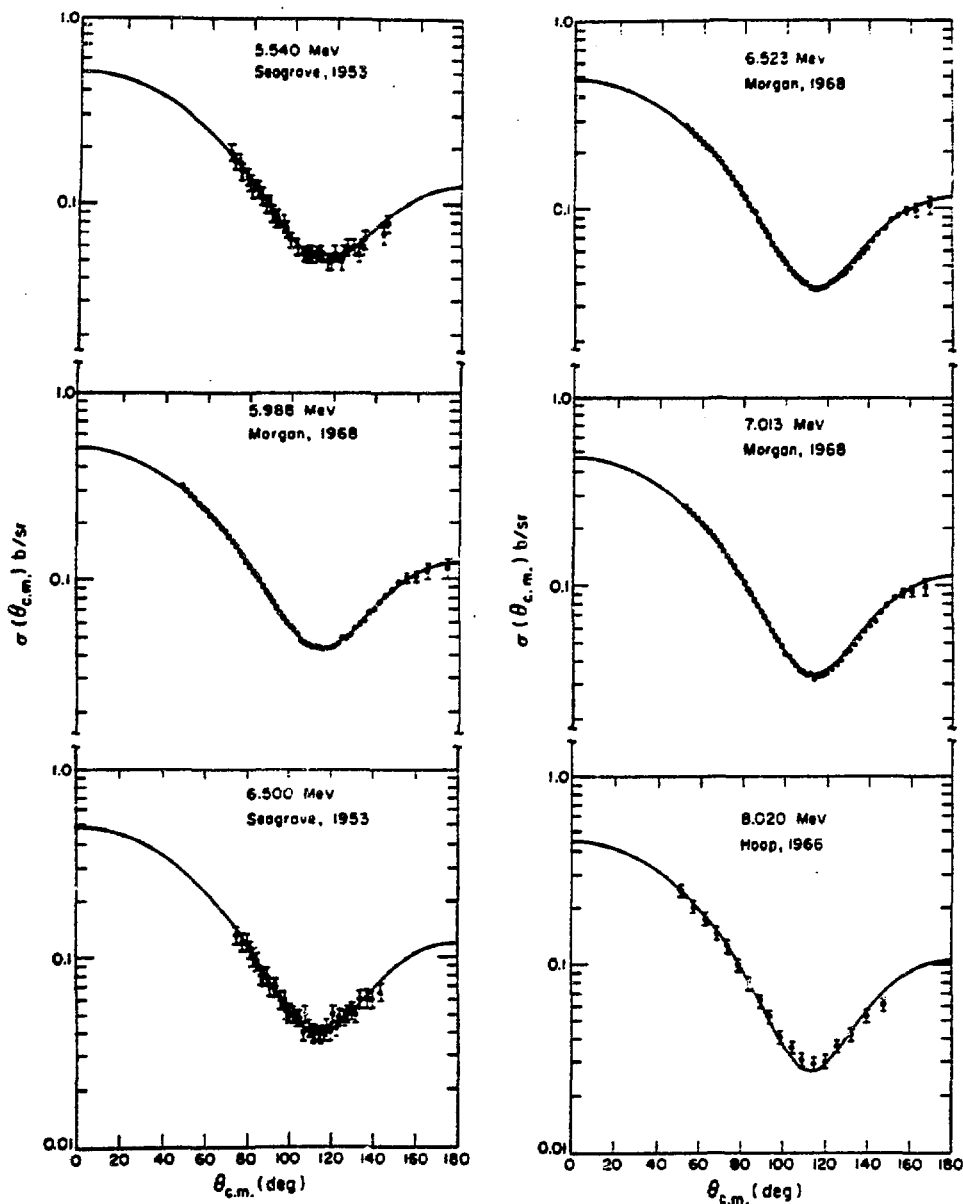


Fig. 9.

Measured and evaluated $n-{}^4He$ differential elastic angular distribution for incident neutron energies between 5.54 and 8.08 MeV.

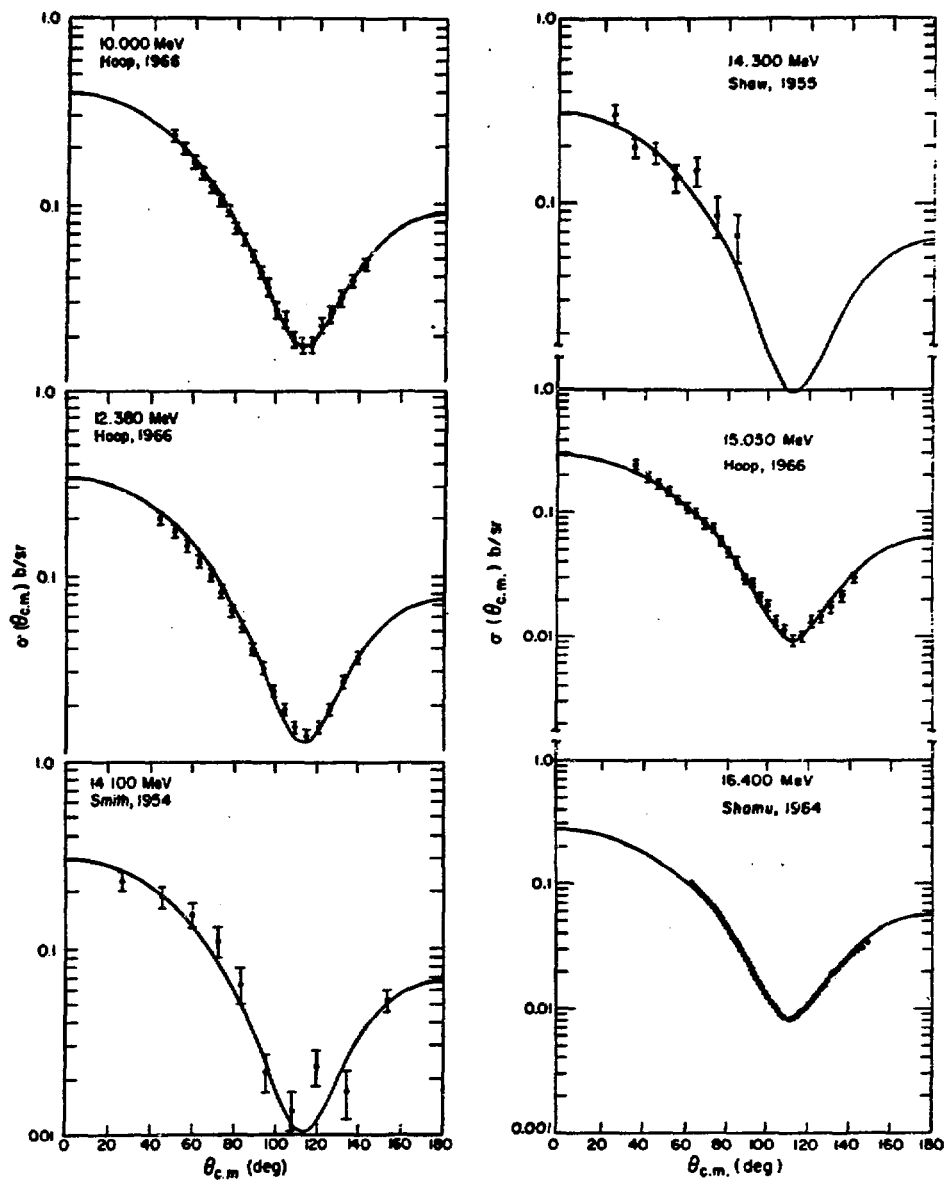


Fig. 10.

Measured and evaluated n-⁴He differential elastic angular distribution for incident neutron energies between 10.0 and 16.4 MeV.

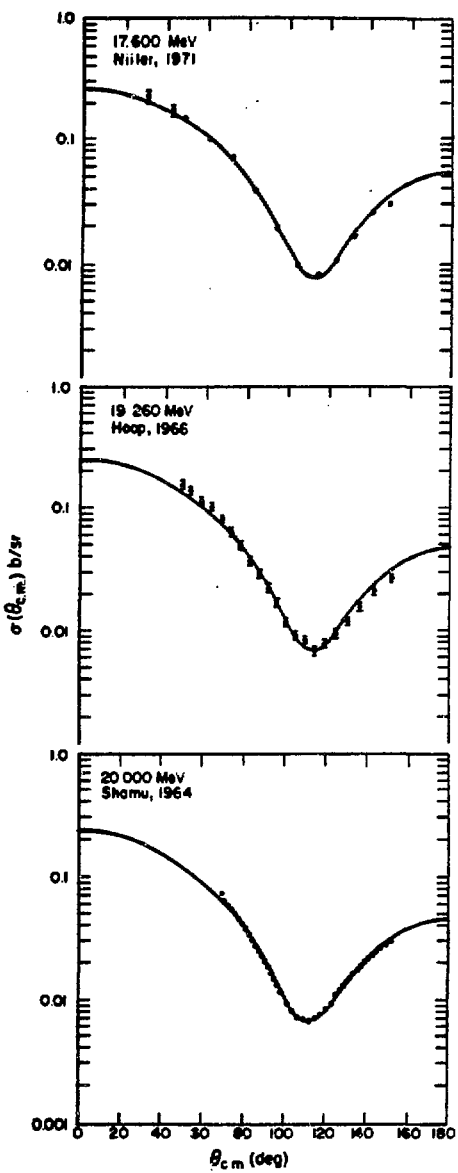


Fig. 11.

Measured and evaluated $n-{}^4He$
differential elastic angular
distribution for incident
neutron energies between
17.6 and 20.0 MeV.

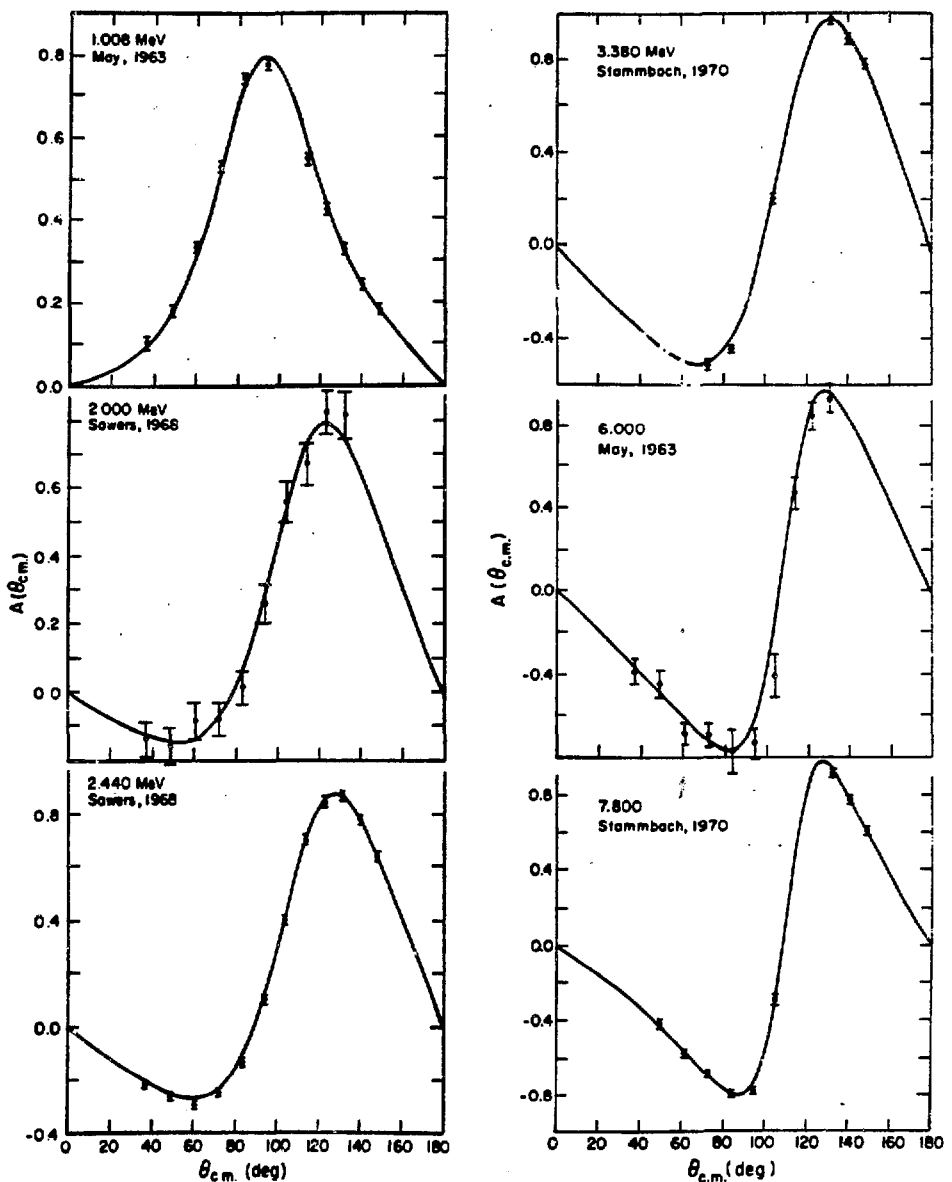


Fig. 12.

${}^4\text{He}(n,n){}^4\text{He}$ neutron polarizations for incident energies between 1.008 and 7.8 MeV.

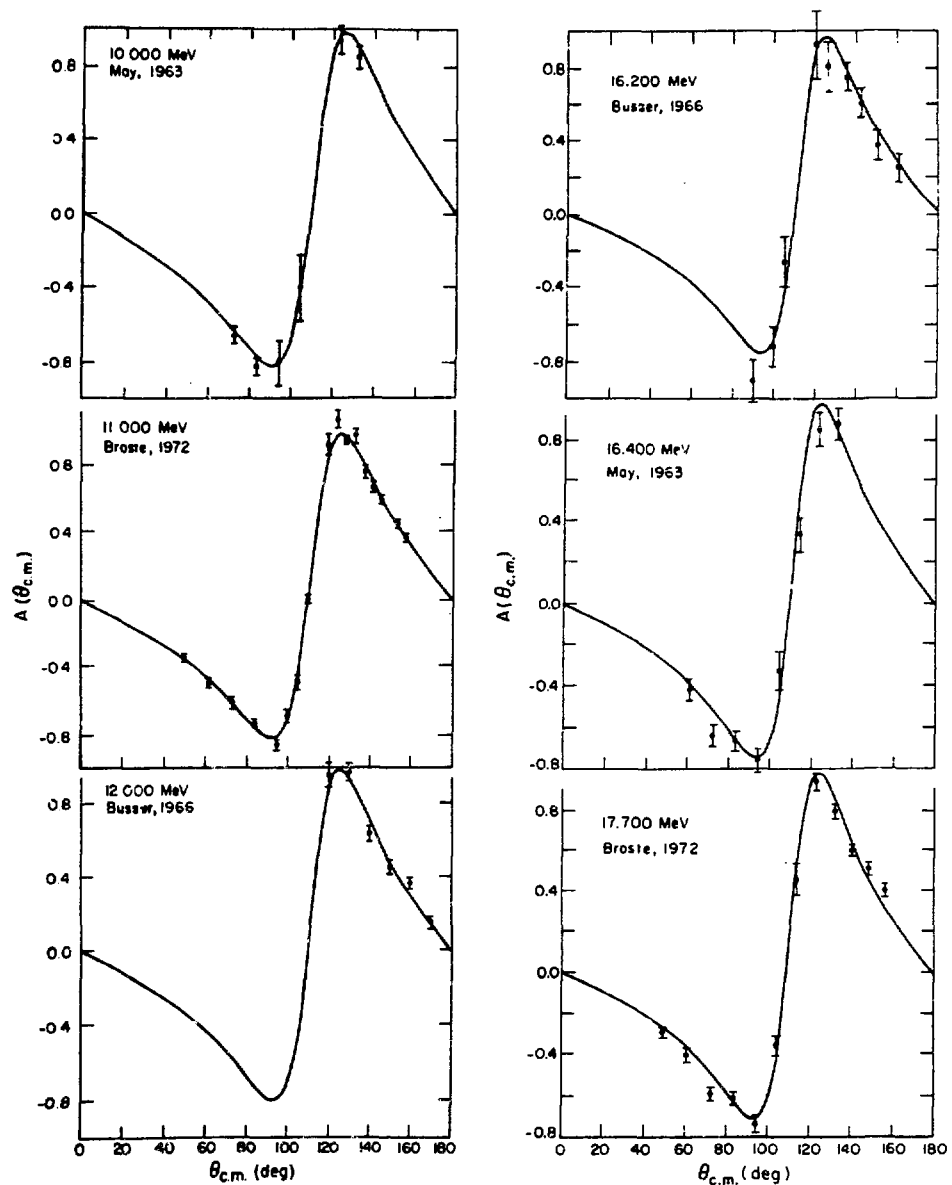


Fig. 13.

${}^4\text{He}(n, n) {}^4\text{He}$ neutron polarizations for incident energies between 10.0 and 17.7 MeV.

SUMMARY DOCUMENTATION FOR ${}^6\text{Li}$

by

G. M. Hale, L. Stewart, and P. G. Young
Los Alamos Scientific Laboratory
Los Alamos, New Mexico

I. SUMMARY

The previous evaluation for ${}^6\text{Li}$ was extensively revised for Version V of ENDF/B (MAT 1303). All major cross-section files except radiative capture were updated. A new R-matrix analysis including recent experimental results was performed up to a neutron energy of 1 MeV, which includes the standards region for the ${}^6\text{Li}(\text{n},\text{t}){}^4\text{He}$ reaction. Extensive revisions were made in the MeV region to include a more precise representation of the $(\text{n},\text{n}'\text{d})$ reaction. In the new representation, the $(\text{n},\text{n}'\text{d})$ cross section is grouped into ${}^6\text{Li}$ excitation energy bins, which preserves the kinematic energy-angle relationships in the emitted neutron spectra. Finally, correlated error data were added up to a neutron energy of 1 MeV, triton angular distributions from the ${}^6\text{Li}(\text{n},\text{t}){}^4\text{He}$ reaction were included below 1 MeV, and radioactive decay data were added to Files 8 and 9. Except for the covariance and (n,t) angular distribution files, the evaluation covers the neutron energy range of 10^{-5} eV to 20 MeV.

II. STANDARDS DATA

The ${}^6\text{Li}(\text{n},\alpha)$ cross section is regarded as a standard below $E_{\text{n}}=100$ keV. The Version V cross sections for ${}^6\text{Li}$ below 1 MeV were obtained from multi-channel, multilevel R-matrix analyses of reactions in the ${}^7\text{Li}$ system, similar to those from which the Version IV evaluation were taken. New data have become available since Version IV was released and most of this new experimental information has been incorporated into the Version V analysis.

For Version IV, the ${}^6\text{Li}(\text{n},\alpha)$ cross section was determined mainly by fitting the Harwell total cross section (reference 3 below), since this was presumably the most accurately known data included in the analysis. However, in addition to the Harwell total, the data base for the analysis included the shapes of the $\text{n}-{}^6\text{Li}$ elastic angular distributions and polarizations, ${}^6\text{Li}(\text{n},\alpha)\text{T}$ angular distributions and integrated cross sections (normalized), and $\text{t}-\alpha$ elastic angular distributions.

Since the time of the Version IV analysis, new data have become available whose precision equals or betters that of the Harwell total cross section. The present analysis includes the following new measurements while retaining most of the data from the previous analysis:

<u>Measurement</u>	<u>References</u>	<u>Approximate Precision</u>
$n-{}^6\text{Li } \sigma_T$	Harvey, ORNL ⁴	0.5-1%
${}^6\text{Li}(n,\alpha)$ integrated cross section	Lamaze, NBS ²¹	1-2% (relative)
${}^4\text{He}(t,t){}^4\text{He}$ differential cross section	Jarmie, LASL ³⁵	0.4-1%
${}^4\text{He}(t,t){}^4\text{He}$ analyzing power	Hardekopf, LASL ³⁶	1%

Fits to the (n,α) data included in the Version V analysis are shown in Figs. 1 and 2. In Fig. 1, the data are plotted as $\sigma \cdot \sqrt{E_n}$; in both figures, the Version IV evaluation is represented by the dashed curves. The good agreement with Lamaze's new ${}^6\text{Li}(n,\alpha)$ integrated cross section measurement²¹ is particularly encouraging, since these are close to the values most consistent with the accurate new $t + \alpha$ measurements.^{35,36} On the other hand, a shape difference persists between the fit and measurements of the total cross section in the region of the precursor dip and at the peak of the 245-keV resonance. However, we feel that including these precise new data in the analysis has reduced the uncertainty of the new ${}^6\text{Li}(n,\alpha)$ cross section significantly (to the order of 3%) over that of previous evaluations in the region of the resonance.

III. ENDF/B-V FILES

File 1. General Information

MT=451. Descriptive data.

File 2. Resonance Parameters

MT=151. Effective scattering radius = 0.23778×10^{-12} cm.

Resonance parameters not given.

File 3. Neutron Cross Sections

The 2200 m/s cross sections are as follows:

MT=1	Sigma =	936.64	b
MT=2	Sigma =	0.71046	b
MT=102	Sigma =	0.03850	b
MT=105	Sigma =	935.89	b

MT=1. Total Cross Section

Below 1 MeV, the values are taken from an R-matrix analysis by Hale, Dodder, Witte (described in Ref. 2) which takes into account data from all reactions possible in ${}^7\text{Li}$ up to 3 MeV neutron energy. Total cross section data considered in this analysis were those of Refs. 3 and 4. Between 1 and 5 MeV, the total was taken to be the sum of MT=2, 4, 24, 102, 103, and 105, which generally follows the measurements of Refs. 5 and 6. Between 5 and 20 MeV, the total was determined by an average of the data of Refs. 6 and 7 which agrees with Ref. 8

except at the lowest energy. In this region, the total exceeds the sum of the measured partial cross sections by as much as 200-300 mb. This difference was distributed between the elastic and total (n, n') d cross sections.

MT=2. Elastic Cross Section

Below 3 MeV, the values are taken from the R-matrix analysis cited for MT=1, which includes the elastic measurements of Refs. 9 and 10. These calculations were matched smoothly in the 3-5 MeV region to a curve which lies about 50 mb above Batchelor (Ref. 26) between 5 and 7.5 MeV, and about 13% above the data of Refs. 14, 27, 28, and 29 at 10 to 14 MeV.

MT=4. Inelastic Cross Section

Sum of MT=51 through MT=81.

MT=24. $(n, 2n)\alpha$ Cross Section

Passes through the point of Mather and Pain (Ref. 11) at 14 MeV, taking into account the measurements of Ref. 12.

MT=51, 52, 54-56, 58-81. (n, n') d Continuum Cross Sections

Represented by continuum-level contributions in ${}^6\text{Li}$, binned in 0.5-MeV intervals. The energy-angle spectra are determined by a 3-body phase-space calculation, assuming isotropic center-of-mass distributions. At each energy, the sum of the continuum-level contributions is normalized to an assumed energy-angle integrated continuum cross section which approximates the difference of Hopkin's measurement (Ref. 13) and the contribution from the first and second levels in ${}^6\text{Li}$. The steep rise of the pseudo-level cross sections from their thresholds and the use of fixed bin widths over finite angles produces anomalous structure in the individual cross sections which is especially apparent near the thresholds. Some effort has been made to smooth out these effects, but they remain to some extent.

MT=53. (n, n_1) d Discrete Level Cross Sections

Cross section has p-wave penetrability energy dependence from threshold to 3.2 MeV. Matched at higher energies to a curve which lies 15-20% above Hopkins (Ref. 13) and passes through the 10-MeV point of Cookson (Ref. 14).

MT=57. $(n, n_2)\gamma$ Cross Section

Rises rapidly from threshold, peaks at 5 mb and falls off gradually to 20 MeV. No data available except upper limits.

MT=102. (n, γ) Cross Sections

Unchanged from Version IV, which was based on the thermal measurement of Jurney (Ref. 15) and the Pendlebury evaluation (Ref. 16) at higher energies.

MT=103. (n,p) Cross Sections

Threshold to 9 MeV, based on the data of Ref. 17. Extended to 20 MeV through the 14-MeV data of Refs. 18 and 19.

MT=105. (n,t) Cross Sections

Below 3 MeV, values are taken from the R-matrix analysis of Ref. 2, which includes (n,t) measurements from Refs. 20-24. Between 3 and 5 MeV, the values are based on Bartle's measurements (Ref. 24). At higher energies, the cross sections are taken from the evaluation of Ref. 16, extended to 20 MeV considering the data of Kern (Ref. 25).

File 4. Neutron Secondary Angular Distributions

MT=2. Elastic Angular Distributions

Legendre coefficients determined as follows:

Below 2 MeV, coefficients up to $L=2$ were taken from the R-matrix analysis of Ref. 2, which takes into account elastic angular distribution measurements from Refs. 9 and 10 above 2 MeV. The coefficients represent fits to the measurements of Refs. 13 and 26 in the 3.5-7.5 MeV range, that of Ref. 14 at 1 MeV, and those of Refs. 27-29 at 14 MeV. Extrapolation of the coefficients to 20 MeV was aided by optical model calculations.

MT=24. $(n,2n)$ Angular Distributions

Laboratory distributions obtained by integrating over energy the 4-body phase-space spectra that result from transforming isotropic center-of-mass distributions to the laboratory system.

MT=51 - 81. (n,n') Angular Distributions

Obtained by transforming distributions that are isotropic in the 3-body center-of-mass system to equivalent 2-body distributions in the laboratory system. MT=53 and 57 are treated as real levels and assumed to be isotropic in the two-body reference system. Data available indicate departure from isotropy for the first real level (MT=53) and this anisotropy will be included in a later update.

MT=105. (n,t) Angular Distributions

Legendre coefficients obtained from the R-matrix analysis of Ref. 2 are supplied at energies below 1 MeV. The analysis takes into account (n,t) angular distribution measurements from Refs. 23 and 30.

File 5. Neutron Secondary Energy Distributions

MT=24. (n,2n) Energy Distributions

Laboratory distributions obtained by integrating over angle the 4-body phase-space spectra that result from transforming isotropic center-of-mass distributions to the laboratory system.

File 8. Radioactive Nuclide Production

MT=103. (n,p) ${}^6\text{He}$

${}^6\text{He}$ beta decays, with a half-life of 808 ms, back to ${}^6\text{Li}$ with a probability of unity.

MT=105. (n,t) ${}^4\text{He}$

Tritium, which is the only radioactive product of this reaction, beta decays to ${}^3\text{He}$ with a probability of unity and with a lifetime of 12.33 years.

File 9. Radioactive Nuclide Multiplicities

MT=103. (n,p) Multiplicity

A multiplicity of one is given for the production of ${}^6\text{He}$.

MT=105. (n,t) Multiplicity

A multiplicity of one is given for the production of tritium.

File 12. Gamma-Ray Multiplicities

MT=57. (n,n₂) γ Multiplicity

Multiplicity of one assumed for the 3.562-MeV gamma ray. Energy taken from reference 31.

MT=102. (n, γ) Multiplicity

Energies and transition arrays for radiative capture taken from Ref. 15, as reported in Ref. 31. The LP flag was used to describe the MT=102 photons.

File 14. Gamma-Ray Angular Distributions

MT=57. (n, n_2) γ Angular Distributions.

The gamma is assumed isotropic.

MT=102. (n, γ) Angular Distributions

The two high-energy gammas are assumed isotropic. Data on the 477-keV gamma indicate isotropy.

File 33. Cross Section Covariances

The relative covariances for MT=1, 2, and 105 below 1 MeV are given in File 33. They are based on calculations using the covariances of the R-matrix parameters in first-order error propagation.

MT=1. Total

Relative covariances are entered as NC-type sub-subsections, implying that they are to be constructed from those for MT=2 and 105. They are not intended for use at energies above 1.05 MeV.

MT=2, 105. Elastic and (n, t)

Relative covariances among these two cross sections are entered explicitly as NI-type sub-subsections in the LB=5 (direct) representation. Although values for the 0.95-1.05 MeV bin are repeated in a 1.05-20 MeV bin, the covariances are not intended for use at energies above 1.05 MeV.

REFERENCES

1. G. M. Hale, L. Stewart, and P. G. Young, LA-6518-MS (1976).
2. G. M. Hale, Proc. Internat. Specialists Symposium on Neutron Standards and Applications, Gaithersburg (1977).
3. K. M. Diment and C. A. Uittley, AERF-PR/NP 15 and AERE-PR/NP 16 (1969). Also private communication to L. Stewart.
4. J. A. Harvey and N. W. Hill, Proc. Conf. on Nuclear Cross Sections and Technology, Vol. 1, 244 (1975).
5. H. H. Knitter, C. Budtz-Jorgensen, M. Mailly, and R. Vogt, CBNM-VG (1976).
6. C. A. Goulding and P. Stoler, EANDC(US)-176U, 161 (1972).
7. D. G. Foster and D. W. Glasgow, Phys. Rev. C3, 576 (1971).
8. A. Bratenahl, J. M. Peterson, and J. P. Stoering, Phys. Rev. 110, 927 (1958), J. M. Peterson, A. Bratenahl, and J. P. Stoering, Phys. Rev. 120, 521 (1960).
9. R. O. Lane, Ann. Phys. 12, 135 (1961).
10. H. H. Knitter and A. M. Coppola, FANDC(E)-57U (1967). Also Ref. 5 above.
11. D. S. Mather and L. F. Pain, AWRE-0-47/69 (1969).
12. V. J. Ashby et al., Phys. Rev. 129, 1771 (1963).
13. J. C. Hopkins, D. M. Drake, and H. Condé, Nucl. Phys. A107, 139 (1968), and J. C. Hopkins, D. M. Drake, and H. Condé, LA-3765 (1967).

14. J. A. Cookson and D. Dandy, Nucl. Phys. A91, 273 (1967).
15. E. T. Jurney, LASL, private communication (1973).
16. E. D. Pendlebury, AWRE-0-60/64 (1964).
17. R. Bass, C. Bindhardt, and K. Kruger, EANDC(E)-57U (1965).
18. G. M. Frye, Phys. Rev. 93, 1086 (1954).
19. M. E. Battat and F. L. Ribe, Phys. Rev. 89, 8 (1953).
20. M. G. Sowerby, B. H. Patrick, C. A. Uttley, and K. M. Diment, J. Nucl. Energy 24, 323 (1970). $^6\text{Li}/^{10}\text{B}$ Ratio Converted Using ENDF/B-IV $^{10}\text{B}(\text{n},\alpha)$ Cross Section.
21. G. P. Lamaze, O. A. Wasson, R. A. Schrack, and A. D. Carlson, Proc. Internat. Conf. on the Interactions of Neutrons with Nuclei, Vol. 2, 1341 (1976).
22. W. P. Poenitz, Z. Phys. 268, 359 (1974).
23. J. C. Overley, R. M. Sealock, and D. H. Ehlers, Nucl. Phys. A221, 573 (1974).
24. C. M. Bartle, Proc. Conf. on Nuclear Cross Sections and Technology, Vol. 2, 688 (1975), and private communication (1976).
25. R. D. Kern and W. E. Kreger, Phys. Rev. 112, 926 (1958).
26. R. Batchelor and J. H. Towle, Nucl. Phys. 47, 385 (1963).
27. A. H. Armstrong, J. Gammel, L. Rosen, and G. M. Frye, Nucl. Phys. 52, 505 (1964).
28. C. Wong, J. D. Anderson, and J. W. McClure, Nucl. Phys. 33, 680 (1962).
29. F. Merchez, N. V. Sen, V. Regis, and R. Bouchez, Compt. Rend. 260, 3922 (1965).
30. I. G. Schroder, E. D. McGarry, G. DeLeeuw-Gierts, and S. DeLeeuw, Proc. Conf. on Nuclear Cross Sections and Technology, Vol. 2, 240 (1975).
31. F. Ajzenberg-Selove, and T. Lauritsen, Nucl. Phys. A227, 55 (1974).
32. M. S. Coates et al., Neutron Standards Reference Data, IAEA, Vienna, p. 105 (1974).
33. S. J. Friesenhahn et al., INTEL-RT-7011-001 (1974).
34. W. Fort and J. P. Marquette, Proceedings of a Panel on Neutron Standard Reference Data, Nov. 20-24 (1972), IAEA, Vienna.
35. N. Jarmie et al., BAPS 20, 596 (1975).
36. R. A. Hardekopf et al., LA-6188 (1977).

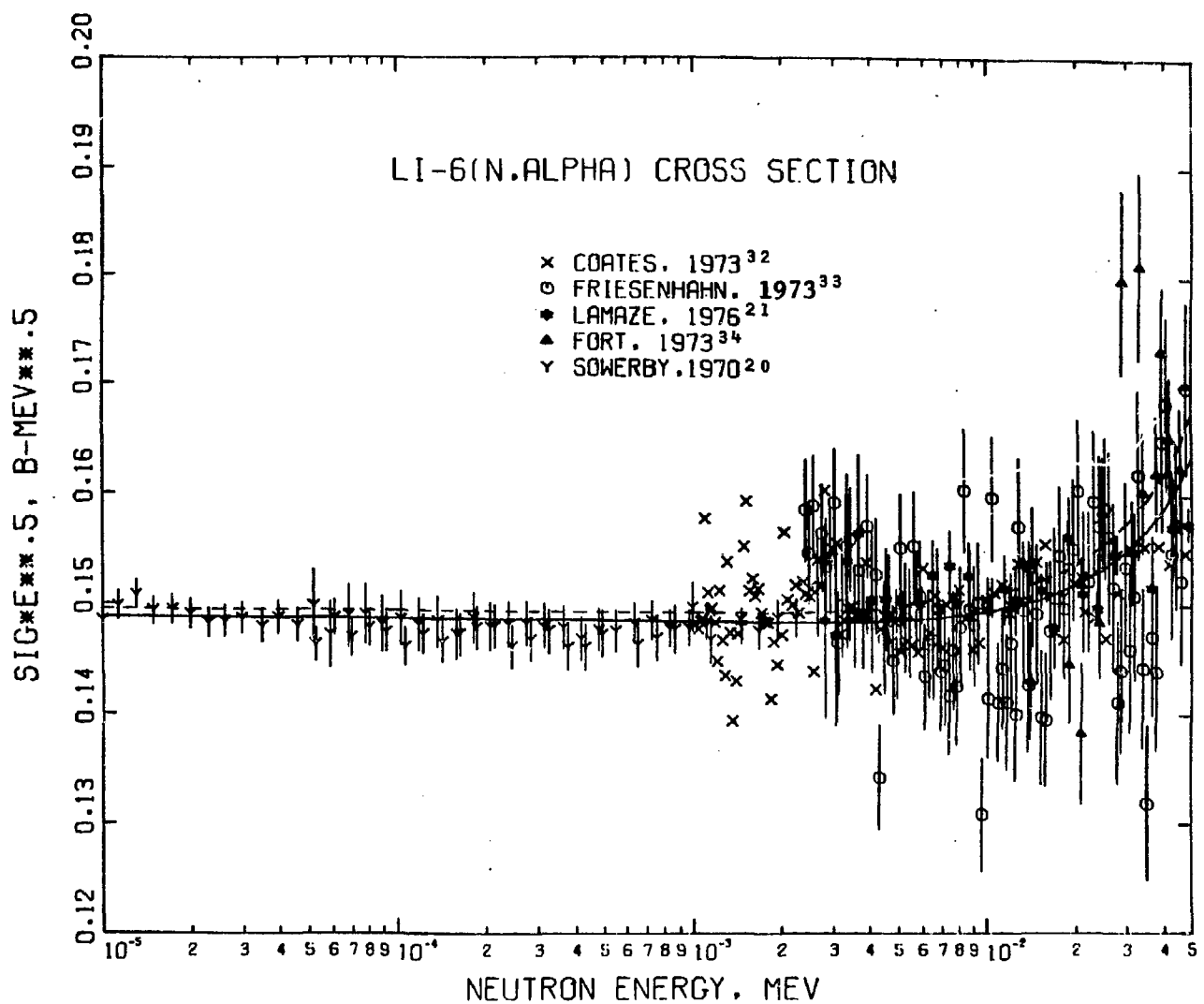


Fig. 1.

The Version V ${}^6\text{Li}(n, t){}^4\text{He}$ cross section times $\sqrt{E_n}$ plotted versus E_n for neutron energies between 10 eV and 50 keV. The dashed curve is ENDF/B-IV; the experimental data are from references 20, 21, 32-34.

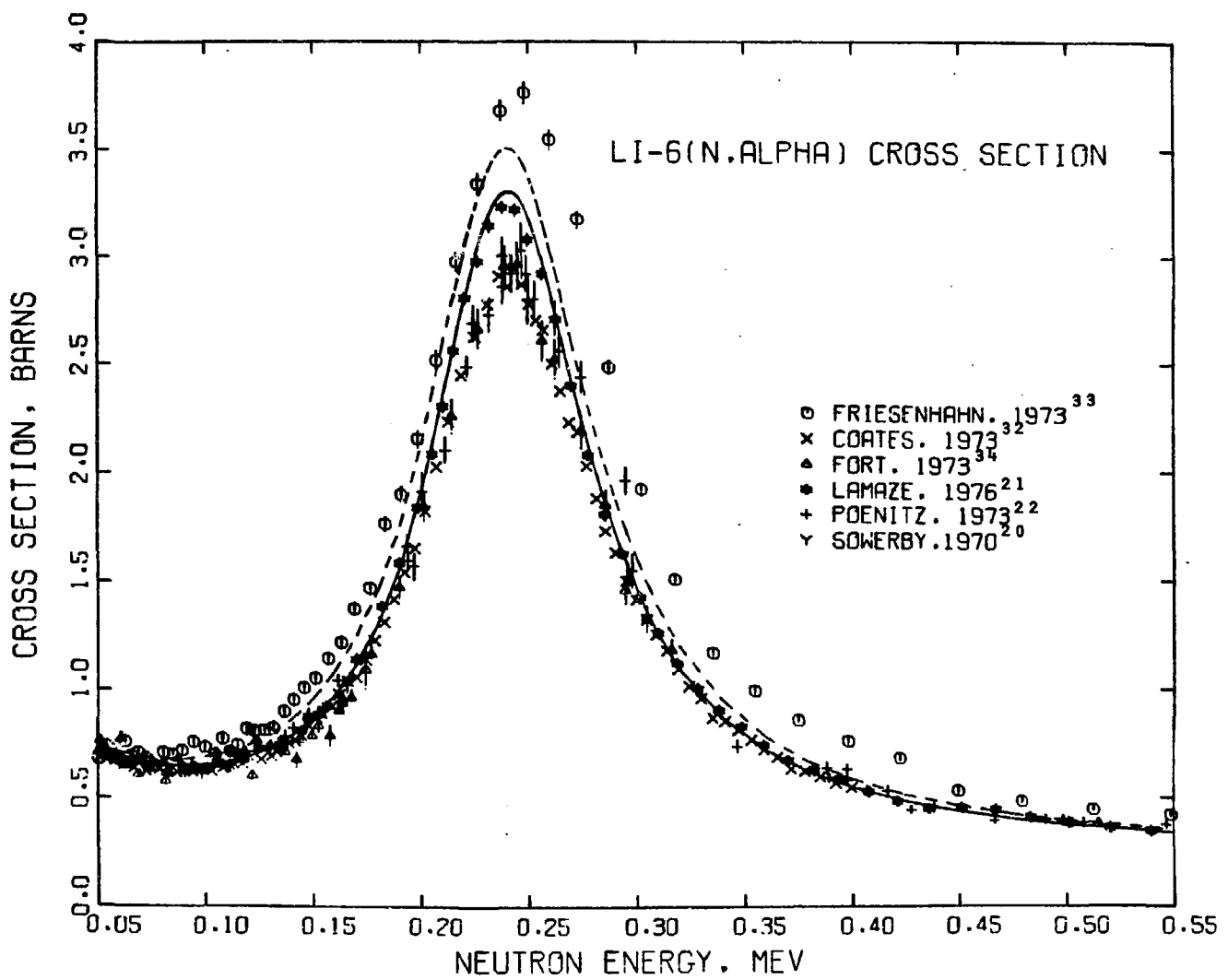


Fig. 2.

The Version V ${}^6\text{Li}(n, t){}^4\text{He}$ cross section from 50 to 550 keV. The dashed curve is ENDF/B-IV; the experimental data are from references 20-22, 32-34.

SUMMARY DOCUMENTATION FOR ^7Li

by

L. Stewart, D. G. Foster, Jr., M. E. Battat, and R. J. LaBauve
Los Alamos Scientific Laboratory
Los Alamos, New Mexico

I. SUMMARY

The ^7Li evaluation for ENDF/B-V (MAT 1272) was carried over from Version IV with only minor format modifications being included. The evaluation of all the neutron data except the total cross section is based upon a 1964 evaluation by Pendlebury (AWRE 0-61/64) as adapted by Battat and LaBauve for Version II of ENDF/B. The total cross section above 0.5 MeV was re-evaluated by Foster as described below and photon production data added by LaBauve and Stewart for Version IV of ENDF/B. The evaluation covers the energy range from 10^{-5} eV to 20 MeV. Covariance data are not included in the file but will be available in a new evaluation forthcoming from LASL.

II. ENDF/B-V FILES

File 1. General Information

MT=451. Descriptive data.

File 2. Resonance Parameters

MT=151. Effective scattering radius = 0.28906×10^{-12} cm.

Resonance parameters not given.

File 3. Neutron Cross Sections

MT=1. Total Cross Section

Below 100 keV, based on analysis of available total cross section and radiative capture measurements (Hu58, Hu60, Ho58, and Ho59) with an expression of the form $\sigma_T = \sigma_{n,n} + \sigma_{n,\gamma}$, where $\sigma_{n,n}$ = constant and $\sigma_{n,\gamma}$ has a $1/V$ energy dependence. The analysis resulted in $\sigma_{n,n} = 1.05$ b and $\sigma_{n,\gamma} = 0.036$ b at thermal.

100 - 500 keV, based on available experimental data (Hu58, Hy60, Ho58, and Ho59).

0.5 - 20 MeV, analysis by Foster (LASL) used. Evaluation from 0.5 to 1.3 MeV based on measurements of Me70. Above 1.3 MeV, based on Go71, slightly normalized to improve agreement with Fo71, Br58, Co52, and Pe60. Accuracy is approximately 2% at 0.5 MeV and 1% above 1 MeV. Polynomial smoothing was used throughout.

MT=2. Elastic Cross Section

0 - 100 keV, see MT=1 summary.

0.1 - 20 MeV, based on experimental data of Ar63, Ba63B, Bo59, Gr59, La61, To56, Wi56, and Wo62.

MT=3. Nonelastic Cross Section (not included in file).

In order to determine the individual reaction cross sections, a total nonelastic cross section was evaluated with the elastic cross section, with each adjusted such that their sum equaled the MT=1 cross section. Experimental nonelastic measurements that were considered include Co59, Go59, Mc63, and Ri53.

MT=4. Inelastic Cross Section

Sum of MT=51 and 91.

MT=16. (n,2n) Cross Section

Threshold - 20 MeV, smooth curve through experimental data of As63 at 10.2 and 14.1 MeV, smoothly extrapolated to 20 MeV, to obtain total (n,2n). Then divided into MT=16 and MT=24 components as described under MT=24.

MT=24. (n,2nd) α Cross Section

Threshold - 20 MeV, the total (n,2n) cross section is divided into (n,2n) ^6Li and (n,2nd) α components assuming that the latter reaction will dominate as the neutron energy increases above its threshold (9.98 MeV).

MT=51. (n,n' γ) Cross Section

Threshold - 20 MeV, the energy-dependent cross section to the 478-keV first-excited state of ^7Li , which is the only ^7Li level stable to particle decay, is based mainly on the experimental data of Ba63B, and Fr55 below 4 MeV and Be62 near 14 MeV, with a smooth interpolation between and extrapolation to 20 MeV.

MT=91. (n,n't) α Cross Section

Threshold - 20 MeV, the cross section to discrete and continuum states in ^7Li unstable to t- α breakup is based mainly on the experimental data of Ba63B, Ro62, and Th54, together with the results of Brown et al., and Osborne (see Hu58, Hu60).

MT=102. (n,γ) Cross Section

Below 150 keV, based on thermal value of 36 mb (Hu60) with $1/V$ energy dependence until the cross section falls to 10 μb .

0.15 - 20 MeV, held constant at 10 μb to 15 MeV, decreasing to 8.6 μb at 20 MeV.

MT=104. (n,d) Cross Section

Threshold - 20 MeV, smooth curve through the experimental data of Ba53, Ba63B, and Mi61.

MT=251. Average Cosine of Scattering Angle

Derived from evaluated files.

MT=252. Average-Logarithmic Energy Decrement

Derived from evaluated files.

MT=253. Gamma

Derived from evaluated files.

File 4. Neutron Angular Distributions

MT=2. Elastic Scattering Angular Distributions

Legendre coefficients given in center-of-mass system with transformation matrix (Al69). See Pe64 for evaluation details.

MT=16. $(n,2n)$ Angular Distributions

Tabular data (isotropic) in the laboratory system. See Pe64 for evaluation details.

MT=24. $(n,2nd)\alpha$ Angular Distributions

Tabular data (isotropic) in the laboratory system. See Pe64 for evaluation details.

MT=51. $(n,n'\gamma)$ Angular Distributions

Tabular data (isotropic) in the cm system. See Pe64 for evaluation details.

MT=91. $(n,n't)\alpha$ Angular Distributions

Tabular data (anisotropic) in the laboratory system. See Pe64 for evaluation details.

File 5. Neutron Energy Distributions

The tabulated spectra of Pendlebury (Pe64) were approximated by use of ENDF/B law 9, as described below.

MT=16. (n,2n) Energy Distribution

Energy range is 8.3 to 20 MeV. Distribution approximated by ENDF/B law 9, with theta (MeV) equal to $0.21\sqrt{E}$. This corresponds to an average theta of 0.7 MeV in the 8.3 to 15 MeV energy interval.

MT=24. (n,2nd) α Energy Distribution

Energy range is 10 to 20 MeV. Distribution approximated by ENDF/B law 9, with theta (MeV) equal to $0.1133\sqrt{E}$. This corresponds to an average theta of 0.4 MeV in the 10 to 15 MeV energy interval.

MT=91. (n,n't) α Energy Distribution

Distributions approximated using law 9. Theta values obtained by linear interpolation between following points:

$E = 2.821 \text{ MeV. Theta} = 0.10 \text{ MeV}$
 $E = 5.8 \text{ MeV. Theta} = 0.70 \text{ MeV}$
 $E = 8.0 \text{ MeV. Theta} = 2.80 \text{ MeV}$
 $E = 15.0 \text{ MeV. Theta} = 5.35 \text{ MeV}$

Data include the cross section to the second level and do not always conserve energy.

File 12. Gamma-Ray Multiplicities

MT=51. (n,n' γ) Multiplicity

The first level in ^7Li is the only known gamma emitter. Multiplicity of 1.0 assumed at all energies.

MT=102. (n, γ) Multiplicity

Thermal capture spectrum measurements are inconclusive. Rough estimates of transition probabilities were made using level energies of Selove and Lauritsen (private communication). LP flag used to indicate primary transitions.

File 14. Gamma-Ray Angular Distributions

MT=51. (n,n' γ) Angular Distributions

Assumed isotropic at all energies.

MT=102. (n, γ) Angular Distributions

Assumed isotropic at all energies.

REFERENCES

A&69 H. Alter, Atomics International, private communication (1969).
Ar63 A. H. Armstrong and L. Rosen, WASH-1042, p. 23 (1963).
As63 V. J. Ashby, H. C. Catron, M. D. Goldberg, R. W. Hill, J. M. LeBlanc, L. L. Newkirk, J. P. Stoering, C. J. Taylor, and M. A. Williamson, Phys. Rev. 129, 1771 (1963).
Ba53 M. F. Battat and F. L. Ribe, Phys. Rev. 89, 80 (1953).
Ba63A J. F. Barry, J. Nuc. Eng. 17, 273 (1963).
Ba63B R. Batchelor and J. H. Towle, Nuc. Phys. 47, 385 (1963).
Be62 J. Benveniste, A. C. Mitchell, C. D. Schrader, and J. H. Zenger, Nucl. Phys. 38, 300 (1962).
Bo59 N. A. Bostrom, I. L. Morgan, J. T. Prud'homme, P. L. Okhuysen, and O. M. Hudson, WADC-TN-59-107 (1959).
Br58 A. Bratenahl et al., Phys. Rev. 110, 927 (1958).
Co52 J. H. Coon et al., Phys. Rev. 88, 562 (1952).
Co59 A. V. Cohen, Unpublished (1959).
Fo71 D. G. Foster, Jr., D. W. Glasgow, Phys. Rev. C3, 576 (1971).
Fr55 J. M. Freeman, A. M. Lane, and B. Rose, Phil. Mag. 46, 17 (1955).
Go59 V. M. Gorbachev and L. B. Poretskii, S. J. At. Eng. 4, 259 (1958), J. Nucl. Eng. 9, 159 (1959).
Go71 C. A. Goulding et al., (RPI), private communication (1971).
Gr59 B. C. Groseclose, Mis. 59-4223 (1959).
Ho58 R. J. Howerton, UCRL 5226 (1958).
Ho59 R. J. Howerton, UCRL 5226 (Revised) (1959).
Hu58 D. J. Hughes and R. B. Schwartz, BNL 325, Second Edition (1958).
Hu60 D. J. Hughes, B. A. Magurno and M. K. Brussel, Supplement No. 1 to BNL 325, Second Edition (1960).
La61 R. O. Lane, A. S. Langsdorf, Jr., J. E. Monahan, and A. J. Elwyn, Annals of Physics 12, 135 (1961).
Mc63 M. H. McGregor, R. Booth, and W. P. Ball, Phys. Rev. 130, 1471 (1963).
Me70 J. W. Meadows and J. F. Whalen, Nucl. Sci. Eng. 41, 351 (1970).
Mi61 K. M. Mikhailina, A. A. Nomofilov, T. A. Romanova, V. A. Sviridov, F. A. Tikhomirov, and K. D. Tolstov, Sov. Progress in Neutron Physics, Ed. P. A. Krupchitskii (1961).
Pe60 J. M. Peterson et al., Phys. Rev. 120, 521 (1960).
Pe64 E. D. Pendlebury, AWRE 0-61/64 (1964).
Ri53 F. L. Ribe, R. W. Davis, and J. M. Holt, LA-1589 (1953).
Ro62 L. Rosen and L. Stewart, Phys. Rev. 126, 1150 (1962).
Th54 R. G. Thomas, LA-1697 (1954).
To56 R. G. Thomas, M. Walt, R. B. Walton, and R. G. Allen, Phys. Rev. 101, 759 (1956).
Wi56 H. B. Willard, J. K. Bair, J. D. Kington, and H. O. Cohn, Phys. Rev. 101, 765 (1956).
Wo62 C. Wong, J. D. Anderson, and J. W. McClure, Nuc. Phys. 33, 680 (1962).

Beryllium-9

DATA SUMMARY AND GENERAL COMMENTS

The experimental data for ${}^4\text{Be}^9$ are summarized in UCRL-50400, Vol. 3. The evaluated data for Be^9 are shown graphically in UCRL-50400, Vol. 15, Part B. The listings for the ECSIL data references are given in UCRL-50400, Vol. 2. This evaluation was done by S. T. Perkins and R. J. Howerton.

There are no measurements for the (n, np) , (n, nd) , $(n, 2t)$ and (n, nt) reactions; since the thresholds for these reactions are very high, their cross sections are considered negligible. Also, since He^5 is unstable (it decays to a neutron and an alpha particle with a ground-state half-life of about 2×10^{-21} s), the (n, na) decay mode is a component of the $(n, 2n)$ reaction; therefore, it does not have to be considered separately. The inelastic scattering reaction is also a component of the $(n, 2n)$ reaction, since the Be^{9*} recoil nucleus always decays to a neutron and two alpha particles.

TOTAL CROSS SECTION

Experimental values of the total cross section are shown graphically on pages 1-58 to 1-70 of UCRL-50400, Vol. 7, Part A, Rev. 1; some tabular values are given on page 1-73.

ELASTIC SCATTERING CROSS SECTION

Experimental values of the elastic cross section are shown graphically on pages 1-71 and 1-72 of UCRL-50400, Vol. 7, Part A, Rev. 1; some tabular values are given on page 1-73. The free-atom cross section is used for all energies less than the usual upper limit set by the molecular binding energy (about 10 eV). Actually, this cross section only represents the nuclear part of the cross section for a stationary target. It should be strongly emphasized that these numbers are meaningless in the absence of a proper thermal treatment, either by the processing code or by the neutronics code that uses these numbers.

From 0.0001 eV to 0.01 MeV, the elastic scattering cross section was set equal to 6 barns. From 0.01 MeV to the (n, α) threshold at 0.67 MeV, the elastic cross section is essentially equal to the total cross section, because the (n, γ) cross section is negligible. The total cross section used here was based on the data of ECSIL Refs. 50-63, 54-92, 62-720, 62-772, and 54-1002.

Above the (n, α) threshold, the scattering cross section was assumed to be the difference between the total and nonelastic cross sections,

Beryllium-9

06/09/78

Beryllium-9 (Cont.)

06/09/78

	REACTION	POINTS	DATE	Q-VALUE	E-MIN	E-MAX
N.G	CROSS SECTION	151	12/14/71	6.8200+ 0	1.0000-10	2.0000+ 1
N.G	G ENERGY-ANGLE DIST.	2	10/25/72	6.8200+ 0	1.0000-10	2.0000+ 1
N.G	G MULTIPLICITY	2	10/25/72	6.8200+ 0	1.0000-10	2.0000+ 1
N.G	TOTAL ENERGY DEP.	2	11/21/76	6.8200+ 0	1.0000-10	2.0000+ 1
N.G	LOCAL ENERGY DEP.	2	11/21/76	6.8200+ 0	1.0000-10	2.0000+ 1

4-Be-9
MAT 1304

4-Be-9

MAT 1304

with the nonelastic cross section set equal to the sum of its parts. From 0.67 to 2 MeV, the evaluated total cross section was based on the previously mentioned references as well as Refs. 51-72, 51-336, and 59-1642. Above 2 MeV, we relied on the results of Ref. 68-3088 for the 2.7-MeV resonance and Ref. 67-750 for the energy region up to 15 MeV. The extension to 20 MeV was based on data from Refs. 54-107, 60-673, and 61-682.

ELASTIC SCATTERING ANGULAR DISTRIBUTIONS

For energies less than 7 MeV, experimental differential scattering data are given in Refs. 55-121, 56-151, 57-231, 55-296, 59-500, 60-571, 58-945, 64-1643, 60-1645, 61-1646, and 64-1647. Experimental elastic scattering angular distributions are shown in UCRL-50400, Vol. 19. These data were used to determine the normalized probabilities. Below the (n,2n) threshold, the scattering consists of only elastic scattering, since there is no inelastic scattering. We took into account the change in shape of the angular distribution in going through the scattering resonances. At 14 MeV, the elastic angular distributions were based on the results of Refs. 59-402, 66-2585, and 68-3106. A smooth extrapolation was made to 20 MeV. The

results at all incident energies are consistent with Wick's limit.

n,2n CROSS SECTION

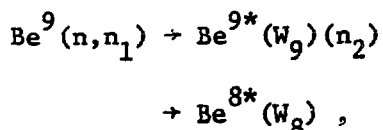
The total (n,2n) cross section is based on the (n,2n) cross sections and nonelastic-minus-absorption cross sections listed by Perkins in AN-1443 (1965). The cross section measurements have been augmented by the more recent (n,2n) data of Refs. 69-763 and 72-3320. The nonelastic measurements of Refs. 68-2595 and 73-3321 were also taken into account. The 20-MeV point was obtained by

- Interpolating nonelastic cross sections between the 14-MeV value and the value at 25.5 MeV (see Ref. 58-356)
- Subtracting the other partial nonelastic reaction cross sections from the interpolated nonelastic cross section.

There have been two recent measurements on the partial cross sections involved in the Be(n,2n) breakup (D. M. Drake *et al.*, *Nucl. Sci. Eng.* 63, 401 [1977]; and F. O. Purser, private communication from Triangle Univ. Nucl. Lab. [1976]). Both references indicated that from about 6 to 12 MeV, the cross section for excitation of the 2.43-MeV level in ⁹Be is substantially lower (up to a factor of two) than was thought previously. In addition, the cross section for excitation of the 1.68-

MeV level has essentially disappeared at 6 MeV. This implies a relatively large cross section for excitation of the 4.7-MeV level when the incident neutron energy lies between 6 MeV and the threshold for excitation of the 6.76-MeV level.

The total $(n,2n)$ cross section is subdivided into five partial reactions, each of which is described by the following time-sequential decay:



where the W_i 's are the level excitation energies, and n_1 and n_2 are the first and second emitted neutrons. The five decay channels are shown below.

Decay channels for the $(n,2n)$ reaction.

W_9 , MeV	W_8 , MeV	Branching fraction, %
1.68	0	100
2.43	0	8-1/3%
	2.94	91-2/3%
4.70	2.94	100
6.76	0	100
11.28	11.4	100

The above branching ratios were measured by Perkins [see AN-1443 (1965)], except for the Be^{9*} (9.1 MeV) transition which has been replaced by Be^{9*} (11.28 MeV) and Be^{9*}

(4.70) decay. The latter measurements are based on the results of C. L. Cocke and P. R. Christensen [see *Nucl. Phys.* 111, 623 (1968)].

Most of the levels in both nuclei are wide. The center-of-mass widths used in the evaluation are given below.

Center-of-mass widths used in the evaluation.^a

W_9 , MeV	Γ_9 , MeV
1.68	0.21
2.43	0
4.70	0.74
6.76	2
11.28	0.575
W_8 , MeV	Γ_8 , MeV
0	0
2.94	1.56
11.4	7

^aF. Ajzenberg-Selove and T. Lauritzen, *Nucl. Phys.* 11, 1 (1959).

ENERGY AND ANGULAR DISTRIBUTIONS FROM THE $n,2n$ REACTION

The five partial $(n,2n)$ reactions include one narrow level and four wide levels. In each of these, the first neutron is described as the result of an inelastic scattering event. The experimental center-of-mass angular distribution of the first neutron from the narrow Be^{9*}

level (2.43 MeV) is described in a P_6 Legendre expansion. The neutrons from the other levels are assumed to be isotropic in their center-of-mass systems. The energy-angle correlation for first neutrons is preserved.

The description of the second neutron from each partial reaction neglects the energy-angle correlation. This is a valid approximation for this reaction, as has been discussed by S. T. Perkins in *Nucl. Sci. Eng.* 31, 156 (1968). All wide levels were described by single-level dispersion theory. After the theoretical level distributions were obtained for Be^{9*} and Be^{8*} , they were integrated, using the equations in AN-1443 (1965), to obtain the Legendre moments of the transference function, $\sigma_\ell(E, E')$, for the second neutron. The integration scheme uses excitation energy bins of equal probability; calculations were performed at the average excitation energy within each bin. (This mode of integration appeared to be the most economical one to use in this case.) This integration scheme introduces some discontinuities into the output spectra, particularly at low incident neutron energies. Since an increase in the number of bins did not appear to be economically feasible, these results were smoothed with a smoothing algorithm. The effective threshold values for the 6.76- and 11.28-MeV

level excitations were assumed to be at incident neutron energies of 7 and 12 MeV, respectively. This allows a better incorporation of the wide-level effects. In these calculations, the center-of-mass angular distribution of the recoiling Be^{9*} nucleus had to be consistent with the description of the first neutron mentioned above. The subsequent decay breakup (into Be^{8*} and a neutron) was assumed to be isotropic in the (Be^{8*}, n) center-of-mass system.

The angular distributions for second neutrons in the laboratory frame-of-reference were obtained from a P_9 Legendre expansion of the transference function. The Legendre moments from the P_9 Legendre expansion were integrated over the energy of the second neutron in order to obtain the Legendre coefficients of the lab-system angular distributions, which then led directly to the angular distributions themselves.

n,p CROSS SECTION

This cross section was estimated from the known threshold value and the single measurement at 15.5 MeV (Ref. 63-913).

n,d CROSS SECTION

This cross section is based on the known threshold value and the measured data between 16.5 and 18.8 MeV (Ref. 69-3101).

n, t CROSS SECTION

The cross section for the (n, t) reaction is divided into (n, t_0) and (n, t_1) components, which proceed through the ground state and the 0.477-MeV level of $^{7*}\text{Li}$, respectively. The total (n, t) cross section near 14 MeV was determined from Refs. 58-496 and 61-650. Except for noting the variation of the cross section with energy, the results of Ref. 58-494 were neglected, due to the large uncertainties in these results.

The (n, t_1) cross section was based on results from F. S. Dietrich *et al.*, *Nucl. Sci. Eng.* 61, 267 (1976). The (n, t_0) cross section was drawn smoothly from zero at threshold to a value at 14 MeV that is the difference between the total (n, t) cross section and the (n, t_1) cross section; above 14 MeV, the (n, t_0) cross section decreases smoothly.

n, α CROSS SECTION

For neutron energies less than 8.6 MeV, the n, α cross section was based on the measurements reported in Refs. 58-494, 57-160, and 61-733. It was then smoothly joined to the three values given at 14 MeV (Refs. 61-650, 53-86, and 67-2367) and extrapolated to 20 MeV. Note that the measured cross section only applies to the production of the ^6He ground state, which beta decays to

^6Li ; for higher states, ^6He decays into an alpha particle and two neutrons.

n, γ CROSS SECTION

The n, γ cross section was assumed to be inversely proportional to incident neutron speed below 100 eV, with a 2200-m/s cross section of 9.5 mbarns. It was extrapolated linearly on a log-log basis to 0.1 mbarn at 1 keV, and then held constant at this value up to 20 MeV.

PHOTON PRODUCTION CROSS SECTIONS AND SPECTRA

Gamma rays in Be^9 are produced by the (n, γ) and (n, t) reactions. At thermal neutron energy, Ref. 70-2415 lists the gamma-ray energies as 0.8535, 2.59, 3.368, 3.444, 5.958, and 6.81 MeV, and it gives the corresponding (n, X γ) cross sections. The photon spectrum was assumed to be independent of incident neutron energy. The multiplicity $M(E_0)$, however, varies with the incident neutron energy E_0 as follows:

$$M(E_0) = M(0)(E_{c-m} + Q_{n,\gamma})/Q_{n,\gamma},$$

where $M(0)$ is the multiplicity at thermal energies, $Q_{n,\gamma}$ is the Q-value for the (n, γ) reaction, and E_{c-m} is the center-of-mass energy:

$$E_{c-m} = \frac{A}{A+1} E_0.$$

By using this recipe, we conserve energy. As the incident neutron energy increases, there are undoubtedly higher levels of Be^{10} that are also excited. However, these higher levels and their transitions have been only partially identified. The component relevant to the (n, t_1) cross section is in

fact equal to this cross section (since its multiplicity is unity).

The angular distribution of gamma rays from the (n, t_1) reaction is isotropic, as reported in Ref. 59-605. The angular distribution of the capture gamma rays is assumed to be isotropic.

SUMMARY DOCUMENTATION FOR ^{10}B

by

G. M. Hale, L. Schwartz, and P. G. Young
Los Alamos Scientific Laboratory
Los Alamos, New Mexico

I. SUMMARY

All cross sections below a neutron energy of 1.5 MeV except the (n,p) and (n,t) reactions were revised for the Version V evaluation of ^{10}B (MAT 1305). The data above 1.5 MeV were carried over from ENDF/B-IV. Other changes to the file include the addition of evaluated cross sections and secondary gamma-ray spectra from the $^{10}\text{B}(\text{n},\gamma)^{11}\text{B}$ reaction, as well as covariance data for cross sections below 1.5 MeV. Except for the covariance file, the evaluated data cover the energy range from 10^{-5} eV to 20 MeV. Partial documentation is provided in LA-6472-PR (1976) and LA-6518-MS (1976).

II. STANDARDS DATA

The $^{10}\text{B}(\text{n},\alpha)^7\text{Li}$ and $^{10}\text{B}(\text{n},\alpha_1\gamma)^7\text{Li}$ reactions are neutron standards at energies below 100 keV. The major reactions below 1 MeV were obtained for the Version V evaluation from multichannel, multilevel R-matrix analyses of reactions in the ^{11}B system, similar to those from which the Version IV evaluation were taken. New data have become available since Version IV was released and most of this new experimental information has been incorporated into the present analyses.

We have added Spencer's measurements of σ_T (Sp73) and Sealock's $^{10}\text{B}(\text{n},\alpha_1)$ angular distributions (Se76) to the data set that was analyzed for Version IV. In addition, we have replaced Friesenhahn's integrated (n,α_1) cross section with the recent measurements of Schrack et al. (both with GeLi and NaI detectors) at NBS (Sc76), and have deleted Friesenhahn's total (n,α) cross section from the data set. The resulting fit to the (n,α) and $(\text{n},\alpha\gamma)$ data is shown in Figs. 1 and 2, respectively. The integrated $^{10}\text{B}(\text{n},\alpha)$ cross section has changed negligibly from the Version IV results at energies below 200 keV. At higher energies, however, the (n,α) cross section has dropped significantly in response to the new NBS data. Unfortunately, the rest of the data in the analysis do not seem particularly sensitive to such changes in the (n,α) cross section, with the result that our calculated cross section must be considered quite uncertain at energies above ~ 300 keV.

5-B-10
MAT 1305

III. ENDF/B-V FILES

File 1. General Information

MT=451. Descriptive data.

File 2. Resonance Parameters

MT=451. Effective scattering radius = 0.40238×10^{-12} cm.

Resonance parameters not included.

File 3. Neutron Cross Sections

The 2200 m/s cross sections are as follows:

MT=1	Sigma =	3839.1	b
MT=2	Sigma =	2.0344	b
MT=102	Sigma =	0.5	b
MT=103	Sigma =	0.000566	b
MT=107	Sigma =	3836.6	b
MT=113	Sigma =	0.000566	b
MT=700	Sigma =	0.000566	b
MT=780	Sigma =	244.25	b
MT=781	Sigma =	3592.3	b

MT=1. Total Cross Section

0 to 1 MeV, calculated from R-matrix parameters obtained by fitting simultaneously data from the reactions $^{10}\text{B}(n,n)$, $^{10}\text{B}(n,\alpha_0)$, and $^{10}\text{B}(n,\alpha_1)$. Total neutron cross-section measurements included in the fit are those of Bo52, Di67, and Sp73.

1 to 20 MeV, smooth curve through measurements of Di67, Bo52, Ts62, Fo61, Co52, and Co54, constrained to match R-matrix fit at 1 MeV.

MT=2. Elastic Scattering Cross Section

0 to 1 MeV, calculated from the R-matrix parameters described for MT=1. Experimental elastic scattering data included in the fit are those of As70 and La71.

1 to 7 MeV, smooth curve through measurements of La71, Po70, and Ho69, constrained to be consistent with total and reaction cross section measurements.

7 to 14 MeV, smooth curve through measurements of Ho69, Co69, Te62, Va70, and Va65.

14 to 20 MeV, optical model extrapolation from 14-MeV data.

MT=4. Inelastic Cross Section

Threshold to 20 MeV, sum of MT=51-85.

MT=51-61. Inelastic Cross Sections To Discrete States

MT=51	Q=-0.717 MeV	MT=55	Q=-4.774 MeV	MT=59	Q=-5.923 MeV
52	-1.740	56	-5.114	60	-6.029
53	-2.154	57	-5.166	61	-6.133
54	-3.585	58	-5.183		

Threshold to 20 MeV, based on (n,n') measurements of Po70, Co69, Ho69, and Va70, and the $(n,x\gamma)$ measurements of Da56, Da60, and Ne70 using a gamma-ray decay scheme deduced from La66, Al66, Se66A, and Se66B. Hauser-Feshbach calculations were used to estimate shapes and relative magnitudes where experimental data were lacking.

MT=62-85. Inelastic Cross Sections to Groups of Levels

These sections were used to group (n,n') cross sections into 0.5-MeV wide excitation energy bins between $E_x=6.5$ and 18.0 MeV. This representation was used in lieu of MF=5, MT=91 to more accurately represent kinematic effects.

Threshold to 20 MeV, integrated cross section obtained by subtracting the sum of MT=2, 51-61, 103, 104, 107, and 113 from MT=1. Cross section distributed among the bands with an evaporation model using a nuclear temperature given by $T = 0.9728 \sqrt{E_n}$ (units MeV), taken from Ir67.

MT=102. (n,γ) Cross Section

0 to 1 MeV, assumed 1/V dependence with thermal value of 0.5 barn.

1 to 20 MeV, assumed negligible, set equal to zero.

MT=103. (n,p) Cross Section

Threshold to 20 MeV, sum of MT=700-703.

MT=104. (n,d) Cross Section

Threshold to 20 MeV, based on $^9\text{Be}(d,n)^{11}\text{B}$ measurements of Si65 and Ba60, and the (n,d) measurement of Va65.

MT=107. (n,α) Cross Section

0 to 20 MeV, sum of MT=780 and 781.

MT=113. $(n,t2\alpha)$ Cross Section

0 to 2.3 MeV, based on a single-level fit to the resonance measured at 2 MeV by Da61, assuming L=0 incoming neutrons and L=2 outgoing tritons.

2.3 to 20 MeV, smooth curve through measurements of Fr56 and Wy58, following general shape of Da61 measurement from 4 to 9 MeV.

MT=700-703. (n,p) Cross Section to Discrete Levels

0 to 20 MeV, crudely estimated from the calculations of Po70 and the (n,xy) measurements of Ne70. Cross section for MT=700 assumed identical to MT=113 below 1 MeV. Gamma-ray decay scheme for ^{10}B from La66.

MT=780. (n,α_0) Cross Section

0 to 1 MeV, calculated from the R-matrix parameters described for MT=1. Experimental (n,α_0) data input to the fit were those of Ma68 and Da61. In addition, the angular distributions of Va72 for the inverse reaction were included in the analysis.

1 to 20 MeV, based on Da61 measurements, with smooth extrapolation from 8 to 20 MeV. Da61 measurement above approximately 2 MeV was renormalized by factor of 1.4.

MT=781. (n,α_1) Cross Section

0 to 1 MeV, calculated from the R-matrix parameters described for MT=1. Experimental (n,α_1) data included in the fit are those of Sc76. In addition, the absolute differential cross-section measurements of Se76 were included in the analysis.

1 to 20 MeV, smooth curve through measurements of Da61 and Ne70, with smooth extrapolation from 15 to 20 MeV. The Da61 data above approximately 2 MeV were renormalized by a factor of 1.4.

File 4. Neutron Angular Distributions

MT=2. Elastic Angular Distributions

0 to 1 MeV, calculated from the R-matrix parameters described for MF=3, MT=1. Experimental angular distributions input to the fit for both the elastic scattering cross section and polarization were obtained from the measurements of La71. Assignments for resonances above the neutron threshold are based on La71.

1 to 14 MeV, smoothed representation of Legendre coefficients derived from the measurements of La71, Ha73, Po70, Ho69, Co69, Va69, and Va65, constrained to match the R-matrix calculations at $E_n=1$ MeV.

14 to 20 MeV, optical model extrapolation of 14-MeV data.

MT=51-85. Inelastic Angular Distributions

Threshold to 20 MeV, assumed isotropic in center-of-mass.

File 12. Gamma Ray Multiplicities

MT=102. Capture Gamma Rays

0 to 20 MeV, capture spectra and transition probabilities derived from the thermal data of Th67, after slight changes in the probabilities and renormalization to the energy levels of Aj75. The LP flag is used to conserve energy and to reduce significantly the amount of data required in the file. Except for the modification due to the LP flag, the thermal spectrum is used over the entire energy range.

MT=781. 0.4776-MeV Photon from the (n, α_1) Reaction

0 to 20 MeV, multiplicity of 1.0 at all energies.

File 13. Gamma-Ray Production Cross Sections

MT=4. $(n, n\gamma)$ Cross Sections

Threshold to 20 MeV, obtained from MT=51-61 using ^{10}B decay scheme deduced from La66, Al66, Se66A, and Se66B.

MT=103. $(n, p\gamma)$ Cross Sections

Threshold to 20 MeV, obtained from MT=701-703 using ^{10}B decay scheme deduced from La66.

File 14. Gamma Ray Angular Distributions

MT=4. $(n, n\gamma)$ Angular Distributions

Threshold to 20 MeV, assumed isotropic.

MT=102. (n, γ) Angular Distributions

0 to 20 MeV, assumed isotropic.

MT=103. $(n, p\gamma)$ Angular Distributions

Threshold to 20 MeV, assumed isotropic.

MT=781. $(n, \alpha_1\gamma)$ Angular Distribution

0 to 20 MeV, assumed isotropic.

File 33. Cross-Section Covariances

The relative covariances for the most important reactions open below 1 MeV are given in File 33. These are calculated directly from the covariances of the R-matrix parameters, using first-order error propagation.

MT=2, 780, 781. (n,n) (n, α_0), and (n, α_1) Covariances.

0 to 1 MeV, relative covariances among these three reactions are entered explicitly using NI-type sub-subsections in the LB=5 (direct) representation.

1 to 20 MeV, all covariances set equal to zero. Not intended for use in this energy range.

MT=1, 107. Total and (n, α) Covariances.

0 to 1 MeV, for compactness, these covariances are constructed from those described above, using NC-type sub-subsections. The constructed covariances for the total cross section therefore neglect contributions from the (n, γ), (n,p), (n,t), and (n,n₁) reactions which are all presumed to be small in magnitude below 1 MeV. Note that although the total cross-section covariances are entered in the NC-type (derived) format, total cross-section data were included in the fit, and they influenced all the calculated covariances.

1 to 20 MeV, set equal to zero. Not intended for use in this energy range.

REFERENCES

Aj75 F. Ajzenberg-Selove, Nucl. Phys. A248, 6 (1975).
Al66 D. E. Alburger et al., Phys. Rev. 143, 692 (1966).
As70 A. Asami and M. C. Moxon, J. Nucl. Energy 24, 85 (1970).
Ba60 R. Bardes and G. E. Owen, Phys. Rev. 120, 1369 (1960).
Be56 R. L. Becker and H. H. Barschall, Phys. Rev. 102, 1384 (1956).
Bo51 C. K. Bockelman et al., Phys. Rev. 84, 69 (1951).
Bo69 D. Bogart and L. L. Nichols, Nucl. Phys. A125, 463 (1969).
Co52 J. H. Coon et al., Phys. Rev. 88, 562 (1952).
Co54 C. F. Cook and T. W. Bonner, Phys. Rev. 94, 651 (1954).
Co67 S. A. Cox and F. R. Pontet, J. Nucl. Energy 21, 271 (1967).
Co69 J. A. Cookson and J. G. Locke, Nucl. Phys. A146, 417 (1970).
Co73 M. S. Coates et al., private communication to L. Stewart (1973).
Da56 R. B. Day, Phys. Rev. 102, 767 (1956).
Da60 R. B. Day and M. Walt, Phys. Rev. 117, 1330 (1960).
Da61 E. A. Davis et al., Nucl. Phys. 27, 448 (1961).
Di67 K. M. Diment, AERE-R-5224 (1967).
Fo61 D. M. Fossan et al., Phys. Rev. 123, 209 (1961).
Fr56 G. M. Frye and J. H. Gammel, Phys. Rev. 103, 328 (1956).
Ha73 S. L. Hausladen, Thesis, Ohio Univ. C00-1717-5 (1973).
Ho69 J. C. Hopkins, private communication to LASL (1969).
Ir67 D. C. Irving, ORNL-TM-1872 (1967).
La66 T. Lauritsen and F. Ajzenberg-Selove, Nucl. Phys. 78, 1 (1966).
La77 R. O. Lane et al., Phys. Rev. C4, 380 (1971).
Ma68 R. L. Macklin and J. H. Gibbons, Phys. Rev. 165, 1147 (1968).
Mo66 F. P. Mooring et al., Nucl. Phys. 82, 16 (1966).
Ne54 N. G. Nereson, LA-1655 (1954).

Ne70 D. O. Nellis et al., Phys. Rev. C1, 847 (1970).
Po70 D. Porter et al., AWRE Q, 45/70 (1970).
Sc76 R. A. Schrack et al., Proc. ICINN (ERDA-CONF-760715-P2), 1345 (1976).
Se76 R. M. Sealock and J. C. Overley, Phys. Rev. C13, 2149 (1976).
Se66A R. E. Segel and R. H. Siemssen, Phys. Lett. 20, 295 (1966).
Se66B R. E. Segel et al., Phys. Rev. 145, 736 (1966).
Si65 R. H. Siemssen et al., Nucl. Phys. 69, 209 (1965).
Sp73 R. R. Spencer et al., EANDC(E) 147, AL (1973).
Te62 K. Tesch, Nucl. Phys. 37, 412 (1962).
Th67 G. E. Thomas et al., Nucl. Instr. Meth. 56, 325 (1967).
Ts63 K. Tsukada and O. Tanaka, J. Phys. Soc. Japan 18, 610 (1963).
Va63 V. Valkovic et al., Phys. Rev. 139, 331 (1965).
Va70 B. Vaucher et al., Helv. Phys. Acta, 43, 237 (1970).
Va72 L. Van der Zwan and K. W. Geiger, Nucl. Phys., A180, 615 (1972).
Wi55 H. B. Willard et al., Phys. Rev. 98, 669 (1955).
Wy58 M. E. Wyman et al., Phys. Rev. 112, 1264 (1958).

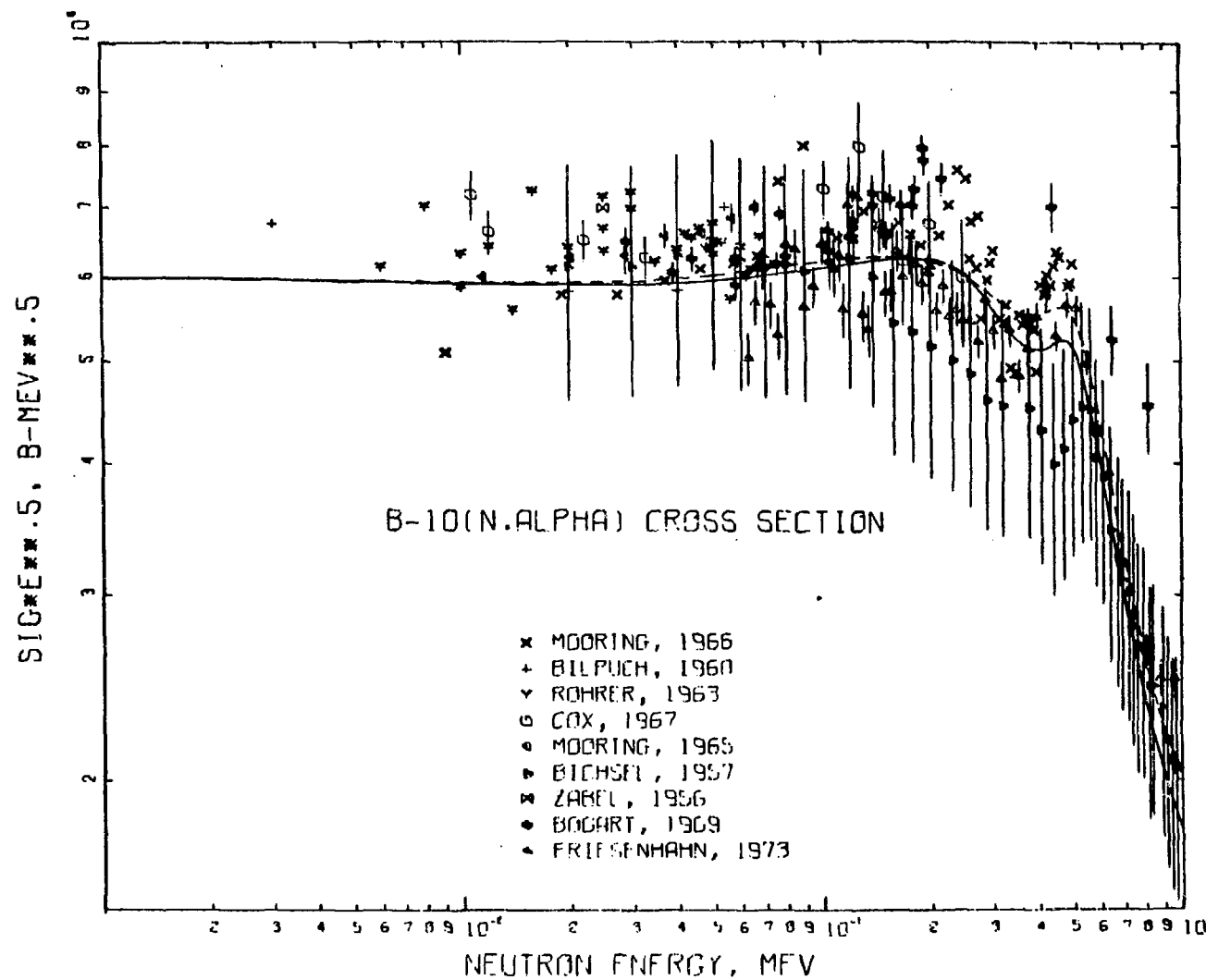


Fig. 1.
Experimental and evaluated data for the $^{10}\text{B}(n,\alpha)^7\text{Li}$ reaction from 1 keV to 1 MeV.
The solid curve is ENDF/B-V and the dashed curve is ENDF/B-IV. References for
experimental data are given in LA-6518-MS.

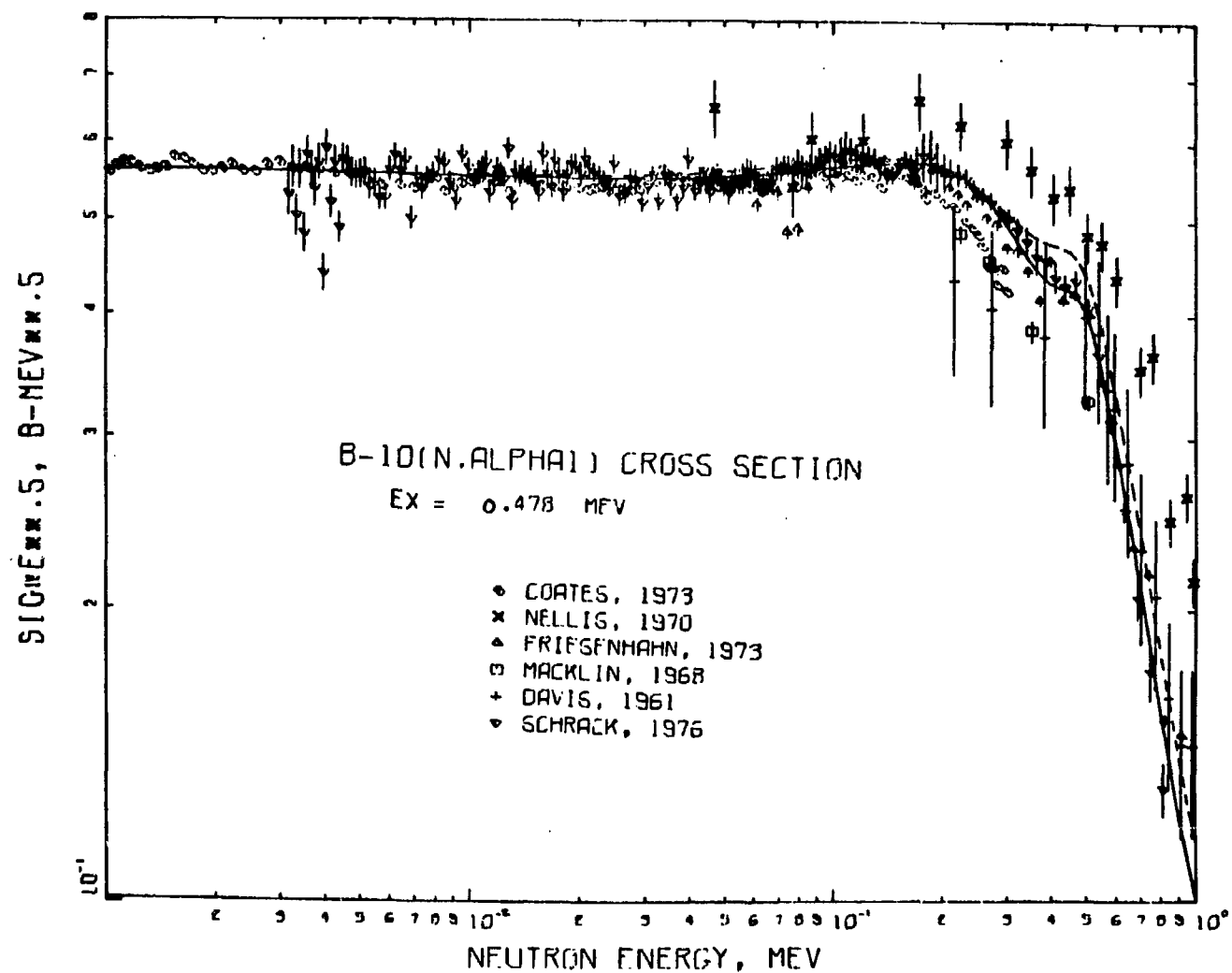


Fig. 2.
 Experimental and evaluated data for the $^{10}\text{B}(\text{n},\alpha\gamma)^7\text{Li}$ reaction from 1 keV to 1 MeV.
 The solid curve is ENDF/B-V and the dashed curve is ENDF/B-IV. References for
 experimental data are Co73, Da61, Ma68, Ne70, Sc76, and those included in LA-6518-M'

Eval-Sep71 C.Cowan
Dist-May74 Rev-Nov74

Extended to 20 MeV for ENDF/B Version-IV

* * * * * * *
Boron-11 Translated from UKAEA Data File (MAT No 49)
* * * * * * *

Data modified Sept 1971 to conform to ENDF/B-III format

* * * * * * *

Revisions to the UKAEA data were made in Sept 1971 by C.Cowan from GE and on temporary assignment at BNL. Revisions include.

- 1) Total and elastic reactions between 0.5 and 2.5 MeV were re-normalized based upon recommended resonance parameters and smooth cross sections from BNL-325
- 2) Angular distributions for elastic scattering (File 4) were normalized at the specified energies between 0.43 and 1.5 MeV to give total probabilities of 1.0

Summary Documentation

Carbon Evaluation

ENDF/B-V MAT 1306

C. Y. Fu and F. G. Perey
Oak Ridge National Laboratory
Oak Ridge, Tennessee

August 1978

New Evaluation for Version V:

1. Total and elastic scattering from thermal to 4.81 MeV.
2. Elastic angular distribution: thermal to 4.81 MeV.
3. New representation for $(n, n3\alpha)$ to yield correct energy angle kinematics.
4. Activation file for (n, p) .
5. Gas production file.
6. Uncertainty file.

Adopted from ENDF/B-IV (by F. G. Perey and C. Y. Fu):

1. (n, α) below 15 MeV and (n, γ) below 1 MeV.
2. Angular distributions of secondary neutrons 4-51.
3. Multiplicity of capture gamma-rays 12-102.
4. All other cross sections and distributions below 8.5 MeV except (n, γ) , (n, α) , and (n, t) .

Adopted from French evaluation¹ which is an extensive revision of ENDF/B-IV:

1. (n, γ) above 1 MeV, (n, α) , and (n, t) .
2. Angular distribution of secondary neutrons 4-52 and 4-53 and gamma rays 14-51.
3. All other cross sections above 8.5 MeV except (n, α) .

Data and evaluation techniques used in the new evaluation, the ENDF/B-IV evaluation, and the French evaluation, as adopted here, are summarized below:

File 3, MT=1. Total

1. E-5 eV to 4.81 MeV — sum of File 3 MT=2 and File 3 MT=102.
2. 4.81 MeV to 20 MeV.²⁻⁴

File 3, MT=2. Elastic Scattering

1.E-5 eV to 4.81 MeV — R-matrix analysis with data.²⁻²⁷
Bayes theorem (or nonlinear least-squares) used for energies
less than 2 MeV. Resulting weights were then used in the
R-matrix analysis. A thermal total cross section of 4.746 + 0.25%
evaluated by Lubitz²⁸ was also used in the R-matrix fit.
4.81 MeV to 8 MeV.^{26,27,29}
8 MeV to 14 MeV.²⁹⁻³¹
14 MeV to 20 MeV.³²

File 3, MT=3. Nonelastic

1.E-5 eV to 4.81 MeV. Same as File 3 MT=102.
4.81 MeV to 20 MeV — File 3 MT=1 minus File 3 MT=2.

File 3, MT=51. Inelastic Scattering to 4.439-MeV Level

4.81 MeV to 6.32 MeV — File 3 MT=3 minus File 3 MT=102.
6.32 MeV to 8.796 MeV — File 3 MT=3 minus File 3 MT=102 minus
File 3 MT=107.
8.796 MeV to 20 MeV — Same references as in File 3 MT=2 and
gamma-ray data of Morgan et al.³³

File 3, MT=52-91. (n,n') and (n,n'3 α) Lumped Together

MT=52 to 55: real levels with physical widths given in File 4.
MT=56 to 58: pseudo levels with 0.25-MeV half width of rectangular
distribution given in File 4.
MT=91: a small evaporation component with T=0.3 to reproduce
threshold effect and the decay of the 2.43-MeV level of ^9Be .
Distribution of secondary neutrons agrees with Refs. 34 and 35.
The sum of File 3 MT=52 to File 3 MT=91 is derived from File 3 MT=3
and all other reaction cross sections, and agrees with Refs. 35-37.

File 3, MT=102. Capture

1.E-5 eV to 1 MeV — 1/V with 3.36 mb at thermal.
1 MeV to 20 MeV — derived from (γ ,n) cross section of Ref. 38.

File 3, MT=103. (n,p)

See Ref. 39.

File 3, MT=104. (n,d)

Derived from (d,n) of Ref. 40.

File 3, MT=107. (n, α)

See Refs. 41-46.

File 3, MT=203. Proton Production

Same as File 3, MT=103.

File 3, MT=204. Deuteron Production

Same as File 3, MT=104.

File 3, MT=207. Alpha Production

Sum of File 3, MT=52 to File 3, MT=91, multiplied by 3,
and added to File 3, MT=107.

File 3, MT=251. Mu Bar

Derived from File 4, MT=2 with code SAD.

File 3, MT=252. Chi

See File 3, MT=251.

File 3, MT=253. Gamma

See File 3, MT=251.

File 4, MT=2. Angular Distribution of Elastically Scattered Neutrons

Same data and analysis as in File 3, MT=2. Legendre coefficients
in center-of-mass with transformation matrix given.

File 4, MT=51. Inelastic Scattering to 4.439-MeV Level

Same data sources as in File 4, MT=2.

File 4, MT=52. Inelastic Scattering to 7.653-MeV Level

See Ref. 47.

File 4, MT=53. Inelastic Scattering to 9.638-MeV Level

See Ref. 47.

File 4, MT=54 to 91. Isotropic in Center-of-Mass

File 5, MT=91. Evaporation Spectrum with T=0.3 MeV.

This is a small component of $(n, n' 3\alpha)$ and is used mainly for the decay of the 2.43-MeV level of ${}^9\text{Be}$ (Ref. 34) and for reproducing the correct threshold effect.³⁵

File 8, MT=103. Activation Data Following (n, p) Reaction.⁴⁸

File 10, MT=103. (n, p) Cross Section Leading to Activation

Same as File 3, MT=103.

File 12, MT=102. Multiplicity of (n, γ) gamma rays.⁴⁹

File 13, MT=51. Production of 4.439-MeV gamma rays.

Same as File 3, MT=51.

File 14, MT=51. Angular Distribution of 4.439-MeV gamma rays.^{33,50-56}

File 14, MT=102. Angular Distribution of Capture gamma rays.

Isotropic in center-of-mass.

File 33, MT=1 to 107. Uncertainty Files for File 3 Data.

References

1. J. Lashkar et al., INDC(F/R)-7/L (1965).
2. R. B. Schwartz, H. T. Heaton, and R. A. Schrack, Bull. Am. Phys. Soc. 15, 567 (1967).
3. S. Cierjacks et al., KFK 1000 and private communication (1969).
4. F. G. Perey, T. A. Love, and W. E. Kinney, ORNL-4823 (1972).
5. H. Ahmed et al., Nucl. Data for Reactors, Helsinki, paper CN-26/23 (1970).
6. R. C. Block et al., J. Nucl. Sci. and Tech. 12, 1 (1975).
7. K. M. Diment and C. A. Uttley, EANDC(UK)94AL (1968).
8. N. C. Francis et al., Neutron Standards and Flux Norm. Symp., Argonne, p. 21 (1970).
9. H. T. Heaton et al., Nucl. Sci. Eng. 56, 27 (1975).
10. A. Langsdorf, Jr. et al., Phys. Rev. 107, 1077 (1957).
11. R. O. Lane et al., Ann. Phys. 12, 135 (1961).
12. R. O. Lane et al., Phys. Rev. 188, 1618 (1969).
13. J. W. Meadows and J. F. Whalen, Nucl. Sci. Eng. 41, 351 (1970).
14. W. E. Kinney, ORNL, private communication (1976).
15. R. J. Holt, Phys. Rev. Lett. 28, 134 (1972).
16. R. J. Holt, Nuclear Cross Sections and Technology, NBS-425, Vol. I, p. 246 (1975).
17. P. Stoler et al., Bull. Am. Phys. Soc. 15, 1668 (1970).
18. R. W. Meier et al., Helv. Phys. Acta 27, 577 (1954).
19. J. E. Wills et al., Phys. Rev. 109, 891 (1958).
20. H. D. Knox et al., Nucl. Phys. A213, 611 (1973).
21. F. O. Purser et al., WASH-1048 (1964).
22. A. J. Elwyn and R. O. Lane, Nucl. Phys. 31, 78 (1962).
23. B. E. Wenzel et al., Phys. Rev. 137, B80 (1965).

24. C. A. Kelsey et al., Nucl. Phys. 68, 413 (1965).
25. G. V. Gorlov et al., Doklady Akad. Nauk. 158, 574 (1964).
26. W. Galati et al., Phys. Rev. C 5, 1508 (1972).
27. F. G. Perey and W. E. Kinney, ORNL-4441 (1969).
28. C. R. Lubitz, KAPL, private communication (1976).
29. D. E. Velkley et al., Phys. Rev. C 7, 1736 (1973).
30. G. Haouat et al., CEA-R 4641 (1975).
31. F. O. Purser, TUNL, private communication (1976).
32. F. Boreli et al., Phys. Rev. 174, 1174 (1968).
33. G. L. Morgan et al., ORNL-TM-3702 (1972).
34. B. Antolkovic and Z. Dolenc, Nucl. Phys. A237, 235 (1975).
35. G. M. Frye et al., Phys. Rev. 99, 1375 (1955).
36. L. L. Green and W. Gibson, Prov. Phys. Soc. A26, 296 (1949).
37. S. S. Vasilev et al., J. E. T. P. 6, 1016 (1958).
38. B. C. Cook, Phys. Rev. 106, 300 (1957).
39. E. M. Rimmer and P. S. Fisher, Nucl. Phys. A108, 567 (1968).
40. O. Ames et al., Phys. Rev. 106, 775 (1957).
41. E. A. Davis et al., Nucl. Phys. 48, 169 (1963).
42. V. V. Verginsky et al., Phys. Rev. 170, 916 (1968).
43. T. Retz et al., Bull. Am. Phys. Soc. 5, 110 (1968).
44. E. R. Graves and R. W. Davis, Phys. Rev. 97, 1205 (1955).
45. A. W. Obst et al., Phys. Rev. C 5, 738 (1972).
46. L. Van der Zwan and K. W. Geiger, Nucl. Phys. A152, 481 (1970).
47. G. A. Grin et al., Helv. Phys. Acta 42, 990 (1969).
48. F. Ajzenberg-Selove, Nucl. Phys. A248, 1 (1975).
49. F. Ajzenberg-Selove, Nucl. Phys. A152, 1 (1970).
50. D. M. Drake et al., Nucl. Sci. Eng. 40, 294 (1969).

51. H. E. Hall and T. W. Bonner, Nucl. Phys. 14, 295 (1959).
52. J. T. Prudhomme et al., AFSWC-TR-30 (1960).
53. D. O. Nellis and I. L. Morgan et al., Texas Nucl. Corp (1964).
54. J. D. Anderson et al., Phys. Rev. 111, 572 (1958).
55. T. Koslowski et al., INR/661/IA/PL (1965).
56. F. C. Engesser, W. E. Thompson, and J. M. Ferguson, USNRDL-TR-791 (1964).

Covariance File for Carbon MAT 306

Covariance data are given for MF=33, MT=1, 2, 3, 51-68, 91, 102, 103, 104, and 107. Derived sections (NC subsections) reflect exactly the way the cross-section files were generated.

For MT=1, MT=2 above 2 MeV, MT=51, and MT=107, covariances were determined from $\pm 2\sigma$ error bands. The error bands were extended and enlarged to cover energy regions lacking experimental data. In general, long range covariances reflect systematic errors common to all data sets. Medium range covariances reflect differences in energy coverage by different data sets and differences in the experimental methods within the same data set. Short range covariances reflect structures in the cross sections and/or threshold effects. Statistical errors are, in principle, nonexistent in the evaluated cross sections.

For MT=2 below 2 MeV, covariances were evaluated individually for each of six data sets. These six data sets and their covariances were averaged by least squares (Bayes theorem). The resulting covariances were further modified by considering the effects of the R-matrix fit which included thermal data, data above 2 MeV, and polarization data. Uncertainties (not covariances) in the angular distributions were also evaluated and are reported in Atomic Data and Nuclear Data Tables (in press).

MT=52-68 are either discrete levels or bands of continuum levels to represent the secondary neutron distributions in $(n, n3\alpha)$ reactions with correct energy-angle kinematics. A 20% fully correlated uncertainty is given to each level or band of levels. This may require improvement in the next round of evaluation.

SUMMARY DOCUMENTATION FOR ^{14}N

by

P. G. Young and D. G. Foster, Jr.
Los Alamos Scientific Laboratory
Los Alamos, New Mexico

I. SUMMARY

The ^{14}N evaluation for ENDF/B-V (MAT 1275) is the same as Version IV except for updating of the covariance data format. Basic documentation for the evaluation is given in LA-4725 (1972), and revisions are described in LA-5375-PR (1973). The evaluation covers the energy range 10^{-5} eV to 20 MeV.

II. ENDF/B-V FILES

File 1. General Information

MT=451. Descriptive Data

Thinning Note: Cross section data in MF=3 and 13 for MT=4, 16, 51-82, 102-108, 700-704, 720-723, 740-741, and 780-790 were thinned using a 2.5% thinning criterion. Similarly, in MF=4 the MT=2, 51-62 angular distributions were thinned using the requirement that the interpolated angular distribution have an RMS average deviation from a fine-grid set of less than 2.5% and that the maximum excursion at any angle be less than 5%.

File 2. Resonance Parameters

MT=151. Effective Scattering Radius = 0.89014×10^{-12} cm.

Resonance parameters not given.

File 3. Neutron Cross Sections

The 2200 m/s cross sections are as follows:

MT=1	Sigma = 11.851 barns
MT=2	Sigma = 9.957 barns
MT=3	Sigma = 1.894 barns
MT= 102	Sigma = 0.075 barns
MT= 103	Sigma = 1.819 barns

MT=1. Total Cross Section

Zero to 1 eV, $\sigma_T = 9.957 + 0.3013/\sqrt{E}$ (b), from absorption of 1.894 b at 2200 m/s and Me49 data above 1 eV.

1 eV to 10 keV, from data of Me49.

10 keV to 0.5 MeV, from Hi52, Bi59, Hu61, and Bi62 with energy scales adjusted to match, normalized separately to join time-of-flight data smoothly at 0.5 MeV.

0.5 MeV to 20 MeV, from Ca70, He70, and Fo71 using Ca70 alone at sharp resonances.

Smoothed by appropriate fits. Log-log interpolation is good to 1.3% to 0.4 MeV. Linear interpolation is good to 0.5% from 0.4 to 20 MeV. Absolute error less than 1% above 0.75 MeV, but may rise to 5% in eV region.

MT=2. Elastic Scattering Cross Section

Zero to 10 MeV, subtracted evaluated non-elastic cross section from the evaluated total, although direct elastic measurements of Fo55, Fo66, Bo57, Ch61, Ba67, Ph61, and Ne70 were considered.

10 to 12 MeV, Transition region.

12 to 20 MeV, Based upon data of Ch61, Ba67, Ne70, Ba63, and Bo68.

MT=4. Total Inelastic Cross Section

Sum of MT=51-82 cross sections

MT=16. (n,2n) Cross Section

Based upon data of Fe60, Br61, Bo65, and Pr60, estimated ± 30 per cent error.

MT=51-62. Inelastic Cross Section to Discrete States

MT=51 Q=-2.313 MeV	MT=55 Q=-5.691 MeV	MT=59 Q=-7.028 MeV
52 -3.945	56 -5.834	60 -7.966
53 -4.913	57 -6.198	61 -8.061
54 -5.106	58 -6.444	62 -8.489

Threshold to 15 MeV, from (n,ny) data of Di69, Or69, Cl69, Bu69, Ny69, Co68, and extensive measurements of Di73.

Above 15 MeV, smooth extrapolations.

MT=63-82 Inelastic Cross Section to Groups of Discrete States

Cross section is grouped into excitation energy bins of 0.5 MeV width centered above Q-values between -9.25 MeV and -18.75 MeV.

The integrated cross section over these bands was adjusted such that the difference between the total and non-elastic cross sections agreed with elastic data (see MT=2). The division of the cross section among the bands is based on Hauser-Feshbach and nuclear temperature calculations. Note that (n,np) and (n,na) reactions are included with the discrete and binned inelastic data through use of LR flags (LR=28 and 22, respectively).

MT=102. Radiative Capture

Zero to 0.25 MeV, 1/V from 75 mb ($\pm 10\%$) at thermal (Ju63).

0.25 to 1 MeV. Transition region.

1 to 20 MeV. Deduced from $^{14}\text{N}(p,\gamma)^{15}\text{O}$ data of Ku70, assuming charge independence. Energy scale adjusted to match foot hills of (p,γ) giant resonance to resonance clusters observed in ^{15}N compound nucleus.

MT=103. (n,p) Cross Section

Sum of MT=700-704.

MT=104. (n,d) Cross Section

Sum of MT=720-723.

MT=105. (n,t) Cross Section

Sum of MT=740-741.

MT=107. (n,a) Cross Section

Sum of MT=780-790.

MT=108. (n,2a) Cross Section

Based on Li52, Mo67, and Hauser-Feshbach calculation.

MT=700. (n,p) Cross Section to ^{14}C Ground State

Zero to 4 MeV, from data of Jo50 and Ga59.

4 to 13 MeV, from inverse reaction data of Wo67.

13 to 20 MeV, smooth extrapolation.

MT=701-704. (n,p) Cross Sections to ^{14}C Excited States

MT=701 Q=-5.468 MeV Ex=6.095 MeV (6.58, 6.89-MeV level excitation cross sections are also included)

MT=702 Q=-6.102 MeV Ex=6.728 MeV

MT=703 Q=-6.385 Ex=7.012 MeV
704 -6.711 7.337

Threshold to 15 MeV, from (n,p γ) data of Or69, Di69, Cl69, Bu69, and Ny69.

15 to 20 MeV, smooth extrapolations.

MT=720. (n,d) Cross Section to ^{13}C Ground State.

Threshold to 15 MeV, from inverse cross section data of Ch61, Be63 near threshold and direct data of Mi68, Fe67, Ca57, and Za63 at 14 MeV.

15 to 20 MeV, smooth extrapolations.

MT=721-723 (n,d) Cross Section to Excited ^{13}C Levels

MT=721 Q=-8.411 MeV Ex=3.086 MeV
722 -9.009 3.684
723 -9.179 3.854

Threshold to 15 MeV, direct data of Fe67, Za63, Ca57 and (n,d γ) data of Or69 and Di69 below 13 MeV.

15 to 20 MeV, smooth extrapolations.

MT=740-741. (n,t) Cross Sections to ^{12}C Ground and 4.439 MeV-Excited State.

Threshold to 15 MeV, direct data of Ga59, Sc66, Re67, and Fe67.

15 to 20 MeV, smooth extrapolations.

MT=780-790. (n, α) Cross Section to Discrete ^{11}B States

MT=780 Q=-0.157 MeV Ex=0.000 MeV
781 -2.282 2.124
782 -4.602 4.444
783 -5.176 5.019
784 -6.900 6.743
785 -6.950 6.793
786 -7.453 7.296
787 -8.153 7.996
788 -8.723 8.566
789 -9.082 8.925
790 -9.342 9.185

Threshold to 6 MeV, from direct data of Jo50, Ga59, and Sc66.

6 to 15 MeV, used above direct data, together with (n,p γ) data of Ha59, Di69, Or69, Ny69, and Bu69. Near 14 MeV, direct (n, α) data of Li52, Ba68, La68, and Ma68 were also used.

15 to 20 MeV, smooth extrapolations.

File 4. Secondary Neutron Angular Distributions

MT=2. Elastic Angular Distributions

Zero to 8 MeV, based upon resonance theory analysis of data of Fo55, Fo66, Bo57, Ch61, and Ba67, using parameters from total and partial cross section analyses and Aj70.

8 to 15 MeV, based upon data of Ch61, Ba67, Ne70, and Ba63.

15 to 20 MeV, based upon optical model calculation.

MT=16. Angular Distribution for (n,2n) Reaction

In the absence of data, isotropy in the cm system is assumed, and the corresponding 3-body phase-space transformed to the laboratory system is given. For any reasonable cm distribution, the strong forward peaking of the transformation will dominate. Normalized for trapezoidal integration.

MT=51 to 62. Angular Distributions for Inelastic Scattering

Above 7 MeV taken from proton data of Do64, Ha70, and Od60 assuming charge symmetry, and neutron data of Ba63. Threshold shapes modeled after Hauser-Feshbach calculations.

MT=63-82. Angular Distributions for Inelastic Scattering

Assumed isotropic in cm at all energies.

File 5. Energy Distribution of Secondary Neutrons

MT=16. Spectrum of (n,2n) Secondary Neutrons

In the absence of data, only the 3-body phase-space distribution is given. Normalized for trapezoidal integration.

File 12. Photon Multiplicities

MT=102. (n, γ) Multiplicities

Zero to 0.25 MeV, thermal spectrum based primarily upon measurements of Th67, Jo69, Gr68, and Mo62. LP flags were used to designate primary gamma rays.

0.25 to 1 MeV. Transition region where thermal spectrum is phased into single ground-state transition.

1 to 20 MeV, deduced from $^{14}\text{N}(\text{p},\gamma)^{15}\text{O}$ data of Ku70, who observed no significant transitions except to ground state.

File 13. Photon-Production Cross Sections

All (n,γ) cross sections agree with the excitation cross sections in MF=3 via the relevant decay scheme (Aj68, Aj70). However, MT=104, 105 include contributions from $(n,np\gamma)$ and $(n,nd\gamma)$.

MT=4. $(n,np\gamma)$ Cross Section

From data of Ha59, Di69, Or69, Cl69, Bu69, Ny69, Co68, and Di73.

MT=103. $(n,nd\gamma)$ Cross Section

From data of Di69, Or69, Bu69, Ny69, and Cl69.

MT=104. $(n,nd\gamma) + (n,np\gamma)$ Cross Section

From data of Di69, Or69, Bu69, Ny69, and Cl69.

MT=105. $(n,t\gamma) + (n,nd\gamma)$ Cross Section

$(n,t\gamma)$ estimated from (n,t) as discussed under MF=3 MT=741.
 $(n,nd\gamma)$ estimated from MT=63-82.

MT=107. $(n,\alpha\gamma)$ Cross Section

From (n,α) data of Ga59, Sc66 and $(n,\alpha\gamma)$ data of Ha59, Di69, Ny69, Or69, and Bu69.

File 14. Photon Angular Distributions

Data on 9 strongest lines from inelastic scattering and particle reactions taken from Mo64.

MT=4. Inelastic Scattering to ^{14}N

The 1.63- and 4.91-MeV gamma are given as anisotropic. All remaining gamma rays are isotropic.

MT=102. (n,γ) Angular Distributions

Zero to 0.4 MeV, all photons are isotropic.

0.4 to 20 MeV, anisotropic distribution for the single ground state transition is based upon $^{14}\text{N}(p,\gamma)^{15}\text{O}$ data by Ku70.

MT=103. $(n,p\gamma)$ Angular Distributions

All isotropic.

MT=104. $(n,np\gamma)$ and $(n,nd\gamma)$ Angular Distributions

All isotropic except 3.85-MeV gamma ray.

MT=105. (n,nd γ) and (n,t γ) Angular Distributions

All isotropic.

MT=107. (n, $\alpha\gamma$) Angular Distributions

All isotropic.

File 33. Neutron Cross Section Covariances

MT=1,2,4,102, 103, and 107. Smooth Cross Section Covariances

Covariances are based upon estimates of the uncertainty in the experimental measurements and theoretical calculations used in in the evaluation. Format updated for Version V. Derived covariances are included explicitly.

REFERENCES

Aj68 F. Ajzenberg-Selove, and T. Lauritsen, (HAV), Nucl. Phys. A114, 1 (1968).
Aj70 F. Ajzenberg-Selove (PEN), Nucl. Phys. A152, 1 (1970).
Ba63 R. W. Bauer et al., (LRL), Nucl. Phys. 47, 241 (1963).
Ba67 R. W. Bauer et al., (LRL), Nucl. Phys. A93, 673 (1967).
Ba68 R. Bachinger and M. Uhl, (IRK), Nucl. Phys. A116, 673 (1968).
Be63 R. E. Benenson and R. Yaramis, (COL), Phys. Rev. 129, 720 (1963).
Bi59 E. G. Bilpuch et al., (DKE), Private communication to BNL (1959);
Bi62 E. G. Bilpuch et al., (DKE), Private communication to R. J. Howerton (1962).
Bo57 N. A. Bostrom et al., (TNC), WADC-TR-57-446 (1957).
Bo65 M. Bormann et al., (HAM), Nucl. Phys. 63, 438 (1965).
Bo68 F. Boreli et al., (TEX), Phys. Rev. 174, 1221 (1968).
Br61 O. D. Brill et al., (RUS), Sov. Phys. Dokl. 6, 24 (1961).
Bu69 P. S. Buchanan (TNC). Private communication (1969).
Ca57 R. R. Carlson (LAS), Phys. Rev. 107, 1094 (1957).
Ca70 A. D. Carlson and R. J. Cerbone, (GGA), Nucl. Sci. Eng. 42, 28 (1970).
Ch61 L. F. Chase et al., (LOK), AFSWC-TR-61-15 (1961).
Cl69 G. Clayeux and G. Grenier (FR), CEA-R-3807 (1969).
Co68 H. Condé et al., (SWD), Neut. Cross Sect. and Tech. Conf., Washington, D.C., p. 763 (1968).
Di69 J. K. Dickens and F. G. Perey, (ORL), Nuc. Sci. Eng. 36, 280 (1969).
Di70 J. K. Dickens et al., ORNL-4864 (1973).
Do64 D. F. Donovan et al., (BNL), Phys. Rev. 133, B113 (1964).
Fe60 J. M. Ferguson and W. E. Thompson, (NRD), Phys. Rev. 118, 228 (1960).
Fe67 P. Fessenden and D. R. Maxson, (BRN), Phys. Rev. 158, 948 (1967).
Fo55 J. L. Fowler and C. H. Johnson, (ORL), Phys. Rev. 98, 728 (1955).
Fo66 J. L. Fowler et al., (ORL), Neut. Cross Sect. and Tech. Conf., Wash. D.C., p. 653 (1968).
Fo71 D. G. Foster, Jr. and W. Glasgow, (PNL), Phys. Rev. C3, 576 (1971).
Ga59 F. Gabbard et al., (RIC), Nucl. Phys. 14, 277 (1959).
Gr68 R. C. Greenwood, (MTR), Phys. Lett. 27B, 274 (1968).
Ha59 H. E. Hall and T. W. Bonner, (RIC), Nucl. Phys. 14, 295 (1959).
Ha70 L. Hansen, (LRL), Private communication (1970).
He70 H. T. Heaton et al., (NBS), Bull. Am. Phys. Soc. 15, 568 (1970).

Hi52 J. J. Hinchey et al., (MIT), Phys. Rev. 86, 483 (1952).
Hu61 C. M. Huddleston and F. P. Mooring, (ANL), ANL-6376, p. 13 (1961).
Jo50 C. H. Johnson and H. H. Barschall, (WIS), Phys. Rev. 80, 818 (1950).
Jo69 L. Jonsson and R. Hardell, (SWD), Symposium on Neutron Capture Gamma Rays, Studsvik (1969).
Ju63 E. T. Jurney and H. T. Motz, (LAS), ANL-9797, p. 241 (1963).
Ku70 H. M Kuan et al., (STF), Nucl. Phys. A151, 129 (1970).
Le68 B. Leroux et al., (FR), Nucl. Phys. A116, 196 (1968).
Li52 A. B. Lillie, (RIC), Phys. Rev. 87, 716 (1952).
Ma68 D. P. Maxson et al., (BRN), Nucl. Phys. A110, 609 (1968).
Me49 E. Melkonian, (COL), Phys. Rev. 76, 1750 (1949).
Mi68 D. Miljanic et al., (YUG), Nucl. Phys. A106, 401 (1968).
Mo62 H. T. Motz et al., (LAS), File Neutron Research in Physics (IAEA, Vienna 1962), p. 225
Mo64 I. L. Morgan et al., (TNC), TNC Nucl. Phys. Div. Ann. Rpt. (Aug. 1964).
Mo67 J. Mosner et al., (GER), Nucl. Phys. A103, 238 (1967).
Ne70 D. O. Nellis, (TNC), Private communication (1970).
Ny69 K. Nyberg, (SWD), Private communication to L. Stewart (1969).
Od60 Y. Oda et al., (TOK), J. Phys. Soc. Japan 15, 760 (1960).
Or69 V. J. Orphan et al., (GGA), GA-8006 (1969).
Ph61 D. D. Phillips (LAS), Private communication to R. J. Howerton (1961).
Pr60 J. T. Prudhomme et al., (TNC), AFSWC-TR-60-30 (1960).
Re67 D. Rendic (YUG), Nucl. Phys. A91, 604 (1967).
Sc66 W. Scobel et al., (HAM), Z. Physik 197, 124 (1966).
Th67 G. F. Thomas et al., (ANL), Nucl. Instr. Meth. 56, 325 (1967).
Wo67 C. Wong et al., (LRL), Phys. Rev. 160, 769 (1967).
Za63 M. R. Zatzick and D. R. Maxson, (BRN), Phys. Rev. 129, 1728 (1963).

SUMMARY DOCUMENTATION FOR ^{15}N

by

E. D. Arthur, P. G. Young, and G. M. Hale
Los Alamos Scientific Laboratory
Los Alamos, New Mexico

I. SUMMARY

The ^{15}N for ENDF/B-V (MAT 1307) is a new evaluation performed originally in 1975 and updated in 1978 for Version V. The data set covers the energy range 10^{-5} eV to 20 MeV and is partially documented in LA-6123-PR (1975) and LA-6164-PR (1975).

II. ENDF/B-V FILES

File 1. General Information

MT=451. Descriptive Data

General approach: The lack of experimental data, with the exception of total cross section measurements, led us to obtain cross sections with a variety of nuclear model codes. We used an energy dependent R-matrix analysis to fit the total cross section data of Ze71 for neutron energies from 0.6 to 5.4 MeV. As a starting point we used the level scheme reported in Ze71. Also used in the R-matrix analysis were the elastic angular distributions of Si62 and Ze71 in the energy range from 1.9 to 3.64 MeV. The parameters of the R-matrix analysis were then used to generate cross sections and to determine Legendre coefficients in the range from 1.0E-05 to 5.4 MeV. In the energy region from 6 to 20 MeV we used two statistical model codes to generate cross sections. With the first, COMNUC, we computed the angular distributions of elastically scattered neutrons. The Legendre coefficients obtained were then joined smoothly with those from the R-matrix analysis. We also obtained angular distributions of neutrons leading to the first seven excited states of ^{15}N . To generate neutron transmission coefficients for this part of the analysis, we used the global optical model parameters of Wilmore and Hodgson as reported by Pe74, and adjusted them to give good agreement with the measured total cross section. The generation of capture, inelastic, and non-elastic cross sections as well as neutron, gamma-ray, and charged-particle spectra was done with the statistical model code, GNASH. This newly developed code (Yo77) is based largely on the statistical model formalism of Uh71. Again, neutron

transmission coefficients were based on the optical model parameters of Wilmore and Hodgson. Transmission coefficients were generated for protons, deuterons, and ^4He , with the appropriate global forms reported in Pe74. For tritons we used the global parameters for ^3He reported in Pe74 since these were consistent with triton optical model parameters for individual light nuclei as compiled by Pe74. The Gilbert-Cameron level density model was used with standard values for level density parameters (Gi64). To account for direct and semi-direct processes we used the pre-equilibrium model of Blann and Cline (Cl71) and assumed a 10% preequilibrium fraction.

File 2. Resonance Parameters

MT=151. Effective scattering radius = 0.592916×10^{-12} cm

Resonance parameters not given.

File 3. Neutron Cross Sections

The 2200 m/s Cross Sections are:

MT= 1 Sigma = 4.4185 b
MT= 2 Sigma = 4.418 b
MT= 102 Sigma = 24.0E-06 b

MT=1. Total Cross Section

From 1.0E-05 eV to 5.4 MeV total cross section values are based on the R-matrix analysis described above. From 5.5 to 20 MeV, the evaluated cross section is based on the smoothed results of Ze71.

MT=2. Elastic Scattering Cross Section

Zero to 20 MeV, subtracted evaluated non-elastic from total to give elastic cross section.

MT=4. Inelastic Cross Section

Sum of MT=22, 28, 51-57, and 91 cross sections.

MT=16. $(n,2n)$ Cross Section

Based on smooth curve drawn through results of the statistical model calculations described before.

MT=22. $(n,n\alpha)$ Cross Section

Based on smoothed results of statistical model calculation.

MT=28. (n,np) Cross Section

Based on smoothed results of statistical model calculation.

MT=51-57. Inelastic Cross Section to Discrete States

MT=51	Q=-5.27 MeV	MT=55	Q=-7.301 MeV
52	-5.299	56	-7.566
53	-6.324	57	-8.313
54	-7.155		

MT=91. (n,n) To Continuum

Continuum defined to begin at 0.1 MeV above last ^{15}N discrete level included in calculation, i.e., continuum begins at 8.413 MeV.

MT=102. (n, γ) Cross Section

Zero to 0.010 MeV, 1/V from 24.0E-06 b at thermal

6 to 20 MeV calculated from statistical model with Axel (Ax62) giant dipole resonance approximation for gamma-ray transmission coefficients.

0.010 to 6 MeV, cross section based on smoothed curve from region where 1/V dependence ends to region where calculated values begin.

MT=103. (n,p) Cross Section

Sum of MT=700, 701, and 718 cross sections.

MT=104. (n,d) Cross Section

Sum of MT=720, 721, 722, and 738 cross sections.

MT=105. (n,t) Cross Section

Sum of MT=740, 741, and 758 cross sections.

MT=107. (n, α) Cross Section

Sum of MT=780-785 and 798 cross sections.

MT=700, 701. (n,p) Cross Section to ^{15}C Ground and First Excited States

MT=700	Q=-8.990 MeV	EX=0. MeV
701	-9.737	0.747

MT=738. (n,p) To Continuum States of ^{15}C

Continuum defined to begin at 0.85 MeV, just above first excited state.

MT=720-722. (n,d) Cross Section to ^{14}C Ground, First, and Second Excited States

7-N-15
MAT 1307

MT=720	Q=-7.984	MeV	EX=0.	MeV
721	-14.079		6.095	
722	-14.567		=6.583	

MT=738. (n,d) To Continuum States of ^{14}C

Continuum defined to begin at 6.681 MeV, just above second excited level in ^{14}C .

MT=740-742. (n,t) Cross Section to ^{13}C Ground, First and Second Excited States

MT=740	Q=-9.902	MeV	EX=0.	MeV
741	-12.992		3.09	
742	-13.586		3.684	

MT=758. (n,t) To Continuum States of ^{13}C

Continuum begins at 3.784 MeV, above second excited level in ^{13}C .

MT=780-785. (n, α) Cross Sections to ^{12}B Ground and First Five Excited States

MT=780	Q=-7.623	MeV	EX=0.	MeV
781	-8.576		0.953	
782	-9.297		1.674	
783	-10.244		2.621	
784	-10.343		2.72	
785	-11.013		3.39	

MT=798. (n, α) To Continuum States of ^{12}B

Continuum begins at 3.49 MeV, just above fifth excited state in ^{12}B .

File 4. Secondary Neutron and Charged Particle Angular Distributions

MT=2. Elastic Angular Distributions

Zero to 5.4 MeV, based on results obtained from R-matrix theory analysis.

6 to 20 MeV, based on optical model calculation

MT=16. Angular Distribution for (n,2n) Reaction

In the absence of data, isotropy in the laboratory system is assumed.

MT=22. Angular Distribution of Neutrons from (n,n α)

Reaction assumed isotropic in the laboratory system.

MT=28. Angular Distribution of Neutrons from (n,np) Reaction

Assumed isotropic in the laboratory system.

MT=51-57. Angular Distribution Calculated Using Hauser-Feshbach Theory.

MT=718. Angular Distribution of Protons from (n,p) Reaction

Assumed isotropic in the laboratory system.

MT=719. Angular Distribution of Protons from (n,np) Reaction

Assumed isotropic in the laboratory system.

MT=738. Angular Distribution of Deutrons from (n,d) Reaction

Assumed isotropic in the laboratory system.

MT=758. Angular Distribution of Tritons from (n,t) Reaction

Assumed isotropic in the laboratory system.

MT=798. Angular Distribution of Alphas from (n,α) Reaction

Assumed isotropic in the laboratory system.

MT=799. Angular Distribution of Alphas from (n,na)

Assumed isotropic in the laboratory system.

File 5. Energy Distribution of Secondary Neutrons and Charged Particles

MT=16, 22, 28, 91, 718, 758, and 798. Calculated with Statistical Model Code, GNASH (Yo77).

MT=719. Used for Proton Spectra from (n,np) Reaction

MT=799. Used for Alpha Spectra from (n,na) Reaction

File 13. Photon Production Cross Sections

MT=4, 16, 103, 104, 105 and 107, (n,n'γ), (n,2nγ), (n,pγ), (n,dγ), (n,tγ), (n,αγ) Cross Sections

Include both discrete and continuum contributions and were generated in the statistical model calculation with the GNASH code (Yo77).

File 14. Photon Angular Distributions

MT=4. (n,n'γ) to ^{15}N , all isotropic

MT=103. (n,pγ) to ^{15}C , all isotropic

7-N-15
MAT 1307

MT=104. $(n, d\gamma)$ to ^{14}C , all isotropic
MT=105. $(n, t\gamma)$ to ^{13}C , all isotropic
MT=107. $(n, \alpha\gamma)$ to ^{12}B , all isotropic
MT=16. $(n, 2n\gamma)$ to ^{14}N , all isotropic

File 15. Energy Distribution of Secondary Photons

MT=4, 16, 103, 104, 105, 107. Generated using statistical model code
GNASH (Yo77).

REFERENCES

Aj70 F. Ajzenberg-Selove, Nucl. Phys. A152, 1 (1973).
Aj71 F. Ajzenberg-Selove, Nucl. Phys. A166, 1 (1971).
Ax62 L. P. Axel, Phys. Rev. 126, 671 (1972).
Cl71 C. K. Cline and M. Blann, Nucl. Phys. A172, 225 (1971).
Fe67 P. Fessenden and D. R. Maxson, Phys. Rev. 158, 948 (1967).
Gi65 A. Gilbert and A. G. L. Cameron, Can. J. of Phys. 43, 1446 (1965).
Pe74 C. M. Perey and F. G. Perey, Atomic and Nucl. Data Tables 13, 293 (1974).
Si62 C. P. Sikkema, Nucl. Phys. 32, 470 (1962).
U71 M. Uhl, Acta Physica Austria 31, 245 (1971).
Yo77 P. G. Young and E. D. Arthur, LA-6947 (1977).
Ze71 B. Zeitnitz et al., Nucl. Phys. A166, 443 (1971).

SUMMARY DOCUMENTATION FOR ^{16}O

by

P. G. Young, D. G. Foster, Jr., and G. M. Hale
Los Alamos Scientific Laboratory
Los Alamos, New Mexico

I. SUMMARY

The ENDF/B-V evaluation for ^{16}O (MAT 1276) is based upon the Version IV evaluation. The only change made from the Version IV data was to update the formats for the correlated error information in File 33. The evaluation covers the energy range 10^{-5} eV to 20 MeV and is partially documented in LA-5759-PR (1974). See also LA-5375-PR (1973) and LA-4780 (1972).

II. ENDF/B-V FILES

File 1. General Information

MT=451. Descriptive Data.

Thinning Note: Cross section data in MF=3 and 13 for MT=4, 51-89, 103, 104, 107, 780-783 were thinned above $E_n=6$ MeV using the requirement that interpolated values between any two points lie within 2% of the fine-grid value, providing that a certain basic grid (200 keV intervals below $E_n=10$ MeV and 500 keV above $E_n=10$ MeV) be maintained. Below $E_n=6$ MeV, a more stringent requirement of 1% was imposed on MT=780 and 107.

In a similar manner, the MT=2 Legendre coefficients in MF=4 were thinned with the requirement that the interpolated angular distribution have an rms deviation from the fine-grid set of less than 2.5% and that the maximum excursion at any angle be less than 5%.

File 2. Resonance Parameters

MT=151. Effective scattering radius = 0.54614×10^{-12} cm.

Resonance parameters not included.

File 3. Neutron Cross Sections

The 2200 m/s cross sections are as follows:

MT=1 Sigma = 3.7483 b

8-0-16
MAT 1276

MT=2 Sigma = 3.7481 b
MT=102 Sigma = 0.1780 mb

MT=1. Total Cross Section

0.0 to 5.7 MeV, essentially calculated from R-Matrix parameters obtained by fitting simultaneously almost all available data for reactions $^{16}\text{O}(\text{n},\text{n})^{16}\text{O}$, $^{16}\text{O}(\text{n},\alpha_0)^{13}\text{C}$, $^{13}\text{C}(\alpha_0,\alpha_0)^{13}\text{C}$ at energies below $E_n=5.7$ MeV. Data for total are smoothed composite of Sc71 and normalized Ci68, with inserts of Ci68, normalized composite Fo73, and normalized Fo61 for narrow structure. Fo73 and Fo61 energy scales adjusted to match Ci68. Resolution corrections applied simultaneously to total and (n,α_0) to give same width and consistent heights to peaks. Level scheme is based on Jo73. 0.44-MeV resonance from normalized data of Ok55. Inserts from the smoothed composite are used over some narrow resonances, and over regions where it appears to better represent the experimental cross section. $^{16}\text{O}(\text{n},\gamma)$ capture cross section has been added at low energies, and the $\text{n}-^{16}\text{O}$ total cross section added in the vicinity of the $\text{n}-^{16}\text{O}$ minimum at $E_n=2.35$ MeV.

5.7 to 20.0 MeV, based on a smoothed, empirical fit to the composite of experimental data described above.

MT=2. Elastic Scattering Cross Section

0.0 to 5.7 MeV, R-matrix calculations.

6 to 11 MeV, obtained by subtracting the sum of MT=4, 102, 103, 104, and 107 from MT=1. However, adjustments were made to certain reaction channels, particularly MT=51, to enhance agreement with the elastic measurements of Ph61, Ch61, and especially Ne72, Ki72, and Bu73.

11 to 14 MeV, smooth curve drawn so as to agree with 14-MeV measurements of Ba63, Mc66, and Be67.

14 to 20 MeV, optical model extrapolation using parameters from fit of 14-MeV data of Ba63, adjusted to give correct total cross sections up to 20 MeV.

MT=4. Inelastic Cross Section

Threshold to 20 MeV, sum of MT=51-89.

MT=51-70. Inelastic Cross Section to Discrete States

	MT=51 Q=-6.052 MeV	MT=58 Q=-10.354 MeV	MT=65 Q=-11.63 MeV
52	-6.131	59 -10.952	66 -12.053
53	-6.917	60 -11.080	67 -12.442
54	-7.119	61 -11.096	68 -12.528
55	-8.872	62 -11.26	69 -12.795
56	-9.597	63 -11.44	70 -12.967
57	-9.847	64 -11.521	

Threshold to 20 MeV, MT=52-55, 59, and 60 are based mainly on (n,ny) data of Di70, Or70, Dr70, Bu71, Ny69, Cl69, and En64 below 15 MeV and were extrapolated to 20 MeV with compound nucleus reaction theory calculations. The remaining MT numbers are based on compound nucleus calculations normalized to give an MT=3 in agreement with elastic data of Ba62, Be67, and Mc66 at 14 MeV. At lower energies, adjustments made, especially to MT=51, to enhance agreement with (n,n') measurements of Ne72, Ki72 and with elastic measurements of Ne72, Ki72, and Bu73. Integral data from sphere transmission measurements (Wo72) were also factored into deriving some of the 14-MeV data.

MT=71-89. Inelastic Cross Section to Groups of Discrete States

Data combined into 0.3-MeV wide excitation energy bins centered about Q-values between -13.15 MeV (MT=71) and -18.55 MeV (MT=89). This representation was used in lieu of MF=5, MT=91, which does not preserve kinematic relationships.

Threshold to 20 MeV, integrated cross section adjusted to give a nonelastic cross section in agreement with the evaluated total and elastic. The cross section was divided among bands according to a nuclear temperature calculation using $T=2$ MeV. Please note that much of the cross section to levels above 9 MeV subsequently results in charged particle emission. MT=56-58, 61-66, 68-70, 72-73, 75, 77-78, 80, 82-83, 85, 87, and 89, are flagged as decaying by alpha emission. This choice leads to a total alpha emission cross section similar to data of Li52, Da68, and Bo66 below 17 MeV. The remaining MT numbers above MT=66 are flagged as being proton emitters.

MT=102. (n,γ) Cross Section

1/V variation from 178 μb at 2200 m/s, from Ju64.

MT=103. (n,p) Cross Section

Threshold to 15 MeV, used evaluation of Sl65, raised 5 per cent above 12 MeV.

15 to 20 MeV, based on experimental data of Bo66, Se62, De62, and Ma54.

MT=104. (n,d) Cross Section

Threshold to 20 MeV, compound nucleus reaction theory calculation normalized to single datum point of Li52 at 14 MeV.

MT=107. (n,α) Cross Section

Threshold to 20 MeV, sum of MT=780-783.

8-0-16
MAT 1276

MT=780. (n,α) Integrated Cross Section to ^{13}C Ground State

0.0 to 5.7 MeV, essentially calculated from R-matrix fit described under MT=1. Energy scale of Ba72 adjusted to match Ci68 total cross section and resolution corrections applied to give width and height of peaks consistent with total. Normalization of 0.85 for Ba72 determined from R-matrix fit and applied. Level scheme based on Jo73.

5.7 to 20 MeV, based on data of Da63, Da68, Si68, Ba73, and composite of Mc66A, Ma68, and Le68 at 14 MeV.

MT=781-783. (n,α) Cross Section to Excited Levels of ^{13}C

Threshold to 15 MeV, used (n,α) data of Da63 and $(n,\alpha\gamma)$ data of Di70, Or70, Cl69, Ny69, En64, and Bu71.

15 to 20 MeV, based on data of Si68.

File 4. Neutron Angular Distributions

MT=2. Elastic Angular Distributions

0.0 to 5.7 MeV, calculated from R-matrix fit (see MF=3, MT=1). Measured angular distributions input to the fit were those of Ch61, Fo58, Fo70, Hi58, Hu62, Jo67, Ki72, La60, Li66, Ma62, and Ph61.

5.7 to 14 MeV, smooth curve through coefficients derived from fits to elastic data of Ph61, Ne72, Ch61, Ba63, Be67, Mc66, Ki72, and Bu73.

14.0 to 20 MeV, from optical model calculation using parameters from fit to 14 MeV data of Ba63, adjusted to give correct total cross sections up to 20 MeV.

MT=51-89. Inelastic Angular Distributions

Threshold to 20 MeV, assumed isotropic in center-of-mass system except for MT=51-55 above 10 MeV which are based on fits of the 14-MeV measurements of Ba63 and Mc66. Note that the sum MT=51 and 52 is consistent with isotropy at 8.56 MeV (Ki72).

File 7. Thermal Scattering Low Data

Provided by D. Finch (SRL). Constrained to match MF=3, MT=2 data.

File 12. Photon Multiplicities

MT=102. Radiative Capture

Based on experimental data from Ju64 and private communication.

File 13. Gamma Ray Cross Sections

MT=4. (n,n γ) Cross Sections

Threshold to 15 MeV, based mainly on data of Di70, Or70, Dr70, Lu70, Bu69, Ny69, Cl69, and En64. Data generated from MF=3 MT=51-60 using an ^{16}O decay scheme from Aj70.

15 to 20 MeV, based on extrapolation of MT=51-60 using compound nucleus reaction theory calculations.

Note that the first excited level of ^{16}O at 6.052 MeV is assumed to decay with emission of two 0.51-MeV gamma rays.

MT=22. (n,n $\alpha\gamma$) Cross Sections

Threshold to 20 MeV, smooth curve based crudely on (n,na) cross section and known levels in ^{12}C , adjusted to agree with composite of 14-MeV data of Cl69, and Or70.

MT=103. (n,p γ) Cross Sections

Threshold to 20 MeV, based on crude division of MF=3, MT=103 cross section among available levels according to $(2*J+1)$.

MT=107. (n, $\alpha\gamma$) Cross Sections

Threshold to 15 MeV, based mainly on (n, $\alpha\gamma$) data of Di70, Or70, Cl69, Ny69, En64, Bu71, and (n, α) data of Da63.

15 to 20 MeV, based on data of Si68.

File 14. Gamma Ray Angular Distributions

MT=4. (n,n γ) Angular Distributions

Assumed isotropic except for the 6.131-MeV gamma, which is based on the angular distribution measurement of Dr70, Lu70, Bu71, and Di70, and the 6.917-MeV gamma, which is based on the two-angle measurements of Di70.

MT=22. (n,n $\alpha\gamma$) Angular Distributions

Assumed isotropic.

MT=103. (n,p γ) Angular Distributions

Assumed isotropic.

MT=107. (n, $\alpha\gamma$) Angular Distributions

Assumed isotropic.

File 33. Neutron Cross Section Covariances

MT=1, 2, 4, 103, 107. Smooth Cross Section

Covariances are based upon estimates of the uncertainty in the experimental measurements and theoretical calculations used in the evaluation. Format updated for Version-V. For more details, see separate summary documentation for covariances.

REFERENCES

Ad49 R. K. Adair et al., Phys. Rev. 75, 1124 (1949).
Aj70 F. Ajzenberg-Selove, Nucl. Phys. A52, 1 (1970).
Ba63 R. W. Bauer et al., Nucl. Phys. 47, 241 (1963).
Ba73 J. K. Bair and F. X. Haas, Phys. Rev. C7, 1356 (1973).
(n, α_0) cross sections obtained by detail balance from this reference.
Be67 P. L. Beach et al., Phys. Rev. 156, 1201 (1967).
Bo66 M. Bormann et al., Proc. IAEA Conf. Nucl. Data, Paris (1966), p.225.
Bu71 P. S. Buchanan et al., ORO-2791-32 (1971).
Bu73 W. P. Bucher et al., BRL-R-1652 (1973).
Ch61 L. F. Chase et al., AFSWC-TR-61-15 (1961).
Ci68 S. Cierjacks et al., KFK-1000 (1960).
Cl69 G. Clayeux and G. Grenier, CEA-R-3807 (1969).
Da63 E. A. Davis et al., Nucl. Phys. 48 169 (1963).
Da68 D. Dandy et al., AWRE 060/68 (1968).
De62 J. A. DeJuren et al., Phys. Rev. 127, 1229 (1962).
Di70 J. K. Dickens and F. G. Perey, Nucl. Sci. Eng. 40, 283 (1970).
Dr70 D. M. Drake et al., Nucl. Sci. Eng. 40, 294 (1970).
En64 F. C. Engesser and W. E. Thompson, J. Nucl. Eng. 21, 487 (1967).
Fo58 J. L. Fowler and H. O. Cohn, Phys. Rev. 109, 89 (1958).
Fo61 D. B. Fossan et al., Phys. Rev. 123, 209 (1961).
Fo70 J. L. Fowler and C. H. Johnson, Phys. Rev. C2, 124 (1970).
Fo73 J. L. Fowler et al., Phys. Rev. C8, 545 (1973).
Hi58 R. W. Hill, Phys. Rev. 109, 2105 (1959).
Hu62 W. Hunzinger and P. Huber, Helv. Phys. Acta 35, 351 (1962).
Jo48 W. B. Jones, Jr., Phys. Rev. 74, 364 (1948).
Jo67 C. H. Johnson and J. L. Fowler, Phys. Rev. 162, 890 (1967).
Jo73 C. H. Johnson, Phys. Rev. C7, 561 (1973).
Ju64 E. T. Jurney and H. T. Motz, Bull. Am. Phys. Soc. 9, 176 (1964).
Ki72 W. E. Kinney and F. G. Perey, ORNL-4760 (1972).
La60 R. O. Lane et al., ANL-6172 (1960).
Le68 B. Leroux et al., Nucl. Phys. A116, 196 (1968).
Li52 A. B. Lillie, Phys. Rev. 87, 716 (1952).
Li66 D. Lister and A. Sayres, Phys. Rev. 143, 745 (1966).
Lu70 B. Lundberg et al., Physica Scripta 2, 273 (1970).
Ma54 H. C. Martin, Phys. Rev. 93, 498 (1954).
Ma62 J. P. Martin and M. S. Zucker, Bull. Am. Phys. Soc. 7, 72 (1962).
Ma68 D. R. Maxson and R. D. Murphy, Nucl. Phys. A110, 555 (1968).
Mc66 W. J. McDonald et al., Nucl. Phys. 75, 353 (1966).
Mc66A W. N. McDonald and W. Jack, Nucl. Phys. 88, 457 (1966).
Me49 E. Melkonian, Phys. Rev. 76, 1750 (1949).
Ne71 D. O. Nellis and P. S. Buchanan, private communication (1971).
Ne72 D. O. Nellis and P. S. Buchanan, DNA-2716 (1972).
Ny69 K. Nyberg, private communication to L. Stewart (1969).
Ok55 A. Okazaki, Phys. Rev. 99, 55 (1955).
Or70 V. J. Orphan et al., Nucl. Sci. Eng. 42, 352 (1970).
Ph61 D. D. Phillips, private communication to BNL (1961).
Sc71 R. B. Schwartz, private communication (1971).
Se62 K. W. Seemann and W. E. Moore, KAPL-2214 (1962).
Si68 Von I. Sick et al., Helv. Phys. Acta 41, 573 (1968).
Sl65 E. L. Slaggie and J. T. Reynolds, KAPL-M-6452 (1965).
Wo72 C. Wong et al., UCRL-51144, Rev. 1 (1972).

Benjamin A. Magurno
Brookhaven National Laboratory

8-0-17
MAT 1317

EVALUATION OF THE NEUTRON CROSS SECTIONS FOR ^{17}O for ENDF/B-V.

The dearth of experimental data associated with ^{17}O necessitated the use of nuclear model codes to calculate neutron cross sections and the utilization of systematics and "rule of thumb" to deduce some of the parameters needed as input to the nuclear model codes. The only available experimental data concerning neutron induced reactions are the coherent scattering amplitude, the thermal (n,α) cross section, a 14.1 MeV (n,p) delayed neutron yield, and a preliminary total cross section measurement in the MeV region. The codes, systematics, and estimates used are outlined in the sections to follow. The general description of the evaluated file is given in Table I.

Thermal Cross Sections and Resonance Integral

The coherent scattering amplitude of 5.78 fm⁽¹⁾ indicates an elastic scattering cross section whose lower limit is 3.74 barns, and for lack of any knowledge of incoherent scattering, is adopted as the total elastic scattering cross section.

The absorption cross section consists of an exoergic (n,α) reaction and possibly a capture cross section.

TABLE I
ENDF/B Description of ^{17}O MAT 1317

<u>FILE (MF)</u>	<u>DESCRIPTION</u>
1	General description of evaluation and references. Contains the dictionary for all files.
2	File 2 contains only the scattering radius. No resonance parameters are provided for MAT 1317.
3	Smooth cross sections for total, elastic, total inelastic, $(\text{n},2\text{n})$, (n,p) , $(\text{n},\text{n}'\text{p})$, (n,d) , (n,α) and $(\text{n},\text{n}'\alpha)$ reactions. Inelastic cross sections are provided for 12 discrete levels, ground state, and the continuum region. The parameters μ , ξ , and γ generated from file 4 angular distributions are included.
4	Angular distributions for elastic scattering expressed as Legendre coefficients, and isotropic inelastic scattering distributions in the center-of-mass-frame of reference.
5	Secondary neutron energy distributions for the inelastic continuum, $(\text{n},2\text{n})$, $(\text{n},\text{n}'\text{p})$ and $(\text{n},\text{n}'\alpha)$ reactions.

On the basis of the quoted errors we have selected the Hanna⁽²⁾ (n,α) measurement for this evaluation. It is in agreement with the values listed in both BNL-325⁽³⁾ and the Chart of the Nuclides⁽⁴⁾. Hanna implies, through rather rough estimates, that the capture cross section should be greater than or equal to the (n,α) cross section; i.e., approximately half the absorption cross section. His evidence is unsubstantiated, however. A recent calculation by S. Mughabghab indicates a value of 3.8 mb, which was adopted for the present evaluation. This value was calculated using methods outlined in BNL-NCS-25086⁽⁵⁾ and is based upon the theory of Lane and Lynn⁽⁶⁾.

The radiative capture resonance integral was calculated with INTER⁽⁷⁾ using a cutoff energy of 0.5 eV.

Energy Dependent Absorption Cross Section

There is considerable structure above $E_n = 150$ keV indicated in the ^{18}O compound nucleus as shown both in Energy Levels of Light Nuclei⁽⁸⁾ and $^{14}C(\alpha, n)$ papers by Bair⁽⁹⁾ et.al., and Morgan⁽¹⁰⁾ et.al. The absorption cross section from thermal energy to approximately 100 keV will therefore be assumed to be $1/v$ and all reactions will be described independently above 100 keV.

Resonance Parameters

There are resonance parameters for two energies listed in BNL-325⁽³⁾, but these are deduced from (α, n) experiments and only total Γ and spins are measured. This is not enough information to do a resonance profile. The described cross sections will, therefore, be construed as average cross sections in the energy ranges that have known structure.

Total Cross Section

From 10^{-5} eV to 100 keV the total cross section is defined to be the sum of the elastic cross section (a constant value of 3.74 barns) and the absorption cross section, a $1/v$ term whose value at thermal is 238.8 mb. For the MeV region the total cross section is derived from a calculation using NUBAK, an inhouse version of ABACUS⁽¹¹⁾. The calculated cross section was plotted on a preliminary experimental curve supplied by Auchampaugh⁽¹²⁾ and was equal to

the average values of the experiment. This procedure provided confidence in the calculation and subsequent use of ABACUS generated transmission coefficients.

Elastic Cross Section

This cross section is provided by subtracting the non-elastic cross section from the total cross section.

Non-Elastic Processes

The non-elastic cross section is defined here to consist of the (n, n') , (n, γ) , $(n, 2n)$, (n, α) , (n, p) , (n, d) , (n, np) and the $(n, n\alpha)$ cross sections. The above cross sections were derived from statistical model calculations with the nuclear model codes COMNUC⁽¹³⁾ and MODNEW⁽¹⁴⁾.

COMNUC uses Hauser-Feshbach theory and width fluctuation corrections to calculate the compound nucleus contributions to the cross sections. The optical model parameters were those of Wilmore-Hodgson⁽¹⁵⁾ as listed in Perey and Perey⁽¹⁶⁾ with the added correction to the square term in V_0 of $0.00118E^2$ MeV. A drawback to the use of the in-house version of COMNUC is that only the incident particle is allowed emission from the compound nucleus.

MODNEW was employed to calculate the n-particle cross sections. This code uses Hauser-Feshbach theory without width fluctuations but has four exit channels, n, p, α , and d, beside the competing γ -channel. Back shifted Fermi gas parameters used in MODNEW, i.e., those of Vonach and Hill⁽¹⁷⁾, did not give satisfactory results for isotopes in the mass range of $A=17$ and the code was subsequently modified⁽¹⁸⁾ to adopt the parameters of Gilbert and Cameron⁽¹⁹⁾.

Inelastic Scattering Cross Section

With no experimental data available for the inelastic cross sections of $^{17}_0$, data for the excited states and the continuum below 8 MeV were generated by COMNUC and for 8 MeV and above, generated by MODNEW.

COMNUC input included 20 discrete energy levels for $^{18}_0$ and a continuum cutoff of 6.9 MeV was employed. Since this version of COMNUC does not account

for n-particle competition the $^{17}\text{O}(n,\alpha)$ reaction (exoergic) was subtracted from the total inelastic and where threshold reactions became important the use of COMNUC was discontinued (i.e., ≈ 8 MeV).

The input for MODNEW is more complicated since MODNEW has four exit channels and will handle up to 6 compound nuclei. Thus, the input must include all pertinent energy level schemes (in this case energy levels for 18 isotopes).

Cross Sections for N-Particle Reaction

The (n,α) cross section calculations (exoergic) from MODNEW shows a relative maximum of 150 mb at ~ 2.5 MeV and another of 275 mb at ~ 12 MeV. This structure, while unexpected, was also produced with the Los Alamos version of COMNUC by E. Arthur ⁽²⁰⁾. The magnitude of the (n,α) cross section was supported by inverse cross section calculations using experimental results from the (α,n) reaction. In the nuclear transition $^{17}\text{O}+n \rightarrow ^{14}\text{C}+\alpha$ the following relationship holds ⁽²¹⁾:

$$(2I_0+1)(2I_n+1)P_n^2 \sigma(n,\alpha) = (2I_C+1)(2I_\alpha+1)P_\alpha^2 \sigma(\alpha,n)$$

Here I is the spin of the nucleus and P is the momentum. Average values read from Bair, et al. ⁽⁹⁾, were substituted in the equation, and for $E_n \sim 3$ MeV (the area of common interest) $\sigma(n,\alpha) \sim 100$ mb.

The calculated (n,p) , (n,d) , $(n,2n)$, $(n,n'\alpha)$ and (n,np) all behaved as expected. The only experimental data available is a cross section for the delayed neutron yield for $^{17}\text{O}(n,p)^{17}\text{N}$ at 14.1 MeV ⁽²²⁾. The value $\sigma_{n,p}$ (activation) = 21.5 ± 1.7 mb is a lower limit for the $^{17}\text{O}(n,p)$ cross section and lends support to the calculated value of $\sigma_{n,p}$ (14.1 MeV) ≈ 40 mb.

Capture Cross Section

The capture cross section was calculated with COMNUC and adjusted to account for competitive reactions. $\Gamma_\gamma \approx 1$ eV was deduced from the extrapolation of systematics for odd A, Γ_γ as a function of A, as shown by Mughabghab ⁽³⁾ on page xxiii of BNL-325, and by investigation of Γ_γ for nearby nuclei. The

average level spacing, $\langle D \rangle$, was determined by inference through investigation of nearby nuclei and from Babba ⁽²³⁾, and was chosen to be 100 keV. The adopted value of $\frac{2\pi\bar{\Gamma}}{\langle D \rangle} \gamma$ was therefore, 0.63×10^{-4} . This choice of $\frac{2\pi\bar{\Gamma}}{\langle D \rangle} \gamma$ was given some support by the resulting calculated 14 MeV capture cross section of 0.1 mb. This is near the expected value deduced from the systematics of Bergqvist ⁽²⁴⁾, of 14-15 MeV capture cross sections as a function of mass number.

Angular Distribution of Secondary Neutrons

The ABACUS-2 ⁽¹¹⁾ code was used to generate the transmission coefficients for use with MODNEW ⁽¹⁴⁾. Also calculated with ABACUS were the differential elastic scattering cross sections. CHAD ⁽²⁵⁾ was used to fit the differential elastic cross sections to a polynomial of the form

$$\frac{d\sigma(E, \mu)}{d\Omega} = \frac{\sigma_s}{4\pi} \sum_{\ell=0}^N (2\ell+1) f_\ell(E) P_\ell(\mu)$$

Assuming $d\sigma(E, \mu)/d\Omega$ may be represented linearly between points, the legendre coefficients $f_\ell(E)$ can be computed analytically. These coefficients appear in the file in the center-of-mass system.

The parameters $\bar{\mu}$, ξ and γ were generated using DUMMY5 ⁽²⁶⁾ with the differential elastic angular distributions calculated with ABACUS. These parameters appear in the ENDF/B file 3, i.e., MF-3, MT-251, 252, 253.

The inelastic angular distributions appear in the file as isotropic in the center-of-mass system.

Energy Distribution of Secondary Neutrons

The energy distributions of secondary neutrons for the $(n, 2n)$ and (n, n') reactions in the continuum have been calculated as an evaporation spectrum.

$$f(E \rightarrow E') \sim E' e^{-E'/\tau}$$

8-0-17
MAT 1317

The nuclear temperature τ is given by equation 13, but the pairing energies given by Gilbert and Cameron were replaced with those of Cook, et al (27). For deformed nuclei the level density parameter "a" was obtained from the equation $a/A = 0.00917S + 0.120 \text{ MeV}^{-1}$. Here $S = S(Z) + S(N)$ is a shell correction. All continuum inelastic temperatures were calculated from the above formula.

The first neutron in the $(n,2n)$ reaction was calculated as above with E being replaced by $E + Q$ of the reaction. The temperature of the second neutron was calculated for the $A - 1$ nucleus with E being replaced by $E + Q - \bar{E}$. Here \bar{E} is the average energy of the first neutron boiled off.

REFERENCES

1. T.M. Valentine, AERE-R5770 (1968).
2. G.C. Hanna, et al., Can. J. Phys. 39, 1784 (1961).
3. S.F. Mughabghab and D.I. Garber BNL-325, Third Edition Vol. I (1973).
4. N.E. Holden and W.F. Walker, G.E. Chart of the Nuclides, Eleventh Edition Revised to 1977 (1972).
5. S.F. Mughabghab, BNL-NCS-25086, Brookhaven National Laboratory (1978) (to be published in Physics Letters).
6. A.M. Lane and E. Lynn, Nucl. Phys. 17, 563, 586 (1960).
7. O. Ozer, "INTER," BNL-17408, Brookhaven National Laboratory (1972).
8. F. Ajzenberg-Selove, Energy Levels of Light Nuclei
A=18 PPP 1-77 (1977)
A=16-17 Nucl. Phys. A281 1 (1977)
A=13-15 Nucl. Phys. A268 1 (1976)
A=11-12 Nucl. Phys. A248 1 (1975)
A= 5-10 Nucl. Phys. A227 1 (1974)
9. J.K. Bair, et al., Phys. Rev. 144, 799 (1966).
10. G.L. Morgan, et al., Nucl. Phys. 148, 480 (1970).
11. E.H. Auerbach, ABACUS-2, BNL-6562 (1964).
12. G. Auchampaugh, Priv. Comm. to NNDC (1977).
13. C.L. Dunford, COMNUC AI-AEC-12931 (1970).
14. M. Uhl, Nuc. Phys. A184, 253 (1972).
15. D. Wilmore and P.E. Hodgson, Nucl. Phys. 55, 673 (1964).
16. C.M. Perey and F.G. Perey, Atomic and Nucl. Data Tables 13, 293 (1974).
17. H.K. Vonach and M. Hille, Nucl. Phys. A127, 289, 1969.
18. P.F. Rose, Brookhaven National Laboratory, Private Communication (1977).
19. A. Gilbert and A.G.W. Cameron, Can. J. Phys. 43, 1446 (1965).
20. E. Arthur, Los Alamos Scientific Laboratory, Private Communication (1977).
21. E. Fermi, Nucl. Phys., U. of Chicago Press pp. 145-146, Revised Edition (1950).
22. H.O. Menlove, et al., Nucl. Sci. and Eng. 40, 136 (1970).
23. H. Babba, Nucl. Phys. A159 625 (1970).
24. I. Bergqvist, Proc. of 2nd International Symposium on Neutron Capture Gamma-Ray Spectroscopy and Related Topics, 199 (Sept. 2, 1974).

8-0-17
MAT 1317

25. R.F. Berland, "CHAD," NAA-SR-11231, Atomics International (1965).
26. DUMMY5, Subroutine of CHAD which manipulates output to ENDF/B format.
27. J.L. Cook, et al., Aus. J. Phys. 20, 477 (1967).

1h

Summary Documentation

Fluorine Evaluation

ENDF/B-V MAT 1309

D. C. Larson and C. Y. Fu
Oak Ridge National Laboratory
Oak Ridge, Tennessee

August 1978

Changes from ENDF/B-IV MAT 1277 were made in sections MF=2/151, MF=3/1,2,3,4,51,52,102,107, MF=13/4,102, MF=15/102, and files MF=8,9 and 33 were added.

A complete evaluation is given for the neutron and photon production cross sections of fluorine from 0.00001 eV to 20 MeV. All data available on the CSISRS data tape [CS76] as of September 1976 were examined; in addition, other data, not yet in CSISRS, were used. Little or no data were available for some important cross sections. In particular, no elastic nor inelastic scattering data exist from 4 to 14 MeV. The results of nuclear model calculations were used where applicable. As gamma-ray branching ratios are mostly known, (n,x) and (n,xγ) cross section data were examined together. In the present case, the better known (n,xγ) cross sections enhanced the reliability of the predicted (n,x) data, particularly inelastic scattering. Activation files (MF=8,9) and uncertainty files (MF=33) have been added for all important reactions. The following files and sections are provided.

File 1. General Information

Section 451. Descriptive Data

File 2. Resonance Parameters

Section 151. General Designation for Resonance Integrals

Effective scattering length was changed from 5.64 Fermi [MJ73] to 5.36 Fermi, which is correct for free atoms.

File 3. Neutron Cross Sections

Section 1. Total Interaction

1.0E-5 to 5 eV: sum of free atom scattering cross section of 3.61 b [MU73] and the capture cross section.

5 eV - 20 MeV: re-evaluated based on data of Larson *et al.* [LA76].

Section 2. Elastic Scattering

Derived by subtracting the nonelastic from the total.

Section 3. Nonelastic Interaction

Sum of the (n,γ) and the (n,x) cross sections. The (n,x) cross sections were obtained from optical model and Hauser-Feshbach calculations up to 12 MeV. Above 12 MeV the calculated (n,x) cross section was shifted upward somewhat as called for by subsequent $(n,2n)$, $(n,n\alpha\gamma)$ and $(n,np\gamma)$ analyses. Both the shifted and the calculated results are within experimental errors. This cross section was used as a constraint for all subsequent calculations.

Section 4. Total Inelastic Scattering

Derived by summing sections 51 through 71 and section 91.

Direct interaction contributions are included in six discrete levels. $(n,n\alpha)$ cross sections are included in sections 61 to 71 and section 91; (n,np) is included in section 91 in order to simplify the representation of the angular and energy distributions of the secondary neutrons.

Section 16. $(n,2n)$ Reaction

Curve drawn through the available data [CS76] up to 15.5 MeV. Data are abundant and generally consistent. The calculation agrees well with the data. Above 15.5 MeV, calculated $[(n,2n) + (n,2nx)]$ cross section was used to avoid the necessity of splitting the secondary neutron distributions.

Section 22. $(n,n\alpha)$ Reaction

Includes calculated $(n,\alpha n)$ cross section only. The $(n,n\alpha)$ cross section is included elsewhere.

Section 28. (n,np) Reaction

Includes calculated (n,np) cross section only

The (n,np) cross section is included elsewhere.

Sections 51-71. Inelastic to lowest 21 Excited States

Hauser-Feshbach and DWBA calculations fitting the (n,n'γ) data [DI74] guided evaluation of these cross sections.

Sections 61 to 71 are dominantly (n,nα) cross sections.

Data of Morgan and Dickens [MO75] for the first two excited states up to 1.5 MeV were used.

Section 91. Inelastic to the Continuum

Statistical model calculation splitting the Hauser-Feshbach [(n,n') + (n,nx)] cross section into (n,n'γ), (n,np), (n,nα) and (n,2n) cross sections. The first three cross sections were lumped together for this section.

Section 102. Radiative Capture

The capture cross sections up to 1.8 MeV were computed from a set of evaluated parameters for 19 resonances [BL68, GAS9, MA65, MA73, MU73, NY71] using the single level Breit-Wigner formula. The 15-keV resonance used in ENDF/B-IV was removed, based on data of MA73. The gamma width of the 270-keV s-wave resonance was adjusted to yield a thermal cross section of 9.5 millibarns [MU73]. All other resonances were assumed to be p-waves. Above 1.8 MeV the capture cross section is very small and was assumed to decrease linearly with energy.

Section 103. (n,p) Reaction

Curve drawn through the available data. Resonances are present.

Calculation agrees with the gross structure up to 16 MeV.

Sections 104, 105. (n,d), (n,t) Reactions

Curves drawn through 14-MeV data.

Section 107. (n,α) Reaction

The curve is drawn through the available data. Resonances are present, but the calculation agrees with the gross structure up to 12 MeV. The region below 4 MeV has been better defined than ENDF/B-IV by adding extra points.

9-F-19
MAT 1309

File 4. Angular Distributions of Secondary Neutrons

All distributions are represented by Legendre coefficients in the center-of-mass frame.

Section 2. Elastic Scattering

0.00001 eV to 10 keV: isotropic

10 keV to 3 MeV: based on measurements made at 7 energies [CS76]

3 MeV to 20 MeV: based on optical model calculations fitting
14-MeV data

Sections 16, 22, 28 and 91. Isotropic

Sections 51 through 71. Based on results from Hauser-Feshbach and
DWBA calculations. Results agree with very limited data.

File 5. Energy Distributions of Secondary Neutrons

Section 16. ($n,2n$) Reaction

Tabulated from calculations. See File 3, Section 91.

Sections 22, 28 and 91. Tabulated from calculations.

File 13. Gamma-Ray Production Cross Section

Section 3. Nonelastic Interaction

From Dickens [DI74]. Includes $(n,x\gamma)$ cross sections for neutrons
from 1.26 to 20 MeV and gamma rays from 0.7 to 10 MeV.

Calculation agrees well with these data except near tertiary
reaction thresholds.

Section 4. Total Inelastic Scattering

110- and 197-keV gamma-ray cross sections were taken from M075
from threshold to 20 MeV.

Section 102. Radiative Capture

Product of capture cross section and gamma-ray multiplicities
evaluated for different neutron energy ranges. See File 15.

The 15-keV resonance included in ENDF/B-IV was removed.

Section 107. (n,α) Reaction

Calculated 120.6-, 297.0- and 397.3-keV gamma rays.

File 14. Angular Distributions of Secondary Gamma Rays

All sections are assumed isotropic.

File 15. Energy Distributions of Secondary Gamma Rays

Section 3. Nonelastic Interaction

From Dickens [DI74].

Section 102. Radiative Capture

The decay scheme of F-20 proposed by Spilling [SP68] was used as a basis for constructing the capture gamma-ray spectra.

The thermal-capture gamma-ray spectrum was constructed by averaging the primary intensities measured by Spilling [SP68] and by Hardell [HA69]. The primary intensities for the 27-keV and the 49-keV resonances measured by Bergqvist et al. [BE67] were used in constructing a gamma-ray spectrum for each resonance respectively. The average primary intensities of these two resonances were used for all other p-wave resonances. These averages were further averaged with their thermal-capture counterparts for the remaining neutron energies. Total energy available was naturally conserved. The 10-keV distribution present in ENDF/B-IV was removed, and the energy of the 19-keV distribution was changed to 15 keV for ENDF/B-V. These changes reflect the removal of the 15-keV resonance.

9-F-19
MAT 1309

References

BE67 I. Bergqvist, et al., Phys. Rev. 158, 1049 (1967).

BL68 R. C. Block et al., Rensselaer Polytechnic Institute, Troy, New York, Annual Technical Report (1968).

CS76 CSISRS Data Tape obtained from Brookhaven National Laboratory in September 1976.

DI74 J. K. Dickens, T. A. Love, and G. L. Morgan, ORNL-TM-4538 (1974).

GA59 F. Gabbard et al., Phys. Rev. 114, 201 (1959).

HA69 R. Hardell and A. Hasselgren, Nucl. Phys. A123, 215 (1969).

LA76 D. C. Larson et al., ORNL-TM-5612 (1976).

MA65 R. L. Macklin and J. H. Gibbons, Rev. Mod. Phys. 37, 166 (1965).

MA73 R. L. Macklin and R. R. Winters, Phys. Rev. C 7, 1766 (1973).

MO75 G. L. Morgan and J. K. Dickens, ORNL-TM-4823 (1975).

MU73 S. F. Mughabghab and D. I. Garber, BNL-325, Third Edition (1973).

NY71 G. Nystrom et al., Phys. Scr. 4, 95 (1971).

SP68 P. Spilling, et al., Nucl. Phys. A113, 395 (1968).

Summary Documentation

Sodium Evaluation

ENDF/B-V MAT 1311

D. C. Larson

Oak Ridge National Laboratory
Oak Ridge, Tennessee 37830

September 1978

The present work supersedes the ENDF/B-IV, MAT 1156 evaluation by Paik, Pitterle and Perey, done in 1971 [PI72]. In almost all sections, substantial revisions have been incorporated, based on recent data and model calculations. The resolved resonance region has been extended and new high resolution total and capture data were used to obtain the resonance parameters. Neutron and photon production data are given from 1.0E-5 eV to 20 MeV. Extensive multistep Hauser-Feshbach calculations were done to fill in data gaps and provide consistency checks for the various cross sections.

File 2, MT=151. Resonance Parameters

The resolved resonance region now includes the region from 600 eV to 500 keV (extended from 160 keV in ENDF/B-IV). Eighteen resonances are included in this range, and in addition, five large resonances above 500 keV are included for the contribution of their tails in the resolved resonance region. The resonance parameters were obtained by using a multilevel Breit-Wigner code [deS78] to fit data of Seltzer and Firk [SE74] for the 2.81-keV resonance, and data of Larson *et al.* [LA76] and Musgrove *et al.* [MU77] for the higher energy resonances. The scattering radius was taken from the resonance parameter fit.

File 3, MT=1. Total Cross Section

From 1.0E-5 to 600 eV the total cross section is based on data of Hodgson *et al.* [HO52], Joki *et al.* [JO55], Lynn *et al.* [LY58] and Rahn *et al.* [RA73], and the addition of a 1/v capture cross section. From 600 eV to 500 keV, a background cross section is given to supplement the cross section generated from the resonance parameters. It is less than

10% of the total cross section. The region around the 300-keV minimum, important for shielding problems, has been carefully done. The thick sample measurements of Brown *et al.* [BR75] were utilized in this region, in addition to data of Larson *et al.* [LA76]. From 500 keV to 20 MeV the evaluation is based on data of Larson *et al.* [LA76]. The data of Cierjacks *et al.* [CI68], Foster and Glasgow [FO71], and Stoler *et al.* [ST71] were also utilized for comparison purposes.

File 3, MT=2. Elastic Scattering Cross Section

In the energy region from 1.0E-5 eV to 600 eV, this file results from subtraction of the nonelastic cross section from the total. From 600 eV to 500 keV it contains the background file which must be added to the elastic scattering cross section generated from the resonance parameters. From 500 keV to 20 MeV, the elastic is again generated by subtracting the nonelastic from the total.

File 3, MT=3. Nonelastic Cross Section

The nonelastic cross section is formed as the sum of MT=4, 16, 102, 103, and 107.

File 3, MT=4. Total Inelastic Cross Section

This cross section is formed by the sum of MT=51 through 68, and MT=91.

File 3, MT=16. n,2n Cross Section

From threshold to 16.5 MeV the evaluation is based mainly on data of Liskien and Paulsen [LI65]. Above 16.5 MeV the evaluation is guided by the data of Paulsen [PA65]. The n,2n evaluation was influenced by calculated results which picked out these data sets from among discrepant measurements.

File 3, MT=51-68. Inelastic Scattering to Discrete Levels

Inelastic scattering to the 440-keV level (MT=51) is the largest contributor to this section. A number of data sets were available, including two high resolution data sets. However, energy shifts and

normalization problems were evident. From threshold up to 2.4 MeV the high resolution excitation function data of Larson and Morgan [LA78] were used, but renormalized down by 8% (within the estimated 10% uncertainty) to be in agreement with energy averaged cross sections of other measurements. Data considered for the energy averaging included that of Smith [SM70,SM77], Fasoli et al. [FA69], Freeman and Montague [FR58], Lind and Day [LI61], Towle and Gilboy [TO62], and Chien and Smith [CH66]. The high resolution data of Perey et al. [PE71], used in ENDF/B-IV, were not used due to a different energy averaged structure than the other sets of data. From 2.4 to 20 MeV, the evaluation is based on data of Donati et al. [DO77], but shifted down in energy by 125 keV above 1 MeV, Fasoli et al. [FA69], Lind and Day [LI61], Perey and Kinney [PE70], Dickens [DI73], and Crawley and Garvey [CR68].

MT=52-55 were changed, based on data of Donati et al. [DO77], Dickens [DI73], and Perey and Kinney [PE70]. MT=56, 59, 60, 61, 62, and 63 were changed, based on data of Dickens [DI73], Perey and Kinney [PE70] and calculated results for these levels. MT=57, 58, 64-68 were thinned, but otherwise unchanged from ENDF/B-IV. Cross sections for all levels except MT=51 are set to zero above approximately 12 MeV. Cross sections for these levels should be extended to 20 MeV at the next update.

File 3, MT=91. Continuum Inelastic

The continuum cross section was estimated by subtracting the sum of MT=51-68 from the calculated total inelastic cross section (less the n,2n component as it is explicitly included in MT=16). Since the consistent calculations were able to reproduce the cross sections to the individual n,n' levels, as well as the total (n,p) and (n, α), this was felt to be an acceptable procedure. However, this should be investigated in more detail for the next update.

File 3, MT=102. Capture Cross Section

The thermal capture cross section of 0.527 b [RY70] is consistent with $\Gamma_\gamma = 0.353$ eV for the 2.81-keV resonance. This capture width is in agreement with recent measurements of Macklin [MA76] and Wilson et al. [WI77]. Thus from 1.0E-5 eV to 600 eV, the capture cross section is calculated from the above Γ_γ using a Breit-Wigner shape. This joins on at

11-Na-23
MAT 1311

600 eV to the capture cross section calculated from the Γ_γ resonance parameters in MF=2, MT=151. These resonance parameters are used up to 500 keV. From 500 keV to 20 MeV the evaluation is based on data of Menlove [ME67a].

File 3, MT=103. (n,p) Cross Section

From threshold to 5.75 MeV the data of Williamson [WI61] were used, from 5.75 to 9.0 MeV the data of Bass et al. [BA66] were used, and from 9 to 10 MeV the data of Williamson were used [WI61]. No data are available from 10 to 14 MeV. Between 14 and 20 MeV a number of (n,p γ) activation measurements exist, but do not include the (n,pn) component of the (n,px) reaction. Thus from 10 to 20 MeV the evaluation is based on calculated results, which split (n,px) into (n,p γ) + (n,pn). The calculation reproduces the (n,p γ) component, and the complete (n,px) reaction is given in this file.

MF=3, MT=107. (n, α) Reaction

The evaluated cross section is based on data of Bass et al. [BA66] and Williamson [WI61] from threshold to 9 MeV. From 12 to 20 MeV a number of (n, $\alpha\gamma$) activation measurements are available. However, at these energies the n, α reaction consists of an (n, $\alpha\gamma$) and a (n, $\alpha\gamma$) component. The evaluation is based on an estimate of the total n, α reaction above 12 MeV, and needs to be looked at again for the next update of this evaluation.

MF=3, MT=251,252,253. Mu-Bar, Xi, Gamma

These files were inserted at Brookhaven National Laboratory.

MF=4, MT=2. Elastic Scattering Angular Distributions

Isotropic angular distributions were used from 1.0E-5 eV to 30 keV. From 30 keV to 300 keV, the data of Lane and Monohan [LA60] were used. The data of Chien and Smith [CH66] were used from 300 to 550 keV. Recent high resolution data of Kinney and Perey [KI76], taken in 1-keV steps, were smoothed and used from 550 keV to 2 MeV. From 2 MeV to 14 MeV, data of various authors [C071,FA69,FA73,KU72,PE70,PO72,T062] were fit with a

Legendre series and used; from 14 to 20 MeV the angular distributions were calculated using optical model parameters obtained from fitting the previously referenced lower energy data.

MF=4, MT=16, 51-68, and 91

All angular distributions are isotropic. Experimental evidence shows no significant anisotropy for the low lying inelastic levels [D077, PE70].

MF=5, MT=16. (n,2n) Energy Distribution

This distribution is given as an evaporation shape, with an estimated energy dependent temperature based on the relation $\theta = 0.2(E - E_{th})$ [PI68] where E_{th} is the threshold energy. This energy distribution could be better predicted from calculation, and should be looked at in future work.

MF=5, MT=91. Continuum Neutron Energy Distribution

This distribution is given as an evaporation shape, with an energy dependent temperature. At 14.6 MeV, the temperature is chosen to reproduce the neutron production data of Hermsdorf et al. [HE75], and scaled approximately as \sqrt{E} [PI68] for other energies. This energy distribution could be better predicted from calculation, and should be looked at in future work.

MF=7, MT=4. Free Gas Law

Taken from ENDF/B-III, based on data of Hockenbury et al. [HO69].

MF=8, MT=16,102,103,107. Radioactive Decay

Data are provided for decay of the reaction products ^{22}Na , ^{24}Na , ^{23}Ne , and ^{20}F . These data are taken from Endt and Van der Leun [EN73].

MF=9, MT=16,102,103,107. Multiplicities for Decay

Multiplicities are all taken to be unity.

MF=12, MT=102. Radiative Capture Multiplicities

This file was carried over from ENDF/B-IV, since no new data were available which would change the previous evaluation. The low energy neutron capture is dominated by the 2.81-keV resonance. There are no data which indicate that the gamma-ray spectrum observed at thermal should not apply to the 2.81-keV resonance [WI77]. A single gamma-ray spectrum has thus been used to describe capture over the entire energy range. The multiplicities were derived from a decay scheme based on consistent thermal capture data of Greenwood et al. [GR66] and Nichol et al. [NI69], which are in agreement with Wilson et al. [WI77].

MF=13, MT=3. Gamma Production Cross Sections

These cross sections are derived from a recent (n,xy) measurement by Larson and Morgan [LA78]. The data were acquired in neutron bins ranging from 300 keV wide at 400 keV to 3 MeV wide at 14 MeV. Gamma rays of energies between 350 keV and 10.5 MeV were measured. Calculated gamma-ray spectra are in good agreement with the measured results. Below $E_n = 14$ MeV, the cross section for gamma rays with energy $< E_\gamma = 350$ keV is very small.

File 14, MT=3,102. Gamma-ray Angular Distributions

Gamma-ray angular distributions are assumed to be isotropic, in agreement with observed results [D077].

File 15, MT=3. Energy Distributions of Gamma Rays

The energy distributions are derived from the (n,xy) measurement of Larson and Morgan [LA78]. The gamma rays were binned in 176 bins ranging in size from 15 keV at 350 keV to 140 keV at 9.4 MeV. The spectra were smoothed to reduce the number of bins, and are in good agreement with the calculated spectra.

File 32, MT=151. Resonance Parameter Uncertainties

Uncertainties in the resonance parameters are based on uncertainties resulting from the least squares multilevel fitting code [deS78], and capture areas. In cases where $\Gamma_n \approx \Gamma_\gamma$, correlations between the parameters are estimated.

File 33, MT=1,2,3,4,16,51-68,91,102,103,107. Uncertainty Files

Uncertainties in the cross sections are estimated from the spread in the available data, and estimated uncertainties in calculated results based on reasonable parameter variations. Short- and long-range correlations are given.

References

BA66 R. Bass, P. Haug, K. Krüger, and B. Staginnus, EANDC(U) 66, p. 64 (1966).

BR75 P. H. Brown, B. L. Quan, J. J. Weiss, and R. C. Block, Trans. Am. Nucl. Soc. 21, 505 (1975).

CH66 J. P. Chien and A. B. Smith, Nucl. Sci. Eng. 26, 500 (1966).

CI68 S. Cierjacks, P. Forti, D. Kopsch, L. Kropp, J. Neve, and H. Unseld, Karlsruhe Report KFK-1000 (June 1968).

CO71 R. E. Coles, Report AWRE/0 (March 1971).

CR68 G. M. Crawley and G. T. Garvey, Phys. Rev. 167, 1070 (1968).

deS78 G. de Saussure, D. K. Olsen, and R. B. Perez, ORNL-TM-6286 (May 1978).

DI73 J. K. Dickens, Nucl. Sci. Eng. 50, 98 (1973).

DO77 D. R. Donati, S. C. Mathur, E. Sheldon, B. K. Barnes, L. E. Beghian, P. Harihar, G.H.R. Kegel, and W. A. Schier, Phys. Rev. C 16, 939 (1977).

EN73 P. M. Endt and C. Van der Leun, Nucl. Phys. A214, 1 (1973).

FA69 U. Fasoli, D. Toniolo, G. Zago, and V. Benzi, Nucl. Phys. A125, 227 (1969).

FA73 U. Fasoli, D. Toniolo, G. Zago, V. Banzi, P. L. Ottaviani, and L. Zuffi, Report CEC(73)7 (1973).

FO71 D. G. Foster, Jr. and D. W. Glasgow, Phys. Rev. C 3, 576 (1971).

FR58 J. M. Freeman and J. H. Montague, Nucl. Phys. 9, 181 (1958).

GR66 R. C. Greenwood, Phys. Lett. 23, 482 (1966).

HE75 D. Hermsdorf, A. Meister, S. Sassonoff, D. Seeliger, K. Seidel, and F. Shahin, Report ZFK-277, INDC(GDR)-2/L (1975).

HO52 E. R. Hodgson, J. F. Gallagher, and E. M. Bowey, PPS/A 65, 992 (1952).

HO69 R. W. Hockenbury, Z. M. Bartolome, J. R. Tatarczuk, W. R. Moyer, and R. C. Block, Phys. Rev. 178, 1746 (1969).

JO55 E. G. Joki, L. G. Miller, and J. E. Evans, Phys. Rev. 99, 610 (1955).

KI76 W. E. Kinney and F. G. Perey, private communication.

KU72 P. Kuijper, J. C. Veefkind, and C. C. Jonker, Nucl. Phys. A181, 545 (1972).

LA60 R. O. Lane and J. E. Monahan, Phys. Rev. 118, 533 (1960).

LA76 D. C. Larson, J. A. Harvey, and N.W. Hill, ORNL-TM-5614 (October 1976).

LA78 D. C. Larson and G. L. Morgan, ORNL-TM-6281 (May 1978).

LI61 D. A. Lind and R. B. Day, Ann. Phys. 12, 485 (1961).

LI65 H. Liskien and A. Paulsen, Nucl. Phys. 63, 393 (1965).

LY58 J. E. Lynn, F.W.K. Firk, and M. C. Moxon, Nucl. Phys. 5, 603 (1958).

MA76 R. L. Macklin, private communication (1976).

ME67 H. O. Menlove, K. L. Coop, H. A. Grench, and R. Sher, Phys. Rev. 163, 1299 (1967).

MU77 A. R. deL. Musgrove, B. J. Allen, and R. L. Macklin, "The Radiative Capture Cross Section of Sodium above 3 keV," preprint (May 1977).

NI69 L. W. Nichol, Can. J. Phys. 47, 953 (1969).

PA65 W. Paulsen, private communication to CCDN (1965).

PE70 F. G. Perey and W. E. Kinney, Report ORNL-4518 (1970).

PE71 F. G. Perey, W. E. Kinney, and R. L. Macklin, Third Conf. Neutron Cross Sections and Technology, Knoxville, p. 191 (1971).

PI68 T. A. Pitterle, Atomic Power Development Associates, Inc. Report APDA-217 (ENDF-121) (June 1968).

PI72 T. A. Pitterle and N. C. Paik, Westinghouse Advanced Reactors Div. Quarterly Prog. Rept. WARD-3045T6B-2, Appendix A (June 1972).

P072 V. I. Popov and V. I. Trykova, CSISRS 40101/001 (1972).

RA73 F. Rahn, H. S. Camarda, G. Hacken, W. W. Havens, Jr., H. I. Liou, J. Rainwater, U. N. Singh, M. Slagowitz, and S. Wynchank, Phys. Rev. C8, 1827 (1973).

RY70 T. B. Ryves and D. R. Perkins, J. Nucl. Energy 24, 419 (1970).

SE74 J. Seltzer and F.W.K. Firk, Nucl. Sci. Eng. 53, 415 (1974).

SM70 D. L. Smith, Report ANL-7710, p. 15 (1971).

SM77 D. L. Smith, "Measurement of Cross Sections for the $^{23}\text{Na}(n,n'\gamma)^{23}\text{Na}$ Reaction near Threshold," preprint (February 7, 1977).

ST71 P. Stoler, P. F. Yergin, J. C. Clement, C. G. Goulding, and R. Fairchild, Third Conf. Neutron Cross Sections and Technology, Knoxville, p. 311 (1971).

TO62 J. H. Towle and W. B. Gilboy, Nucl. Phys. 32, 610 (1962).

WI61 C. F. Williamson, Phys. Rev. 122, 1877 (1961).

WI77 W. M. Wilson, H. E. Jackson, and G. E. Thomas, Nucl. Sci. Eng. 63, 55 (1977).

Summary Documentation
Natural Magnesium Evaluation
ENDF/B-V MAT=1312

D. C. Larson
Oak Ridge National Laboratory
Oak Ridge, Tennessee

September 1978

The present evaluation supersedes the ENDF/B-IV, MAT 1280 evaluation by M. K. Drake and M. P. Fricke [DR74]. New data have been incorporated for the total cross section (MF=3/MT=1), inelastic scattering to the first excited level in $^{24}\text{Mg}(3/53)$ and the photon production cross sections (13/3, 15/3). In addition, all MF=3 data were thinned to 1%, greatly reducing the number of points, and shortened formats were used for MF=4 data. The remainder of the evaluation is taken from ENDF/B-IV. The evaluation contains neutron and gamma-ray production cross sections for natural magnesium. Energy and angular distributions are given for all secondary neutrons and gamma rays produced by neutron interactions. Cutoff date for new material was December 1977.

File 2 (Resonance Parameters)

Resonance parameters were not considered necessary. An effective scattering radius of 0.5E-12 cm is given.

File 3 (Neutron Cross Sections)

File 3, MT=1 (Total Cross Section)

From 1.0E-5 eV to 10 eV, ENDF/B-IV results were used, which were based mainly on the data of Newson *et al.* [NE59]. From 10 eV to 10 keV, and over the 83-keV resonance, the data of Singh *et al.* [SI74] were used. In the region from 10 to 500 keV (where the Singh *et al.* measurement stopped), the data of Singh *et al.* and Larson *et al.* [LA78] were in good agreement, but the Larson data had much higher resolution. Thus, the latter data were used from 10 keV to 20 MeV, except over the 83-keV resonance, where the sample in the Larson measurement was too thick to observe the peak cross section.

File 3, MT=2 (Elastic Scattering Cross Section)

The elastic scattering cross section was obtained everywhere by subtracting the non-elastic cross section from the evaluated total cross section. This cross section was compared to the results from the available experimental data [KI70, TH62, ST65, CL64, KO64]. These measurements were typically made at low energy resolution and therefore the results represent averages over the structure in the elastic scattering cross section. There was fairly good agreement between the measured and evaluated data, with the exception that the evaluated data were slightly higher than the results obtained by Kinney and Perey [KI70] for neutron energies between 4 and 8.5 MeV.

File 3, MT=3 (Non-Elastic Cross Section)

The non-elastic cross section was taken as the sum of (MF/MT = 3/4, 3/16, 3/22, 3/28, 3/102, 3/103, and 3/107.

File 3, MT=51-91 (Inelastic Scattering Cross Section)

The inelastic scattering cross section for magnesium has been given as the total inelastic scattering cross section, level excitation cross sections for the first 40 levels, and a continuum portion. The cross sections for the element were obtained by combining the evaluated cross sections for the individual isotopes.

The level excitation cross sections for the first level in ^{24}Mg , $Q = -1.37$ MeV, were based on a measurement of the excitation function for this level by Dickens [DI74] et al. up to 4.3 MeV. Between 4.3 and 9 MeV, the experimental data of Kinney and Perey [KI70], Thomson, et al. [TH62], Broder, et al. [BR64], and Mathur, et al. [MA65] were used. Near 14 MeV, the data of Clarke and Cross [CL64] and Stelson, et al. [ST65] were used. Interpolation and extrapolation of data to higher energies was done using calculated results from the HELENE and JUPITOR codes.

The excitation functions for the 4.12 and 4.23 levels in ^{24}Mg were based on calculations. The sum of these two levels was consistent with the ORNL data [KI70] between 6 and 8.6 MeV and the Stelson data [ST65] at 14 MeV, but the individual levels were higher than the ORNL data at 8.6 MeV.

All other level excitation functions were based on calculations and results agreed with the limited experimental data [BR64, EN65, MA65].

File 3, MT=16 [(n,2n) Cross Section]

The (n,2n) cross section for the element was obtained from the (n,2n) cross sections for the individual isotopes. The (n,2n) cross section for ^{24}Mg was based on a measurement made by Arnold [AR65]. The (n,2n) cross sections for ^{25}Mg and ^{26}Mg were based on statistical model calculations made by Pearlstein [PE64].

File 3, MT=103,28 [(n,p) and (n,n-p) Cross Sections]

The (n,p) and the (n,n-p) cross sections for the element were obtained from the cross sections for the individual isotopes. Almost no experimental data were available for the (n,n-p) reaction; therefore these cross sections were evaluated to be consistent with the (n,p) cross sections for the individual isotopes.

^{24}Mg : Between 5.0 and 12 MeV the (n,p) cross section was based on measurements by Butler and Santry [BU63] and by Liskien and Paulsen [LI66]. In the energy region of over-lap for these two measurements, 6 to 8 MeV, their results were in good agreement. Numerous sets of experimental results were available for the energy region from 12 to 14 MeV and the data were not in good agreement ($\pm 30\%$). In this energy region, the data measured by Ferguson and Albergotti were used [FE67]. Considerable structure had been observed in the (n,p) cross section and the recommended data were evaluated to have the same structure as seen in the total and (n,p) cross section. Between 14 and 15 MeV, the structure as observed by Paulsen and Liskien [PA65] were used. The magnitude was based on this and other measurements [BA69, IM64, PA67]. Above 15 MeV, the (n,p) cross section decreased fairly rapidly and the recommended data were based on measurements by Imhof [IM64] and Paulsen and Liskien [PA65].

No experimental data were available for the (n,n-p) reaction. The recommended values were based on semi-theoretical arguments. The sum of the (n,p) and (n,n-p) was assumed to have the same energy dependence as the non-elastic cross section. The threshold for the (n,n-p) reaction was at 12.2 MeV. The recommended (n,n-p) cross section was taken to be

zero at 12.6 and reach a maximum value of 90 mb at 20 MeV. The resulting cross section was very uncertain.

^{25}Mg : No experimental results were available for neutron energies less than 13 MeV. The recommended data were based on several sets of experimental data sets that were available for the energy region from 13 to 17 MeV. The shape of the recommended cross section was taken from the measurement by Bormann [B066]. The cross section at 14.5 MeV was an average of the results by Bormann [B066], Pasquarelli [PA67], and Prasd and Sarkar [PR66]. From the effective threshold at 4.5 MeV to 13 MeV the recommended cross section was assumed to have the same shape as calculated from a statistical model and was normalized to the experimental data at 13 MeV. The same procedure was used to obtain the $(n, n-p)$ cross section as for ^{24}Mg .

^{26}Mg : Almost no experimental data were available for the (n, p) and $(n, n-p)$ reactions. Very crude estimates of these cross sections were made. These estimates were based on statistical model calculations and the experimental data measured by Nurmia and Fink [NU58] and Allan [AL61].

File 3, MT=107, 22 [(n, α) and $(n, n-\alpha)$ Cross Sections]

These cross sections were evaluated in the same manner as the (n, p) and $(n, n-p)$ cross sections. However, far less experimental data were available. The (n, α) cross section for the element was tied almost exclusively to the experimental data for ^{26}Mg . Experimental data measured by Bormann [B066], Prasd and Sarkar [PR66], and Pasquarelli [PA67] were used to define the $^{26}\text{Mg}(n, \alpha)$ cross section for the energy range from 13 to 17 MeV. Statistical model calculations were used to obtain the cross section for this isotope from its effective threshold at about 7.5 MeV up to 13 MeV and above 17 MeV. From 2.1 to 3.0 MeV the inverse cross section, NE-22(α, n -zero) Mg-25 , as measured by Ashery [AS69], was used to determine the $^{25}\text{Mg}(n, \alpha)$ cross section. Above 3 MeV, statistical model calculations were used to predict the shape of the cross section. The magnitude of the $^{25}\text{Mg}(n, \alpha)$ cross section at 14.5 MeV was based on the evaluated $^{26}\text{Mg}(n, \alpha)$ cross section at this energy and a calculated ratio for $^{25}\text{Mg}/^{26}\text{Mg}$ [GA64]. Since there were no useable experimental data for

^{24}Mg , the evaluated cross section for this isotope was based on a statistical model calculation, normalized to a calculated ratio [GA64].

As a result of calculated comparisons to the LLL pulsed-sphere measurements [H073], the inelastic scattering was increased by 150 mb at 14 MeV incident energy, and in a systematic way, everywhere between 8 and 20 MeV. Since the (n,α) cross section was the most uncertain, it was decreased by the amount that the inelastic cross section was increased, to preserve the non-elastic cross section.

The $(n,n\alpha)$ cross section for the isotope was obtained in the same manner as the $(n,n-p)$ cross section. The (n,α) and $(n,n\alpha)$ cross sections are very uncertain due to the lack of experimental data and the reliance on nuclear model calculations.

File 3, MT=102 (The Radiative Capture Cross Section)

The radiative capture cross section was taken to be the same as that evaluated by Drake [DR67] for neutron energies less than 500 keV. This was based on a thermal cross section of 0.063 barns and was $1/V$ up to 1.0 keV. Between 1.0 keV and 500 keV, the capture cross section for the element was calculated from the evaluated resonance parameters for the isotopes [DR67]. Above 500 keV, the cross section was taken to be $1/E$ up to about 3 MeV where direct capture mechanisms predominate. Above 5 MeV, the capture cross section was taken to be relatively constant and the recommended cross section at 14 MeV was based on experimental results obtained by Cvelbar [CV69].

File 4 (Angular Distributions of Secondary Neutrons)

File 4, MT=2 [Elastic Scattering (MT=2) Legendre Coefficient Representation]

The angular distribution of elastically scattered neutrons was assumed to be isotropic up to 25 keV. Just above 25 keV several p-wave resonances have been observed and the angular distributions are peaked in the backward direction. Between 25 and 300 keV, the recommended angular distributions were based on a measurement made by Langsdorf, et al. [LA56]. Between 0.3 and 1.0 MeV, the distributions were based on measurements by Langsdorf [LA56], Cox [CO66], and Korzh [KO64]. Between 2.0 and 4.0 MeV, the data

measured by Thomson [TH62] were used. Between 5 and 8.5 MeV, the ORNL [KI70] measurements were used. Near 14 MeV, the experimental data measured by Stelson, et al. [ST65], Clarke and Cross [CL64], and Berko, et al. [BE58] were used. Between 8.5 and 14 MeV and above 15 MeV, the recommended angular distributions were obtained from deformed nucleus model calculations.

File 4, MT=51-91 (Angular Distribution of Inelastically Scattered Neutrons)

The angular distributions for neutrons that lead to the 1.37-MeV level in ^{24}Mg were based on the experimental data of Thomson, et al. [TH62] for points at 2.84, 3.79, and 4.76 MeV, data of Kinney and Perey [KI70] at 5.44 and 7.55 MeV, data of Stelson, et al. [ST65] and Clarke and Cross [CL64] at 14 MeV. The angular distribution for all other incident energy points was based on HELENE and JUPITOR calculations. The distribution data for the 4.12- and 4.23-MeV levels in ^{24}Mg were based on calculations. The angular distributions for all other levels and the continuum were assumed to be isotropic in the cm system.

File 4, MT=16, 28, 22 [(n,2n), (n,n-p), and (n,n α) Angular Distributions]

Neutrons from these reactions were assumed to be isotropic in the cm system.

File 5, MT=91, 16 (Energy Distributions for Inelastic Scattering and n,2n Reactions)

Secondary neutron energy distributions for inelastic scattering to the continuum are based on a statistical model calculation below 10 MeV. Above 10 MeV, an evaporation spectrum was used, with a temperature chosen to reproduce the LLL pulsed-sphere measurements. An effective nuclear temperature was used for each isotope for the second neutron.

File 12, MT=102 (Radiative Capture Gamma-Ray Multiplicities)

The multiplicities for gamma rays from radiative capture have been based on the data measured by Orphan, et al. [OR70] at thermal neutron energies. The data measured by Bird, et al. [BI71] have been used to

describe the gamma rays from capture in the 83-keV resonance. The multiplicities for all other energies were based on values at thermal and they increase as a function of incident neutron energy to preserve total energy released.

File 13, MT=3 (Gamma-Ray Production Cross Sections)

The gamma-ray production cross sections were taken from the 125 degree (n,xy) measurement by Dickens, Love and Morgan [DI74]. Gamma rays with energy $E_g = 0.7$ to 10.5 MeV are included.

File 15, MT=3, 102 (Energy Distribution of Secondary Gamma Rays)

The energy distributions for the secondary gamma-ray production were obtained by binning the data of Dickens et al. [DI74]. The energy distributions for (n,γ) reactions were based on measurements by Orphan et al. [OR70] and Bird, et al. [I71]. Histogram representations have been used to describe the energy distributions.

References

AL61 D. L. Allan, Nucl. Phys. 24, 274 (1961).

AR65 D. M. Arnold, Ph.D. Thesis, Univ. Georgia, 1965.

AS69 D. Ashery, Nucl. Phys. A136, 481 (1969).

BA69 R. C. Barrall et al., Report AFWL-TR-68-134 (1969).

BE58 S. Berko et al., Nucl. Phys. 6, 210 (1958).

BI71 J. R. Bird, et al., Report ORNL-TM-3379 (1971).

BO66 M. Bormann, et al., Proc. Conf. Nucl. Data for React., Paris, Vol. I, p. 225 (1966).

BR64 D. L. Broder, et al., Atomic Energy 16, 103 (1964).

BU63 J. P. Butler and D. C. Santry, Can. J. Phys. 41, 372 (1963).

CL64 R. C. Clarke and W. G. Cross, Nucl. Phys. 53, 177 (1964).

CO66 S. A. Cox (ANL), private communication (1966).

CV69 F. Cvelbar, Nucl. Phys. A138, 412 (1969).

DI74 J. K. Dickens, T. A. Love, and G. L. Morgan, ORNL-TM-4544 (1974).

DR67 M. K. Drake, Report NDL-TR-89, part 3 (1967).

DR75 M. K. Drake and M. P. Fricke, Report DNA 3479F (1975).

EN65 F. C. Engesser and W. E. Thompson, Report USNRDL-TR-916 (1965).

FE67 J. M. Ferguson and J. C. Albergotti, Nucl. Phys. 98, 65 (1967).

GA64 D. G. Gardner and Yu-Uen Yu, Nucl. Phys. 60, 49 (1964).

HO73 R. J. Howerton (LLL), private communication (1973).

IM64 W. L. Imhof (Lockheed), private communication (1964).

KI70 W. E. Kinney and F. G. Perey, ORNL-4550 (1970).

KO64 I. A. Korzh et al., Atomic Energy 16, 260 (1964).

LA56 A. Langsdorf, et al., Report ANL-5567 (1956).

LA78 D. C. Larson, J. A. Harvey, N. W. Hill, and H. Weigmann, ORNL-TM-6420 (1978).

LI66 H. Liskien and A. Paulsen, Nukleonik 8, 315 (1966).

MA65 S. C. Mathur et al., Nucl. Phys. 73, 561 (1965).

OR70 V. J. Orphan et al., Report 6A-10248 (1970).

NE59 H. W. Newson et al., Ann. Phys. 8, 211 (1959).

NU58 M. J. Nurmia and R. W. Fink, Nucl. Phys. 8, 139 (1958).

PA65 A. Paulsen and H. Liskien, J. Nucl. Energy a/b 19, 907 (1965).

PA67 A. Pasquarelli, Nucl. Phys. 93, 218 (1967).

PE64 S. Pearlstein, Report BNL-897 (1964).

PR66 R. Prasd and D. C. Sarkar, Nucl. Phys. 85, 476 (1966).

SI74 U. N. Singh et al., Phys. Rev. C 10, 2150 (1974).

ST65 P. H. Stelson, et al., Nucl. Phys. 68, 97 (1965).

TH62 D. B. Thomson, et al., Phys. Rev. 125, 2049 (1962).

SUMMARY DOCUMENTATION FOR ^{27}Al

by

P. G. Young and D. G. Foster, Jr.
Los Alamos Scientific Laboratory
Los Alamos, New Mexico

I. SUMMARY

The ENDF/B-IV evaluation for ^{27}Al was carried over for Version V as MAT 1313. Besides minor format changes, the only new data included are correlated errors in File 33. The evaluation covers the energy range 10^{-5} eV to 20 MeV. Documentation for the evaluation is LA-4726 (1972), as updated by LA-5759-PR (1974).

II. ENDF/B-V FILES

File 1. General Information

MT=451. Descriptive data.

File 2. Resonance Parameters

MT=151. Effective scattering radius = 0.32752×10^{-12} cm.

Resonance parameters not given.

File 3. Neutron Cross Sections

The 2200 m/s cross sections are:

MT=1 $\sigma = 1.580$ b
MT=2 $\sigma = 1.348$ b
MT=102 $\sigma = 0.232$ b

MT=1. Total Cross Section

Below 4.6 keV: 1/V fit to Me52 and H150 (normalized to Me52), using thermal capture σ of 232 mb (Go71) and resulting in a total of 1.580 b.

4.6 - 189 keV: From Ga65 normalized to Me52 via H159 at low energies and to Pe72 at high energies.

209 - 475 keV: From Pe72 with energy scale corrected to match Ci68 at higher energies.

13-Al-27
MAT 1313

475 - 11.5 MeV: Composite of Pe72 and Sc69, normalized to their weighted average, with inserts of normalized Ci68 where needed to preserve resolution.

11.5 - 20 MeV: Composite of Pe72, Fo71, Al66, and Pe60 normalized to their weighted average. Slope at 20 MeV includes guidance from Ta55.

Smoothing between 4.6 keV and 2 MeV by approximate Breit-Wigner fits where possible, connected by polynomial fits. 2 - 12 MeV smoothed by running cubic polynomial fits. Above 12 MeV fitted secondary polynomial to middles of running polynomial fits.

MT=2. Elastic Scattering Cross Section

Below 5 MeV: Subtracted nonelastic from total.

5 to 16 MeV: Mainly based on elastic data of Ho69, St59, Ki70, St65, Co58, Co59, Be58, Mi68, Be56, and Ka72 together with the evaluated total and the nonelastic measurements listed below.

16 to 20 MeV: Smooth extrapolation to 1/2 the total at 20 MeV.

MT=3. Nonelastic Cross Section (implicit - not in file)

Below 9 MeV: Based on the nonelastic measurements of Ba58, Be56, Ta55, De65, on the sum of MT=4, 102, 103, 107, and on the difference between the evaluated total and the elastic measurements of Ho69, Ki70, Be56, and Mi68.

9 to 16 MeV: Based on nonelastic measurements of Ba58, Ta55, Gr55, Ph52, Ma57, De61, Fl56, Ch67, and on the difference between MT=1 and MT=2 data of St59, St65, Co58, Co59, and Be58.

16 to 20 MeV: Difference between MT=1 and MT=2.

MT=4. Inelastic Cross Section

Threshold to 5 MeV: Sum of MT=51-63.

5 to 9 MeV: Based on (n,n') data of Th63, To67, the evaluated (n,n') data of Di71 which includes consideration of several other measurements, and the (n,ny) data of Di71, Or71, and Di73.

9 to 20 MeV: The difference between MT=1 and the sum of MT=2, 16, 102, 103, 104, 105, and 107.

MT=16. (n,2n) Cross Section

Threshold to 20 MeV: Estimated using a nuclear temperature calculation assuming that highly excited states in ^{27}Al decay 50 per cent by neutron emission.

MT=51 - 63. Inelastic Cross Section to Discrete States

MT=51 Q=-0.843 MeV	MT=56 Q=-3.001 MeV	MT=60 Q=-4.409 MeV
52 -1.013	57 -3.678	61 -4.508
53 -2.210	58 -3.956	62 -4.580
54 -2.732	59 -4.055	63 -4.811
55 -2.980		

Threshold to 5 MeV: Based on the (n, n') data of To62, Wi63, Ts61, and the $(n, n\gamma)$ data of Ch68, Ma65, Di71, Or71, and Di73.

5 to 9 MeV: Based on an evaluation of several measurements given in Di71 (Table B1).

9 to 20 MeV: Smooth extrapolation passing through 14 MeV data of St65, and Bo65A.

MT=64 - 90. Inelastic Cross Section To Groups Of Discrete States
in Energy Bins Centered About Q-values Between
-5.25 MeV and -18.875 MeV.

Threshold to 20 MeV: Integrated cross section over bands obtained by subtracting MT=51-63 from MT=4. Cross section divided among bands according to a nuclear temperature calculation using temperatures based on (n, n') data of Th63, and Gr53. The cross section to the bands with MT=64-71 was adjusted extensively to produce agreement with the 14-MeV measurements of secondary neutron spectra by Ka72.

(Please note that much of the cross section to bands above $E_x=9$ MeV subsequently results in charged particle emission. Since these data are not included explicitly as (n, n_x) reactions, it is important that users involved in certain calculations (e.g., local heating) be aware of this information.)

MT=102. (n, γ) Cross Section

Below 1 keV: 1/V from thermal value of 232 mb (Go71).

1 to 140 keV: From B168, 6-keV resonance has width deduced from total cross section. Small resonances nearby also from total.

Above 140 keV: Mainly from He50, He53, and Ca62.

MT=103. (n, p) Cross Section (see Yo72 for more details)

Threshold to 4 MeV: Based on the measurements of He54 and Gr67, extrapolated from 3 MeV to threshold with an L=0 penetrability function for the outgoing $p + {}^{27}\text{Mg}$ channel.

4 to 20 MeV: Smooth curve through the measurements of He54, Gr67, Ca62, Ba66, and Ma60.

13-A1-27
MAT 1313

MT=104. (n,d) Cross Section

Threshold to 20 MeV: Smooth curve through single datum of G&61.

MT=105. (n,t) Cross Section

Threshold to 20 MeV: Smooth curve with same shape as MT=104.
Reaching maximum of 15 mb at 20 MeV.

MT=107. (n, α) Cross Section (see Yo72 for more details)

Threshold to 20 MeV: Based on a smooth curve through experimental data, mainly those of Bu63, Pa65, and Li66, with results from Gr67, Sc61, Gr58, Ba61, Ma65, Ga62, Im64, Ke59 and several 14-MeV points also being considered. The curve was extrapolated from 6 MeV to threshold with an L=0 penetrability function for the outgoing $\alpha + {}^{24}\text{Na}$ channel.

File 4. Neutron Angular Distributions

MT=2. Elastic Angular Distributions

From smooth curves through plots of coefficients from fits to all available data above .25 MeV, without evaluation of measurements. Mainly from Ta57, Ch66, To62, Ts61, Ki70, and Be58, with optical-model bridge to Si62. Some of data augmented before fitting by zero-degree point slightly above Wick limit, and coefficients adjusted empirically afterwards to obey Wick limit. But only barely at higher energies.

MT=16. (n,2n) Angular Distributions

Assumed isotropic in CM, using 2-body kinematics to estimate transformation to laboratory system.

MT=51 - 63. Inelastic Neutron Angular Distributions

Anisotropic distributions based on measurements by Ts61, To62, Wi63, Mi68, Ta70, G&72, St65, Bo65A, and Ka72 were incorporated over varying energy ranges from threshold to 20 MeV. In several regions where data were lacking, isotropy was assumed.

MT=64 - 90. Inelastic Neutron Angular Distributions

Assumed isotropic in the center-of-mass system.

File 5. Neutron Energy Distributions

MT=16. (n,2n) Energy Distributions

Based on statistical theory.

File 12. Gamma Ray Multiplicities

MT=102. (n,γ) Capture Multiplicities

The ^{26}Al decay scheme for excitation by radiative capture with thermal neutrons from Ha69 was adopted after some modification to enhance agreement with experiment. The results have been compared with the less detailed data of Ba67, Ju71, and Ma69, and are reasonably consistent. Some of the lines in Ra70 below 1 MeV appear to be spurious and have been dropped. Spectrum for thermal neutrons is assumed to apply at all energies.

File 13. Gamma Ray Smooth Cross Sections

MT=4. $(n,n\gamma)$ Cross Sections

Threshold to 5 MeV, based on the (n,n') data of To62, Wi63, Ts61, and the $(n,n\gamma)$ data of Ch68, Ma65, Di71, Or71, and Di73.

5 to 20 MeV. Mainly from $(n,n\gamma)$ data of Di73, Or71, and Di71, Dr73, Pe64, Be66, Cl69, En67, Bo65, Ma68, Ca60 and Pr60, supplemented by statistical theory calculations.

MT=28. $(n,np\gamma)$ Cross Sections

Threshold to 20 MeV, based on the measurements of Di73, Or71, En67, Pr60, Cl69, Be66, Bo65, and on statistical theory.

MT=103. $(n,p\gamma)$ Cross Sections

Threshold to 9 MeV, used data of Di71.

9 to 20 MeV. Smooth Extrapolation.

File 14. Gamma Ray Angular Distributions

MT=4. $(n,n\gamma)$ Angular Distributions Assumed Isotropic.

MT=28. $(n,np\gamma)$ Angular Distributions Assumed Isotropic.

MT=103. $(n,p\gamma)$ Angular Distributions Assumed Isotropic.

File 15. Gamma Ray Energy Distributions

MT=4. $(n,n\gamma)$ Energy Distributions

Statistical theory calculation adjusted to fit measurement of Di73.

MT=28. $(n,np\gamma)$ Energy Distributions

Statistical theory calculation adjusted to fit measurement of Di73.

File 33. Neutron Cross Section Covariances

Based on revised version of Table 6 in LA-4726. Errors are given only for MT=1, 2, 4, 16, 102, 103, and 107. MT=2 is taken from experiment between 9 and 17 MeV, and derived everywhere else. MT=4 is derived above 9 MeV. The derivation formulas are given by NC-type sub-subsections with LTY=0 in MT=2 and MT=4.

REFERENCES

Ba58 W. P. Ball et al., (LRL), Phys. Rev. 110, 1392 (1958).
Ba61 B. P. Bayhurst and R. J. Prestwood, (LAS), Phys. Rev. 121, 1438 (1961).
Ba66 R. Base, EANDC(E)-66U, p. 64, and Private communication (1966).
Ba67 G. A. Bartholomew et al., Nucl. Data A3, 367 (1967).
Be55 J. R. Beyster et al., (LAS), Phys. Rev. 98, 1216 (1955).
Be56 J. R. Beyster et al., (LAS), Phys. Rev. 104, 1319 (1956).
Be58 S. Berko et al., Nucl. Phys. 6, 210 (1958).
Be66 V. M. Bezotosnyi et al., (RUS), Sov. J. Nucl. Phys. 3, 632 (1966).
B168 R. C. Block, Private communication to R. J. Howerton (1968).
Bo59 N. A. Bostrom et al., (TNC), WADC-TN-59-107 (1959).
Bo65 V. N. Bockharev and V. V. Napedov (LEB), Sov. J. Nucl. Phys. 1, 574 (1965).
Bo65A G. C. Bonazzola et al., (TUR), Phys. Rev. 140, 835 (1965).
Bu63 J. P. Butler and D. C. Santry, Can. J. Phys. 41, 372 (1963).
Ca60 R. L. Caldwell et al., (SOC), Nucl. Sci. Eng. 8, 173 (1960).
Ca62 G. Calvi et al., Nucl. Phys. 39, 621 (1962).
Ca67 A. D. Carlson and H. H. Barschall, Phys. Rev. 158, 1142 (1967).
Ch66 J. P. Chien and A. B. Smith, Nucl. Sci. Eng. 26, 500 (1966).
Ch67 A. Chatterjee and A. M. Ghose (BOS), Phys. Rev. 161, 1181 (1967).
Ch68 K. C. Chung et al., (KTY), Nucl. Phys. 68, 476 (1968).
C168 S. Cierjacks et al., KFK-1000 (1968).
Cl69 G. Clayeux and G. Grenier (FR), CEA-R-3807, (1969).
Co58 J. H. Coon et al., (LAS), Phys. Rev. 111, 250 (1958).
Co59 J. H. Coon (LAS), Private communications to R. J. Howerton (1959).
De61 Yu. G. Degtyarev and V. G. Nadtochii, Sov. J. At. Energy 11, 1043 (1961).
De65 Yu. G. Degtyarev (RUS), J. Nucl. Energy 20, 818 (1965).
Di71 J. K. Dickens (ORL), ORNL-TM-3284, 1971.
Di73 J. K. Dickens et al., ORNL-TM-4232 (1973).
Dr70 D. M. Drake et al., (LAS), Nucl. Sci. Eng. 40, 294 (1970).
En67 F. C. Engesser and W. E. Thompson (NRD), J. Nucl. Energy 21, 487 (1967).
Fe67 J. M. Ferguson and J. C. Albergotti (NRD), Nucl. Phys. 98, 65 (1967).
Fl56 N. N. Flerov and V. M. Talyzin (RUS), Atomnaya Energiya 1, 155 (1956).
Fo71 D. G. Foster, Jr. and D. W. Glasgow, Phys. Rev. C3, 575 (1971).
Ga62 F. Gabbard and B. D. Kern (KTY), Phys. Rev. 128, 1276 (1962).
Ga65 J. B. Garg et al., Private communication to R. J. Howerton (1965).
Gl61 R. N. Glover and E. Wilgold (GBR), Nucl. Phys. 24, 630 (1961).
Gl72 D. W. Glasgow, Private communication (1972).
Go71 D. T. Goldman, Unpublished evaluation (1971).
Gr53 E. R. Graves and L. Rosen (LAS), Phys. Rev. 89, 343 (1963).
Gr55 E. R. Graves and R. W. Davis (LAS), Phys. Rev. 97, 1205 (1955).
Gr58 J. A. Grundl et al., (LAS), Phys. Rev. 109, 425 (1958).
Gr67 J. A. Grundl (LAS), Nucl. Sci. Eng. 30, 69 (1967).
Ha69 R. Hardell et al., Nucl. Phys. A126, 392 (1969).

He50 R. L. Henkel and H. H. Barschall, Phys. Rev. 80, 145 (1950).
He53 R. L. Henkel, Private communication to Sigma Center (1953).
Hi59 C. T. Hibdon, Phys. Rev. 114, 179 (1959).
Ho69 B. Holmqvist and T. Wiedling (AE), AE-366 (1969).
Im64 W. L. Imhog (LOK), private communication to NNCSC (1964).
Jo64 G. D. Joanou and C. A. Stevens (GA), GA-5884 (1964).
Ju71 E. T. Journey, Private communication (1971).
Ka72 J. L. Kammerdiener, Thesis, University of California at Davis (1972).
Ke59 B. D. Kern et al., (NRD), Nucl. Phys. 10, 226 (1959).
Ki70 W. E. Kinney and F. G. Perey (ORL), ORNL-4516 (1970).
La57 A. Langsdorf et al., Phys. Rev. 107, 1077 (1957).
Li66 H. Liskien and A. Paulsen, Nucleonics 8, 315 (1966).
Ma57 M. H. MacGregor et al., (LRL), Phys. Rev. 108, 726 (1957).
Ma60 G. S. Mani et al., (HAR), Nucl. Phys. 19, 535 (1960).
Ma65 S. C. Mathur et al., (TNC), Nucl. Phys. 73, 561 (1965).
Ma68 G. N. Maslov et al., (RUS), Sov. J. At. Energy 24, 704 (1968).
Ma69 R. E. Maerker and F. J. Muckenthaler, ORNL-4382 (1969).
Me52 A. W. Merrison and E. R. Wiblin, Proc. Roy. Soc. (L) 215, 278 (1952).
Mi68 A. Mittler et al., (KTY), Bull. Am. Phys. Soc. 13, 1420 (1968).
Or71 V. J. Orphan and C. G. Hoot, Gulf-RT-A10743 (1971).
Pa65 A. Paulsen and H. Liskien (GEL), J. Nucl. Energy 19, 907 (1965).
Pe64 J. L. Perkin (ALD), Nucl. Phys. 60, 561 (1964).
Pe72 F. G. Perey et al., ORNL-4823 (1972).
Ph52 D. D. Phillips et al., (LAS), Phys. Rev. 88, 600 (1952).
Pr60 J. T. Prudhomme et al., (TNC), AFSWC-TR-60-30 (1960).
Ra70 N. C. Rasmussen et al., GA-10248 (1970).
Sc61 H. W. Schmitt and J. Halperin (ORL), Phys. Rev. 121, 827 (1961).
Sc70 R. B. Schwartz, private communication (1970).
St59 C. St. Pierre et al., (MON), Phys. Rev. 115, 999 (1959).
St62 T. P. Stuart et al., Phys. Rev. 125, 276 (1962).
St65 P. H. Stelson and R. L. Robinson (ORL), Nucl. Phys. 68, 97 (1965).
Ta55 H. L. Taylor et al., (RIC), Phys. Rev. 100, 174 (1955).
TA70 S. Tanaka et al., Nucl. Data for Reactors, IAEA p. 317 (1970).
Th63 D. B. Thompson (LAS), Phys. Rev. 129, 1649 (1963).
To62 J. H. Towle and W. B. Gilboy, Nucl. Phys. 39, 300 (1962).
To67 J. H. Towle and R. O. Owens (ALD), Nucl. Phys. A100, 257 (1967).
Ts61 K. Tsukada et al., Physics of Fast and Intermediate Reactors, Vienna (1961).
Wi63 D. Winterhalter (ZAG), Nucl. Phys. 43, 339 (1963).
Yo72 P. G. Young, LASL Memo T-2-99 to the Norm. and Standards Subcommittee of
CSEWG (1972).

14-Si-0
MAT 1314

Summary Documentation
Natural Silicon Evaluation
ENDF/B-V MAT 1314
D. C. Larson
Oak Ridge National Laboratory
Oak Ridge, Tennessee 37830
September 1978

The present work supersedes the ENDF/B-IV MAT 1194 evaluation by Larson and Perey. Neutron and photon production data are given for neutron energies between 10^{-5} eV and 20 MeV. New data were incorporated for the total cross section, inelastic scattering to the first two excited levels in ^{28}Si , capture cross section, elastic scattering angular distributions, and gamma-ray production. The remainder of the evaluation was left unchanged. Detailed information regarding charged particle reactions, including angular and energy distributions, is carried over from ENDF/B-IV.

File 2. Resonance Parameters

No resonance parameters are given for silicon. The effective scattering length was changed from 0.41363 E-12 cm to 0.40311 E-12 cm, reflecting the more accurate measurement of Dilg [DI71].

File 3, MT=1. Total Cross Section

From 1.0E-5 eV to 730 keV, the evaluation has been updated from ENDF/B-IV. The cross section from 1.0E-5 eV to 5 eV is given by the sum of 2.042 b scattering [DI71] (changed from 2.15 b) and a 1/v capture contribution. From 5 eV to 730 keV the recent high resolution data of Larson et al. [LA76] was used. The region from 730 keV to 20 MeV is unchanged from ENDF/B-IV, and is based on a spline fit to the data of Schwartz et al. [SC71], which was in good agreement with data of Perey et al. [PE72].

File 3, MT=2. Elastic Scattering

A scattering cross section of 2.042 b (changed from 2.15 b in ENDF/B-IV) is used from 1.0E-5 eV to 5 eV [DI71]. From 5 eV to 20 MeV the scattering cross section was derived by subtracting the nonelastic from the total.

File 3, MT=3. Nonelastic Cross Section

This file is a sum of MT=4, 16, 22, 28, 102, 103, 104 and 107. There are some changes in this file due to changes in MT=4 and 102.

File 3, MT=4. Total Inelastic

This file is based on a sum of MT=51 through 72, and MT=91. It differs from ENDF/B-IV due to changes in MT=52 and 61.

File 3, MT=16. n,2n Cross Section

Same as ENDF/B-IV; it is estimated via a statistical model for each isotope, and the results combined for the element.

File 3, MT=22. n,no Reaction

Taken from ENDF/B-IV; it was formed by calculating the n,no and n,αn cross sections for each isotope, and combining the results.

File 3, MT=28. n,np Reaction

Taken from ENDF/B-IV; it was formed by calculating the n,np and n,pn cross sections for each isotope, and combining the results.

File 3, MT=51 through 72. Inelastic Scattering to Discrete Levels

The largest inelastic cross sections are for the 1.78 and 4.61 MeV levels in ^{28}Si . Evaluation for these levels is based mainly on data of Dickens et al. [DI70,DI74], and Perey and Kinney [PE71]. Other data sets considered include CL64, DR69, KI70, DN67, MA68, NE72, OB73, and PE66. In addition to these references, data for the higher-lying levels were taken from BA66, GI65, and PE73. Model calculations were used for interpolation and extrapolation where necessary. Levels in ^{29}Si and ^{30}Si are included.

File 3, MT=91. Continuum Inelastic

Tertiary reaction calculations [FU73] were used to split the n, n' reaction into $n, n'\gamma + n, 2n + n, np + n, n\alpha$. Only the $n, n'\gamma$ component is included in MT=91. References include CL72, MA67, MA69, and FU73, GI65, PE73.

File 3, MT=102. Radiative Capture

From $1.0E-5$ eV to 1.0 keV, a $1/v$ dependence is assumed, normalized to 0.16 b at 0.0253 eV. This region is unchanged from ENDF/B-IV. A smooth line was drawn from 1.0 to 2.6 keV, where the data of Boldeman et al. [BO75] were used up to 1.18 MeV. From 1.18 to 20 MeV, the evaluation smoothly decreases through 0.49 mb at 14.1 MeV [CV69] to 0.43 mb.

File 3, MT=103. (n,p) Reaction

This reaction is unchanged from ENDF/B-IV. The (n,p) reaction is well defined by experiment [BA66,FO70,MA56] from threshold up to 9 MeV, and at 14 MeV by activation measurements. The calculated (n,p) cross section was in good agreement with experiment, and was used from 9 to 20 MeV. Above 13 MeV, the (n,pn) component was removed, leaving only the $(n,p\gamma)$ component.

File 3, MT=104. (n,d) Reaction

This cross section is unchanged from ENDF/B-IV, was estimated by Drake [DR68] in an earlier evaluation, and is considered speculative.

File 3, MT=107. (n,\alpha) Reaction

This cross section is unchanged from ENDF/B-IV. The (n,α) cross section is well defined from threshold up to 8.4 MeV by experiment [BE65,BI63,GR69 and MA63 reduced by 30%]. Above 8.4 MeV there are no reliable measurements of the total (n,α) cross section. The evaluation above 8.4 MeV is based on calculations which reproduce the average measured (n,α) up to 8.4 MeV as well as the $^{30}\text{Si}(n,\alpha)$ cross section measured at 14 MeV [SI70]. Above 13 MeV the $(n,\alpha n)$ component is removed, leaving only the $(n,\alpha\gamma)$ component.

14-S1-0
MAT 1314

File 3, MT=251-253. Mu-Bar, Xi, Gamma

Derived from the elastic scattering angular distribution and kinematics using computer code SAD (done at BNL).

File 3, MT=700-714. (n,p) Reaction to Discrete Levels

Unchanged from ENDF/B-IV, these cross sections are based on calculations for ^{28}Si , and comparison to averaged data of BA66, GR69, MA56, MI67, MI71.

File 3, MT=718. (n,p) Continuum Protons

Unchanged from ENDF/B-IV, this cross section from threshold to 9 MeV is taken as the difference between the sum of MT=700-714, and the evaluated total (n,p) cross section in MT=103. From 9 to 20 MeV, it is based on calculated results.

File 3, MT=719. (n,np) + (n,pn) Reaction

This file is same as MT=28.

File 3, MT=780-791. (n, α) Reaction to Discrete Levels

Unchanged from ENDF/B-IV, this cross section is based on calculated results for ^{28}Si and comparison to averaged data of BI63, GR69, MA63, MI67 and MI71.

File 3, MT=798. (n, α) Continuum Alphas

Unchanged from ENDF/B-IV, this cross section from threshold to 8.4 MeV is taken as the difference between the sum of MT=780-791, and the evaluated total (n, α) cross section in MT=107. From 8.4 to 20 MeV, it is based on calculated results.

File 3, MT=799. (n,n α) + (n, α n) Reaction

This file is same as MT=22.

File 4, MT=2. Elastic Scattering Angular Distributions

From 1.0E-5 eV to 40 keV, the angular distributions are isotropic. High resolution data of Kinney and Perey [KI76] are used from 40 keV to 3.0 MeV. The data were taken in 1-keV steps, but have been thinned for this evaluation. From 3 to 11 MeV, measured distributions [BR72, DR69, KI70, KN67, MA68, NE72, OB73, TA64, TA69 and VE72] were used. From 11 to 20 MeV, results of optical model calculations were used. All angular distributions are given as Legendre coefficients.

File 4, MT=16,22,28

Outgoing neutrons assumed isotropic.

File 4, MT=51-72. n,n' to Discrete Levels

These angular distributions are taken from ENDF/B-IV. For MT=52 and 61 (first and second excited states in ^{28}Si) the angular distributions are a weighted sum of Hauser-Feshbach and direct interaction calculations. Generally, they are in good agreement with existing data referenced under MF=3, MT=51-72. Angular distributions for remaining states are taken from Hauser-Feshbach calculations.

File 4, MT=91. (n,n') to Continuum

This angular distribution is assumed isotropic.

File 4, MT=700-714. (n,p) Proton Angular Distributions

Distributions were taken from Hauser-Feshbach results, and compared with data of Debertin [DE67].

File 4, MT=718,719. Proton Angular Distributions

Assumed isotropic.

File 4, MT=780-791. (n, α) Alpha Angular Distributions

Taken from Hauser-Feshbach calculations.

File 4, MT=798,799. Alpha Angular Distributions

Assumed isotropic.

File 5, MT=16. (n,2n) Reaction

Energy distributions are taken from ENDF/B-IV. The secondary neutrons are assumed to have a Maxwellian shape.

File 5, MT=22. Secondary Neutrons

The calculated neutron energy distributions from the $(n,n\alpha)$ and $(n,\alpha n)$ reactions were weighted by their cross sections and combined. They are given as histogram probability distributions.

File 5, MT=28. Secondary Neutrons

The calculated neutron energy distributions from the (n,np) and (n,pn) reactions were weighted by their cross sections and combined. They are given as histogram probability distributions.

File 5, MT=91. Continuum Neutrons

The continuum neutron energy distributions are given as histogram probability distributions.

File 5, MT=718. Continuum Protons

The continuum proton energy distributions are given as histogram probability distributions, estimated from calculations.

File 5, MT=719. Secondary Protons

The calculated proton energy distributions from the (n,np) and (n,pn) reactions were weighted by their cross sections and combined. They are given as histogram probability distributions.

File 5, MT=798. Continuum Alphas

The continuum alpha energy distributions are given as histogram probability distributions, estimated from calculations.

File 5, MT=799. Secondary Alphas

The calculated alpha energy distributions from the $(n,n\alpha)$ and $(n,\alpha n)$ reactions were weighted by their cross sections and combined. They are given as histogram probability distributions.

File 12, MT=102. Radiative Capture

Energies and multiplicities for gamma rays resulting from capture of neutrons from 1.0E-5 eV to 50 keV were taken from thermal capture data [BL69, LY67, SP70]. Multiplicities for gamma rays resulting from 50 keV to 1 MeV neutrons were taken from Lundberg and Bergquist [LU70]. From 1 to 20 MeV, the average of the above multiplicities was used. These results are taken from ENDF/B-IV.

File 13, MT=4,22,28,103,107. Gamma Production Cross Sections

Discrete gamma-ray cross sections are given up to a neutron energy of 3 MeV. The largest gamma-ray cross sections are from $^{28}\text{Si}(n,n'\gamma)$ to the 1.78-MeV level. Updates from ENDF/B-IV up to 3 MeV have been made for this gamma ray, based on data of Dickens *et al.* [DI73]. This results in much more structure than previously present. The remainder of the gamma-ray cross sections result from calculations, and when summed, reproduce the $(n,x\gamma)$ measurement of Dickens *et al.* [DI73]. Gamma rays from all neutron-induced reactions from all three isotopes are included in these files.

File 14, All MT Sections. Gamma-Ray Angular Distributions

All gamma-ray angular distributions are assumed isotropic.

File 15, MT=4,22,28,103,107. Energy Distributions of Secondary Gamma Rays

Energy distributions are given as histogram probability distributions from $E_n = 3$ to 20 MeV, and include gamma rays from 0.0 to 15.0 MeV.

File 33, MT=1,2,3,4,52,61,103,107. Uncertainty Files

Uncertainty files are given for all major reactions. They are estimates based on spread in available data sets, and estimates of uncertainties in the various calculations. Long- and short-range correlations are given.

References

BA66 Bass, EANDC(E)66,64; see also CSISRS Accession No. 60228.

BE65 Betz and Rossle, EANDC(E)57U (February 1965).

BI63 Birk, Goldering, and Hillman, NIM 21, 197 (1963).

BL69 Blichert-Toft and Tripathy, 69 Studsvik, STI/PUB/235 (1969).

BO75 Boldeman et al., Nucl. Phys. A252, 62 (1975).

BR72 Brandenberger et al., Nucl. Phys. A196, 65 (1972).

CL64 Clarke and Cross, Nucl. Phys. 53, 177 (1964).

CL72 Clayeux and Volgnier, CEA-R-4279 (March 1972).

CV69 Cvelbar, Hudoklin, and Potokar, Nucl. Phys. A138, 412 (1969).

DE67 Debertin, Nucl. Phys. A101, 473 (1967).

DI70 Dickens, Phys. Rev. C2, 990 (1970).

DI71 Dilg, ZN/A 26, 442 (1971).

DI73 Dickens, Love, and Morgan, ORNL Report TM-4389.

DI74 Dickens and Morgan, Phys. Rev. C 10, 958 (1974).

DR68 Drake, Gulf Atomic Report GA-8628 (original evaluation of Si).

DR69 Drake et al., Nucl Phys. A128, 209 (1969).

FO70 Foroughi and Durisch, HPA 43, 432 (1970).

FU73 Fu, Computer Code NNNGAM, ORNL (1973).

GI65 Gilbert and Cameron, Can. J. Phys. 43, 1446 (1965).

GR69 Grimes, Nucl. Phys. A124, 369 (1969).

KI70 Kinney and Perey, ORNL Report 4517 (July 1970).

KI76 Kinney and Perey, to be published.

KN67 Knitter and Coppola, Zeits. Phys. 207, 56 (1967).

LA76 Larson et al., ORNL-TM-5618 (1976).

LU70 Lundberg and Bergqvist, Phys. Scripta 2, 265 (1970).

LY67 Lycklama et al., Can. J. Phys. 45, 1871 (1967).

MA56 Marion et al., Phys. Rev. 101, 247 (1956).

MA63 Mainsbridge et al., Nucl. Phys. 48 83 (1963).

MA67 Mathur et al., Texas Nuclear Report NDL-TR-86 (1967).

MA68 Martin et al., Nucl. Phys. A113, 564 (1968).

MA69 Mathur et al., Phys. Rev. 186, 1038 (1969).

MI67 Miller and Kavanagh, NIM 48, 13 (1967).

MI71 Mingay et al., NIM 94, 497 (1971).

NE72 Nellis et al., DNA Report 2716, Texas Nuclear (February 1972).

OB73 Obst and Weil, Phys. Rev. C 7, 1076 (1973).

PE66 Pettit et al., Nucl. Phys. 79, 231 (1966).

PE71 Perey et al., Proc. 3rd Conf. Neutron Cross Section Tech., Knoxville, Tennessee (1971).

PE72 Perey, Love, and Kinney, ORNL Report 4823.

PE73 Penny, Hauser-Feshbach Computer Code HELGA (1973).

SC71 Schwartz et al., BAPS 16, 495 (AH3) (1971).

SI70 Singh, BAPS 15 (BG5) (1970).

SP70 Spits et al., Nucl. Phys. A145, 449 (1970).

TA64 Tanaka, J. Phys. Soc. Japan 19, 2249 (1964).

TA69 Tanaka et al., JAERI (May 1969).

VE72 Velkley, BAPS 17, 555 (1972) and private communications.

Phosphorus-31

DATA SUMMARY AND GENERAL COMMENTS

The experimental data for $^{31}_{15}\text{P}$ are summarized in UCRL-50400, Vol. 3; they are listed in UCRL-50400, Vol. 10. The evaluated data for this isotope are shown graphically in UCRL-50400, Vol. 15, Part B. R. J. Howerton did the evaluation.

TOTAL CROSS SECTION

Experimental and evaluated total cross sections for ^{31}P are shown graphically on pages 2-75 to 2-79 of UCRL-50400, Vol. 7, Part A, Rev. 1; some tabular experimental values are given on page 2-80. The evaluated total cross sections are shown in UCRL-50400, Vol. 15, Part B. These cross sections are based on the following specific ECSIL data sets: ECSIL-15 from 6 to 20 keV; ECSIL-819 from 40 to 90 keV; ECSIL-99 from 100 to 800 keV; ECSIL-455 from 800 keV to 1.2 MeV; and ECSIL-750 from 2 to 20 MeV. These ECSIL data references are given in UCRL-50400, Vol. 2.

ELASTIC SCATTERING CROSS SECTION

Two elastic scattering data points are listed on page 2-80 of UCRL-50400, Vol. 7, Part A, Rev. 1. In view of the scarcity of experimental data, the elastic cross section was obtained by differencing the evaluated total

cross sections and the sums of the evaluated nonelastic cross sections.

ELASTIC SCATTERING ANGULAR DISTRIBUTIONS

Measurements of the elastic scattering angular distributions are shown in UCRL-50400, Vol. 19. In the evaluation, the elastic scattering angular distributions were assumed to be isotropic for all neutron energies below 100 keV. Above 100 keV, the evaluated elastic scattering angular distributions were based on experimental data, supplemented at the higher energies by spherical optical model calculations, in which the best-fit optical model parameters of Becchetti and Greenlees were used [*Phys. Rev.* 182, 1190 (1969)].

INELASTIC SCATTERING CROSS SECTION

Some inelastic scattering cross section data are shown graphically on pages 2-109 and 2-110 of UCRL-50400, Vol. 8, Rev. 1, Part A. In view of the scarcity of experimental data, inelastic scattering was represented in the evaluation by a continuum contribution that starts at 1.31 MeV. The evaluated n, n' continuum cross sections are shown graphically in UCRL-50400, Vol. 15, Part B.

15-P-31
MAT 1315

Phosphorus-31

06/09/78

REACTION	POINTS	DATE	Q-VALUE	E-MIN
N-ELASTIC	CROSS SECTION	123	8/19/72	0.0000+ 0
N-ELASTIC	ANGULAR DIST.	20	1/03/72	0.0000+ 0
N-ELASTIC	TOTAL ENERGY DEP.	30	11/12/74	0.0000+ 0
N-ELASTIC	LOCAL ENERGY DEP.			1.0000- 10
N,N'	CROSS SECTION	10	8/19/72	0.0000+ 0
N,N'	ENERGY-ANGLE DIST.	10	8/19/72	0.0000+ 0
N,N'	TOTAL ENERGY DEP.	13	12/03/76	0.0000+ 0
N,N'	LOCAL ENERGY DEP.	11	12/03/76	0.0000+ 0
N,N'	CROSS SECTION	8	8/19/72	0.0000+ 0
N,N'	ENERGY-ANGLE DIST.	4	8/19/72	-1.2310+ 1
N,N'	TOTAL ENERGY DEP.	4	12/03/76	-1.2310+ 1
N,N'	LOCAL ENERGY DEP.	4	12/03/76	-1.2310+ 1
N,N'	CROSS SECTION	8	8/19/72	-1.2310+ 1
N,N'	ENERGY-ANGLE DIST.	5	8/19/72	-7.3000+ 0
N,N'	TOTAL ENERGY DEP.	10	12/03/76	-7.3000+ 0
N,N'	LOCAL ENERGY DEP.	10	12/03/76	-7.3000+ 0
N,P	CROSS SECTION	29	9/29/77	-7.3000+ 0
N,P	TOTAL ENERGY DEP.	2	12/03/76	-7.1000- 1
N,P	LOCAL ENERGY DEP.	2	12/03/76	-7.1000- 1
N,A	CROSS SECTION	8	9/28/77	-1.9400+ 0
N,A	TOTAL ENERGY DEP.	2	12/03/76	-1.9400+ 0
N,A	LOCAL ENERGY DEP.	2	12/03/76	-1.9400+ 0
N,G	CROSS SECTION	68	4/03/76	-1.9400+ 0
N,G	ENERGY DIST.	2	11/01/72	7.9300+ 0
N,G	MULTIPLICITY	2	11/01/72	7.9300+ 0
N,G	TOTAL ENERGY DEP.	2	11/2/76	7.9300+ 0
N,G	LOCAL ENERGY DEP.	2	11/2/76	7.9300+ 0
N,XG	CROSS SECTION	5	2/21/73	0.0000+ 0
N,XG	ENERGY-ANGLE DIST.	5	1/11/73	0.0000+ 0
N,XG	CROSS SECTION	9	1/11/73	0.0000+ 0
N,XG	ANGULAR DIST.	2	5/31/73	0.0000+ 0
N,XG	CROSS SECTION	5	1/11/73	0.0000+ 0
N,XG	ANGULAR DIST.	2	5/31/73	0.0000+ 0

PHOTON = 1.2660+ 0 MEV
PHOTON = 1.2660+ 0 MEV
PHOTON = 2.2310+ 0 MEV
PHOTON = 2.2310+ 0 MEV

INELASTIC SCATTERING ANGULAR AND ENERGY DISTRIBUTIONS

The angular distributions for the continuum inelastic scattering were assumed to be isotropic. The energy distributions for incident neutron energies below 5 MeV were chosen so as to reproduce the average and maximum secondary neutron energies for the reaction. The energy distributions at 5 MeV and above were obtained from temperature model calculations, with contributions from preequilibrium processes estimated (see UCRL-50400, Vol. 15, Part A, pages 19 to 22).

n,2n CROSS SECTION

The threshold for the n,2n reaction is 12.70 MeV. Experimental values of the n,2n cross section are shown graphically on page 2-111 of UCRL-50400, Vol. 8, Rev. 1, Part A; some tabulated values are given on page 2-116. The evaluated n,2n cross sections are shown on page 98 of UCRL-50400, Vol. 15, Part B.

ANGULAR AND ENERGY DISTRIBUTIONS FOR THE n,2n REACTION

The angular distribution of secondary neutrons produced by the n,2n reaction was assumed to be isotropic in the laboratory system. Energy distributions of the secondary neutrons, which are presented in tabular form, are derived from temperature

model calculations, with the assigned temperatures consistent with nuclear systematics (see UCRL-50400, Vol. 15, Part A, page 24).

n,n'p CROSS SECTION

The threshold for the n,n'p reaction is 7.53 MeV. Two experimental n,n'p data points are listed on page 1-116 of UCRL-50400, Vol. 8, Rev. 1, Part A. The evaluated n,n'p cross sections are shown in UCRL-50400, Vol. 15, Part B.

ANGULAR AND ENERGY DISTRIBUTIONS FOR THE n,n'p REACTION

The angular distribution of secondary neutrons produced by the n,n'p reaction was assumed to be isotropic in the laboratory system. Energy distributions of the secondary neutrons, which are presented in tabular form, are derived from temperature model calculations, with the assigned temperatures consistent with nuclear systematics (see UCRL-50400, Vol. 15, Part A, page 24).

n,p CROSS SECTION

The threshold for the n,p reaction is 0.73 MeV. Experimental and evaluated n,p cross sections are shown graphically on pages 2-112 and 2-113 of UCRL-50400, Vol. 8, Rev. 1, Part A; some tabulated experimental values are given on page 2-117. The evaluated n,p cross sections are shown in UCRL-50400, Vol. 15, Part B.

15-P-31
MAT 1315

n,α CROSS SECTION

The threshold for the n,α reaction is 2.01 MeV. Experimental values of the n,α cross section are shown graphically on pages 2-114 and 2-115 of UCRL-50400, Vol. 8, Rev. 1, Part A; some tabular values are given on page 2-117. The evaluated n,α cross sections are shown graphically in UCRL-50400, Vol. 15, Part B.

n,γ CROSS SECTION

A few experimental values of the neutron capture cross section are given on page 2-80 of UCRL-50400, Vol. 7, Part A, Rev. 1. The evaluated capture cross sections are shown in UCRL-50400, Vol. 15, Part B. They are based mainly on nuclear systematics.

PHOTON PRODUCTION FROM n,γ REACTIONS

The neutron capture gamma-ray spectrum at thermal neutron energies was taken from the data of V. J. Orphan, N. C. Rasmussen, and T. L. Harper, Gulf General Atomic Rept. GA-10248 (1970). This spectrum was assumed to apply at all neutron energies, since there are no data for incident neutron energies higher than thermal. To conserve the total energy of the reaction, the gamma-ray multiplicity was assumed to vary as a linear function of neutron energy.

$n,X\gamma$ CROSS SECTION

A few $n,X\gamma$ angular and energy distributions are listed on page 1-60 of UCRL-50400, Vol. 3, Rev. 2. In the P^{31} evaluation, the $n,X\gamma$ cross section was assumed to include all photons except those produced in the neutron capture reaction. The evaluated $n,X\gamma$ cross sections include two discrete lines plus a continuum component that starts at 3.3 MeV. The discrete lines were evaluated as shown below.

1.266 MeV

This gamma ray arises from the transition of the 1.266-MeV level to the ground state in P^{31} . For incident neutron energies below 2.234 MeV, the gamma ray is produced entirely from the n,n' reaction. Thus, the $n,X\gamma$ cross section for producing this line was set equal to the n,n' cross section for energies below 2.234 MeV. At higher energies, the inelastic scattering data of K. Tsukada *et al.*,* G. C. Bonazzola and E. Chiavassa,† and A. Mittler *et al.*** were used as guides in the evaluation.

*Paper SM-18/12 of the Vienna Conf. on "Physics of Fast and Intermediate Reactors" (1961).

†*Nucl. Phys.* 68, 369 (1965).

***Bull. Am. Phys. Soc.* 13, 1420 (1968).

2.234 MeV

This gamma ray originates from the transition of the 2.234-MeV level to the ground state in P^{31} . The cross section for producing this gamma ray was calculated based on the inelastic-scattering data of K. Tsukada *et al.*, and R. L. Caldwell *et al.*, *Nucl. Sci. Eng.* 8, 173 (1960), as well as data obtained from the evaluated n, n' cross section.

The $n, X\gamma$ cross sections for the continuum component were calculated with the NXGAMEL code, using the systematics developed by Perkins, Haight, and Howerton, *Nucl. Sci. Eng.* 57, 1 (1975). A summary of this method of evaluating photon production data is discussed in UCRL-50400, Vol. 15, Part A, pages 38 to 41. In the evaluation, the continuum was assumed to start at 3.3 MeV, to

become 50% of the calculated value at 8 MeV, and to continue at 50% to 20 MeV; between 3.3 and 8 MeV, it was assumed that the interpolation was linear. This procedure gives results that are in reasonable agreement with the experimental data of Caldwell *et al.* at 14.8 MeV.

SPECTRA OF PHOTONS FROM THE $n, X\gamma$ PROCESS

The angular distributions of the photons produced by the $n, X\gamma$ reaction were assumed to be isotropic. The energy distributions of the discrete photons were estimated using the kinematics of the reaction. The energy distributions of the photons from the continuum component of the reaction were calculated with the nuclear systematics of Perkins, Haight, and Howerton cited above.

SUMMARY DOCUMENTATION FOR SULFUR

M. Divadeenam

National Nuclear Data Center

Brookhaven National Laboratory

June 20, 1979

ABSTRACT

The following neutron and gamma production data are given for Sulfur in the energy range 1.0×10^{-5} to 20 MeV. (MAT No. 347).

File 1: General description of the evaluation and relevant references.

File 2: Resonance parameters for Sulfur isotopes from 1.0×10^{-5} eV to 1091 keV (^{32}S), 550 keV (^{33}S) and 642 keV (^{34}S).

File 3: Smooth cross sections for total, elastic, total inelastic, inelastic cross sections to 40 discrete levels; the inelastic continuum, $(n,2n)$, $(n,\alpha n')+(n,n'\alpha)$, $(n,pn')+(n,fip)$, (n,p) , (n,d) , (n,t) , (n,α) , $(n,2p)$ and capture cross sections. Extracted data for $\bar{\mu}$, ξ and γ are also included. In addition, Hydrogen, Deuterium, Tritium and Helium production cross sections are generated.

File 4: Angular distributions for elastic scattering are given in terms of Legendre Polynomial coefficients in the c.m. system. Isotropic inelastic angular distributions are given in the file.

File 5: Secondary neutron energy distributions for the inelastic continuum, $(n,2n)$, $(n,n'\alpha)$, and $(n,n'p)$ reactions with precompound effects are given.

File 12: Multiplicity for gamma-ray production due to capture from 1.0×10^{-5} eV to 2.53×10^{-2} eV.

16-S-0
MAT 1347

File 13: ($n, x\gamma$) production cross sections from 2.53×10^{-2} eV to 20 MeV.

File 14: Angular distributions of photons assumed to be isotropic.

File 15: Normalized energy distribution of photons up to 2.53×10^{-2} eV and due to non-elastic processes at higher energies.

Introduction

This is a completely new evaluation, in particular, the secondary neutron cross sections and angular distributions as well as the secondary neutron energy distribution for the continuum inelastically scattered neutrons have been included. In addition, the isotopic cross sections for the various (n , particle) cross sections were evaluated to construct the corresponding natural S files. Precompound effects were included. The least abundant isotope ^{36}S was not considered in the evaluation.

The resolved resonance region extends from 1.0×10^{-5} eV to 1091.0 keV, and the resonance parameters for the three sulfur isotopes ^{32}S , ^{33}S , ^{34}S have been evaluated from experimentally determined resonance parameters.

The KFK S total cross section data extending up to 20 MeV were used to construct smooth cross section file. Measurements due to other investigators were also used in the evaluation.

File 1: General Comments

A brief summary of the data along with the references is given. Details will be presented in a report based on this evaluation.

File 2: Resonance Parameters

^{32}S , ^{33}S and ^{34}S resonance parameters were evaluated from references 1-3. Due to lack of experimental data no resonance parameters for the minor isotope ^{36}S are given. Bound level parameters ^{4,5} were determined by fitting the thermal scattering and absorption cross sections.

File 3: Smooth Neutron Cross Sections(i) Total Cross Section

The KFK total cross section data⁶ on Sulfur were used for the evaluation. Spline fit of the data published in BNL-325 was adopted to represent the smooth cross section set. Weight to other data sets⁷⁻²⁴ was also given.

(ii) Elastic Cross Section

This was obtained by subtracting the non-elastic cross section³³⁻³⁸ from the total.

(iii) Total Inelastic Cross Section

Model (Ref. 92) calculated results for 40 levels were adopted. These were weighted with isotopic abundances together with the isotopic (n,p), (n,2n), (n,fp)+(n,pn), (n,αn + n, nα), (n,d), (n,t), (n,α), (n,2p) and (n,γ) evaluated cross sections and the sum of these partial cross sections was subtracted from the non-elastic cross section to give the total inelastic cross section of the remaining discrete levels and the inelastic continuum. The resulting cross section is designated as the inelastic continuum cross section.

(iv) (n,2n) Cross Section

Only few experimental points³⁹⁻⁴¹ are available for ³²S. For the other isotopes, model⁹⁴ calculated excitation functions were adopted.

(v) (n,fp) + (n,pn') Cross Section

The experimental (n,fp) + (n,pn') cross section values around 14 MeV were used to check the corresponding model⁹⁴ calculated results. The isotopic contributions to (n,fp) and (n,pn') were combined to give the cross section for Sulfur.

(vi) Inelastic Cross Section to the Discrete Levels and the Continuum*

COMNUC results were used for 40 inelastic levels given below:

<u>NO.</u>	<u>E_x (MeV)</u>	<u>J^π</u>	<u>Isotope</u>
1	0.8404	$1/2+$	33
2	1.9664	$5/2+$	33
3	2.12740	$2+$	34
4	2.23020	$2+$	32
5	2.31260	$3/2+$	33
6	2.86630	$5/2+$	33
7	2.9337	$7/2-$	33
8	2.96870	$7/2+$	33
9	3.21990	$3/2-$	33
10	3.30350	$2+$	34
11	3.77900	$0+$	32
12	3.83160	$5/2+$	33
13	3.91400	$0+$	34
14	3.93460	$3/2+$	33
15	4.04780	$9/2+$	33
16	4.07200	$1+$	34
17	4.11500	$2+$	34
18	4.28200	$2+$	32
19	4.45900	$4+$	32
20	4.62200	$3-$	34
21	4.68800	$4+$	34

*The inelastic continuum was obtained from the difference

$$\sigma_{\text{non}} - \left[\sum_{k=1}^{40} \sigma_{nn}^k + (n, p) + (n, 2n) + (n, np) + (n, pn) + (n, \alpha n) + (n, \alpha \alpha) + (n, d) + (n, t) + (n, \alpha) + (n, 2p) + (n, \alpha) \right]$$

16-S-0
MAT 1347

(iv) Inelastic Cross Section to the Discrete Levels and the Continuum (cont)

<u>NO.</u>	<u>E_x(MeV)</u>	<u>J^π</u>	<u>Isotope</u>
22	4.69530	1+	32
23	4.87500	3+	34
24	4.89100	2+	34
25	5.00620	3-	32
26	5.2300	2-	34
27	5.31800	2-	34
28	5.38300	1+	34
29	5.41300	3+	32
30	5.54900	2+	32
31	5.68000	2-	34
32	5.68900	5-	34
33	5.75300	1-	34
34	5.79800	1-	32
35	5.85000	0+	34
36	5.99300	2+	34
37	6.12000	2+	34
38	6.17300	3-	34
39	6.2240	2-	32
40	6.4100	4+	32

(vii) Capture Cross Section

Thermal capture cross sections were fit with bound level parameters for ^{32}S , ^{33}S and ^{34}S . Beyond 1 MeV the effect of the Giant Dipole Resonance is considered in calculating (n, γ) cross sections with COMNUC.⁹² COMNUC results were normalized to average resonance capture cross section obtained from RESEND output.

(viii) (n,p) Cross Section

$^{32}\text{S}(n,p)$ reaction was evaluated by Duddley and Kennerly⁵⁸ for ENDF/B-IV. The $^{32}\text{S}(n,p)$ cross section was evaluated using extensively available data⁵⁶⁻⁷⁰. Allen's $^{32}\text{S}(n,p)$ data were renormalized to the ENDF/B-V $^{238}\text{U}(n,f)$ cross sections. The structure in $^{32}\text{S}(n,p)$ cross section ($E_n < 6$ MeV) observed by Hurliman et al.⁶⁶ and Luscher⁶⁷ has been retained. A smooth curve through the experimental points is drawn beyond 12 MeV. There are significant differences below 12 MeV between Duddley-Kennerly and the present evaluated file. For the $^{34}\text{S}(n,p)$ reaction model calculated results were combined with experimental data of Bormann beyond 14 MeV. Contribution due to ^{33}S was adopted from model⁹⁴ calculations.

(ix) (n,d) and (n,t) Reactions

Model⁸⁴ calculated results for the (n,d) reaction were adopted for the three S isotopes. $^{32}\text{S}(n,t)$ experimental data⁷¹⁻⁸⁰ were evaluated while $^{33}\text{S}(n,t)$ cross sections based on model⁹⁴ predictions were used. Contribution due to $^{34}\text{S}(n,t)$ reaction was negligible (based on model calculations).

(x) (n,α), (n,αn) and (n,n'α) Cross Sections

The available experimental data⁸¹⁻⁹¹ for $^{32}\text{S}(n,\alpha)$ and $^{34}\text{S}(n,\alpha)$ reactions were used in the evaluation. Model⁹³ calculations were used beyond the range of experimental data. MODNEW⁹³ calculated results were adopted for $^{33}\text{S}(n,\alpha)$ reaction. ALICE⁹⁴ calculated results were used for (n,αn) and (n,n'α) reactions for the three Sulfur isotopes.

(xi) (n,2p) Cross Section

Model⁹⁴ calculated cross sections for ^{32}S were adopted for the

file assuming that the other isotopes have negligible cross section due to high Q values.

(xii) Gas Production Cross Sections

Hydrogen, Deuterium, Triton and Helium Production cross sections were generated from (n,p), (n,pn') and (n,2p); (n,d); (n,t); (n,α) and (n,αn) cross sections respectively.

(xiii) $\bar{\mu}$, ξ , γ

These were generated using the code DUMMY5⁹⁷.

File 4: Secondary Neutron Angular Distribution

(i) Elastic Angular Distributions

Model⁹⁸ calculated angular distributions were adopted. These were fitted with the code CHAD⁹⁶ to obtain Legendre coefficients in the c.m. system.

(ii) Inelastic Angular Distributions

Isotropic angular distributions assumed.

File 5: Secondary Neutron Energy Distributions

(i) Continuum Inelastic Neutrons

The secondary energy distributions were based on model predicted⁹⁴ results. Both the pre-compound and compound effects were included.

(ii) (n,2n'), (n,αn') and (n,pn') Neutron Distributions

Code EVAHYB⁹⁵ was used to give the neutron energy distributions.

File 12: Gamma Ray Multiplicities

Gamma ray multiplicities due to capture are given from 10×10^{-5} eV to 2.53×10^{-2} eV based on both Maerker's data⁵³ and Rasmussen's data⁵⁴.

16-S-0
MAT 1347

File 13: (n,xy) Production Cross Section

This is based on Howerton's ^{32}S ENDF/B-V evaluation⁵⁵. It covers the energy range from 9.0×10^5 eV to 20 MeV.

File 14: Photon Angular Distributions

These are assumed to be isotropic.

File 15: Photon Energy Distributions

These are based on files 12 and 13.

REFERENCES

1. HELPERIN, JOHNSON, WINTERS AND MACKLIN, PRIVATE COMMUNICATION AND TO BE PUBLISHED.
2. G.F.AUCHAMPAUGH, J.HALPERIN, R.L.MACKLIN, W.M.HOWARD, PHYS. REV. C12, 1126(1975)
3. F.SIEBEL, PH.D. THESIS(DUKE UNIVERSITY) UNPUBLISHED(197).
4. S.F.MUGHABGHAB, D.I.GARBER, BNL-325 VOL I (THIRD EDITION, 1973).
5. KOSTER ET. AL., PRIVATE COMMUNICATION TO S.F.MUGHABGHAB
-----TOTAL CROSS SECTION-----
6. C. CIERJACKS ET. AL., KFK-1000, 1968
7. FOSTER ET. AL., PHYS.REV. C3,576, 1971
8. ANGELI ET. AL., ACTA PHYS. AC., 28,87(1970) .
9. FILIPOV ET.AL., DUBNA-ACC-68/17(1968).
10. FERGUSON, NUCL.PHYS. A117,472(1968).
11. KAO ET. AL., CHIN.J.PHYS. 5,43(1967).
12. CARLSON ET. AL., PHYS. REV. 13136,695(1964)
13. FASOLI ET. AL., NUOVO CIMENTO, 44,455(1966).
14. TSUKADA ET. AL., J .PHYS.SOC.JAP., 18,610(1963).
15. CABE, ET. AL., EANDC(E)-49,66,63
16. DECONNINCK, ET. AL., NUCL. CHEM. 18, 671(1960)
17. CUZZOCREA, ET. AL.,NUCL. CHEM. 18,671(1960)
18. HUIJER ET.AL., PHYSICA, 24,331(1958)
19. COOK ET. AL., PHYS.REV. 94,651(1954)
20. NERESON ET. AL., PHYS.REV. 89,775(1953)
21. COON ET. AL., PHYS. REV., 88,562(1952)
22. STAFFORD, PROC. PHYS. SOC. 64,388(1951)
23. FREIER, ET.AL., PHYS.REV. 78,508(1950)
24. PETERSON ET.AL., PHYS.REV.79,593(1950)
----ELASTIC CROSS SECTION----
25. LANGSDORF PHYS. REV. 107,1077(1957)
26. OBST. ET AL PHYS. REV. C 7,1076(1973)
27. HOLMQVIST ET. AL. AE-366(1969)
28. CLARK ET.AL, NUCL. PHYS. 53,177(1964)
29. TESCH, NUCL. PHYS. 37,412(1962)
30. TSUKADA ET. AL. VIENNA 1,75(1961)
31. MACHWE ET. AL., PHYS. REV. 114,1563(1959)
32. PIERRE ET. AL., PHYS. REV. 115,999(1959)
-----NON ELASTIC-----
33. MACHWE ET. AL., PHYS. REV. 114,1563 (1959)
34. MAC GREGOR PHYS. REV.108, 726(1957)
35. STRIZHAK, ATOM. EN. 2,68(1957)
36. BEYSTER ET. AL., PHYS. REV. 108,726(1957)
37. FLEROV.ET.AL.,ATOM. EN. 1,155(1956)
38. STRIZHAK,ZH. EKSP. TEOR. FIZ., 31,907(1956)
----- (N,2N) REACTION-----
39. BORMANN ET. AL., AFWL-TR-68-134(1969)
40. BARRALL ET. AL., NUCL.PHYS. 138A, 387(1967).
41. ARNOLD (1965), CSIRS A/N,11520
----- (N,PN') REACTION -----
42. ALLAN, NUCL. PHYS., 24,274(1961)
43. HASSLER AND PECK JR.,PHYS. REV. 125,1011(1962)

16-S-0

MAT 1347 ----- (N,GAMMA) -----

44. BOUZYK, SUWALSKI, TOPA, REACTOR CONF. BUCHAREST(1961)
45. POMERANCE, PHYS. REV., 83, 641(1951)
46. COLMER AND LITTLER, PROC. PHYS. SOC. A63, 1176(1950)
47. HARRIS, MUELHAUSE, RASMUSSEN, SCHROEDER, THOMAS, PHYS. REV. 80, 342 (1950)
48. RAINWATER, HAVENS, DUNNING, WU, PHYS. REV., 73, 733(1948)
49. SEREN, FRIEDLANDER, AND TURKELL, PHYS. REV. 72, 888(1947)
50. DURHAM, GIRARDI, NUO CIMENTO, SUPPLEMENT, VOL. 19, 4(1961)
51. GIBBONS, MACKLIN, MILLER AND SCHMIDT, PHYS. REV. 122, 182(1961)
52. MACKLIN, PASMA AND GIBBONS, PHYS. REV. 136B, 695(1964).
53. MAERKER, ORNL-TM-5203-ENDF-227
54. RASMUSSEN, ORHAN, HARPER, CUNNINGHAM, AND ALI, DASA 2570(GA-10248)
55. HOWERTON, PRELIMINARY ENDF/BV MAT 1316 AND PRIVATE COMMUNICATION

----- (N,P) CROSS SECTION -----

56. SESSI, THESIS, UNIV. OF IDAHO(1956)
57. WESTERMARK, PHYS. REV. 88, 573(1952).
58. DUDLEY AND KENNERLEY, IN ENDF/B-IV DOSIMETRY FILE, BNL-NCS-50446, EDITED BY MAGURNO
59. BARRAL ET.AL., AFWL-TR-68-134(1969) AND NUCL.PHYS. A138, 387(1969).
60. PASQUARELLI, NUCL.PHYS. A93, 218(1967)
61. KHURANA ET.AL., NUCL.PHYS. 69, 153(1965)
62. SANTRY ET. AL., CAN J. CHEM. 41, 123, (1963)
63. LEVKOSKII, ZH. EKSP. TEOR. FIZ., 45, 305(1963)
64. ALLAN NUCL. PHYS. 24, 274(1961)
65. ALLEN JR. ET. AL., PHYS. REV. 107, 1308(1957)
66. HURLIMANN, ET. AL., HELV. PHYS. ACTA, 28, 33(1955)
67. LUSCHER ET. AL., HELV. PHYS. ACTA, 23, 561(1950)
68. PAUL ET.AL., CAN. J. PHYS. 31, 267(1953)
69. KLEMA ET.AL., PHYS. REV. 106, (1948)
70. ANTOLKOVIC, NUCL.PHYS. 44, 123(1963)

----- (N,T) REACTION -----

71. DIKSIC ET. AL, INDC(SEC)-18, 193, 71
72. SACHER ET. AL, OESTER. AKAD. WISS., 176, 305(1968)
73. BORMANN ET. AL INT.NAT. CONF., PARIS 1, 225(1966)
74. KHURANA ET., NUCL. PHYS. 69, 153(1965)
75. POULARIKAS, ARKANSAS, 14(1963)
76. WEIGOLD ET. AL., NUCL. PHYS. 32, 106, (1962)
77. BAERG ET.AL., CAN. J. CHEM. 39, 684(1961).
78. PRASAD ET. AL., NUCL. PHYS. 85, 476(1966)
79. BORMANN. ET. AL., INT.NAT.CONF., PARIS, 1, 225(1966).
80. PAUL ET. AL., CAN. J. PHYS. 31, 267(1953)

----- (N,ALFA) REACTION -----

81. MUNNICH, Z. PHYSIK, 153, 106(1958)
82. SESSI, THESIS, UNIV. OF IDAHO(1956)
83. KUNABE, J. PHYS. SOC. JAP., 13, 325(1958)
84. SCHMITT BULL. AM.PHYS. SOC. 3, 37(N6), 58
85. HURLIMANN ET. AL., HELV.PHYS. ACTA, 28, 33(1955)
86. BARRAL ET. AL., AFWL-TR-68-134(1969)
87. PASQUARELLI, NUL.PHYS. A, 93, 218(1967)
88. KHURANA ET. AL., NUCL. PHYS. 69, 153(1965)
89. ALLEN JR. ET. AL., PHYS. REV. 107, 1368(1957)
90. PAUL ET. AL., CAN. J. PHYS. 31, 267(1953)
91. AUCHAMAUGH ET. AL., PHYS. REV., 12C, 1126(1975)

16-S-0
MAT 1347

-----NUCLEAR MODEL CODES-----

- 92. C. R. DUNFORD, COMMUC: AI-AEC-12931(1970)
- 93. MODNEW: UHL'S CODE(REF.NUCL. PHYS.)MODIFIED TO
RUN ON NNDC PDP-10 AT BNL
- 94. M.BLANN,OVERLAID ALICE; UNIV. OF ROCHESTER REPORT C003494-29
(1975).
- 95. M.BLANN,EVAHYB;EARLY VERSION OF ALICE(UNPUBLISHED)
- 96. BERLAND,CHAD; NAA-SR-11231(1965)
- 97. R.R. KINSEY,DUMMY5,PRIVATE COMMUNICATION
- 98. AUERBACH, ABACUSII. BNL-6562(1964)

Sulfur-32

DATA SUMMARY AND GENERAL COMMENTS

The references to the experimental data for $^{16}\text{S}^{32}$ are summarized in UCRL-50400, Vol. 3. They are listed in UCRL-50400, Vol. 10. The data consist primarily of measurements for natural sulfur, but they also include measurements for isotopes S^{32} and S^{34} . The evaluated data are shown graphically in UCRL-50400, Vol. 15, Part B.

TOTAL CROSS SECTION

Experimental and evaluated total cross sections for S^{32} are shown graphically on pages 2-81 to 2-91 of UCRL-50400, Vol. 7, Part A, Rev. 1; some tabular experimental values are given on pages 2-92 and 2-93. The evaluated total cross sections are shown in UCRL-50400, Vol. 15, Part B.

ELASTIC SCATTERING CROSS SECTION

Some experimental elastic scattering data are shown graphically on page 2-92 of UCRL-50400, Vol. 7, Part A, Rev. 1; additional tabulated values are given on page 2-93. The evaluated elastic scattering cross sections are shown in UCRL-50400, Vol. 15, Part B. These evaluated elastic cross sections were obtained for the most part by differencing the evaluated total cross sections and the sums of the evaluated nonelastic cross sections.

ELASTIC SCATTERING ANGULAR DISTRIBUTIONS

Measurements of the elastic scattering angular distributions are shown in UCRL-50400, Vol. 19. In the evaluation, the elastic scattering angular distributions were assumed to be isotropic for all neutron energies below 50 keV. Above 50 keV, the evaluated elastic scattering angular distributions were based on experimental data, supplemented at the higher energies by spherical optical model calculations in which the best-fit optical model parameters of Bechetti and Greenlees were used [*Phys. Rev.* 182, 1190 (1969)].

INELASTIC SCATTERING CROSS SECTION

Inelastic scattering data for natural sulfur are shown on pages 2-119 (graphical) and 2-121 (tabular) of UCRL-50400, Vol. 8, Rev. 1, Part A; corresponding quantities for S^{32} are shown on pages 2-123 and 2-130. In view of the scarcity of the experimental data, inelastic scattering was represented in the evaluation by a continuum contribution that starts at 213. MeV. The evaluated n, n' continuum cross sections are shown graphically in UCRL-50400, Vol. 15, Part B.

16-S-32
MAT 1316

Sulfur-32

05/09/78

16-S-32
MAT 1316

INELASTIC SCATTERING ANGULAR AND ENERGY DISTRIBUTIONS

The angular distributions for the continuum inelastic scattering were assumed to be isotropic. The energy distributions for incident neutron energies below 5 MeV were chosen so as to reproduce the average and maximum secondary neutron energies for the reaction. The energy distributions at 5 MeV and above were obtained from temperature model calculations; contributions from preequilibrium processes were estimated (see UCRL-50400, Vol. 15, Part A, pages 19 to 22).

calculations, with the assigned temperatures consistent with nuclear systematics (see UCRL-50400, Vol. 15, Part A, page 24).

n,n'p CROSS SECTION

The threshold for the n,n'p reaction is 9.14 MeV. One experimental data point for natural sulfur is listed on page 2-122 of UCRL-50400, Vol. 8, Rev. 1, Part A; a data point for S^{32} is listed on page 2-131. The evaluated n,n'p cross sections, which are shown in UCRL-50400, Vol. 15, Part B, were estimated by using nuclear systematics.

n,2n CROSS SECTION

The threshold for the n,2n reaction is 15.56 MeV. Experimental values of the n,2n cross section are shown graphically on page 2-124 of UCRL-50400, Vol. 8, Rev. 1, Part A; some tabulated values are given on page 2-130. The evaluated n,2n cross sections are shown graphically in UCRL-50400, Vol. 15, Part B.

ANGULAR AND ENERGY DISTRIBUTIONS FOR THE n,2n REACTION

The angular distribution of secondary neutrons from the n,2n reaction was assumed to be isotropic in the laboratory system. Energy distributions of the secondary neutrons, which are presented in tabular form, are derived from temperature model

ANGULAR AND ENERGY DISTRIBUTIONS FOR THE n,n'p REACTION

The angular distribution of secondary neutrons produced by the n,n'p reaction was assumed to be isotropic in the laboratory system. Energy distributions of the secondary neutrons, which are presented in tabular form, are derived from temperature model calculations, with the assigned temperatures consistent with nuclear systematics (see UCRL-50400, Vol. 15, Part A, page 24).

n,p CROSS SECTION

The threshold for the n,p reaction is 0.96 MeV. Experimental n,p cross sections are shown graphically on pages 2-120 (natural sulfur), 2-126 and 2-127 (S^{32}), and 2-133 (S^{34}) of

16-S-32

MAT 1316

UCRL-50400, Vol. 8, Rev. 1, Part A; some tabulated experimental values are given on pages 2-122 (natural sulfur), 2-131 (S^{32}), and 2-134 (S^{34}). The evaluated n,p cross sections for S^{32} are based on the experimental data, and are shown in UCRL-50400, Vol. 15, Part B.

n,t CROSS SECTION

The threshold for the n,t reaction is 13.09 MeV. Experimental values of the n,t cross section are shown graphically on page 2-128 of UCRL-50400, Vol. 8, Rev. 1, Part A; some tabular values are given on page 2-132. The evaluated n,t cross sections are shown graphically in UCRL-50400, Vol. 15, Part B.

n, α CROSS SECTION

The threshold for the n,α reaction is -1.53 MeV, so this reaction is exothermic. Experimental n,α cross sections for S^{32} are shown on pages 2-129 (graphical) and 2-132 (tabular) of UCRL-50400, Vol. 8, Rev. 1, Part A; some corresponding cross sections for S^{34} are given on pages 2-133 and 2-134. The evaluated n,α cross sections for S^{32} are shown in UCRL-50400, Vol. 15, Part B.

n, γ CROSS SECTION

A few capture cross section data points for natural sulfur, S^{32} , and

S^{34} are given on pages 2-93, 2-95, and 2-96, respectively, of UCRL-50400, Vol. 7, Part A, Rev. 1. The evaluated neutron capture cross sections for S^{32} , which are based in large part on nuclear systematics, are shown in UCRL-50400, Vol. 15, Part B.

PHOTON PRODUCTION FROM n,γ REACTIONS

The neutron capture gamma-ray spectrum at thermal neutron energies was taken from the data of V. J. Orphan, N. C. Rasmussen, and T. L. Harper, Gulf General Atomic Rept. GA-10248 (1970). This spectrum was assumed to apply at all neutron energies, since there are no data for incident neutron energies higher than thermal. To conserve the total energy of the reaction, the gamma-ray multiplicity was assumed to vary as a linear function of neutron energy.

n, $X\gamma$ CROSS SECTION

The only experimental $n,X\gamma$ data points for sulfur are listed on page 2-122 of UCRL-50400, Vol. 8, Rev. 1, Part A. In the evaluation for sulfur, the $n,X\gamma$ cross section was assumed to include all photons except those produced in the neutron capture reaction. Also, although the evaluation for sulfur is listed as S^{32} (the reason being that S^{32} is by far the dominant isotope in natural sulfur), some

16-S-32
MAT 1316

gamma ray lines from the scarce isotopes S^{33} , S^{34} , and S^{36} were also considered in the evaluation of the $n, X\gamma$ cross sections. The evaluated $n, X\gamma$ cross sections include five discrete lines plus a continuum contribution that starts at 0.9 MeV. The discrete lines were evaluated as follows.

2.237 MeV

This gamma ray arises from the transition of the 2.237-MeV level to the ground state in S^{32} . For incident neutron energies below approximately 4 MeV, the gamma ray is produced entirely from the n, n' reaction. Thus, the $n, X\gamma$ cross section for producing this gamma ray was set equal to the n, n' cross section for energies below 4 MeV. The corresponding cross section at 14 MeV was taken from the study by J. Benveniste *et al.*, UCID-4619 (1963). Cross sections at the other energies were obtained by interpolation and extrapolation.

1.54 MeV

This gamma ray arises from the transition of the second to the first excited state in S^{32} . At 14 MeV, the cross section for producing this gamma ray was assumed to be 6% of the cross section for producing the 2.237-MeV gamma ray. The assumption was based on the inelastic proton scattering data of G. Crawley and

G. T. Garvey, *Phys. Rev.* 160, 981 (1967) and 167, 1070 (1968). At other neutron energies, the cross section was guessed.

3.78 MeV

This gamma ray arises from the transition of the 3.78-MeV level to the ground state in S^{32} . The cross section at 7.6 MeV was given in a private communication from F. G. Perey (1968). The cross section at other energies was guessed.

4.29 MeV

This gamma ray arises from the transition of the 4.29-MeV level to the ground state in S^{32} . The cross section at 7.6 MeV was given in the private communication of F. G. Perey cited above. The cross section at 14 MeV was deduced by making the same assumptions for the 4.29-MeV line as for the 1.54-MeV line; the data of Crawley and Garvey were used as a guide.

2.77 MeV

This gamma ray arises from the transition of the 5.01-MeV level to the 2.237-MeV level in S^{32} . Two references* give different values for the cross section at 14 MeV.

*W. E. Thompson and F. C. Engesser, USNRDL-TR-1043 (1966), and V. N. Bochkarev and V. V. Neféдов, *Yad. Fiz.* 1, 803 (1965).

16-S-32

MAT 1316

Bochkarev's value was chosen, using Crawley and Garvey's p,p' data, cited above, as a guide. At other energies the cross section was guessed.

All discrete lines in the n,XY evaluation came from the S^{32} isotope. However, gamma rays from S^{33} , S^{34} , and S^{36} were considered in the evaluation of the continuum component. The n,XY cross sections for the continuum component were obtained from the NXGAMEL code, using the systematics developed by Perkins, Haight, and Howerton, *Nucl. Sci. Eng.* 57, 1 (1975). A summary of this method of evaluating photon production data is discussed in UCRL-50400, Vol. 15, Part A, pages 38 to 41. In the evaluation, the continuum was assumed to start at 0.9 MeV, becoming 0.4% of the calculated value at 3 MeV, 2% at 5 MeV, and 41% at 10 MeV and above. The continuum gamma rays at the lower energies come from n,n' reactions in the rare isotopes S^{33} , S^{34} , and S^{36} .

At 14.8 MeV, the procedure followed here gives results that are in reasonable agreement with the results of W. E. Tucker, ORO-2791-30 (1969) and ORO-2791-32 (1971).

SPECTRA OF PHOTONS FROM THE n,XY PROCESS

The angular distributions of the 2.237-, 4.29-, and 3.78-MeV gamma rays were taken from the measurements of F. G. Perey (private communication, 1968) at 7.6 MeV. The angular distributions of the 1.54- and 2.77-MeV gamma rays were assumed to be isotropic. The energy distributions of these discrete photon lines were estimated based on the kinematics of the reaction. The angular distributions of the continuum photons were assumed to be isotropic, and the corresponding energy distributions were calculated from the systematics of Perkins, Haight, and Howerton cited above.

Eval-Feb67 M.S.Allen and M.K.Drake

Ga-7829 vol-4(1967) Dist-May74
extended to 20 MeV for ENDF/B version

1V 1149 1451

* * * * * * *

Natural Chlorine

The evaluation is described in GA-7829 vol-iv (Feb.1967)
(NDL-TR-89, part iv)

* * * * * * *

The low energy radiative capture (MT=102) and (n,p) (MT=103)
cross sections were modified Jan.1972 to conform to the
recommended 2200 M/Sec values (CSEWG normalization and standards
subcommittee) the 2200 M/Sec values were

n,gamma = 32.85 barns

n,proton = 0.355 barns

* * * * * * *

file 3

Total Cross Section

Up to 4 keV the data of Brugger, et al(1) were used
from 4 to 50 keV the data of Garg et al (2) were used
from 50 to 200 keV the data of Newson, et al (3) were used
from 200 to 1000 keV the data of Kiehn, et al (4) were used
above 1.0 MeV the recommended curve was basically based on the
measurement of Glasgow and Foster (5)

*

N, Gamma Cross Section

The cross section was taken to be $1/V$ near thermal neutron energies
above 20 eV the data of Kashukeev (6) and Macklin (7) were used

Inelastic Cross Sections

Up to 7.0 MeV the total and discrete level excitation cross
sections were obtained using the ABACUS-11 code
above 7.0 MeV the total inelastic cross section was obtained
by subtracting other partial ./s from the non-elasting cross
section which was based on data measured by Pasechnik (8) and
Frasca (9)

*

n,p Cross Section

Up to 10 eV the cross-section was taken to be $1/V$
from 10 eV to 10 keV the data shown in BNL-325 (1964) were used
from 3.0 MeV to 20 MeV a smooth curve was drawn through the 1
experimental data measured by Mathur and Morgan (10), Cohen and
White (11), and Paul and Clarke (12)

*

n,2n Cross Section

The n,2n cross section was based on experimental measurements
of each isotope

* * * * * * *

file 4

Elastic Scattering

The results from optical model calculations were used (see report
Other Reactions)

17-Cl-0
MAT 1149

Angular distributions of neutrons from discrete level inelastic scattering were obtained using the ABACUS code.

Other neutrons were assumed to be isotropic.

* * * * *

file 5

A statistical model was used to describe all secondary neutrons except discrete level inelastic

* * * * *

file 12

Radiative Capture

These gamma rays were obtained by analyzing measurements of thermal neutron capture. The recommended transition probabilities were taken from Endt and Van der Leun (13) and Hazewindus (14). Since no epithermal data were available the same secondary gamma spectra was used for all incident neutron energies

Discrete Inelastic

The recommended data were obtained by using the level excitation cross sections and the recommended branching ratios (see Ga-7829)

* * * * *

file 14

Angular distribution of gamma rays from discrete level inelastic were calculated using the MANDY code. all other gamma rays were assumed to be isotropic

* * * * *

* * * * *

References

- (1) R.M.Brugger, et al., Phys.Rev.104,1054(1956)
- (2) J.B.Garg, et al., paper 74 Conf. on nuclear structure, Antwerp, July 1965.
- (3) H.W.Newson, et al., Phys.Rev.105,198 (1957)
- (4) R.M.Kiehn, et al., Phys.Rev.91,66 (1953)
- (5) D.W.Glasgow and D.G.Foster, jR., Baps 8, 321 (1963)
- (6) N.T.Kashukeev, et.al., J.Nucl.Eng. parts A and B 14,76 (1961)
- (7) R.L.Macklin, et.al., Phys.Rev.129,269(1963)
- (8) M.V.Pasechnik, Gen Conf.vol.2. p.3 (1955)
- (9) A.J.Frasca, et.al., Phys.Rev.144,854(1966)
- (10) S.C.Mathur and I.L.Morgan, Nucl.Phys. 75,561 (1966)
- (11) A.V.Cohen and P.H.White, Nucl.Phys. 1, 73 (1956)
- (12) E.P.Paul and R.L.Clarke, Can.J.Phys. 31,267 (1953)
- (13) P.M.Endt and C.Van der Leun, Nucl.Phys.34,1 (1962)
- (14) N.Hazewindus, et.al., Physica 29, 681 (1963)

* * * * *

Chlorine**translated at U.Va. from GA evaluation by Drake, et al. Please refer comments or questions regarding errors in translation or in format, or concerning the translation code (late.) to

Donald J. Dudziak, University of California, Los Alamos
Scientific Laboratory Los Alamos NM 87544

Any comments regarding the data evaluation should be referred to M.K. Drake, et al, the authors of Ga-7829 (NDL-TR-89). The permission of Mr. Drake to translate his evaluation is gratefully acknowledged. Transition probability arrays for inelastic scat-

17-C1-0
MAT 1149

tering were taken from diagrams in Ga-7829, part iv. Data for rtn 1032 and 3032 were assigned MT=28, as recommended by Drake. Translation completed July, 1969.

Photon production files converted to new format in LA-4549(ENDF-102, revised, vol. 11) by Donald J. Dudziak October 1970.

Neutron and photon production files converted to ENDF/B-11 format for the radiation shielding information center by Singletary, Penny, and Roussin. File 2 and file 23 also added in March 1971.

Eval-1967 M.K.Drake
Ga-7829 vol-5 (1967) Dist-may74

extended to 20 MeV for ENDF/B version-IV

* * * * *

Natural Potassium

* * * * *

file 3

Total Cross Section

Up to 10 eV a smooth curve was drawn through the data of Joki(1) from 10 eV to 17 keV the total cross section was obtained from a resolved resonance calculation based on the two principle isotopes. Parameters of Good,et al (2) were used between 17 keV and 315 keV a smooth curve was drawn through the 1958 data measured by Newson (3).

The total cross section was very poorly measured between 0.3 and 1.0 MeV. The recommended curve was drawn through data measured by Peterson (4).

Between 0.9 and 2.10 MeV an average was taken of data measured by Vaughn (5). Structure in the cross section is present but could not be analyzed from Vaughns data.

Above 2.1 MeV data measured by Foster (6) and Deconninck ,(7) were used.

Radiative Capture Cross Section

The low energy cross section was modified to agree with the CSEWG normalization and standards subcommittee recommended 2200 M/Sec value of *(2.10 barns)*

From 1.0-5 eV to 20 keV the cross section was obtained from the resolved resonance parameters (see Ga-7829 vol-4) plus additional 1/V component to obtain the desired 0.0253 eV value

Above 20keV the cross section was drawn through the experimental points at 30.5 and 65.0 keV measured by Macklin et al (8). The slope was taken to be the same as was measured for K-41 activation by Stupegia (9).

Inelastic Scattering

The first three level excitation cross sections were based on measurements by Lind and Day (10) and Towle and Gilboy (11) for neutron energies up to 4.0 MeV. Other level excitation cross sections were obtained using the ABACUS-11 code (see report) Calculations were made for neutron energies up to 6.8 MeV Above 6.8 MeV the total inelastic cross section was taken as the difference between the non-elastic cross section and the sum of $(n,p) + (n,np) + (n,a) + (n,na) + (n,2n)$. See report for the non-elastic cross section.

n,proton Cross sections

Up to 700 keV the (n,p) cross section is 1/V with a 2200 M/Sec value of 0.051 barns (normalization and standards subcommittee recommendation).From 700 keV to 4.0 MeV measured values for the $(n,p0) + (n,p1) + (n,p2)$ cross sections were used, based on measurements by Bass et al (12,13).

19-K-0
MAT 1150

Between 4.0 and 8.0 MeV the data of Bass et al (13) were used. The recommended curve was extrapolated through to data measured by Langkau (14) (12.6 to 19.4 MeV). The (n,np) cross section was based on measurements made by Langkau (14) and Bormann (15).

n, alpha Cross Sections

Up to 1.0 MeV the cross section was taken to be $1/V$ with a 2200 M/Sec value of 0.0046 barns (normalization and standards subcommittee recommendation). From 1.0 MeV to 3.5 MeV the (n,a) cross section was based on (n,alph-zero) measurements of Bass (12,13). From 3.5 to 8.0 MeV data of Bass (14) were used. Above 8.0 MeV the data of Bormann (15,16) were used. The (n,an) cross section was based on data measured by Bormann(15)

n,2n Cross Section

The n,2n cross section was based on measurements made by Bormann (17,18) for the K-39(n,2n) K-38g reaction and by Arnold (19) and Bormann (17) for the K-39 (n,2n) K-38m reaction

* * * * * * *

file 4 (Angular Distributions)

Elastic Scattering

From 0.03 to 1.3 MeV the data of Langsdorf, et al (20) were used from 1.5 to 3.8 MeV the data of Towle and Gilboy (11) were used above 4.0 MeV the ABACUS-11 code was used

Non-elastic Reactions

Angular distributions for (n,2n), (n,np), (n,na), an (n,inelastic continuum) neutrons have been assumed to be isotropic.

Ang Distr. for neutrons from discrete level excitation reactions have been calculated using the ABAUS-11 code.

* * * * * * *

file 5 (Energy Distributions)

An evaporation model has been used for MT=16,22,28, and 91 the effective nuclear temperature was based on

$$t(e) = b * \sqrt{e/a}$$

e= incident neutron energy

a= nuclear mass

b= 2.5 for MT=91, = 1.59 for MT= 16, 22, and 28

(see vol-1 of Ga-7829)

* * * * * * *

file 12 and 13 Photon Production Cross Sections

Gamma rays from thermal neutron capture were obtained from data summarized by Endt and Van der Leun (21) and Groshev et al (22) and measurements of Rudolph and Gersch (23).

Since no epi-thermal measurements were available the same spectra was assumed for all incident neutron energies.

Photons from discrete inelastic level excitation were obtained from the level cross section. All six levels were assumed to decay to the ground state.

Photons from (n,p1), (n,p2) and (n,a1) reactions were obtained by analyzing the individual reactions.

*

Photons from neutron reaction above 7.0 MeV was based on a measurement by Caldwell for Phosphorous. These data are poorly known.

The angular distributions for discrete photons was calculated using the MANDY code.

The angular distributions for continuum photons was assumed to be isotropic.

* * * * *

References

- (1) E.G.Joki, et.al., Phys.Rev.99,610 (1955)
- (2) W.M.Good, et.al., Phys.Rev.109,926 (1958)
- (3) H.W.Newson (Duke U.) pri.comm.(see BNL-883,1964)
- (4) R.E.Peterson, Phys.Rev. 77, 747 (1950)
- (5) F.J.Vaughn, et.al., Nucl.Sci.Eng. 17, 325 (1963)
- (6) D.G.Foster,Jr. (pri.comm 1966)
- (7) G.Deconninck, et.al., J.Phys.(Paris) 22, 652 (1961)
- (8) R.L.Macklin, et.al., Phys.Rev. 129, 2695 (1963)
- (9) D.C.Stupegia, et.al., IAEA Conf.on nuclear data (Oct.1966)
- (10) D.A.Lind and R.B.Day, Ann.Phys. 12, 485 (1961)
- (11) J.H.Towle and W.B. Gilboy, Nucl.Phys. 72, 515 (1965)
- (12) R.Bass, et.al., Nucl.Phys. 28, 478 (1961)
- (13) R.Bass, et.al., Endc(e)-57, 1965
- (14) R.Langkau, Z.Naturforsh, 18a, 914 (1963)
- (15) M.Bormann, et.al., Z.Naturforsh, 15a, 200 (1960)
- (16) M.Bormann, et.al., Z.Phys.166, 477 (1962)
- (17) M.Bormann, Nucl.Phys. 65, 257(1965)
- (18) M.Bormann, et.al.,Nucl.Phys. 63, 438 (1965)
- (19) D.M.Arnold, Thesis, U. of Georgia (1965)
- (20) A.Langsdorf, et.al.,Phys.Ref.107,1077 (1957)
- (21) P.M.Endt and C.Van der Leun, Nucl.Phys. 34, 1 (1962)
- (22) L.V.Groshev, et.al.,Atlas of gamma-ray Spectra from Radiative Capture (trans),pergamon press, 1959
- (23) W.Rudolph and H.V.Gersch, Nucl.Phys. 71, 221 (1965)
- (24) R.L.Caldwell, et.al., Nucl.Sci.Eng. 8, 173 (1960)

* * * * *

Potassium--translated Jun 69 from Ga evaluation (Ga-7829, 1967)
Please refer comments or questions regarding errors in translation or in format, or concerning the translation code (latex)

to**Donald J. Dudziak, University of California, Los Alamos 1
Scientific Laboratory, Los Alamos, NM 87544

Any comments regarding the data evaluation should be referred to M.K. Drake, et al, the authors of Ga-7829 (NDL-tr-89). The permission of Mr. Drake to translate his evaluation is gratefully acknowledged. Transition probability arrays for inelastic scattering were taken from diagrams in Ga-7829,part v. Data for rtn 1032 and 3032 were assigned MT=28, as recommended by Drake.
Translation completed July, 1969.

Photon production files converted to new format in LA-4549(ENDF-102,revised,vol. II) by Donald J. Dudziak July 1970.

Neutron and photon production files converted to ENDF/B-II format for the radiation shielding information center by Singletary, Penny, and Roussin. File 2 and file 23 also added in March 1971.

20-Ca-0
MAT 1320

Summary Documentation

Calcium Evaluation

ENDF/B-V Preliminary

MAT = 1320

C. Y. Fu and F. G. Perey
Oak Ridge National Laboratory
Oak Ridge, Tennessee

August 1978

The following revisions are made to the ENDF/B-IV evaluation
(Fu and Perey, 1973):

Total cross sections from 100 eV to 50 keV were decreased by about 200 mb according to a new measurement.¹ Both the new data and the earlier evaluation are given graphically in BNL-325.²

Capture cross sections from 2.5 keV to 200 keV were increased by a factor of 2 to 5 according to new ORELA data.^{3,4} The capture cross sections were assumed to decrease above 200 keV, reach a minimum near 5 MeV, then increase to go through a 14-MeV datum by Cvelbar *et al.*⁵

(n,x) and (n,xy) cross sections for MT=4, 22, 28, 103, and 107 above 10 MeV were revised based on the calculation reported in Ref. 6. The calculated (n,xy) cross sections agree with the ORELA measurement by Dickens *et al.*,⁷ but were separately given for each reaction.

In addition, two minor changes were made: Q(n,2n) was changed to that of ⁴⁸Ca to include a small contribution from this isotope. Three points were added to the total cross section from 1.18 to 1.19 MeV to define a cross-section minimum better.

The following summary for each file and section is for ENDF/B-V:

File 1. General Information

Section 451. Descriptive Data

File 2. Resonance Parameters

Section 151. General Designation for Resonance Integrals

Effective scattering length of 4.88 fermi² is given.

File 3. Neutron Cross Sections

Section 1. Total Interaction

0.00001 eV to 10 eV: Sum of the free atom scattering cross section of 2.99 barns⁸ and the capture cross section.

10 eV to 10 keV: Magleby et al.⁹

10 keV to 180 keV: Refs. 1 and 10.

180 keV to 480 keV: ORNL measurement.¹¹

480 keV to 500 keV: ORNL¹¹ and NBS¹² measurements.

500 keV to 20 MeV: Magnitude based on ORNL¹¹ and NBS.¹²
Resonance structure based on Karlsruhe.¹³

Section 2. Elastic Scattering

Derived by subtracting the nonelastic from the total.

Section 3. Nonelastic Interaction.

Sum of the (n,γ) and the (n,x) cross sections.

The (n,x) cross sections were obtained from optical model and Hauser-Feshbach calculations fitting both the nonelastic data¹⁴ and the differences between the smoothed total cross sections and the measured elastic scattering data.^{14,15} The result was used as a constraint for the subsequent calculations.

Section 4. Total Inelastic Scattering

Derived by summing Sections 51 through 73 and Section 91.

Direct interaction contributions are included in 16 discrete levels and in the gamma-ray production calculations.

Section 16. (n,2n) Reaction

Curve drawn through the available data¹⁴ for ⁴⁰Ca and ⁴⁸Ca.

Cross sections are less than 2 mb below 16 MeV, thus no calculation was attempted.

Section 22. (n,nα) Reaction

Sum of calculated (n,nα) and (n,αn) cross sections.

Available data¹⁴ near 14 MeV are for the (n,nα) channel only.

See also Sections 91 and 108 for related calculations.

Section 28. (n,np) Reaction

Sum of calculated (n,np) and (n,pn) cross sections.

Available data¹⁴ near 14 MeV are for the (n,np) channel only.

The cross section (the sum) is the largest nonelastic component at 14 MeV.

Section 51. Inelastic Scattering to First Excited State in ^{44}Ca

Data given were estimated.

Sections 52-64. Inelastic Scattering to First 13 Excited States in ^{40}Ca
Hauser-Feshbach and DWBA calculations⁶ fitting both the (n,n') and the (n,n' γ) data.¹⁴⁻¹⁶

Sections 65-73. Inelastic Scattering to 14th Through 48th Excited States in ^{40}Ca

Excitation functions for these 35 levels were calculated and grouped into 9 bands. The Q-value given for each section is that of the lowest level in the band.

Section 91. Inelastic Scattering to the Continuum

Statistical model calculation⁶ splitting the Hauser-Feshbach [(n,n') + (n,nx)] cross section into (n,n' γ), (n,np), and (n,na) cross sections. The cross section for the formation of the compound nucleus by gamma rays was that of a giant dipole.

Section 102. Radiative Capture

The 0.0253-eV cross section is 0.43 barns¹⁷ which agrees with the average of several old measurements.¹⁸ 1/v up to 1 keV.

Above 1 keV, data of Refs. 3-5 were used.

Section 103. (n,p) Reaction

Calculations fitting both the (n,p) and the (n,p γ) data.¹⁴⁻¹⁶

Available (n,p) data are discrepant, thus (n,p γ) data were emphasized.

Sections 104, 105, 106. (n,d), (n,t), (n,He-3) Reactions

Calculations using an empirical formalism modified from that of Pearlstein.¹⁹

Section 107. (n, α) Reaction

Calculations fitting both the (n, α) and the (n, $\alpha\gamma$) data.¹⁴⁻¹⁶

Available (n, α) data are discrepant, thus (n, $\alpha\gamma$) data were emphasized.

Sections 108, 111, 112. $(n,2\alpha)$, $(n,2p)$, $(n,p\alpha)$ Reactions
Statistical model calculations⁶ splitting the Hauser-Feshbach
 $[(n,p) + (n,px)]$ cross section into $(n,p\gamma)$, (n,pn) , $(n,2p)$,
and $(n,p\alpha)$ cross sections. Similarly for the (n,α) channel.
Sections 251, 252, 253. $\bar{\mu}$, X , γ
Derived from elastic scattering angular distributions.

File 4. Angular Distributions of Secondary Neutrons

All distributions are represented by Legendre coefficients in the center-of-mass frame.

Section 2. Elastic Scattering

0.00001 eV to 10 keV: Isotropic.
10 keV to 4 MeV: From measurements¹⁴ made at 46 energies.
4 MeV to 20 MeV: Optical model calculations⁶ fitting
18 data sets^{14,15} at 11 energies.
Sections 16, 22, 28, 51, 65 through 73, and 91. Isotropic
Sections 52 through 64
Hauser-Feshbach and DWBA calculations⁶ using optical model
parameters determined in File 4, Section 2.
Results agree with available data.^{14,15}

File 5. Energy Distributions of Secondary Neutrons

Section 16. $(n,2n)$ Reaction

Maxwellian distribution with temperatures derived from level
density of ^{40}Ca and LeCouteur theory.²⁰

Sections 22, 28, 91

Tabulated from calculations (see File 3 descriptions).

File 12. Multiplicity of Gamma Rays Produced by Neutron Reaction

Section 4. Total Inelastic Scattering

Calculations fitting both the (n,n') and the $(n,n'\gamma)$ data.¹¹
The production cross section of the 1.158-MeV gamma ray from
 ^{44}Ca (n,n') reaction was obtained by subtracting that of the
calculated 1.159-MeV gamma ray from ^{40}Ca (n,p) reaction from
the measured sum¹⁶ of both.

Sections 22, 28. $(n, n\alpha)$, (n, np) Reactions
Predicted from calculations.⁶

Section 102. Radiative Capture

Only gamma rays from thermal neutron capture are included.

Spectrum was constructed from a proposed decay scheme of ^{41}Ca .²¹

Sections 103, 107. (n, p) , (n, α) Reactions

See File 3, Sections 103 and 107.

File 14. Angular Distributions of Secondary Gamma Rays

All sections are assumed isotropic.

File 15. Energy Distributions of Secondary Gamma Rays

See File 12.

References

1. U. N. Singh et al., Phys. Rev. C 10, 2143 (1974).
2. D. I. Garber and R. R. Kinsey, BNL-325, 3rd Ed., Vol. II, 1976.
3. B. J. Allen et al., Conf. on Nucl. Cross Sections and Technology, NBS-SP-425, Vol. 2, p. 360 (1975).
4. A. R. de L. Musgrove et al., "Odd-Even Effects in Radiative Neutron Capture by ^{42}Ca , ^{43}Ca , ^{44}Ca ," (submitted April 1976 for publication in Nucl. Phys.).
5. Cvelbar et al., NIJS-R-505 (1967).
6. C. Y. Fu, Atomic Data and Nuclear Data Tables 17, 127 (1976).
7. J. K. Dickens et al., Nucl. Sci. Eng. 53, 277 (1974).
8. J. R. Stehn et al., "Neutron Cross Sections - Vol. I, Z=1 to 20," BNL-325 (1964).
9. E. H. Magleby et al., Bull. Am. Phys. Soc. 3, 110 (1958).
10. H. W. Newson et al., Ann. Phys. 14, 365 (1961);
C. D. Bowman et al., Ann. Phys. 17, 319 (1962).
11. F. G. Perey, W. E. Kinney, and T. A. Love, Oak Ridge National Laboratory, private communication (1972).
12. R. B. Schwartz, National Bureau of Standards, private communication (1971).
13. S. Cierjacks, Karlsruhe Nuclear Research Center, Germany, private communication (1971).
14. CSISRS data tape, obtained from the National Neutron Cross Section Center of the Brookhaven National Laboratory, November 1970.
15. F. G. Perey and W. E. Kinney, "Calcium Neutron Elastic- and Inelastic-Scattering Cross Sections from 4.0 to 8.5 MeV," ORNL-4519 (1970).
16. J. K. Dickens, Nucl. Sci. Eng. 48, 78 (1972).
17. F. P. Cranston and D. H. White, Nucl. Phys. A169, 95 (1971).
18. D. J. Hughes and R. B. Schwartz, "Neutron Cross Sections," BNL-325 (1958).
19. S. Pearlstein, "Neutron-Induced Reactions in Medium Mass Nuclei," Brookhaven National Laboratory Report No. BNL-16271 (1971).
20. K. J. LeCouteur, in Nuclear Reactions, Vol. 1, p. 318, edited by P. M. Endt and M. Demur, North-Holland (1959).
21. H. Gruppelaar and P. Spilling, Nucl. Phys. A102, 226 (1967).

ANL/NDM-28
TITANIUM-II: AN EVALUATED NUCLEAR DATA FILE*
by
C. Philis
Centre d'Etudes de Bruyères-le-Châtel
R. Howerton
Lawrence Livermore Laboratory
A. B. Smith
Argonne National Laboratory
June 1977

ABSTRACT

A comprehensive evaluated nuclear data file for elemental titanium is outlined including definition of: the data base, the evaluation procedures and judgments, and the final evaluated results. The file describes all significant neutron-induced reactions with elemental titanium and the associated photon-production processes to incident neutron energies of 20.0 MeV. In addition, isotopic-reaction files, consistent with the elemental file, are separately defined for those processes which are important to applied considerations of material-damage and neutron-dosimetry. The file is formulated in the ENDF format. This report formally documents the evaluation and, together with the numerical file, is submitted for consideration as a part of the ENDF/B-V evaluated file system.

*This work is supported by the "Commissariat à l'Energie Atomique" (France) and the U. S. Department of Energy.

I. INTRODUCTION

Herein, the data base, physical concepts and models and the methodology of the evaluated nuclear data file of elemental titanium are outlined. The evaluated file is presented in detailed graphical form with estimates of uncertainties. This evaluation is submitted as an elemental component of the ENDF/B-V evaluated-nuclear-data-file system (I-1). The evaluation is comprehensive in reaction type and energy scope (10^{-5} eV to 20 MeV). Particular attention is given to those aspects of most importance in the analysis of fission- and fusion-based energy systems (I-2). In addition to the primary elemental file, a secondary isotopic file is provided for selected reactions of interest in dosimetry and radiation-damage studies. This isotopic file is consistent with the primary elemental file.

The data base for this evaluation was derived from the literature as generally available to October 1976 with an extension to January 1977 in some selected areas. In the several MeV region an extensive measurement and calculational program was correlated with the evaluation providing an improved data base and nuclear models for extrapolation. This measurement and calculational program and associated models are defined in the companion document; Titanium-I (I-3). Subsequent portions of this document deal with: resonance properties, neutron total cross sections, neutron scattering, neutron emission, radiative neutron capture, various charged-particle-emitting reactions and photon production processes. The neutron-reaction Q-values of these various components are summarized in Table I-1. The entire numerical file is available from the National Nuclear Data Center (I-4) and the NEA Center for the Compilation of Nuclear Data (I-5). As available from either of these Centers, the numerical file

22-Ti-0
MAT 1322

takes alternate forms with the discrete-point or parameter representation of the resonance region. The (n;p) isotopic dosimetry files have previously been submitted as a component of the ENDF/B-V Dosimetry File and are discussed in more detail in Ref. I-6.

REFERENCES-Section I

- I-1. Evaluated Nuclear Data File-B, ENDF/B, Brookhaven Natl. Lab. Report, ENDF-102, Eds. D. Garber, C. Dunford and S. Pearlstein (1975).
- I-2. See, for example, WRENDA, INDC(SEC)-55/URSF, World Request List for Nuclear Data, Ed. R. Lessler, Inter. Atomic Energy Agency (1976).
- I-3. P. Guenther et al., Argonne Natl. Lab. Report, ANL/NDM-31 (1977).
- I-4. National Nuclear Data Center, Brookhaven Natl. Lab.
- I-5. Centre de Compilation de Données Neutroniques, Saclay, France.
- I-6. C. Philis et al., Argonne National Lab. Report, ANL/NDM-27 (1977).

ANL/NDM-24

FAST NEUTRON CROSS SECTIONS OF VANADIUM AND
AN EVALUATED NEUTRONIC FILE

by

P. Guenther^a, D. Havel^a, R. Howerton^b, F. Mann^c
D. Smith^a, A. Smith^a and J. Whalen^a
May 1977

ABSTRACT

Energy-averaged total cross sections of elemental vanadium were measured from 1.5 to 5.5 MeV. Differential elastic and inelastic neutron scattering cross sections were measured from 1.8 to 4.0 MeV. Neutrons corresponding to the excitation of states in vanadium at 321 ± 10 , 938 ± 15 , 1603 ± 19 , 1811 ± 21 , 2409 ± 27 , ≈ 2500 , 2706 ± 30 and 2773 ± 30 keV were observed. From these experimental results an energy-average model was deduced suitable for extrapolating and interpolating the measured values. These results and those reported elsewhere were used to construct a comprehensive Evaluated Neutronic File in the ENDF format with particular attention to higher-energy processes having an impact on FBR, CTR, dosimetry and gas production applications.

* This work supported by the U.S. Energy Research and Development Administration.

- a. Argonne National Laboratory, Argonne, Ill.
- b. Lawrence Livermore Laboratory, Livermore, Calif.
- c. Hanford Engineering Development Laboratory, Richland, Wash.

I. INTRODUCTION

Vanadium is a promising structural metal for use in high-temperature neutronic systems particularly where tritium containment is a concern (e.g., in fusion power systems). The element is essentially monoisotopic (> 99% ^{51}V), "magic" in neutron number, an odd nucleus near the peak of the s-wave strength function and the spectroscopic structure is relatively well known to excitations of several MeV (1). These unusual characteristics make the interaction of fast neutrons with vanadium of physical interest and, in some ways, simplify experimental studies of the associated fast- neutron interactions and their interpretation. At incident energies of \approx 1.0 MeV the respective neutron cross sections are known to fluctuate with energy and to have some aspects characteristic of intermediate structure (2). Between 1.0 and 5.0 MeV there is a transitional region where the character of the neutron interactions change from a discrete-resonance to an energy-averaged behavior. Compound-nucleus processes in this mass-energy region remain a matter of physical interest (3). Moreover, experimental information in the few-MeV region is useful in establishing nuclear models which subsequently can be applied to extrapolate and interpolate difficult to measure cross sections. This is particularly true for vanadium as a number of important $(n;X)$ cross sections are not well measured; and, as a consequence, model-based theory must be used to extrapolate the measured values over wide energy ranges in order to obtain

cross section values important to many applied calculations.

The primary objective of the present work is the provision of a good contemporary data base for applied use. It was an intent of the measurements to better define the fast neutron interaction with vanadium in the few-MeV range and thus provide a basis for the development of a realistic energy-average model for subsequent extrapolation and interpolation. The present results and those reported elsewhere in the literature were used to develop a comprehensive Evaluated Neutronic File in the ENDF format (4). Particular attention was given to the higher-energy processes of importance in FBR and CTR applications and to the dosimetry and gas-production aspects of the data file. Subsequent portions of this paper outline the present experimental and calculational results and the construction of the evaluated file. The complete numerical contents of the file are given in the Appendix.

REFERENCES

1. Nuclear Data Sheets, A=51, M. Rao and J. Rapaport (1970).
2. A. Smith, J. Whalen and K. Takeuchi, Phys. Rev., C1 581 (1970).
3. P. Moldauer, Proc. Inter. Conf. on Interaction of Neut. with Nuclei, Univ. Lowell, (1976), CONF-760715.
4. Evaluated Nuclear Data File ENDF/B-IV, Brookhaven National Lab. Report, NCS-50496 (1975).

SUMMARY DOCUMENTATION
NATURAL CHROMIUM EVALUATION
ENDF/B-V
MAT=1324

A. Prince and T.W. Burrows

The present work supersedes the ENDF/B-IV, MAT=1191 evaluation by A. Prince (ENDF-246 [1976]). Neutron and photon production data are given between 10^{-5} eV and 20 MeV. The cross sections included are total, elastic, nonelastic, inelastic, $(n, n'\gamma)$, (n, p) , (n, d) , (n, t) , $(n, {}^3\text{He})$, (n, α) , $(n, 2n)$, $(n, 3n)$, $(n, n\alpha)$, (n, np) and gas production. The photon data include multiplicities, photon production cross sections, and secondary energy spectra.

File 2

The resonance parameters and background used in determining the total, elastic, and capture cross sections up to 642.85 keV are the same as ENDF/B-IV. The 0.0253 eV values are $\sigma_{\text{Tot}} = 7.44576$ b, $\sigma_{\text{elas}} = 4.34190$ b, $\sigma_{n\gamma} = 3.10386$ b, and

File 3, MT=1

The total cross section from E=648 keV to 20 MeV is the same as ENDF/B-IV where experimental data¹ and the model calculations were used. From 10^{-5} eV to 648 keV background cross sections are given and are the same as ENDF/B-IV.

File 3, MT=2 and 3

The elastic and nonelastic cross sections are the same as ENDF/B-IV.

For the statistical model code² calculations noted below, an attempt was made to find the best set of parameters based on the work of Dilge et al.³ which would reproduce the experimental data available.

File 3, MT=4

The total inelastic section is completely new based on recent data⁵ and model calculations.²

24-Cr-0
MAT 1324

File 3, MT=16

The $(n,2n)$ is a new evaluation based on the isotopic data of references 6-11 and the natural $(n,2n)$ data of Frehaut and Mosinski¹² and on statistical model calculations² with preequilibrium considered.

File 3, MT=17, 22, and 104

The $(n,n\alpha)$, $(n,3n)$, and (n,d) data are all based completely on model calculations,² including preequilibrium

File 3, MT=28

The (n,np) section is based on references 6, 11, and 13, and on model code calculations.

File 3, MT=51 through 90

The discrete inelastic sections are based on new calculations for all isotopes employing Hauser-Feshbach calculations for compound processes^{3,14} and coupled-channel codes for interpretation of the direct reaction.¹⁵ The calculations were normalized to recent data¹⁶ and other data^{5,17-26} were also considered. For ^{50}Cr and ^{54}Cr only the first-excited states are included with the remaining contribution placed into the continuum. For the major isotopes ^{52}Cr and ^{53}Cr , there are 19 levels represented for each isotope.

File 3, MT=91

The continuum inelastic data were calculated using the statistical mode code.² All discrete level data exceeding the 40 level ENDF/B limitations are included in the continuum. The results were adjusted to conform with the non-elastic.

File 3, MT=102

The capture calculations cover the same energy range and form as the total. At 0.0253 eV the capture cross section = 3.10386 b (resonance parameters plus background) compared to an experimental value of 3.1 b.²⁷

File 3, MT=103

The (n,p) data are based on references 13, 28-37 and on statistical model calculations² including preequilibrium.

File 3, MT=107

The (n,α) data are based on the preliminary experimental data of Dolya³⁸ and on statistical model code calculations.²

File 3, MT=203 through 207

The total gas production sections (MT=203-207) are based on the results in MT=103-107 and on statistical model calculations.²

File 3, MT=251 through 253

MT=251-253 are taken from ENDF/B-IV.

File 4, MT=2, 16, 17, 22, 28 and 51-91

The angular distributions of secondary neutrons were derived as follows. The elastic distribution is the same as ENDF/B-IV. The angular distributions for $(n,2n)$, $(n,3n)$, $(n,n\alpha)$, (n,np) and continuum inelastic (MT=16, 17, 22, 28 and 91) were assumed to be isotropic. The discrete inelastic angular distributions (MT=51-90) are the results of compound-nucleus Hauser-Feshbach calculations¹⁴ and direct reaction calculations¹⁵ combined to describe angular distributions and of experimental data.¹⁶

File 5, MT=16, 17, 22, 28, and 91

The secondary energy distributions for $(n,2n)$, $(n,3n)$, $(n,n\alpha)$ and (n,np) (MT=16, 17, 22 and 28) are presented as nuclear temperature histograms based on the Gilbert-Cameron formalism.³⁹ Since the threshold for the $(n,3n)$ reaction is so high, it was necessary to arbitrarily renormalize the temperatures to conserve energy. The continuum inelastic secondary energy distributions are presented as histograms based on the experimental data of Salnikov et al.⁴⁰

File 12, MT=4

Between 600 keV and 1 MeV the discrete photon production was calculated from File 3, MT=4, 51, 52, and 53. These calculations were also used to adjust the data of Morgan and Newman.⁴⁵

File 12 and 15, MT=102

Three sets of data⁴¹⁻⁴³ were combined in a consistent manner to obtain the thermal capture- γ spectrums with the final total multiplicity adjusted to conserve energy. The spectrum at 10^{-5} eV was assumed to be the same as thermal. Between thermal and 200 keV, the spectrum average data of Allen et al⁴⁴ were employed with the assumption that the distribution did not vary with energy and the final total multiplicity adjusted to conserve energy. In the 200 to 600 keV range, the (n,xy) data of Morgan and Newman⁴⁵ were used assuming it to be pure capture and adjusting the multiplicity to conserve energy. After subtracting the discrete photons (see above) from the 600 keV to 1 MeV data of Morgan and Newman in an energy-conserving manner, the resultant data were assumed to be due to capture only and the multiplicity adjusted to conserve energy.

File 13 and 15, MT=3

For $E_n \geq 1$ MeV the photon production cross sections and energy spectra were determined by integrating the data of Morgan and Newman⁴⁵ over the photon energy range given.

File 14, MT=3, 4 and 102

All photon production angular distributions were assumed to be isotropic.

References

1. CSISRS from F. G. Perey (ORNL). Private Communication, 1973.
2. M. Uhl, Acta Phys. Austrica 31, 245 (1970).
3. W. Dilge, et al., Nucl. Phys. A217, 259 (1973).
4. T. W. Burrows and A. Prince, Proceedings Intl. Conf. on the Interactions of Neutrons with Nuclei, Lowell, Mass., July, 1976.
5. CSISRS from G. P. Couchell (Univ. of Lowell). Private Communications, 1977.
6. BNL-325 (2nd Edition) Suppl. 2 (1966).
7. S. M. Qaim et al., Proc. Int'l Conf., British Nucl. Energy Soc. (1971).
8. M. Bormann et al., Nucl. Phys. A115, 309 (1968).
9. S. M. Qaim, Nucl. Phys. A115, 309 (1968).
10. B. T. Kenna and P. E. Harrison, SLA-73-0637 (1973).
11. P. Hille et al., translated from Mitteilung des Inst. fuer Radium for Schung No. 573 (1965).
12. J. Frehaut and G. Mosinski, Fifth Intl. Symposium on the Interaction of Fast Neutrons with Nuclei, Gaussig, DDR (Nov., 1975).
13. L. Husain and P. K. Kuroda, J. Inorg. Nucl. Chem. 29, 2665 (1967).
14. C. L. Dunford, AI-AEC-12931 (1970).
15. T. Tamura, Computer Program JUPITOR-1 for Coupled-Channel Calculations, ORNL-4152 (1967).
16. W. E. Kinney and F. G. Perey, ORNL-4806 (1974).
17. J. B. Weddel, Phys. Rev. 104, 1069 (1956).
18. P. H. Stelson et al., Nucl. Phys. 68, 97 (1965).
19. D. M. Van Patter et al., Phys. Rev. 128, 1246 (1962).
20. Yu. G. Degtyarev and U. N. Protopov, J. At. Energy 23, 1350 (1967).
21. O. A. Salnikov, Atomnaya En. 3, 106 (1957).
22. L. Crandberg and J. S. Levin, Phys. Rev. 103, 343 (1956).
23. L. E. Beghian et al., Phil. Mag. 8 (1), 261 (1956).
24. D. L. Broder et al., Sov. J. At. En. 16, 113 (1965).

25. V. E. Scherrer et al., Phys. Rev. 96, 386 (1954).
26. R. M. Kiehn and C. Goodman, Phys. Rev. 95, 989 (1954).
27. S. F. Mughabghab and D. I. Garber, BNL-325 (3rd Ed.), Vol. I, 1973.
28. B. D. Kern et al., Nucl. Phys. 10, 226 (1959).
29. I. G. Clator, Priv. Comm. (1969).
30. E. B. Paul and R. L. Clark, Can. J. Phys. 31, 267 (1953).
31. D. L. Allan, Nucl. Phys. 24, 274 (1961).
32. B. Mitra and A. M. Ghose, Nucl. Phys. 83, 157 (1966).
33. J. K. Mukherjee, Proc. Phys. Soc. (London) 77, 508 (1961).
34. J. Dressler, et al., INR-1464, 12 (1973).
35. C. J. Khurana and I. M. Gavil, Nucl. Phys. 69, 153 (1965).
36. P. Holmberg et al., J. Inorg. Nucl. Chem. 36, 715 (1974).
37. D. V. Aleksandrov et al., Sov. J. At. En. 39, 736 (1976).
38. G. P. Dolya et al., Kiev. Conf. (USSR) (YK-11,9) (1973).
39. A. Gilbert and A. G. W. Cameron, Can. J. Phys. 43, 1446 (1965).
40. O. A. Salnikov et al., 2nd Conf. on Nucl. Data for Reactors, Helsinki, Vol. 2, 359 (1970).
41. D. L. Broder et al., Sov. J. Nucl. Phys. 13, 129 (1971).
42. V. J. Orphan et al., GA-10248 (1970).
43. D. C. Kocher, Nucl. Data Sheets 18, 463 (1976).
44. B. J. Allen et al., AAEC/E-200 (1969).
45. G. L. Morgan and E. Newman, ORNL-TM-5098 (1976).

SUMMARY OF THE COVARIANCE FILES
FOR NATURAL CHROMIUM, MAT=1324

A. Prince and T.W. Burrows

MF=32

Since the resonance parameters and background used in determining the total, elastic, and capture cross sections up to 642.85 keV are the same as ENDF/B-IV and no uncertainties were assigned,¹ there is no covariance file for the resonance parameters.

MF=33, General

Due to the complexity of the reactions and the model codes used, no attempt has been made to estimate the off-diagonal covariance elements between sections.

The evaluation of chromium was independent of any other ENDF evaluations. Therefore, there is no need for covariance matrices relating this material to other ENDF materials.

Model code uncertainties were estimated by varying the input parameters.

MT=33, MT=1, 2, 3, and 102

Since these sections are unchanged from ENDF/B-IV, the covariance matrices were taken from the estimated uncertainties in Table 12 of Reference 1.

The representation of 33/1 and 33/3 as derived from 33/2 and 33/102 throughout the resonance region and of 33/2 derived from 33/1 and 33/3 above the resonance region is the way we evaluated these sections. That is, in the resonance region, the total was considered to be the sum of the elastic and the capture; and the nonelastic, equal to the capture; above the resonance region, the elastic was obtained by subtracting the nonelastic from the total.

MF=33, MT=4

This section is represented as two "NC-type" and one "NI-type" sub-sub-sections. The "NI-type" sub-subsection covers the energy range up to the first non-zero cross section and the variance is set to 0. The two "NC-type" sub-subsections cover the energy ranges of 0.71-3.97 MeV and 3.97 MeV to 20.0 MeV, respectively.

The first sub-subsection represents the derivation of the total inelastic from the first 31 discrete levels. The second represents the derivation of the total inelastic from the total non-elastic and the various reaction channels. This is essentially the way in which 3/4 was evaluated.

The user should be warned that the above representation may cause large processing times for some codes such as NJOY. An alternative representation would be the removal of the first "NC-type" sub-subsections and changing the second "NC-type" to cover the energy range 0.71-20.0 MeV. However, this would no longer represent the best estimate of the authors.

MF=33, MT=26

Below 15 MeV, this section represents an estimate of the uncertainty in the model calculations. Above 15 MeV, it represents a comparison between the calculations and experimental data, both for the natural and for the isotope.

MF=33, MT=17, 22, 104, and 106

These sections represent an estimate of the uncertainty in the model calculations.

MF=33, MT=28

Between 13.5 and 15.0 MeV, the section represents a comparison between calculations and experiment. For the other energy ranges, the representation is an estimate of the uncertainty in the model code calculations.

MF=33, MT=51 and 90

These sections represent a comparison between calculations and available experimental data. Where no data were available, the representation is an estimate of the model code uncertainties.

MF=33, MT=91

Although this section was derived from the total inelastic and the discrete inelastic (MT=51-90), we have represented it as "evaluated". We have followed this representation since we have not included the correlations between the discrete inelastic sections. Without these correlations the continuum inelastic uncertainty would tend to blow up if represented as "derived".

MF=33 and 103

The region from 12 MeV to 17 MeV represents a comparison between experiment and calculations. The remainder is a representation of the model uncertainties.

MF=33, MT=107

The 14- to 15- MeV region represents a comparison between experiment and model; the remainder, model uncertainties.

MF=33, Gas Production

The covariance matrices for gas production (MT=203-207) have not been included. The gas production sections of File 3 were derived from the appropriate (n,particle) sections of File 3, except near 20 MeV where some more esoteric reactions made a small contribution. Therefore, they could be easily added with the following "NC-type" representations.

203	(1.) 28 + (1.) 103
204	(1.) 104
205	(1.) 102
206	(1.) 106
207	(1.) 22 + (1.) 107

References:

1. A. Prince, "Evaluations of Chromium Neutron and Gamma Production Cross-Sections for ENDF/B-IV" BNL-NCS-50593 (ENDF-246) (1976).

SUMMARY DOCUMENTATION
of
The Neutron and Gamma Ray Production Cross Sections of Mn

S. F. Mughabghab

I. INTRODUCTION

Because of the importance of ^{55}Mn as a structural material in reactors and its use as a standard in cross section measurements in the thermal energy range, the present evaluation of the ^{55}Mn cross sections for ENDF/B-V was undertaken. In addition, in this evaluation, theoretical calculations of the $(n,2n)$, (n,p) , (n,α) and (n,d) reactions were carried out within the framework of the compound (Hauser-Feshbach) and precompound (Griffin-Blan) models. Another new feature of this evaluation is the basing of the γ -ray production cross sections on experimental data.

II. THERMAL CROSS SECTIONS AND RESONANCE PARAMETERS

A multilevel Breit-Wigner formalism was adopted in fitting [1] the total cross sections of Cote, et al. [2] (.0095 eV-2 keV), Garg, et al. [3] (0.58-200 keV) and Rohr and Friedland [4] (48-260 keV). As a starting point, the resonance parameters recommended in BNL-325, Third Edition [5] were considered, and changes were subsequently made until an acceptable fit to the experimental data was achieved in the high energy region. This necessitated using a scattering radius of 5.5 fm. Furthermore, the weak levels observed in the capture data of Garg, et al. [6] were adopted as p-wave resonances. To obtain a capture resonance integral of 14.2 b (a weighted average of the experimental data), a radiative width of 0.459 eV was deduced for the first positive energy resonance at 337 eV.

In the low neutron energy region, the calculated cross sections were at first constrained to reproduce a capture cross section of 13.3 b and to describe

25-Mn-55

MAT 1325

the polarization data of Bernstein et al. [7]. Two bound levels of different spins (2 and 3) were invoked. The capture cross sections for spin 2 resonances is 9.05 b while that for spin 3 resonances is 4.21 b. The fractional change in the capture cross section in changing from an antiparallel to a parallel spin configuration is given by:

$$R = \frac{\sigma(\uparrow \downarrow) - \sigma(\uparrow \uparrow)}{\sigma(\uparrow \downarrow)} = \frac{2f_n f_N (1 - \frac{5}{7} \frac{\sigma_3}{\sigma_2})}{1 + f_n f_N + \frac{\sigma_3}{\sigma_2} (1 - \frac{5}{7} f_n f_N)}$$

The neutron and target nuclei polarization f_n and f_N measured by Bernstein et al. [7] were respectively 0.32 and 0.16. A possible 15% neutron depolarization due to neutron scattering will reduce f_n to 0.27.

Inserting these values in the above equation gives a fractional change in the cross section of 0.039. This is to be compared with a measured value [7] of 0.034.

III. FAST NEUTRON CROSS SECTIONS

A. Total Cross Section

The total cross section from 10^{-5} eV to 130 keV is represented by the resolved resonance parameters; from 130-210 keV it is based on Rohr et al.'s data [8]; from 210-500 keV on Stubbin's data [9]; and from 500 keV to 20 MeV on Cierjacks' data [10].

B. Elastic Cross Section

This cross section is obtained by subtracting the nonelastic from the total cross section. The nonelastic cross section is derived by summing up all cross sections except the elastic cross section.

C. (n,particle) Cross Sections

In the evaluation of the (n,particle) cross sections guidance was obtained by using Uhl's nuclear model code [11] which allows for secondary and tertiary reactions and gamma-ray competition. It was possible to make simultaneous theoretical fits to the (n,p), (n,d), (n,2n), (n,α), (n,np), and (n,nα) reactions. These calculations are valuable particularly in the energy regions where experimental data is either sparse or not available. In order to fit the experimental data in the energy region from 14-20 MeV, it was necessary to apply a pre-equilibrium fraction of about 20%.

1. (n,2n) Cross Section:

This cross section is based on the data contained in References [12-22]. In the energy region from 13-20 MeV the evaluation is based on nuclear model calculations based on Uhl's code. The cross section near threshold is 30% lower than ENDF/B-IV. A computation of the average fission neutron cross section of the present evaluated (n,2n) reaction yields a value of 0.30 mb. This is to be compared with a measured value of 0.25 ± 0.01 mb [23]. It is interesting to compare this value with a reactor fission value of 0.26 ± 0.02 mb [24].

2. (n,3n) Cross Section

This is taken over from ENDF/B-IV.

3. (n,p) Cross Section

Experimental data [25-27] are only available at 14.7 MeV. The evaluation is based essentially on nuclear model calculation which shows that the cross section attains a peak value of about 46 mb at 13 MeV.

4. (n,d) cross section

The evaluation is based on nuclear model calculations [11].

The measured value [28] at 14 MeV (4.2 mb) is in very good agreement with the calculations. This evaluation differs significantly from ENDF/B-IV which describes this cross section as approaching an asymptotic value of about 5 mb at 20 MeV. The present evaluation indicates that this (n,d) cross section has a peak at 19.8 MeV of magnitude 23.4 mb.

5. (n,a) cross section

From threshold to 12 MeV, this cross section is based on nuclear model calculations [11]; from 12 to 20 MeV, it is based on experimental data [26,29-31]. The calculations are in better agreement with the data of Bormann, et al., [29].

6. (n,na) and (n,np) cross sections

These are based on nuclear model calculations [11].

D. Inelastic Cross Sections

The cross sections for the excitation of discrete levels (126 keV-2.42 MeV) are evaluated by considering the experimental data [32-34] and carrying out Hauser-Feshbach calculations to estimate the cross sections in the threshold regions and above 4.0 MeV. The inelastic scattering to the continuum of levels is obtained by using Uhl's code [11].

E. Radiative Capture Cross Section

The capture cross section in the energy region up to 100 keV is represented by the resolved resonance parameters. From 100 keV to 20 MeV, the evaluation is based on data of Garg, et al., [3], Stupegia, et al., [37], Menlove, et al., [38], Dovbenko, et al., [39], Johnsrud, et al., [40] and Stavisskii, et al., [41].

IV ANGULAR DISTRIBUTION OF SECONDARY NEUTRONS

These are taken over from ENDF/B-IV

V ENERGY DISTRIBUTION OF SECONDARY NEUTRONS

These are the same as ENDF/B-IV

VI GAMMA RAY PRODUCTION CROSS SECTIONS

These are based on data of Morgan [42].

REFERENCES

1. S.F. Mughabghab, Transactions of American Nuclear Society, 22, 661 (1975).
2. R.E. Cote, L.M. Bollinger, and G.E. Thomas, Phys. Rev. 134, B1047 (1964).
3. J.B. Gorg, J. Rainwater, and W.W. Havens, Jr., private communication, See also J.B. Gorg, Nucl. sci and Eng. 65, 76 (1978).
4. G. Rohr and E. Friedland, Nucl. Phys. A104, 1 (1967).
5. S.F. Mughabghab and D.I. Garber, BNL-325, Volume 1, Third Edition (1973).
6. J.B. Garg, R. Macklin, and J. Halperin, Phys. Rev. C, 18, 2079 (1978).
7. S. Bernstein, et al., Phys. Rev. 94, 1243 (1954).
8. G. Rohr and E. Friedland, Nucl. Phys. A104, 1 (1967).
9. W. Stubbins, Phys. Rev. 84, 902 (1951).
10. S. Cierjacks, et al., KFK-100/Supp. 1 (1968).
11. M. Uhl's, Nucl. Phys. A184, 253 (1972).
12. H. Paulsen and H. Liskien, J. Nucl. Energy, 19, 907, (1965).
13. H. Menlove, et al., Phys. Rev., 163, 1308 (1967).
14. M. Bormann, et al., Nucl. Phys., A130, 195 (1969).
15. J. Araminowicz and J. Dresler, P. INR-1464, 14 (1973).
16. G.N. Maslov, et al., INDC (CCP)-42/U, 10, 1974.
17. J. Csikai and G. Peto, Acta. Physica Hungaricae, 23, 87 (1967).
18. J. Benveniste, 58 Geneva, 15, 3, (1958).
19. E. Weigold, Aust. Jour. Phys., 13, 186 (1960).
20. R.C. Barrel, et al., Nucl. Phys./A, 138, 387 (1969).
21. R. Wenusch and H. Vonach, See BNL-325, Goldberg, et al., (1966).
22. F. Deak, et al., Acta. Physica Hungaricae, 38, 209 (1975).
23. A. Fabry, BLG-465, Centre d'Etude de L'Energie Nucleaire (1972).

24. E. Steinnes, Radiochemica Acta 13, 169 (1970).
25. D.L. Allan, Nucl. Phys. 24, 274 (1961).
26. B. Minetti and A. Pasquarelli, Zeit Phys. 199, 275 (1967).
27. R. Prasad and D.C. Sarkas, El Nuovo Cimento 3A, N3, 467 (1971).
28. L. Colli, et al., Nucl. Phys. 46, 73 (1963).
29. M. Bormann, et al., Nucl. Phys. 63, 438 (1965).
30. K. Rusek, et al., INDC(POL)-6/G, 10 (1976).
31. F. Gabbard and B.D. Kern, Phys. Rev. 128, 1276 (1962).
32. E. Almen-Ramstrom, AE-503 (1975).
33. E. Barnard, et al., Contribution B22, Conference On Nuclear Structure Study with Neutrons, 1972, p.176.
34. M.A. Etemad, AE-481 (1973).
35. N.P. Glazkov, Jour. Nucl. Energy 18, 656 (1964).
36. J.J. Van Loef and D.A. Lind, Phys. Rev. 101, 103 (1956).
37. D.C. Stupegia, et al., J. Nucl. Energy 22, 267 (1968).
38. H.D. Menlove, et al., Phys. Rev. 163, 1299 (1967).
39. A.G. Dovbenko, et al., Atom. Energiya 26, 67 (1969).
40. A. Johnsrud, et al., Phys. Rev. 116, 927 (1959).
41. Yu Stavisskii and Toltikov, At Energy 10, 508, (1961).
42. G.L. Morgan, ORNL/TM-553 (1976).

Summary Documentation

Iron Evaluation

ENDF/B-V MAT = 1326

C. Y. Fu and F. G. Perey
Oak Ridge National Laboratory
Oak Ridge, Tennessee

October 1978

ORNL-4617¹ describes ENDF/B-III. Major revisions for ENDF/B-IV and ENDF/B-V are summarized below.

PART I: SUMMARY FOR ENDF/B-V
(C. Y. Fu and F. G. Perey, 1977)

File 2, MT=151

Resonance parameters for ^{54}Fe , ^{56}Fe , and ^{57}Fe from 1 to 400 keV were examined in detail by C. M. Perey.² Parameters for ^{58}Fe were taken from ENDF/B-V dosimetry file.³

File 3, MT=1

Broad structures in the resonance range (155 eV to 400 keV) were kept unchanged from ENDF/B-IV values. Narrow resonances were better defined.

File 3, MT=2

Similar to File 3, MT=1.

File 3, MT=51

Revised according to the recommendation of Kinney and Perey⁴ up to 1300 keV.

File 3, MT=102

The capture cross sections from 155 eV to 400 keV are well-represented by the resonance parameters. From 400 keV to 1 MeV average cross sections measured by Allen *et al.*,⁵ which agree well with those measured by Le Rigoleur,⁶ were adopted. Above 2 MeV the capture cross sections were increased substantially to go through a data point near 14 MeV.⁷

26-Fe-0
MAT 1326

File 4, MT=2

High-resolution data of Kinney and Perey⁸ from 40 keV to 1.4 MeV were adopted. The broad trend of the Legendre coefficients are in good agreement with ENDF/B-IV values.

File 13, MT=3

Taken from Chapman and Morgan.⁹ This is a repeat measurement using ORELA which resolves the long-standing discrepancies discussed below.

File 15, MT=3

Similar to File 13, MT=3. The lowest three neutrons energies (up to 2.122 MeV) are for capture gamma rays.

File 15, MT=102

Restructured by using variable-energy bins to make shorter files and truncated to 0.85 MeV. Above 0.85 MeV the capture gamma rays are included in File 15, MT=3.

File 32, MT=151

Covariances for the resonance parameters evaluated by C. M. Perey.²

File 33, MT=1 through 107

Covariances for File 3 data.

PART II: SUMMARY FOR ENDF/B-IV

(F. G. Perey, C. Y. Fu, S. K. Penney, W. E. Kinney, R. Q. Wright, 1974)

This modification supersedes the previous evaluation, ENDF/B-III MAT 1180, evaluated by S. K. Penny, W. E. Kinney, R. Q. Wright, F. G. Perey, and C. Y. Fu or ORNL.

It was primarily intended for a revision of the secondary neutron distributions as new data^{10,11} have become available and as the pulsed sphere measurements¹² and related calculations^{12,13} indicated that the

previous neutron distributions were inadequate, and for a reevaluation of the gamma-ray-production cross sections since the recently available data¹⁴ disagree substantially with the data set¹⁵ upon which the previous evaluation was largely based. These purposes were consistently achieved by an extensive calculation for ⁵⁶Fe which also led to the refinement of all reaction cross sections except capture. Significant changes are summarized below.

1. Total cross section between 30 keV and 2 MeV — peaks and valleys were refined based on three sets of ORELA measurements¹⁶ using 1-, 4-, and 12-inch samples.

2. Nonelastic — obtained by compromising three pieces of information, namely, the measured nonelastic cross section, the difference between the evaluated total cross section and the available elastic scattering cross section, and the theoretical interpretation of the total gamma-ray-production cross section. The calculated nonelastic cross section was normalized to this result for constraining the subsequent calculations.

3. Inelastic scattering — six more discrete levels were added based on the Hauser-Feshbach¹⁷ and DWBA¹⁸ calculations in order to include the 4.505-MeV collective state as a discrete level. The direct-interaction components were included in 15 of the 26 discrete levels.¹⁹ The direct-interaction component was included in the continuum using an empirical treatment.²⁰ MT=51 (0.846-MeV level) was changed between 2 and 5 MeV according to an evaluation by Smith²¹ which was based on all available data and his recent measurement. MT=52 (the 1.408-MeV level in ⁵⁴Fe) was revised based on recently available data.²²

4. The Hauser-Feshbach method was used to calculate the $[(n,n') + (n,nx)]$, $[(n,p) + (n,px)]$, and $[(n,\alpha) + (n,\alpha x)]$ cross sections. The $[(n,n') + (n,nx)]$ cross section above 4.531 MeV was split into the (n,n') continuum, $(n,2n)$, (n,np) , and $(n,n\alpha)$ cross sections using a statistical-empirical model.²⁰ The empirical aspects include giant-dipole gamma-ray competition, angular-momentum correction for the second outgoing particle, and direct or preequilibrium emission of the first particle.

5. The (n,p) cross section was well defined by measurements^{23,24} and that of ⁵⁶Fe was well fitted by calculation up to 13 MeV. The (n,pn)

cross section was taken to be the difference between the calculated ^{56}Fe $[(n,p)+(n,px)]$ cross section and the measured ^{56}Fe (n,p) cross section. Neutron distribution for the (n,pn) reaction was calculated and was averaged with that of the (n,np) reaction for MT=28.

6. There is no measured ^{56}Fe (n,α) cross section. The calculated ^{56}Fe (n,α) cross section was restrained by the 14-MeV empirical value and the measured fission-spectrum averages. The ^{54}Fe (n,α) cross section was taken from a calculation by Kirouac and Slavik.²⁵ The $(n,\alpha n)$ cross section and neutron distribution were calculated and were combined with those of the $(n,n\alpha)$ reaction for MT=22.

7. The (n,d) , (n,t) , and $(n,^3\text{He})$ cross sections were based on calculations using the Pearlstein empirical model and parameters.²⁶

8. The two major sets^{14,15} of the gamma-ray-production cross sections agree within experimental errors for incident neutron energies below 6 MeV and then start to diverge, the GRT set¹⁵ being 1.6 barns larger than the ORNL set¹⁴ in the 11 to 15 MeV region. Other available data were too limited to resolve this discrepancy. The calculated results are intermediate between the two, being closer to the GRT measurement below 12 MeV and closer to the ORNL data above 12 MeV. For a tentative evaluation the ORNL data were used for the energy distributions (File 15) as these were given in adequate neutron bins and were the only data available from 15 to 20 MeV. The gamma rays below 0.69 MeV were not measured and were filled in using the calculated values. Up to 10 MeV incident neutron energy the energy conservation law relating the calculated outgoing particle energy and the evaluated gamma-ray energy was applied to determine the gamma-ray multiplicities. From 10 to 16 MeV the calculated multiplicities were used and were extrapolated to 20 MeV according to the shape given by the ORNL measurement.

PART III: GENERAL DESCRIPTION FOR ENDF/B-V

The following description for each file and section is for ENDF/B-V. The references given are only the more important ones. Where a computer code is referred to, it means that interpolation extrapolation of the given experimental data were based on calculations.

File 2. Resonance Parameters

Multilevel Breit-Wigner parameters are given for all isotopes in the energy range 155 eV to 400 keV.^{2,3}

File 3. Neutron Cross Sections

Section 1. Total Interaction

.00001 eV to 330 keV^{16,27-29}

330 keV to 20 MeV^{16,30-32}

Section 2. Elastic Scattering

Derived by subtracting the non-elastic cross section from the total cross section.

Section 3. Non-Elastic Interaction

See summary given above.

Section 4. Total Inelastic Scattering

Derived by adding inelastic scattering cross sections for exciting discrete levels and the continuum.

Section 16. (n,2n) Reaction

See summary given above and Ref. 33.

Section 22. (n,n α) Reaction

See summary given above.

Section 28. (n,np) Reaction.

See summary given above and Refs. 28 and 34.

Section 51. Inelastic Scattering Exciting First Level in ^{56}Fe

.8611 MeV to 1.5 MeV^{4,35}

1.5 MeV to 2.122 MeV^{35,36}

2.122 MeV to 20 MeV^{17-19,21,37-40}

Section 52. Inelastic Scattering Exciting First Level in ^{54}Fe

See Ref. 22.

Sections 53-76. Inelastic Scattering Exciting Second Through 25th Levels in ^{56}Fe

See Refs. 17-19, 37, and 39.

Section 91. Inelastic Scattering Exciting the Continuum

See summary given above and Refs. 10, 11, 20, 23, 38, and 41-43.

Section 102. Radiative Capture

See Refs. 5-7, 27, and 29.

Section 103. (n,p) Reaction

See summary given above and Refs. 23 and 24.

Section 104. (n,d) Reaction

See summary given above.

Section 105. (n,t) Reaction

See summary given above.

Section 106. (n,³He) Reaction

See summary given above.

Section 107. (n, α) Reaction

See summary given above and Refs. 23 and 25.

File 4. Angular Distribution of Secondary Neutrons

All distributions are given in the center-of-mass system in the Legendre polynomial representation.

Section 2. Elastic Scattering

.00001 eV to 1.23 MeV^{8,44-47}

1.23 MeV to 4 MeV^{8,44,48-52}

4 MeV to 20 MeV^{38,44,53}

Section 16. (n,2n) Reaction

Both neutrons are assumed to be isotropic.

Section 22. (n,n α) Reaction

Assumed isotropic.

Section 28. (n,np) Reaction

Assumed isotropic.

Section 51. Inelastic Scattering Exciting First Level in ⁵⁶Fe

See Refs. 17, 18, and 37-39.

Section 52. Inelastic Scattering Exciting First Level in ⁵⁴Fe

Assumed isotropic.

Sections 53-76. Inelastic Scattering Exciting Second through 25th Levels in ⁵⁶Fe

See Refs. 17-19 and 37-39.

Section 91. Inelastic Scattering Exciting the Continuum

Assumed isotropic.

File 5. Energy Distributions of Secondary Neutrons

Section 16. $(n,2n)$ Reaction

See summary given above and Refs. 33 and 43.

Section 22. $(n,n\gamma)$ Reaction

See summary given above.

Section 28. (n,np) Reaction

See summary given above.

Section 91. Inelastic Scattering Exciting the Continuum

See Refs. 10-12, 20, 38, and 40-43.

File 12. Multiplicities of Gamma Rays Produced by Neutron Reactions

Section 51. Inelastic Scattering Exciting First Level in ^{56}Fe

Neutron energy is 0.8611 to 2.122 MeV. One discrete gamma ray is given.

Section 52. Inelastic Scattering Exciting First Level in ^{54}Fe

Energy range is 1.433 to 2.122 MeV. One discrete gamma ray is given.

Section 102. Radiative Capture

These gamma rays are representative of neutron energy ranges. 54

File 13. Gamma-Ray-Production Cross Sections

See summary given above and Ref. 9.

File 14. Angular Distributions of Secondary Gamma Rays

Assumed isotropic.

File 15. Energy Distributions of Secondary Gamma Rays

See summary given above and references of files 12 and 13.

File 32. Covariances for Resonance Parameters

See Ref. 2.

File 33. Covariances for File-3 Data

References

1. S. K. Penny and W. E. Kinney, ORNL-4617 (1971).
2. C. M. Perey, private communication, 1977 (to be published).
3. Fred Mann, HEDL, private communication (1977).
4. W. E. Kinney and F. G. Perey, Nucl. Sci. Eng. 63, 418 (1977).
5. B. J. Allen et al., Nucl Phys. A269, 408 (1976); also "Valence Neutron Capture in Fe-54," to be published.
6. C. le Rigoleur et al., CEA-R-4788 (1976).
7. D. I. Garber and R. R. Kinsey, BNL-325, Third Edition, Vol. 2 (1976).
8. W. E. Kinney and F. G. Perey, private communication (1977).
9. G. T. Chapman and G. L. Morgan, ORNL-TM-5416 (1976).
10. J. L. Kammerdiener, UCRL-51232 (1972).
11. G. Clayeux et al., CEA-R-4279 (1972).
12. L. F. Hansen et al., Nucl. Sci. Eng. 51, 278 (1973).
13. S. N. Cramer et al., ORNL-TM-4072 (1973).
14. J. K. Dickens et al., Nucl. Sci. Eng. 50, 311 (1973).
15. V. J. Orphan et al., GRT-A10743 (1971), rev. by V. Rogers, IRT, private communication (1973).
16. J. A. Harvey, USAEC Conf-720901, p. 1075 (1972).
17. S. K. Penny, Computer Code HELGA, ORNL (1973).
18. R. H. Bassel et al., Computer Code JULIE, ORNL (1966).
19. G. S. Mani, Nucl. Phys. A165, 225 (1971).
20. C. Y. Fu, Computer Code NNNGAM, ORNL (1973).
21. A. B. Smith, private communication (1973).
22. W. E. Kinney and F. G. Perey, ORNL-4907 (1973).
23. M. D. Goldberg et al., BNL-325 (1966).
24. J. C. Robertson et al., J. Nucl. Energy 27, 139 (1973).
25. G. J. Kirouac and C. J. Slavik, private communication (1972).
26. S. Pearlstein, BNL-16271 (1971).
27. J. J. Schmidt, KFK-120 (1966).
29. J. S. Story, UDAEA Winfrith, private communication (1970).
30. A. D. Carlson and R. J. Cerbone, GA-9149 (1969).
31. S. Cierjacks et al., KFK-1000 (1968).
32. D. C. Irving and E. A. Straker, ORNL-TM-2891 (1970).
33. O. A. Salnikov et al., Soviet J. of Nucl. Phys. 12, 620 (1971).

34. D. L. Allan, Nucl. Phys. 24, 274 (1961).
35. F. Voss et al., USAEC Conf-710301, p. 218 (1971).
36. W. B. Gilboy and J. B. Towle, Nucl. Phys. 64, 130 (1965).
37. A. Gilbert and A. G. W. Cameron, Can. J. Phys. 43, 1446 (1965).
38. W. E. Kinney and F. G. Perey, ORNL-4515 (1970).
39. M. N. Rao, Nucl. Data Sheets B3-3, 4-43 (1970).
40. R. J. Peterson, Annals of Physics 53, 40 (1969).
41. G. C. Bonazzola et al., Nucl. Phys. 51, 353 (1963).
42. R. M. Schechtman and J. D. Anderson, Phys. Rev. 77, 241 (1965).
43. S. C. Mathur et al., Phys. Rev. 186, 1038 (1969).
44. E. Barnard et al., PEL-180, Pelindaba, Pretoria (1968).
45. S. A. Cox, Bull. Am. Phys. Soc. 8, 478 (1963).
46. I. O. Korzh and M. T. Skylar, UKR. Fiz. Zh. 8, 1389 (1963).
47. M. V. Pasechnik et al., At. En. USSR 16, 207 (1964).
48. J. R. Beyster et al., Phys. Rev. 104, 1319 (1956).
49. R. L. Becker et al., Nucl Phys. 89, 154 (1966).
50. N. A. Bostrom et al., WADC-TR-59-31 (1959).
51. L. Cranberg and J. S. Levin, Phys. Rev. 103, 343 (1969).
52. B. Holmqvist, Arkiv Fysik 38, 403 (1968).
53. F. G. Perey, Computer Code GENOA, ORNL (1970).
54. J. E. White et al., Nucl. Sci. Eng. 51, 496 (1973).

Covariance File for Iron MAT 326

Covariance data are given for MF=32, MT=151 and MF=33, MT=1, 2, 3, 4, 16, 22, 28, 51-76, 91, 102-107. Derived sections (NC subsections) reflect exactly the way the cross-section files were generated.

In general, covariances were determined from $\pm 2\sigma$ error bands. The error bands were extended and enlarged to cover energy regions lacking experimental data. Long range covariances reflect systematic errors common to all data sets. Medium range covariances reflect differences in energy coverage by different data sets and differences in experimental techniques within the same data sets. Short range covariances reflect meaningful structures in the cross sections and/or threshold effects. Statistical errors are, in principle, nonexistent in the evaluated cross sections.

For all threshold reaction cross sections, covariances have at least two components -- an absolute and a fractional. The absolute component represents with few numbers the usually large variation of uncertainties near threshold and for the high-energy tail. The fractional component picks up the rest of the covariances. For the more important reactions, such as MT=51, 2 absolute and 2 fractional components were used.

A constant uncertainty of 50 mb was used to represent the total cross section minima. This corresponds to about 12% for the 24-keV minimum.

The uncertainties for the resonance parameters were taken from the evaluation by C. M. Perey who will report it in detail.

SUMMARY DOCUMENTATION for ^{59}Co
S.F. Mughabghab

I. Introduction

The present evaluation of ^{59}Co is based on that of ENDF/B-IV updating those files for which new experimental data is available. These include the resonance parameters, the inelastic cross sections, the capture cross section, and (n, particle) cross sections. For the (n, particle) cross sections, guidance was obtained by theoretical calculations based on Uhl's code¹.

II. Thermal Cross Sections and Resonance Parameters

The resonance parameters from 132 eV to 84.4 keV are adopted from the evaluation of Mughabghab and Krieger² with minor changes. The parameters of the bound level have to be modified from Reference 2 in order to satisfy the recent polarization data of Abragam, et al,³ and the scattering data of Koester, et al,⁴ and the total cross section measurements of Dilg, et al,⁵. In addition, weak resonances observed in the capture data of Spencer, et al,^{6,7} are assumed to be p-wave resonances. The spins of the weak resonances are assigned randomly in order to obey the $(2J+1)$ law for level density. The scattering widths for these resonances are derived from the reported $g\Gamma_{n\gamma}/\Gamma$ values by assuming a radiative width of 0.22 eV. When the $g\Gamma_{n\gamma}/\Gamma$ values approach a value of $g\Gamma_\gamma$, a scattering width of 2.0 eV is arbitrarily assumed for these resonances.

The resonance region was terminated in this evaluation at about 85 keV because of the important contribution of p-wave capture as measured in References^{6,7}.

In the present evaluation the following 2200 m/sec cross sections and resonance capture integral results are obtained:

capture	=	37.233 b
scattering	=	5.364 b
total	=	42.597 b
resonance capture integral	=	73.78 b

III. Fast Neutron Cross Sections

A. Total Cross Section

From 10^{-5} eV to 85 keV, the total cross section is represented by s- and p-wave resonance parameters. Between 85 to 100 keV, it is based on the data of Garg, et al,⁸; between 100 keV and 20 MeV, it is taken over from ENDF/B-IV. For details, see Reference⁹ on the high energy region.

B. Elastic Neutron Scattering Cross Section

The elastic scattering cross section in the energy region 85-100 keV is obtained by subtracting the capture from the total cross section. From 0.10-20 MeV, it is taken over from ENDF/B-IV.

C. Inelastic Cross Sections

The total inelastic cross section is derived by summing up the inelastic cross sections to discrete levels and the continuum.

The inelastic cross sections to the discrete levels 1.099, 1.190 1.291, 1.430, 1.459, 1.7445, 2.0645, 2.0876, 2.153, 2.184, 2.206 MeV is based on the experimental data of Guenther, et al,⁹ in the neutron energy region 1.8-3.1 MeV and Etemad¹⁰ in the neutron energy region 2.0-4.5 MeV. Outside these energy ranges, the evaluation is based on Hauser-Feshbach calculations¹¹. The data of Egan, et al, was considered¹² but not much weight was given to it because of uncertainties associated with unfolding the photon production cross sections into inelastic cross sections. The inelastic neutron scattering to the continuum region (effective threshold = 2.244 MeV) is adopted from ENDF/B-IV.

D. (n, particle) Cross Sections

1. (n,2n) Reaction Cross Section

Considerable experimental data is available for this reaction. For a brief summary of the older data sets, refer to BNL-325 (1966)¹³. In this evaluation, emphasis is placed on the more recent data sets of Frehaut and Mosinski¹⁴ and Veeser and Arthur¹⁵. As in the case of ⁵⁵Mn, guidance was obtained with aid from nuclear model calculations based on

Uhl's code¹⁶.

2. (n,p) Cross Sections

Between threshold (0.796 MeV) and 10 MeV, the evaluation is based on the experimental data of Smith and Meadows^{17,18}. Other measurements are reported by Maslov, et al,¹⁹ and Levodoskii, et al,²⁰. Measurements prior to 1966 are summarized in BNL-325¹³. The data of Jeronymo, et al,²¹ seems to be in error by a factor of about 10 on the high side. At 14.7 MeV there is a wide discrepancy between the various reported values.

Nuclear model calculations were carried out using Uhl's code¹⁶. A pre-equilibrium fraction of 20 percent was applied. Level density parameters were adjusted to fit the other (n, particle) reaction. A value of 63.3 mb is predicted at 14.7 MeV.

3. (n,d) Cross Sections

The only available data are at 14.8 MeV²² which reports a value of about 2 mb. The present evaluation is based on nuclear model calculations¹⁶.

4. (n,t) Cross Sections

Only 14.6 MeV values are available, ranging from 2.1 to 0.019 mb^{23,25}. A value of 20 μ b is adopted at 14.9 MeV and extrapolated to 20 MeV.

5. (n,³He) Cross Sections

Recent measurements at 14.6 MeV by Diksic, et al,²⁶ and Qaim²⁷ report values ranging from 62 to 4.6 μ b. The latter value is adopted on the basis of systematics and extrapolated to 20 MeV.

6. (n,⁴He) Cross Sections

Although two new data sets^{28,29} are available, it was felt that these would not significantly alter the previous ENDF/B-IV evaluations.

7. (n,np) and $(n,n\alpha)$ Cross Sections

These are based on nuclear model calculations¹⁶.

E. Radiative Capture Cross Section

In the energy region 10^{-8} - 85 keV, the capture cross section is represented by resonance parameters; from 85-1000 keV it is based on Spencer and Macklin's data⁷. Between 1.0-6.2 MeV, it is based on data of Johnsrud, et al,³⁰ and Paulsen³¹ data. In the higher energy region (1.0-20 MeV) the evaluation is based on nuclear model calculations¹¹ with guidance from the systematics of neighboring nuclei. The 14.7 MeV value is normalized to a weighted average value of 0.83 mb^{32,33}.

IV. Angular Distribution of Secondary Neutrons

These are adopted from ENDF/B-IV.

V. Energy Distribution of Secondary Neutrons

These are taken over from ENDF/B-IV.

VI. Photon Production Cross Sections

This is taken over from ENDF/B-IV with minor changes. In the resonance region, multiplicities are included.

References

1. M. Uhl, Nucl. Phys. A184, 253 (1972).
2. S.F. Mughabghab and T.J. Krieger, BNL-NCS-50468.
3. A. Abragam, et al, Jour. de Physique - Letters, 36, L263 (1975) and private communication.
4. L. Koester, et al, Z. Physik, 271, 201 (1974).
5. W. Dilg, et al, Z. Physik, 264, 427 (1973).
6. R.R. Spencer and H. Beer, Nucl. Sci. Eng. 60, 390 (1976).
7. R.R. Spencer and R.L. Macklin, Nucl. Sci. Eng. 61, 346 (1976).
8. J.B. Garg, J. Rainwater and W.W. Havens, Bull. Am. Phys. Soc. 8, 334 (1963). See also J.B. Garg, Nucl. Sci. Eng. 65, 76 (1978) and private communication.
9. P.T. Guenther, P.A. Moldauer, A.B. Smith, D.L. Smith and J.F. Whalen, ANL/NDM-1, June 1973. See also Nucl. Sci. Eng. 54, 273 (1974).
10. M.A. Etemad, Report AE-481 (1973).
11. C. Dunford, Report AI-AEC-12931 (1970).
12. J.J. Egan, R.V. Leclair, M.A. Doyle, and L.E. Beghian, Bull. Am. Phys., Soc. 22, 631 (1977) and private communication.
13. M.D. Goldberg, et al, BNL-325, Second Ed., Supp. 2 (1966).
14. J. Frehaut and G. Mosinki, Report CEA-R-4627 (1974).
15. L.R. Veeser and E.D. Arthur, Proc. of the International Conference on Interactions of Neutrons with Nuclei, 1351 (1976) (Lowell) and private communication.
16. M. Uhl, Nucl. Phys., A184, 253 (1972).
17. D.L. Smith and J.W. Meadows, Nucl. Sci. Eng. 58, 314 (1975).
18. D.L. Smith and J.W. Meadows, Nucl. Soc. Eng. 60, 187 (1976).
19. G.N. Maslov, F. Nasyrov, N.F. Pashkin, INDC (CCP). 42/U page 10 (1974).
20. V. Levodoskii, et al, Sov. Jour. Nucl. Phys. 8, 4 (1969).
21. J.M.F. Jeronymo, et al, Nucl. Phys. 47, 157 (1963).
22. L. Colli, et al, Nuovo Cimento 20, 94 (1961).
23. C.S. Khurana and I.M. Govil, Nucl. Phys. 67, 153 (1965).

24. A. Pouliarikas and D. Gardner, Am. Prog. Rep. Nucl. Chem (Arkansas).
25. T. Biro, et al, Jour. Inorg. Nucl. Chem. 37, 1583 (1975).
26. M. Diksic, P. Strohal, and I. Slauss, Jour. Ing. Nucl. Chem. 36, 477 (1974).
27. S.M. Qaim, Jour. Ing. Nucl. Chem. 36, 239 (1974).
28. J.C. Robertson, B. Audric, and P. Kolowski, Jour. Nucl. Energy 27, 531 (1973).
29. K. Rusek, et al, INDC (POL)-61G, page 10 (1976).
30. A.E. Johnsrud, M.G. Silbert, and H.H. Berchall, Phys. Rev. 116, 927 (1959).
31. A. Paulsen, Ziet., Physik, 205, 226 (1967).
32. F. Rigaud, J.L. Irigaray, and G.Y. Petit, Nucl. Phys. A173, 551 (1971).
33. F. Cvelbar, et al, Nucl. Phys. A130, 401 (1969).

SUMMARY DOCUMENTATION FOR Ni

M. Divadeenam

National Nuclear Data Center
Brookhaven National Laboratory

ABSTRACT

The following neutron and gamma production data are given for Ni in the energy range 1.0×10^{-5} to 20 MeV. (MAT No.1328).

File 1: General description of the evaluation and relevant references.

File 2: Resonance parameters for $^{58,60,62,64}\text{Ni}$ from 1.0×10^{-5} to 690.0 keV.

File 3: Smooth cross sections for total, elastic, total inelastic, inelastic cross sections to 26 discrete levels; the inelastic continuum, $(n,2n)$, $(n,\alpha n')+(n,n'\alpha)$, $(n,pn')+(n,np')$, (n,p) , (n,d) , (n,α) , $(n,2p)$ and capture cross sections. Extracted data for $\bar{\mu}$, ξ , and γ are also included. In addition, Hydrogen, Deterium and Helium production cross sections are generated.

File 4: Angular distributions for elastic and inelastic scattering are given in terms of Legendre Polynomial coefficients in the c.m. system. In particular the direct interaction effects (channel coupling) are considered for the inelastic angular distributions for the two lowest excited states of the even Ni isotopes.

File 5: Secondary neutron energy distribution for the inelastic continuum with precompound effects, $(n,2n)$, $(n,n'\alpha)$, and $(n,n'p)$ reactions are given.

File 12: Multiplicity for gamma-ray production due to capture from 1.0×10^{-5} eV to $1.00 \times 10^{+6}$ eV.

File 13: $(n,x\gamma)$ production cross sections from 1.00×10^{-6} eV to 20 MeV.

File 14: Angular distributions for photons assumed to be isotropic.

File 15: Normalized energy distribution of photons up to $1.00 \times 10^{+6}$ eV and due to non-elastic processes at higher energies.

Introduction

This is almost a completely new evaluation, in particular, the secondary neutron cross sections and angular distributions as well as the secondary neutron energy distribution for the continuum inelastically scattered neutrons have been updated. In addition, the isotopic cross sections for the various (n, particle) cross sections were evaluated to construct the corresponding natural Ni files. Precompound effects were included.

From 1.0×10^{-5} eV to 690.0 keV, the resolved resonance region and the resonance parameters along with the smooth background cross sections have been taken from the ENDF/B-IV Ni evaluation (MAT=1190), which, in turn, was adopted from ENDF/B-III Ni (MAT=1123) evaluation.

The Ni total cross section data of Perey, Love and Kinney extending up to 20 MeV was used to construct smooth cross section file.

File 1: General Comments

A brief summary of the data, along with the references is given. Details will be presented in a report based on this evaluation.

File 2: Resonance Parameters

A complete discussion is presented in Ref. 1. Due to the lack of experimental data (extending up to 690 keV) no resonance parameters for the odd minor isotope ^{61}Ni are given.

File 3: Smooth Neutron Cross Section

(i) Total Cross Section

Both the thin and thick sample data of Perey, Love and Kinney were used to make a spline fit to the experimental cross sections from 0.690-20 MeV. These are new data with an accuracy of $\sim 2\%$. Good agreement is found between the ENDF-IV and $V\sigma_t$.

(ii) Elastic Cross Section

This was obtained by subtracting the non-elastic cross section³⁻¹⁵ from the total. At higher energies the extracted cross sections agree well with the calculated (ABACUS-II; Ref. 16) results.

(iii) Total Inelastic Cross Section

There are extensive data^{41-49,89} on the excitation cross section for the first excited states in^{58,60,62} Ni. These were combined with the available data for the other excited levels ($E_n < 3.5$ MeV) and model (Ref. 50) calculated results for levels, which have no experimental data. These were weighted with isotopic abundances together with the isotopic (n,p), ($n,2n$), ($n,n'p$) + (n,pn'), ($n,\alpha n' + n,n'\alpha$), (n,d) and ($n,2p$) evaluated cross sections and the sum of these partial cross sections was subtracted from the non-elastic cross section to give the total inelastic cross section of the remaining discrete levels and the inelastic continuum. The resulting cross section is designated as the inelastic continuum cross section.

(iv) ($n,2n$) Cross Section

There are extensive data¹⁷⁻²⁷ only for⁵⁸ Ni.* For the other isotopes, model²⁸ calculated excitation functions were normalized to THRESH²⁹ predictions which are based on systematics at 14 MeV neutron energy.

(v) ($n,n'p$) + (n,pn') Cross Section

The⁵⁸ Ni experimental ($n,n'p$) + (n,d) cross section data around 14 MeV were used to normalize the corresponding model²⁸ calculated results. Similar data for the other isotopes were used to normalize the theoretical results. The isotopic contributions to ($n,n'p$) and (n,pn') were combined to give the cross section for Ni.

(vi) Inelastic Cross Section to the Discrete Levels and the Continuum
Experimental data^{41,49,89} including the lastest measurements by

* (cf. Appendix A)

Smith, et al.⁸⁶ were combined with COMNUC⁵⁰ calculated cross sections to the levels listed below:

E(MeV)	J ^π (Isotope)
1.172	2 ⁺ (62)
1.332	2 ⁺ (60)
1.452	2 ⁺ (58)
2.158	2 ⁺ (60)
2.286	2 ⁺ (60)
2.459	2 ⁺ (58)
2.506	2 ⁺ (60)
2.625	2 ⁺ (60)
2.775	2 ⁺ (58)

For the two lowest excited states of even Ni isotopes, JPLX (JUPITOR: Ref. 51), calculated results were joined with the COMNUC results at 10 MeV. COMNUC results were used for the additional 17 levels.

(vii) Capture Cross Section

The corresponding ENDF/IV-B file⁵² was retained without any changes below 1 MeV. COMNUC calculated results were adopted above 1 MeV.

(viii) (n,p) Cross Section

⁵⁸Ni(n,p) cross section was evaluated* using the extensively available data⁵³⁻⁶⁸. Similarly, there are extensive data⁶⁹⁻⁸² on ⁶⁰Ni and an evaluated† smooth curve was drawn to arrive at the evaluated cross section curve. Model calculated cross sections were normalized for the other minor isotopes, when the experimental data were available.

(ix) (n,α), (n,αn') and (n,n'α) Cross Sections

For each isotope the model²⁸ generated (n,α), (n,αn') and (n,n'α) cross sections were added to estimate the corresponding fission spectrum average, which was normalized to Farrar's experimental data.³¹ The resulting factor was used to normalize the model calculated (n,α) and (n,αn') + (n,n'α) cross section components.

* (cf. Appendix B)

† (cf. Appendix C)

x) (n,2p) Cross Section

Model calculated cross sections for ^{58}Ni were adopted for the file assuming that the other Ni isotopes have negligible cross sections due to high Q values.

(xi) Gas Production Cross Sections

Hydrogen, Deterium and Helium Production cross sections were generated from (n,p), (n,n'p) and (n,2p) (n,d) and (n, α) and (n,an') respectively.

(xii) μ , ξ , γ

These were generated using the code DUMMY5.⁸³

File 4: Secondary Neutron Angular Distributions

(i) Elastic Angular Distributions

Evaluated angular distribuitons given in Version IV were adopted. In addition, the recent data by Smith, et al⁸⁹ ($E_n \leq 4$ MeV) were also included. These were fitted with the code CHAD⁸⁴ to obtain Legendre coefficients. Model calculated angular distributions were used above 4 MeV neutron energy to supplement Smith's data.

(ii) Inelastic Angular Distributions

Compound nuclear (COMNUC) and direct inelastic angular distributions (JP1X) were combined for the first two excited states of the even-even isotopes. For the high lying states as well as for the ^{61}Ni levels, only compound nuclear angular distributions were used. CHAD was used to generate the Legendre coefficients.

File 5: Secondary Neutron Energy Distributions

(i) Continuum Inelastic Neutrons

The secondary energy distributions were based on the relevant parameters (extracted from the measured⁹⁰ distributions at 14 MeV) and the model predicted⁸⁴ pre-compound fraction. Both the pre-compound and compound effects were included.

(ii) (n,2n), (n,an') and (n,pn') Neutron Distributions

Code THETA⁸⁵ was used to give the temperature dependent energy distributions.

File 12: Gamma Ray Multiplicities

Gamma ray multiplicities due to Capture are given from 10×10^{-5} eV to 1.0×10^6 eV based on both Maerker's data⁸⁸ and ENDF/B-IV evaluation.

File 13: (n,x γ) Production Cross Section

This is based on the ENDF/B-IV evaluation and covers the energy range from 1.00×10^6 eV to 20 MeV, (cf. ref. 52).

File 14: Photon Angular Distributions

These are assumed to be isotropic.

File 15: Photon Energy Distributions

These are based on files 12 and 13.

REFERENCES

1. R.G. Stieglitz, J.T. Reynolds, C.J. Slavik, C.R. Lubitz, KAPL-M-7156 (1973).
2. F.G. Perey, T.A. Love and W.E. Kinney, CSISRS AN10342 (1973).
3. R.W. Bauer et al, COO-1573-33, 2.
4. H.L. Tailor et al, Phys. Rev. 100, 174 (1955).
5. V.I. Strizhak et al, Sovt. J. At. Energy, 2, 72 (1957).
6. M.T. MacGregor et al, Phys. Rev. 108, 7261 (1957).
7. M. Walt and H. Barschall, Phys. Rev. 93, 1062 (1954).
8. J.R. Beyster et al, Phys. Rev. 98, 1216 (1955).
9. J.R. Beyster et al, Phys. Rev. 104, 1319 (1956).
10. I.A. Korzh et al, Sovt. J. At. Energy, 20, 8, (1966).
11. M.K. Machwe et al, Phys. Rev. 114, 1563 (1959).
12. A.I. Abromov, Sovt. J. At. Energy, 12, 65 (1962).
13. M.V. Paschenik, Geneva Conf. 2, 3 (1955).
14. V.I. Strizhak, et al, JETP. 4, 769 (1957).
15. B. Holmqvist, et al, AE-303 (1967).
16. E.H. Auerbach, ABACUS-2 (Rev.) BNL-65621 (1962).
17. J.D. Hemingway, Jour. Nucl. Energy, 27, 241 (1973).
18. W. Lu and R.W. Fink, Phys. Rev. C4, 1173 (1971).
19. R.C. Barral and M. Silbergeld, Nucl. Phys. A113, 387 (1969).
20. R.C. Barral, SUPH-69-2 (1969).
21. J.K. Temperley, Nucl. Sci. Eng. 32, 195 (1968).
22. M. Bormann, EANDC(E), 66, 42 (1969).
23. A. Paulsen, Nuk, 7, 117 (1965).
24. W.E. Gross et al, Bull. Am. Phys. Soc. 7, 335 (1962).
25. R.N. Glover and Weigold, Nucl. Phys. 29, 309 (1962).
26. R.J. Prestwood and B.P. Bayhurst, Phys. Rev. 121, 1438 (1961).
27. B.P. Bayhurst et al, Phys. Rev. 12, 451 (1975).
28. Uhl's code adapted and modified to run on NNDC PDP-10 at BNL.
29. S. Pearlstein, Jour. Nucl. Energy, 27, 81 (1973).
30. O. Ozer, Modified Version of INTER, BNL-17408 (1972).

31. H. Farrar et al, Private Communication (1973, 1976).
32. W.J. Cross, R.L. Clark, K. Morin, G. Slinn, N.M. Ahmed and K. Beg, AECL 1542, 6 (1962).
33. S.M. Qaim and G. Stocklin, Proc. 8th Symp. on Fusion Tech. Eur 5182E (1974).
34. J.K. Temperley, Nucl. Sc. and Eng. 32, 195 (1968).
35. J.D. Hemingway, Journ. of Nucl. Energy 27, 241 (1973).
36. G.N. Maslov et al, Yad, K, 9, 50 (1972).
37. P.V. March and W.T. Morton, Phil. Mag. 3, 577 (1958).
38. D.L. Allan, Nucl. Phys. 24, 274 (1961).
39. A.V.N. Levikoskii et al, SJNP. 8, 4 (1968).
40. B.C. Spira and J.M. Robson, N.P. 127, 81 (1967).
41. P. Boshung et al, Nucl. Phys. A161, 593 (1971).
42. V.C. Rogers et al, Nucl. Sci. and Eng. 45, 297 (1971).
43. E.S. Konobeevskii et al, IZV, AKAD, NAUK, SSSR 35, 2345 (1971).
44. W.E. Kinney and F.G. Perey, ORNL-4807, (1973).
45. J.H. Towle, Nucl. Phys. A100, 257 (1967).
46. K. Nishimura et al, Nucl. Phys. 70, 421 (1965).
47. D.L. Border et al, Sovt. J. Nucl. Phys. 18, 645 (1964).
48. R.B. Day, Phys. Rev. 117, 1330 (1960).
49. W.L. Rodgers et al, COO-1573-33, 2
50. C.L. Dunford AI-AEC-12931 (1970).
51. JPIX Version of JUPITOR: T. Tamura, ORNL, 4152 (1967).
52. M.R. Bhat, BNL 50435 (1974).
53. D.L. Smith and J.W. Meadows, Trans. Am. Nucl. Soc. 16, 1, (1973).
54. D.L. Smith and J.W. Meadows, Private Communication to M.R. Bhat
55. J.W. Meadows and T.F. Whalen, Phys. Rev. 130 (1963).
56. J.K. Temperely, Nucl. Sci. and Eng. 40, 331 (1970).
57. A. Paulsen and Widera, EANDC(E) 1504, (1972).
58. K. Nakai, H. Gotoh and H. Amano, J. Phys. Soc. Japan, 17, 1215 (1962).
59. J.F. Barry, J. Nucl. Energy Parts A/B, 16, 467 (1962).
60. M. Borman, Z. Naturforsch, 21A, 988 (1966).
61. P. Decowski et al, Nucl. Phys. A112, 513 (1968).

62. R.W. Fink, D. Lu, BAP, 15, 1372 (1970).
63. S. Okumura, Nucl. Phys. 493, 74 (1967).
64. J. Dresler et al, Inst. Nucl. Research (Polish), INR. 1464, 12 (1973).
65. I.L. Preiss and R.W. Fink, NP, 15, 326 (1960).
66. R.N. Glover and E. Weigold, Nucl. Phys. 29, 309 (1962).
67. J.D. Hemingway, Journ. Nucl. Eng. 27, 241 (1973).
68. L. Gonzales et al, Phys. Rev. 120, 1319 (1960).
69. H. Liskien and A. Paulsen, Nucl. Phys. 63, 393 (1965).
70. H. Liskien and A. Paulsen, Nukleonik, 8, 315 (1966).
71. A. Paulsen, Nukleonik 10, 91 (1967).
72. A. Paulsen, Z. Physik 205, 226 (1967).
73. R.S. Storey, W. Jack and A. Ward, Proc. Phys. Soc. 75, 526 (1960).
74. J.D. Hemingway, Jour. Nucl. Energy 27, 241 (1973).
75. V.N. Levkovskii, G.P. Vinitskaya, G.E. Kovilskaya and V.M. Stepanov, Sovt. Jour. Nucl. Phys. 10, 25 (1969).
76. D.L. Allan, Proc. Phys. Soc. A70, 195 (1957).
77. I.L. Preiss and R.W. Fink, Nucl. Phys. 15, 326 (1960).
78. P.V. March and W.T. Morton, Phil. Mag. 3, 577 (1958).
79. Ligensa and W. Greiner, Ann. of Physics 51, 28 (1969).
80. M. Divadeenam and M.R. Bhat, BAPS. 21, 536 (1975).
81. A.K. Volter et al, IZV 26, 1079 (1962).
82. A.M. Bormann et al, EANDC(E), 66, 42 (1966).
83. R.R. Kinsey, DUMMY5, Private Communication.
84. NUCHAD, Modified Version of CHAD: R.F. Berland (NAA-SR-11231 (1965).
85. C.R. Dunford, THETA, Private Communication (1977).
86. M. Blann, OVERLAID ALICE, Univ. of Rochester Report COO-3494-29.
87. M. Divadeenam and M.R. Bhat, Proceedings of the Int. Conf. on the Int. of Neutrons with Nuclei, I, 1348 (1976).
88. R.E. Maerker, ORNL-TM-5203-ENDF-227 (1976), and Private Communication.
89. A.B. Smith et al, CSISRS AN11680.
90. D. Hermsdorf et al, KE. 16, 252 (1973).

28-Ni-0
MAT 1328

APPENDIX A

$^{58}\text{Ni}(\text{n},2\text{n})$ EVALUATION FOR ENDF/B-V

$^{58}\text{Ni}(\text{n},2\text{n})$ $Q = 12.415$ MeV

Since the last evaluation of $^{58}\text{Ni}(\text{n},2\text{n})$ reaction only one set of new measurements were done by Bayhurst, et al.¹⁷ They used the radio chemical method for measuring the cross section. $^{27}\text{Al}(\text{n},\alpha)$ reaction cross section was measured to determine the fluency. $^{58}\text{Ni}(\text{n},2\text{n})$ measured cross sections were renormalized to the ENDF-IV $^{27}\text{Al}(\text{n},\alpha)$ cross section.

There are extensive measurements (in addition to the one referred to above) on the $^{58}\text{Ni}(\text{n},2\text{n})$ cross section. Paulsen and Liskien and Borman, et al, measured over a wide energy range. Details of their data and other data has been discussed by Bhat¹⁸ in his evaluation.

We like to point out that some of the cross sections which required renormalization have been corrected for the ENDF-IV cross sections. The exception being that of Prestwood and Bayhurst who measured with respect to $^{238}\text{U}(\text{n},\text{f})$. The $^{238}\text{U}(\text{n},\text{f})$ cross sections are not listed in their paper for use in renormalization.

Paulsen and Liskien and Borman's data are in good agreement with each other below 16 MeV, they diverge above this energy with the Paulsen data being larger than the other set.

There are three other sets that extend up to 20 MeV: one by Prestwood and Bayhurst, the second by Bayhurst, et al, and the third one by Jeronymo, et al. These data agree with the general trend up to 14 MeV; above this energy they are very high. Particularly that of Bayhurst, et al, which are recent measurements. From their paper it is not clear whether they had done any multiple scattering corrections, etc.

Jeronymo data are too low to be considered for evaluation. Similarly Lu and Fink, Ross, et al, and Csikai, et al, measure around 14 MeV. All of these three measured cross sections are higher than the rest. They are not given any weight in the evaluation.

Glover and Weigold's measurement follow the general trend of other data.

The evaluated curve was drawn following the general trend of the Borman data at higher energies and lying in between Paulsen-Liskien and Borman data. Near the threshold HF calculated values were used to draw the curve. Essentially, the present evaluation is the same as the earlier one, done by Bhat, except near the threshold. Bibliography of the data used in the evaluation are given in the reference.

<u>E-range (MeV)</u>	<u>Method</u>	<u>Renormalized</u>	<u>Standard</u>	<u>Reference</u>
16.2 - 20	Radiochemical	yes	A (n,α)	Bayhurst
12.9 - 19.6	Activation	-	Absolute	Paulsen-Liskien
12.9 - 19.6	Activation	not required	Hydrogen	Borman
13.7 - 14.8	Activation	-	Absolute	Temperley
13.5 - 19.8	Radiochemical	measured $^{238}\text{U}(n,f)$ not available	$^{238}\text{U}(n,f)$	Prestwood Bayhurst
13.8 - 14.9	Activation	-	Absolute	Glover-Weigold

Errors:

<u>Ni(n,2n)</u>	<u>Errors</u>
12. - 14	10%
14. - 15	10%
15 - 17	7%
17 - 20	12%

REFERENCES

1. A. Paulsen and H. Liskien *Nuk* 7, 117 (1965).
2. M. Bormann, F. Dreyer and V. Zielinski *EANDC (E)* 66, 42 (1966).
3. R.J. Prestwood and B.P. Bayhurst, *Phys. Rev.* 121, 1438 (1961).
4. J.M.F. Jeronymo, G.S. Marri, J. Olkowsky, A. Sadeghi and G.F. Williamson, *Nucl. Phys.* 47 157 (1963).
5. Wen-deh Lu and R.W. Fink, *Phys. Rev.* C4, 1173 (1971).
6. W.G. Cross, R.L. Clarke, K. Morin, G. Slinn, N.M. Ahmed and K. Beg, *Bull. American Phys. Soc. Ser. II*, 7, 335 (1962).
7. J. Csikai *EANDC-50*, 2 (1965), *Conf. on Study of Nuclear Structure with Neutrons, Antwerp*, paper 102 (1965).
8. M.D. Goldberg, S.F. Mughabghab, B.A. Magurno and V.M. May, BNL-325, Second Ed., Supplement No. 2, II-A, (1966).
9. J.K. Temperley, *Nucl. Sci. & Eng.* 32, 195 (1968).
10. R.C. Barrall, M. Silbergeld and D.G. Gardner, *Nucl. Phys.* A138, 387 (1969).
11. R.C. Barrall, M. Silbergeld and D.G. Gardner SUPH-69-2 (1969).
12. R.C. Barrall, J.A. Holmes and M. Silbergeld AFWL-TR-68-134 (1969), CSIRS AN/SN-10022/14.
13. L.A. Rayburn, *Phys. Rev.* 122, 168 (1961).
14. I.L. Preiss and R.W. Fink, *Nucl. Phys.* 15, 326 (1960).
15. E.T. Bramlett and R.W. Fink, *Phys. Rev.* 131, 2649 (1963).
16. R.N. Glover and E. Weigold, *Nucl. Phys.* 29, 309 (1962).
17. B.P. Bayhurst, J.S. Gilmore, R.J. Prestwood, J.B. Wilhelmy, N. Jarmie, B.H. Erkkila and R.A. Hardekopf, *Phys. Rev.* 12, (1975).
18. M.R. Bhat, in *ENDF/B-IV Dosimetry File*, Edited by B. Magurno, BNL-NCS-50446 (1975).

APPENDIX B

$^{58}\text{Ni}(\text{n},\text{p})$ EVALUATION FOR ENDF/B-V

$^{58}\text{Ni}(\text{n},\text{p})$ Reaction $Q = .3947$ MeV

The previous $^{58}\text{Ni}(\text{n},\text{p})$ evaluation was done by Schenter.¹ In the low energy region, his evaluation closely follows the experimentally measured values of Smith and Meadows,² in that local fluctuations of the cross section were retained in the evaluated curve. In addition, the 6-13 MeV range had only four measured points. However, for the present evaluation, extended measurements by Smith and Meadows³ are available.

The data on $^{58}\text{Ni}(\text{n},\text{p})$ cross section is extensive, and of reliable quality. This reaction is used in dosimetry applications, and also treated as a secondary standard for measuring other neutron induced reactions.

The most extensive sets of data on $^{58}\text{Ni}(\text{n},\text{p})$ reaction are:

1. Smith and Meadows ^{2,3}	0.44 - 10 MeV
2. Meadows and Whalen ⁴	1.04 - 2.67 MeV
3. Barry, et al ⁸	1.6 - 15 MeV
4. Paulsen and Widera ⁶	1-2 and 12.7 - 16.4 MeV
5. Okumura ¹⁵	13.4 - 15 MeV
6. Borman ⁹	13 - 19.6 MeV

In addition, there are other measured data sets at a few energy points ranging from 2-15 MeV.

For the purpose of evaluation, we have looked at the entire experimental data in detail in the following energy ranges.

0.4 - 1.0 MeV
1.0 - 2.0 MeV
2.0 - 4.0 MeV
4.0 - 6.0 MeV
6.0 - 10. MeV
10.0 - 12.7 MeV
<u>Gap - no data</u>
12.7 - 15.0 MeV
15.0 - 20.0 MeV

0.4 - 1.0 MeV

In this low energy region, only the data of Smith and Meadows³ is available. There are some deviations from the expected¹ smooth energy dependence of the low energy (n,p) cross section. The 0.5 MeV and 1 MeV cross section values were determined from the simple prescription (given in Fermi's book) for exothermic neutron-induced and outgoing charge-particle reactions. Most of the experimental points at these low energies follow this prescription.

1.0 - 2.0 MeV

In this energy range, Smith-Meadows,³ Meadows-Whalen,⁴ Paulsen-Widera,⁶ Temperley⁵ and Nakai⁷ data are used. Temperley points are too high compared to the general trend of the Smith-Meadows and Meadows-Whalen data. Furthermore, Nakai's points have very large errors. Temperley's and Nakai's data were not considered in the evaluation.

2.0 - 4.0 MeV

There are several data sets in this energy range. Smith Meadows data covers most of the range Gonzalez's²⁰ points, and some of the Konijn's⁹ points are high and a few of the latter ones are low beyond 3.5 MeV from the general trend of most of the data points, while Nakai's points are low. Some structure (fluctuation) is evident in the 2.5-4 MeV range 3.0 MeV, and 3.25 MeV in the Smith- Meadows data. For the purpose of evaluation, it was decided to draw a smooth curve to indicate the increasing trend of the experimental points. Schenter's evaluation retained all of the details of local fluctuations.

4 - 6 MeV

Three data sets cover this energy range -there is some paucity of the data which suggests some fluctuations, however, a smooth curve indicating the increasing trend of the data is drawn as an evaluated curve. As in the other energy regions considered, the ENDF/B-IV evaluation retains most of the observed structure in the evaluated curve.

6 - 10 MeV

As in the previous energy region, three data sets span this energy

range. Barry's points are higher than that of Smith-Meadows, whereas Smith-Meadows has some point scatter. For the evaluation purpose a smooth curve with a value of 600 mb at 8.5 MeV is suggested as the evaluated curve. Schenter's curve is higher than the present evaluation.

10 - 12.7 MeV

Unfortunately, no experimental data exists in this energy region.

12.7 - 15 MeV

We note that there are plenty of experimentally measured σ_{np} cross sections in the 14-15 MeV range. Point scatter is very large in the measured cross sections. Decowski's points are way high - above the general trend of the other points in this energy region. A curve through most of the points in the 14-15 MeV range is drawn in this region. The choice to draw an evaluated curve is not unique.

15 - 20 MeV

Two data sets cover this energy range, that of Paulsen-Widera and Borman⁹ extending only up to 18 MeV. A curve through midway between these two sets is drawn. This is justified on the basis that HF calculations with 0.3 pre-compound fraction predicts a similar trend.

Errors:

$^{58}\text{Ni}(n,p)$	errors:
0 - 1 MeV	25%
1 - 2 MeV	10%
2 - 4 MeV	9%
4 - 6 MeV	5%
6 - 10 MeV	5%
10 - 12.7 MeV	- (10%)
12.7 - 15 MeV	15%
15.0 - 20 MeV	13%

REFERENCES

1. R. Schenter, in ENDF/B-IV Dosimetry File, Edited by B. Magurno, BNL-NCS-50446 (1975).
2. D.L. Smith and J.W. Meadows, Trans. Am. Nucl. Soc. 16, 1 (1973).
3. D.L. Smith and J.W. Meadows, private communication to M.R. Bhat.
4. J.W. Meadows and T.F. Whalen, Phys. Rev. 130, (1963).
5. J.K. Temperley, Nucl. Sci. and Eng. 40, 331 (1970).
6. A. Paulsen and Widera, EANDC(E) 1504, (1972).
7. K. Nakai, H. Grotob and H. Amano, J. Phys. Soc. Japan, 17, 1215 (1962).
8. J.F. Barry, J. Nucl. Energy Parts A/B, 16, 467 (1962).
9. J. Konijn and A. Lauber, Nucl. Phys. 48 191 (1963).
10. J.J. Van Lueff, N.P. 24, 340 (1961).
11. M. Borman, Z. Naturforsch, 21A, 988 (1966).
12. R.C. Barral, Nucl. Phys. A138, 387 (1969).
13. G.N. Maslov, F. Nasyrov and Paslikin, YK-9-50 (1972).
14. P. Decowski, et al, Nucl. Phys. A112, 513 (1968).
15. R.W. Fink, BAP 15, 1372 (1970).
16. W. Cross, R.L. Clark, K. Morin, G. Slinn, N.M. Ahmed and K. Beg, AECL 1542 (1962) and BAP 7, 335 (1962).
17. S. Okumura, Nucl. Phys. A93, 74 (1967).
18. J. Dresler, et al, INR 1464, 12 (1973).
19. I.L. Preiss and R.W. Fink, Nucl. Phys. 15, 326 (1960).
20. R.N. Glover and E. Weigold, Nucl. Phys. 29, 309 (1962).
21. J.D. Hemingway, JNE, 27, 241 (1973).
22. L. Gonzales, et al, Phys. Rev. 120, 1319 (1960).

APPENDIX C

$^{60}\text{Ni}(\text{n},\text{p})$ EVALUATION FOR ENDF/B-V

$^{60}\text{Ni}(\text{n},\text{p})$ $Q = 2.0411 \text{ MeV}$

Extensive data for this reaction is measured by Paulsen and Liskien. The covered energy range is 6-19.6 MeV. In addition to this set of data, there are some spotty measurements around 14 MeV. Except Allan's the rest of the 14 MeV data is high compared to the general trend indicated by the Paulsen and Liskien data.

Bhat¹ has done the previous (ENDF/B-IV version) $^{60}\text{Ni}(\text{n},\text{p})$ evaluation. The present evaluation differs from that of Bhat's in two respects.

1. The low energy (< 6 MeV) part of the $^{60}\text{Ni}(\text{n},\text{p})$ cross section was extrapolated with the help of the HF predicted (n,p) cross section from threshold to 6 MeV neutron energy.
2. The dominant structure suggested by Paulsen-Liskien set is retained in the evaluated curve. Justification for such a procedure is based on good comparison with Liqensa and Grieners p-h calculations¹⁴ in the neighboring compound nucleus ^{60}Ni .

Errors:

$^{60}\text{Ni}(\text{n},\text{p})$

Range	Error
Thresh - 6.0 MeV	5%
6.0 - 8.0 MeV	11%
8.0 - 9.5 MeV	9%
9.5 - 1.0 MeV	9%
10.0 - 12.5 MeV	9%
12.5 - 15.0 MeV	7%
15 - 20.0 MeV	8%

28-N1-0
MAT 1328

REFERENCES

1. M.R. Bhat, in ENDF/B-IV Dosimetry File, Edited by B. Magurno, BNL-NCS-50446 (1975).
2. H. Liskien and A. Paulsen, Nucl. Phys. 63, 393 (1965).
3. H. Liskien and A. Paulsen, Nukleonik, 8, 315 (1966).
4. A. Paulsen, Nukleonik 10, 91 (1967).
5. A. Paulsen, Z. Physik 205, 226 (1967).
6. W.G. Cross, R.L. Clarke, K. Morin, G. Slinn, N.M. Ahmed and K. Beg, EANDC (Can)-16 (1963).
7. D.L. Allan, Nucl. Phys. 24, 274 (1961).
8. R.S. Storey, W. Jack, and A. Ward, Proc. Phys. Soc. 75, 526, (1960).
9. J.D. Hemingway, Jour. Nucl. Energy 27, 241 (1973).
10. V.N. Levkovskii, G.P. Vinitskaya, G.E. Kovilskaya and V.M. Stepanov, Sov. Jour. Nucl. Phys. 10, 25 (1969).
11. I.L. Preiss and R.W. Fink, Nucl. Phys. 15, 326 (1960).
12. P.V. March and W.T. Morton, Phil. Mag. 3, 577 (1958).
13. D.L. Allan, Proc. Phys. Soc. A70, 195 (1957).
14. Ligensa and W. Greiner, Ann. of Physics 51, 28 (1969).

Summary Documentation

Copper Evaluation

ENDF/B-V MAT 1329

C. Y. Fu

Oak Ridge National Laboratory
Oak Ridge, Tennessee

August 1978

PART I. REVISIONS FOR ENDF/B-V

File 3, MT=1

Total cross sections from 0.2 to 2.0 MeV were replaced by the high-resolution cross sections measured by Perey.¹ These data seemed to be of the highest quality available.

File 3, MT=2

Elastic scattering cross sections were obtained by subtracting the nonelastic from the total.

File 3, MT=3

Nonelastic cross sections were changed due to revisions in (n,p), (n,α), (n,np), and (n,nd) cross sections.

File 3, MT=22

(n,nd) cross sections were changed due to revisions in both isotopes. ^{63}Cu (n,nd) cross sections were based on our calculated curve² normalized at 14.8 MeV to the helium production cross sections for ^{63}Cu measured by Grimes and Haight³ with fixed ^{63}Cu (n,α) cross sections (see File 3, MT=107). ^{65}Cu (n,nd) cross sections were based on the data of Santry and Butler.⁴

File 3, MT=28

(n,np) cross sections were modified due to revisions in both isotopes. ^{63}Cu (n,np) cross sections were based on our analysis⁵ of the proton spectrum from 14.8-MeV neutrons incident on ^{63}Cu measured by Grimes and Haight.³ ^{65}Cu (n,np) cross sections below 12 MeV were based

on the calculation of Mann;⁶ from 12 to 20 MeV Mann's calculation was slightly modified to reproduce the 14.8-MeV hydrogen production cross section of ⁶⁵Cu measured by Grimes and Haight³ with fixed ⁶⁵Cu(n,p) cross sections (see File 3, MT=103).

File 3, MT=102

(n,γ) cross sections were thinned to 1%, reducing the number of energy entries from 408 to 48. This automatically shortened Files 3-1, 3-2, and 3-3.

File 3, MT=103

(n,p) cross sections were changed due to revision of ⁶³Cu(n,p) cross sections, which were based on model analysis⁵ of the proton spectrum from 14.8-MeV neutrons incident on ⁶³Cu measured by Grimes and Haight.³ ⁶⁵Cu(n,p) cross sections were taken from the evaluation by Drake and Fricke⁷ which has adequate data basis.

File 3, MT=107

⁶³Cu(n,α) cross sections were taken from ENDF/B-IV dosimetry file MAT 6411.⁸ ⁶⁵Cu(n,α) cross sections below 10 MeV were taken from the calculation by Mann.⁶ From 10 to 20 MeV Mann's calculation was altered to reproduce the 14.8-MeV helium production cross section measured by Grimes and Haight³ with fixed ⁶⁵Cu(n,α) cross sections (see 3-22). File 3 MT=107 and File 3 MT=22 together yield a helium production cross section of 51 mb at 14.8 MeV for natural copper, in good agreement with a measured value of 52 ± 4 mb by Farrar *et al.*⁹

File 12, MT=102

Capture gamma-ray multiplicities from 0.2 to 1.25 MeV were revised according to the measurement by Chapman¹⁰ and File 3 MT=102. File 15 MT=102 two energy distributions of the secondary gamma rays from capture for incident neutron energies from 0.2 to 1.25 MeV were added.¹⁰ In the previous evaluation, thermal capture gamma rays were used in the above energy range.

References for Part I

1. F. G. Perey, Oak Ridge National Laboratory, private communication (1977).
2. C. Y. Fu and F. G. Perey, J. Nucl. Mater. 61, 153 (1976).
3. S. M. Grimes and R. C. Haight, Lawrence Livermore Laboratory, private communication (1977).
4. D. C. Santry and J. P. Butler, Can. J. Phys. 44, 1153 (1965).
5. C. Y. Fu, ORNL-TM (to be published).
6. F. M. Mann, Hanford Engineering Development Laboratory, private communication (1977).
7. M. K. Drake and M. P. Fricke, Science Applications Inc., DNA-3356F (1974).
8. H. Alter, in ENDF/B-IV Dosimetry File, Ed. B. A. Magurno, BNL-NCS-50446, ENDF-216 (1975).
9. H. Farrar et al., Atomics International, private communication, (1977).
10. G. T. Chapman, Oak Ridge National Laboratory, ORNL-TM-5215 (1976).

PART II. SUMMARY FOR ENDF/B-IV (M. K. DRAKE AND M. P. FRICKE, 1974)

File 2, MT=151

Resonance parameters and File 3 cross sections below 30 keV were taken from ENDF/B-III¹ which was based on BNL-325.²

File 3, MT=1

Between 30 keV and 100 keV, the total cross sections measured by Garg *et al.*³ were used. In this energy range there was considerable structure in the experimental data, but it was not measured well enough to obtain resolved resonance parameters. In the energy region from 100 keV to 1.5 MeV, the ANL results obtained by Meadows and Whalen⁴ were used. In the upper portion of this energy range (1.2 to 1.5 MeV) the experimental data were averaged over 200 keV energy bands since the variations in the experimental data appeared to be more statistical than structure in cross section.

Very poor quality data were available for the region from 1.5 to 2.3 MeV.^{5,6} A smooth curve was drawn for the total cross section. The curve did not go through the average of the data; rather the curve was drawn to fit the better data below 1.5 MeV and above 2.3 MeV. Between 2.3 and 12 MeV, a smooth curve was drawn through the Foster and Glasgow⁷ data. An average of the data measured by Foster and Glasgow,⁷ Albergotti and Ferguson,⁸ and Robinson, *et al.*⁹ were used for neutron energies between 12 and 15 MeV. Above 15 MeV a smooth and slowly decreasing curve was drawn through the available data.¹⁰⁻¹³

File 3, MT=2

The elastic scattering cross section was obtained by subtracting the non-elastic cross section from the evaluated total cross section. The resulting cross section was compared to the available experimental data for elastic scattering. In the energy region from 0.3 to 4.0 MeV, the evaluated cross section agreed very well with the available measurements.¹⁴⁻¹⁷ Between 4 and 8 MeV, the evaluated curve was slightly higher than the measured data of Holmqvist.¹⁷

File 3, MT=3

Below 600 keV, the non-elastic cross section was the same as the radiative capture cross section. Between 600 keV and 5 MeV, the non-elastic cross sections for the isotopes were obtained by summing the components. Above 5 MeV, the non-elastic cross sections for the isotopes were taken to be the same as the element which was evaluated by drawing a smooth curve through the existing experimental data.¹⁸⁻²⁷ In the energy range from 6 to 9 MeV, there was a discrepancy between the available experimental data for elastic scattering¹⁷ and non-elastic cross section.^{18,20} The evaluated cross section for both the elastic and non-elastic cross sections were slightly higher than the experimental data. This was done to preserve the total cross section which was measured more accurately.

File 3, MT=16

Many sets of (n,2n) cross sections were available for ^{63}Cu . Some were absolute and others were relative. The relative measurements²⁸⁻³² were re-normalized to 0.568 barns at 14.7 MeV, consistent with the $^{65}\text{Cu}(n,2n)$ cross section at this energy. The absolute values³³⁻³⁶ along with the results from 14 MeV measurements and the re-normalized cross section values were used to obtain the recommended cross section.

The $^{65}\text{Cu}(n,2n)$ cross section was taken from the ENDF/B dosimetry library. This evaluation was based on measurements by Santry and Butler,³⁷ Prestwood and Bayhurst,³⁸ Paulsen and Liskien,³⁹ Rayburn,³¹ and Bormann and Lammers.³⁶

File 3, MT=28 and MT=103

Very little experimental data were available for $^{63}\text{Cu}(n,p)$ or $^{63}\text{Cu}(n,np)$. These cross sections were obtained from statistical model calculations. The calculated results were normalized at 14.5 MeV to the sparse experimental data.⁴⁰⁻⁴³

The (n,p) cross section for ^{65}Cu has been measured from threshold (about 3 MeV) to 20 MeV. The data of Santry and Butler³⁷ were used for the complete energy range. The magnitude of the cross section near 14 MeV was well established by several other measurements. Few and widely

disagreeing values have been measured for the (n,np) cross section. The same procedure for $^{63}\text{Cu}(n,np)$ was used for $^{65}\text{Cu}(n,np)$ cross section.

File 3, MT=22 and MT=107

The $^{63}\text{Cu}(n,\alpha)$ cross section was taken from the ENDF/B dosimetry file. This evaluation was based on the data of Paulsen and Liskien.⁴⁴ The $(n,n\alpha)$ cross section for ^{63}Cu was based on a statistical model calculation which was normalized to an experimental value at 14.8 measured by Irfan and Jack.⁴⁵

The (n,α) cross section for ^{65}Cu was based on a statistical model calculation and the calculated curve was normalized to the available experimental data⁴⁶⁻⁴⁸ at 14 MeV. The $(n,n\alpha)$ cross section was based on the experimental data of Santry and Butler,³⁷ Bramlitt and Fink,⁴⁶ and Kantele and Gardner.⁴⁹

File 3, MT=102. Radiative Capture Cross Section

Above 30 keV, the radiation capture cross section was obtained by evaluating this cross section for the isotopes. Between 30 keV and 3 MeV, the $^{63}\text{Cu}(n,\gamma)$ cross section was based on the experimental data of Dovbenko et al.⁵⁰ and Zaikin et al.⁵¹ The recommended curve was drawn slightly higher than the Dovbenko data and lower than the Zaikin data. At 14 MeV, the curve was drawn through Perkin⁵² and a recent Columbia value.⁵³

The $^{65}\text{Cu}(n,\gamma)$ cross section curve was drawn through 46 mb at 25 keV, which was an average of several mono-energetic measurements between 20 and 25 keV. Above 30 keV, the recommended curve was drawn on the low side of values measured by Tolstikov⁵⁴ and Stavisskii and Tolstikov.⁵⁵ Between 600 keV and 3 MeV, the data measured by Zaikin et al. were used.

File 3, MT=4, and MT=51 to 91. Inelastic Scattering Cross Sections

The inelastic scattering cross section was made up of 11 discrete levels and a continuum. Several sets of inelastic scattering and gamma-ray production cross section measurements were used to obtain the level excitation cross sections for neutron energies up to 1.5 MeV^{14,56-59} for the 0.67- and 0.912-MeV levels in ^{63}Cu and the 0.77 and 1.115 MeV levels in ^{65}Cu . From 5.5 to 8 MeV, the data of Kinney⁶⁰ were used. Extrapolation to other energies was based on Helene and Dwuck calculations.

File 4, MT=2

Angular distributions for secondary neutrons from elastic scattering were taken to be isotropic below 100 keV. Between 100 and 600 keV the data of Lane, *et al.*⁶¹ were used. Between 600 keV and 1.2 MeV, the data measured by Cox⁶² were used and between 1.5 and 8 MeV the measurement made by Holmqvist¹⁷ was used. Near 14 MeV the results from several measurements were used.⁶³⁻⁶⁵ From 8 to 14 MeV and above 16 MeV, the angular distributions were calculated using the Helene and Dwinsk codes.

File 4, MT=16 to 91

Angular distributions for neutrons from inelastic level reactions were obtained from the Helene code (compound nucleus part) and the Dwinsk code (direct interaction part). Calculations were made for the first three levels in each isotope. There was reasonably good agreement between the calculated distributions for the 0.77 and 1.115 MeV levels at 2.33 MeV and a measurement by Rogers *et al.*⁶⁶ All other levels, the continuum, and all other neutron producing reactions were assumed to have isotropic distributions in the C.M. system.

File 5, MT=16 to 91

The energy distributions for inelastic scattering continuum (MT=91) and (n,2n) (MT=16) were based on the statistical model. An effective nuclear temperature of 1.02 MeV at 14.1 MeV was used. The effective nuclear temperature of the second neutron for the (n,2n) reaction was 0.4 MeV at 14 MeV.

File 12, MT=102

The multiplicities for radiative capture gamma rays were taken from a thermal neutron measurement made by Orphan *et al.*⁶⁷

File 13, MT=16 and MT=102

(n,n γ) and (n,2n γ) gamma-ray production cross sections were obtained from SPEC-10 calculations fitting data of Jcnsson⁶⁸ and Dickens.⁶⁹

29-Cu-0
MAT 1329

File 15, MT=3 and MT=102

Orphan et al.⁶⁷ for capture gamma rays; Dickens et al.⁶⁹ for gamma rays from all reactions above 1.25 MeV.

References for Part II

1. J. M. Otter, et al., Report AI-AEC-1271 (1968).
2. M. D. Goldberg, et al., BNL-325, 2nd Ed., Suppl. 2, Vol. IIA (1966).
3. J. B. Garb, J. Rainwater, and W. W. Havens, Jr., Report EANDC(US)-54L (1964).
4. J. W. Meadows and J. F. Whalen (ANL), private communication (1972).
5. M. N. Nikolayev, et al., Phys. of Fast and Intermediate Reactors, Vol. I (1961).
6. D. W. Miller, et al., Phys. Rev. 88, 1042 (1952).
7. D. G. Foster, Jr. and D. W. Glasgow, Phys. Rev. 3, C576 (1971).
8. J. C. Albergotti and J. M. Ferguson, Nucl. Phys. 82, 652 (1966).
9. W. K. Robinson, et al., American J. Phys. 37, 482 (1969).
10. P. H. Bowen, et al., Nucl. Phys. 22, 640 (1960).
11. J. M. Peterson, et al., Phys. Rev. 120, 521 (1960).
12. R. B. Day and R. L. Henkel, Phys. Rev. 92, 358 (1958).
13. M. Mazari, et al., Phys. Rev. 100, 972 (1955).
14. A. B. Smith, et al., Phys. Rev. 135, 76 (1964).
15. I. A. Korzh, et al., At. En. 16, 260 (1964).
16. L. Ya. Kasakova, et al., Conf. on Nuclear Structure Study with Neutrons, p. 200, Antwerp (1965).
17. B. Holmqvist, Arkiv Fysik 38, 403 (1968).
18. J. R. Beyster, et al., Phys. Rev. 104, 1319 (1956).
19. H. L. Taylor, et al., Phys. Rev. 100, 174 (1955).
20. W. P. Ball, et al., Phys. Rev. 110, 1392 (1958).
21. T. W. Bonner and J. C. Slattery, Phys. Rev. 113, 1088 (1959).
22. G. M. Haas and P. L. Okhuyzen, Phys. Rev. 132, 1211 (1963).
23. D. D. Phillips, et al., Phys. Rev. 88, 600 (1952).
24. M. H. MacGregor, et al., Phys. Rev. 108, 726 (1957).
25. D. Didier, et al., Report EANDC(E) - 49L (1963).
26. A. Chatterjee and A. M. Ghose, Phys. Rev. 161, 1181 (1967).
27. Yu. G. Degtyarev and V. G. Nadtochii, At. En. 11, 397 (1961).
28. D. R. Kohler and W. L. Alford, Report AOMC-RR-62-1 (1969).
29. A. V. Cohen and P. H. White, Nucl. Phys. 1, 73 (1956).
30. J. C. Csikai and G. Peto, Actaphys. Acad. Sci. Hungaricae 23 87 (1967).

31. L. A. Rayburn, Phys. Rev. 130, 731 (1963).
32. R. N. Glover and E. Weigold, Nucl. Phys. 29, 309 (1962).
33. W. E. Thomson and J. M. Ferguson, Phys. Rev. 118, 228 (1960).
34. M. Bormann, et al., Z. Physik 166, 477 (1962).
35. H. Liskien and A. Paulsen, J. Nucl. Energy A/B 19, 73 (1965).
36. M. Bormann and B. Lammers, Nucl. Phys. A130, 195 (1969).
37. D. C. Santry and J. P. Butler, Can. J. Phys. 44, 1183 (1966).
38. R. J. Prestwood and B. P. Bayhurst, Phys. Rev. 121, 1438 (1961).
39. A. Paulsen and H. Liskien, Nukleonik 7, 117 (1965).
40. D. L. Allan, Nucl. Phys. 24, 274 (1961).
41. R. S. Storey, et al., Proc. Phys. Soc. 75, 526 (1960).
42. L. Colli, et al., Nuovo Cimento 13, 730 (1959).
43. D. L. Allan, Proc. Phys. Soc. 70, 195 (1957).
44. A. Paulsen, Nukleonik 10, 91 (1967).
45. M. Irfan and W. Jack, Proc. Phys. Soc. 81, 808 (1963).
46. E. T. Bramlett and R. W. Fink, Phys. Rev. 131, 2649 (1963).
47. I. L. Priess and R. W. Find, Nucl. Phys. 15, 626 (1960).
48. D. L. Claytor, Dissertation Abstr. 30B, 2850 (1969).
49. J. Kantele and D. G. Gardner, Nucl. Phys. 35, 353 (1962).
50. A. G. Dovbenko, et al., Report INDC-260 E, p. 11 (1969).
51. G. G. Zaikin, et al., At. En. 25, 526 (1968).
52. J. L. Perkin, Proc. Phys. Soc. 72, 505 (1958).
53. M. Stamatelatos, private communication (1972).
54. V. A. Tolstikov, et al., At. En. 17, 505 (1964).
55. Yu. Ya. Stavisskii and V. A. Tolstikov, At. En. 10, 508 (1961).
56. N. P. Glazkov, At. En. 15, 416 (1963).
57. A. B. Tucker, et al., Phys. Rev. 137, 1181 (1965).
58. B. Holmqvist and T. Wiedling, Arkiv Fysik 35, 71 (1967).
59. K. Nishimura, et al., Nucl. Phys. 70, 421 (1965).
60. W. E. Kinney, ORNL-4908 (1974).
61. R. O. Lane, et al., Ann. Phys. 12, 135 (1961).
62. S. A. Cox, Bull. Am. Phys. Soc. 8, 478 (1963).
63. J. H. Coon, et al., Phys. Rev. 111, 250 (1958).
64. S. Berko, et al., Nucl. Phys. 6, 210 (1958).

29-Cu-0
MAT 1329

65. B. Ya. Guzhovski, At. En. 11, 395 (1961).
66. W. L. Rogers, et al., Report COO-1573-33 (1967).
67. V. J. Orphan, et al., Report GA-10248 (1970).
68. B. Jonsson, et al., Arkiv Fysik 39, 295 (1969).
69. J. K. Dickens et al., ORNL-4840 (1973).

SUMMARY DOCUMENTATION FOR THE KRYPTON ISOTOPES

A. Prince

National Nuclear Data Center

Brookhaven National Laboratory

Reviewed by R. Schenter (HEDL) May 1978

I. Introduction

The major differences between the ENDF/B-IV evaluation and ENDF/B-V, are related to the recent experimental resonance parameter data of Block et al.² New data on the level schemes of the various isotopes and residual nuclei resulting from neutron interactions also prompted a more detailed treatment of the various reaction cross sections. The evaluation covers all significant possible neutron-induced reactions from 10^{-5} ev to 20.0 MeV.

The isotopes and their corresponding MAT numbers are given below for ENDF/B-V. A capsule summary is given in the Appendix.

<u>Isotope</u>	<u>MAT</u>
78Kr	1330
80Kr	1331
82Kr	1332
83Kr	1333
84Kr	1334
86Kr	1336

2.0 RESONANCE REGION

78Kr MAT (10^{-5} ev to 865.0 ev)

The recent experimental data of Block et al.,² were used for calculating the cross section and resonances integral in this energy region. Block et al., concluded that the ^{78}Kr and ^{80}Kr form a doublet around $E = 106.0$ ev, an assumption that was made in ENDF/IV. In addition, since neither Block² nor Mann and Watson³ could definitely assign the 640-eV level to any particular isotope, although they designated the possibilities to be ^{78}Kr , ^{80}Kr ,^{1,3} and a doublet in ^{82}Kr ,² this resonance was used in both ^{78}Kr and ^{80}Kr .

A negative resonance at $E_R = -120.6$ ev produced a thermal capture cross section.

$$\sigma(0.0253 \text{ ev}) = 4.85 \text{ b}$$

which compares favorably with the experimental

$$\sigma(0.0253 \text{ ev}) = 4.7 \pm 0.68 \text{ b.}^{4,5}$$

There are no experimental data for the absorption resonance integral for ^{78}Kr . The calculated value, based on the resonance parameters given in Table 1, is $I_{ab}(E_{cutoff} = 0.5 \text{ ev}) = 23.67 \text{ b}$. Block et al., estimated that $I_{ab} = 20.0 \pm 1.0 \text{ b}$ between 20.0 and 1200 ev. Both these values are about five times as large as the value quoted in Ref. 6, the reason being that in Ref. 6, only the 640.0-eV resonance was used.

36-Kr-78/86

MAT 1330+

The potential scattering cross section was estimated to be 7.00 b on the basis of several measurements ranging from 6.2 ± 0.1 b⁷ to 7.61 ± 0.04 b⁸ (also see Refs. 6 and 9) for Kr(Nat).

^{80}Kr MAT 1331 (10⁻⁵ eV to 1.0 keV)

Use of the resonance parameters shown in Table 1, where a bound level is located $E = -118.0$ eV, yielded a thermal capture cross section $\sigma_{ny} = 11.74$ b, which may be compared with the range of values given in Table 2.

The resonance integral calculated by using the parameters in Table 1 produced a value of I_y (0.5-eV cutoff) = 68.6 b, which, although somewhat higher than those recommended in Refs. 2, 6, and 10, is preferred since the most recent quoted value² is based on data in the region 20.0 to 1200.0 eV which clearly underestimate the evaluated value that goes from 0.05 eV to the MeV range.

The potential scattering cross section is taken to be the same as that of ^{78}Kr .

^{82}Kr MAT 1332 (10⁻⁵ eV to 100.0 eV)

Only one resonance at an energy of ~ 40 eV has been firmly established for ^{82}Kr .^{2,6} Block et al.,² have concluded that there is a doublet belonging to ^{82}Kr around 640.0 eV, but, since they give no neutron width (Γ_n), this resonance has been ignored.

The radiation width Γ_{yr} was determined by the method proposed by Malecky et al.,¹¹ in which it is assumed that the main contribution to Γ_{yr} is due to the electric dipole radiation; from a semi-empirical analysis it may be estimated as

$$\Gamma_{yr} = 10.5 U/A (a^{-1/2}) (1.0 - 0.01 I^2) \text{ eV} \quad (1)$$

where

A = mass of nucleus,

U = effective energy of excitation ($U = E_B - \Delta$)

E_B = binding energy of compound nucleus,

$\Delta = \delta(N)$ and $\delta(p)$ the pairing energies,

I = spin of target nucleus, and

a = single-particle state density parameter near the Fermi surface.

The relation between a and A is based on the analysis of Cook et al.,¹² where

$$a/A = 0.00917S + 0.142, \text{ and}$$

$S = S(N) + S(Z)$ shell correction parameter.

A value of $\Gamma_{yr} = 236$ mV was calculated from Eq. (1) for ^{82}Kr .

In addition to the reported resonance at 39.8 eV, it was necessary to assume a bound level at -42.83 eV (Table 1) to yield a thermal capture cross section $\sigma_{ny} = 30.17$ b. The experimental value leading to the metastable state in ^{83}Kr of $\sigma_{ny}^m = 20.0 \pm 3.5$ b has been reported in Ref. 4. The value calculated here is barely within the recommended value of

$\sigma_{n\gamma}^{(m+g)} = 45 \pm 15$ b.⁶ A value $\sigma_{n\gamma} = 25.0$ b has been estimated by Iijima.¹³ as with ^{78}Kr , the potential scattering cross section was chosen to be $\sigma_{\text{pot}} = 7.0$ b. The resonance integral calculated from the data in Table 1 is $I_{\gamma} = 183.56$ b ($E_{\text{cutoff}} = 0.5$ eV). The recommended value calculated from a single resonance at 39.8 eV has been given as 200 ± 40 b.⁶ A calculated $I_{\gamma} = 190.0$ b where 13.7 b is due to the unresolved region was reported in Ref. 13.

^{83}Kr MAT 1333 (10⁻⁵ to 520.625 eV)

The resonance parameters given Ref. 3 yielded a thermal capture cross section of the only 16 b, which is much too small compared with the various recommended values 200 ± 30 b⁶ and 205 b.¹³

Calculating the radiation width by Eq. (1) yielded $\Gamma_{\gamma\gamma} = 233.0$ mV;

assuming a bound level at -3.9 eV gives a thermal capture cross section $\sigma_{n\gamma} = 207.67$ b.

The calculated resonance integral is $I_{\gamma} = 188.65$ b, which is lower than the value $I_{\gamma} = 170.2$ b in Ref. 13.

As earlier, the potential scattering cross section is the same as that of Kr(Nat), namely 7.0 b.

^{84}Kr MAT 1334 (10⁻⁵ to 2.0 keV)

An unassigned resonance reported by Mann and Watson³ was assumed to be due to ^{84}Kr at an energy of 1625.0 eV, with a neutron width $\Gamma_n = 2.84.0$ mV and $\Gamma_{\gamma} = 226.0$ mV (Eq. 1). This resonance along with the other two low-lying resonances at 519.0 and 580.0 eV yielded a thermal capture cross section $\sigma_{n\gamma} (0.0253 \text{ eV}) = 0.0864$ b. Kondaiah et al.,⁴ reported an experimental value of 0.09 ± 0.013 b for the 4.4-h ^{85}Kr and a value of 0.042 ± 0.004 b for the 10.74- γ ^{85}Kr . A recommended value of $\sigma_{n\gamma} = 0.130 \pm 0.014$ b ^{85}Kr (m+g) is given in Ref. 6, and $\sigma_{n\gamma} = 0.16$ b is reported in Ref. 14.

The calculated resonance integral of magnitude 3.27 b is in good agreement with the calculated value of 2.7 ± 0.7 b reported in Ref. 6, and in excellent agreement with $I_{\gamma} = 3.54$ given in Ref. 14.

^{86}Kr MAT 1336 (10⁻⁵ eV to 13 keV)

Since no resonance parameters have been experimentally verified for ^{86}Kr , it was necessary to make certain assumptions. From Mann et al.,³ there is an unassigned resonance at an energy of 2700 eV. Since the thermal capture cross section and resonance integral for ^{86}Kr have been estimated to be very small (see following references) this resonance was taken to be due to this isotope.

On the basis of an estimated s-wave strength function, $s_0 = 0.5 \times 10^{-4}$, and assuming $\Gamma_n / \Gamma_r \ll 1$, the resonance parameters given in Table 1 were derived. These parameters produced a thermal captive cross section equal to 0.0635 b , which is not too far from the value $0.06 \pm 0.02 \text{ b}^6$ and is consistent with the estimate of 0.062 b .¹⁴ Again, a potential scattering radius of 7.0 was used.

The resonance integral was calculated to be 0.122 b , which may be compared with the calculated value of $0.03 \pm 0.03 \text{ b}^3$, and 0.07 quoted in Ref. 14 (also see Ref. 13).

3.0 CONTINUUM REGION CROSS SECTION

The cross sections (total, elastic, inelastic capture, n-proton, and $n-^4\text{He}$) in the keV to 20-MeV region were calculated by using the code CERBERO-2.¹⁶

The n, γ, n, n' , n, p , and $n-^4\text{He}$ reaction calculations were carried out in the Hauser-Feshbach formalism with width fluctuation correction and with the Q values given in Table 4. The level schemes used in these calculations are given in Table 5 (these levels were taken from Ref. 17 unless otherwise stated). The calculations were then modified to take into account other threshold reaction cross section ($n, 2n$, $n, 3n$, n, d , n, t) which were calculated for ENDF/IV (see Ref. 1).

4.0 ANGULAR DISTRIBUTION OF SECONDARY NEUTRONS

The angular distribution of the elastically scattered neutrons was interpreted in terms of a Legendre polynomial fit using CHAD¹⁸ for File 4. For the inelastically scattered neutrons and the $n, 2n$ reactions, the distribution was assumed to be isotropic.

5.0 ENERGY DISTRIBUTION OF SECONDARY NEUTRONS

The energy distributions of neutrons due to the $n, 2n$, $n, 3n$, and continuum inelastic scattering were expressed in terms of a normalized probability distribution having an evaporation spectrum given by

$$f(E + E') = E'/I e^{-E'/\theta}$$

where I = normalization constant, and θ = nuclear temperature. The energy dependence of θ was formulated according to Gilbert and Cameron.¹⁹

Table 1
Adopted Resonance Parameters

Isotope	E_R (eV)	Γ_T (mV)	Γ_n (mV)	Γ_γ (mV)	Ref.
^{78}Kr	-120.6*	936.0	706.0	230.0	-
	108.4	279.0	49.0	230.0	2
	450.9	460.0	230.0	230.0	2
	640.0	1730.0	1500.0	230.0	2
^{80}Kr	-118.0*	1460.0	1230.0	230.0	-
	89.2	234.0	4.0	230.0	2
	106.0	670.0	440.0	230.0	2
	927.0	2530.0	2300.0	230.0	2
^{82}Kr	-42.83	496.0	260.0	236.0	1
	39.80	324.3	88.3	236.0	1
^{83}Kr	-3.9	245.44	12.44	233.0	1
	27.9	300.0	67.0	233.0	1
	233.0	523.0	290.0	233.0	1
^{84}Kr	519.0	571.0	345.0	226.0	1
	580.0	313.0	87.0	226.0	1
	1625.0	2410.0	2184.0	226.0	1
^{86}Kr	2730.0	3568.0	3400.0	168.0	1

*See text.

Table 2
Experimental and Recommended Thermal Capture Cross Sections for ^{80}Kr

$\sigma_{n\gamma}$ (b)	Reference
14.0±1.5	BNL 325, Vol. 1 (3rd ed.), 1973.
11.3±0.4	G. Bondley and W.H. Johnson, NSE 47, 151 (1972).
15.6±2.8	I.R. Barabanov et al., JETP Lett. 15, 456 (1972).
11.5±0.6	N.E. Holden and F.W. Walker, G.E. Chart of Nuclides (11th ed.), 1972.
11.5±0.5	N.E. Holden (BNL), Private Communication, 1978.
12.6	F.W. Walker et al., G.E. Chart of Nuclides (12th ed.), 1977.
11.74	This work.

36-Kr-78/86
MAT 1330+

Table 3
Natural Abundance and Mass of Krypton Isotopes

Isotope	% Abundance	Mass (amu)	S_n (MeV)*
78	0.35	77.920401	8.368
80	2.25	79.916376	7.850
82	11.60	81.913482	7.467
83	11.50	82.914131	10.518
84	57.00	83.911506	7.111
86	17.30	85.910616	5.511

* S_n = Binding energy of last neutron in compound nucleus.

Table 4
 Q Values for Nuclear Reactions

Reaction	78_{Kr}	80_{Kr}	82_{Kr}	83_{Kr}	84_{Kr}	86_{Kr}	ENDF
	-Q (MeV)	MT					
(n, p)	-0.089	1.228	2.306	0.187	3.920	6.520	103
(n, ^3He)	5.752	7.730	9.695	10.461	11.707	14.202	106
(n, n'd)	17.129	17.581	17.884	15.151	18.067	18.669	
(n, n' ^4He)	4.358	5.066	5.990	6.479	7.101	7.511	22
(n, ^4He , n')	4.358	5.066	5.990	6.479	7.101	7.511	22
(n, p, ^4He)	4.931	7.252	5.990	7.942	12.322	14.308	
(n, 2n)	11.981	11.525	10.980	7.467	10.518	9.860	16
(n, d)	5.974	6.886	7.766	7.548	8.480	9.655	104
(n, ^4He)	-3.665	0.969	-1.111	-1.526	-1.168	-1.384	107
(n, n't)	19.942	19.610	19.468	19.052	19.410	19.194	
(n, p, n')	8.199	9.111	9.907	9.773	10.705	11.880	28
(n, ^4He , p)	4.931	7.252	9.475	7.942	12.322	14.208	
(n, 3n)	21.14	19.893	18.839	18.450	17.985	16.971	71
(n, t)	10.87	11.322	11.585	8.892	11.808	12.410	105
(n, n'p)	8.199	9.111	9.907	9.773	10.705	11.880	28
(n, n' ^3He)	16.913	18.226	19.590	17.162	20.978	22.753	
(n, 2p)	6.052	8.470	10.711	8.907	13.500	17.111	
(n, d, n')	17.129	17.581	17.884	15.151	18.067	18.669	

Table 5 (a)
Energy Levels for Hauser-Feshbach Calculations: ^{76}Kr

^{79}Kr		Residual Nucleus:				^{75}Sc	
$\sigma_{n\gamma}$	E (MeV)	$\sigma_{nn'}$	E (MeV)	I^π	σ_{np}	E (MeV)	I^π
0.000	1/2 ⁻	0.000	0 ⁺		0.000	1 ⁺	0.000
0.300	7/2 ⁺	0.455	2 ⁺		0.032	2 ⁻	0.110
0.147	5/2 ⁻	1.119	4 ⁺		0.180	4 ⁺	0.285
0.183	3/2 ⁻	1.978	6 ⁺				0.420
0.291	5/2 ⁻						0.610
0.384	3/2 ⁻						0.750
0.402	5/2 ⁻						0.860
0.450	7/2 ⁻						0.903
0.534	1/2 ⁺						1.030
0.660	5/2 ⁻						
0.689	5/2 ⁻						
0.695	3/2 ⁺						
0.720	7/2 ⁻						
0.810	3/2 ⁻						
1.038	7/2 ⁺						
1.912	1/2 ⁺						
2.060	3/2 ⁺						
2.768	7/2 ⁺						

36-Kr-78/86
MAT 1330+

Table 5(b)
Energy Levels for Hauser-Feshbach Calculations: ^{86}Kr

^{81}Kr		Residual Nucleus: ^{80}Kr				^{80}Br		^{77}Sc	
$\sigma_{n\gamma}$	I^π	$\sigma_{nn'}$	I^π	σ_{np}	I^π	σ_{na}	I^π	E (MeV)	
E (MeV)		E (MeV)		E (MeV)		E (MeV)			
0.000	$7/2^+$	0.000	0^+	0.000	1^+	0.000	$1/2^-$		
0.190	$1/2^-$	0.616	2^+	0.037	2^-	0.162	$7/2^+$		
0.457	$3/2^-$	1.252	2^+	0.085	5^-	0.175	$9/2^+$		
0.549	$1/2^+$	1.320	0^-	0.256	2^+	0.239	$3/2^-$		
0.608	$5/2^-$	1.436	4^+	0.271	2^-	0.250	$5/2^-$		
0.636	$7/2^-$	2.390	6^+	0.281	3^-	0.440	$5/2^-$		
0.701	$3/2^+$	3.400	8^-	0.314	1^-	0.521	$3/2^+$		
0.919	$3/2^-$			0.366	1^-	0.680	$5/2^-$		
1.025	$3/2^+$			0.381	3^-	0.818	$1/2^+$		
1.108	$1/2^+$			0.468	1^-	0.912	$3/2^+$		
1.280	$3/2^+$			0.684	2^-	0.956	$1/2^-$		
1.677	$5/2^+$			0.722	1^-	1.006	$3/2^+$		
1.803	$3/2^+$			0.760	1^-	1.126	$1/2^-$		
				0.835	1^-	1.412	$1/2^-$		
				1.139	1^-	1.623	$1/2^-$		
				1.200	2^-	1.819	$1/2^-$		
				1.410	3^-	2.393	$3/2^-$		
				1.700	2^-				
				1.880	2^-				

Table 5 (c)
Energy Levels for Hauser-Feshbach Calculations: ^{82}Kr

^{83}Kr		Residual Nucleus: ^{82}Kr				^{82}Br		^{79}Sc	
$\sigma_{n\gamma}$	I^π	$\sigma_{nn'}$	I^π	σ_{np}	I^π	σ_{na}	I^π		
E (MeV)		E (MeV)		E (MeV)		E (MeV)			
0.000	$9/2^+$	0.000	0^+	0.000	5^-	0.000	$7/2^-$		
0.009	$7/2^+$	0.777	2^+	0.046	2^+	0.096	$1/2^+$		
0.042	$1/2^-$	1.475	2^+	0.078	1^+	0.130	$9/2^-$		
0.562	$5/2^-$	1.820	4^-			0.365	$5/2^-$		
0.571	$3/2^+$	2.094	3^+			0.526	$1/2^+$		
0.690	$3/2^-$	2.172	0^-			0.620	$3/2^+$		
0.798	$7/2^-$	2.427	3^-			0.720	$3/2^-$		
		2.648	4^-			0.974	$1/2^+$		
		2.828	5^+			1.160	$1/2^+$		
		2.920	6^+			1.490	$1/2^+$		
						1.670	$3/2^-$		
						2.040	$1/2^-$		
						2.280	$3/2^-$		
						2.590	$3/2^+$		
						2.960	$1/2^+$		
						3.280	$1/2^+$		
						3.440	$3/2^-$		

Table 5 (d)
Energy Levels for Hauser-Feshbach Calculations: ^{83}Kr

^{84}Kr		Residual Nucleus: ^{83}Kr				^{83}Br		^{80}Sc	
$\sigma_{n\gamma}$	I^π	$\sigma_{nn'}$	I^π	σ_{np}	I^π	σ_{na}	I^π		
E (MeV)		E (MeV)		E (MeV)		E (MeV)			
0.000	0^+	0.000	$9/2^+$	0.000	$3/2^-$	0.000	0^+		
0.882	2^+	0.009	$7/2^+$	0.357	$5/2^-$	0.686	2^+		
1.834	0^+	0.042	$1/2^-$	0.988	$1/2^-$	1.449	2^+		
1.900	2^+	0.562	$5/2^-$	1.030	$3/2^-$	1.479	0^-		
2.086	4^+	0.571	$3/2^-$	1.700	$1/2^-$	1.960	2^+		
2.337	4^-	0.690	$5/2^-$	2.050	$3/2^-$	2.310	2^+		
2.705	3^-	0.798	$7/2^-$	2.450	$7/2^+$	2.514	2^+		
2.775	2^+			2.646	$7/2^-$	2.814	2^+		
3.048	4^-			2.738	$1/2^-$	3.126	2^+		
3.225	1^-			2.946	$7/2^-$	3.248	2^+		
3.477	1^-			3.09	$1/2^-$	3.350	1^+		
3.570	3^-					3.390	2^-		
3.650	5^-					4.063	0^-		
3.721	3^-								

*Reference 24.

Table 5 (e)
Energy Levels for Hauser-Feshbach Calculations: ^{84}Kr

^{85}Kr		Residual Nucleus: ^{84}Kr				^{84}Br		^{81}Sc	
$\sigma_{n\gamma}$	I^π	$\sigma_{nn'}$	I^π	σ_{np}	I^π	σ_{na}	I^π		
E (MeV)		E (MeV)		E (MeV)		E (MeV)			
0.000	$9/2^+$	0.000	0^+	0.000	2^-	0.000	$1/2^-$		
0.305	$1/2^-$	0.822	2^+	0.408	1^-	0.103	$7/2^+$		
1.050	$3/2^-$	1.834	0^+	0.557	6^-	0.294	$9/2^+$		
1.230	$5/2^-$	1.900	2^+	0.873	2^-	0.468	$1/2^-$		
1.767	$3/2^+$	2.086	4^+	0.979	3^-	0.625	$5/2^-$		
2.108	$1/2^-$	2.337	4^-	1.196	4^-	1.053	$3/2^+$		
2.166	$1/2^+$	2.705	3^+			1.232	$1/2^+$		
2.237	$7/2^+$	2.775	2^+			1.303	$3/2^+$		
2.418	$5/2^-$	3.048	4^-			1.406	$1/2^-$		
3.380	$7/2^-$	3.225	1^-			1.725	$3/2^+$		
		3.477	1^-			1.828	$5/2^+$		
		3.570	3^-			2.174	$3/2^+$		
		3.650	5^-			2.550	$5/2^+$		
		3.721	3^-			2.680	$1/2^+$		
						3.070	$3/2^+$		
						3.310	$5/2^+$		
						3.490	$3/2^+$		
						3.570	$1/2^+$		
						3.670	$3/2^+$		
						3.720	$5/2^+$		

*Reference 21.

Table 5(f)
Energy Levels for Hauser-Feshbach Calculations: ^{86}Kr

^{87}Kr		Residual Nucleus:				^{83}Sc	
		^{86}Kr		^{86}Br			
$\sigma_{n\gamma}$	I^π	$\sigma_{nn^*}^*$	I^π	σ_{np}	I^π	σ_{na}	I^π
E (MeV)		E (MeV)		E (MeV)		E (MeV)	
0.000	$5/2^+$	0.000	0^+	0.000	2^-	0.000	$9/2^-$
0.529	$1/2^+$	1.563	2^+	0.196	1^-	0.220	$1/2^-$
1.468	$3/2^+$	2.248	4^+	0.268	4^-	1.050	$3/2^-$
1.873	$5/2^+$	2.355	2^+	0.390	2^-	1.230	$5/2^-$
1.996	$3/2^+$	2.733	0^-	0.862	1^-	1.767	$3/2^+$
2.080	$5/2^+$	3.109	3^-	1.210	1^-	2.108	$1/2^+$
2.112	$3/2^+$	3.542	0^+	2.232	1^+	2.166	$1/2^+$
2.250	$9/2^-$	3.832	0^-	2.392	1^+	2.237	$7/2^+$
2.277	$1/2^+$	3.959	4^+	2.772	1^+	2.418	$5/2^-$
2.515	$7/2^+$	4.111	2^+			3.380	$7/2^-$
2.775	$3/2^+$	4.194	2^-				
2.825	$3/2^+$	4.298	3^-				
3.015	$5/2^+$	4.668	4^+				
3.223	$3/2^+$	4.826	2^+				
3.237	$5/2^-$	4.948	2^-				

*References 21 and 22.

36-Kr-78/86
MAT 1330+

Appendix A1

Capsule Summary for Kr Isotopes

Isotope KR-78

MAT 1330

File 2

Resonance parameters based on new experimental data of Block et al.²

File 3

<u>Reaction Type</u>	<u>MT</u>	<u>Comments</u>
Total	1	
Elastic	2	
Non-Elastic	3	Based on new model calculations
Total Inelastic	4	
(n,2n)	16	Same as Version 4
Discrete & Cont. Inel.	51 to <u>53</u> and 91	based on new model calculations
(n,γ)	102	
(n,p)	103	Based on new model calculations
(n,d)	104	
(n,t)	105	Same as Version 4
(n, ³ He)	106	
(n, ⁴ He)	107	Based on new model calculations

Files 4 and 5 same as ENDF/IV

Appendix A2

Isotope KR-80

MAT 1331

File 2

Resonance parameters based on new experimental data of Block et al.²

File 3

<u>Reaction Type</u>	<u>MT</u>	<u>Comments</u>
Total	1	
Elastic	2	
Non-Elastic	3	Based on new model calculations.
Total Inelastic	4	
(n,2n)	16	Same as Version 4
Discrete & Cont. Inel.	51 to <u>56</u>	and 91 New level scheme.
(n,γ)	102	
(n,p)	103	Based on new model calculations.
(n,d)	104	
(n,t)	105	Same as Version 4
(n, ³ He)	106	
(n, ⁴ He)	107	Based on new model calculations.

Files 4 and 5 same as ENDF/IV

36-78/86-12

Appendix A3

Isotope KR-82

MAT 1332

File 2

Resonance parameters same as Version 4

File 3

<u>Reaction Type</u>	<u>MT</u>	<u>Comments</u>
Total	1	
Elastic	2	
Non-Elastic	3	Based on new model calculations
Total Inelastic	4	
(n,2n)	16	Same as Version 4
Discrete & Cont. Inel.	51 to <u>59</u> and 91	
(n, γ)	102	
(n,p)	103	Based on new model calculations
(n,d)	104	
(n,t)	105	
(n, ³ He)	106	Same as Version 4
(n, ⁴ He)	107	Based on new model calculations

Files 4 and 5 same as ENDF/IV

Appendix A4

Isotope KR-83

MAT 1333

File 2

Resonance parameters same as Version 4.

File 3

<u>Reaction Type</u>	<u>MT</u>	<u>Comments</u>
Total	1	
Elastic	2	
Non-Elastic	3	Based on new model calculations
Total Inelastic	4	
(n,2n)	16	Same as Version 4
(n,3n)	17	
Discrete & Cont. Inel.	51 to <u>56</u> and 91	
(n, γ)	102	
(n,p)	103	Based on new model calculations
(n,d)	104	
(n,t)	105	Same as Version 4
(n, ³ He)	106	
(n, ⁴ He)	107	Based on new model calculations

Files 4 and 5 same as ENDF/IV

36-78/86-13

36-Kr-78/86
MAT 1330+

Appendix A5

Isotope KR-84

MAT 1334

File 2
Resonance parameters same as Version 4.

File 3

<u>Reaction Type</u>	<u>MT</u>	<u>Comments</u>
Total	1	
Elastic	2	
Non-Elastic	3	Based on new model calculations
Total Inelastic	4	
(n,2n)	16	Same as Version 4
Discrete & Cont. Inel.	51 to <u>63</u> and 91	
(n,γ)	102	
(n,p)	103	Based on new model calculations
(n,d)	104	
(n,t)	105	Same as Version 4
(n, ³ He)	106	
(n, ⁴ He)	107	Based on new model calculations

Files 4 and 5 same as ENDF/IV

Appendix A6

Isotope KR-86

MAT 1336

File 2
Resonance parameters same as Version 4.

File 3

<u>Reaction Type</u>	<u>MT</u>	<u>Comments</u>
Total	1	
Elastic	2	
Non-Elastic	3	Based on new model calculations
Total Inelastic	4	
(n,2n)	16	Same as Version 4
(n,3n)	17	
Discrete & Cont. Inel.	51 to <u>64</u> and 91	
(n,γ)	102	
(n,p)	103	Based on new model calculations
(n,d)	104	
(n,t)	105	Same as Version 4

Files 4 and 5 same as ENDF/IV

36-78/86-14

REFERENCES

1. A. Prince, BNL-NCS-50503, 1974.
2. R.C. Block et al., Int. Conf., Harwell, England, 1978.
3. D.P. Mann and W.W. Watson, Phys. Rev. 116, 1516 (1959).
4. R. Kondaiah et al., Nucl. Phys. A120, 329 (1968).
5. F.W. Walker et al., G.E. Chart of Nuclides (12th ed.) 1977.
6. S.F. Mughabghab and D.I. Garber, BNL 325 (3rd ed.), Vol. 1, 1973.
7. D.C. Rorer et al., Nucl. Phys. A133, 410 (1969).
8. V.E. Krohn and G.R. Ringo, Phys. Rev. 148, 1303 (1966).
9. S.J. Cocking, J. Nucl. Eng. 6, 113 (1958).
10. J. G. Bradley and W.H. Johnson, NSE 47, 151 (1972).
11. H. Malecky et al., Sov. J. Nucl. Phys. 13, 133 (1971).
12. J.L. Cook, Austr. J. Phys. 20, 477 (1967).
13. S. Iijima et al., JAERI 1206, (1971).
14. H. Saketa et al., JAERI, 1194, 1970.
15. R. Genin et al, J. Phys. Radium 24, 21 (1963).
16. F. Fabbri et al., CERBERO-2, RT/F(77)6, 1977.
17. Nuclear Data Sheets. Series B, Vol. 15, Academic Press, New York, 1975.
18. R. F. Berland, CHAD, NAA-SR-11231 (1965).
19. A. Gilbert and A.G.W. Cameron, Can. J. Phys. 43, 1446 (1965).
20. S. Vaisala et al., Phys. Rev. C13, 372 (1976).
21. B.K. Arora et al., Phys. Rev. C10, 2301 (1974).
22. E.B. Flynn et al., Phys. Rev. C13, 568 (1976).

Evaluated Neutron Cross Sections for Natural Zirconium and
the Zirconium Isotopes 90, 91, 92, 94, and 96.

M. K. Drake, D. A. Sargis, Tin Maung
Science Applications, Inc.

Additions and Editing by
S. Pearlstein, Brookhaven National Laboratory

A complete evaluation for natural zirconium and information on evaluated data for the separate isotopes were provided to the National Nuclear Data Center (NNDC) by Science Applications, Inc. (SAI). Evaluations for the separated isotopes consistent with the evaluation for natural zirconium were prepared by NNDC. Sources of the data are documented in EPRI NP-250.

Resonance Parameters

Resolved resonance parameters primarily taken from the recommended values given in BNL-325 (1). Parameters obtained for negative energy levels in Zr-90, Zr-91, Zr-92, Zr-94 and Zr-96 by fitting 2200 M/SEC cross sections in isotopes and the element. No unresolved parameters are given. The 2200 M/S cross sections and resonance integrals for natural zirconium and its isotopes are given in Table I.

TOTAL CROSS SECTION

Below 5 keV, the total cross is represented by the resolved resonance parameters. Between 5 keV and 82 keV the total cross section is the difference between the evaluated cross section and a resolved resonance calculation. The evaluated cross section was based on measurements by Newson, et al (2) and Seth (3). Between 82 keV and 500 keV the data of Seth were used between 500 keV and 2 MeV. The evaluated data were based on measurements of Green and Mitchell (4) and Stooksberry and Anderson (5). Above 2 MeV, the measurements of Green and Mitchell (4), Foster and Glasgow (6), Carlson and Barschall (7) and Peterson, et al (8).

N,2N CROSS SECTION

The cross section for the element was based on estimates for the isotopes. Except for Zr-90, the results from a statistical model were used. The (n,2n) cross section for Zr-90 was based on measurements by Prestwood and Bayhurst (9), Nethaway (10) and several measurements near 14 MeV.

N,ALPHA CROSS SECTION

The (n, alpha) cross section was based on estimates for the isotopes. The energy dependent measurements by Bayhurst and Prestwood (11), statistical model calculations and several measurements at 14 MeV were used.

(N,P) CROSS SECTION

The (n,p) cross section for Zr-90 was based on measurements by Carroll and Stooksberry (12) and Bayhurst and Prestwood (11). The (n,p) cross section for Zr-91 was based on measurements by Carroll and Stooksberry (12) Reed (13) and Levkovskii (14). The (n,p) cross section for Zr-92 and Zr-94 were based on measurements by Carroll and Stooksberry (12), Reed (13), Bramlitt and Fink (15), Lu, et al (16), Levkovskii (14) and Prasad and Sarkar (16) and Paul and Clarke (17).

THE (N,GAMMA) CROSS SECTION

The data recommended by Benzi (18) were used.

INELASTIC SCATTERING CROSS SECTION

19 level excitation cross sections and a continuum cross section has been given for the natural element. The isotopic contributions of the excited levels are given in Table II. The cross sections were based on a previous evaluation by KAPL and the experimental data of Tessler, et al (19),

Day (20), McDaniel, et al (21), Brandenberger and Glasgow, Smith and Whalen (22), Lind and Day (23), Tessler and Glickstein (24), Guenther, et al (22), Glazkov (25).

ELASTIC SCATTERING CROSS SECTION

Basically, the elastic scattering cross section was taken as the difference between the total cross section and the non-elastic cross section. The experimental data used, including Engelbrecht and Smith (26) Hans and Snowdon (27), Kent, et al (28), Walt and Beyster (29), Walt and Barschall (30), Gilboy and Towle (31) and Clark and Cross (32).

REFERENCES

- (1) Mughabghab, S.F. and Garber, D.I., BNL-325, Vol. I, Third Ed. (June, 1973)
- (2) Newson, H.W., et al, Annals of Phys. 8, 211 (1959)
- (3) Seth, K.K., Phys. Letters 16, 306 (1965)
- (4) Green, L. and Mitchell, J.A. WAPD-TM-1073 (April 1973)
- (5) Stooksberry, R.W. and Anderson, J.H., Nuc. Sci. and Eng. 51, 235, 73
- (6) Foster, D.C., Jr., and Glasgow, D.W., Phys. Rev. C3, 576 (1971)
- (7) Carlson, A.D. and Barschall, H.H., Phys. Rev. 158, 1142 (1967)
- (8) Peterson, J.M., et al, Phys. Rev. 120, 521 (1960)
- (9) Prestwood, R.J. and Bayhurst, B.P., Phys. Rev. 121, 1438 (1961)
- (10) Nethaway, D.R. Nucl. Phys. A190, 635 (1972)
- (11) Bayhurst, B.P. and Prestwood, R.J., J. Inorg. Nucl. Chem. 23, 173 (1961)
- (12) Carroll, E.E. and Stooksberry, R.W., Nucl. Sci. Eng. 25, 285 (1966)
- (13) Reed, C.H., UC-34 (1960)
- (14) Levkovskii, V.N., Sov. Phys., JETP 18, 213 (1964)
- (15) Bramlitt, E.T. and Fink, R.W., Phys. Rev. 131, 2649 (1963)

- (16) Prasad, R. and Sarkar, D.C., Nuovo Cimento 3A, 467 (1971)
- (17) Paul, E.B. and Clarke, R.L., Can. J. Phys. 31, 268 (1953)
- (18) Benzi, V., et al, Cec (71) 9, Nov. 1971
- (19) Tessler, G., et al. Phys. Rev. C2, 2390 (1970)
- (20) Day, R.B. Pri. Comm. (1965)
- (21) Mc Daniel, R.D. et al, Phys. Rev. C10, 1087 (1974)
- (22) Guenther, P., et al, ANL/NDM-4 (1974)
- (23) Lind, D.A. and Day, R.B. Annals Phys. 12, 485 (1961)
- (24) Tessler, G. and Glickstein, S., Bull. Am. Phys. Soc. 20, 174 (1975)
- (25) Glazkov, N.P. A.E. 15, 416 (1963)
- (26) Reitman, et al. Nucl. Phys. 48, 593, (1963)
- (27) Hans, H.S. and Snowdon, S.C., Phys. Rev. 108, 1028 (1957)
- (28) Kent, D.W., Phys. Rev. 125, 331 (1962)
- (29) Walt, M. and Beyster, J.R., Phys. Rev. 98, 677 (1955)
- (30) Walt, M. and Barschall, H.H., Phys. Rev. 93, 1062 (1954)
- (31) Gilboy, W.H. and Towle, J.H., Nucl. Phys. 42, 86 (1963)
- (32) Clarke, R.L. and Cross, W.G., Nucl. Phys. A95, 320 (1967)

40-Zr-Nat/Iso
MAT 1340+

Table I

2200 M/S Cross Sections and Resonance Integrals

Isotope	E-Cutoff (eV)	R.I. (Barns)	Therm X/S (Barns)
Zr-90	8.2	+04	0.219
Zr-91	5.0	+03	5.144
Zr-92	5.4	+04	0.595
Zr-94	5.4	+04	0.304
Zr-96	6.6	+04	5.202
Zr	--		0.993
			0.1807

Table II

Inelastic Levels Used in the Evaluation

<u>Level Number</u>	<u>Energy (MeV)</u>	<u>Isotope</u>
1	0.9182	94
2	0.9345	92
3	1.2049	91
4	1.30	94
5	1.383	92
6	1.46	91,92,94,96
7	1.669	94
8	1.7607	90,96
9	1.85	91,92,96
10	2.05	91,92,94
11	2.15	90,91,94,96
12	2.261	91
13	2.319	90
14	2.32	91
15	2.35	91,92,94
16	2.557	91
17	2.61	91,94
18	2.738	90,91
19	2.748	90

Evaluated Neutronic Cross Section File for Niobium
(ENDF-IV, Preliminary)

by

R. Howerton
Lawrence Livermore Laboratory

and

A. Smith, P. Guenther and J. Whalen
Argonne National Laboratory

I. Introductory Comment

This resumé is intended for qualitative guidance only. A full report of the file content and physical basis is given in ANL/NDM-6. Any serious user of the file should refer thereto.

II. Outline of File

This evaluation gives primary emphasis to fast neutron induced reactions wherein there is a prompt emission of particles or quanta. No attention is given to gamma-ray induced processes nor to properties associated with a residual activity of measurable lifetime. Experimental information is often incomplete in the latter areas and recourse must be made to theoretical calculation (e.g. isomer-ratio calculations). At incident neutron energies of - 100 keV this evaluation is explicitly identical to that of Allen and Drake given in ENDF/B MAT-1164 (1). From 100 keV to 8.0 MeV this evaluation is primarily based on recent experimental results (2). Above 8.0 MeV it is founded on experimental results where available. In the difficult high-energy region a major reliance was placed upon physical understanding, associated calculational models and on available systematic experimental knowledge.

A. Total Neutron Cross Sections

The evaluated total neutron cross sections were deduced from the weighted averages of experimental values available from 0.1 to 15.0 MeV and extended to 20.0 MeV using the model described in Ref. 2. The experimental information was obtained from the open literature and the files of the National Neutron Cross Section Center. The primary differences between the present evaluation and that of ENDF (MAT-1164) are below energies of 2.0 MeV. The differences are both positive and negative and amount to as much as 10% in some energy ranges. Comparisons at energies of - 100 keV are, of course, meaningless as the present evaluation explicitly employs the ENDF MAT-1164 values in this lower energy range.

B. Elastic Scattering Cross Section

The model calculations described in Ref. 2 are in excellent agreement with a number of experimental results at energies of \sim 5.0 MeV and in

41-Nb-93
MAT 1189

reasonable agreement with the observed distribution at 8.05 MeV. The above considerations justify the use of the Model for the determination of the relative shape of elastic-scattering angular distributions for the present evaluation. However, there remain appreciable uncertainties at higher energies (> 10 MeV). Improved experimental information is needed.

C. Inelastic Scattering Cross Sections

The evaluation of discrete inelastic neutron excitation cross sections was largely based upon the neutron detection measurements described in Refs. 2 and 3. The onset of the continuum inelastic excitation cross section is at ~ 2.5 MeV (i.e. the energy of the last discrete-ly observed excited state) and becomes the entire inelastic cross section at 6.0 MeV. Throughout this evaluation the continuum inelastic scattering cross section was treated as a free parameter adjusted to assure consistency with the evaluation of non-elastic and other partial cross sections. The present file uses a point-wise distribution in the continuum region inclusive of a high energy tail consistent with the expected contributions from pre-compound processes. The spectral distributions at 14 MeV were determined from the work of Kammerdiener (4) and are consistent with the systematic results of an extensive integral test program based upon 14 MeV pulsed-sphere experiments carried out at Lawrence Livermore Laboratory (5). The inelastic cross sections of the present file differ from those of ENDF-III by 20% or more over much of the energy range including the region below 8.0 MeV where experimental results give good guidance. Above ~ 9.0 MeV both evaluations become more speculative but a very large difference remains.

D. Neutron Radiative Capture; $^{93}\text{Nb}(n;\gamma)^{94}\text{Nb}$ Cross Sections

The (n,γ) evaluated cross sections at energies of ~ 0.1 MeV were taken directly from ENDF-III MAT-1164. At higher energies the evaluation is consistent with recent measurements by W. Poenitz.

E. The $^{93}\text{Nb}(n;2n')^{92}\text{Nb}$ Cross Section

A number of measurements have determined the cross section for the activation of the ~ 10 day isomer of ^{92}Nb by means of the $(n;2n')$ process and these results are relatively consistent. There have been three recent measurements of the total $(n;2n')$ cross section. These two types of results were combined using isomer ratio calculations to obtain the present file.

F. The $^{93}\text{Nb}(n;3n')^{91}\text{Nb}$ Cross Section

The evaluation is based upon considerations of systematics.

G. The $^{93}\text{Nb}(n;p)^{93}\text{Zr}$ Cross Section

The present evaluation uses the energy dependence of the reaction as given in MAT-1164, renormalized to the 40 mb value at 14.0 MeV. This

procedure is consistent with the body of experimental knowledge of the (n;p) processes and with the reported direct observation of the proton product. The evaluated result is subject to large uncertainties.

H. The $^{93}\text{Nb}(n;d)^{92}\text{Zr}$ and $^{93}\text{Nb}(n;p,n')^{92}\text{Zr}$ Cross Sections

The $^{93}\text{Nb}(n;d)^{92}\text{Zr}$ cross sections will probably be small and are not considered in the present evaluation. The (n;p,n') reaction is included with the (n;n').

I. The $^{93}\text{Nb}(n;2p)^{92}\text{Y}$, $^{93}\text{Nb}(n;^3\text{He})^{91}\text{Y}$ and $^{93}\text{Nb}(n;T)^{91}\text{Zr}$

Ignored.

J. The $^{93}\text{Nb}(n;\alpha)^{90}\text{Y}$ Cross Section

Taken from MAT-1164.

K. The $^{93}\text{Nb}(n;\alpha,n')^{89}\text{Y}$ Cross Section

In view of the relatively large error associated with the measured quantities and the relatively small upper limit to the cross section, the evaluation smoothly interpolates the total reaction cross section from zero at threshold to 5 mb at 20.0 MeV.

L. Gamma-Ray Production Cross Sections

For neutron energies less than 100 keV the only photon producing reaction is the (n, γ) reaction. This evaluation assumes a constant photon spectrum from neutron capture for all neutron energies and adjusts the multiplicity to conserve energy. For neutron energies less than 100 keV photon production from neutron capture is presented explicitly. For neutron energies - 100 keV the capture reaction is included with all other reactions. For energies - 100 keV the present evaluation relies upon gamma-ray production files calculated from the formalism of Howerton and Plechaty (6) as modified by Perkins, Haight and Howerton (7). The calculations included contributions from all photon producing processes and were consistent with the known energetics. The emission spectra are complexes of exponential forms reducing in the limiting case of very large incident energies to a single exponential. The spectra are known to be complex at even rather low energies (~ 1.0 MeV) with no dominant single line thus the simple continuum distribution should be reasonably suitable for most fast neutron applications, since the neutron interaction data are energetically consistent.

41-Nb-93
MAT 1189

References

1. M. S. Allen and M. K. Drake, Gulf General Atomic Report GA-8133 (1967).
See also ENDF-III, MAT-1164, National Neutron Cross Section Center,
Brookhaven National Laboratory.
2. Fast Neutron Processes in Niobium--Measurements and Evaluation, A. Smith
et al., Argonne National Laboratory Report AP/CTR/TM-4.
3. A. Smith et al., Zeits. Phys., 264 379 (1973).
4. J. L. Kammerdiener, Neutron Spectra Emitted by Pu-239, U-238, U-235,
Pb, Nb, Ni, Al and C Irradiated by 14 MeV Neutrons.
5. C. Wong et al., Livermore Pulsed Sphere Program; Program Summary Through
July 1971, Lawrence Livermore Report, UCRL-51144 Rev. 1, (1972).
6. R. Howerton and E. Plechaty, Nucl. Sci. and Eng., 32 178 (1968).
7. S. Perkins, R. Haight and R. Howerton, to be published (1974).

Molybdenum

DATA SUMMARY AND GENERAL COMMENTS

The experimental data for natural molybdenum and its various isotopes are listed in UCRL-50400, Vol. 3. The evaluated data for natural molybdenum are shown graphically in UCRL-50400, Vol. 15, Part B. R. J. Howerton did the evaluation.

TOTAL CROSS SECTION

Experimental total cross sections for natural molybdenum are shown graphically on pages 5-17 to 5-27 of UCRL-50400, Vol. 7, Part A, Rev. 1; some tabulated values are given on page 5-32. Total cross sections for ^{92}Mo are shown on page 5-34; total cross sections for ^{94}Mo are shown on pages 5-35 and 5-36; total cross sections for ^{95}Mo are shown on page 5-37; total cross sections for ^{96}Mo are shown on pages 5-38 and 5-39; total cross sections for ^{98}Mo are shown on pages 5-41 and 5-42; and total cross sections for ^{100}Mo are shown on page 5-45. The evaluated total cross sections, which are based on these experimental data, are shown in UCRL-50400, Vol. 15, Part B.

ELASTIC SCATTERING CROSS SECTION

Elastic scattering cross sections for natural Mo are shown graphically on page 5-28 of UCRL-50400, Vol. 7, Part A, Rev. 1; some tabular values

are given on pages 5-32 and 5-33. Elastic cross sections for ^{92}Mo are shown on page 5-35; elastic cross sections for ^{94}Mo are given on pages 5-36 and 5-37; elastic cross sections for ^{96}Mo are given on pages 5-39 and 5-40; elastic cross sections for ^{98}Mo are shown on page 5-43; and elastic cross sections for ^{100}Mo are given on pages 5-46 and 5-48. The evaluated elastic scattering cross sections are shown in UCRL-50400, Vol. 15, Part B. These evaluated elastic cross sections were obtained by taking differences between the evaluated total cross sections and the sums of the evaluated nonelastic cross sections, with the experimental elastic scattering data used as a guide.

ELASTIC SCATTERING ANGULAR DISTRIBUTIONS

Elastic scattering differential cross section measurements for neutron energies up to 8 MeV and at 14 MeV are shown in UCRL-50400, Vol. 19. In the evaluation, the elastic scattering angular distributions were assumed to be isotropic for neutron energies up to 50 keV. Between 50 keV and 8 MeV the angular distributions were based on the experimental data. Above 8 MeV the elastic scattering angular distributions were taken from spherical optical model

Molybdenum

06/09/78

REACTION	POINTS	DATE	Q-VALUE	E-MIN	E-MAX
N,ELASTIC	CROSS SECTION	119	9/05/72	0.0000*	2.0000*
N,ELASTIC	ANGULAR DIST.	12	1/03/72	0.0000*	5.0000-
N,ELASTIC	TOTAL ENERGY DEP.	30	1/14/74	0.0000*	2.0000-
N,ELASTIC	LOCAL ENERGY DEP.	30	1/14/74	0.0000*	1.0000-10
N,N	CROSS SECTION	19	9/22/72	0.0000*	2.0000*
N,N	ENERGY-ANGLE DIST.	12	9/22/72	0.0000*	2.5000-
N,N	TOTAL ENERGY DEP.	16	12/03/76	0.0000*	2.5000-
N,N	LOCAL ENERGY DEP.	11	12/03/76	0.0000*	2.5000-
N,2N	CROSS SECTION	16	9/22/72	0.0000*	2.0000*
N,2N	ENERGY-ANGLE DIST.	7	9/22/72	0.0000*	2.0000*
N,2N	TOTAL ENERGY DEP.	13	12/03/76	0.0000*	2.0000*
N,2N	LOCAL ENERGY DEP.	8	12/03/76	0.0000*	2.0000*
N,3N	CROSS SECTION	7	9/22/72	-1.4800*	1.5000-
N,3N	ENERGY-ANGLE DIST.	4	9/22/72	-1.4800*	1.5000-
N,3N	TOTAL ENERGY DEP.	3	12/03/76	-1.4800*	1.5000-
N,3N	LOCAL ENERGY DEP.	3	12/03/76	-1.4800*	1.5000-
N,G	CROSS SECTION	400	9/05/72	0.7500*	1.0000-10
N,G	ENERGY DIST.	2	2/23/78	0.7500*	1.0000-10
N,G	MULTIPOLICITY	2	2/23/78	0.7500*	1.0000-10
N,G	TOTAL ENERGY DEP.	2	1/21/76	0.7500*	1.0000-10
N,G	LOCAL ENERGY DEP.	2	1/21/76	0.7500*	1.0000-10
N,XG	CROSS SECTION	15	2/23/78	0.0000*	2.5000-
N,XG	ENERGY-ANGLE DIST.	15	2/23/78	0.0000*	2.5000-

calculations, in which the best-fit optical model parameters of Beccetti and Greenlees were used [Phys. Rev. 182, 1190 (1969)].

INELASTIC SCATTERING CROSS SECTION

The experimental n, n' data for natural molybdenum are shown graphically on pages 6-34 to 6-39 of UCRL-50400, Vol. 8, Rev. 1, Part A; some tabulated values are given on page 6-41. A single n, n' data point for ^{92}Mo is given on page 6-47; n, n' data for ^{94}Mo are given on pages 6-49 and 6-50; n, n' data for ^{96}Mo are given on page 6-51; n, n' data for ^{98}Mo are given on page 6-53; and n, n' data for ^{100}Mo are given on pages 6-54 and 6-55. The evaluated inelastic scattering cross section for natural Mo is represented by a continuum contribution that has a threshold at 0.25 MeV, which is just above the energy of the first excited state in ^{95}Mo . The evaluated inelastic continuum cross section, which is based on a combination of the experimental data and nuclear systematics, is shown in UCRL-50400, Vol. 15, Part B.

INELASTIC SCATTERING ANGULAR AND ENERGY DISTRIBUTIONS

The angular distributions for inelastic scattering were assumed to be isotropic in the laboratory system for all incident energies. While this

assumption is incorrect for the pre-equilibrium and direct-interaction portions of the reaction, the alternative of entering anisotropic angular distributions into the evaluation is also incorrect because the uncertainties in the reaction cross section are so large. For energies below the onset of the preequilibrium process, at about 8 MeV, the energy distributions of the secondary neutrons were derived from a temperature model. For incident neutron energies above 8 MeV, the energy distributions of the secondary neutrons were characterized by a two-component model - a "temperature" component plus a "preequilibrium and unresolved direct-interaction" component. The method used in selecting the fraction of the inelastically scattered neutrons to be associated with the preequilibrium process is described in UCRL-50400, Vol. 15, Part A, pages 19 to 22.

$n, 2n$ CROSS SECTION

The dominant even-A isotopes in Mo have $n, 2n$ thresholds that are somewhat above 8 MeV, and the trace odd-A isotopes in Mo have thresholds that are generally below 8 MeV. Thus, 8 MeV was selected as an effective $n, 2n$ threshold for natural Mo. A single $n, 2n$ data point for natural Mo is given on page 6-41 of UCRL-50400, Vol. 8, Rev. 1, Part B; $n, 2n$ data for ^{92}Mo are shown graphically on pages

6-43 to 6-45. Some tabular values are given on page 6-48; $n,2n$ data for Mo¹⁰⁰ are given on page 6-56. The evaluated $n,2n$ cross sections are shown in UCRL-50400, Vol. 15, Part B. Because of the scarcity of experimental data, these evaluated $n,2n$ cross sections were determined, in part, from nuclear systematics.

ANGULAR AND ENERGY DISTRIBUTIONS FOR THE $n,2n$ REACTION

The angular distribution of secondary neutrons from the $n,2n$ reaction was assumed to be isotropic in the laboratory system. Energy distributions of the secondary neutrons, which are presented in tabular form, are derived from temperature model calculations, with the assigned temperatures consistent with systematics (UCRL-50400, Vol. 15, Part A, page 24).

$n,3n$ CROSS SECTION

The Mo isotopes with $A \leq 98$ have $n,3n$ thresholds above 15 MeV; the Mo isotopes with $A \geq 99$ have $n,3n$ thresholds below 15 MeV. Thus, 15 MeV was selected as an effective $n,3n$ threshold. Since there are no experimental $n,3n$ data for Mo, the evaluated $n,3n$ cross sections were determined entirely from nuclear systematics. The evaluated $n,3n$ cross sections are shown in UCRL-50400, Vol. 15, Part B.

ANGULAR AND ENERGY DISTRIBUTIONS FOR THE $n,3n$ REACTION

The same evaluation procedures were used for the $n,3n$ reaction as for the $n,2n$ reaction described above.

n,γ CROSS SECTION

Experimental neutron capture cross sections for natural Mo are given on pages 5-29 to 5-31 (graphical) and on page 5-33 (tabular) of UCRL-50400, Vol. 7, Part A, Rev. 1; neutron capture data for Mo⁹⁵ are given on page 5-38; neutron capture data for Mo⁹⁶ and Mo⁹⁷ are given on page 5-40; neutron capture data for Mo⁹⁸ are given on pages 5-43 to 5-45; and capture data for Mo¹⁰⁰ are given on pages 5-46 to 5-48. The evaluated neutron capture cross sections for natural Mo, which were largely based on these experimental data, are shown in UCRL-50400, Vol. 15, Part B.

PHOTON PRODUCTION FROM n,γ REACTIONS

The spectrum of photons from the neutron capture process at thermal neutron energies was taken from the measurements of V. J. Orphan *et al.*, Gulf General Atomic Rept. GA-10248 (1970). This spectrum was assumed to apply at all incident neutron energies up to 20 MeV, but the photon multiplicity was adjusted so as to conserve the total energy of the reaction.

$n, X\gamma$ CROSS SECTION

Experimental $n, X\gamma$ data for natural Mo are given on page 6-40 (graphical) and on page 6-42 (tabular) of UCRL-50400, Vol. 8, Rev. 1, Part B. Since these are the only available $n, X\gamma$ cross sections for Mo, the evaluated $n, X\gamma$ cross sections were based, in part, on these experimental data and in part on calculations with the NXGAMEL code, using the systematics developed by Perkins, Haight, and Howerton [*Nucl. Sci. Eng.* 57, 1 (1975)]. A summary of this method of

evaluating photon production data is discussed in UCRL-50400, Vol. 15, Part A, pages 38 to 41. The evaluated $n, X\gamma$ cross section is represented as a continuum that has a threshold at 0.25 MeV.

SPECTRA OF PHOTONS FROM THE $n, X\gamma$ PROCESS

The photon angular distributions were assumed to be isotropic. The photon energy distributions were obtained from the systematics of Perkins, Haight, and Howerton cited above.

ENDF/B-V Summary Documentation

Isotope: 43-Tc-99 MAT=1308, Tape 510

HEDL	R.E. Schenter and D.L. Johnson	(Fast Capture)	Nov. '78
HEDL	F.M. Mann and F. Schmittroth	(Fast Capture)	Nov. '78
RCN	H. Gruppelaar	(Fast Capture)	Apr. '78
INEL	R. Bunting and C. R. Reich	(Decay)	Mar. '78
BAW	A.Z. Livolsi	(ENDF/B-IV)	Oct. '71

The present work supersedes the ENDF/B-IV evaluation, MAT = 1137 by Livolsi (Summary of MAT 1137 given on page 43-99-4). Only the capture cross section and the resolved resonance parameters were changed for this evaluation. The new thermal cross sections are given as:

Cross Section Values at E = 0.0253 eV

Total	24.58	B
Scatter	5.09	B
Capture	19.49	B

Capture Resonance Integral (E_C = .5 eV) 350.1 B

The following indicates the changes from ENDF/B-IV:

MF = 2 MT = 151

Resolved resonance parameters were obtained from capture measurements at RPI (Private Communication - Letter Robert C. Little to Sol Pearlstein, July 13, 1977)

43-Tc-99
MAT 1308

MF = 3 MT = 102

Capture cross section evaluations were obtained using a generalized least-squares approach with calculations being performed with the computer code FERRET. Results of these calculations are shown in Figure 1, where the a priori curve is from ENDF/B-IV and the adjusted curve was used as the final evaluated ENDF/B-V cross section. Input for these adjustment calculations included both integral and differential experimental data results. Figure 1 also includes the differential data values and their uncertainties which were obtained from the CSIRS library. Integral measurement results came from CFRMF and STEK Assemblies 500, 1000, 2000, 3000, 4000. References for this work include:

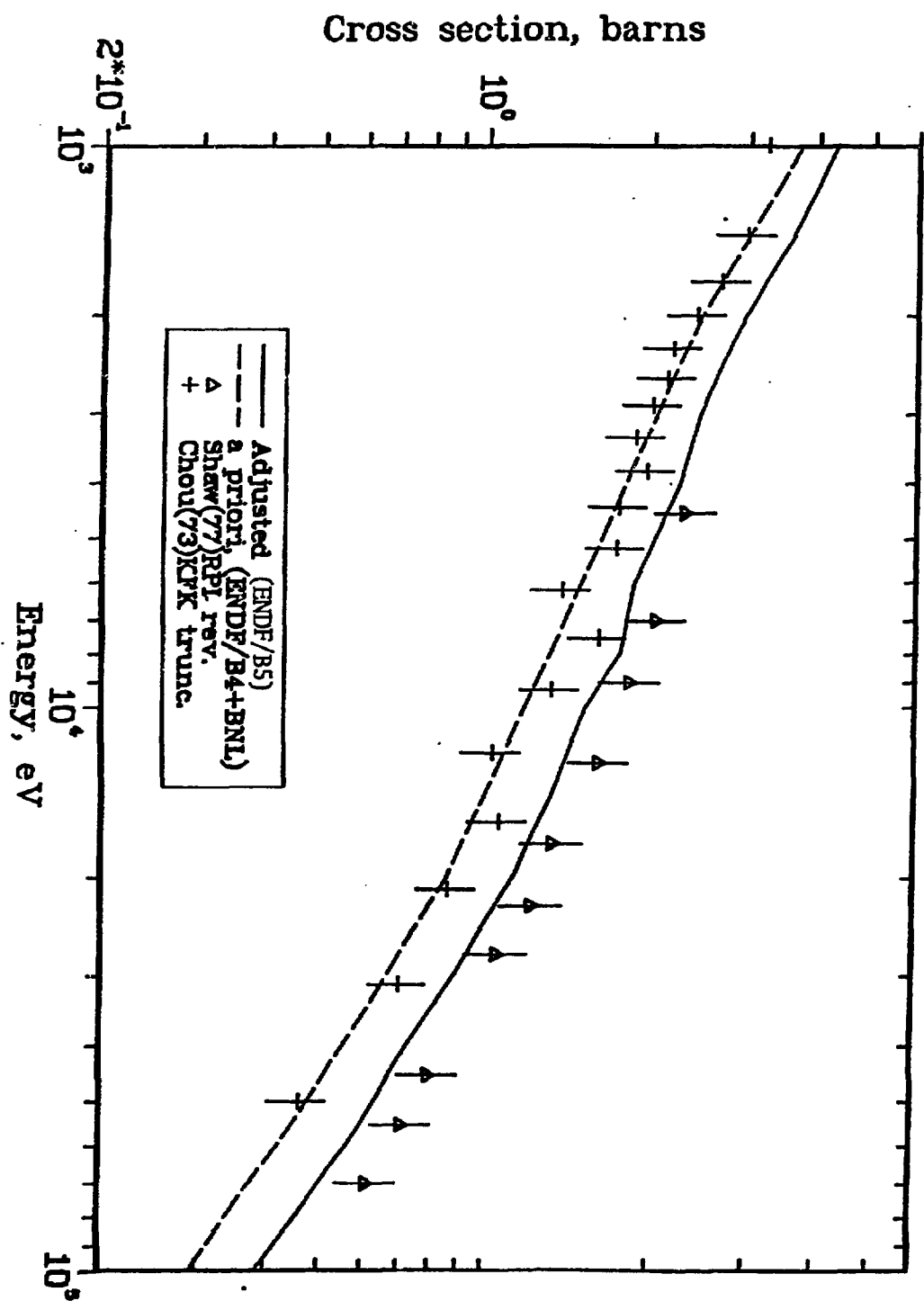
1. F. Schmittroth, "FERRET Data Analysis Code," HEDL TME-79-40, September 1979.
2. J.W.M. Dekker, ECN-14, February 1977. (STEK information)
3. Y.D. Harker, et. al., TREE 1259, March 1978. (CFRMF information)

MF = 8 MT = 457

Decay data evaluation by Bunting and Reich using Nuclear Data Sheets 12, 431 (1974) by L. D. Medsker and Atomic Data File Entry (8/6/76) by Wapstra and Bos.

Tc 99 evaluation

Case PK 3.5



MAI 1308
43-Tc-99

Eval-Oct71 Z.Livolsi
BAW-1367 Dist-May74
Extended to 20 MeV for ENDF/B Version-IV
* * * * *

Technetium-99 evaluated by Zizo Livolsi Babcock+Wilcox October 71

Sigma-Total 2200m/sec= 24.07 b
Sigma-Scat. 2200m/sec= 5.04 b
Sigma-Capt. 2200m/sec= 19.03 b
1/E weighted capt.integral above .5eV= 353.35 b

For all pertinent information regarding these data, please refer to BAW-1367 (or ENDF-144)

File Contents

- 1-453 Decay chain (1,2,3)
- 2-151 Resolved resonances and bound level (4) all s-wave
Unresolved resonances (5) s and p-waves
- 3-001 Total cross section calculated by optical model (6) converging on experiment (7) above 2. MeV
- 3-002 Elastic scattering Xsection resultant of compound (8) and shape elastic (6)

- 3-004 Total (n,n*) scattering (8)
- 3-016 (n,2n) scattering (9,10)
- 3-051 Excited discrete (n,n*) levels (1,8)
thru excited discrete (n,n*) levels (1,8)
- 3-061 Excited discrete (n,n*) levels (1,8)
- 3-091 (n,n*) levels described by continuum (8)
- 3-102 Capture xsection below 300eV due to resolved resonances(4)
up to 140keV correction imposed on unresolved Xsection(5)
up to 15MeV in competition with excited levels and correctd
for energy variation of gamma strength function (8,11) above
5MeV contribution from direct + collective capture (12)
- 4-002 Diff. elastic calculated by MR Bhat for Ag (no exp data)
- 5-016 Maxwellian evaporation spectrum for (n,2n)
- 5-091 Maxwellian evaporation spectrum for (n,n*)

References

- 1- CM Lederer, JM Hollander, I Perlman, 6th ed(1967)
- 2- G Cenacchi, T/Fima(68)4
- 3- THE Mattauch, W Thiele, AH Wapstra, Nucl.Phys 67(1965)
- 4- T Watanabe, SD Reeder, NSE 41, 188(1970)
- 5- Jen-Chang Chou, INR-4/70-28 (N/1970)
- 6- ABACUS- EH Auerbach, BNL-6562 (1964)
- 7- W Foster, SCISRS File (BNW-1967)
- 8- COMNUC- CL Dunford, AI-AEC-12931
- 9- S Pearlstein, Nucl.Data 3A, 327(1967)
- 10- JM Blatt, VF Weisskopf, Theor.Nucl.Physics, P.484
- 11- GgOD- AZ Livolsi, A Prince (not released)
- 12- FISPRO2- V Benzi, GC Panini, G Reffo, CEC(69)24

ENDF/B-V Summary Documentation

Isotope: 45-Rh-103 MAT=1310, Tape 510

HEDL	R.E. Schenter and D.L. Johnson	(Fast Capture)	Nov. '78
HEDL	F.M. Mann and F. Schmittroth	(Fast Capture)	Nov. '78
RCN	H. Gruppelaar	(Fast Capture)	Apr. '78
BAW	A.Z. Livolsi	(ENDF/B-IV)	Oct. '71

The present work supersedes the ENDF/B-IV evaluation, MAT = 1125 by Livolsi (Summary of MAT 1125 given on page 45-103-4). Only the capture cross section and the resolved resonance parameters were changed for this evaluation. The new thermal cross sections are given as:

Cross Section Value at E = 0.0253 eV

Total	150.18	B
Scatter	3.88	B
Capture	146.31	B

Capture Resonance Integral (E_c = .5 eV) 1032. B

The following indicate the changes from ENDF /B-IV:

MF=2 MT=151

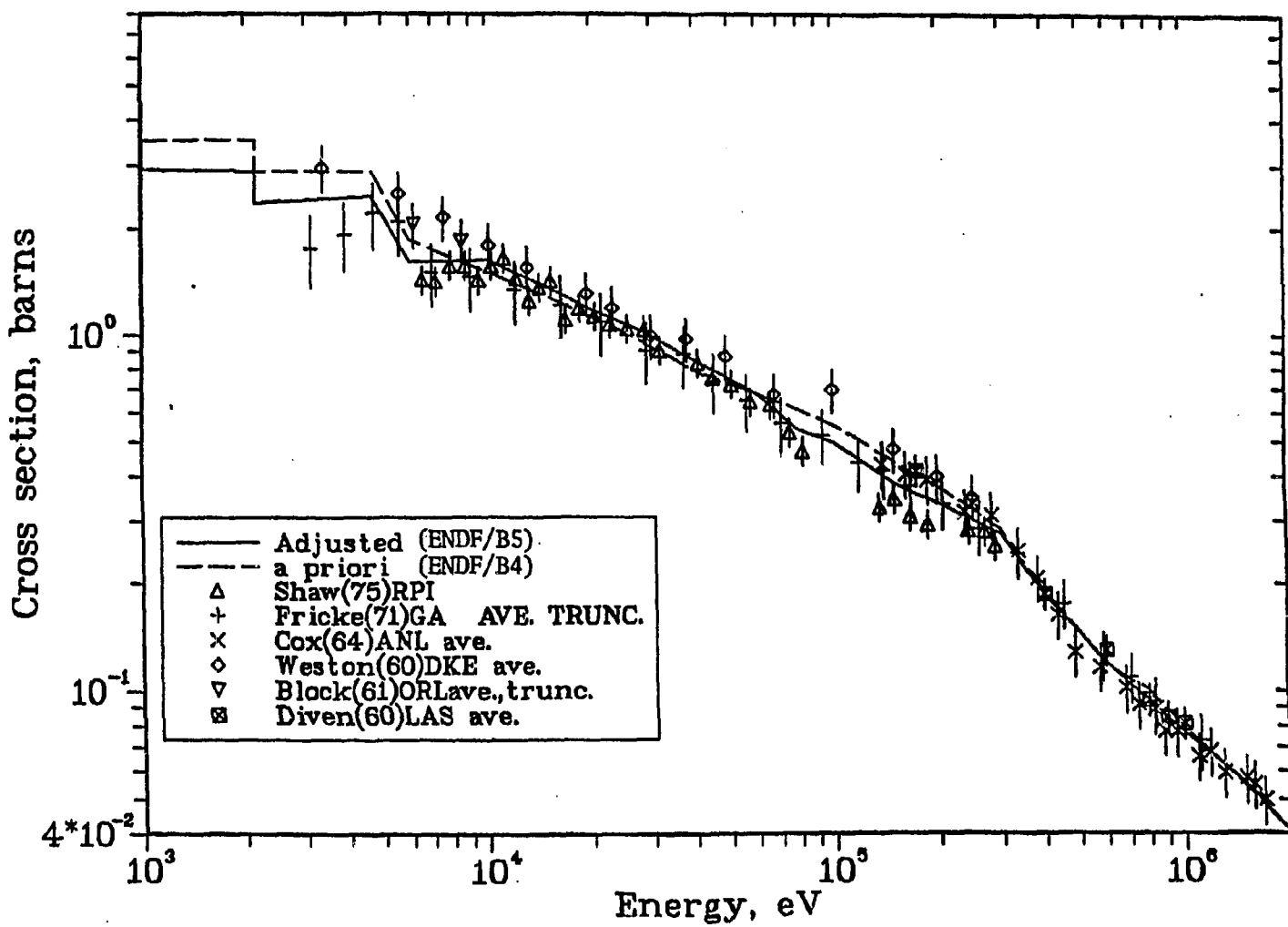
Resolved resonance parameters were obtained from BNL-325 (Third Edition, Volume 1, June 1973).

MF = 3 MT = 102

Capture cross section evaluations were obtained using a generalized least-squares approach with calculations being performed with the computer code FERRET. Results of these calculations are shown in Figure 1, where the a priori curve is from ENDF/B-IV and the adjusted curve was used as the final evaluated ENDF/B-V cross section. Input for these adjustment calculations included both integral and differential experimental data results. Figure 1 also includes the differential data values and their uncertainties which were obtained from the CSIRS library. Integral measurement results came from CFRMF and STEK Assemblies 500, 1000, 2000, 3000, 4000. References for this work include:

1. F. Schmittroth, "FERRET Data Analysis Code," HEDL TME-79-40, September 1979.
2. J.W.M. Dekker, ECN-14, February 1977. (STEK information)
3. Y.D. Harker, et. al., TREE 1259, March 1978. (CFRMF information)

RH 103 CROSS SECTION EVALUTION
 (ENDF/B4)-APRIORI
 Case PK 2.6



45-Rh-103
 MAT 1310

45-Rh-103
MAT 1310

45-RH-103 (MAT=1125)
by Livolsi at B+W
Reviewed by D.T.S.

Eval-Oct71 Z.Livolsi
BAW-1367 (ENDF-144) Dist-May74
Extended to 20 MeV for ENDF/B Version-IV
* * * * *

Rhodium - 103 Evaluated by Zizo Livolsi Babcock+Wilcox October 71

Sigma-Total 2200M/Sec= 151.68 b
Sigma-Scat. 2200M/Sec= 3.46 b
Sigma-Capt. 2200M/Sec= 148.21 b
1/E weighted capt.integral above .5eV=1048.34 b

For all pertinent information regarding these data, please refer to BAW-1367 (or ENDF-144)

File Contents

- 1-453 Decay chain (1,2,3)
- 2-151 Resolved resonances (4,5) set P-waves
unresolved resonances (4) set P-waves, obs.lv1.spac.(5)
- 3-001 Total cross section calculated by optical model (6) converging on experiment below (7) and above (8) 2MeV
- 3-002 Elastic scattering Xsection resultant of compound (9) and shape elastic (6)
- 3-004 Total (n,n*) scattering (9,10,11,12)
- 3-016 (n,2n) scattering (13,14)
- 3-051 Excited discrete (n,n*) levels (1,9,10)
thru excited discrete (n,n*) levels (1,9,10)
- 3-064 Excited discrete (n,n*) levels (1,9,10)
- 3-091 (n,n*) levels described by continuum (9)

- 3-102 Capture Xsection below 40keV due to resolved and unresolved resonances (4,5) up to 15MeV in competition with excited levels and corrected for energy variation of gamma-strength function (9,15) above 5MeV contribution from direct and collective capture (16,17)
- 3-102 Metastable state capture given as histogram below 1.855eV of 0.15164 lethargy width up to 4.15keV 0.07713 du above 4.15keV Xsection continuous. isomeric ratio from Ponitz(18)
- 4-002 Diff. elastic calculated by MR Bhat for Ag (no exp. data)
- 5-016 Maxwellian evaporation spectrum for (n,2n)
- 5-091 Maxwellian evaporation spectrum for (n,n*)

References

- 1- CM Lederer, JM Hollander, I Perlman, 6th ed(1967)
- 2- G Cenacchi, T/Fima(68)4
- 3- THE Mattauch, W Thiele, AH Wapstra, Nucl.Phys 67(1965)
- 4- AD Carlson, MP Fricke, UC-34 (6/1971)
- 5- P Ribon, CEA-N-1149 (1969)
- 6- ABACUS- EH Auerbach, BNL-6562 (1964)
- 7- CA Uttley, KM Diment, AERE-PR/NP9 (1966)
- 8- W Foster, SCISRS File, (BNW-1967)
- 9- COMNUC- CL Dunford, al-AEC-12931
- 10- MA Rothman et al., Phys.Rev.107,155(1957)

45-Rh-103
MAT 1310

- 11- KK Seth, SCISRS File (Duke-1965)
- 12- JP Butler, DC Santry, Neut.Xsect.Conf,2,802(1968)
- 13- H Bissem et al. EANDC(E)127U,P.38
- 14- HA Tewes et al. UCRL-6038-T (1960)
- 15- GGOD- AZ Livolsi, A Prince (not released)
- 16- FISPRO2- V Benzi, GC Panini, G Reffo, CEC(69)24
- 17- G Longo et al (To be published in Nucl.Physics)
- 18- W Ponitz, EANDC(e)66(u)

47-Ag-107
MAT 1371

ENDF/B-V Summary Documentation

Isotope: 47-Ag-107 MAT=1371, Tape 510

HEDL	R.E. Schenter and D.L. Johnson	(Fast Capture)	Nov. '78
HEDL	F.M. Mann and F. Schmittroth	(Fast Capture)	Nov. '78
BNL	M.R. Bhat and A. Prince	(ENDF/B-IV)	Oct. '71

The present work supersedes the ENDF/B-IV evaluation, MAT - 1138 by Bhat and Prince (Summary of MAT 1138 given on page 47-109-4). Only the capture cross section was changed for this evalution. The thermal cross sections are given as:

Cross Section Value at E - 0.0253 eV

Total	42.47	B
Scatter	5.62	B
<u>Capture</u>	<u>36.85</u>	B

Capture Resonance Integral (E_c=.5 eV) 115.2 B

The following indicates the changes from ENDF/B-IV:

47-107-107
MAT 1371

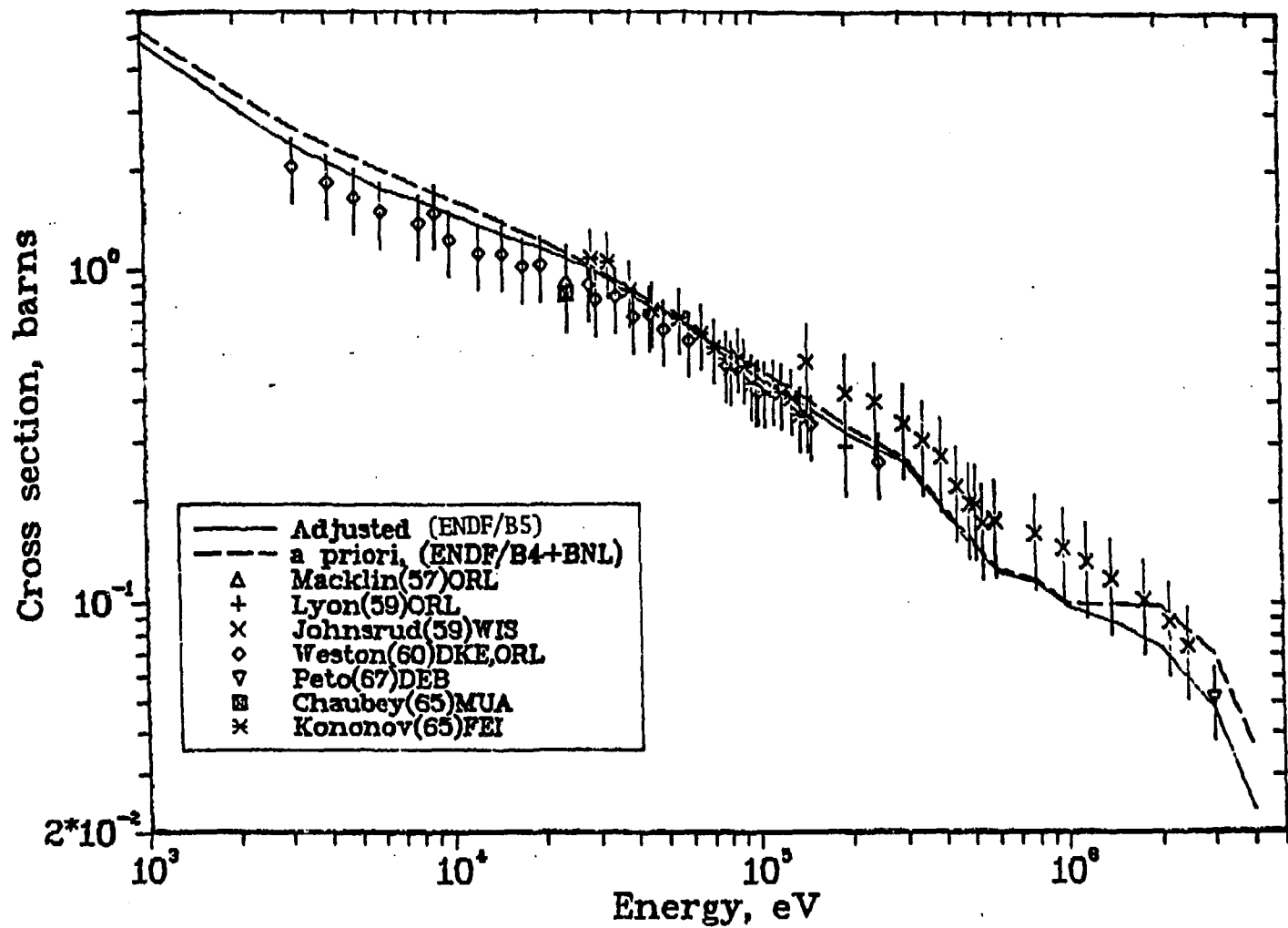
MF = 3 MT = 102

Capture cross section evaluations were obtained using a generalized least-squares approach with calculations being performed with the computer code FERRET. Results of these calculations are shown in Figure 1, where the a priori curve is from ENDF/B-IV and the adjusted curve was used as the final evaluated ENDF/B-V cross section. Input for these adjustment calculations included both integral and differential experimental data results. Figure 1 also includes the differential data values and their uncertainties which were obtained from the CSIRS library. Integral measurement results came from CFRMF. References for this work include:

1. F. Schmittroth, "FERRET Data Analysis Code," HEDL TME-79-40, September 1979.
2. Y.D. Harker, et. al., TME 1259, March 1978. (CFRMF information)

Ag 107 evaluation

Case PK 35.2



E-101-14

47-Ag-107
MAT 1371

ENDF/B-V Summary Documentation

Isotope: 47-Ag-109 MAT=1373, Tape 510

HEDL	R.E. Schenter and D.L. Johnson	(Fast Capture)	Nov. '78
HEDL	F.M. Mann and F. Schmittroth	(Fast Capture)	Nov. '78
RCN	H. Gruppelaar	(Fast Capture)	Apr. '78
BNL	M.R. Bhat and A. Prince	(ENDF/B-IV)	Oct. '71

The present work supersedes the ENDF/B-IV evaluation, MAT = 1139 by Bhat and Prince (Summary of MAT 1139 given on page 47-109-4). Only the capture cross section was changed for this evaluation. The thermal cross sections are given as:

Cross Section Value at E = 0.0253 eV

Total	93.47	B
Scatter	1.68	B
Capture	91.79	B

Capture Resonance Integral (E_c = .5 eV) 1459. B

The following indicates the changes from ENDF/B-IV:

47-Ag-109
MAT 1373

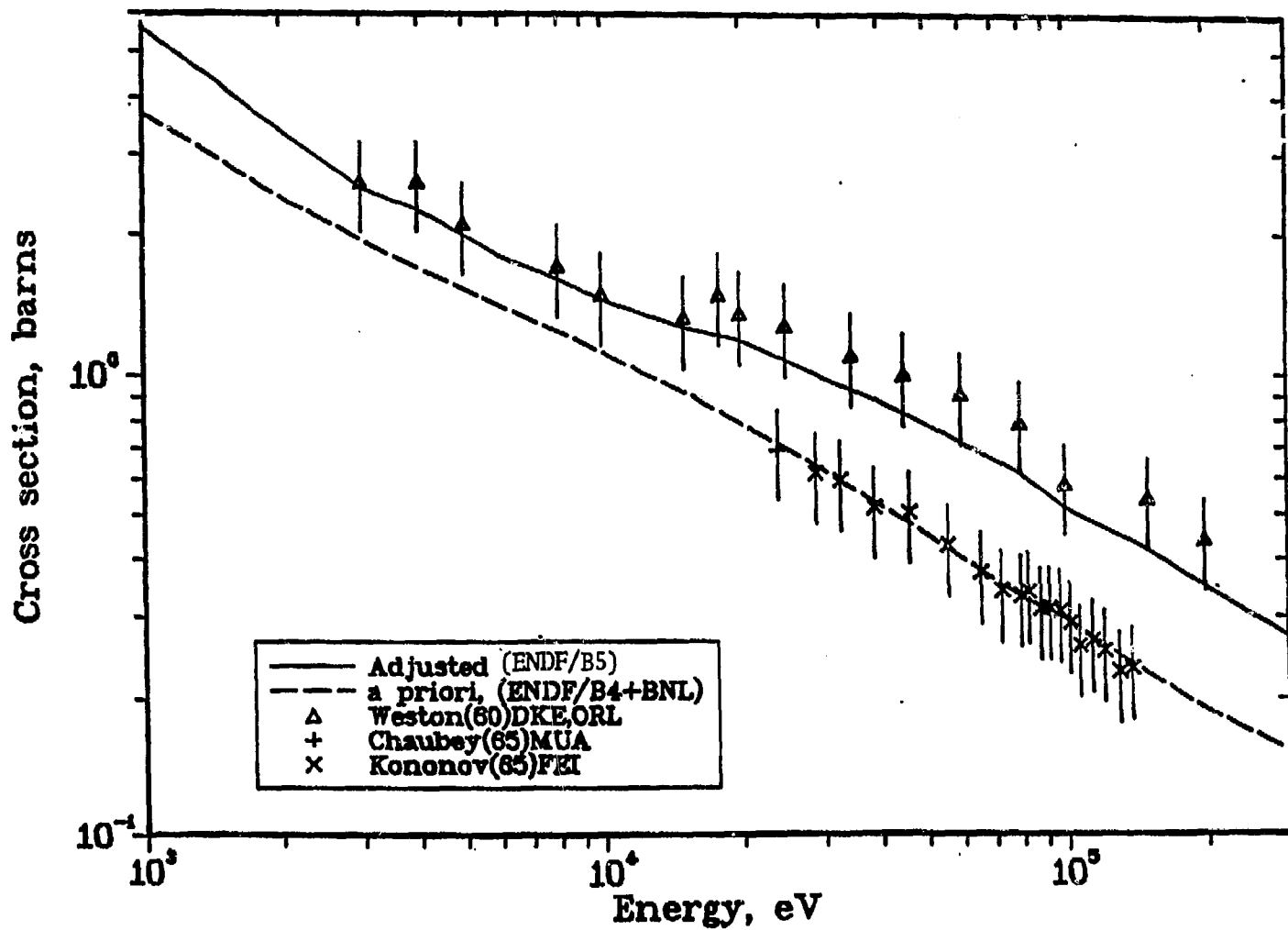
MF = 3 MT = 102

Capture cross section evaluations were obtained using a generalized least-squares approach with calculations being performed with the computer code FERRET. Results of these calculations are shown in Figure 1, where the a priori curve is from ENDF/B-IV and the adjusted curve was used as the final evaluated ENDF/B-V cross section. Input for these adjustment calculations included both integral and differential experimental data results. Figure 1 also includes the differential data values and their uncertainties which were obtained from the CSIRS library. Integral measurement results came from CFRMF and STEK Assemblies 500, 1000, 2000, 3000, 4000. References for this work include:

1. F. Schmittroth, "FERRET Data Analysis Code," HEDL TME-79-40, September 1979.
2. J.W.M. Dekker, ECN-14, February 1977. (STEK information)
3. Y.D. Harker, et. al., TREE 1259, March 1978. (CFRMF information)

Ag 109 evaluation

Case PK 12.4



47-Ag-109
MAR 1373

47-109-109
MAT 1373

SUMMARY DOCUMENTATION FOR THE EVALUATION OF ^{107}Ag , ^{109}Ag , AND ^{133}Cs

M. R. Bhat and A. Prince
NNCSC, Brookhaven National Laboratory

1. INTRODUCTION

This report describes the evaluation of Ag-107, Ag-109 and Cs-133 for the Evaluated Nuclear Data File, Version III (ENDF/B-III). The choice of the several pieces of experimental data used in the evaluation and the justification for such a choice are discussed in this report. The energy range covered by these evaluations is from 10^{-5} eV to 1.5×10^7 eV. The experimental data has been supplemented by the results of nuclear model calculations in the energy regions where such data were not available. These codes and the results of their calculations are described in the following pages.

2. LOW ENERGY CROSS SECTIONS

2.1. Resolved Resonance Parameters:

Ag-107, Ag-109

The most extensive measurements of the resonance parameters on the separated isotopes of silver are due to Muradyan and Adamchuk⁽¹⁾. These authors give the resonance parameters of Ag-107 up to 915 eV and for Ag-109 up to 903 eV. We have made use of these parameters as well as those recommended in BNL-325, 2nd Edition.⁽²⁾ Resonance spins where available are indicated as given in the latter reference. The gamma widths given explicitly in BNL-325 for some resonances have been used; otherwise we have set $\Gamma_\gamma = 0.140$ eV. The nuclear radius used for Ag-107 is 0.71365×10^{-12} cm. which gives a $\sigma_p = 6.4$ barns; a value obtained in the measurements of Shull and Wollan.⁽³⁾ This experimental value also agrees with the measurements of Zimmerman and Hughes⁽⁴⁾ who obtained $\sigma_p = 6.5 \pm 0.5$ barns. The nuclear radius used for Ag-109 is

0.63×10^{-12} cm a value given by Chrien⁽⁵⁾ from an analysis of the transmission data on low energy resonances. It is quite possible that some of the resonances given are p-wave resonances. However, since none of them has been specifically identified as such all the resonances have been grouped together as s-wave resonances.

Cs-133

We have used the resonance parameters of Cs-133 as given by Garg, et al.⁽⁶⁾ The measured resonances extend up to an energy of 3.5 keV. The assumed value of Γ_γ was 0.110 eV. None of the resonance spins are known. Hence, we have put the resonance spins as 7/2; the spin of the target nucleus. The nuclear radius used here 0.75166×10^{-12} cm. Which corresponds to a $\sigma_p = 7.1$ barns as measured by Shull and Wollan⁽³⁾. Since none of these resonances has been designated as p-wave resonances we have listed all of them as s-wave resonances.

2.2. 2200 m/sec Neutron Capture Cross Section

Ag-107, Ag-109

We have used a value of 92 barns for the 2200 m/sec neutron capture cross section for Ag-109 as suggested by Walker.⁽⁷⁾ The contribution to the capture cross section from the resonance parameters is 89.96 barns and we have added the difference as a 1/v contribution. For Ag-107 we have used a value of 36.8 barns for the capture cross section. This value was obtained by taking 63.4 barns for the capture cross section of natural silver as measured by Tattersall, et al.⁽⁸⁾ and calculating the contribution of Ag-107 by assuming 92 barns for Ag-109.

47-Ag-109
MAT 1373

In the case of Ag-107 the resonance parameters contribution 2.56 barns for the capture cross section and the difference has been added on as a 1/v contribution.

Cs-133

The thermal capture cross section recommended by Walker⁽⁹⁾ for this nucleus is 29.5 barns. We have used this value in the evaluation; this is made up of 16.06 barns from the resonance parameters and the rest being added on as a 1/v contribution.

3. HIGH ENERGY CROSS SECTIONS

3.1. Optical Model Parameters

The high energy cross section data available for these nuclei consists of capture and total cross section measurements over limited energy ranges with a few values of the (n , particle) reaction cross sections. Hence, the gaps in the experimental data have to be filled by nuclear model calculations. Therefore, one has to decide on a set of optical model parameters suitable for the nuclei under consideration. Such a choice of optical model parameters was made by fitting the total cross section data of Foster⁽⁹⁾ for natural silver and cesium between 2.5 - 15.0 MeV. It is found that the optical parameters of Wilmore and Hodgson⁽¹⁰⁾ give total cross sections which agree quite well with the experimental data. The calculations were done with the ABACUS-NBARREX Code.⁽¹¹⁾ The optical model parameters used are shown in Table I.

3.2. Capture Cross Sections

Ag-107

The calculations of the capture cross section of Ag-107 were done using the code COMMNUC by C. Dunford.⁽¹²⁾ The excited states of Ag-107 used in these calculations are given in Table V along with their spins and parities. One other input data needed by this program is $2\pi \frac{\Gamma_v}{\langle \Delta \rangle} = 0.05965$ where $\langle \Delta \rangle$ is the average level spacing as determined from the neutron resonance parameter data for this nucleus. This parameter may also be considered as a normalizing parameter whose value is so adjusted as to get a fit to the experimental capture cross sections. In the case of Ag-107 we obtain a value of $2\pi \frac{\Gamma_v}{\langle \Delta \rangle} = 0.05965$ from the resonance parameters. However, it was found that the experimental capture data could be fitted with a value of 0.04029. The experimental data chosen for the fit was from Obninsk⁽¹³⁾ from 29keV to 146keV and from the University of Wisconsin,⁽¹⁴⁾

from 145 keV to 2.45 MeV. These measurements agree quite well with the Duke University (15) capture data above 60 keV or so though the Duke data seems to be consistently lower for lower energies. There is no experimental data on capture cross sections of Ag-107 at higher energies of 14-15 MeV. Hence, one could not estimate the contribution of direct and semi-direct capture at these higher energies. The capture cross section is therefore shown as a monotonically decreasing function of energy and is shown compared with the experimental data in Figure 1.

Ag-109

The experimental capture cross sections used for this isotope is again due to Kononov, et al. (13) from Obninsk. The cross section at 24 keV in this set agrees quite well with the single measurement due to Chaubey, et al. (16). However, all the values of capture cross sections in this set are lower than the Duke values as read off from their published curve. Also, if we combine the Obninsk values for Ag-107 and Ag-109 in the proportion of the natural abundance of these isotopes we get a capture cross section for natural silver which is about 16% lower systematically than the Karlsruhe measurements. (17) These discrepancies indicate need for further accurate measurements on separated isotopes of silver to resolve them. One could obtain a fit for the Obninsk capture data with $2\pi \frac{\Gamma}{D} = 0.02$ though the resonance parameters give a value of 0.0586. The calculated and experimental cross sections for Ag-109 are shown in Figure 2.

Cs-133

The most recent and careful measurements of the capture cross section of cesium in the keV region seem to be those due to Kompe (17) from Karlsruhe. We could fit this data by using $2\pi \frac{\Gamma}{D} = 0.03831$; a value obtained from the resonance parameter data. The calculated and experimental

cross sections are shown in Figure 3. In the case of this nucleus we do have an (n, γ) cross section measurement due to Qaim⁽¹⁸⁾ at 14.8 MeV. Therefore calculations of the direct and semi-direct capture cross sections were made using FISSPRO Code of Benzi, et al.⁽¹⁹⁾ and normalized to the experimental value of 7.1 mbarn at 14.8 MeV. This contribution to the capture cross section was added on to the capture cross section due to compound nuclear processes above 4.0 MeV.

3.3. Differential Elastic Scattering

Since there is no experimental data on the angular distribution of elastically scattered neutrons from these three nuclei we used the ABACUS-NEARREX Code to calculate the angular distribution. The calculated cross sections were then fitted to a number of Legendre polynomials using the Code CHAD⁽²⁰⁾ to obtain the corresponding coefficients of a Legendre fit.

3.4. Inelastic Scattering

There is no experimental data on inelastic scattering for any of these three nuclei. The relevant cross section were therefore calculated using COMMNUC and the energy level scheme shown in Table II.

3.5. $(n, \text{particle})$ Reactions

Ag-107

Amongst all the measurements of the $(n, 2n)$ cross sections on Ag-107, there is only one experiment due to Minetti and Pasquarelli⁽²¹⁾ who measure simultaneously the cross sections for populating the 6^+ ($T_{1/2} = 8.3$ days) metastable state in Ag-106 as well as the 1^+ ($T_{1/2} = 24$ min) ground state. They find these two cross sections to be 653 ± 30 mb and 870 ± 40 mb

respectively at 14.7 MeV. We have chosen then values for normalizing the $(n,2n)$ reaction cross section curve as calculated by Pearlstein⁽²²⁾ using the code THRESH. This code uses the standard evaporation model of a highly excited nucleus to calculate the various $(n, \text{ particle})$ reaction cross sections. The cross sections calculated with this code using a $Q = 9.531$ MeV give a curve which passes through the experimental value of 1523 ± 70 mb at 14.7 MeV; hence we did not have to renormalize the calculated curve. Using the same code and $Q = -0.752, -4.354$ for the (n,p) and (n,α) reactions respectively the corresponding cross sections were calculated. Since there were no experimental data available on these reactions for Ag-107, the same normalization constants as had been used to normalize the calculated curves of Ag-109 to its experimental points were used here.

Ag-109

Minetti and Pasquarelli⁽²¹⁾ obtained a cross section of 797 ± 50 mb for the $(n,2n)$ reaction on Ag-109 leading to the 1^+ ground state of the final nucleus Ag-108. However, they did not measure the cross section leading to the 6^+ metastable state in the final nucleus. In the case of the $(n,2n)$ reaction on Ag-107 we populate a 1^+ ground state and a 6^+ metastable state in Ag-106. The ratio of these two cross sections are 0.751. Since we have states of the same spin in Ag-108 we can assume the same ratio for these two cross sections. Assuming $\sigma^{(g)} = 797$ we get $\sigma^{(m)} = 598$ mb giving the total $(n,2n)$ cross section as 1395 mb at 14.7 MeV. The $(n,2n)$ reaction cross section curve as calculated from the THRESH code with $Q = 9.182$ MeV was normalized to this experimental value. Using the same code we also calculated the

(n,p) cross section curve with a $Q = 0.538$ MeV. This curve was normalized to an experimental value of 15 mbarn at 14.5 MeV. This value was estimated from the measurements of Bayhurst and Prestwood⁽²³⁾ and Coleman.⁽²⁴⁾ The (n, α) cross section was similarly calculated with $Q = -3.403$ and the calculated curve normalized to a value due to Mukerjee, et al.⁽²⁵⁾

Cs-133

The experimental values for the (n,2n) cross sections used in the evaluation are 1620 ± 150 mb at 14.8 MeV by Qaim⁽¹⁸⁾ and 1598 ± 160 mb by Nagel⁽²⁶⁾ at 14.6 MeV. Their mean of 1609 mb was used to normalize the curve calculated using THRESH with $Q = 9.038$. The (n,p) cross section curve was calculated using a $Q = 0.121$ MeV and normalized to 10.5 mb at 14.8 MeV due to Qaim.⁽¹⁸⁾ The (n, α) cross section values were similarly calculated with $Q = -3.695$ MeV and normalized to a mean of the experimental values of $1.96 \pm .15$ mb at 14.4 MeV due to Lu, et al.⁽²⁷⁾ and $1.14 \pm .2$ mb at 14.8 MeV due to Qaim.⁽¹⁸⁾

3.6. Energy Distributions of Secondary Neutrons

For the nuclei under consideration, energy distributions of secondary neutrons originating from (n,2n) processes and by inelastic scattering to a continuum of levels was also calculated. These energy distributions are expressed as normalized probability distributions. The energy distributions for these nuclei have been specified as an evaporation spectrum of the type

$$f(E \rightarrow E') = \frac{E'}{I} e^{-E'/\theta}$$

where I is the normalization constant and

$$I = \theta^2 \left[1 - e^{-(E-U)/\theta} \left(1 + \frac{E-U}{\theta} \right) \right]$$

Where θ is a temperature tabulated as a function of neutron energy E and U defines the upper limit for the final neutron energy such that $0 \leq E' \leq E - U$. To calculate θ as a function of neutron energy, we used the nuclear level density formulation of Gilbert and Cameron (28) with shell corrections. The basic idea of their approach is to match two types of level density formulae:

$$\rho_1 = \frac{1}{T} e^{-(E-E_0)/T}$$

which holds true for energies lower than a characteristic energy E_x and

$$\rho_2 = \frac{\sqrt{\pi}}{12} \frac{\exp(2\sqrt{aU})}{a^{1/4} U^{5/4}} \frac{1}{\sqrt{2\pi}\sigma}$$

applicable to energies greater than E_x . E_x may be determined from the nuclear systematics given in this paper and T and E_0 are determined by fitting ρ_1 and ρ_2 at $E = E_x$. For energies where the formula ρ_2 is applicable the nuclear temperature τ is

$$\frac{1}{\tau} = \sqrt{\frac{a}{U}} - \frac{3}{2U}$$

where again a and U may be determined from the tables given by Gilbert and Cameron. In the low energy density expression, the nuclear temperature is considered a constant whereas in the high energy expression it is energy dependent as shown by the expression for τ .

References

1. G. V. Muradyan and Yu. V. Adamchuk, IAEA Conf. on Nuclear Data, Paris, Vol. I (1966) 79.
2. Neutron Cross Sections, Vol. II B, Z=41-60, BNL-325, 2nd Edition, Supplement No. 2, M. D. Goldberg, S. F. Mughabghab, S. N. Purohit, E. A. Magurno, and V. M. May, 1966.
3. G. G. Shull and E. O. Wollan, Phys. Rev. 81 (1951) 527.
4. R. L. Zimmerman and D. J. Hughes, Bull. Am. Phys. Soc. 3 (1958) 176.
5. R. E. Chrien, Phys. Rev. 141 (1966) 1129.
6. J. B. Garg, J. Rainwater, and W. W. Havens, Jr., Phys. Rev. 137 B (1965) 547.
7. W. H. Walker, AECL-3037 and Memo to Fission Products Subcommittee, April 8, 1970.
8. R. B. Tattersall, H. Rose, S. K. Pattenden, and D. Jowitt, Journal Nuclear Energy A12 (1960) 32.
9. D. G. Foster, Jr., and D. W. Glasgow, Phys. Rev. C3 (1971) 576, and SCISRS -I File.
10. D. Wilmore and P. E. Hodgson, Nuc. Phys. 55 (1964) 673. There is an error in Eqn(10), p. 676 of this paper where $W = 9.52 - 0.53E$ should be $W = 9.52 - 0.053$. See P. E. Hodgson, Ann. Rev. Nucl. Sci. 17, 1. Also P. Marmier and E. Sheldon, "Physics of Nuclei and Particles" Vol. II, p. 1107, Academic Press, 1970.
11. P. A. Moldauer and S. A. Zawadzki, Private Communication.
12. C. Dunford, COMMNUC, AI-AEC-12931.
13. V. N. Kononov, Yu. Ya Stavisskii; S. R. Chistozvonov, V. S. Shorin IAEA, Conf. on Nuclear Data, Paris, Vol. I (1966) 469, and SCISRS-I File.
14. A. E. Johnsrud, M. G. Silbert, and H. H. Barschall, Phys. Rev. 116 (1959) 927, and SCISRS-I File.

47-Ag-109
MAT 1373

15. L. W. Weston, K. K. Seth, E. G. Bilpuch, and H. W. Newson, *Annals of Physics* 10 (1960) 477.
16. A. K. Chaubey and M. L. Sehgal, *Phys. Rev.* 152 (1966) 1055.
17. D. Kompe, *Nucl. Phys.* A133 (1969) 513, and SCISRS-I File.
18. S. M. Qaim, *Jour. Inorg. and Nucl. Chem.* 32 (1970) 1799.
19. V. Benzi, G. C. Panini, and G. Reffo, *GEC(69)24*.
20. R. F. Berland, CHAD, (NAA-SR-11231).
21. B. Minetti and A. Pasquarelli, *Nucl. Phys.* A118 (1968) 449.
22. S. Pearlstein, *Neutron-Induced Reactions in Medium Mass Nuclei, J. Nucl. Energy* 27 (1973) 81.
23. B. P. Bayhurst and R. J. Prestwood, *Jour. Inorg. and Nucl. Chem.* 23 (1961) 173.
24. R. F. Coleman, B. E. Hawker, L. P. O'Connor, and J. L. Perkin, *Proc. Phys. Soc.* 73 (1959) 215.
25. S. K. Mukherjee, A. K. Ganguly and N. K. Majumdar, *Proc. Phys. Soc.* 77 (1961) 508.
26. W. Nagel and A. H. W. Aten, Jr. *Physica* 31 (1965) 1097.
27. W. Lu, N. Ranakumar, and R. W. Fink, *Phys. Rev.* 1C (1970) 358.
28. A. Gilbert and A. G. W. Cameron, *Can. Jour. Phys.* 43 (1965) 1446.

47-Ag-109
MAT 1373

Table I. Optical Model Parameters

$$V(r) = Uf(r) + iWg(r)$$

$$f(r) = \left[1 + \exp(r-R)/a_U \right]^{-1}$$

$$g(r) = 4\exp\{(r-R)/a_W\} \left[1 + \exp(r-R)/a_W \right]^{-2}$$

$$r_0 = 1.26 \text{ fm} \quad a_U = 0.66 \text{ fm} \quad a_W = 0.48 \text{ fm}$$

$$R = r_0 A^{1/3} \text{ fm}$$

$$U = 47.01 - 0.267 - 0.00118E^2 \text{ MeV}$$

$$W = 9.52 - 0.053 \text{ MeV}$$

Spin orbit term = 0.

47-109-15

47-Ag-109
MAT 1373

Table II. Energy Levels

Ag-107		Ag-109		Cs-133	
<u>E_{ex} (keV)</u>	<u>J^π</u>	<u>E_{ex} (keV)</u>	<u>J^π</u>	<u>E_{ex} (keV)</u>	<u>J^π</u>
0.0	1/2-	0.0	1/2-	0.0	7/2+
93.0	7/2+	88.0	7/2+	81.0	5/2+
126.0	9/2+	133.0	9/2+	161.0	5/2+
325.0	3/2-	311.0	3/2-	384.0	3/2+
423.0	5/2-	415.0	5/2-	437.0	1/2+
787.0	3/2-	702.0	3/2-	633.0	9/2+
922.0	5/2+	Continuum ≥ 950 keV		Continuum ≥ 710 keV	

47-109-16

47-AG-109
MAT 1373

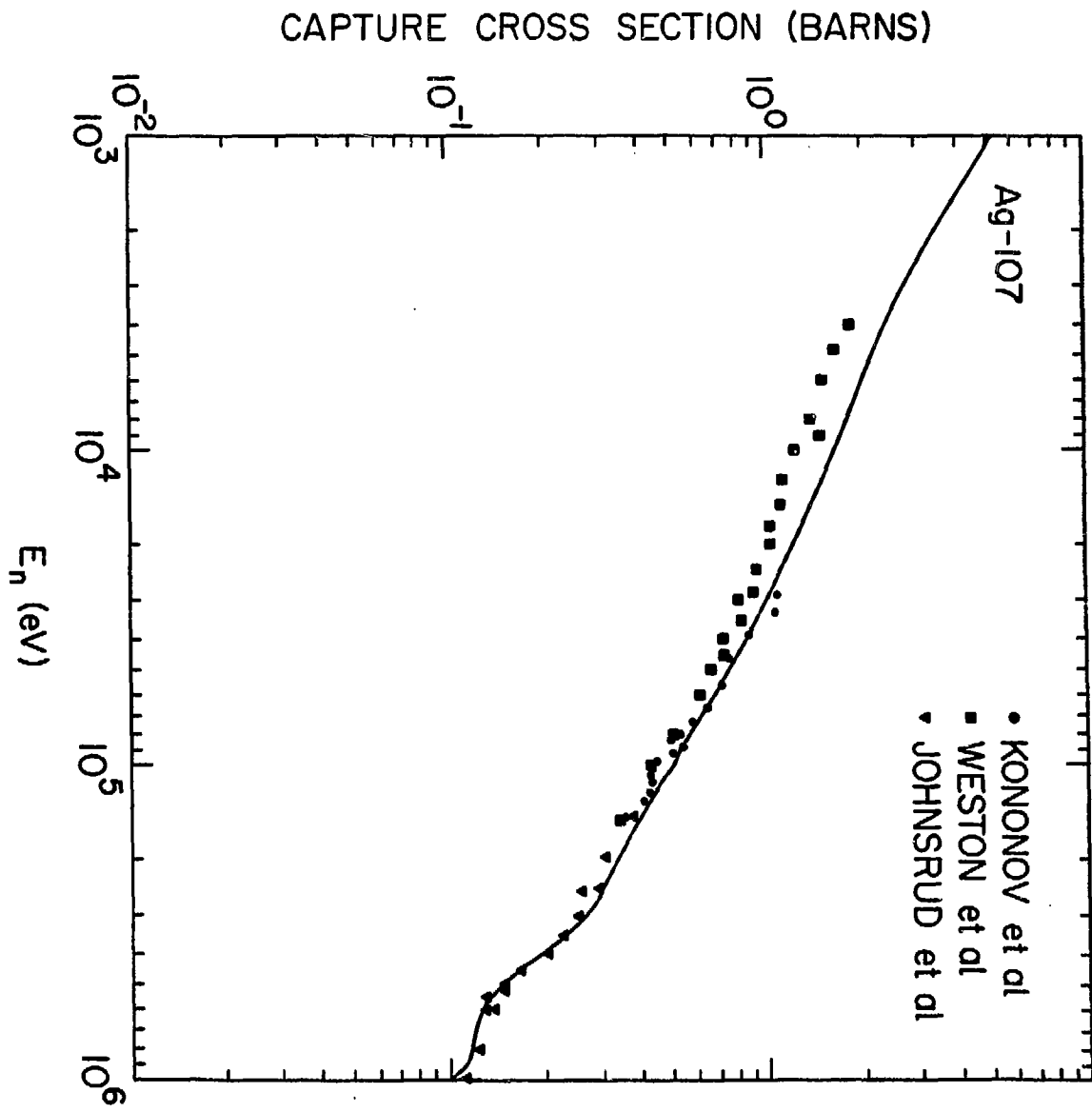


FIG. 1

47-109-17

47-Ag-109
MAT 1373

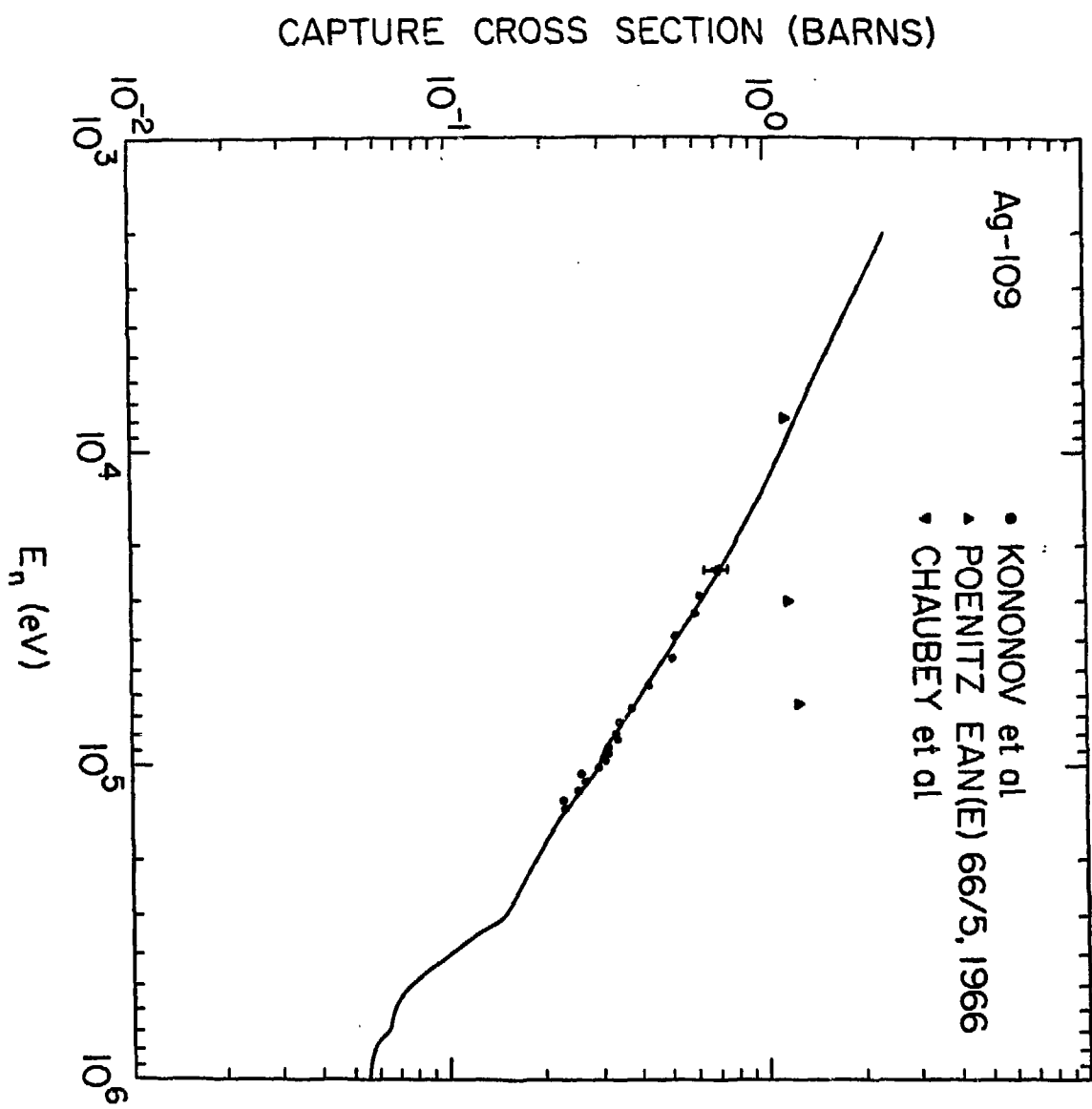


Fig. 2

47-109-109
MAT 1373

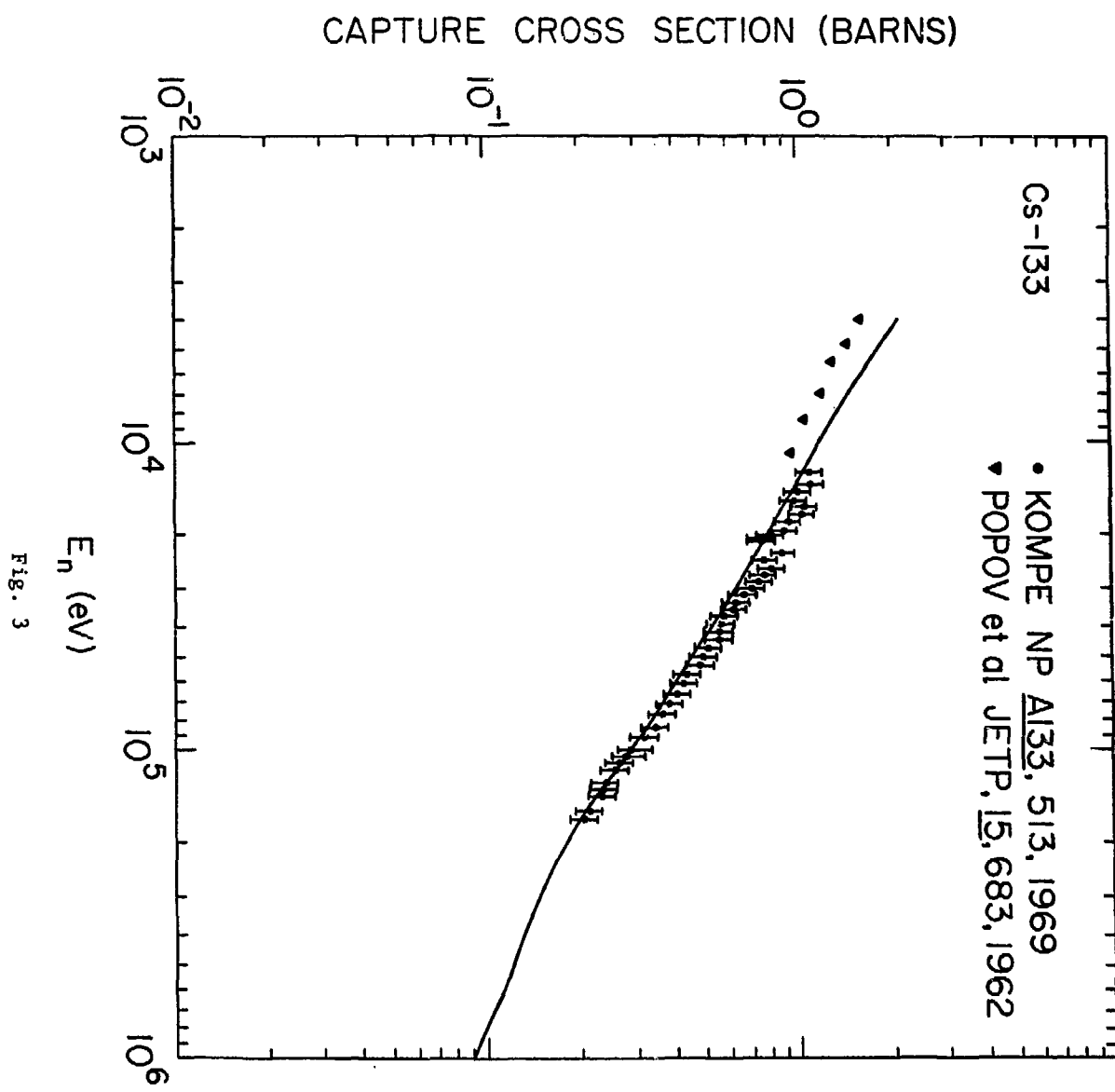


Fig. 3

Natural Cadmium (MAT 1281) and Cadmium-113 (MAT 1282)

Source

United Kingdom Nuclear Data Library (UKNDL) - Received 1973.
Natural Cadmium originally DFN 70. Cadmium-113 originally DFN 71.
Translated to ENDF formats using UKE⁽¹⁾.

Evaluators

The resonance region was evaluated by M. F. James (Winfrith) in 1969.
The high energy data was taken from the work of M. K. Drake (General Atomic).
The energy range was extended from 10^{-6} eV to 20 MeV by Pearlstein (Brookhaven)
in 1973.

Documentation

Work of James unpublished. This summary documentation based on notes
provided by J. Story⁽²⁾ (Winfrith). Data above the resolved resonance region
is mainly that of Drake⁽³⁾.

Resonance Region

For natural cadmium a fictitious resonance introduced at -0.5 eV to adjust
cross section in the eV range and achieve consistency with the 20 barn Cd-111-
thermal capture cross section⁽⁴⁾. The nuclear properties of the cadmium
isotopes are described in table I. The preferred S-wave resonance parameters
and .0253 capture cross sections are described in Tables II and III respectively.

As a post mortem Story⁽²⁾ offered the opinion that recent data might lead
him to prefer 6.3 ± 1.1 b and 9.6 ± 3.0 b for the Cd-110 and Cd-111 g σ_{γ} values
respectively, but regards the data to be very poor and new measurements desirable.

Table I

Exact masses, atomic abundances, and ground state spin & parity quantum numbers of the isotopes of natural cadmium

Mass No.	Exact mass AMU	Atomic abundance %	I II
106	105.906463(4)	1.22 ± 0.01	0+
108	107.904189(4)	0.90 ± 0.04	0+
110	109.903010(3)	12.37 ± 0.04	0+
111	110.904186(3)	12.77 ± 0.07	$\frac{1}{2}+$
112	111.902703(3)	24.00 ± 0.13	0+
113	112.904407(3)	12.28 ± 0.05	$\frac{1}{2}+$
114	113.903367(3)	28.84 ± 0.07	0+
116	115.904762(3)	7.62 ± 0.03	0+

From the abundances and mass data may be derived the atomic mass of natural cadmium

$$112.423662 \pm 0.00292 \text{ AMU}$$

Table II

Preferred resolved resonance parameters for S-wave neutrons

Isotope	Energy (eV)	Spin J	Γ_n (MeV)	Γ_γ (MeV)
106	None	Resolved		
108	None	Resolved		
110	89.6	$\frac{1}{2}$	115	130
	372	$\frac{1}{2}$	23	130
	-0.5	(0)	0.04204	103
111	27.6	1	5.1	(103)
	69.0	(1)	0.091	(103)
	86.3	(1)	2.67	(103)
	99.6	1	13.0	72
	103.2	(0)	2.88	(103)
	115.0	(1)	0.44	(103)
	138.3	1	9.7	100
	164.2	1	59.0	104
	225.45	(1)	33.4	(103)
	233.7	0	233	160
	275.8	(1)	22.7	(103)
	314.0	(1)	3.6	(103)
	332.2	(1)	8.0	(103)
	356.5	1	49.0	93
	389.5	0	124	90
	439	(1)	16	(103)
	480	(0)	28	(103)
	541	(1)	84	(103)

Table II (Contd.)

48-Cd-0
MAT 1281

Isotope	Energy (eV)	Spin J	Γ_n (MeV)	Γ_γ (MeV)
111	578	0	296	150
	606	(1)	60	(103)
	625	(1)	694	(103)
112	66.7	$\frac{1}{2}$	6.1	95
	83.3	$\frac{1}{2}$	0.76	(95)
	226.7	$\frac{1}{2}$	25	(95)
	444.3	$\frac{1}{2}$	60	(95)
	743	$\frac{1}{2}$	180	(95)
	935	$\frac{1}{2}$	220	(95)
	1125	$\frac{1}{2}$	600	(95)
113	0.1777	1	0.6244	112.9*
	18.4	1	0.198	(111)
	56.3	(0)	0.212	(111)
	63.9	1	3.8	90
	84.9	1	29	121
	108.5	1	1.2	128
	143.2	(1)	4.54	(111)
	159.0	(1)	12.15	(111)
	193.3	0	224	112
	215.6	1	33	114
	261.5	1	45	106
	270.0	0	64	124
	292.2	(1)	76	(111)
	415.8	1	140	116
	433.8	1	36	110
	503	1	80	95
	527	1	44	100
	552	1	137	110
	625	(0)	160	(111)
	675	(1)	127	(111)
	724	1	53	(111)
	858	1	660	(111)
114	58.7	$\frac{1}{2}$	12	115
	120.1	$\frac{1}{2}$	57	100
	226.0	$\frac{1}{2}$	1.8	100
	394.1	$\frac{1}{2}$	760	100
	673	$\frac{1}{2}$	220	100
	756	$\frac{1}{2}$	140	100
	1107	$\frac{1}{2}$	1500	100
116	29.3	$\frac{1}{2}$	0.042	100

Potential scattering cross-section for all isotopes taken as 6.53 b.

Nuclear scattering radius for all isotopes taken as 7.2 fm

Table III

Preferred capture cross sections at 0.0253 eV

Isotope	Preferred	σ_{γ}^0 (barns)		
		Derived from parameters	Difference equals contribution from distant levels	Correction at Energy E(ev)
106	1.0 ± 0.5	-	1.0	$0.159/\sqrt{E}$
108	1.0 ± 0.2	-	1.0	$0.159/\sqrt{E}$
110	3.5 ± 1.0	0.825	2.7	$0.429/\sqrt{E}$
111	23.5 ± 3.0	23.52	-	-
112	0.54 ± 0.5	0.103	0.44	$0.070/\sqrt{E}$
113	$19,878 \pm 74$	-	-	-
114	0.34 ± 0.15	0.499	-	-
116	0.08 ± 0.02	0.00377	0.076	$0.0121/\sqrt{E}$
Nat.	2446 ± 9			

References

1. ENDF-134R(ORNL-TM 2880, Rev.) October 1973. R. Q. Wright, S. N. Cramer and D. C. Irving.
2. Private communication February 1974. J. Story.
3. GA-6997, March 1966. M. K. Drake.
4. ORNL-3994, September 1966. Baldock et al.

48-Cd-113
MAT 1318

ENDF/B-V Summary Documentation

Isotope: 48-Cd-113 MAT=1318, Tape 510

BNL	S. Pearlstein	(ENDF/B-IV)	1973
HEDL	F.M. Mann and R.E. Schenter	(Resonance Region)	Nov. '78
INEL	R. Bunting and C.W. Reich	(Decay)	Apr. '78

The present work is the same as the ENDF/B-IV evaluation, MAT = 1282 by Pearlstein (Summary of MAT 1282 given on page 48-0-1), except the resonance region was changed. The ENDF/B-IV evaluation was obtained from a translation of the UKNDL DFN-71 file into ENDF/B format. Above the resonance region ($E > 1.0$ Kev) mainly Drake GA-6997 was used. The new thermal cross sections are given as:

Cross Section Value at $E = 0.0253$ eV

Total	19912.	B
Scatter	22.	B
Capture	19890.	B

Capture Resonance Integral ($E_c = .5$ eV) 380.3 B

The following indicates the changes from ENDF/B-IV:

MF=2 MT=151

Resonance parameters were obtained from the results of time of flight spectroscopy measurements at Columbia University (H.I. Liou, et. al., Phys. Rev. 10, 2, August 74).

48-113-1

48-Cd-113
MAT 1318

Unresolved parameters (300<E<1000 eV) were obtained using the computer code RESPAR.

MF=8 MT=457

Decay data evaluations by Bunting and Reich using ENSDF decay data file (ENSDF Dated 770503).

Summary Documentation for the Stable Xenon Isotopes

by

M. R. Bhat and S. F. Mughabghab

1. Introduction

Evaluations of the neutron cross-sections of the nine stable isotopes of xenon were originally assembled for ENDF/B-IV and the details have appeared in a report [1]. These data files are for studies using the xenon isotopes as tag materials. The data files have been updated to include new data and some minor errors have been corrected. In the following, details of the sections for each isotope significantly modified are described.

2. Xe-124 (MAT=1335)

(i) Resolved Resonance Parameters

The resonance parameters of the 5.16 eV resonance and the newly assigned 9.88 eV resonance have been set equal to the new values obtained by Kane [2]. In addition, the 0.0253 eV capture cross-section was set equal to 164.5 ± 15 b [2] and the parameters of a bound level at -10 eV were adjusted to give the desired thermal capture. The other resolved resonance is from the work of Ribon [3]. The capture integral (0.5 to $2.0E+7$ eV) is also calculated to be 3046 b which agrees quite well with the experimental value of 3600 ± 500 b [7].

(ii) (n,2n) Cross-Section

The (n,2n) cross-section as calculated using FASCRO [4] was normalized to 957 mb at 14.5 MeV which is a mean of the data of Kondaiah et al., [5] and the new data of Sigg et al., [6].

3. Xe-126 (MAT=1339)

(i) Resolved Resonance Parameters

The thermal (0.0253 eV) capture cross-section was set equal to 2.2b, a value measured by Bresesti et al., [7]. Two resonances at 86.56 eV and 100.17 eV from the list of unassigned resonances in Ribon's Thesis [3] are assigned to Xe-126 to give a capture integral of 44b and the experimental value is 38.0 ± 3.8 b [7]. A bound level at 75 eV was also included to give the evaluated thermal capture of 2.2b.

3. Xe-126 (MAT=1339) (cont'd)

(ii) (n,2n) Cross Section

The (n,2n) cross section as calculated using FASCRO [4] was normalized to 1.481b at 14.5 MeV. This is a mean of the data of Kondaiah et al., [5] and the new measurements of Sigg et al., [6].

4. Xe-128 (MAT=1348)

(i) Resolved Resonance Parameters

The thermal capture cross-section was evaluated to be 5.36b. This was obtained by assigning 0.36b for the cross section to the metastable state which is a mean of 0.29b measured by Kondaiah et al., [5] and 0.43b obtained by Tilbury et al., [8]. To this was added 5b, the capture cross section to the ground state as measured by MacNamara and Thode [9]. The resonance parameters are mainly based on Ribon's Thesis [3] and a bound level at -10 eV was invoked and its parameters adjusted to give the evaluated thermal capture cross-section. The calculated capture resonance integral (0.5 eV to 20.0 MeV) is 11.3b.

(ii) (n,2n) and (n,p) Cross Sections

The (n,2n) cross section calculated from FASCRO [4] was normalized to 1.814b at 14.5 MeV, which is a mean of the data of Kondaiah et al., [5] and Sigg et al., [6]. The (n,p) cross section also calculated using FASCRO was normalized to 28 mb at 14.6 MeV as measured by Sigg et al., [6].

5. Xe-129 (MAT=1349)

Resolved Resonance Parameters

The thermal capture cross section was evaluated to be 18b. This was obtained by lowering the measured value of 21 ± 7 b by Eastwood and Brown [10] by half their quoted error to allow for the fact that their measurements were made in a reactor spectrum with contributions from epithermal neutrons. The resonance parameters are mainly from Ribon's Thesis [3] and where the resonance spins were not determined from direct measurements, they were arbitrarily assigned to follow the $(2J+1)$ law for level density. A bound

5. Xe-129 (MAT=1349) Cont'd)

Resolved Resonance Parameters (cont'd)

level at - 23.0 eV was also included to give the evaluated capture cross-section. The calculated resonance capture integral (0.5-2.0E+07 eV) is 255.2b.

6. Xe-130 (MAT=1350)

(i) Resolved Resonance Parameters

The thermal capture cross-section was evaluated to be 6.2b. This was obtained by assigning 0.42b for the cross-section for the metastable state which is a mean of 0.495b by Kondaiah et al., [5] and 0.34b by Tilbury et al., [8]. To determine the capture cross-section to the ground state, it was assumed that the ratio $\sigma_{n\gamma g}/\sigma_{n\gamma m}$ for Xe-130 is the same as that observed for Xe-132 by Kondaiah et al., [5] viz 13.83. The resolved resonance parameters are mainly based on Ribon's Thesis [3] with a bound state at -10 eV whose parameters were adjusted to give the evaluated thermal capture cross section. The calculated resonance capture integral (0.5-2.0E+07 eV) is found to be 4.5b.

(ii) (n,p) Cross Section

The (n,p) cross-section calculated from FASCRO was normalized to the Kondaiah data [5] of 6.7 ± 0.8 mb at 14.4 MeV. This value cannot be reconciled with the data of Sigg et al., [6] who obtain a value higher by about 66%.

7. Xe-131 (MAT=1351)

(i) The Resolved Resonance Parameters

The resolved resonance parameters are based mainly on the work of Ribon [3]. For the resonances where spins were not known, spin values of either 1 or 2 were arbitrarily assigned to follow the $(2J+1)$ law for level density. A bound level at - 41 eV was also added and its parameters adjusted to give an evaluated thermal capture of 90b. The calculated resonance capture integral is 1020b.

54-Xe-Stable
MAT 1335+

7. Xe-131 (MAT=1351) (cont'd)

(ii) The (n,p) Cross Section

The (n,p) cross-section was obtained by normalizing FASCRO [4] calculations to 6.2 mb at 14.5 MeV which is a mean of the data of Kondaiah et al., [5] and of Sigg et al., [6].

8. Xe-132 (MAT=1352)

(i) Resolved Resonance Parameters

A mean of the capture cross-section to the metastable state as measured by Eastwood et al., [10] and by Kondaiah et al., [5] is 26 mb. Kardon et al., determined $\sigma_{n\gamma m}/\sigma_{n\gamma g} = 0.063$. [11]. With this ratio and $\sigma_{n\gamma m} = 26$ mb, one obtains $\sigma_{n\gamma g} = 413$ mb. This agrees quite well with the Kondaiah value of 415mb [5]. Their mean is 414mb which added to 26mb gives 440mb. The resolved resonances are from Ribon's Thesis [3] and a bound level was introduced at -100 eV and its parameters adjusted to obtain the evaluated thermal capture cross-section. The resonance capture integral (0.5 to 2.0E+7 eV) is 1.75b.

(ii) The (n,p) Cross Section

The (n,p) cross-section calculated using FASCRO [4] was normalized to 3.3mb at 14.5 MeV. This is a mean of the measured data of Kondaiah et al., [5] and Sigg et al., [6].

9. Xe-134 (MAT=1354)

(i) Resolved Resonance Parameters

The thermal cross-section was evaluated to be 0.25b, this is a mean of the value of 0.265 ± 0.020 b by Kondaiah et al., [5] and 0.228 ± 0.020 b by Eastwood et al., [10]. The resonance parameters are by Ribon [3] and a bound level was inserted at -25.0 eV and its parameters adjusted to give the evaluated thermal capture cross section. The calculated resonance capture integral (0.5-2.0E+07 eV) is 0.8b.

9. Xe-134 (MAT=1354) (cont'd)

(ii) The (n,2n) Cross Section

The (n,2n) cross section was obtained from FASCRO and has not been renormalized to experimental data since the Kondaiah et al., renormalized data [5] of 2541 ± 259 mb at 14.4 MeV and the Sigg [6] renormalized data of 1509 ± 14 mb at 14.6 MeV are discrepant.

(iii) The (n,p) Cross Section

The (n,p) cross section obtained from FASCRO was normalized to 2.1 mb at 14.5 MeV; this being the mean of the data of Kondaiah et al., [5] and of Sigg et al., [6].

10. Xe-136 (MAT=1356)

This evaluation is the same as in ENDF/B-IV (MAT=1178). All available data were reviewed including the new (n,2n) data by Sigg et al., [6] which were found to be consistent with the previous evaluation.

References

1. M.R. Bhat and S.F. Mughabghab, BNL-50374 (ENDF-185) 1973.
2. W.R. Kane et al., Private Communication (1978).
3. P. Ribon, Thesis, Univ. of Paris, Jan. 16, 1969.
4. S. Pearlstein, FASCRO (Private Communication) (1973).
5. E. Kondaiah et al., Nuc. Phys. A120, 329, 337 (1968).
6. R.A. Sigg and P.K. Kuroda, Nuc. Sci and Eng. 60, 235 (1976).
7. M. Bresesti et al., Jour. of Inorg. Nucl. Chem. 27, 1175 (1965).
8. R.S. Tilbury & H.H. Kramer, Nuc. Sci. & Eng. 31, 545 (1968).
9. J. MacNamara and H.G. Thode, Phys. Rev. 80, 296 (1950).
10. T.A. Eastwood and F. Brown, EANDC(CAN), 16, 6 (1963).
11. B. Kardon et al., Sovt. Nuc. Phys. 10, 15 (1970).

54-Xe-135
MAT 1294

Eval-Jun67 B.R.Leonard,Jr. and K.B.Stewart
Dist-May74 Rev-Nov74

ENDF/B Version-IV modifications (Apr74)
File extended from 1.0 keV to 20.0 MeV by F.Schmittroth and
R.E.Schenter (HEDL)

Radioactive decay data evaluated by C.W.Reich (ANC)

Added same angular distribution (MF=4,MT=2) as for
Cs-133(MAT=1141)

Data modified June,1970 to conform to ENDF/B-II Formats

Xenon-135 entry by B.R.Leonard,Jr. and K.B.Stewart ref.1
June 1967

Xe 135 Evaluation updated for energies from 1 keV to
20 MeV

F Schmittroth and R.E.Schenter
Westinghouse Hanford Company (February 1974)

MT=1 Total cross section was obtained from Moldauers
optical potential, ref.6.

MT=2 Elastic cross section was obtained by subtracting
the inelastic and capture cross sections from
total.

MT=4,51,91 Inelastic cross sections were obtained
from the compound nucleus code COMNUC,ref.7.

MT=102 Neutron capture obtained from the code NCAP,
ref.8.

MF=1 General Information

MT=451 Atomic mass = 134.907 ref.2

MT=457 Q- 1973 Revision of Wapstra-Gove mass tables
Half-life N.E.Holden, Chart of the Nuclides(1973)
and private communication (Sept.,1973)

Other- M.J.Martin,(Radioactive atoms-Supplement 1),
ORNL-4923 (1973)

MF=3 Smooth Cross Sections

MT=1 The Resonance Parameters of Summer(ref.4) have been

MT=2 accepted as the best estimate of the cross section.

MT=102 These parameters have been used in the program
UNICORN(ref.5) to calculate point values at 0 deg.K
from 0.0001 eV to 1 keV. The calculations give
sigma capture = 2.636E+06 barns at 0.0253 eV.

Q-value ref. J.Mattauch et al, Nuc.Phys 67(1965 No.1)

54-Xe-135
MAT 1294

References

1. Leonard,B.R.,Steward,K.B. , PNL June 1967
2. Everling,F.,et.al., Nucl.Phys.18,529(1960)
4. Sumner,H.M. ,AEEW-R-116(June 1962)
5. Otter,J.M. ,NAA-SR.11980,Vol.6(June 1966)
6. P.A.Moldauer, Phys.Rev.,Vol.135(1964)B642.
7. C.Dunford, COMMUC-3,Private Comm. to A.Prince.
8. F.Schmittroth, HEDL-TME-71-106, August 1971

NOTE: For 54-Cs-133 Documentation see 47-Ag Section

ENDF/B-V Summary Documentation

Isotope: 55-Cs-133 MAT=1355, Tape 510

HEDL	R.E. Schenter and D.L. Johnson	(Fast Capture)	Nov. '78
HEDL	F.M. Mann and R. Schmitroth	(Fast Capture)	Nov. '78
RCN	H. Gruppelaar	(Fast Capture)	Apr. '78
BNL	M.R. Bhat and A. Prince	(ENDF/B-IV)	Oct. '71

The present work supersedes the ENDF/B-IV evaluation, MAT = 1141 by Bhat and Prince (Summary of MAT 1141 given on page 47-109-4). Only the capture cross section and the resolved resonance parameters were changed for this evaluation. The new thermal cross sections are given as:

Cross Section Value at E = 0.0253 eV

Total	34.57	B
Scatter	4.96	B
Capture	29.61	B

Capture Resonance Integral (E_c = .5 eV) 382.7 B

The following indicates the changes from ENDF/B-IV:

MF = 2 MT = 151

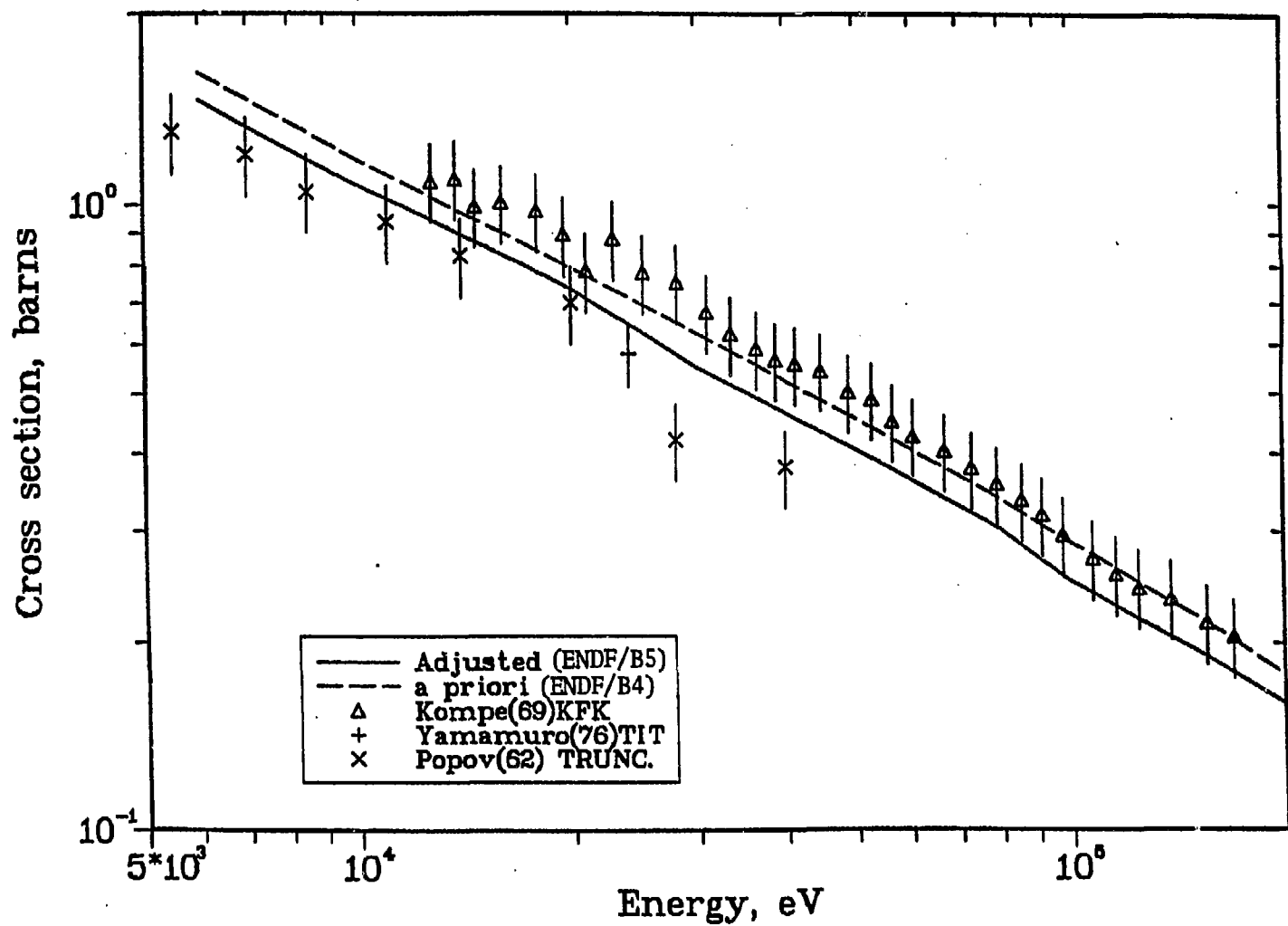
Γ_{γ} was changed for most resonances to .135 eV to give better agreement with integral results described in the following section.

MF = 3 MT = 102

Capture cross section evaluations were obtained using a generalized least-squares approach with calculations being performed with the computer code FERRET. Results of these calculations are shown in Figure 1, where the a priori curve is from ENDF/B-IV and the adjusted curve was used as the final evaluated ENDF/B-V cross section. Input for these adjustment calculations included both integral and differential experimental data results. Figure 1 also includes the differential data values and their uncertainties which were obtained from the CSIRS library. Integral measurement results came from CFRMF and STEK Assemblies 500, 1000, 2000, 3000, 4000. References for this work include:

1. F. Schmittroth, "FERRET Data Analysis Code," HEDL TME-79-40, September 1979.
2. J.W.M. Dekker, ECN-14, February 1977. (STEK information)
3. Y.D. Harker, et. al., TREE 1259, March 1978. (CFRMF information)

CS 133 CROSS SECTION EVALUATION
(ENDF/B4)-APRIORI
Case PK 5.6



Barium-138

DATA SUMMARY AND GENERAL COMMENTS

The experimental data for natural Ba and its various isotopes are listed in UCRL-50400, Vol. 3. The evaluated data for Ba¹³⁸ are shown graphically in UCRL-50400, Vol. 15, Part B. R. J. Howerton did the evaluation.

TOTAL CROSS SECTION

Total cross section data for natural Ba are shown graphically on pages 7-1 to 7-3 of UCRL-50400, Vol. 7, Part B, Rev. 1; some tabular values are given on page 7-4. There are no experimental data for the separate isotopes of barium. The evaluated total cross sections for Ba¹³⁸ are shown in UCRL-50400, Vol. 15, Part B. These evaluated total cross sections were based on the experimental data for natural Ba, in particular on ECSIL data sets ECSIL-498, ECSIL-728, ECSIL-748, and ECSIL-750.

ELASTIC SCATTERING CROSS SECTION

A few elastic scattering data points for natural barium are listed on page 7-4 of UCRL-50400, Vol. 7, Part B, Rev. 1. The evaluated elastic cross sections for Ba¹³⁸ are shown graphically in UCRL-50400, Vol. 15, Part B. In view of the scarcity of experimental data, the evaluated

elastic cross sections for Ba¹³⁸ were obtained by taking differences between the evaluated total cross sections and the sums of the evaluated nonelastic cross sections.

ELASTIC SCATTERING ANGULAR DISTRIBUTIONS

Elastic scattering differential cross section measurements on natural barium for neutron energies up to 5 MeV and at 14 MeV are shown in UCRL-50400, Vol. 19. The evaluated elastic scattering angular distributions were assumed to be isotropic for neutron energies below 100 keV. Above 100 keV, the angular distributions were obtained from the available experimental data and from spherical optical model calculations, in which the best-fit optical model parameters of Becchetti and Greenlees were used [Phys. Rev. 182, 1190 (1969)].

INELASTIC SCATTERING CROSS SECTION

Experimental n,n' data for natural barium are listed on page 7-45 of UCRL-50400, Vol. 8, Rev. 1, Part B; data for Ba¹³⁷ and Ba¹³⁸ are given on pages 7-46 and 7-47. In view of the scarcity of the experimental data, the evaluated n,n' cross sections were represented by a continuum cross section with a threshold at 1.44 MeV. These evaluated n,n' cross sections,

Barium-138

06/09/78

REACTION	POINTS	DATE	Q-VALUE	E-MIN	E-MAX
N.ELASTIC	CROSS SECTION	104	2/27/76	0.0000+ 0	1.0000-10
N.ELASTIC	ANGULAR DIST.	13	1/03/76	0.0000+ 0	1.0000- 1
N.ELASTIC	TOTAL ENERGY DEP.	35	1/14/74	0.3600+ 0	1.0000-10
N.ELASTIC	LOCAL ENERGY DEP.	35	1/14/74	0.0000+ 0	2.0000+ 1
N.N.	CROSS SECTION	20	10/03/72	0.0000+ 0	1.4400+ 0
N.N.	ENERGY-ANGLE DIST.	11	10/03/72	0.0000+ 0	1.4400+ 0
N.N.	TOTAL ENERGY DEP.	14	12/03/76	0.0000+ 0	2.0000+ 1
N.N.	LOCAL ENERGY DEP.	13	12/03/76	0.0000+ 0	2.0000+ 1
N.2N	CROSS SECTION	13	10/03/72	-8.5700+ 0	0.6500+ 0
N.2N	ENERGY-ANGLE DIST.	7	10/03/72	-8.5700+ 0	0.6500+ 0
N.2N	TOTAL ENERGY DEP.	11	12/03/76	-8.5700+ 0	0.6500+ 0
N.2N	LOCAL ENERGY DEP.	7	12/03/76	-8.5700+ 0	0.6500+ 0
N.3N	CROSS SECTION	6	10/03/72	-1.5620+ 1	1.5620+ 1
N.3N	ENERGY-ANGLE DIST.	4	10/03/72	-1.5620+ 1	1.5620+ 1
N.3N	TOTAL ENERGY DEP.	3	12/03/76	-1.5620+ 1	1.5620+ 1
N.3N	LOCAL ENERGY DEP.	3	12/03/76	-1.5620+ 1	1.5620+ 1
N.P	CROSS SECTION	4	10/03/72	-4.0400+ 0	6.0000+ 0
N.P	TOTAL ENERGY DEP.	2	5/29/78	-4.0400+ 0	6.0000+ 0
N.P	LOCAL ENERGY DEP.	2	5/29/78	-4.0400+ 0	6.0000+ 0
N.A	CROSS SECTION	5	10/03/72	3.8700+ 0	2.2500+ 0
N.A	TOTAL ENERGY DEP.	2	5/29/78	3.8700+ 0	2.0000+ 0
N.A	LOCAL ENERGY DEP.	2	5/29/78	3.8700+ 0	2.0000+ 0
N.G	CROSS SECTION	121	4/03/76	4.7100+ 0	1.0000-10
N.G	ENERGY DIST.	2	2/23/78	4.7100+ 0	1.0000-10
N.G	MULTIPOLICY	2	2/23/78	4.7100+ 0	1.0000-10
N.G	TOTAL ENERGY DEP.	2	1/12/76	4.7100+ 0	2.0000+ 1
N.G	LOCAL ENERGY DEP.	2	1/12/76	4.7100+ 0	2.0000+ 1
N.XG	CROSS SECTION	15	2/23/78	0.0000+ 0	1.4400+ 0
N.XG	ENERGY-ANGLE DIST.	2/23/78	0.0000+ 0	2.0000+ 1	
G					

which were obtained mainly from nuclear systematics, are shown in UCRL-50400, Vol. 15, Part B.

INELASTIC SCATTERING ANGULAR AND ENERGY DISTRIBUTIONS

The angular distributions for inelastic scattering were assumed to be isotropic in the laboratory system for all incident energies. While this assumption is incorrect for the preequilibrium and direct interaction portions of the reaction, the alternative of entering anisotropic angular distributions in the evaluation would also be incorrect because the uncertainties in the reaction cross section are so large. For energies below the onset of the preequilibrium process, at about 7 MeV, the energy distributions of the secondary neutrons were derived from a temperature model. Above 7 MeV, the energy distributions of the secondary neutrons were characterized by a two-component model - a "temperature" component plus a "preequilibrium and unresolved direct-interaction" component. The method used in selecting the fraction of the inelastically scattered neutrons to be associated with the preequilibrium process is described in UCRL-50400, Vol. 15, Part A, pages 19 to 22.

$n,2n$ CROSS SECTION

The $n,2n$ threshold for Ba^{138} is

8.65 MeV. Experimental $n,2n$ cross sections for Ba^{138} are given on page 7-48 of UCRL-50400, Vol. 8, Rev. 1, Part B. The $n,2n$ cross sections for Ba^{132} , Ba^{134} , and Ba^{136} are given on pages 7-45 and 7-46. The evaluated $n,2n$ cross sections, which are based on a combination of experimental data and nuclear systematics, are shown in UCRL-50400, Vol. 15, Part B.

ANGULAR AND ENERGY DISTRIBUTIONS FOR THE $n,2n$ REACTION

The angular distribution of secondary neutrons from the $n,2n$ reaction was assumed to be isotropic in the laboratory system. Energy distributions of the secondary neutrons, which are presented in tabular form, are derived from temperature model calculations, with the assigned temperatures consistent with systematics (see UCRL-50400, Vol. 15, Part A, p. 24).

$n,3n$ CROSS SECTION

The $n,3n$ threshold in Ba^{138} is 15.65 MeV. There are no experimental data for this reaction. The evaluated $n,3n$ cross sections, which were based on nuclear systematics, are shown in UCRL-50400, Vol. 15, Part B.

ANGULAR AND ENERGY DISTRIBUTIONS FOR THE $n,3n$ REACTION

The same evaluation procedures were used for the $n,3n$ reaction as for the $n,2n$ reaction described above.

56-Ba-138

MAT 1353

n, p CROSS SECTION

An effective threshold of 6 MeV was chosen for the n, p reaction in Ba^{138} . Experimental n, p data for Ba^{138} are listed on page 7-48 of UCRL-50400, Vol. 8, Rev. 1, Part B; some n, p data for Ba^{136} are listed on page 7-46. The evaluated n, p cross sections, which were based on these experimental data and on nuclear systematics, are shown in UCRL-50400, Vol. 15, Part B.

n, α CROSS SECTION

The n, α reaction in Ba^{138} is exo-ergic. In the evaluation, an effective n, α threshold of 2.25 MeV was chosen. Experimental n, α data for Ba^{138} are listed on page 7-49 of UCRL-50400, Vol. 8, Rev. 1, Part B. The evaluated n, α cross sections, which were based on a combination of experimental data and nuclear systematics, are shown in UCRL-50400, Vol. 15, Part B.

n, γ CROSS SECTION

Experimental neutron capture cross sections for Ba^{138} are shown graphically on page 7-7 of UCRL-50400, Vol. 7, Part B, Rev. 1; some tabular values are given on page 7-8. Some capture cross sections for natural barium are given on page 7-4. The evaluated neutron capture cross sections, which were based partly on the

experimental data and partly on nuclear systematics, are shown in UCRL-50400, Vol. 15, Part B.

PHOTON PRODUCTION FROM n, γ REACTIONS

The spectrum of photons from the neutron capture process at thermal neutron energies was taken from the measurements of V. J. Orphan *et al.*, Gulf General Atomic Rept. GA-10248 (1970). This spectrum was assumed to apply at all incident neutron energies up to 20 MeV, but the photon multiplicity was adjusted so as to conserve the total energy of the reaction.

n, $X\gamma$ CROSS SECTION

There are no experimental n, $X\gamma$ data for barium. In the evaluation, the n, $X\gamma$ cross section was represented by a continuum with a threshold at 1.44 MeV. The evaluated n, $X\gamma$ cross sections were obtained from calculations with the NXGAMEL code, using the systematics developed by Perkins, Haight, and Howerton [*Nucl. Sci. Eng.* 57, 1 (1975)]. A summary of this method of evaluating photon production data is discussed in UCRL-50400, Vol. 15, Part A, pages 38 to 41.

SPECTRA OF PHOTONS FROM THE n, $X\gamma$ PROCESS

The photon angular distributions were assumed to be isotropic. The

56-Ba-138
MAT 1353

photon energy distributions were
obtained from the systematics of

Perkins, Haight, and Howerton cited
above.

62-Sm-149
MAT 1319

ENDF/B-V Summary Documentation

Isotope: 62-Sm-149 MAT=1319, Tape 510

HEDL	R.E. Schenter and D.L. Johnson	(Fast Capture)	Nov. '78
HEDL	F.M. Mann and F. Schmittroth	(Fast Capture)	Nov. '78
RCN	H. Gruppelaar	(Fast Capture)	Apr. '78
CRNL	W.H. Walker	(Thermal Region)	Jun. '79
BNL	B.R. Leonard and K.B. Stewart	(ENDF/B-I - ENDF/B-IV)	Jun. '67

The present work supersedes the ENDF/B-IV evaluation which is also the ENDF/B-I evaluation, MAT = 1027 by Leonard and Stewart (Summary of MAT 1027 given on page 62-149-5). Thermal cross sections (1.E-5 to 2.361 eV) were changed by Walker. Fast capture cross sections (100 ev to 20 MeV) and resolved resonance parameters were also changed. The new thermal cross sections are given as:

Cross Section Values at E = 0.253 eV for 0° K

Total 39446.4 B

Scatter 135.8 B

Capture 39310.6 B

Capture Resonance Integral (E_c = .5 eV) 3256.3 B

The following indicates the detailed changes from ENDF/B-IV:

MF=2 MT=151 - (Resolved Region - 2.361 to 100 eV)

The resolved resonance parameters have been changed to multi-level parameters for ENDF/B-V. J values were corrected using BNL-325, Vol I (1973). The value of 2.361 eV was chosen to match the cross section from the single level calculation of Walker to that of the multi-level cross section. The parameters of the $E_r = .285$ and .0981 eV resonances were modified by Walker.

MF = 3 MT = 1

Total cross sections (1.E-5 to 2.361 eV) were calculated by Walker considering data from References 1-4.

MF = 3 MT = 2

Calculations were made (1.E-5 to 2.361 eV) by Walker which include no Bragg effects.

References

1. Leonard, B. R., Stewart, K. B., PNL June 1967.
2. Goldman, D. T., Chart of the Nuclides (June 1964).
3. Marshak, H., Sailor, V. L., Phys. Rev. 109, 1219 (1958).
4. BNL-325, Second Edition, Suppl. 2, Vol. 2c (1966).

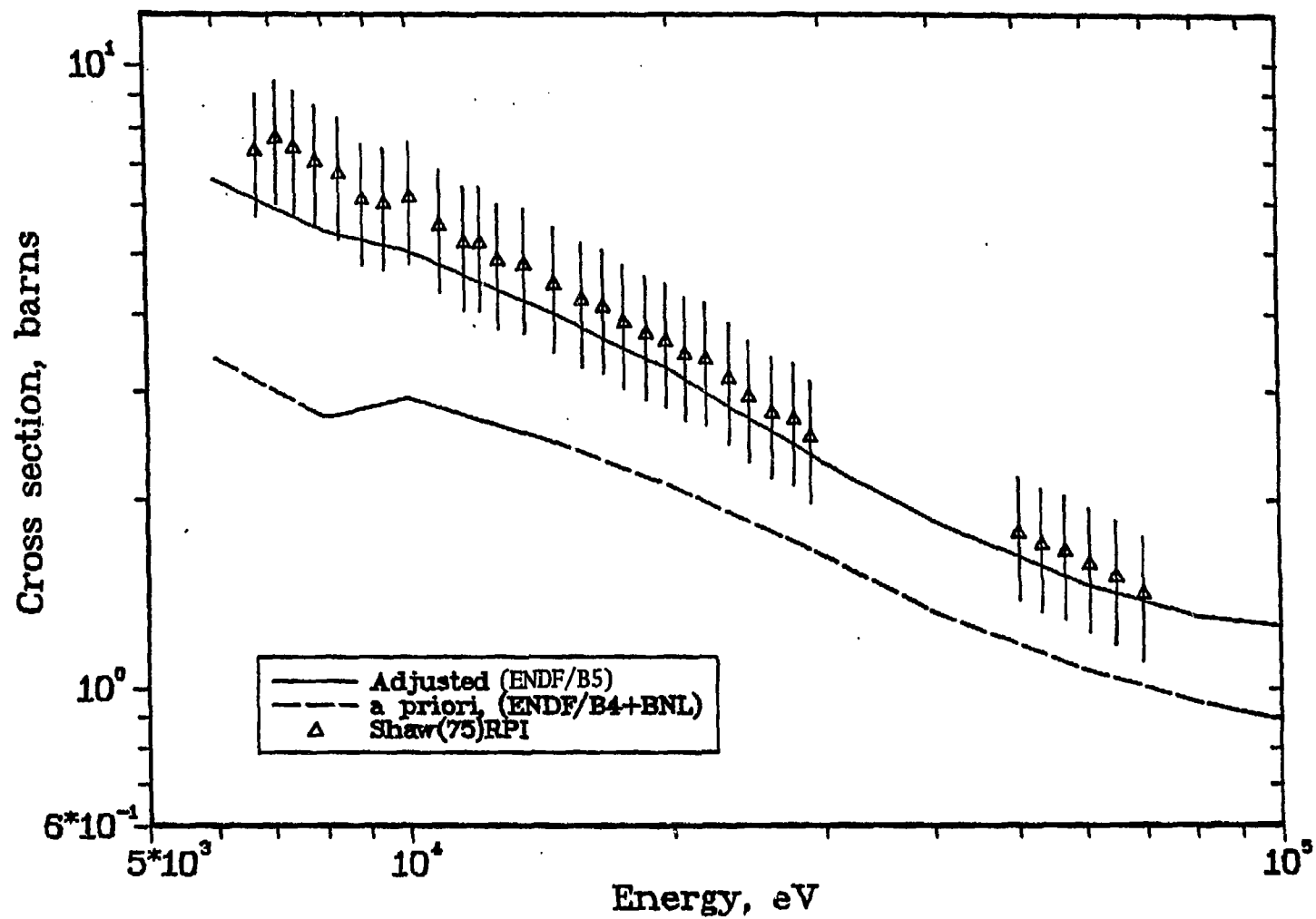
MF = 3 MT = 102

Capture cross section evaluations were obtained using a generalized least-squares approach with calculations being performed with the computer code FERRET. Results of these calculations are shown in Figure 1, where the a priori curve is from ENDF/B-IV and the adjusted curve was used as the final evaluated ENDF/B-V cross section. Input for these adjustment calculations included both integral and differential experimental data results. Figure 1 also includes the differential data values and their uncertainties which were obtained from the CSIRS library. Integral measurement results came from STEK Assemblies 500, 1000, 2000, 3000, 4000. References for this work include:

1. F. Schmittroth, "FERRET Data Analysis Code," HEDL TME-79-40, September 1979.
2. J.W.M. Dekker, ECN-14, February 1977. (STEK information)

Sm 149 evaluation

Case PK 7.4

62-Sm-149
MAT 1319

SAMARIUM-149

General Identification

MAT = 1027
ZA = 62149.0
AWR = 147.638
I = 3.5

[Everling] (1)

$$\frac{\text{MSm}^{149}}{\text{Mn}} = \frac{148.9169}{1.008665} = 147.638$$

Introduction

The primary objective of establishing the data file for Sm-149 was to provide a best estimate of cross sections in the thermal and epithermal energy range for the calculation of absorptions in thermal systems. The ENDF/B entries as of this date consequently include smooth cross sections in the thermal region, resonance parameters from 3.55 to 100 eV, and average parameters for the region of 100 eV to 10,000 eV.

Cross Sections

Low-energy

Although a great deal of effort has gone into measurement of resonance parameters of Sm¹⁴⁹, there is a paucity of precise data in the thermal region. The measurements which exist show that although the resonance at 0.0976 eV dominates the thermal region there is a significant contribution from a bound level (~10% at 0.025 eV). The parameters of the bound level have never been precisely determined. [Pattenden] (2), for example, added a 1/v component which gave much too large a contribution in the low cross section regions between resonances at higher energies. To establish the low energy behavior the following data sources were considered:

62-Sm-149
MAT 1319

<u>Source</u>	<u>Sample</u>	<u>Energy Range</u>
Pattenden (2)	Sm ¹⁴⁹	0.01 - 1 eV
McReynolds (3)	Sm	0.005 - .2 eV
Sailor (4)	Sm	0.04 - 1 eV
Marshak (5)	Sm	0.06 - .19 eV

The following resonance parameters of [Marshak]⁽⁵⁾ were then used in the program UNICORN⁽⁶⁾ to calculate the cross section throughout the thermal range:

<u>E_0</u>	<u>Γ_n^0</u>	<u>Γ_γ</u>	<u>J</u>	<u>R</u>
0.0976 eV	1.642 meV	63.6 meV	4	$.5093 \times 10^{-12}$ cm
0.873	0.7747	59.9	4	.5093

The resonance parameters listed in file 2 were also used in the calculation. The calculated cross section was then used with the measured data listed above, corrected for the contributions of other Sm isotopes where necessary, to establish the residual cross section. The residual cross section was then fitted by standard graphical techniques to establish the parameters of the bound level. The resulting fit was not very precise but was well within the rather large scatter of the data. The following resonance parameters were derived:

<u>E_0</u>	<u>Γ_n^0</u>	<u>Γ_γ</u>	<u>J</u>	<u>R</u>
-0.285 eV	2.167 meV	64 meV	3	$.5093 \times 10^{-12}$ cm

The value of Γ_γ , of course, could not be determined for a level so far removed but was input as the approximate average value of the lowest-lying resonances. Similarly, the value of $J = 3$ was input, having been determined by others.⁽⁷⁾

The negative energy resonance parameters were then added to the UNICORN input. The resulting cross sections were recalculated, found to be

in reasonable agreement with expectations and no further adjustment was made. The calculated cross sections gave the following values for σ_γ at 0.0253 eV:

	ENDF/B	[BNL-325(1966)] ⁽⁷⁾
Sm ¹⁴⁹	41,200	41,000 \pm 2,000
Sm	5,780	5,820 \pm 100

The ENDF/B data file consists of 82 point values for σ_T (MT=1), σ_n (MT=2), and σ_γ (MT=102) over the energy range 10^{-4} to 3.554 eV. The point values were calculated by UNICORN for 0°K. Sm¹⁴⁹ was given a mass of 10^{-4} in the calculations to remove the center-of-mass term. Ln σ vs E interpolation is specified because the energy mesh calculated by UNICORN is designed for minimum interpolation error in that fashion. Point values were continued to the minimum cross-section region (3.554 eV) between the 0.873 eV and 4.98 eV resonances to minimize discontinuities from joining smooth cross section values to values calculated from resonance parameters in the presence of interference.

Smooth cross sections in the resonance region 3.554 eV to 10^{-4} eV are specified to be zero in the ENDF/B file.

Resonance Region

Resolved

A preliminary version of [BNL-325 (1966)]⁽⁷⁾ lists resonance parameters for 27 resonances from 4.98 to 99 eV. The recommended parameters were used in most cases except where rounding had reduced precision. In the case of the 4.98 eV resonance the recommended value⁽⁷⁾ of $\Gamma_n^0 = 0.90$ meV is inconsistent with the determination of $J = 4$. The value used in the ENDF/B file of $\Gamma_n^0 = .7854$ meV is

consistent with the results of Marshak.⁽⁵⁾ In the case of the 9.0 eV resonance the value given by Marshak⁽⁵⁾ and quoted in [BNL-325 (1966)]⁽⁷⁾ for Γ_n^0 is in error. The correct Marshak value, for $J = 4$, of $\Gamma_n^0 = 3.093$ meV is used in the ENDF/B data file. This corrected value is to be applied to the value of Γ (not to Γ_γ as done in Ref 7) to obtain the value of $\Gamma_\gamma = 58.6$ meV used in the ENDF/B file.

In the ENDF/B file the value of $J = I = 3.5$ was used to generate the value $g = .5$ for those resonances where J has not been determined.

Unresolved

The transmission coefficient constant was determined from

$$\rho = c \int E = kR = 1.118 \cdot 10^{-3} \int E.$$

The following average parameters were specified in ENDF/B as determined from the resolved parameters and assuming the same values for $J = 3$ and $J = 4$ resonances:

$$\begin{aligned} D &= 6.8 \text{ eV} \\ \langle \Gamma_n^0 \rangle &= 5.1 \times 10^{-3} \text{ eV} \\ \langle \Gamma_\gamma \rangle &= 62 \text{ meV} \end{aligned}$$

where the value of $\langle \Gamma_\gamma \rangle$ was determined from the average of the lowest energy resonances where precise determinations exist. The high-energy cutoff of the unresolved region was arbitrarily set at 10^4 eV in ENDF/B.

REFERENCES

1. F. Everling, L. A. König, J. E. H. Mattauch, and A. H. Wapstra, Nuclear Physics 18, 520 (1950).
2. N. J. Pattenden, P.I.C., Vol. 16, 66 (Geneva 1958).
3. A. W. McReynolds and E. Andersen, Phys. Rev. 93, 195 (1954).
4. V. L. Sailor, H. H. Landon, and H. Foote, Phys. Rev. 96, 1014 (1954).
5. H. Marshak and V. L. Sailor, Phys. Rev. 109, 1219 (1958).
6. J. M. Otter, NAA-SR-11980, Vol. VI (June 1966).
7. BNL-325, Second Edition, Suppl. 2, Z = 41-80 (1966) (Preliminary Draft).

SUMMARY DOCUMENTATION:

Neutron and Gamma-Ray Production

Cross Sections of ^{151}Eu

S.F. Mughabghab

I. INTRODUCTION

Because the europium isotopes are significant fission product nuclides, an accurate knowledge of their neutron capture cross sections is very important. In addition, data on the europium isotopes is important for fast breeder reactors. Recent measurements of the capture cross sections of natural europium and its separated isotopes appeared in the literature, which fact warranted a new re-evaluation of the isotopes ^{151}Eu and ^{153}Eu . In this report, a summary documentation of the ^{151}Eu evaluation will be presented.

II. THERMAL CROSS SECTIONS AND RESONANCE PARAMETERS

The resolved resonance parameters recommended in BNL-325, vol. 1, Third Edition¹ are adopted. Where spin values are not determined, assignments are made randomly with the restriction of obeying the $(2J+1)$ level density law and the J-independence of the strength functions. Since the resolved positive energy resonances contribute 1430.5b to the thermal capture cross section (2200 m/sec), a negative energy resonance is invoked in order to fit a measured capture cross section of $9200 \pm 100 \text{b}^1$.

The unresolved resonance region, 98.81 eV to 10 keV, is described by average resonance parameters obtained from reference⁷. The

average radiative width for s-wave resonances was increased from 91.17 eV (in the resolved region) to 98 eV (in unresolved region) in order to fit the experimental data in the energy region of 100 eV to 10 keV. The average resonance parameters are summarized in Table 1.

Table 1

Average S-and P-Wave Resonance Parameters

Resonance Spin	s-wave			p-wave		
	$S_0 \times 10^{-4}$	D(eV)	$\langle \Gamma_\gamma \rangle$ (eV)	$S_1 \times 10^{-4}$	D(eV)	$\langle \Gamma_\gamma \rangle$ (eV)
1				0.80	2.363	0.92
2	4.07	1.418	0.98	0.80	1.418	0.92
3	4.07	1.013	0.98	0.80	1.013	0.92
4				0.080	0.788	0.92

The final 2200 m/sec cross sections and capture resonance integral are:

$$\text{Capture} = 9197 \text{ b}$$

$$\text{Scattering} = 3.4 \text{ b}$$

$$\text{Total} = 9200 \text{ b}$$

$$\text{Capture Resonance Integral} = 3305 \text{ b} \quad (0.5 \text{ eV cutoff})$$

The latter value is in agreement with the recommendations¹, but not with the recent measurement of Kim, et al,².

III. FAST NEUTRON CROSS SECTIONS

A. Total Cross Section

In the neutron energy region 10^{-5} eV to 98.8 eV it is represented by multilevel Breit-Wigner resonance parameters. From 98.8 eV to 10 keV, it is described by average resonance parameters summarized in Table 1. From 10 keV to 20 MeV it is taken over from ENDF/B-IV.

Konk's, et al,⁴, Moxon, et al,⁵, Hockenbury, et al,⁶, Yurlov, et al,⁷ and Czirr⁸. There is reasonable agreement between the data sets of Moxon, et al,⁵, Hockenbury, et al,⁶, Yurlov, et al,⁷ and Czirr⁸. However, these data sets are significantly higher than those of Konk, et al,⁴. It was decided to downgrade Konk, et al's data⁴ (on which ENDF/B-IV evaluation is based), and base the present evaluation on the other data sets. In addition, the recent capture measurements of Asami, et al,⁹ (the results of which were received after the completion of this evaluation) are in agreement with Moxon, et al,⁵, Hockenbury, et al,⁶ and Yurlov, et al,⁷. Another observation that could be made is that the high energy data points of Moxon, et al,⁵ (35-100 keV) seem to be on the high side.

Between 160 keV and 2.5 MeV, Johnsrud, et al,¹⁰, measured the activation cross section of ^{152m}Eu (9.3 hr. metastable state). To represent the total capture cross section in this energy region, this activation cross section was normalized by a factor of 2.3 in order to agree with Yurlov, et al's data⁷ in the overlap region. This procedure had some justification in view of the integral results of Anderl, et al,¹¹ (see below).

Above 2.5 MeV, where experimental measurements are not yet available, the capture cross section is based on COMNUC calculations¹² normalized to a value of 1 mb at 14.7 MeV. The latter value is obtained from the systematics of capture cross sections of various isotopes at 14.7.

B. Elastic Scattering Cross Section

The elastic scattering cross section above 10 keV is obtained by subtracting the nonelastic cross section from the evaluated total cross section. The non-elastic cross section is derived by summing all the neutron cross sections except the elastic cross section.

C. Inelastic Cross Sections

This is the same as ENDF/B-IV.

D. (n, particle) Cross Sections

The (n,p), (n,n'p), (n,α), (n,n'α), (n,2n) and (n,3n) cross sections are taken over from the previous evaluation which are based on model calculations of GROGI-3 code

The (n,d), (n,t), and (n,³He) reaction cross sections are based on THRESH calculations³.

E. Radiative Capture Cross Section

Considerable emphasis is placed on the present evaluation of the capture cross section of ¹⁵³Eu.

The capture cross section in the low energy region, 10⁻⁵ to 98.8 eV is represented by the resonance parameters. The unresolved energy region from 98.8 eV to 10 keV is described by the average resonance parameters summarized in Table 1. In the energy region 10 keV to 360 keV, the following experimental data sets were considered:

After the completion of the evaluation, the capture cross section was averaged over a 620-point-CFRMF spectrum. The CFRMF average capture cross section of ^{151}Eu obtained is 2.38 b. This compares favorably with a measured value of 2.61 ± 0.16 b¹¹.

IV. ANGULAR DISTRIBUTION OF SECONDARY NEUTRONS

These are taken over from ENDF/B-IV. For the elastic scattering of neutrons, the values are obtained from ABACUS-2 calculations¹³. The secondary neutrons due to (n,n'), (n,2n), (n,3n), (n,n'p), (n,n'a) reactions were assumed to be isotropic in the center of mass system.

V. ENERGY DISTRIBUTION OF SECONDARY NEUTRONS

These are adopted from ENDF/B-IV. The energy distribution of secondary neutrons due to the reactions (n,2n), (n,3n), and (n,n') are represented by Maxwellians with effective temperatures and based on the Weisskopf Formula¹⁴.

VI. GAMMA-RAY MULTIPLICITIES AND TRANSITION PROBABILITY

These are taken over from ENDF/B-IV.

References

1. S.F. Mughabghab and D.I. Garber, BNL-325, Vol. 1, third edition (1973).
2. J.I. Kim, E.M. Gryntakis, and H.J. Horn, Radiochimica Acta, 22, 20 (1975).
3. S. Pearlstein, J. Nucl. Energy 27, 81 (1973).
4. V.A. Konks, Yu P. Popov, and Yu. I. Fenin, Sov. J. Nuc. Phys. 7, 310 (1968) AN 80279/4.
5. M.C. Moxon, D.A. J. Endacott, and J.E. Jolly, Annals of Nucl. Energy, 3, 399 (1976) AN 20489/3.
6. R.W. Hockenbury, H.R. Knox, and N.N. Kaushal, private communication .
7. B.D. Yurlov, V.N. Konokov, and E.D. Popetsev, Conference on Neutron Phys., Vol. 3, 190 (1975) KieV.
8. J.B. Czirr, UCRL-5804, report UCRL-5804 (1970) AN 10169/6.
9. A. Asami, et al, private communications, 1978.
10. A.R. Johnsrud, M.G. Silbert, and H.H. Barchall, Phys. Rev. 11b, 927 (1959) AN 11675/22.
11. R.A. Anderl, Y.D. Harker, E. H. Turk, R. G. Nisle, and J.R. Berreth, Nuclear Cross Sections and Technology, Vol. 2, 908 (1975).
12. C.L. Dunford, COMNUC-1, report AI-AEC-12931 (1970) .
13. E. H. Auerbach, report BNL-6562 (1962) .
14. A. Weinberg and E. Wigner, The Physical Theory of Reactors (1959), The University of Chicago Press.

SUMMARY DOCUMENTATION FOR ^{152}Eu and ^{154}Eu

H. Takahashi
National Neutron Cross Section Center
Brookhaven National Laboratory

ABSTRACT

This is a summary of the evaluation of the neutron cross sections of ^{152}Eu and ^{154}Eu from 1.0×10^{-5} eV to 20 MeV. (^{152}Eu MAT = 1292, ^{154}Eu MAT = 1293).

File 1: General Information.

File 2: Resolved and unresolved resonance parameters.

File 3: Smooth cross sections for total, elastic, non-elastic, total inelastic, inelastic cross-section to discrete levels as well as the continuum of levels. In addition are given the various (n, particle) and capture cross sections.

File 4: Angular distributions for elastic scattering are given in terms of Legendre coefficients in the c-of-m system; the inelastic scattering is assumed to be isotropic.

File 5: Secondary neutron energy distributions are given as an evaporation spectrum.

INTRODUCTION

There are very few experimental data available on these unstable isotopes of europium; as such the evaluations described here are heavily dependent on nuclear model calculations and systematics. These two evaluations are discussed together as both of them deal with the odd-odd isotopes of europium.

File 1: GENERAL INFORMATION

This contains a description of the evaluation and information on the nuclear model calculations.

File 2: RESONANCE PARAMETERS

(i) Resolved Resonances

The resolved resonance parameters for ^{152}Eu and ^{154}Eu are respectively given up to 61.5eV and 60eV. These were generated by a procedure similar to that of Cook¹. The values of average level spacing and the reduced neutron width were determined by a method similar to that of Barr and Devaney² in which the ratios of the average values of these parameters for odd-even to odd-odd nuclei are determined for nuclei in this mass region for which experimental data are available. These ratios and the measured values for ^{151}Eu and ^{153}Eu are then used to obtain $\langle D \rangle$ and $\langle \Gamma_n^0 \rangle$ for ^{152}Eu and ^{154}Eu .

(ii) Unresolved Resonance Region

The unresolved resonance parameters are given from the upper end of the resolved resonance region to 10 keV. These were again determined using the method of Barr and Devaney.²

File 3: SMOOTH NEUTRON CROSS SECTIONS

(i) Total Cross Section

The total cross-section for ^{152}Eu and ^{154}Eu between 10keV and 2.5 MeV were calculated using the optical model code ABACUS-2³ and the Beccchetti Greenless⁴ parameters. Above 2.5 MeV the total cross-sections of ^{152}Eu and ^{154}Eu were assumed to be the same and equal to the Foster and Glasgow data⁵ for natural europium. The cross-section from 15.0 to 20.0 MeV were determined from optical model calculation and this experimental data up to 15.0 MeV.

(ii) Elastic Scattering Cross Section

The elastic scattering cross section from 10 keV to 20 MeV were obtained by subtracting the non-elastic cross-section from the total.

(iii) Inelastic Scattering Cross Section

As there are no input data the inelastic scattering cross-section for the first five levels in ^{152}Eu and ^{154}Eu were calculated using the Code COMMNUC-III⁶ up to 3.0 MeV. Above 3.0 MeV the inelastic scattering is mostly the excitation of the continuum of levels; hence, the discrete level cross-section were assumed to be zero. The inelastic scattering to the continuum was calculated using the code GROGI-III.⁷ The level density parameters were taken from Cook's data⁸ for the deformed nuclei using the Gilbert-Cameron formula⁹.

(iv) (n, particle) Cross Sections

There are no experimental data available on any of the (n, particle) reactions. Hence, they were calculated using the semi-empirical statistical model code THRESH¹⁰ and for cascade reactions with the code GROGI-III⁷. In evaluating ^{151}Eu and ^{153}Eu (n,p) and (n,a) cross-sections it was found that the cross-section calculated by THRESH were small

63-Eu-152, 154
MAT 1292, 1293

compared to the experimental data at 14.0 MeV and the calculation had to be normalized to the experimental data. A similar normalization of the calculated values were carried out for ^{152}Eu and ^{154}Eu using respectively the factors obtained for ^{151}Eu and ^{153}Eu . Cross-sections for $(n, n'p)$, $(n, n'\alpha)$, $(n, 2n)$ and $(n, 3n)$ reactions were calculated using GROGI-III.

(v) The Capture Cross Section

This was calculated using the code COMMNUC-III up to 3.0 MeV. From 3 to 20 MeV it was obtained from GROGI-III for compound nuclear processes and Cvelbar's formula¹¹ to calculate the capture cross section due to direct and semi-direct reaction.

File 4: ANGULAR DISTRIBUTION OF SECONDARY NEUTRON

The differential elastic angular distributions were calculated using ABACUS-2³ and they were fitted with Legendre coefficients in the c-of-m system. Secondary neutrons due to other reactions were assumed to have isotropic distribution in the c-of-m system.

File 5: ENERGY DISTRIBUTION OF SECONDARY NEUTRONS

The energy distributions of neutrons from the $(n,2n)$ $(n,3n)$ and the continuum inelastic scattering were assumed to be Maxwellian. The effective temperatures for them were obtained from the Weisskopf formula.¹²

References

1. J. L. Cook, Australian Atomic Energy Commission Report AAEC/TM-549, 1969.
2. D. W. Barr and J. J. Devaney, Kilovolt Europium Capture Cross Sections. LA-3643 (1967).
3. E. H. Auerbach. ABACUS-2, BNL 6562 (1964).
4. F. D. Becchetti and G. W. Greenlees, Phys. Rev. 182, 1190 (1969).
5. D. G. Foster and D. W. Glasgow. CSISRS Library AN-10047 (1967).
6. C. L. Dunford, COMMNUC-III Private Communication (1971).
7. H. Takahaski, GROGI-III Modified from GROGI-II by J. Gilat BNL-50246 (T-580) (1969).
8. J. Cook, H. Ferguson and A. Musgrove AAEC/TM-392 (1967).
9. A. Gilbert and A. G. W. Cameron, Can. Jour. Phys. 43, 1446, 1965.
10. S. Pearlstein. Journ. Nucl. Energy 27, 81 (1973).
11. F. Cvelbar, A. Hudoklin, M. V. Michailovic, M. Nazzir and M. Petrisic, NIJS Report - T-529 (1968).
12. A. M. Weinberg and E. P. Wigner, The Physical Theory of Neutron Chain Reactors p. 104. Univ. of Chicago Press (1959).

SUMMARY DOCUMENTATION

NEUTRON AND GAMMA RAY PRODUCTION CROSS SECTIONS

OF ^{153}Eu

S. F. Mughabghab

I. INTRODUCTION

This material deals with the evaluation of the neutron- and gamma-ray production cross sections of the isotope ^{153}Eu . The emphasis is placed on the low-energy region because of the importance of Eu in control rods in nuclear reactors. In addition, since the europium isotopes ^{151}Eu and ^{153}Eu are significant fission product nuclides, accurate knowledge of their neutron cross sections is important. A close reexamination of the thermal capture cross sections of ^{153}Eu indicated that a previous recommended value of $390 \pm 30 \text{ b}$ is overestimated¹ because of an error in the half-life of ^{154}Eu .

II. THERMAL CROSS SECTIONS AND RESONANCE PARAMETERS

The resonance parameters recommended in BNL-325 (1973)¹ were adopted in this evaluation with minor changes. Only the spin of the resonance at 2.45 eV was previously determined. For the other resonances, spin assignments were made randomly with the restriction of satisfying the $(2J+1)$ law-level density and the spin independence of the neutron strength function.

A reexamination of the recent thermal capture cross section measurements of Moxon et al.,² Widder,³ Kim et al.,⁴ Sims and Juhnke,⁵ Vertebny et al.⁶ and Razbudej et al.⁷ brought out some of the problems associated with an accurate determination of the thermal cross section of ^{153}Eu . These problems are related to the lack of an accurate knowledge of the ^{151}Eu ($\sigma_{\gamma} = 9200 \pm 100 \text{ b}$) content in the ^{153}Eu samples and use of an inaccurate value of the half-life of ^{154}Eu in the activation measurements.

The half-life of ^{154}Eu seems to have undergone a major change with time as illustrated in Table 1. Because of large uncertainties in this quantity

Table 1
Half-life of ^{154}Eu

Halflife (years)	Reference
5.4	Hayden et al.-49 ⁸
<u>16</u> ⁺ <u>4</u>	Karraker et al.-52 ⁹
7.84 ± 0.35	Grisham-68 ¹⁰
8.7 ± 0.7	McHugh-59 ¹¹
8.5 ± 0.5	Emery et al.-72 ¹²

and the fact that two of the recent measurements are not published,¹⁰⁻¹¹ it was decided to derive a recommended value for the half-life of ^{154}Eu by an intercomparison of the activation and non-activation measurements.

Accordingly as shown in Table 2, the following procedure was followed: (1) the activation (16 years half-life was used by these authors) and non-activation measurements were separated, (2) the reported thermal cross sections were adjusted for ^{151}Eu content in ^{153}Eu samples when enough information was furnished by the measurers, (3) a weighted-average value of $\sigma_{\gamma} = 303 \pm 6$ b of references 2,4,6,7, and 13 was obtained, and equal weights were applied to the activation measurements to obtain $\sigma_{\gamma} = 618 \pm 18$ b (for $T_{1/2} = 16$ years). From Steps (3) and (4), one obtains a half-life for ^{154}Eu of:

$$T_{1/2} = 7.84 \pm 0.38 \text{ years.}$$

Table 2
Thermal Capture Cross Section of ^{153}Eu

Reported		Adjusted		Method	Author	
	σ_{γ} (b)	I'_{γ} (b)	σ_{γ} (b)	I'_{γ} (b)		
Non-activation	$\sigma_t = 448 \pm 16$		296 ± 16		Total C/S	Pattenden ¹⁸
	317 ± 5	$I'_{\gamma} = 1280 \pm 100$	317 ± 5	1416 ± 100	pile oscillator	Tattersall ¹⁴
	382 ± 15				Capture	Widder ³
	317 ± 15		317 ± 15		Capture	Moxon ²
	275 ± 14		292 ± 11		Total C/S	Vertebny-Razbudej ^{6,7}
Activation	639 ± 7	$I'_{\gamma} = 3667 \pm 58$	311 ± 4	1918 ± 30	activation	Sims ⁵
	603 ± 23	3147 ± 196	296 ± 11	1678 ± 100	activation	Kim ⁴

This value is in excellent agreement with Grisham's¹⁰ determinations, and gives additional support for recommended capture cross section of 303 ± 6 b for ^{153}Eu .

The positive energy resonances contribute 58 b to the thermal capture cross section. The difference is accounted for by a negative energy resonance with a spin of $J=2$, which is derived from thermal γ ray spectra measurements.¹⁵

The final 2200 m/sec cross sections and capture resonance integral are:

$$\text{Capture} = 299.85 \text{ b}$$

$$\text{Scattering} = 6.75 \text{ b}$$

$$\text{Total} = 306.60 \text{ b}$$

$$\text{Capture Resonance Integral} = 1448 \text{ b}$$

The capture resonance integral derived in this evaluation is in very good agreement with the determination of Tattersall et al.¹⁴ The scattering cross

63-Eu-153
MAT 1359

section obtained in this evaluation (6.75 b) is on the low side when compared to the measurement of Vertebny et al.,⁶ 8.0 \pm 0.2 b.

The unresolved energy region from 97.22 eV-1.0 keV is represented by average resonance parameters as recommended in ref. 1.

$$S_0 = 2.50 \times 10^{-4}$$

$$S_1 = 0.60 \times 10^{-4}$$

$$\langle \Gamma_\gamma \rangle = 0.958 \text{ eV}$$

III. FAST NEUTRON CROSS SECTIONS

A. Total Cross Sections

In the energy region from 10^{-5} to 97.22 eV, the total cross section is represented by multilevel-Breit-Wigner resonance parameters; in the unresolved region, 97.22 eV to 10 keV, it is represented by average resonance parameters. In the high energy region 10 keV to 20 MeV, it is taken over from ENDF/B-IV.

B. Elastic Cross Section

The elastic scattering cross section below 10 keV is dealt with in the same manner as the total cross section. Above 10 keV, it is derived by the usual procedure of subtracting the non-elastic cross sections from the total cross section.

C. Inelastic Cross Sections

This is taken over from ENDF/B-IV.

D. (n,particle) Cross Sections

1. (n,2n) and (n,3n) Cross Sections

Several 14.7 MeV cross sections in which residual nucleus is left in the metastable states $^{152m1}\text{Eu}$ (9.3 hours) and $^{152m2}\text{Eu}$ (96 min) have been measured.¹⁶⁻¹⁹ Recently, Qaim¹⁹ measured the cross section leading to the 12.4 year

ground state of ^{152}Eu , as well as the cross sections to the two metastable states. The total $(n,2n)$ cross section is 2047 ± 171 b.¹⁹ The GROGI-3 code calculations of ENDF/B-IV are normalized to this value at 14.7 MeV. For the $(n,3n)$ reaction, experimental results are not available. As a result, the values calculated by GROGI-3 were adopted.

2. (n,p) and $n,n'p$ Cross Sections

Experimental data are available only for a neutron energy 14.7 MeV.^{18,20-22} The ENDF/B-IV evaluation, based on semiempirical statistical model code THRESH²³ is renormalized to a value of 5.6 mb at 14.7 MeV.

For the $(n,n'p)$ reaction cross section, no data are available. This cross section is based on GROGI-3 calculations of ENDF/B-IV.

3. (n,α) and $(n,n'\alpha)$ Cross Sections

Two discrepant values at 14.7 MeV (2.2 ± 0.3 and 9 ± 2 mb) are available.^{21,24} In this evaluation, a value of 9 mb is adopted. This choice is based on: (1) systematics which indicate that the (n,α) reaction has a maximum value of about 9 mb at atomic weight $A=155$, and (2) estimates obtained from the double differential data of Glowka et al.²⁵ Therefore, the (n,α) evaluation of ENDF/B-IV, which is based on THRESH calculations is renormalized to a value of 9 mb at 14.7 MeV. The thermal (n,α) cross section is set equal to 1 μb .²⁶

Since no experimental data are available for the $(n,n'\alpha)$ reaction, this cross section was adopted from ENDF/B-IV, which is based on GROGI-3 calculations.

4. (n,d) , (n,t) , and $(n,^3\text{He})$ Reaction Cross Sections

Since no experimental data are available for these reactions, the values calculated by GROGI-3 for ENDF/B-IV were adopted.

5. The Radiative Capture Cross Section

The radiative capture cross section in the energy range 10^{-5} to 97.7 eV is represented by the resonance parameters. Between 97.7 eV and 10 keV, it is described by the average resonance parameters. In the higher energy region (10 to 360 keV), the capture cross section is based on the experimental data of Moxon et al,² Konks and Fenin,²⁷ Hockenbury et al,²⁸ and Yurlov et al.²⁹ These data are in general agreement. Above 360 keV, the evaluation is based on COMNUG calculations³⁰ and normalized to a value of 1 mb at 14.7 MeV.

After the completion of this evaluation, the capture cross section was averaged over a 620-point CFRMF spectrum. The value obtained is 1.585 b, which is in excellent agreement with a measured value of 1.5 ± 0.12 b.³¹

IV. ANGULAR DISTRIBUTION OF SECONDARY NEUTRONS

These were taken over from ENDF/B-IV and depend on ABACUS and CHAD calculations.

V. ENERGY DISTRIBUTION OF SECONDARY NEUTRONS

These are adopted from ENDF/B-IV.

VI. MULTIPLICITIES AND TRANSITION PROBABILITIES

These are based on ENDF/B-IV.

VII. ANGULAR DISTRIBUTION OF GAMMA RAYS

These are taken from ENDF/B-IV.

Acknowledgments

Discussions with N. Holden about the half-life of ^{154}Eu are gratefully acknowledged.

REFERENCES

1. S.F. Mughabghab and D.I. Garber, BNL-325, Vol. 1, 3rd ed., 1973.
2. M.C. Moxon, D.A. Endacott, J.E. Jolly, Annals Nucl. Energy 3, 399 (1976).
3. J.E. Widder, Nucl. Sci. Eng. 60, 53 (1976).
4. J.I. Kim, E.M. Gryntakis, and H.J. Born, Radiochimica Acta 22, 20 (1975).
5. G.H.E. Sims and O.G. Juhnke, J. Inorg. Nucl. Chem. 29, 2671 (1967).
6. V.P. Vertebny et al., Proc. 1st Neutron Physics Conf., Kiev, USSR, part 2, 239 (1973).
7. V.F. Razbudej, A.F. Fedorova, A.V. Muravitskij, Rpt. INDC(CCP)-100/U, 23 (1977).
8. R.J. Hayden, J.H. Reynolds, and M.G. Ingram, Phys. Rev. 75, 1500 (1949).
9. D.G. Karrakar, R.J. Hayden, and M.G. Ingram, Phys. Rev. 87, 901 (1952).
10. G. Grisham (LASL), Private Communication with N.E. Holden (Dec. 5, 1968).
11. J. McHugh (KAPL), Private Communication with N.E. Holden (June 1962).
12. J.F. Emery, S.A. Reynolds, E.I. Watt, and G.I. Gleason, Nucl. Sci. Eng. 48, 319 (1972).
13. N.J. Pattenden, Sec. Geneva Conf., Vol. 16, 45, Paper P/11 (1958).
14. R.B. Tattersall, H. Rose, N.J. Pattenden, and D. Jewitt, J. Nucl. Energy 12, 32 (1960).
15. W. Stoffl, D. Rabenstein, K. Schrechenbach, and T. von Egidy, A. Physik, A282, 97 (1977).
16. R.G. Wille and R.W. Fink, Phys. Rev. 118, 292 (1960).
17. P. Rama Prasad, J. Rama Rad, and E. Kondaiah, Nucl. Phys. A125, 57 (1967).
18. A. Bari, DA/B, 32, 5901, CSIRS A/N 10431/2,4,5.
19. S.M. Qaim, Nucl. Phys. A224, 319 (1974).
20. S.M. Qaim, Radiochem. Radioanal. Letts 25, 335 (1976).

63-Eu-153
MAT 1359

21. H.S. Pruys, E.A. Hermes, and H.R. von Gunter, *J. Inorg. Chem.* 37, 1587 (1975).
22. R.F. Colman, B.E. Hawker, L.P. O'Connor, and J.L. Perkin, *Proc. Phys. Soc.* 73, 215 (1959).
23. S. Pearlstein, *J. Nucl. Energy* 27, 81 (1973).
24. C.S. Khurana and I.M. Covil, *Nucl. Phys.* 69, 153 (1969).
25. L. Glowacka et al., *Nucl. Phys.* A244, 117 (1975).
26. A. Emsalem, Do Huu Phuoc and R. Chery, *Nucl. Phys.* A231, 437 (1974).
27. V.A. Konks and Yu.I. Fenin, Conf. Interaction of Neutrons with Nuclii, Dubna (USSR) Rept. No. 1845, p. 100 (1964).
28. R.W. Hockenbury, H.R. Knox, and N.N. Kaushal, Conf. Nucl. Cross Sections and Technology, Vol. 2, 905 (1975) CSISRS AN 1043518.
29. B.D. Yurlov, V.N. Konokov, and E.D. Popetaev, *Proc. 2nd Conf. on Neutron Physics*, Kiev, USSR, Vol. 3, 190 (1975).
30. C. Dunford, *Atomics Intern. Rpt. AI-AEC-1293* (1970).
31. Y.D. Harker, *Private Communication*, Jan. 1978; see also, R.A. Anderl et al., *Nucl. Cross Sections and Technology*, Vol. 2, 908 (1975).

Benjamin A. Magurno
Brookhaven National Laboratory

64-Gd-152/160
MAT 1362+

SUMMARY DOCUMENTATION
FOR THE ISOTOPES OF GADOLINIUM*

I. INTRODUCTION

TABLE I
Gadolinium Isotopes Evaluated in This Study

Isotope	Stability	Mass	Abundance (%) [1]	ENDF/B MAT No.
^{152}Gd	Naturally Occuring Radioactive	151.91982	0.2	1362
^{154}Gd	Stable	153.92069	2.2	1364
^{155}Gd	Two Isomeric States One Stable	154.92264	14.9	1365
^{156}Gd	Two Isomeric States One Stable	155.92214	20.6	1366
^{157}Gd	Stable	156.92397	15.7	1367
^{158}Gd	Stable	157.92412	24.7	1368
^{160}Gd	Stable	159.92707	21.7	1370

All available experimental data for these isotopes were examined, and for the most part, used in the evaluations. Where data was lacking or deemed "unusable", theoretical calculations were employed. This is a new set of evaluations except in the case of radiative capture above 5 MeV where the evaluated data of R. Schenter [2] were renormalized and added to the files.

While these isotopes are in the region where the nucleus goes from spherical to deformed ($N \sim 90$) all isotopes were treated as deformed when optical model calculations were performed.

* This description is a summary extracted from EPRI NP-556, October, 1977.

II THERMAL CROSS SECTIONS AND RESONANCE PARAMETERS

The thermal cross section values and resonance parameters in BNL-325 Third Edition, Volume 1 [3] were used as a starting point for these evaluations. In order to reproduce the required thermal capture cross section and resonance capture integrals in the resolved resonance region the resonance parameters were processed by RESEND [4] and the appropriate bound levels and/or $1/v$ contributions were added where necessary. The bound levels were calculated according to the approximate Breit-Wigner recipe:

$$\sigma_{\gamma} (.0253 \text{ eV}) = \frac{4.099 \times 10^6 g \Gamma_n^0 \Gamma_{\gamma}}{E_0^2}$$

$$\text{where } \Gamma_n = \Gamma_n^0 \sqrt{|E_0|}$$

A. ^{152}Gd

BNL-325 lists values of 1100 ± 100 barns for the capture cross section and 3000 ± 300 barns for the resonance capture integral. These values are based upon the ratio measurements of Steinnes [5]. Steinnes used a Gd_2O_3 sample and assumed a 0.2% isotopic abundance for ^{152}Gd , but did not determine the samarium content. Instead he assumed a samarium content $\leq 0.05\%$, and ignored possible activity from ^{153}Sm (^{153}Sm has a line at 103 keV) [6]. The activity measurements were based on the sum of the 97 keV and 103 keV peaks, both only partially resolved with a Ge(Li) detector.

The contribution of the positive levels to the thermal capture cross section is 7.2 barns. There are no resonances < 3.3 eV tabulated in BNL-325, so a bound level was indicated. Using a "picket fence" model and assuming $\langle D \rangle \approx 15$ eV the bound level E_0 is approximately -12 eV. Using the Steinnes value of 1100 barns the calculated Γ_n of the bound level would be 2.4 eV. Possible samarium contamination and the overly large value of Γ_n led to the decision to ignore the Steinnes data for ^{152}Gd . A capture cross section of

14.4 barns was assumed, which includes a bound contribution equal to the contribution from the positive levels. For the bound level $\Gamma_n = 0.016$ eV, is a more reasonable neutron width.

Positive levels from 3.31 eV to 231 eV were used in the evaluation, and $\Gamma_\gamma = 0.056$ eV was assumed where no value of Γ_γ was listed in BNL-325. The last 3 resonances in BNL-325 from 238 to 293 eV were ignored, since only E_0 was identified, and no parameters were listed. No unresolved resonance parameters were evaluated for this isotope. The calculated resonance integral was 388 barns.

B. ^{154}Gd

In order to maintain the thermal capture cross section of 85 barns listed in BNL-325 a bound level was introduced. $E_0 = -7$ eV assuming equally spaced levels with $\langle D \rangle = 15.5$ eV. Using $\Gamma_\gamma = 0.0870$ eV (the same as that used for the positive Γ_γ) a $\Gamma_n = 0.030$ eV was calculated. The resolved resonance region terminates at 1 keV, and no unresolved parameters were evaluated for this isotope.

C. ^{155}Gd and ^{157}Gd

^{155}Gd and ^{157}Gd were the only odd A isotopes of the seven evaluated. It was necessary to supply spins where they were not listed (i.e. not measured) in BNL-325. D_J , the mean spacing for $\ell = 0$ resonances of spin 1 or 2 was used as a guide in selecting unknown spins. Here $D_J = D_{\text{obs}}/g_J$ where $g_J = 3/8$ for $J = 1$ resonances and $5/8$ for $J = 2$ resonances. Values of D_{obs} were taken from BNL-325.

The resonance parameters for ^{155}Gd were taken from BNL-325 up to 183 eV. Above this an unresolved resonance parameter region was added up to 10 keV.

The spins for ^{157}Gd are not those listed in BNL-325. The first two are from Moller [7] and the other experimentally determined spins are from Karzhavina [8]. Undetermined spins were assigned as above. The resolved resonance region ends at 306 eV. Above this energy range an unresolved resonance parameter region was added up to 10 keV. The unresolved parameters for both ^{155}Gd and ^{157}Gd were calculated with the computer program UR by E. Pennington. [9].

D. ^{156}Gd

The parameters used for ^{156}Gd are the same as those appearing in BNL-325 with the addition of a level at 80.2 eV. This level was measured by Mughabghab and Chrien [10] and inadvertently omitted in the compilation. The values for σ_γ (.0253 eV) and I_γ calculated here are in good agreement with those appearing in BNL-325. The resolved energy range extends to 1.4 keV for this isotope. The adopted $\bar{\Gamma}_\gamma = 0.086$ eV. No unresolved region was calculated for this isotope.

E. ^{158}Gd

The thermal capture cross section in BNL-325 is 2.5 ± 0.5 barns. This number comes from the Steinnes [5] ratio measurements using the calculated I_γ from the resonance parameters. Recomputing the cross section using a weighted mean of the ratio measurements of Steinnes and those of Van der Linden [11] and the calculated I_γ from the resonance parameters a value of 2.0 barns was calculated for the thermal capture cross section. The resonance contribution to the cross section was 1.26 barns. A $1/V$ cross section term was added to make up the difference. The resolved energy range extends to 10 keV, so no unresolved energy region was calculated for this isotope. The adopted $\bar{\Gamma}_\gamma = 0.105$ eV.

F. ^{160}Gd

The resonance parameters for this isotope came from BNL-325. The value of I_{γ} is in good agreement with BNL-325. The thermal capture cross section in BNL-325 is 0.77 barns which was measured from the 3.7 min ^{161}Gd activity. The resonance contribution to the thermal cross section was 0.217 barns. A $1/V$ term was added to make up the difference and the results appear in Table II. The resolved energy range extends to 10 keV as in ^{158}Gd , and so no unresolved resonance region was evaluated. The adopted $\bar{\Gamma}_{\gamma} = 0.108$ ev.

III. FAST NEUTRON CROSS SECTIONS

A. Total Cross Section

The total cross section of each gadolinium isotope in the resonance region is determined by the resonance parameters. Above the resonance region a least squares spline fit was constructed from the experimental data for natural gadolinium. On the basis of systematics and optical model theory it was felt that this curve would well represent individual isotopes.

B. Elastic Cross Sections

The elastic scattering cross sections from 10^{-5} ev to the end of the resonance region were handled in a manner similar to the total cross section (i.e., generated from resonance parameters). Above the resonance energy region the elastic cross sections were obtained by subtracting all non-elastic processes in the file from the total cross section.

C. $(n, \text{particle})$ Cross Section

The n -particle cross sections $(n,2n)$, (n,p) and (n,α) were calculated for all isotopes using the statistical model code THRES2 [12]. The theoretical curves were normalized to experimental data where available. In most cases

data was not available, but in a few cases single 14 MeV data points were measured. In the latter case the output of THRES2 was renormalized to the data point with a few minor exceptions. A fair amount of 14 MeV experimental data exists for the ^{160}Gd ($n,2n$) reaction.

D. Inelastic Cross Sections

There is no experimental data available for the total inelastic scattering. Data for the excited states and the continuum were obtained by nuclear model calculations using the code COMNUC [13]. COMNUC uses Hauser-Feshbach theory and width fluctuation corrections to calculate the compound nuclear contributions to the cross sections. The optical model parameters used in these calculations were supplied by A. Prince. [14].

^{155}Gd calculations were run with 15 levels including the ground state. This is the limit imposed by the in-house version of COMNUC. The continuum started at 0.67 MeV. ^{157}Gd was calculated using 15 levels up to 0.839 MeV. Spin and parity for levels in the region of 0.6-0.7 MeV were doubtful, so the threshold for the continuum was set at the same threshold as ^{155}Gd (i.e., 0.67 MeV). Cross sections for levels higher than 0.67 MeV were subtracted from the continuum. The continuum in the above cases, as with all the calculations for the gadolinium isotopes is described in COMNUC by a continuous distribution of levels whose density is calculated by an expression of the type given by Gilbert and Cameron [15]:

All the even isotopes of gadolinium were calculated in the same manner. Also levels for all even isotopes except ^{156}Gd were calculated beyond the threshold of the continuum. As in ^{157}Gd the excited state cross sections beyond the continuum threshold were subtracted from the calculated continuum.

E. Radiative Capture Cross Section

The capture cross sections of all gadolinium isotopes from 10^{-5} ev to the top of the resonance region are described by resonance parameters, and in the case of ^{158}Gd and ^{160}Gd a thermal 1/V contribution. Above the resonance region and up to approximately 5 MeV the shape of the curve was determined using the COMNUC code. The COMNUC generated data set was renormalized to the data of Shorin et al [16]. Shorin measured all the gadolinium isotopes except ^{152}Gd . The measurements were made by the detection of prompt gamma-rays and time of flight techniques. The energy range for his measurements was 5.0 to 70 keV. His relative cross sections (measured against the $\text{B}(\text{n},\alpha\gamma)$ cross section) were normalized to the 30 keV gold cross section of 596 mb \pm 4%. The abundance weighted experimental data is in good agreement with the capture cross section of natural gadolinium as measured by Fricke et al [17].

The capture cross sections from the Schenter evaluation [2] were renormalized to the above evaluation at 1 MeV. This data was used between 5 and 20 MeV.

IV. ANGULAR DISTRIBUTION OF SECONDARY NEUTRONS

Using the optical model parameters supplied by Prince [14] and the code ABACUS-2 [18] the differential elastic scattering cross sections were calculated. The calculated cross sections were then fed into the CHAD code [19]. CHAD fits this data as a polynomial of the form:

$$\frac{d\sigma_s(E;\mu)}{d\Omega} = \frac{\sigma_s}{4\pi} \sum_{l=0}^n (2l+1) f_l(E) P_l(\mu)$$

By use of the assumption that $d\sigma_s(E,\mu)/d\Omega$ may be represented by a linear function between the input points, the Legendre scattering coefficients $f_l(E)$ can be computed analytically. These coefficients appear in the file in the center of mass system.

64-Gd-152/160
MAT 1362+

The parameters $\bar{\mu}$, ξ and γ were generated using the code DUMMY5 [20] with the differential elastic angular distributions calculated with ABACUS. These appear in ENDF/B File 3.

The inelastic angular distributions appear in the file as isotropic in the center-of-mass system.

V. ENERGY DISTRIBUTIONS OF SECONDARY NEUTRONS

The energy distributions of secondary neutrons for the $(n,2n)$ and (n,n') reactions in the continuum have been calculated as a nuclear temperature energy in MeV. From Gilbert and Cameron [15].

$$\frac{1}{\Theta} = \sqrt{\frac{a}{U}} - \frac{3}{2U}$$

a = nuclear level density parameter (MeV^{-1})

U = $E - P(Z) - P(N)$ MeV

P = Pairing Energy

The Pairing Energies given by Gilbert and Cameron were replaced with those of Cook et al. [21]. For deformed nuclei, the equation $a/A = 0.00917S + 0.120 \text{ MeV}^{-1}$ was used. Here $S = S(Z) + S(N)$ is a shell correction. All continuum inelastic temperatures were calculated from the above formula.

The first neutron in the $(n,2n)$ reaction was calculated as above with E being replaced by $E + Q$ of the reaction. The temperature of the second neutron was calculated for the $A - 1$ nucleus with E being replaced by $E + Q - \bar{E}$. Here \bar{E} is the average energy of the first neutron boiled off.

REFERENCES

1. N.E. Holden and F.W. Walker, "Chart of the Nuclides", Eleventh Edition Revised to April 1972, Knolls Atomic Power Laboratory, General Electric Corporation, October, 1972.
2. R.E. Schenter and F. Schmittroth, Hanford Engineering and Development Laboratories Gadolinium Isotopes Evaluated for ENDF/B-IV, Distributed, December, 1974.
3. S.F. Mughabghab and D.I. Garber, "Neutron Cross Sections, Volume 1, Resonance Parameters", BNL-325, Third Edition, Volume 1, Brookhaven National Laboratory, June, 1973.
4. O. Ozer, "RESEND", BNL-17134, Brookhaven National Laboratory, 1972.
5. E. Steinnes, J. Inorg. and Nuc. Chem. 34, 2699, 1972.
6. E. Steinnes, Private Communication to S.F. Mughabghab, February, 1976.
7. H.B. Moller, et al., Nuc. Sci. and Eng. 8, 183, 1960.
8. E.N. Karzhavina, et al., JINR P3-6948, 1973.
9. E. Pennington, "Interim Documentation of Unresolved Resonance Program UR", Argonne National Laboratory Internal Memorandum, April, 1969.
10. S.F. Mughabghab and R.E. Chrien, Phys. Rev. 180, 1151, 1969.
11. R. Van der Linden, F. De Corte and J. Hoste, Journal of Radioanalytical Chemistry 20, 695, 1974.

64-Gd-152/160
MAT 1362+

12. S. Pearlstein, Nuc. Cross Section and Tech. Conf. Volume II, 332, 1975.
13. C.L. Dunford, AI-AEC-12931, 1970.
14. A. Prince, Private Communication, 1975.
15. A. Gilbert and A.G.W. Cameron, Can. J. Phys. 43, 1446, 1965.
16. V.S. Shorin et al., Yad. Fiz. 19, 5, 1974.
17. S.J. Friesenhahn et al., Nuc. Phys. A146, 337, 1970.
18. E.H. Auerbach, ABACUS-2, BNL-6562, Brookhaven National Laboratory, 1964.
19. R.F. Berland, CHAD, NAA-SR-11231, Atomics International, 1965.
20. DUMMY5, Subroutine of CHAD (above) modified to output in ENDF format.
21. J.L. Cook, et al., Aus. J. Phys. 20, 477, 1967

66-Dy-164
MAT 1031

PRI.COMM.1967

JUN67 B.R.LEONARD.JR. AND K.B.STEWART

DYS PROS IUM-164

General Identification

MAT = 1031
ZA = 66164.0
AWR = 162.52
I = 0
R = $.77 \times 10^{-12}$ cm

[Everling] (1)

Ref. 2

$$\frac{163.9281}{1.008665} = 162.52$$

Radioactive Decay

MT = 102 $\text{Dy}^{165} \rightarrow \text{Ho}^{165}$ $\lambda = 8.309 \times 10^{-5} \text{ sec}^{-1}$ Ref 3.

Cross Sections

Low Energy

The cross sections of Dy^{164} are rather non-controversial. The July 1, 1966, edition of CINDA (3) shows three monoenergetic measurements: 1) σ_T measured from 10^{-3} to 1.5×10^{-2} eV by Moore (4), 2) σ_T and σ_{act} measured from .02 to 1.5 eV by Sher (5) and 3) resonance parameters for a resonance at 146 eV by Zimmerman. (6)

Sher used his data and those of Moore to derive parameters for the bound level that dominates the thermal cross section. The parameters quoted by Sher are rather confusing. He quotes a value of $\Gamma = 166 \pm 4$ meV. Since the resonance is at -1.89 eV the analysis is very insensitive to the value of Γ . Consequently we have refitted the data preserving the quoted parameters as much as possible, particularly hoping to improve the fit to the activation cross section. We found no significant improvement. Our derived parameters are:

$$\begin{aligned} E_C &= -1.89 \\ \Gamma_n^0 &= 0.0420 \text{ eV} \\ \Gamma_\gamma &= 0.0538 \text{ eV} \\ R &= .77 \times 10^{-12} \text{ cm} \end{aligned}$$

where the value of Γ_γ was chosen to agree with the value obtained for the 146 eV resonance.

The program UNICORN⁽⁷⁾ was used to calculate the low-energy cross sections using our parameters for the -1.89 eV resonance and the parameters of Zimmerman for the 146 eV resonance. The calculation was done for 0°K and the center-of-mass term removed from UNICORN. The point values are given in file 3 as 40 values from 10^{-4} to 2.229 eV. Ln σ -E interpolation is specified.

Resonance Region

The parameters of Zimmerman for the 146 eV resonance are given in file 2. The resolved resonance region is specified from 2.229 to 272 eV. The smooth cross section file is specified to be zero in this energy range.

The UNICORN calculation yields a capture resonance integral of 352 barns from 0.45 eV to 10^3 eV. This is to be compared with a recent measured value of 377 ± 34 barns.⁽⁸⁾

Fast-Neutron Region

Foster and Glasgow⁽⁹⁾ have recently measured the total cross section of elemental dysprosium from 3 to 15 MeV. These results form the basis for 18 point values given in file 3 from 3 to 20 MeV.

REFERENCES

1. F. Everling, L. A. König, J. E. H. Matteauch, and A. H. Wapstra, Nuclear Physics 18, 529 (1960).
2. Chrien, Col. Univ., Private Communication.
3. D. Strominger, J. M. Hollander, and G. T. Seaborg, Rev. Mod. Phys. 30, 585 (1958).
4. W. E. Moore, KAPL, quoted in Ref 5.
5. R. Sher, S. Tassan, E. V. Weinstock, and A. Hellsten, Nucl. Sci. Engr. 11, 369 (1961).
6. R. L. Zimmerman, Bull. Am. Phys. Soc. II, 2, 42 (1957).
7. J. M. Otter, NAA-SR-11980, Vol. VI (June 1966).
8. J. J. Scoville, E. Fast, and J. W. Rogers, Nucl. Sci. Engr. 25, 12 (1966).
9. D. G. Foster, Jr. and D. W. Glasgow, PNWL, Unpublished Data (1966)
Available from BNL Sigma Center.

LUTETIUM-175General Identification

MAT = 1032		
ZA = 71175.0		
AWR = 173.438	Ref 1.	<u>174.9409</u>
I = 3.5		1.008665
R = $.73 \times 10^{-12}$ cm	Ref 2.	

Radioactive Decay

MT = 102 $\text{Lu } 176^m \rightarrow \text{Hf } 176$ $\lambda = 5.20 \times 10^{-5} \text{ sec}^{-1}$ Ref 3

Introduction

The primary objective was to provide a set of evaluated data for low-energy neutrons since the primary interest in Lu-175 is in application as a neutron spectrum indicator. However, since new data were available on the fast-neutron total cross sections we have also entered σ_T and σ_γ in the fast-neutron range. Hopefully these data will provide a basis for model calculations to complete the data set on this nucleus.

Cross SectionsLow Energy

Although Lu¹⁷⁵ is the major isotope in elemental Lutetium (97.41%) the Lu¹⁷⁵ cross section at low energies constitutes only about 1/3 of the elemental cross section. In a literature search through July 1, 1966 [CINDA]⁴ we have found only one attempt to establish the low energy cross section of Lu¹⁷⁵. In this work of [Baston]⁵ measurements of σ_T were made over the energy region 0.01 to 1.0 eV with a time-of-flight spectrometer. The authors made no attempt to fit the observed cross section but presented a best fit 1/v behavior from which they inferred a value of σ_γ (.0253 eV) = 23 \pm 3 barns. The data which they presented were, however, noticeably non-1/v. Consequently, we have fitted these data in order to provide

an improved estimate of the energy variation of the cross section. The resonance parameters given in file 2 were used to calculate the resonance contribution to the low energy cross section using the program UNICORN. The residual cross section was then analyzed by standard graphical techniques to obtain parameters for a bound level. Our evaluation of the parameters gives:

$$E_0 = -.1785 \text{ eV}$$

$$2g\Gamma_n = 3.907 \times 10^{-6} \text{ eV}$$

$$\Gamma_\gamma = 0.060 \text{ eV}$$

$$R = .73 \times 10^{-12} \text{ cm}$$

The values of R and Γ_γ are, of course, input values. The resonance is sufficiently far removed that the analysis is insensitive to the value of Γ_γ so we have used the value established for the observed parameters.

The parameters of the bound level plus the parameters contained in file 2 were used to calculate the final cross section. The calculations as performed by UNICORN for 0°K. The results of the calculations are given in file 3 as 33 point values for $\sigma_T(MT=1)$, $\sigma_n(MT=102)$, and $\sigma_\gamma(MT=102)$ over the energy range of 10^{-4} to 1.075 eV.

The results of these calculations gave the following values at $E = .0253 \text{ eV}$:

$$\sigma_T = 28.2 \text{ barns}$$

$$\sigma_\gamma = 23.5 \text{ barns}$$

$$\sigma_p = 4.7 \text{ barns}$$

The cross section values in the low energy range which are calculated

for elemental lutetium using the ENDF/B data for Lu¹⁷⁵ and Lu¹⁷⁶ are seriously discrepant with recent total cross section measurements.^(2,7) The contribution of Lu¹⁷⁵ to the elemental cross section is so small that it would require a factor of 2 or more error in the absolute scale of the Lu¹⁷⁵ cross section to explain the discrepancy.

Resonance Region

No new information on the resonance parameters of Lu¹⁷⁵ has appeared⁽⁴⁾ since the 1960 Supplement to INNL-325.⁽⁸⁾ The parameters for the 16 resonances extending from 2.61 to 57.4 eV are given in file 2. The value $J = I = 3.5$ is specified for each resonance so that $g = .5$.

The unresolved parameters were obtained from averaging the resolved parameters. The unresolved region is specified in file 2 from 60 to 10^5 eV with the following parameters for each of the $J = 3$ and $J = 4$ states for $L = 0$:

$$\rho = c \int_E = kR = 3.2 \times 10^{-3} \int_E$$

$$D = 7.25 \text{ eV}$$

$$\langle \Gamma_n^0 \rangle = 1.27 \times 10^{-3} \text{ eV}$$

$$\langle \Gamma_\gamma \rangle = .060 \text{ eV}.$$

The smooth cross sections in file 3 are specified to be zero through the resonance region $E = 1.075$ to 10^5 eV.

Fast Neutron Region

Fast-neutron values of σ_T are specified for 29 energy values from 10^5 to 2×10^7 eV in file 3. The values for $E > 2.5$ MeV are based on the measurements of Foster and Glasgow⁽⁹⁾ and the lower energy values are guessed from systematics.

The fast capture cross section σ_γ is specified in file 3 from 10^5 to 2×10^7 eV based on the data shown in Ref 8. The extrapolated behavior falls off slightly faster than $1/v$.

REFERENCES

1. G. E. Chart of the Nuclides (8/64).
2. M. Atoji, Phys. Rev. 121, 610 (1961).
3. D. Strominger, J. M. Hollander, and G. T. Seaborg, Rev. Mod. Phys. 30, 585 (1958).
4. CINDA, EANDC-60U (July 1, 1966).
5. A. H. Baston, J. C. Lisle, and G. S. G. Tuckey, Journ. Nucl. Energy A 13, 35 (1960).
6. J. M. Otter, NAA-SR-11980, Vol. VI (June 1966).
7. L. G. Amaral, M. Abreu, F. G. Bianchini, and M. C. Mattos, IEA-86 (1963).
8. D. J. Hughes, B. A. Magurno, and M. K. Brussel, BNL-325, Second Ed., Suppl. 1 (Jan. 1, 1960).
9. D. G. Foster, Jr. and D. W. Glasgow, PNWL, Unpublished Data (1966)
Available from BNL Sigma Center.

LUTETIUM-176General Identification

MAT = 1033

ZA = 71176.0

AWR = 174.43

Ref 1

 $\frac{175.94}{1.008665}$

I = 7

R = $.73 \times 10^{-12}$ cm

Ref 2

Radioactive Decay

MT = 102

Lu¹⁷⁷ \rightarrow Hf¹⁷⁷ $\lambda = 1.20 \times 10^{-6}$ sec⁻¹ Ref 3Introduction

The primary objective was to provide a set of evaluated data for low-energy neutrons since the primary interest in Lu-176 is in application as a neutron spectrum indicator. However, since new data were available on σ_T for fast neutrons for elemental lutetium we have included the same fast-neutron data for σ_T and σ_γ as is contained in the Lu¹⁷⁵ ENDF/B file.

Cross SectionsLow Energy

Roberge and Sailor⁽⁴⁾ have published the results of precision measurements which they made on σ_T from 0.02 to 0.25 eV for a sample enriched in Lu¹⁷⁶. Their data were used to derive very precise values of the parameters of the 0.142 eV resonance which dominates the thermal cross section of Lu¹⁷⁶. Their data apparently show that essentially all of the thermal cross section is due to this resonance. In the ENDF/B file we have used the parameters determined by Roberge plus the resonance parameters listed in file 2 to calculate the low energy cross sections of Lu¹⁷⁶. The calculations were performed by UNICORN⁽⁵⁾ for a temperature of 0°K with the center-of-mass term removed since laboratory energy coordinates were used. The results of this calculation are entered in

ENDF/B file 3 as 37 point values of σ_T (MT=1), σ_n (MT=2), and σ_γ (MT=102) from 10^{-4} to 0.88 eV. The results give the following values for a neutron energy of 0.0253 eV:

$$\begin{aligned}\sigma_T &= 1955 \text{ barns} \\ \sigma_n &= 3.04 \text{ barns} \\ \sigma_\gamma &= 1952 \text{ barns}\end{aligned}$$

There are other measurements of lutetium cross sections at low energies which are discrepant with the low energy cross sections given in the ENDF/B file. These other measurements imply a significant contribution at thermal energies from a bound level.

Atoji⁽²⁾ measured a value of $\sigma_T = 105 \pm 2$ barns for elemental lutetium at an energy of 0.0735 eV. If this discrepancy were due to Lu¹⁷⁶ it would require a value of $\sigma_T = 3430$ barns at 0.0735 eV. The precise measurements of Roberge give a value of about 2950 barns at this energy.

Amaral, et al⁽⁶⁾ have measured the total cross section from 0.0185 to 0.203 eV with a crystal spectrometer. Although they obtained 0.142 eV resonance parameters that were sensibly the same as those of Roberge they report a value of $\sigma_T = 118 \pm 1$ barns at 0.0253 eV for elemental lutetium. Subtracting the Lu¹⁷⁵ cross section from this value would leave a Lu¹⁷⁶ cross section of 3500 barns. However, Baston⁽⁷⁾ has made measurements on an enriched sample of Lu¹⁷⁶ in this region with a time-of-flight spectrometer. Baston's resonance parameters again agree well with those of Roberge. Baston's data in the low energy region lie somewhat higher on the average than the values calculated from the resonance parameters but his average values in the region of 0.0253 eV are only about 2200 barns.

Thus it is concluded that the results of Roberge are the best estimate of the low energy cross sections of Lu¹⁷⁶ at this time.

Resonance Region

A search of CINDA (1966)(8) shows no new information on the resonance parameters of Lu¹⁷⁶. Thus the values given in the 1960 supplement to BNL-325⁽⁹⁾ have been incorporated in the ENDF/B file. The resolved resonance region extends from 0.8796 to 48 eV and contains 20 resonances. The value of $J = I = 7.0$ is specified to obtain $g = 0.50$.

The unresolved resonance region is specified from 48 eV to 100 keV. The average resonance parameters are assumed the same for each spin state and $L = 0$:

$$\rho \approx c\sqrt{E} = kR = 3.2 \times 10^{-3} \sqrt{E}$$

$$D = 4.66 \text{ eV}$$

$$\langle \Gamma_n^0 \rangle = 8.47 \times 10^{-4} \text{ eV}$$

$$\langle \Gamma_\gamma \rangle = 0.060 \text{ eV}$$

The smooth cross sections in file 3 are specified to be zero throughout the resonance range 0.88 to 1×10^5 eV.

Fast-Neutron Range

Values of σ_T and σ_γ are specified in file 3. These are the same values given for Lu¹⁷⁵ (MAT = 1032).

71-Lu-176

MAT 1033

1. F. Everling, L. A. König, J. E. H. Mattauch, and A. H. Wapstra, Nuclear Physics 18, 529 (1960).
2. M. Atoji, Phys. Rev. 121, 610 (1961).
3. G. Goldstein and S. A. Reynolds, Nuclear Data A 1, 435 (1966).
4. J. P. Roberge and V. L. Sailor, Nucl. Sci. Engr. 7, 502 (1960).
5. J. M. Otter, NAA-SR-11980, Vol. VI (June 1966).
6. L. A. Amaral, M. Abreu, F. G. Bianchini, and M. C. Mattos, IEA-86 (1963).
7. A. H. Baston, J. C. Lisle, and G. S. G. Tuckey, Journ. Nucl. Energy A, 13, 35 (1960).
8. CINDA, EANDC-60U, July 1, 1966.
9. D. J. Hughes, B. A. Magurno, and M. K. Brussell, BNL-325, Second Edition, Suppl. 1 (Jan. 1, 1960).

Evaluated Neutron Cross Sections for Natural Hafnium and
the Hafnium Isotopes 174, 176, 177, 178, 179, and 180.

M. K. Drake, D. A. Sargis, Tin Maung, Science Applications, Inc.

Additions and Editing by
S. Pearlstein, Brookhaven National Laboratory

A complete evaluation for natural hafnium and information on evaluated data for the separate isotopes were provided to the National Nuclear Data Center (NNDC) by Science Applications Incorporated (SAI). Evaluations for the separate isotopes consistent with the evaluation for natural hafnium were prepared by NNDC. The evaluations were extended to 20 MeV by the NNDC following total cross section measurements ⁽¹³⁾ for Ta and W corrected for nuclear size.

RESONANCE PARAMETERS

The resolved resonance parameters are based on data compiled by Perkins and Gyulassy ⁽¹⁾, plus Hf-177 and Hf-178 data by Liou, et al ⁽²⁾ Hf-178 and Hf-180 data by Moxon, et al ⁽³⁾. The unresolved resonance parameters are based on statistical properties of resolved resonances and fit of keV cross sections measured by Kapchigaseev ⁽⁴⁾ and Moxon ⁽⁵⁾. The 2200 M/S cross sections and resonance integrals for natural hafnium and its isotopes are given in Table I.

TOTAL CROSS SECTION

For energies less than 1.0 eV - data for the element by Moore ⁽⁶⁾ and Joki ⁽⁷⁾ and data for the isotopes by Conrad, et al ⁽⁸⁾ were used. For energies between 1.0 eV and 100 keV, resolved and unresolved resonance parameters between 100 and 500 keV data by Sherwood, et al ⁽⁹⁾ and Green and Mitchell ⁽¹⁰⁾ were used. Above 2.5 MeV data by Foster and Glasgow ⁽¹¹⁾ were adopted.

ELASTIC SCATTERING CROSS SECTION

For energies below 500 keV, the elastic scattering cross sections was taken as the total cross sections minus the non-elastic cross section.

For energies between 500 keV and 2.5 MeV, data of Sherwood, et al ⁽⁹⁾ and Walt and Barschall ⁽¹²⁾ were used. Above 2.5 MeV, the total cross section minus the non-elastic cross section was adopted.

INELASTIC SCATTERING CROSS SECTION

12 excitation levels were adopted based on data of Sherwood, et al ⁽⁹⁾. The isotopic contributions to the excited levels are given in Table II.

RADIATIVE CAPTURE CROSS SECTION

The 2200 M/SEC values were obtained by weighted ave, of experimental data (values given above). A 1/v contribution were used for Hf-174, 176, 178, and negative energy resonances given for Hf-180.

REFERENCES

- (1) Perkins, S.T. and Gyulassy, UCRL-50400, Vol 12 (1972)
- (2) Liou, H.I. et al, Phys. Rev. C11, 2022 (1975)
- (3) Moxon, M.C., et al, Pri. Comm. (1975)
- (4) Kapchigashev, S.P., Atomizdat, Moscow, 1970
- (5) Moxon, M.C., et al, AERE-PR/NP21 (1974)
- (6) Moore, W.E., Bul-Am-Phys-Soc, 6, 70 (1961)
- (7) Joki, E.G., et al. Nucl-Sci-Eng, 11, 298 (1961)
- (8) Conrad, C.A., et al, Bull-Am-Phys-Soc, 14, 496 (1969)
- (9) Sherwood, G.L. et al, Nucl-Sci-Eng 39, 461 (1970)
- (10) Green, L. and Mitchell, J.A., WAPD-TM-1073 (1973)
- (11) Foster, D.G. and Glasgow, D.W., Phys. Rev. C3, 576 (1971)
- (12) Walt, M. and Barschall, H.H., Phys. Rev. 93, 1062 (1954)
- (13) Peterson, et al, Phys. Rev. 120, 521 (1960)

72-Hf-Nat/Iso
MAT 1372+

Table I

Resonance Integrals and 2200 M/SEC Capture X/S

	RI(BARNS)	2200 M/SEC X/S (BARNS)
Hf-174	446	391
Hf-176	337	21.8
Hf-177	7220	376
Hf-178	1747	84.6
Hf-179	451	40.4
Hf-180	29	13.0
Element	1900	104.5

Table II

Inelastic Levels Used in the Evaluation

<u>Level Number</u>	<u>Energy (MeV)</u>	<u>Isotope</u>
1	0.0932	174,176,178,180
2	0.113	177,179
3	0.250	177,179
4	0.307	174,176,178,179,180
5	0.321	177
6	0.385	177,179
7	0.409	177
8	0.427	177
9	0.509	177
10	0.555	177
11	0.591	177
12	0.632	174,176,177,178,180

Eval-Jan72 Howerton, Perkins, MacGregor
UCRL-51306 (1975) Dist-Sep74 Rev-Nov74

*** DNA 4179 MOD 3 with ENDF/B-III resonance parameters *****

Ta-181 evaluated neutron cross sections
R.J.Howerton, S.T.Perkins, R.C.Haight and M.H. MacGregor
Lawrence Livermore Laboratory, Livermore, California

General Comments

The neutron energy range extends from .00001 eV to 20 MeV. In addition to elastic scattering, which occurs at all energies, the following reactions have threshold (UCRL-50400, Vol. 9) energies less than 20 MeV.

Reaction	Threshold (MeV)
n,n*	0.00623
n,2n	7.69
n,3n	14.30
n,p	0.24
n,np	5.97
n,d	3.73
n,nd	11.16
n,t	4.87
n,nt	11.00
n,he3	6.20
n,nhe3	13.24
n,alpha	exoergic (q = 7.41)
n,n alpha	exoergic (q = 1.53)
n,gamma	exoergic (q = 6.06)

All charged particle producing reactions, except the (n,p) process will be neglected as there are essentially no measurements. The cross sections for (n,n), (n,n*), (n,2n), (n,3n), (n,p), (n,gamma), and (n,x gamma) reactions are discussed below, as are the secondary neutron angular and energy distributions for these reactions. Discussions are also included for photon and electron production cross sections, multiplicities, energy distributions, and angular distributions. To provide a mechanism for entering electron production data into the ENDF/B format, files 32, 33, 34, and 35 were defined exactly analogous to files 12, 13, 14, and 15. For documentation see LA-4549 (ENDF-102, Rev., Vol. II) and read electron for photon in that reference.

The data base for the evaluation is given in UCRL-50400, vol. 2 and 3. References not specifically cited here are given in these two volumes.

73-Ta-181
MAT 1285

MF = 2

ENDF/B-III resolved and unresolved resonance parameters have been married onto this evaluation below 5kev (MAT-1126).

Neutron cross sections

Elastic scattering cross section

MF = 3 MT = 2

The elastic scattering cross sections is equal to 6.25 barns at 0.0253 eV, the difference between the total and n,gamma cross sections, and is essentially constant over the thermal energy region. In the resolved resonance region, up to about 300 eV, the cross section was determined from a single level analysis for zero degrees Kelvin material temperature. The parameters used were the recommended set in BNL-325, Suppl. 2, Vol. IIC (1966).

At higher energies, the elastic scattering cross section was taken as the difference between the total and the nonelastic cross section. The nonelastic was derived from the sum of its parts where data were available, from measurements of the nonelastic c/s where available and otherwise from systematics.

Elastic scattering angular distributions,

MF = 4 MT = 2

Normalized probabilities

The elastic scattering was assumed to be isotropic in the center of mass system for energies less than 50 keV. From 50 keV to 14.6 MeV the evaluations were based on experimental data where such data exist. For energies equal to or greater than one MeV optical model calculations were done to obtain an estimate of the inelastic scattering to low lying levels included in the experimental results. To provide a reasonable number of angular distributions, optical model calculations were used at intermediate energies and for energies greater than 14.6 MeV. The optical model results agreed very well with the experiments except at the minima where one would expect the low lying level excitations to cause a filling of the minima. The Wick limit was tested against all distributions and it was found that the criterion was met.

Inelastic scattering cross section

MF = 3 MT = 51-60 and 91

The excitation function for the 6 keV level was based on calculations done by Donald Gardner using the COMNUC code. the excitation functions for the next 9 levels were obtained from Ref. 885 and from recent ORNL data (Dickens and Morgan (1973)). The results were smoothly extrapolated to 10 mb at 2-4 MeV and kept constant to 20 MeV.

The total inelastic cross section was based on individual level data at energies of the order of one MeV. From 1 to 20 MeV there are few measurements and the excitation function was estimated from nuclear systematics. The difference between the total inelastic and the level data was assigned to the inelastic Continuum cross section. The experiment reported in Ref. 885 could not resolve certain doublets so a mean energy was assigned which, of course, differs from the energies presented in all tabulations of levels or level diagrams for Ta-181.

Inelastic scattering angular distributions,
MF = 4 MT = 51-60 and 91

Normalized probabilities

The level data were assumed isotropic in the center of mass system and the continuum component was assumed isotropic in the Laboratory System for energies less than 8.0 MeV. For higher energies the distributions were peaked forward.

Inelastic scattering energy distributions
MF = 5 MT = 91

The continuum inelastic scattering energy distribution is composed of an evaporation component plus a high energy pre-equilibrium component. This latter portion decreases with increasing secondary energy and its contribution increases with the incident neutron energy. The evaporation temperature was assumed to vary as the square root of the incident neutron energy. In the detailed evaluation, a separation was made into neutrons with incident energies above the $(n,2n)$ threshold, and those with energies below. The former were assumed to emit primarily high energy neutrons in the (n,n^*) reaction.

$(n,2n)$ cross section
MF = 3 MT = 16

The $(n,2n)$ cross section near threshold was determined from the observed dip in gamma ray production (Oak Ridge Report ORNL-TM-3702, Feb. 1972), using the formalism of Howerton and Plechaty (Nucl. Sci. Eng. 32, 178 (1968)). The overall shape for the excitation function was set equal to that of U238, with suitable adjustments to match the systematics of tantalum.

$(n,2n)$ energy distributions
MF = 5 MT = 16

The formalism of the temperature model was used for convenience in the absence of measurement.

$(n,3n)$ cross section
MF = 3 MT = 17

The $(n,3n)$ excitation function was based on the difference between a constant nonelastic cross section of 2.45 barns and the sum of the inelastic and $(n,2n)$ cross sections.

(n,3n) energy distributions

MF = 5 MT = 17

The formalism of the temperature model was used for convenience in the absence of measurement.

(n,p) cross section

MF = 3 MT = 103

The (n,p) cross section was based on the data of Ref. 2887, with smooth extrapolations to threshold and to 20 MeV.

(n,gamma) cross section

MF = 3 MT = 102

The (n,gamma) cross section is equal to 21.9 barns at .0253 eV and is 1/V over the thermal region. In the resolved resonance region, the cross section (at zero degrees Kelvin) was obtained from a single level analysis - see section under elastic scattering cross section.

From about 300 eV to 10 keV, the lead slowing-down-time spectrometer data of Ref. 1960 was used. This was merged smoothly into the relatively large amount of data available for energies below 5 MeV, and smoothly extrapolated to 20 MeV.

Gamma ray production cross sections

(n,x gamma) cross section from the
(n,gamma) reaction

MF = 12 MT = 102

The multiplicity for gamma rays, $m(e)$, from the (n,gamma) reaction was obtained below 35 keV neutron energy by normalizing the spectral shapes to the binding energy (be) plus the neutron energy E minus the energy diverted by internal conversion. Above 35 keV, this cross section is included in the (n,xgamma) cross section. Note that the assumed energy variation of the multiplicity conserves energy for the reaction with the energy distribution described below.

(n,x gamma) energy distribution from
The (n,gamma) reaction

MF = 15 MT = 102

The distributions are expressed as normalized probability distributions.

At $(10^{**}(-11))$ MeV neutron energy, this energy distribution was taken to be that of Ref. 2415 for photons between 2.5 and 5. MeV. above 5. MeV the thermal capture data of Ref. 3211 were used after having been normalized to Ref. 2415. Below 0.5 MeV photon energy, the data of Ref. 3211 were used, normalized at 402 keV to Ref. 2415. The production of K and L x-rays following internal conversion was taken from the internal conversion cross sections discussed below. A fluorescence yield of 100 was assumed for each K and L vacancy. Between 0.5 and 2.5 MeV, the energy distribution was taken from a gamma cascade calculation.

At 2 keV neutron energy the same procedure was followed except that the 2 keV data of Ref. 3211 was used for the photon energies above 5. MeV. At 35 keV neutron energy the energy distribution was assumed to be the same as at 2 keV.

(n,x gamma) cross section

MF = 13 MT = 3

This component includes all gamma rays except those from the capture process discussed above. Four discrete lines were entered explicitly. The measurements of Dickens and Morgan (1973), Larsen (1973), and of Rogers et al (1971) were used as guides for lines at 0.108, 0.1361, 0.152, 0.165, 0.179, 0.1937, 0.205 0.259, 0.288, 0.301, 0.331, 0.345, 0.3589, 0.482, 0.80, 0.99, 1.08, 1.150, 1.206, 1.245, 1.308, 1.382, and 1.426 MeV. K and L x-rays following internal conversion were also included. gamma rays from the other discrete (n,n*) levels were lumped into the Continuum.

Continuum contributions were handled by using the Howerton and Plechaty recipe with measured gamma ray temperatures (ORNL-TM-3702) for each reaction. The average photon energy in the spectra were chosen to give overall energy conservation for the combined neutron-plus-gamma production processes.

(n,x gamma) energy distributions

MF = 15 MT = 3

Experimental gamma ray temperatures (ORNL-TM-3702) were used with the Howerton and Plechaty recipe (loc. Cit.) in a calculation that was matched to gamma ray production data (ORNL-TM-3702) and to neutron systematics, with energy being conserved on the average for all neutron and gamma ray production processes.

References

Reference numbers quoted here refer to data in the 111 experimental neutron cross section library. See UCRL-50400, vol. 2 and 3 for comments and indexes to the data, as well as for other experimental results that were used in the evaluation.

- 885. Private communication (1966) A.B.Smith (ANL)
- 1019 Private communication (1968) W.E.Tucker (Texas Nuclear)
- 1497 Nuclear Sci. Eng. 40, 294 (1970) D.M.Drake et al. (LASL)
- 1960 J.Exptl.Theoret.Phys. (USSR) 46, 80 (1964) V.A.Konks et al.
- 2402 INR-795/I/PL (1967) J.Brzosko et al. (Poland)
- 2415 GA-10248 (DASA-2570) (1970) N.C.Rasmussen et al. (Gga)
- 2887 Nuclear Phys. 123, 603 (1969) J.S.Brzosko et al. (Poland)
- 3211 Nuclear Phys. A168, 449 (1971) R.G. Helmer, R.C. Greenwood and C.W. Reich (Mtr)
- 3212 P.F.A. Goudsmit, Thesis, Univ. Amsterdam (1969)
- 3213 Bull. Acad. Sci. (Phys. Ser.) 32, 1833 (1968) Ya K. Alkenis, M.K. Balodis, and P.T. Prokof@ev

Eval-Apr71 J.Otter,C.Dunford, and E.Ottewitte

AI-AEC-12990 (1971) Dist-May74

Extended to 20 MeV for ENDF/B Version-IV

* * * * *

Tantalum-182 ENDF/B MAT 1127, May 1971 (Ref) AI-AEC-12990
Thermal Xscx and resonance parameters evaluated by John Otter.
fast cross sections evaluated by Charles Dunford and Eric
Ottewitte. File assembly by Philip Rose.

MF=1 MT=451. Descriptive Information

Atomic mass/ Mattauch,Thiele,Wapstra. Nucl.Phys. 67,1(65).

MF=2 MT=151. Resonance Parameters

Resolved resonances - e, $2g^*(\gamma, n)$, and gamma gamma where known from NSE 33,16. Unknown gamma gamma equal to average of known values. J assigned in proportion to $2j+1$. Negative energy resonance parameters from fit to total cross sections at one and three eV. Calculated 2200 M/S cross sections are capture=8249b, scattering=31b, and total=8280b. Potential scattering assumed same as Ta-181, = 8.3b.

Unresolved resonance parameters energy independent. Dobs and gamma gamma from resolved resonance range S0, S1, and S2 same as Ta-181. D(J)/Dobs from AAEC/TM 392.

Resonance integral - capture (0.5eV-100keV) = 1020b. There is no experimental comparison.

MF=3 MT=1. Total Cross Section

2PLUS and COMNUC calculational results were used directly.

MF=3 MT=2. Elastic Cross Section

2PLUS and COMNUC calculational results were used directly.

MF=3 MT=4. Total Inelastic Cross Section

Equal to the sum of the level excitation and continuum Xscs.

MF=3 MT=16. n-2n Cross Section

The adopted cross section is the Ta-181 n-2n cross section shifted in energy to the Ta-182 threshold.

MF=3 MT=17. n-3n Cross Section

The n-3n cross section was obtained by subtracting the n-2n and inelastic continuum from the non-elastic cross section.

MF=3 MT=51. Inelastic Excitation (direct and compound nucleus) to the 97 keV level.

Cross sections calculated by the computer programs 2PLUS and COMNUC have been adopted without change at energies well above the threshold. Seemingly unphysical structure calculated by the COMNUC code was smoothed out near the threshold.

73-Ta-182
MAT 1127

MF=3 MT=52-58,91. Inelastic Excitation (compound nucleus only)
Calculation by 2PLUS-COMNUC for 114, 173, 237, 270, 292, 315
and 360 keV levels plus the continuum. Structure in the 114 keV
level near threshold smoothed out. Structure caused by
competition for open channels due to 1st level weakly coupled
and 2nd level strongly coupled to the ground state.

MF=3 MT=102. n-Gamma Cross Section
2PLUS-COMNUC results used to 5 MeV. above 5 MeV the theory of
V. Benzi and G. Reffo was used. Ref CCDN-nw/10 ENEA Data Center

MF=3 MT=107. n-Alpha Cross Section
same as Ta-181 (MAT 1126)

MF=4 MT=2. Angular Distribution of Elastically-Scattered Neuts.
transformation matrix calculated for mass 182. Legendre
coefficients taken directly from 2PLUS-COMNUC runs. 1

MF=4 MT=51-58,91. Angular Distribution of Neutrons Inelastically
scattered to discrete levels.

The level distributions were made isotropic in the CM frame.
the continuum was made isotropic in the lab frame.

MF=5 MT=16,17. Nuclear Temperatures - (n,2n), (n,3n) Reactions.
Temperature of first emitted neutron same as for MT=91.
Temperature of second and third emitted neutrons deduced by
conservation of energy, assuming the kinetic energy of an
emitted neutron is 2*Kt.

MF=5 MT=91. Nuclear Temperature - Inelastic Continuum
Maxwellian distribution used to describe nuclear temperature.
Level spacing same as Ta-181 (MAT 1126). U specified for Ta-182
thresholds.

SUMMARY DOCUMENTATION FOR ^{182}W

by

P. G. Young, J. Otter,[†] E. Ottewitte,[†] and P. Rose[†]
Los Alamos Scientific Laboratory
Los Alamos, New Mexico

I. SUMMARY

The ^{182}W evaluation for ENDF/B-V (MAT 1128) was carried over intact from Version IV with only minor format changes being made. The evaluation of the neutron files was performed at Atomics International and is documented in TI-707-130-026 (1973). The gamma-ray production data were evaluated at Los Alamos Scientific Laboratory and are documented in LA-5793 (1975). The ENDF/B-V data span the energy range 10^{-5} eV to 20 MeV.

II. ENDF/B-V FILES

File 1. General Information

MT=451. Descriptive Data

Atomic mass and Q-values taken from Ref. 1.

File 2. Resonance Parameters

MT=151. (A) Resolved Resonances Evaluation

Potential scattering cross section = 8.0 ± 1.0 b at E=0.

2200 m/s Cross Sections (barns)

	<u>CALC</u>	<u>MEAS (Ref. 2)</u>
CAP	20.5	20.7 ± 0.5
SCAT	11.6	

Resolved Resonance Parameters

- 100 eV	from	fit to capture
4.16 eV	from	Ref. 2
5 - 250 eV	from	evaluation, Refs. 2, 3, and 4
250 -1250 eV	from	evaluation, Refs. 3 and 4
1250 -4500 eV	from	Ref. 4
1920 -2198 eV	from	Ref. 3

[†] Atomics International

MT=151. (B) Unresolved Resonances Evaluation

Potential scattering cross section = 8.5 ± 1.0 b at $E_n=0$.
Total cross section = 8.85 b at $E_n=100$ keV (calculated).

Unresolved resonance parameters from automated optimized fit to
the evaluated measured capture cross section.

AV L=0 level spacing ($E_n=0$) = 57.45 eV, energy dep. from Ref. 5.

AV Capture level width = 0.0901 eV, energy independent

L=0 Strength function = 1.8E-4, energy independent

L=1 Strength function = 0.272E-4, energy independent

L=2 Strength function = 0.0

Average capture cross section uncertainty at energy E

<u>E (keV)</u>	<u>Uncertainty (%)</u>
100	15
90	10
10	10
4.5	17

Resonance integral (capture) 596 b calculation, 590 ± 10 b measurement (Ref. 6).

File 3. Neutron Cross Sections

MT=1. Total Cross Section

The total cross section was evaluated using a least squares spline fit to experimental data for this isotope. Spline fits of experimental data for natural tungsten were also factored into the evaluation (see MAT 1129 for Refs). The total cross section curve was smoothly joined to the evaluated total cross section in the unresolved resonance range below 100 keV. Isotopic data references are Whalen⁷ (100-650 keV), Martin⁸ (0.65-20 MeV), and Foster and Glasgow⁹ (2.5-15 MeV). General references for the total cross section are Goldberg et al.² and Devaney and Foster.¹⁰ The uncertainty in the total cross section is probably less than 7% over the energy range from 600 keV to 20 MeV. Between 300 keV and 600 keV the uncertainty increases to 10% and from 100 to 200 keV the uncertainty is estimated to be 15%.

MT=2. Elastic Cross Section

The elastic cross section was obtained by subtracting the nonelastic cross sections from the evaluated total cross section. The elastic cross section is in good agreement with the data of Lister¹¹ between 300 keV and 1.5 MeV. Between 1 MeV and 9 MeV the evaluated curve lies above 2PLUS-COMNUC results. At 4.3 MeV the cross section is some 15% lower than the experimental data point of Kinney and Perey¹² for natural tungsten. Our evaluation is, however, in agreement with their data above 5 MeV.

MT=4. Total Inelastic Cross Section

Equal to the sum of the level excitation and continuum cross sections. The total inelastic cross section for this isotope is in general agreement with the data of Owens et al.¹³ for natural tungsten between 5 and 7 MeV.

MT=16. (n,2n) Cross Section

The semi-empirical techniques of Pearlstein¹⁴ and W. D. Lu et al.¹⁵ were used to deduce the n,2n cross section. The evaluated curve at 14.8 MeV is in agreement with Dilg et al.¹⁶ and Druzhinin et al.¹⁷

MT=17. (n,3n) Cross Section

The n,3n cross sections were deduced using the semi-empirical techniques of S. Pearlstein¹⁴ and W. D. Lu.¹⁵ An effective threshold for the n,3n reaction was set 1.25 MeV above the theoretical threshold.

MT=28. (n,pn) Cross Section

The shape of the n,pn excitation curve is based upon the experimental data of J. F. Barry et al.¹⁸ for ¹⁸⁶W (see MAT 1131). The curve has been shifted in energy by the difference in the reaction Q for this isotope and ¹⁸⁶W. The cross section contains contributions from the n,np and n,d reactions.

MT=51. Inelastic Excitation (Direct and Compound Nucleus) to the 2⁺ Level

The cross sections were calculated using 2PLUS-COMNUC. They have been renormalized via a least squares fit to data of D. Lister et al.¹⁹ with a 10% uncertainty in the adjusted curve.

MT=52-58, 91. Inelastic Excitation (Compound Nucleus Only,..

Calculation by the COMNUC code for the 329, 680, 1220, 1258, 1289, 1331, and 1374 keV levels plus the continuum. The 329-keV level excitation curve was renormalized to the data of D. Lister.¹⁹ The uncertainty in the adjusted cross sections is about 10%.

MT=102. Radiative Capture Cross Section

The radiative capture cross section was evaluated between 10 keV and 150 keV using a least squares fit to experimental data (see MF=2, MT=151). This fit was combined and joined to the theoretical cross sections computed between 100 keV and 4 MeV using the COMNUC code. Above 4 MeV the COMNUC results were joined to the collective and direct interaction capture cross sections calculated using the theory of V. Benzi and G. Reffo.²⁰ The uncertainty in the radiative capture cross section is probably less than 15% for energies between 100 keV and 200 keV. Above 200 keV the cross

section is reliable only to the extent of the validity of the theoretical models.

MT=103. (n,p) Cross Section

The shape of the n,p excitation curve is based upon the experimental data of J. F. Barry et al.¹⁸ for ¹⁸⁶W (see MAT 1131). The curve has been shifted in energy to pass through the data point reported by M. Lindner et al.²¹ (3.5 ± 0.35 mb at 14.1 MeV).

MT=107. (n,α) Cross Section

The n,α cross section evaluation is based upon data of A. Rubinc and D. Zubke²² for ¹⁸¹Ta. The few experimental data points for isotopes of tungsten between 14 and 15 MeV qualitatively substantiate the use of this curve. The evaluation has not been extended below 11 MeV.

File 4. Neutron Angular Distributions

MT=2. Elastic Angular Distributions

The angular distributions for elastic scattering are given as Legendre polynomial coefficients in the cm system. These data were calculated by 2PLUS-COMNUC codes for each isotope. As little isotopic experimental data existed, the calculated data were averaged according to abundance and compared to natural tungsten data. The comparison indicated that the experimental data contained direct inelastic reactions to the first level. With the calculated first-level direct inelastic included, agreement within experimental error was generally indicated over all energies. This agreement also supports the validity of the inelastic angular file below. The natural tungsten experimental data were taken from Refs. 23-30. Error estimates for this section are difficult because it appears that pure elastic scatter has not been measured except at low energies. Because of the good agreement overall with the combined data, this file is estimated to be accurate to 15% at energies below 1 MeV, and within a factor of two at energies above 1 MeV for all scattering angles.

MT=51-58, 91. Angular Distribution of Inelastic Scattered Neutrons

Angular distributions are given as Legendre polynomial coefficients in the laboratory frame of reference. These data are based upon 2PLUS-COMNUC calculations. They include anisotropic contributions from direct inelastic excitation of the 2⁺ level. Compound level and continuum excitations are isotropic in the laboratory system. Errors are small simply due to the predominance of isotropy.

File 5. Neutron Energy Distributions

MT=16, 17. Nuclear Temperatures for the (n,2n) and (n,3n) Reactions

Temperature of first emitted neutron same as for MT=91. Temperatures of second and third emitted neutrons deduced by conservation of energy assuming the kinetic energy of an emitted neutron is 2^*KT .

MT=91. Nuclear Temperature for Inelastic Continuum

References 31-34 were used in deriving temperatures. Least squares Weisskopf level spacing was fit to natural tungsten data. Isotopic data adjusted using deformed nucleus level density formula of Gilbert and Cameron.³⁴

File 12. Gamma Ray Multiplicities

MT=102. Multiplicities for Gamma Ray Production from Radiative Capture

Multiplicities at neutron energies below 1 eV are based on a preliminary thermal measurement for natural W by Jurney³⁵ and from 1 eV to 1000 eV on calculations by Yost et al.³⁶ At higher energies the multiplicities are based on an analysis of natural W measurements (Dickens,³⁸ $E_n=1-20$ MeV) using statistical calculations similar to those described by Troubetzkoy,³⁷ with the multiplicities chosen to give rough agreement with the measurements. The theory was used at all energies to divide the natural W data into isotopic components.

File 13. Gamma Ray Production Cross Sections

MT=4. Gamma Ray Production Cross Sections from Inelastic, (n,2n), and (n,3n) Reactions

The cross sections for discrete photons are based on the level excitation cross sections in MF=3, MT=51-58, mainly using the level decay scheme of Way.³⁹ The cross sections for continuum gamma rays are based on a statistical theory analysis of the Dickens³⁸ measurements on natural W. The theory was used for interpolation, smoothing, and separation of the data into isotopic components.

File 14. Gamma Ray Angular Distributions

MT=4, 102. Angular Distributions of Gamma Rays from Radiative Capture, Inelastic, (n,2n), and (n,3n) Reactions

Gamma rays from all reactions are assumed isotropic in the laboratory system.

File 15. Gamma Ray Energy Distributions

MT=4. Energy Distributions of Gamma Rays from Inelastic, (n,2n), and (n,3n) Reactions

The spectra at all energies are based on a statistical theory analysis of the Dickens³⁸ measurements with natural W. The theory was used as described above (MF=13, MT=4). Arbitrary adjustments were made to the theoretical fits in regions where agreement with experiment was poor (mainly below $E_n=5$ MeV).

MT=102. Energy Distributions of Gamma Rays From Radiative Capture

Spectra at neutron energies below 1 eV are based on a preliminary thermal measurement by Jurney³⁵ and from 1 eV to 1000 eV on calculations by Yost et al.³⁶ At higher energies the spectra are based on statistical calculations using parameters obtained by analyzing the Dickens³⁸ measurement for $E_n=1-3$ MeV. The theory was used at all energies to divide the natural W data into separate isotopic components.

(Note: No information is provided in this evaluation on electron production from internal conversion. Such information might be important for local heating and radiation damage problems.)

REFERENCES

1. A. H. Wapstra and N. B. Gove, Nucl. Data Tables 9, 267 (1971).
2. M. D. Goldberg et al., BNL-325, 2nd Edition, Supplement 2, (1966).
3. Z. M. Bartolome et al., Nucl. Sci. Eng. 37, p. 137 (1969).
4. F. J. Rahn and H. Camarda, personal communication, Columbia (1970).
5. J. L. Cook et al., AAEC/TM-392 (1967).
6. M. Drake, (1968) for American Institute of Phys. Handbook (1972).
7. J. F. Whalen, ANL-7210, 16 (1966).
8. R. C. Martin, PhD Thesis, RPT (1967).
9. D. G. Foster and D. W. Glasgow, Phys. Rev. 3C, 576 (1971).
10. J. J. Devaney and D. G. Foster, Jr., Los Alamos report LA-4928 (1972).
11. D. Lister et al., ANL-7288 (1967).
12. W. E. Kinney and F. G. Perey, ORNL-4803 (1973).
13. R. O. Owens et al., Nucl. Phys. A112, 337 (1968).
14. S. Pearlstein, Nucl. Sci. Eng. 23, 238 (1965).
15. W. D. Lu et al., Phys. Rev. C1, 350 (1970).
16. Dilg et al., Nucl. Phys. A118, 9 (1968).
17. Druzhinin et al., Sov. J. Nucl. Phys. 4, 515 (1966).
18. J. F. Barry et al., Proc. Phys. Soc. 74, 632 (1959).
19. D. Lister et al., Phys. Rev. 162, 1077 (1967).
20. V. Benzi and G. Reffo, CCDN-NW10, ENEA Neutron Compilation Center (1969).
21. M. Lindner et al., Lawrence Livermore Laboratory, private communication (1972).
22. A. Rubino and D. Zubke, Nucl. Phys. 85, 606 (1966).
23. A. B. Smith and P. A. Moldauer, BAPS 5, 409 (1960).
24. F. T. Kuchnir et al., Phys. Rev. 176, 1405 (1968).

25. W. Walt and H. Barschall, Phys. Rev. 93, 1062 (1954).
26. K. Tsukada et al., Nucl. Phys. A125, 641 (1966).
27. R. W. Hill, Phys. Rev. 109, 2105 (1958).
28. W. Kinney, private communication (1972).
29. D. B. Thomson, Phys. Rev. 129, 1649 (1963).
30. H. Nauta, Nucl. Phys. 2, 124 (1956).
31. S. G. Buccino et al., Nucl. Phys. 60, 17 (1964).
32. R. O. Owens and J. H. Towle, Nucl. Phys. A112, 337 (1968).
33. W. E. Kinney, ORNL, private communication (1972).
34. A. Gilbert and A. G. W. Cameron, Can. J. Phys. 43, 1446 (1965).
35. E. T. Jurney, private communication (1973).
36. K. J. Yost, J. E. White, C. Y. Fu, and W. E. Ford, Nucl. Sci. Eng. 47, 209 (1972).
37. E. S. Troubetzkoy, Phys. Rev. 122, 212 (1961).
38. J. K. Dickens, private communication (1972).
39. K. Way, Nuclear Data Bl-1, 1 (1966).

SUMMARY DOCUMENTATION FOR ^{183}W

by

P. G. Young, J. Otter,[†] E. Ottewitte,[†] and P. Rose[†]
Los Alamos Scientific Laboratory
Los Alamos, New Mexico

I. SUMMARY

The ^{183}W evaluation for ENDF/B-V (MAT 1129) was carried over intact from Version IV with only minor format changes being made. The evaluation of the neutron files was performed at Atomics International and is documented in TI-7Q7-130-026 (1973). The gamma-ray production data were evaluated at Los Alamos Scientific Laboratory and are documented in LA-5793 (1975). The ENDF/B-V data span the energy range 10^{-5} eV to 20 MeV.

II. ENDF/B-V FILES

File 1. General Information

MT=451. Descriptive Data

Atomic mass and Q-values taken from Ref. 1.

File 2. Resonance Parameters

MT=151. (A) Resolved Resonances Evaluation

Potential scattering cross section = 8.0 ± 1.0 b at $E_n=0$.

2200 m/s Cross Sections (barns)

	<u>CALC</u>	<u>MEAS (Ref. 2)</u>
CAP	10.0	10.2 ± 3.0
SCAT	3.4	

Resolved Resonance Parameters

-1.5 eV from fit to capture
0 - 150 eV from Ref. 2
150 - 175 eV from evaluation, Refs. 2 and 3
175 - 760 eV from Ref. 3

[†] Atomics International

MT=151. (B) Unresolved Resonances Evaluation

Potential scattering cross section = 8.5 ± 1.0 b at $E_n=0$.
Total cross section = 11.3 b at $E_n=45$ keV (calculated).

Unresolved resonance parameters from automated optimized fit to the evaluated measured capture cross section. The competitive reaction width for $L=2$, $J=1$ is for the L to $L=2$ elastic scattering process.

AV $L=0$ level spacing ($E_n=0$) = 12.53 eV, energy dep. from Ref. 4.
AV Capture level width = 0.0801 eV, energy independent
 $L=0$ Strength function = 2.125E-4 eV, energy independent
 $L=1$ Strength function = 0.227E-4 eV, energy independent
 $L=2$ Strength function = 2.56E-4 eV, energy independent

Average capture cross section uncertainty at energy E

E (keV)	Uncertainty (%)
45	11
10	12
5	20
2.5	40

Resonance integral (capture) 355 b calculation, 380 ± 15 b measurement (Ref. 5).

File 3. Neutron Cross Sections

MT=1. Total Cross Section

There are no experimental data for ^{183}W . The total cross section was evaluated using a least squares spline fit to experimental data for natural tungsten.⁶⁻¹⁰ The total cross section curve was smoothly joined to the evaluated total cross section in the energy range below 100 keV. The lack of direct experimental data introduces a large uncertainty in the total cross section between 100 keV and 700 keV (see Ref. 10).

MT=2. Elastic Cross Section

The elastic cross section was obtained by subtracting the nonelastic cross sections from the evaluated total cross section. Between 1 MeV and 9 MeV, the evaluated curve lies above 2PLUS-COMNUC results. At 4.3 MeV the cross section is some 15% lower than the experimental data point of Kinney and Percy¹¹ for natural tungsten. Our evaluation is, however, in agreement with their data above 5 MeV.

MT=4. Total Inelastic Cross Section

Equal to the sum of the level excitation and continuum cross sections. The total inelastic cross section for this isotope is in general agreement with the data of Owens et al.¹² for natural tungsten between 5 and 7 MeV.

MT=16. (n,2n) Cross Section

The semi-empirical techniques of Pearlstein¹³ and W. D. Lu et al.¹⁴ were used to deduce the n,2n cross section.

MT=17. (n,3n) Cross Section

The n,3n cross sections were deduced using the semi-empirical techniques of S. Pearlstein¹³ and W. D. Lu.¹⁴ An effective threshold for the n,3n reaction was set 1.25 MeV above the theoretical threshold.

MT=28. (n,pn) Cross Section

The shape of the n,pn excitation curve is based upon the experimental data of J. F. Barry et al.¹⁵ for ^{186}W (see MAT 1131). The curve has been shifted in energy by the difference in the reaction Q for this isotope and ^{186}W . The cross section contains contributions from the n,np and n,d reactions.

MT=51, 52. Inelastic Excitation (Direct and Compound Nucleus) to the 46.5 and 99 keV Levels.

The cross sections were calculated using the 2PLUS-COMNUC codes. No experimental data has been reported.

MT=53-59, 91. Inelastic Excitation (Compound Nucleus Only).

Calculation by the COMNUC code for the 207, 209, 292, 309, 412, 453, and 595-keV levels plus the continuum. The theoretical cross sections were used without modification.

MT=102. Radiative Capture Cross Section

The radiative capture cross section was evaluated between 10 keV and 100 keV using a least squares fit to experimental data (see MF=2, MT=151). This fit was combined and joined to the theoretical cross sections computed between 100 keV and 4 MeV using the COMNUC code. Above 4 MeV the COMNUC results were joined to the collective and direct interaction capture cross sections calculated using the theory of V. Benzi and G. Reffo.¹⁶ The uncertainty in the radiative capture cross section is 11% between 45 keV and 90 keV. Between 90 keV and 200 keV the uncertainty is probably less than 25%. Above 200 keV the cross section is reliable only to the extent of the validity of the theoretical models.

MT=103. (n,p) Cross Section

The shape of the n,p excitation curve is based upon the experimental data of J. F. Barry et al.¹⁵ for ^{186}W (see MAT 1131). The curve has been shifted in energy to pass through the data point reported by M. Lindner et al.¹⁷ (4.2 \pm 0.42 mb at 14.1 MeV).

MT=107. (n, α) Cross Section

The n,α cross section evaluation is based upon data of A. Rubino and D. Zubke¹⁸ for ^{181}Ta . The few experimental data points for isotopes of tungsten between 14 and 15 MeV qualitatively substantiate the use of this curve. The evaluation has not been extended below 11 MeV.

File 4. Neutron Angular Distributions

MT=2. Elastic Angular Distributions

The angular distributions for elastic scattering are given as Legendre polynomial coefficients in the cm system. These data were calculated by 2PLUS-COMNUC codes for each isotope. As little isotopic experimental data existed, the calculated data were averaged according to abundance and compared to natural tungsten data. The comparison indicated that the experimental data contained direct inelastic reactions to the first 2 levels. With the calculated first-and second-level direct inelastic included, agreement within experimental error was generally indicated over all energies. This agreement also supports the validity of the inelastic angular file below. The natural tungsten experimental data were taken from Refs. 19-26. Error estimates for this section are difficult because it appears that pure elastic scatter has not been measured except at low energies. Because of the good agreement overall with the combined data, this file is estimated to be accurate to 15% at energies below 1 MeV, and within a factor of two at energies above 1 MeV for all scattering angles.

MT=51-59, 91. Angular Distribution of Inelastic Scattered Neutrons

Angular distributions are given as Legendre polynomial coefficients in the laboratory frame of reference. These data are based upon 2PLUS-COMNUC calculations. They include anisotropic contributions from direct inelastic excitation of the $^{3/2}+$ and $^{5/2}+$ levels. Compound level and continuum excitations are isotropic in the laboratory system. Errors are small simply due to the predominance of isotropy.

File 5. Neutron Energy Distributions

MT=16, 17. Nuclear Temperatures for the (n,2n) and (n,3n) Reactions

Temperature of first emitted neutron same as for MT=91. Temperatures of second and third emitted neutrons deduced by conservation of energy assuming the kinetic energy of an emitted neutron is $2*KT$.

MT=91. Nuclear Temperatures For Inelastic Continuum

References 27-30 were used in deriving temperatures. Least squares Weisskopf level spacing was fit to natural tungsten data.

Isotopic data adjusted using deformed nucleus level density formula of Gilbert and Cameron.³⁰

File 12. Gamma Ray Multiplicities

MT=102. Multiplicities for Gamma Ray Production from Radiative Capture

Multiplicities at neutron energies below 1 eV are based on a preliminary thermal measurement for natural W by Jurney³¹ and from 1 eV to 1000 eV on calculations by Yost et al.³² At higher energies the multiplicities are based on an analysis of natural W measurements (Dickens,³⁴ $E_n=1-20$ MeV) using statistical calculations similar to those described by Troubetzkoy,³³ with the multiplicities chosen to give rough agreement with the measurements. The theory was used at all energies to divide the natural W data into isotopic components.

File 13. Gamma Ray Production Cross Sections

MT=4. Gamma Ray Production Cross Sections from Inelastic, (n,2n), and (n,3n) Reactions

The cross sections for discrete photons are based on the level excitation cross sections in MF=3, MT=51-59, mainly using the level decay scheme of Artna.³⁵ The cross sections for continuum gamma rays are based on a statistical theory analysis of the Dickens³⁴ measurements on natural W. The theory was used for interpolation, smoothing, and separation of the data into isotopic components.

File 14. Gamma Ray Angular Distributions

MT=4, 102. Angular Distributions of Gamma Rays from Radiative Capture, Inelastic, (n,2n), and (n,3n) Reactions

Gamma rays from all reactions are assumed isotropic in the laboratory system.

File 15. Gamma Ray Energy Distributions

MT=4. Energy Distributions of Gamma Rays from Inelastic, (n,2n), and (n,3n) Reactions

The spectra at all energies are based on a statistical theory analysis of the Dickens³⁴ measurements with natural W. The theory was used as described above (MF=13, MT=4). Arbitrary adjustments were made to the theoretical fits in regions where agreement with experiment was poor (mainly below $E_n=5$ MeV).

MT=102. Energy Distributions of Gamma Rays from Radiative Capture

Spectra at neutron energies below 1 eV are based on a preliminary thermal measurement by Jurney³¹ and from 1 eV to 1000 eV on

calculations by Yost et al.³² At higher energies the spectra are based on statistical calculations using parameters obtained by analyzing the Dickens³⁴ measurement for $E_n=1-3$ MeV. The theory was used at all energies to divide the natural W data into separate isotopic components.

(Note: No information is provided in this evaluation on electron production from internal conversion. Such information might be important for local heating and radiation damage problems.)

REFERENCES

1. A. H. Wapstra and N. B. Gove, Nucl. Data Tables 9, 267 (1971).
2. M. D. Goldberg et al., BNL-325, 2nd Edition, Supplement 2 (1966).
3. Z. M. Bartolome et al., Nucl. Sci. Eng. 37, p. 137 (1969).
4. J. L. Cook et al., AAEC/TM-392 (1967).
5. M. Drake, (1968) for American Institute of Phys. Handbook (1972).
6. J. F. Whalen, ANL-7210, 16 (1966).
7. M. Davadeenam, PhD Thesis Duke University (1967).
8. W. H. Kao et al., Chinese J. Phys. 5, 43 (1967).
9. J. M. Peterson et al., Phys. Rev. 120, 521 (1960).
10. J. J. Devaney and D. G. Foster, Jr., Los Alamos report LA-4928 (1972).
11. W. E. Kinney and F. G. Perey, ORNL-4803 (1973).
12. R. O. Owens et al., Nucl. Phys. A112, 337 (1968).
13. S. Pearlstein, Nucl. Sci. Eng. 23, 238 (1965).
14. W. D. Lu et al., Phys. Rev. C1, 350 (1970).
15. J. F. Barry et al., Proc. Phys. Soc. 74, 632 (1959).
16. V. Benzi and G. Reffo, CCDN-NW10, ENEA Neutron Compilation Center (1969).
17. M. Lindner et al., Lawrence Livermore Laboratory, private communication (1972).
18. A. Rubino and D. Dubke, Nucl. Phys. 85, 606 (1966).
19. A. B. Smith and P. A. Moldauer, BAPS 5, 409 (1960).
20. F. T. Kuchnir et al., Phys. Rev. 176, 1405 (1968).
21. W. Walt and H. Barschall, Phys. Rev. 93, 1062 (1954).
22. K. Tsukada et al., Nucl. Phys. A125, 641 (1966).
23. R. W. Hill, Phys. Rev. 109, 2105 (1958).
24. W. Kinney, private communication (1972).
25. D. B. Thomson, Phys. Rev. 129, 1649 (1963).
26. H. Nauta, Nucl. Phys. 2, 124 (1956).
27. S. G. Buccino et al., Nucl. Phys. 60, 17 (1964).
28. R. O. Owens and J. H. Towle, Nucl. Phys. A112, 337 (1968).
29. W. E. Kinney, ORNL, private communication (1972).
30. A. Gilbert and A. G. W. Cameron, Can. J. Phys. 43, 1446 (1965).
31. E. T. Jurney, private communication (1973).
32. K. J. Yost, J. E. White, C. Y. Fu, and W. E. Ford, Nucl. Sci. Eng. 47, 209 (1972).
33. E. S. Troubetzkoy, Phys. Rev 122, 212 (1961).
34. J. K. Dickens, private communication (1972).
35. A. Artna, Nuclear Data Bl-1, 37 (1966).

SUMMARY DOCUMENTATION FOR ^{184}W

by

P. G. Young, J. Otter,[†] E. Ottewitte,[†] and P. Rose[†]
Los Alamos Scientific Laboratory
Los Alamos, New Mexico

I. SUMMARY

The ^{184}W evaluation for ENDF/B-V (MAT 1130) was carried over intact from Version IV with only minor format changes being made. The evaluation of the neutron files was performed at Atomics International and is documented in TI-707-130-026 (1973). The gamma-ray production data were evaluated at Los Alamos Scientific Laboratory and are documented in LA-5793 (1975). The ENDF/B-V data span the energy range 10^{-5} eV to 20 MeV.

II. ENDF/B-V FILES

File 1. General Information

MT=451. Descriptive Data

Atomic mass and Q-values taken from Ref. 1.

File 2. Resonance Parameters

MT=151. (A) Resolved Resonances Evaluation

Potential scattering cross section = 8.0 ± 1.0 b at $E_n=0$.

2200 m/s Cross Sections (barns).

	<u>CALC</u>	<u>MEAS (Ref. 2)</u>
CAP	1.8	1.8 ± 0.2
SCAT	3.9	

Resolved Resonance Parameters

-11.76 eV	from	fit to capture
102 eV	from	evaluation, Refs. 2 and 3
150 - 2060 eV	from	evaluation, Refs. 2, 3, and 4
2080 - 2110 eV	from	Ref. 3
2200 - 2650 eV	from	Ref. 4

[†] Atomics International

74-W-184
MAT 1130

MT=151. (B) Unresolved Resonances Evaluation

Potential scattering cross section = 8.5 ± 1.0 b at $E_n=0$.
Total cross section = 9.1 b at $E_n=100$ keV (calculated).

Unresolved resonance parameters from automated optimized fit to
the evaluated measured capture cross section.

AV L=0 level spacing ($E_n=0$) = 80.3 eV, energy dep. from Ref. 5.

AV Capture level width = 0.0731 eV, energy independent

L=0 Strength function = $2.3E-4$, energy independent

L=1 Strength function = $0.18E-4$, energy independent

L=2 Strength function = $1.45E-4$, energy independent

Average capture cross section uncertainty at energy E

<u>E (keV)</u>	<u>Uncertainty (%)</u>
100	15
90	10
10	10
4.5	20

Resonance integral (capture) 16.2 b calculation, 13 ± 2 b measure-
ment (Ref. 6).

File 3. Neutron Cross Sections

MT=1. Total Cross Section

The total cross section was evaluated using a least squares spline
fit to experimental data for this isotope. Spline fits of exper-
imental data for natural tungsten were also factored into the
evaluation (see MAT 1129 for references). The total cross section
curve was smoothly joined to the evaluated total cross section
in the unresolved resonance range below 100 keV. Isotopic data
references are Whalen⁷ (100-650 keV), Martin⁸ (0.65-20 MeV), and
Foster and Glasgow⁹ (2.5-15 MeV). General references for the
total cross section are Goldberg et al.² and Devaney and Foster.¹⁰
The uncertainty in the total cross section is probably less than
7% over the energy range from 600 keV to 20 MeV. Between 300 keV
and 600 keV the uncertainty increases to 10% and from 100 to 200
keV the uncertainty is estimated to be 15%.

MT=2. Elastic Cross Section

The elastic cross section was obtained by subtracting the nonelastic
cross sections from the evaluated total cross section. The elastic
cross section is in good agreement with the data of Lister¹¹
between 300 keV and 0.8 MeV. Between 0.8 MeV and 1.5 MeV, the
elastic cross section is somewhat higher than the experimental
data. Between 1 MeV and 9 MeV the evaluation curve lies above
2PLUS-COMNUC results. At 4.3 MeV the cross section is some 15%
lower than the experimental data point of Kinney and Perey¹² for
natural tungsten. Our evaluation is, however, in agreement with
their data above 5 MeV.

MT=4. Total Inelastic Cross Section

Equal to the sum of the level excitation and continuum cross sections. The total inelastic cross section for this isotope is in general agreement with the data of Owens et al.¹³ for natural tungsten between 5 and 7 MeV.

MT=16. (n,2n) Cross Section

The semi-empirical techniques of Pearlstein¹⁴ and W. D. Lu et al.¹⁵ were used to deduce the n,2n cross section.

MT=17. (n,3n) Cross Section

The n,3n cross sections were deduced using the semi-empirical techniques of S. Pearlstein¹⁴ and W. D. Lu.¹⁵ An effective threshold for the n,3n reaction was set 1.25 MeV above the theoretical threshold.

MT=28. (n,pn) Cross Section

The shape of the n,pn excitation curve is based upon the experimental data of J. F. Barry et al.¹⁶ for ¹⁸⁶W (see MAT 1131). The curve has been shifted in energy by the difference in the reaction Q for this isotope and ¹⁸⁶W. The cross section contains contributions from the n,np and n,d reactions.

MT=51. Inelastic Excitation (Direct and Compound Nucleus) to the 2⁺ Level

The cross sections were calculated using 2PLUS-COMNUC. They have been renormalized via a least squares fit to data of D. Lister et al.¹⁷ with a 10% uncertainty in the adjusted curve.

MT=52-59, 91. Inelastic Excitation (Compound Nucleus Only).

Calculation by the COMNUC code for the 365, 748, 904, 1007, 1135, 1223, 1270, and 1287 keV-levels plus the continuum. The 365-, 904-, and 1007-keV level excitation curves were renormalized to the data of D. Lister.¹⁷ The uncertainty is about 10% in the 365-keV level data and 15% in the 904- and 1007-keV level data.

MT=102. Radiative Capture Cross Section

The radiative capture cross section was evaluated between 10 keV and 150 keV using a least squares fit to experimental data (see MF=2, MT=151). This fit was combined and joined to the theoretical cross sections computed between 100 keV and 4 MeV using the COMNUC code. Above 4 MeV the COMNUC results were joined to the collective and direct interaction capture cross sections calculated using the theory of V. Benzi and G. Reffo.¹⁸ The uncertainty in the radiative capture cross section is probably less than 15% for energies between 100 keV and 200 keV. Above 200 keV the cross

section is reliable only to the extent of the validity of the theoretical models.

MT=103. (n,p) Cross Section

The shape of the n,p excitation curve is based upon the experimental data of J. F. Barry et al.¹⁶ for ¹⁸⁶W (see MAT 1131). The curve has been shifted in energy to agree with the ratio of (n,p) measurements reported by Coleman¹⁹ for ¹⁸⁴W and ¹⁸⁶W at 14.5 MeV.

MT=107. (n,α) Cross Section

The n,α cross section evaluation is based upon data of A. Rubino and D. Zubke²⁰ for ¹⁸¹Ta. The few experimental data points for isotopes of tungsten between 14 and 15 MeV qualitatively substantiate the use of this curve. The evaluation has not been extended below 11 MeV.

File 4. Neutron Angular Distributions

MT=2. Elastic Angular Distributions

The angular distributions for elastic scattering are given as Legendre polynomial coefficients in the cm system. These data were calculated by 2PLUS-COMNUC codes for each isotope. As little isotopic experimental data existed, the calculated data were averaged according to abundance and compared to natural tungsten data. The comparison indicated that the experimental data contained direct inelastic reactions to the first level. With the calculated first-level direct inelastic included, agreement within experimental error was generally indicated over all energies. This agreement also supports the validity of the inelastic angular file below. The natural tungsten experimental data were taken from Refs. 21-28. Error estimates for this section are difficult because it appears that pure elastic scatter has not been measured except at low energies. Because of the good agreement overall with the combined data, this file is estimated to be accurate to 15% at energies below 1 MeV, and within a factor of two at energies above 1 MeV for all scattering angles.

MT=51-59, 91. Angular Distribution of Inelastic Scattered Neutrons

Angular distributions are given as Legendre polynomial coefficients in the laboratory frame of reference. These data are based upon 2PLUS-COMNUC calculations. They include anisotropic contributions from direct inelastic excitation of the 2⁺ level. Compound level and continuum excitations are isotropic in the laboratory system. Errors are small simply due to the predominance of isotropy.

File 5. Neutron Energy Distributions

MT=16, 17. Nuclear Temperatures for the (n,2n) and (n,3n) Reactions

Temperature of first emitted neutron same as for MT=91. Temperatures of second and third emitted neutrons deduced by conservation of energy assuming the kinetic energy of an emitted neutron is $2*KT$.

MT=91. Nuclear Temperature for Inelastic Continuum

References 29-32 were used in deriving temperatures. Least squares Weisskopf level spacing was fit to natural tungsten data. Isotopic data adjusted using deformed nucleus level density formula of Gilbert and Cameron.³²

File 12. Gamma Ray Multiplicities

MT=102. Multiplicities for Gamma Ray Production from Radiative Capture

Multiplicities at neutron energies below 1 eV are based on a preliminary thermal measurement for natural W by Journey³³ and from 1 eV to 1000 eV on calculations by Yost et al.³⁴ At higher energies the multiplicities are based on an analysis of natural W measurements (Dickens,³⁶ $E_n=1-20$ MeV) using statistical calculations similar to those described by Troubetzkoy,³⁵ with the multiplicities chosen to give rough agreement with the measurements. The theory was used at all energies to divide the natural W data into isotopic components.

File 13. Gamma Ray Production Cross Sections

MT=4. Gamma Ray Production Cross Sections from Inelastic, (n,2n), and (n,3n) Reactions

The cross sections for discrete photons are based on the level excitation cross sections in MF=3, MT=51-59, mainly using the level decay scheme of Martin.³⁷ The cross sections for continuum gamma rays are based on a statistical theory analysis of the Dickens³⁶ measurements on natural W. The theory was used for interpolation, smoothing, and separation of the data into isotopic components.

File 14. Gamma Ray Angular Distributions

MT=4, 102. Angular Distributions of Gamma Rays from Radiative Capture, Inelastic, (n,2n), and (n,3n) Reactions

Gamma rays from all reactions are assumed isotropic in the laboratory system.

File 15. Gamma Ray Energy Distributions

MT-4. Energy Distributions of Gamma Rays from Inelastic, (n,2n), and (n,3n) Reactions

The spectra at all energies are based on a statistical theory analysis of the Dickens³⁶ measurements with natural W. The theory was used as described above (MF=13, MT=4). Arbitrary adjustments were made to the theoretical fits in regions where agreement with experiment was poor (mainly below $E_n=5$ MeV).

MT-102. Energy Distributions of Gamma Rays from Radiative Capture

Spectra at neutron energies below 1 eV are based on a preliminary thermal measurement by Jurney³³ and from 1 eV to 1000 eV on calculations by Yost et al.³⁴ At higher energies the spectra are based on statistical calculations using parameters obtained by analyzing the Dickens³⁶ measurement for $E_n=1-3$ MeV. The theory was used at all energies to divide the natural W data into separate isotopic components.

(Note: No information is provided in this evaluation on electron production from internal conversion. Such information might be important for local heating and radiation damage problems).

REFERENCES

1. A. H. Wapstra and N. B. Gove, Nucl. Data Tables 9, 267 (1971).
2. M. D. Goldberg et al., BNL-325, 2nd Edition, Supplement 2, (1966).
3. Z. M. Bartolome et al., Nucl. Sci. Eng. 37, p. 137 (1969).
4. F. J. Rahn and H. Camarda, personal communication, Columbia (1970).
5. J. L. Cook et al., AAEC/TM-392 (1967).
6. M. Drake, (1968) for American Institute of Phys. Handbook (1972).
7. J. F. Whalen, ANL-7210, 16 (1966).
8. R. C. Martin, PhD Thesis, RPT (1967).
9. D. G. Foster, and D. W. Glasgow, Phys. Rev. 3C, 576 (1971).
10. J. J. Devaney and D. G. Foster, Jr., Los Alamos report LA-4928 (1972).
11. D. Lister et al., ANL-7288 (1967).
12. W. E. Kinney and F. G. Perey, ORNL-4803 (1973).
13. R. O. Owens et al., Nucl. Phys. A112, 337 (1968).
14. S. Pearlstein, Nucl. Sci. Eng. 23, 238 (1965).
15. W. D. Lu et al., Phys. Rev. C1, 350 (1970).
16. J. F. Barry et al., Proc. Phys. Soc. 74, 632 (1959).
17. D. Lister et al., Phys. Rev. 162, 1077 (1967).
18. V. Benzi and G. Reffo, CCDN-NW10, ENEA Neutron Compilation Center (1969).
19. R. F. Coleman, Proc. Phys. Soc. 73, 215 (1959).
20. A. Rubino and D. Zubke, Nucl. Phys. 85, 606 (1966).
21. A. B. Smith and P. A. Moldauer, BAPS 5, 409 (1960).
22. F. T. Kuchnir et al., Phys. Rev. 176, 1405 (1968).
23. W. Walt and H. Barschall, Phys. Rev. 93, 1062 (1954).
24. K. Tsukada et al., Nucl. Phys. A125, 541 (1966).
25. R. W. Hill, Phys. Rev. 109, 2105 (1958).

26. W. Kinney, private communication (1972).
27. D. B. Thomson, Phys. Rev. 129, 1649 (1963).
28. H. Nauta, Nucl. Phys. 2, 124 (1956).
29. S. G. Buccino et al., Nucl. Phys. 60, 17 (1964).
30. R. O. Owens and J. H. Towle, Nucl. Phys. 112, 337 (1968).
31. W. E. Kinney, ORNL, private communication (1972).
32. A. Gilbert and A. G. W. Cameron, Can. J. Phys. 43, 1446 (1965).
33. E. T. Jurney, private communication (1973).
34. K. J. Yost, J. E. White, C. Y. Fu, and W. E. Ford, Nucl. Sci. Eng. 47, 209 (1972).
35. E. S. Troubetzkoy, Phys. Rev. 122, 212 (1961).
36. J. K. Dickens, private communication (1972).
37. M. J. Martin, Nuclear Data Bl-1, 63 (1966).

SUMMARY DOCUMENTATION FOR ^{186}W

by

P. G. Young, J. Otter,[†] E. Ottewitte,[†] and P. Rose[†]
Los Alamos Scientific Laboratory
Los Alamos, New Mexico

I. SUMMARY

The ^{186}W evaluation for ENDF/B-V (MAT 1131) was carried over intact from Version IV with only minor format changes being made. The evaluation of the neutron files was performed at Atomics International and is documented in TI-707-130-026 (1973). The gamma-ray production data were evaluated at Los Alamos Scientific Laboratory and are documented in LA-5793 (1975). The ENDF/B-V data span the energy range 10^{-5} eV to 20 MeV.

II. ENDF/B-V FILES

File 1. General Information

MT=451. Descriptive Data

Atomic mass and Q-values taken from Ref. 1.

File 2. Resonance Parameters

MT=151. (A) Resolved Resonances Evaluation

Potential scattering cross section = 8.0 ± 1.0 b at $E_n=0$.

2200 m/s Cross Sections (barns).

	<u>CALC</u>	<u>MEAS (Ref. 2)</u>
CAP	37.5	38 ± 2
SCAT	0.39	

Resolved Resonance Parameters

18.81 eV from evaluation of Refs. 2 and 4 plus
adjustment from fit to capture cross
section

100 - 250 eV from evaluation of Refs. 2-4
250 - 3200 eV from evaluation of Refs. 3-4

[†] Atomics International

MT=51. (B) Unresolved Resonances Evaluation

Potential scattering cross section = 8.5 ± 1.0 b at $E_n=0$.
Total cross section = 9.1 b at $E_n=100$ keV (calculated).

Unresolved resonance parameters from automated optimized fit to
the evaluated measured capture cross section.

AV L=0 level spacing (E=0) = 99.1 eV, energy dep. from Ref. 5

AV Capture level width = 0.0530 eV, energy independent

L=0 Strength function = 2.2E-4, energy independent

L=1 Strength function = 0.252E-4, energy independent

L=2 Strength function = 1.45E-4, energy independent

Average capture cross section uncertainty at energy E

<u>E (keV)</u>	<u>Uncertainty (%)</u>
----------------	------------------------

100	11
90	8
45	8
22.5	14
10	11
4.5	17

Resonance integral (capture) 522 b calculation, 490 ± 50 b measure-
ment (Ref. 6).

File 3. Neutron Cross Sections

MT=1. Total Cross Section

The total cross section was evaluated using a least squares spline
fit to experimental data for this isotope. Spline fits of exper-
imental data for natural tungsten were also factored into the
evaluation (see MAT 1129 for Refs). The total cross section
curve was smoothly joined to the evaluated total cross section
in the unresolved resonance range below 100 keV. Isotopic data
references are Whalen⁷ (100-650 keV), Martin⁸ (0.65-20 MeV), and
Foster and Glasgow⁹ (2.5-15 MeV). General references for the
total cross section are Goldberg et al.² and Devaney and Foster.¹⁰
The uncertainty in the total cross section is probably less than
7% over the energy range from 600 keV to 20 MeV. Between 300 keV
and 600 keV the uncertainty increases to 10% and from 100 to 200
keV the uncertainty is estimated to be 15%.

MT=2. Elastic Cross Section

The elastic cross section was obtained by subtracting the nonelastic
cross sections from the evaluated total cross section. The elastic
cross section is in good agreement with the data of Lister¹¹
between 300 keV and 0.7 MeV. Between 0.7 MeV and 1.5 MeV, the
elastic cross section is some 10% higher than the experimental
data. Between 1 MeV and 9 MeV the evaluated curve lies above
2PLUS-COMNUC results. At 4.3 MeV the cross section is some 15%
lower than the experimental data point of Kinney and Perey¹² for
natural tungsten. Our evaluation is, however, in agreement with
their data above 5 MeV.

MT=4. Total Inelastic Cross Section

Equal to the sum of the level excitation and continuum cross section. The total inelastic cross section for this isotope is in general agreement with the data of Owens et al.¹³ for natural tungsten between 5 and 7 MeV.

MT=16. (n,2n) Cross Section

The semi-empirical techniques of Pearlstein¹⁴ and W. D. Lu et al.¹⁵ were used to deduce the n,2n cross section. The evaluated curve at 14.8 MeV is in agreement with Druzhinin et al.¹⁶

MT=17. (n,3n) Cross Section

The n,3n cross sections were deduced using the semi-empirical techniques of S. Pearlstein¹⁴ and W. D. Lu.¹⁵ An effective threshold for the n,3n reaction was set 1.25 MeV above the theoretical threshold.

MT=28. (n,pn) Cross Section

The shape of the n,pn excitation curve is based upon the experimental data of J. F. Barry et al.¹⁷ The uncertainty in the cross section is 25% at energies well above the observed threshold. The cross section contains contributions from the n,np and n,d reactions.

MT=51. Inelastic Excitation (Direct and Compound Nucleus) to the 2⁺ Level

The cross sections were calculated using 2PLUS-COMNUC. They have been renormalized via a least squares fit to data of D. Lister et al.¹⁸ with a 10% uncertainty in the adjusted curve.

MT=52-59, 91. Inelastic Excitation (Compound Nucleus Only).

Calculation by the COMNUC code for the 401, 730, 840, 850, 960, 1040, 1110, and 1250 keV levels plus the continuum. The 401, 730, and 942-keV level excitation curves were renormalized to the data of D. Lister.¹⁸ The uncertainty in the adjusted cross sections is about 10%. The sum of the 840 and 850 keV level COMNUC results were renormalized to the 863 ± 10 keV excitation data of D. Lister. Likewise, the sum of the 1040 and 1110 keV levels were renormalized to the 1035 ± 10 keV experimental data. The summed levels have a 15% cross section uncertainty.

MT=102. Radiative Capture Cross Section

The radiative capture cross section was evaluated between 10 keV and 4 MeV using a least squares spline fit to experimental data (see MF=2, MT=151). Comparisons with COMNUC theoretical results were excellent. Adjustments were made, however, to the data fit

in the neighborhood of the 2^+ threshold to better fit the theoretical calculations. These adjustments improved the reconstructed elemental file comparison with experiment. Above 4 MeV the data fit was joined to theoretical capture cross sections calculated between 4 and 20 MeV. The theory of Benzi and Reffo¹⁹ was used to determine the collective and direct interaction cross section.

MT=103. (n,p) Cross Section

The n,p cross section evaluation is based upon experimental data of J. F. Barry et al.¹⁷ Uncertainty is 25% at energies well above the observed threshold.

MT=107. (n, α) Cross Section

The n, α cross section evaluation is based upon data of A. Rubino and D. Zubke²⁰ for ^{181}Ta . The few experimental data points for isotopes of tungsten between 14 and 15 MeV qualitatively substantiate the use of this curve. The evaluation has not been extended below 11 MeV.

File 4. Neutron Angular Distributions

MT=2. Elastic Angular Distributions

The angular distributions for elastic scattering are given as Legendre polynomial coefficients in the cm system. These data were calculated by 2PLUS-COMNUC codes for each isotope. As little isotopic experimental data existed, the calculated data were averaged according to abundance and compared to natural tungsten data. The comparison indicated that the experimental data contained direct inelastic reactions to the first level. With the calculated first-level direct inelastic included, agreement within experimental error was generally indicated over all energies. This agreement also supports the validity of the inelastic angular file below. The natural tungsten experimental data were taken from Refs. 21-28. Error estimates for this section are difficult because it appears that pure elastic scatter has not been measured except at low energies. Because of the good agreement overall with the combined data, this file is estimated to be accurate to 15% at energies below 1 MeV, and within a factor of two at energies above 1 MeV for all scattering angles.

MT=51-59, 91. Angular Distribution of Inelastic Scattered Neutrons

Angular distributions are given as Legendre polynomial coefficients in the laboratory frame of reference. These data are based upon 2PLUS-COMNUC calculations. They include anisotropic contributions from direct inelastic excitation of the 2^+ level. Compound level and continuum excitations are isotropic in the laboratory system. Errors are small simply due to the predominance of isotropy.

File 5. Neutron Energy Distributions

MT=16, 17. Nuclear Temperatures for the (n,2n) and (n,3n) Reactions

Temperature of first emitted neutron same as for MT=91. Temperatures of second and third emitted neutrons deduced by conservation of energy assuming the kinetic energy of an emitted neutron is $2*KT$.

MT=91. Nuclear Temperature for Inelastic Continuum

References 29-32 were used in deriving temperatures. Least squares Weisskopf level spacing was fit to natural tungsten data. Isotopic data adjusted using deformed nucleus level density formula of Gilbert and Cameron.³²

File 12. Gamma Ray Multiplicities

MT=102. Multiplicities for Gamma Ray Production from Radiative Capture

Multiplicities at neutron energies below 1 eV are based on a preliminary thermal measurement for natural W by Jurney³³ and from 1 eV to 1000 eV on calculations by Yost et al.³⁴ At higher energies the multiplicities are based on an analysis of natural W measurements (Dickens,³⁶ $E_n=1-20$ MeV) using statistical calculations similar to those described by Troubetzkoy,³⁵ with the multiplicities chosen to give rough agreement with the measurements. The theory was used at all energies to divide the natural W data into isotopic components.

File 13. Gamma Ray Production Cross Sections

MT=4. Gamma Ray Production Cross Sections from Inelastic, (n,2n), and (n,3n) Reactions

The cross sections for discrete photons are based on the level excitation cross sections in MT=3, MT=51-59, mainly using the level decay scheme of Gove.³⁷ The cross sections for continuum gamma rays are based on a statistical theory analysis of the Dickens³⁶ measurements on natural W. The theory was used for interpolation, smoothing, and separation of the data into isotopic components.

File 14. Gamma Ray Angular Distributions

MT=4, 102. Angular Distributions of Gamma Rays from Radiative Capture, Inelastic, (n,2n), and (n,3n) Reactions

Gamma rays from all reactions are assumed isotropic in the laboratory system.

File 15. Gamma Ray Energy Distributions

MT=4. Energy Distributions of Gamma Rays from Inelastic, (n,2n), and (n,3n) Reactions

The spectra at all energies are based on a statistical theory analysis of the Dickens³⁶ measurements with natural W. The theory was used as described above (MF=13, MT=4). Arbitrary adjustments were made to the theoretical fits in regions where agreement with experiment was poor (mainly below $E_n=5$ MeV).

MT=102. Energy Distributions of Gamma Rays from Radiative Capture

Spectra at neutron energies below 1 eV are based on a preliminary thermal measurement by Jurney³³ and from 1 eV to 1000 eV on calculations by Yost et al.³⁴ At higher energies the spectra are based on statistical calculations using parameters obtained by analyzing the Dickens³⁶ measurement for $E_n=1-3$ MeV. The theory was used at all energies to divide the natural W data into separate isotopic components.

(Note: No information is provided in this evaluation on electron production from internal conversion. Such information might be important for local heating and radiation damage problems.)

REFERENCES

1. A. H. Wapstra and N. B. Gove, Nucl. Data Tables 9, 267 (1971).
2. M. D. Goldberg et al., BNL-325, 2nd Edition, Supplement 2, (1966).
3. Z. M. Bartolome et al., Nucl. Sci. Eng. 37, p. 137 (1969).
4. F. J. Rahn and H. Camarda, personal communication, Columbia (1970).
5. J. L. Cook et al., AAEC/TM-392 (1967).
6. M. Drake, (1968) for American Institute of Phys. Handbook (1972).
7. J. F. Whalen, ANL-7210, 16 (1966).
8. R. C. Martin, PhD Thesis, RPT (1967).
9. D. G. Foster and D. W. Glasgow, Phys. Rev. 3C, 576 (1971).
10. J. J. Devaney and D. G. Foster, Jr., Los Alamos report LA-4928 (1972).
11. D. Lister et al., ANL-7288 (1967).
12. W. E. Kinney and F. G. Perey, ORNL-4803 (1973).
13. R. O. Owens et al., Nucl. Phys. A112, 337 (1968).
14. S. Pearlstein, Nucl. Sci. Eng. 23, 238 (1965).
15. W. D. Lu et al., Phys. Rev. C1, 350 (1970).
16. Druzhinin et al., Sov. J. Nucl. Phys. 4, 515 (1966).
17. J. F. Barry et al., Proc. Phys. Soc. 74, 632 (1959).
18. D. Lister et al., Phys. Rev. 162, 1077 (1967).
19. V. Benzi and G. Reffo, CCDN-NW10, ENEA Neutron Compilation Center (1969).
20. A. Rubino and D. Zubke, Nucl. Phys. 85, 606 (1966).
21. A. B. Smith and P. A. Moldauer, BAPS 5, 409 (1960).
22. F. T. Kuchnir et al., Phys. Rev. 176, 1405 (1968).
23. W. Walt and H. Barschall, Phys. Rev. 93, 1062 (1954).
24. K. Tsukada et al., Nucl. Phys. A125, 641 (1966).
25. R. W. Hill, Phys. Rev. 109, 2105 (1958).

26. W. Kinney, private communication (1972).
27. D. B. Thomson, Phys. Rev. 129, 1649 (1963).
28. H. Nauta, Nucl. Phys. 2, 124 (1956).
29. S. G. Buccino et al., Nucl. Phys. 60, 17 (1964).
30. R. O. Owens and J. H. Towle, Nucl. Phys. A112, 337 (1968).
31. W. E. Kinney, ORNL, private communication (1972).
32. A. Gilbert and A. G. W. Cameron, Can. J. Phys. 43, 1446 (1965).
33. E. T. Jurney, private communication (1973).
34. K. J. Yost, J. E. White, C. Y. Fu, and W. E. Ford, Nucl. Sci. Eng. 47, 209 (1972).
35. E. S. Troubetzkoy, Phys. Rev. 122, 212 (1961).
36. J. K. Dickens, private communication (1972).
37. N. B. Gove, Nuclear Data Bl-2, 1 (1966).

GE-NMPO GEMP-587

JAN68 W.B.HENDERSON, J.W.ZWICK

RHENIUM-185 (MAT 1083) and RHENIUM-187 (MAT 1084)

Background

This work* was undertaken specifically to supply ENDF/B with evaluated neutron cross sections of Re-185 and Re-187. It is an extension of an earlier evaluation* by A. Prince to include more recent data and make use of improved nuclear models. Most remarks below pertain to both isotopes. Where the information applies to only one isotope, it is so identified. Formal documentation will be published as ENDF 115.

MF = 1, MT = 451 - GENERAL INFORMATION AND INTEGRAL DATA

The weight of the atom and neutron in the ratio, AWR, were taken from the Chart of the Nuclides.¹

The absorption integral above 0.5 ev was computed from resolved and unresolved resonance parameters in File 2 and smooth absorption cross sections in File 3. For Re-185 the calculation gives 1748.3 barns versus 1726 ± 68^2 , 1650 ± 90^3 , 1753 ± 90^3 , and 1828 ± 120^4 measured. For Re-187 the calculation gives 287.7 barns versus 292 ± 42^2 , 308 ± 20^3 , and 312 ± 22^4 measured. Using the abundances⁵ of 0.3707 for Re-185 and 0.6293 for Re-187 the calculated value for natural rhenium is 829.1 barns versus 823 ± 52^2 , 856 ± 65^3 , 842 ± 50^3 , 874 ± 58^4 , and 694 ± 125^6 measured.

The calculated absorption cross section at 0.0253 ev for Re-185 is 114.0 barns versus 114 ± 3^2 measured and 105 ± 10^7 evaluated by Goldberg, et al. For Re-187** the calculation gives 74.8 barns versus 75 ± 4^2 and 73 ± 7^7 . For natural rhenium the calculation gives 89.3 barns versus 89 ± 5^2 .

The calculated scattering cross section at 0.0253 ev for Re-185 is 20.6 barns and for Re-187, 10.1 barns. For natural rhenium this corresponds to 14.0 barns versus 14 ± 4^5 evaluated by Hughes and Schwartz.

The calculated total cross section at 0.0253 ev for Re-185 is 134.6 barns versus 118 ± 2^8 measured. The calculated value for Re-185 is a consequence of producing the 114.0 barns absorption from resonance parameters, which requires strong (or many) bound levels. The calculated scattering is the free atom cross section while the measured values contain solid state effects. The calculated total cross section for Re-187 is 84.8 barns versus 90 ± 2^8 measured. For natural rhenium the calculation gives 103.3 barns versus 100 ± 1^2 and 100 ± 2^8 measured.

The calculated reactivity worth of core-length natural rhenium samples in the fast-spectrum, refractory metal 710 Basic Critical Experiment No. 1⁹ using the ENDF/B rhenium cross sections is -7.1×10^{-5} per gram versus $(-5.7 \pm 1.0) \times 10^{-5}$

*Work performed under U.S. Atomic Energy Commission Contract No. At(40-1)-2847.

**The capture cross section of Re-187 includes that leading to the 18.6 minute excited state.

75-Re-185/187
MAT 1083, 1084

measured. Although this evaluation produces natural rhenium absorption cross sections which are lower than most measured values above 100 ev, no change is recommended, pending further data testing, since absorption cross sections in agreement with those measurements lead to predictions of reactivity worth more negative than measured in both the 710 and the ZPR-9¹⁰ fast critical experiments.

MF = 1, MT = 453 - RADIOACTIVE DECAY DATA

The data were taken from the Chart of Nuclides¹. The decay constants were computed from the half lives of the ground states. Lacking a means of specifying branching ratios in the ENDF/B format, OS-186 was made the daughter of Re-186, since 95% of the decays³¹ go that way.

MF = 2, MT = 151 - RESONANCE PARAMETERS

Resolved resonance parameters of Friesenhahn, et al² were used except for bound levels, which were determined from a multi-level Breit-Wigner fit to the low energy capture and total cross sections of Friesenhahn, et al². The J values are from Goldberg, et al⁷, where given; otherwise they were arbitrarily assigned 3 or 2 in the ratio 7 to 5 to facilitate multi-level calculations. In Re-185 a single bound level with J = 3 provided an adequate fit to the data. In Re-187 two bound levels were required and results were very insensitive to the J assignments. The spin-independent radii correspond to potential scattering cross sections of 7.45 and 7.55 barns in Re-185 and Re-187 respectively and were assigned to fit the measured low energy² total cross section of natural rhenium, as well as intermediate energy^{2,11,12} values.

In the unresolved resonance region the average capture width and observed level spacing were taken from Friesenhahn, et al². Strength functions for s, p, and d waves were assigned to be in approximate agreement with average optical model values and to fit the total cross section at intermediate energies. The resulting capture cross sections are somewhat lower than most measured^{2,13-20} values, as mentioned in the description of MF = 1, MT = 451.

In the resolved resonance region the single-level Breit-Wigner formula is specified, and a "smooth" correction is supplied in File 3 to correct the resulting scattering and total cross sections to the values obtained by the multi-level evaluation. The capture cross sections in this region are also corrected by File 3 to correct for the contribution of unresolved resonances, which were included in the evaluation.

In the unresolved resonance region smooth File 3 cross sections correct for use of energy-independent level spacing and ignoring contributions of higher order than p-wave, both of which are presently limitations of ENDF/B. Since the threshold for inelastic scattering is above the upper boundary (10⁵ ev) of the unresolved region, no difficulties are encountered by the ENDF/B exclusion of inelastic competition in the unresolved resonance formulation.

MF = 3, MT = 1 - SMOOTH TOTAL CROSS SECTION

The values in the resolved resonance region, E \leq 99.8 ev in Re-185 and 93.8 ev in Re-187, correct the single-level Breit-Wigner results to multi-level values, and correct capture for the omission of unresolved resonance contributions.

The values in the unresolved resonance region, to 100 keV, correct for use of constant level spacing and omission of contributions of higher order than p-wave.

The values above 100 keV were obtained from ABACUS-NEARREX²¹ calculations, where the optical model parameters, which are given in File 1, were adjusted to provide a good fit to the measured total cross section^{11,12,22,23} of natural rhenium (and to the measured partial cross sections, but not at the expense of agreement with the total).

MF = 3, MT = 2 - SMOOTH ELASTIC CROSS SECTION

The values in the resolved resonance region correct the single-level results to multi-level values.

The values in the unresolved resonance region correct for use of constant level spacing and omission of d-wave contributions.

From 100 keV to 5 MeV the sum of shape and compound elastic cross sections from ABACUS-NEARREX was used. Above 5 MeV the compound elastic cross section was negligible and only the shape elastic cross section was used. The calculated values are somewhat higher than measured²⁴ at energies between 0.6 and 1.5 MeV and may indicate the need for an energy-dependent Moldauer Q value in the ABACUS-NEARREX calculation. The calculated values were nevertheless used since they provide an internally consistent set of partial isotopic cross sections.

MF = 3, MT = 4 - INELASTIC CROSS SECTION

From 100 keV to 1.5 MeV the cross sections for individual inelastic level excitations were computed in ABACUS-NEARREX. The energy, spin, and parity of 8 levels plus ground state of Re-185²⁴⁻²⁶ and 11 levels plus ground state of Re-187^{10,27} were used. From 100 keV to 1.0 MeV the $\sigma_{n,\gamma}$ cross section from ABACUS-NEARREX was also included. Above 1.0 MeV the $\sigma_{n,\gamma}$ and $\sigma_{n,\gamma n}$ cross sections from ABACUS-NEARREX could not be used because lack of inelastic level data precludes correct competition. From 1 to 5 MeV the inelastic cross section was computed as the reaction cross section minus compound elastic and capture, the latter obtained as described in MF = 3, MT = 102 below. Above 5 MeV the inelastic cross section is $\sigma_{\text{reaction}} - \sigma_{\text{capture}} - (\sigma_{n,2n} + \sigma_{n,3n})$.

Comparison with Smith's measurements²⁴ shows underpredictions near threshold which again may indicate need for an energy-dependent Moldauer Q value.

MF = 3, MT = 16 - n,2n CROSS SECTION

The threshold and shape were taken from values supplied by Pearlstein²⁸. The amplitudes were normalized to best fit measured values^{7,29}.

MF = 3, MT = 17 - n,3n CROSS SECTION

The threshold and shape were taken from values supplied by Pearlstein²⁸. The normalization factor is the same as determined for the corresponding n,2n cross section.

75-Re-185/187
MAT 1083, 1084

MF = 3, MT = 27 - SMOOTH ABSORPTION CROSS SECTION

Same as MT = 102, smooth capture cross section. The n,p and n,α cross sections⁷ over the energy range covered by this evaluation were considered negligible and were not included.

MF = 3, MT = 102 - SMOOTH CAPTURE CROSS SECTION

In the resolved resonance region the correction for the contribution of unresolved resonances is given.

In the unresolved resonance region the corrections for use of constant level spacing and omission of contributions of higher order than p-wave are given.

From 100 keV to 1 MeV the values were obtained from ABACUS-NEARREX calculations. Above 1 MeV the shape of the ENDF/B Ta-181 (MAT 1035) capture cross section was used, normalized to the isotopic rhenium capture cross sections evaluated at 1 MeV.

MF = 3, MT = 251, 252, and 253 - ELASTIC $\bar{\mu}$, ξ , and γ

These were computed from the differential elastic cross sections calculated by ABACUS-NEARREX. A modified version of the CHAD³⁰ code was used.

MF = 4, MT = 2 - ELASTIC SECONDARY ANGULAR DISTRIBUTIONS

The transformation matrix and the Legendre coefficients for 19 moments were computed by CHAD as above. Comparison with Smiths measurements²⁴ shows good correlation of the odd moments and a tendency to overpredict the even moments which may stem from the deformed nature of the Re nuclei.

MF = 5, MT = 4, 16, 17 - SECONDARY ENERGY DISTRIBUTIONS

The fractional contributions of the discrete levels and $\sigma_{n,\gamma n'}$ to the total inelastic cross section were computed from threshold to 1.5 MeV using ABACUS-NEARREX results.

The $(n,n'\gamma)$ secondary neutron energy distributions above 1.5 MeV and all $(n,\gamma n')$, $(n,2n)$ and $(n,3n)$ secondary neutron distributions were described as Maxwellian with $T = \sqrt{E}/25$ MeV (same as Ta-181, MAT 1035). This spectrum is no doubt harder than the $n,\gamma n'$ secondaries and the secondaries following the first inelastic neutron emitted, but softer than the inelastic neutrons from direct reactions, which constitute the major portion of inelastic reactions above the onset of the $n,2n$ reaction. An accurate calculation of these effects was beyond the scope of this evaluation.

MF = 7, MT = 4 - THERMAL NEUTRON SCATTERING LAW

The free gas law was specified below 1.0 ev. The free atom scattering cross section was specified as the value at 0.0253 ev, although in Re-185 the calculated value varies from 20.7 to 15.0 barns between 10^{-5} to 1.0 ev and in Re-187 it varies from 10.1 to 8.9 barns.

REFERENCES

1. D. T. Goldman and J. R. Roesser, "Chart of the Nuclides, Ninth Edition," Knolls Atomic Power Laboratory, November 1966.
2. S. J. Friesenhahn, et al., "Neutron Capture Cross Sections and Resonance Parameters of Rhenium from .01 ev to 30 kev," GA-8189, August 16, 1967.
3. R. Sher, et al., "The Resonance Integrals of Rhenium and Tungsten," Trans. Am. Nucl. Soc. 9, 248 (1966).
4. D. F. Shook and C. R. Pierce, "Resonance Integrals of Rhenium for a Wide Range of Sample Sizes," Trans. Am. Nucl. Soc. 10, 261 (1967). Data taken from Friesenhahn, et al².
5. D. J. Hughes and R. B. Schwartz, "Neutron Cross Sections," BNL-325, Second Edition, July 1, 1958.
6. R. A. Karam and T. F. Parkinson, "The Resonance Absorption Integral of Rhenium," Conf. on Neutron Cross Section Technology, March 22-24, 1966, CONF-660303, p. 171.
7. M. D. Goldberg, et al., "Neutron Cross Sections," Vol. IIC, Z=61 to 87, BNL-325, Second Edition, Supplement No. 2, August 1966.
8. V. P. Vertebny, et al., "Total Neutron Cross Sections of Re-185 and Re-187," Atomnaya Energiya 19, 250 (1965). [Transl. Soviet Atomic Energy 19, 1162].
9. F. L. Sims, et al., "Fast-Spectrum Refractory-Metal Critical Experiment Measurements," Trans. Am. Nucl. Soc. 9, 488 (1966).
10. R. C. Doerner, et al., "Physics Measurements in Tungsten-Based, Aluminum-Reflected Fast Reactors," ANL-7007, March 1967.
11. D. C. Stupegia, A. A. Madson, and M. Schmidt, private communication to BNL Sigma Center (1966). Data taken from SCISRS file.
12. R. H. Tabony, K. K. Seth, and E. G. Bilpuch, private communication to BNL Sigma Center. Data taken from SCISRS file.
13. R. C. Block, et al., "Neutron Radiative Capture Measurements Utilizing a Large Liquid Scintillator Detector at the ORNL Fast Chopper," Neutron Time of Flight Methods, Saclay Conf. (1961). Data taken from BNL SCISRS file.
14. D. C. Stupegia, et al. "Fast Neutron Capture in Rhenium," J. Nucl. Energy Parts A/B 19, 767 (1965).
15. Yu. Ya Stavisskii, et al., "Fast Neutron Capture Cross Sections for Rhenium," Atomnaya Energiya 19, 42 (1965). [Transl. Soviet Atomic Energy 19, 935 (1965)]. Data taken from BNL SCISRS file.
16. D. Kompe, "Capture Cross Section Measurements for Some Medium and Heavy Weight Nuclei Using a Large Liquid Scintillator," KFK-455, October, 1966.

75-Re-185/187
MAT 1083, 1084

17. V. N. Kononov and Yu. Ya. Stavisskii, "Cross Sections for the Radiative Capture of Fast Neutrons in Rhenium and Tantalum," *Atomnaya Energiya* 19, 457 (1955). [Transl. Soviet Atomic Energy 19, 1428 (1965)]. Data taken from BNL SCISRS file.
18. R. L. Macklin, et al., "Average Radiative Capture Cross Sections for 30- and 65- keV Neutrons," *Phys. Rev.* 129, 2695 (1963).
19. R. L. Macklin, et al., "Neutron Activation Cross Sections with Sb-Be Neutrons," *Phys. Rev.* 107, 504 (1957).
20. A. K. Chaubey and M. L. Seghal, "Test of Statistical Theory of Nuclear Reactions at 24 keV," *Phys. Rev.* 152, 1055 (1966).
21. Unpublished. See P. A. Moldauer, et al., "NEARREX, A Computer Code for Nuclear Reaction Calculations," ANL-6978, December, 1964.
22. A. B. Smith, private communication to BNL Sigma Center (1964). Data taken from SCISRS file.
23. D. G. Foster and D. W. Glasgow, private communication to BNL Sigma Center (1967). Data supplied by B. A. Magurno, BNL.
24. A. B. Smith, et al., "Fast Neutron Scattering from Tantalum, Rhenium, and Platinum," ANL-7363, August 1967.
25. Nuclear Data, Section B. Vol. 1, No. 1, Academic press, February, 1966.
26. Nuclear Data Sheet NRC 59-6-127, National Research Council.
27. K. Maack Bisgard, et al., "The Level Structure of ^{187}Re ," *Nucl. Phys.* 71, 192 (1965).
28. S. Pearlstein, private communication.
29. A. A. Druzhinin, et al., "The Fast Neutron (n, γ) and $(n, 2n)$ Reaction Cross-Sections on Rhenium Isotopes," *J. Nucl. Phys. (USSR)* 5, 18 (1967).
30. R. Berland, "CHAD - Code to Handle Angular Data," NAA-SR-11231, December 31, 1965.
31. Nuclear Data, Section B. Vol. 1, No. 2, Academic press, June, 1966.

SUMMARY DOCUMENTATION
of
 ^{197}Au

S.F. Mughabghab

I INTRODUCTION

Because of its monoisotopic nature, its chemical purity, its large thermal neutron capture cross section and absorption resonance integral [1] and the simple decay scheme of the product nucleus formed by neutron capture, the capture cross section of gold has become one of the primary basic standards. The evaluation of the capture cross section of gold in the energy region 200 keV-3.5 MeV, subject to the requirement for a consistent set of primary standards on (n,p) , $^6\text{Li}(n,\alpha)$, $^{10}\text{B}(n,\alpha)$ and $^{235}\text{U}(n,f)$ for ENDF/B-V, was carried out in conjunction with the Standards and Normalization Subcommittee of CSEWG and its Task Force. (a)

II THERMAL CROSS SECTIONS AND RESONANCE PARAMETERS

The recommended resonance parameters in the energy range 4.9 eV-2 keV, which appeared in BNL-325, Third Edition [1] were adopted with minor changes and additions. The spin assignments of Lottin and Jain [2] were incorporated, and the parameters of a bound level with spin $J=2$ were derived in order to fit the experimental capture and total cross sections at low neutron energies. This spin value of the bound level was deduced by Wasson et al [3] from interference analysis of neutron capture γ -rays.

Because of the presence of structure in the gold capture cross section up to 100 keV [4], it was decided by the Standards and Normalization Subcommittee of CSEWG to extend the resolved energy region from 2.0 to 4.8 keV. Unfortunately, individual resonance parameters (T_n, Γ_γ, J values) were not

(a) The Au Capture Task Force members are: B.R. Leonard, Jr. (BNL), Chairman, M.R. Bhat (BNL), A.D. Carlson (NBS), M.S. Moore (LASL), S.F. Mughabghab (BNL), R.W. Peelle (ORNL), W.P. Poenitz (ANL), L. Stewart (LASL).

available as yet. The $g\Gamma_n\Gamma_\gamma/\Gamma$ values of Macklin et al [4] were combined with the renormalized $g\Gamma_n^2/\Gamma$ values of Hoffman et al [5] to obtain J , Γ_n, Γ_γ values for the individual resonances. The renormalization factors were estimated by a comparison of the $g\Gamma_n^2/\Gamma$ values of Hoffman et al [5] with those derived from BNL-325 [1] in the overlap region. This procedure indicated that the values of these authors are under-estimated by about a factor of 3.5 for the strong resonances.

The thermal cross sections at .0253 eV are:

capture	=	98.71 b
scattering	=	6.84 b
total	=	105.55 b

The absorption resonance integral with a 0.5 eV cutoff is 1559 b.

III FAST NEUTRON CAPTURE CROSS SECTIONS

A. Total Cross Section

As pointed out previously, the total cross section from 10^{-5} eV to 4.8 keV is represented by the resonance parameters. The total cross section from 4.8-10 keV was derived from the average resonance parameters; from 1.0 kev-2.3 MeV, it is based on data of Ref. [6-10], from 2.3-15.0 MeV on data of Foster et al [11]. In the high energy region, 15.0 to 20.0 MeV, the evaluation is based on data of Peterson [12].

B. Elastic Cross Section

The elastic cross section from 4.8 keV to 20 MeV is obtained by subtracting the sum of all the nonelastic cross sections from the total cross section.

C. Total Inelastic Cross Section

This is obtained by the sum of all the discrete level excitation (77 keV-1.24 MeV) cross sections and the continuum cross section. The latter is derived by nuclear model calculations.

D. $(n, \text{particle})$ Cross Section

$(n, 2n)$ cross section is based on the experimental data contained in References [13-16]. The $(n, 3n)$ evaluation is based on the experimental

data of Veeser et al [16]. The (n,p) and (n,α) evaluation is based on data of Prestwood and Bayhurst [14].

E. Inelastic Cross Sections

The inelastic scattering cross section data of Devilliers et al [17], Barnard et al [18] and Nelson et al [19] were considered. In the neutron energy region where experimental information is not available, i.e. near threshold and above $E_n = 1.6$ MeV, the evaluation is based on a properly normalized statistical model calculation following the formalism of Hauser and Feshbach. Nuclear model calculations were carried out with the aid of the code COMNUC-1 [20] using basically the level diagram scheme of ^{197}Au as reported by the Nuclear Data Group (vintage 1973), and Barnard et al [18]. Inelastic scattering cross section to the continuum of levels, specified by a low energy cut off of 1.25 MeV, is obtained by using COMNUC-1. The derived values are normalized to the difference between non-elastic and the sum of discrete inelastic and (n,particle) reaction cross sections.

F. Capture Cross Section

The capture cross section of gold in the energy region from 10^{-5} eV to 4.8 keV is represented by the resolved resonance parameters. In the energy regions from 4.8 keV to 200 keV, the evaluation is based on Macklin et al's data [4].

In the energy region from 200-3500 keV, a great deal of effort was placed on the evaluation. The following procedure was adhered to. At first, the totality of the old and recent data were divided into two groups depending on whether the measurement is designated as absolute or relative. Subsequently, the relative gold capture cross sections were separated into four groups corresponding to one of the adopted standards (n,p), $^6\text{Li}(n,\alpha)$, $^{10}\text{B}(n,\alpha)$ or $^{235}\text{U}(n,f)$. In those cases where the ratio values were not reported by the authors, these were reconstructed whenever enough information was provided by the authors. As an example, the $^6\text{Li}(n,\alpha)$ cross section adopted by Macklin, et al, [4] in his flux measurements, was derived here from the reported prescription and the ratio values of the gold capture cross section to the $^6\text{Li}(n,\alpha)$ cross section

were obtained. Then various ratio values corresponding to each standard were plotted separately and were initially compared with the ratio values derived from ENDF/B-V. Such a procedure is helpful in discerning any systematic trends in the data as may be indicated by high or low values or possible changes in the shape of the relative cross sections. Ratio values which deviated by more than two standard deviations from ENDF/B-V or the average of the experimental values were rejected.

The following observations could be made regarding these data:

1. Data of Macklin, et al., [4], Lindner, et al., [21] and Fort and Le Rigoleur [22] are generally in very good agreement.
2. As shown by Fort and Le Rigoleur [22], the activation and nonactivation measurements are in reasonable agreement with each other particularly in the energy region 400-500 keV where the deviation is only about 2%.
3. Data of Paulsen, et al., [23] Fricke, et al., [24] and Barry, et al., [25] measured relative to the (n,p) cross section are consistently high with respect to the ENDF/B-IV evaluation and with the data of Macklin, et al., [4], Lindner, et al., [21], Poenitz [26] and Fort and Le Rigoleur [22].
4. In the energy range 1000-3500 keV, the data of Paulsen, et al., [23] appear to converge, particularly at the high energy end, with that of Poenitz [26] and Lindner, et al., [21].
5. The Robertson, et al., [27] cross section value at 966 keV is about 12% high with respect to Poenitz [26], Lindner, et al., [21] and ENDF/B-IV evaluation, but somehow in agreement with the data point of Paulsen, et al., [23]. Since it is believed that there is no structure in the gold

capture cross section at this energy, the result of Robertson, et al., [27] was down-graded.

6. The data of Czirr and Stelts [28] is high when compared with other data, and with the ENDF/B-IV evaluations. It is to be noted that the data points at 319, 412 and 532 keV were withdrawn by the authors.

On the basis of these observations, it was decided to base the ENDF/B-V evaluation on the data sets of Macklin, et al., [4], Fort and Le Rigoleur [22], Poenitz [26], and Lindner, et al., [21] in the energy range 100-1000 keV. Above 100 keV, the ENDF/B-IV evaluation is based on Poenitz [26], Lindner's et al.'s [21] and Paulsen et al.'s [23] data. The result of this is essentially to decrease the capture cross section of gold by not more than about 4%. This is about the magnitude of the uncertainty of the gold capture cross section in this energy range.

In the energy region 3.5-2.0 MeV, experimental data is sparse. These include the data of Johnsrud et al [29] and Miskel et al [30], both of which used the activation technique and measured the flux with a fission chamber. Between 4 MeV and 20 MeV, only 14 MeV data by Drake et al [31] and Schwerer et al [32] are available, which indicate that the capture cross section of gold at 14 MeV is about 1 mb. As a result, the ENDF/B-V evaluation between 3.5-20 MeV is based on COMNUC calculations which are normalized to a value of 14 mb at 4.4 MeV (renormalized Johnsrud et al [29] data point) and 1 mb at 14 MeV.

It is of interest to calculate the fission spectrum average of the capture cross section and compare it with experimental measurements. Absolute capture cross section measurements for ^{197}Au for ^{252}Cf spontaneous fission neutrons were carried out recently by Green [33] and Mannhart [34] who reported values of 79.9 ± 2.9 and 76.2 ± 1.8 mb respectively. In addition, Fabry, et al., [35] reported an integral cross section ratio measurement of $^{197}\text{Au}(n,\gamma)$ relative to $^{238}\text{U}(n,f)$ for a thermal-induced ^{235}U fission neutron spectrum. Adopting a value of 295.4 mb for $^{238}\text{U}(n,f)$ fission spectrum average from the ENDF/B-IV dosimetry file [36], (ENDF/B-V

file as yet unavailable), one obtains a value of $85 + 4$ mb for $^{198}\text{Au}(N, \gamma) ^{199}\text{Au}$.

A Maxwellian fission spectrum of characteristic temperature T and represented by:

$$\Phi(E) = C \sqrt{\frac{E}{T}} e^{-\frac{E}{T}} \quad (1)$$

was employed (C is a normalizing constant). Values for T of 1.32 MeV (ENDF/B-IV) and 1.39 MeV were used in the calculations for ^{235}U and ^{232}Cf fission spectra respectively.

The ^{235}U and ^{252}Cf fission spectrum averages of the ENDF/B-V gold capture cross section are calculated with the aid of Eq. 1, and are shown in Table I. The evaluated values are compared with experimental numbers [33-35, 37].

TABLE I
Comparison with Integral Measurements

Fission Spectrum	Experimental Values (mb)	Present Evaluation (mb)	Reference
$^{235}\text{U}(T=1.32 \text{ MeV})$	$84.8 + 4.1$	81.3	Fabry [34]
$^{252}\text{Cf}(T=1.39 \text{ MeV})$	79.9 ± 2.9	78.1	Green [33]
	76.2 ± 1.8		Mannhart [34]
	95.5 ± 2.3		Pauw [36]

IV ANGULAR DISTRIBUTION OF SECONDARY NEUTRONS

The elastic scattering angular distribution in the energy range up to 8.05 MeV are based on experimental data. With the aid of the optical model parameters derived by Holmqvist and Wiedling [38], optical model calculations were carried out by using ABACUS-2. The calculations were compared with measurements at the following neutron energies: 0.5, 1.0, 2.0, 2.5, 5.0, and 8.05 MeV. The agreement between calculations and measurements is

reasonably good enough to warrant extrapolating them above 8.1 MeV where experimental data are not available. In addition, the graphic display code Tiger [39] was used to fit the experimental data with a least-squares spline procedure, check Wick's limit, and then extract Legendre coefficients of various orders for the angular distribution of scattered neutrons.

Because of the absence of experimental data, the angular distributions for the (n,particle) reactions have been specified as isotropic.

V. ENERGY DISTRIBUTION OF SECONDARY NEUTRONS

The energy distribution of secondary neutrons for the (n,2n), (n,n') reactions have been calculated as a nuclear temperature energy in MeV using code THETA [40]. For more detail, see documentation on Gd isotopes by B.A. Magurno.

79-Au-197
MAT 1379

REFERENCES

1. S.F. Mughabghab and D.I. Garber, BNL-325, Third Edition, Volume 1 (1973).
2. A. Lottin and A. Jain, Journal de Physique, 34, 123, (1973).
3. O.A. Wasson et al, Phys. Rev. 173, 1170 (1968).
4. R.L. Macklin, J. Halperin, and R.R. Winters, Phys. Rev/C, 11, 1270 (1975).
5. M.M. Hoffman, et al, Neutron Cross Sections and Technology Vol. 2, p. 868 (1971), Knoxville, Tenn.
6. K.K. Seth, Phys. Letters, 16, 306 (1965).
7. W. Bilpuch, private communication (1959).
8. J.F. Whalen, ANL-7210, 16 (1966).
9. M. Walt and R.L. Becker, Phys. Rev. 89, 1271 (1953).
10. R.B. Day, private communication (1965).
11. D.G. Foster, Jr., private communication (1967). See also Phys. Rev/C 3, 576 (1971).
12. J.M. Peterson, Phys. Rev. 110, 927 (1958); ibid, 120, 521 (1960).
13. H. Tewes, et al, private communication (1960).
14. R.J. Prestwood and B.D. Bayhurst, Phys. Rev. 121, 1438, (1961).

15. H. Liskin, et al, Atomkernenergie 26, 34 (1975).
16. L.R. Veeser, E.D. Arthur and P.G. Young, Phys. Rev/C, 16, 1792 (1977)
17. J.A.M. DeVilliers, et al., Zeit. Physik 183, 323 (1965).
18. E. Barnard, et al., Nucl. Phys., A107, 612 (1968).
19. J.A. Nelson et al., Phys. Rev. C3, 307 (1971).
20. C.L. Dunford, AI-AEC-12931 (1970).
21. M. Lindner, R.J. Nagle, and J.H. Landrum, Nucl. Sci. Eng. 59, 381 (1976).
22. E. Fort and C. Le Rigoleur, NBS Special Publication 425, Vol. 2, 957, (1975). This represents two data sets, one by Fort using the activation technique, the other by Le Rigoleur using prompt gamma rays.
23. A. Paulsen, R. Widera, and H. Liskien, Atomkernenergie 26, 80 (1975).
24. M.P. Fricke, et al, Nuclear Data for Reactors, Helsinki, Vol. 2, 281 (1970).
25. J.F. Barry, J. Nucl. Energy 18, 491 (1964).
26. W.P. Poenitz, Nucl. Sci. Eng. 57, 300 (1975).
27. J.C. Robertson et al, Jour. Nucl. Energy 23, 205 (1969).
28. J.B. Czirr and M.L. Stelts, Nucl. Sci. Eng. 52, 299 (1973).

29. A.E. Johnsrud, M.G. Silbert, and H.H. Barshall, Phys. Rev. 116, 927 (1959).
30. J.A. Miskel, et al, Phys. Rev. 128, 2717 (1962).
31. D. Drake, I. Berqvist and D.K. McDaniels, Phys. Letters 36B, 557 (1971).
32. O. Schwerer, et al, Nucl. Phys. A264, 105 (1976).
33. L. Green, Nucl. Sci. Eng. 58, 361 (1975).
34. W. Mannhart, Proceedings of the IAEA Consultant's Meeting on Integral Cross Section Measurements in Standard Neutron Fields, Vienna, November 15-18, 1976.
35. A. Fabry, J.A. Grundl, and C. Eisenhauer, NBS special publication 425, Vol. 1, 254 (1975), Nuclear Cross Sections and Technology.
36. ENDF/B-IV Dosimetry File BNL-NCS-50446 (1975). Ed. B.A. Magurno.
37. H. Pauw and A.H.W. Aten, Nucl. Energy 25, 457 (1971).
38. B. Holmqvist and T. Wiedling, Nucl. Phys. A188, 24 (1971), AE-403 (1971).
39. R.R. Kinsey, DUMMY-5, private communication.
40. C. Dunford, private communication.

Summary Documentation

Lead Evaluation

ENDF/B-V MAT 1382

C. Y. Fu and F. G. Perey
Oak Ridge National Laboratory
Oak Ridge, Tennessee

August 1978

The following revisions are made to the ENDF/B-IV evaluation¹
(Fu and Perey, 1973):

Gamma-ray-production cross sections (Files 12, 13, 15) from 0.6 to
20 MeV were revised according to the measurements of Chapman and Morgan.²

Capture cross sections above 3 MeV were revised by using the available
²⁰⁸Pb data.³

The (n,2n) cross sections from 7 to 15 MeV were revised according
to the recent measurement of Frehaut and Mosinski.⁴ The extrapolations
to above 15 MeV were guided by the ²⁰⁴Pb data.³ The inelastic cross
sections above 7 MeV and the (n,3n) cross sections were revised to con-
serve the total cross sections.

The following files and sections are included. Experimental data
were taken from CSISRS data tape⁵ unless otherwise stated.

File 1. General Information

Section 451. Descriptive data and dictionary

File 2. Resonance Parameters

Section 151. General designation for resonance information

Only effective scattering length given.

Taken from BNL-325.⁶

File 3. Neutron Cross Sections

Section 1. Total Interaction

0.00001 eV to 1 keV from BNL-325.⁶

1 keV to 0.47 MeV mostly from Good.⁷

0.47 MeV to 20.0 MeV from Schwartz.⁸

82-Pb-0
MAT 1382

Section 2. Elastic Scattering

Derived by subtracting the non-elastic cross section from the total cross section.

Section 3. Non-Elastic Interaction

Calculated.¹ Very good agreement with experiment.

Section 4. Total Inelastic Scattering

Calculated.¹ Very good agreement with experiment.

Section 16. (n,2n) Reaction

See Introduction.

Section 17. (n,3n) Reaction

See Introduction.

Sections 51 through 85. Inelastic Scattering Exciting Levels

Calculated.¹ Compared favorably with experiment.

48 levels in 206, 49 levels in 207, and 22 levels in 208 are merged to form 35 levels in natural lead.

Section 91. Inelastic Scattering Exciting Continuum

Derived by subtracting the level contribution from the total inelastic cross section.

Section 102. Radiative Capture

0.00001 eV to 10 eV--1/v dependence assumed with 0.198 barns

at 0.0253 eV. Resonance data of Allen et al.⁹ to 200 keV.

Curve drawn through limited data for higher energy.³

Section 251. Mu Bar

Derived from elastic angular distributions and kinematics using the computer program SAD.

Section 252. Xi

See Section 251.

Section 253. Gamma

See Section 251.

File 4. Angular Distribution of Secondary Neutrons

All distributions are given in the legendre polynomial representations.

Section 2. Elastic Scattering

0.00001 eV to 5 MeV--coefficients obtained by fitting data
5 MeV to 20 MeV--optical model calculation.¹ Optical model
parameters best fit data at 7 and 14 MeV.
Representation is in center of mass system.
Transformation matrix is given.

Sections 51 through 85. Inelastic Scattering Exciting Levels
Calculated¹ and compared favorably with data.
Representation is in center of mass system.

Section 91. Inelastic Scattering Exciting Continuum
Assumed isotropic.

File 5. Energy Distribution of Secondary Neutrons

Section 16. (n,2n) Reaction
Calculated. Parameters deduced from 14-MeV data.¹⁰⁻¹³

Section 17. (n,3n) Reaction
Calculated. See File 5, Section 16.

Section 91. Inelastic Scattering Exciting the Continuum
Calculated. See File 5, Section 16.

File 12. Multiplicities of Gamma Rays Produced by Neutron Reaction

Section 102. Radiative Capture
0.00001 eV to 10 eV--thermal neutron capture assumed.
10 eV to 573--one average resonance capture spectrum assumed.¹⁴

File 13. Gamma-Ray Production Cross Sections

Section 3. Non-Elastic Interaction

Combined from contributions from radiative capture,
inelastic scattering, (n,2n), and (n,3n) reactions.²

File 14. Angular Distributions of Secondary Gamma Rays

Section 3. Non-elastic Interaction

Assumed isotropic

File 15. Energy Distribution of Secondary Gamma Rays

Section 3. Non-Elastic Interaction

573 keV to 20 MeV--composite spectra resulting from radiative capture, inelastic, $(n,2n)$, and $(n,3n)$ reactions were taken from Ref. 2.

Section 102. Radiative Capture

0.00001 eV to 10 eV--one single spectrum resulting from thermal neutron capture is assumed valid.

1 keV to 573 keV--one single spectrum is assumed valid which was derived from rather limited resonance capture data.¹⁴

10 eV to 1 keV--linear interpolation between above two spectra.

File 33. Covariances

Sections 1, 2, 3, 4, 16, 17, 51, 52, 64, 102.

References

1. C. Y. Fu and F. G. Perey, *Atomic Data and Nuclear Data Tables* 16, 409 (1975).
2. G. T. Chapman and G. L. Morgan, ORNL/TM-4822 (1975).
3. D. I. Garber and R. R. Kinsey, BNL-325, 3rd Ed., Vol. 2 (1976).
4. J. Frehaut and G. Mosinski, *5th International Symposium on the Interaction of Fast Neutrons with Nuclei*, Gaussig, DDR, November 17-21, 1975.
5. CSISRS data tape obtained November 1970 from Brookhaven National Laboratory.
6. M. D. Goldberg et al., BNL-325 (1966).
7. W. M. Good, Oak Ridge National Laboratory, private communication (1971).
8. R. B. Schwartz, National Bureau of Standards, private communication (1971).
9. B. J. Allen et al., *Phys. Rev. C* 8, 1504 (1973).
10. J. L. Kammerdiener, UCRL-51232 (1972).
11. G. Clayeaux et al., CEA-R-4279 (1972).
12. C. Wong et al., UCRL-51144 (1972).
13. E. D. Cashwell, private communication to CSEWG (1973).
14. J. A. Biggerstaff et al., *Phys. Rev.* 154, 1136 (1967).

Covariance File for Lead MAT 382

Covariance data were given for MF=33, MT=1, 2, 3, 4, 16, 17, 51, 52, 64, and 102. Derived sections (NC subsections) reflect exactly the way the cross-section files were generated.

In general, covariances were determined from $\pm 2\sigma$ error bands. The error bands were extended and enlarged to cover energy regions lacking experimental data. Long range covariances reflect systematic errors common to all data sets. Medium range covariances reflect differences in energy coverage by different data sets and differences in experimental techniques within the same data sets. Short range covariances reflect meaningful structures in the cross sections and/or threshold effects. Statistical errors are, in principle, nonexistent in the evaluated cross sections.

As in the case of iron, absolute uncertainties were used in addition to fractional uncertainties to help keep the files short. The absolute components are the most useful for total cross-section minima and near thresholds.

Except for the total and capture cross sections, all other cross sections were evaluated with guidance from model calculations. However, in energy regions in which model calculations were used directly, uncertainty estimates were based on a general understanding of the adequacy or inadequacy of various models rather than on model parameter variations.

M. R. Bhat

I. Introduction

This describes the evaluation of Th-232 for ENDF/B-V. The evaluation was a joint effort to which many persons from a number of institutions contributed. Some of these have been described by their authors in a number of reports. Reference will be made to these reports in appropriate sections without discussing their contents in detail.

2. File 1

(i) Nu-bar Total (MT=452)

This section is consistent with the evaluations on delayed and prompt neutrons in sections MT=455 and 456 respectively.

(ii) Nu-bar Delayed (MT=455)

Delayed neutron yields were evaluated by Kaiser and Carpenter [1].

(iii) Nu-bar Prompt (MT=456)

This evaluation is by R. Gwin [2]. Evaluation of R, the ratio of $\bar{\nu}_p(\text{Th-232})/\bar{\nu}_p(\text{Cf-252})$ in this report was multiplied by the recommended $\bar{\nu}_p(\text{Cf-252})=3.757$ to obtain the evaluated data.

(iv) Energy Released in Fission (MT=458)

Energy released in fission and its partition into the different modes of decay was evaluated by Sher et al [3].

3. File 2

(i) The resolved resonance parameters were evaluated by B.R. Leonard et al [4] which are essentially the same as those in BNL-325 (3rd Edition) [5] except for the two negative energy resonances whose parameters were adjusted to obtain a fit to the data in the thermal range from 1.0 E-05 to 5.0 eV. In assembling the present data file, the neutron widths of the first two positive energy s-wave resonances were set equal to the values given by Derrien [6]. A ladder plot of the p-wave resonances indicated that a number of them were missing and they were replaced by a smooth background. This was calculated as follows. Cross sections in the resolved region were calculated using the p-wave resonances given in the data file and they were

averaged over 100 eV bins. Using the code UR [7], cross sections were calculated with a p-wave strength function of $S_1=1.6 \times 10^{-4}$ and a $\Gamma_\gamma = 21.1$ meV. The difference in the areas under the cross-sections curves calculated by these two methods was determined and put in File 3 as a smooth straight-line background to represent the missing p-wave resonances.

(ii) Unresolved Resonance Region (MT=151)

The unresolved resonance region extends from 4 to 50 keV. From 4 to 25 keV, the capture cross section as evaluated by de Saussure and Macklin [8] was used. This was joined smoothly to the Poenitz [9] evaluation above 25 keV. The capture cross section was read off at intervals of 1 keV and the input data from 4 to 50 keV at 1 keV intervals used to extract the unresolved resonance parameters is: 1.130, 0.982, 0.908, 0.850, 0.803, 0.764, 0.730, 0.702, 0.677, 0.655, 0.636, 0.618, 0.601, 0.585, 0.571, 0.557, 0.545, 0.533, 0.521, 0.511, 0.500, 0.491, 0.482, 0.473, 0.465, 0.459, 0.452, 0.448, 0.443, 0.439, 0.435, 0.431, 0.429, 0.426, 0.424, 0.422, 0.420, 0.420, 0.420, 0.417, 0.414, 0.411, 0.407, 0.401, 0.395, 0.390. The code UR [7] was used to obtain the unresolved resonance parameters. The s-wave and d-wave strength functions were set equal to 0.888×10^{-4} and 0.882×10^{-4} as evaluated by de Saussure and Macklin [8] and the $\Gamma_\gamma = 21.3$ meV was used. The p-wave Γ_γ was increased to 25.2 meV and the reduced neutron width varied to fit the capture cross section.

4. File 3

(i) Thermal Region (1.0E-05 - eV)

This is mainly based on the Leonard evaluation [4] with the following changes. The capture cross section from this reference was used from 1.0E-05 to 2.53E-02 eV after renormalizing it to 7.40b at 2.53-02 eV. From 2.6E-02 to 5 eV the fit of Chrien and Liou [10] to their low energy capture data was used after renormalizing it to 7.40b at 2.53-02 eV. The total cross section in this energy region is the sum of the Leonard scattering cross section and his capture cross section renormalized to 7.40b at 2.53E-02 eV. The final scattering cross section given in the data files is the difference between this total and the capture cross section evaluated as described above. The dilute resonance capture integral from 0.5 eV to 20 MeV is 84.0b.

(ii) Cross Section from 50 keV to 20 MeV

The evaluations of total, elastic, capture, fission inelastic, $(n,2n)$, and $(n,3n)$ cross sections are by Meadows et al [11] and have been fully discussed in their published report.

5. File 4

(i) Elastic and Inelastic Scattering Angular Distributions

Angular distributions are based on available experimental data supplemented by nuclear model calculations details of which are given in Ref. 11. The secondary neutrons from $(n,2n)$, $(n,3n)$ and fission are assumed to be isotropic.

6. File 5

(i) Secondary Neutrons from $(n,2n)$ and $(n,3n)$ Reactions (MT=16, 17)

These were determined using the statistical model of Segev [12] with a precompound component [11].

(ii) Fission Neutron Spectrum (MT=18)

The energy variation of the mean energy of the fission spectrum was calculated using the Howerton and Doyas method [13] and the evaluated \bar{v}_p and the $\Gamma_{nn'f} / \Gamma_{n,f}$, $\Gamma_{n,2nf} / \Gamma_{n,f}$ and $\Gamma_{n,3nf} / \Gamma_{nf}$ ratios [14]. This was normalized to $\bar{E} = 2.255$ MeV obtained by Vasil'ev at 14.3 MeV [15] and energy dependent Watt spectrum parameters were obtained.

(iii) Secondary Neutrons Scattered into the Continuum (MT=91)

The evaluation is based on experimental data [11] with a harder precompound component varying from 0.0% at 6 MeV to 20% at 20 MeV added.

(iv) Delayed Neutron Spectrum (MT=455)

Delayed neutron spectra were evaluated by Kaiser and Carpenter [1].

7. File 8

(i) Fission Product Yields (MT=454 and 459)

The fission product direct yields before delayed neutron emission (MT=454) and cumulative yields along each isobaric chain after delayed neutron emission (MT=459) were evaluated, reviewed and recommended by the the Fission Product Yield Data Subcommittte (T.R. England, Chairman). Data files were prepared by T.R. England[16].

(ii) Radioactive Decay Data (MT=457)

The radioactive decay data were evaluated by C.W. Reich [17]. The reaction Q-values are based on the Wapstra Mass Tables [18] and also the data in Ref. 19, 20 and 21.

8. Files 12 and 13

Photon production cross sections were evaluated by Howerton [22].

(i) Photons from Fission (MF=12, MT=18)

The multiplicity of photons from fission for all incident energies was derived from the data of Peelle and Maienschein [23]. It was assumed that the multiplicity is independent of incident neutron energy.

(ii) Photons from Capture (MF=12, MT=102)

This is represented by an energy dependent multiplicity and an energy independent spectrum. The spectrum is based on some undocumented measured data for ^{238}U [22] with minor adjustment for the small differences in the Q-value between ^{232}Th and ^{238}U . Details of multiplicity calculations are given in Ref. 24.

(iii) Photons from Non-Elastic processes (MF=13, MT=3)

Explicit representation of three photons (0.04971, 0.1632 and 0.3344 MeV) from inelastic scattering was derived from File 3 data and known branching ratios. For incident neutron energies > 0.7251 MeV the method of Ref. 25 was used to calculate photon production cross sections and spectra from all reactions except photons from the first three inelastic groups, neutron capture and neutron induced fission.

9. File 14

All photons are assumed to be isotropic

10. File 15

For MT=3, photon spectra were obtained using the method of Ref. 25. For fission produced photons (MT=18) the data of Ref. 23 were used for all incident neutron energies because there are no experimental data for ^{232}Th . For photons due to capture, the spectrum is assumed to remain unchanged for all incident neutron energies and is based on undocumented measured photon spectrum of ^{238}U at thermal energy with a minor adjustment for the small Q-value differences between ^{238}U and ^{232}Th .

11. File 31

This file contains only one section corresponding to the uncertainties in total $\bar{\nu}$ (MT=452) and is by R. Gwin [2, 26].

12. File 33

This file contains two sections on fission (MT=18) and capture (MT=102) cross sections. The data uncertainties are represented by a matrix with only diagonal elements and are partly based on the error estimates in Ref. 11. It is estimated that the thermal capture cross section is known to about one percent and the Chrien data from .035 ev to about 15 ev have errors from 3% to 14% and are estimated to have about 8% error in the energy band from thermal to 15 ev. Uncertainties in the capture cross section are estimated to be 10% from 15 eV to 1 MeV and about 20% above 1 MeV.

References

1. R.E. Kaiser and S.G. Carpenter (ANL-West) Private Communication (1978).
2. R. Gwin ORNL/TM-6245 (ENDF-262) (1978).
3. R. Sher, S. Fiarman and C. Beck, Private Communication (1977).
4. D.F. Newman, B.R. Leonard, Jr., et al., EPRI NP-222 (1977).
5. S.F. Mughabghab and D.I. Garber, BNL-325 (3rd Edition 1973).
6. H. Derrien, NEANDC (E) 163U (1975).
7. E. Pennington, Private Communication.
8. G. de Saussure and R.L. Macklin ORNL/TM-6161 (ENDF-255) (1977).
9. W.P. Poenitz, Private Communication (1978).
10. R.E. Chrien et al. To be published (1978).
11. J.W. Meadows et al., ANL/NDM-35, Argonne National Laboratory (1978).
12. M. Segev et al., Trans. Am. Nuc. Soc. 22, 679 (1975).
13. R.J. Howerton and R.J. Doyas, Nuc. Sci. and Eng. 46, 414 (1971).
14. W.P. Poenitz, Private Communication (1977).
15. Yu. A. Vasil'ev et al., Physics of Nuclear Fission, N.A. Perfilov and V.P. Eismont (Eds.), Israel Program of Science Trans. Jerusalem (1964).
16. T.R. England, Private Communication (1978).
17. C.W. Reich, Private Communication (1978).
18. Wapstra-Bos-Grove Mass Table, 1974 Version.
19. M.R. Schmorak, Nuclear Data Sheets, 20, 165 (1977).
20. C.M. Lederer et al., Table of Isotopes (7th Edition), Preliminary Data, Private Communication to C.W. Reich (1978).
21. A. Rytz, Atomic Data and Nucl. Data Tables 12, 479 (1973).
22. R.J. Howerton, Private Communication.
23. R.W. Peelle and F.C. Maienschein, Nuc. Sci. and Eng. 40, 485 (1970).
24. R.J. Howerton et al., "The LLL Evaluated Nuclear Data Library (ENDL): Evaluation Techniques, Reaction Index and Description of Individual Evaluations" UCRL-50400, Vol. 15, Part A, Lawrence Livermore Laboratory (1975).
25. S.T. Perkins, R.C. Haight and R.J. Howerton, Nuc. Sci. and Eng. 57, 1 (1975).
26. R. Gwin, Private Communication, (1978).

91-Pa-233
MAT 1391

ENDF/B-V Summary Documentation
Isotope: 91-Pa-233 MAT - 1391

F.M. Mann	(HEDL)	Apr '78
C.R. Reich	(INEL)	Apr '78

No new cross section data have been measured since the last evaluation for ENDF/B-II by P.C. Young. That evaluation was checked against resonance data and systematics of near-by nuclei and made consistent with ENDF/B-V procedures. The summary documentation for that evaluation follows on the next page.

C. R. Reich supplied the radioactive decay data.

Eval-Jan70 P.C.Young
Dist-Jul74

* * * * *

Data modified October 70 to conform to ENDF/B-version II formats
* * * * *

Data modified Jan 74 at General Atomic(DRM) to use BNL-325 (ed.3)
resolved resonance parameters below 18eV. 0.0253ev capt xsect =
41.4605 b.

* * * * *

Data modified May 74 at Brookhaven (BNL) by R. Kinsey
Decay data added, files extended to 20 MeV, and initial point
of threshold reactions corrected.

* * * * *

MF=1,MT=451 Comments and Dictionary

MF=1,MT=452 nu(E)=c1+c2*E, where c1 and c2 were obtained from a
derived empirical relation dependent on Z and A

MF=1,MT=457 Decay data eval-Feb74 C.W.Reich ANC

References Q- 1973 revision of the Wapstra-Gove Mass Tables

Half-life- N.E. Holden, Chart of the Nuclides (1973)
and private communication (Jan., 1974)

Other- Y.A. Ellis, Nuclear Data b 6, no.3, 257(1971)

MF=2,MT=151 Reson parameters from * Ref.1(28 reson, up to 17.5eV),
Ref.2(12 reson, 17.5-37.5eV). Resolved reson energy range- 0.001
to 38.5 eV. ave reson parameters deduced from the 27 positive
reson given in Ref.1. Unresolved reson energy range- 38.5 eV to
10 keV. The 12 gn0 from Ref.2 adjusted to yield same reson int
contrib implied by the ave reson parameters. The resulting gn0
for the 40 resolved reson and the ave gn0 for the unresolved
reson adjusted to yield a capt reson int(0.5eV-10MeV)=859.96bn(
including the contrib of the MF=3,MT=102 data). The gn0 for the
neg reson then adjusted to yield a 0.0253eV capt xsect= 39.79bn

file 3 contains smooth data in the energy range 10 keV to 15 MeV
MF=3,MT=1 Total cross section - required to be consistent in
both magnitude and energy variation with the total x-section
of neighboring nuclides, e.g. Th232,U233,U235,U238, and Pu239.

MF=3,MT=2 Elastic scattering cross section = Total x-section
minus Nonelastic x-section. In addition, required to be consistent
in energy variation with elastic scattering x-section of
neighboring nuclides (Th232,U235,U238) and to join smoothly at
10 keV with a value nearly equal to the potential scattering
x-section (=9.995 barns, Ref.2).

MF=3,MT=3 Nonelastic cross section = Sum of the (n,f),
(n,np prime), (n,2n), (n,3n) and (n,gamma) cross sections.

MF=3,MT=4 inelastic scat xsect - taken from Ref.3 . Q-value =
- 18.7 keV (energy of the first excited state in 91Pa233)

MF=3,MT=16 and 17 (n,2n) and (n,3n) xsect - taken from Ref.3
Q-value calculated using atomic masses from Ref.4.

MF=3,MT=18 Fission cross section - composite curve as follows -
0.48-1.00MeV 233Pa(n,f)= 238U(n,f) from Ref.5.
1.00-1.50MeV log(233Pa(n,f)) linear in log(E)
1.50-5.00MeV 233Pa(n,f)= (c1/c2)*238U(n,f) from Ref.5.
c1=0.832 = calc. plateau value of 233Pa(n,f) Ref.6.

c2=0.511 = avg. value of 238U(n,f) (Ref.5), 2.6-5.6 MeV
5.00-9.00MeV 233Pa(n,f) has energy variation similar to that
for (n,f) of U234, U236 and NP237 from Ref.5.
9.00-12.5MeV 233Pa(n,f)=(c1/c2)*238U(n,f) from Ref.7.
c1=1.56 = derived value of 233Pa(n,f) for the second plateau
near 9.0 MeV.
c2=1.02 = 238U(n,f)(Ref.7) at the second plateau.
12.5-15.0MeV 233Pa(n,f) has same energy variation as that for
236U(n,f)(Ref.7)
Q-value = calculated energy release per fission
MF=3,MT=51,52,53,54,55,91 Partial inelastic scat xsect-from Ref.3
MF=3,MT=102 Capture cross section - composite curve as follows -
0.01-0.08MeV 233Pa(n,gamma) selected to join smoothly with the
(n,gamma) calculated from average resonance parameters
0.08-15.0MeV 233Pa(n,gamma) = 2*238U(n,gamma) from Ref.8.
Normalization factor(=2) chosen so that 233Pa(n,gamma) =
236U(n,gamma)(Ref.8) at 0.9 MeV
MF=3,MT=251 mu-bar (avg.cosine of the scattering angle in the lab
system for elastic scattering), calculated from the U(1,m) and
Legendre coefficients given in file 4
MF=3,MT=252 xi (avg.logarithmic energy decrement).
MF=3,MT=253 gamma (slowing down parameter).
The energy dependence of the two above quantities is determined
by the Legendre coefficients given in file 4. Completely
general expressions in powers of AWR**-1 have been derived for
the constants which determine the contribution of each of the
Legendre coefficients.
MF=4,MT=2 Transfer Matrix U (from c.m. To lab). A general ex-
pression for U(1,m) in powers of AWR**-1 has been derived. The
Legendre coefficients were taken directly from Ref.3, and are
based on the data for Th232.
MF=4,MT=51,52,53,54,55 Ang Dist of neutrons scat inelastically
from 5 discrete levels assumed isotropic in the cm system
MF=5,MT=16,17,91 Energy dependence of secondary neutrons defined
by an evaporation spectrum . Energy dependence of theta calcu-
lated using the formulation in Ref.9
MF=5,MT=18 Simple fission spectrum - theta (constant) calculated
using the formulation given in Ref.10.
MF=7,MT=4 Thermal scattering law - free atom x-section=10barns.
References
1. Simpson and Codding, Nucl Sci and Eng, 28, 133 (1967)
2. Harris D.R. , Wapd-TM-814 (1969)
3. Drake and Nichols, Ga-7462 (1967)
4. Mattauch, et al, Nuclear Physics, 67, 1 (1965)
5. Davey , Nucl Sci and Eng , 32, 35 (1968)
6. Lalovic , Lectures on Nucl Interactions, vol II,207 (1962)
7. Hart , Ahsb(s) r 169 (1969)
8. Stehn,et al, BNL-325, 2nd ed, suppl 2 , vol III (1965)
9. Smith and Grimesey, IN-1182 (1969)
10.Terrell, Phys and Chem of Fiss, vol II, 3 (1965)

SUMMARY DOCUMENTATION FOR ^{233}U

by

L. Stewart, D. G. Madland, and P. G. Young
Los Alamos Scientific Laboratory
Los Alamos, New Mexico

and

L. Weston and G. de Saussure
Oak Ridge National Laboratory
Oak Ridge, Tennessee

and

F. Mann
Hanford Engineering and Development Laboratory
Richland, Washington

and

N. Steen
Bettis Atomic Power Laboratory
West Mifflin, Pennsylvania

I. SUMMARY

A new evaluation of neutron-induced reactions on ^{233}U was carried out for Version V of ENDF/B (MAT 1393). The analysis was divided among several laboratories. The thermal data evaluation was performed at BAPL and LASL, the resolved and unresolved resonance regions were evaluated at ORNL and HEDL, and evaluation of the data from 10 keV to 20 MeV and assembly of the composite file was carried out at LASL. In addition, fission product yield data were provided by the CSEWG Yield Subcommittee (T. England, chairman), and radioactive decay data by C. Reich (INEL). Partial documentation of the evaluation is provided in LA-7200-PR³ and in reference 16. The evaluation covers the energy range 10^{-5} eV to 20 MeV. Gamma-ray production and covariance data will be added to the file in a later MOD 1 update.

II. ENDF/B-V FILES

File 1. General Information

MT=451. Descriptive data.

MT=452. $\bar{\nu}$ Total

Sum of prompt plus delayed $\bar{\nu}$. Used thermal value recommended by CSEWG Standards Subcommittee of 2.4947 on 5-27-78. This value is 1% larger than recommended by Lemmel¹ and 0.13% smaller than Version IV.

MT=455. $\bar{\nu}$ Delayed

The delayed yields and spectra were evaluated by Kaiser and Carpenter at ANL-Idaho (see Ref. 2 for technical details). The same six-group yields appear in Version IV but the spectra have been changed for Version V.

MT=456. $\bar{\nu}$ Prompt

The energy dependence of prompt $\bar{\nu}$ is changed significantly from Version IV. Although the thermal value is slightly lower, the value around 1.5 MeV is significantly higher and has a different shape with three slightly different slopes. This evaluation relies heavily on the measurements with respect to ^{235}U and ^{252}Cf using the CSEWG recommended standards. In particular, the data of Boldeman, Sergachev, Nurpeisov, and Block⁵⁻⁷ were weighted at all energies while the Mather⁸ measurements were relied upon only at high energies. Smirenkin, Flerov, and Protopopov⁹⁻¹¹ also contributed in the high-energy range. This evaluation decouples the thermal value based on η measurements from the fast range. Otherwise, the $\bar{\nu}$ - η discrepancy would be perpetuated to 20 MeV.

MT=458. Energy Release in Fission

These values were taken directly from an evaluation by R. Sher¹² (Stanford).

File 2. Resonance Parameters

MT=151. (a) Resolved Resonance Region

Resolved range extends to 60 eV. Multi-level parameters provided by de Saussure (ORNL) in Adler-Adler formalism from analysis by Reynolds (KAPL). Version IV used single-level Breit-Wigner representation but had large fluctuations in fission in File 3 background.

(b) Unresolved Resonance Region

Unresolved range extends to 10 keV. Version IV was pointwise over this range. A reevaluation of the point-wise cross sections begun by Mann (HEDL) were used as the starting point by Weston (ORNL), who obtained new average cross sections for fission and capture which require no File 3 backgrounds. Cross sections based on Carlson and Behrens,⁴ Weston,¹⁷ Cao,¹⁸ and Nizamuddin¹⁹ for fission. Weston's data²⁰ were used for capture using a potential

scattering radius of 0.9893. Reasonable agreement with Patten-den's total cross section²¹ was obtained, especially below 1 keV. New measurements are needed in this range.

File 3. Neutron Cross Sections

Thermal Range

The 2200 m/s ($E_n=0.0253$ eV) data are as follows:

Eta	2.2959	Capture	45.76 b
Alpha	0.0866	Fission	528.45 b
γ Prompt	2.4873	Absorption	574.21 b
γ Total	2.4947	Elastic	12.6 b
		Total	586.81 b

The capture and fission cross sections were renormalized by N. Steen (BAPL). The elastic scattering in the thermal range changed significantly from Version IV to conform to Leonard's thermal and Weston's evaluation in unresolved range. The total was adjusted accordingly. Elastic and total changes made by LASL.

10 keV - 20 MeV

Much of the File 3 data above 50 keV relied heavily on model calculations performed by Madland (LASL). Calculations were particularly important for this isotope since experimental information was often insufficient if not completely missing. A detailed description of the methods used can be found in reference 3. Note that for convenience, many of the specific references found in BNL-325 are not repeated here.

MT=1. Total Cross Section

No measurements exist from 10 to 40 keV; therefore, an extrapolation was made to give reasonable agreement with recent ANL data¹³ above 40 keV and cross sections predicted by Madland. The present evaluation is based on recent ANL measurements¹³ and earlier work of Green (Bettis) and Foster (Hanford). See BNL-325 (Ref. 5). No measurements exist above 15 MeV. This reevaluation resulted in an increased total cross section up to 7 MeV, the increase near 1.6 MeV being as large as 8%. Use of the Foster data resulted in a decrease of 4.8% near 14 MeV.

MT=2. Elastic Cross Section

(Obtained from total minus reaction). The increased total cross section required a significant increase in the elastic cross section over the energy range to 7 MeV. At 14 MeV the elastic was decreased due to the decrease in the total.

MT=4. Inelastic Cross Section

Sum of MT=51-54 and MT=91. These data were taken from model calculations of discrete and continuum compound inelastic scattering and coupled-channel direct inelastic scattering.

MT=16, 17. (n,2n) and (n,3n) Cross Sections

Taken from Hauser-Feshbach statistical model calculations performed by Madland.

MT=18. (n,f) Cross Sections

Data from 10 keV to 100 keV sparse and reasonably discrepant.

Above 100 keV, we relied heavily on the ratio measurements of Carlson and Behrens⁴ and those of Meadows,¹⁴ normalized to Version V ²³⁵U fission. The absolute data of Poenitz¹⁵ were also employed, although good agreement among the sets was lacking. The evaluated curve was drawn as smoothly as possible due to the magnitude of the discrepancy among the sets.

MT=51-54. Discrete Inelastic Cross Sections

Taken from compound and direct inelastic scattering model.

MT=102. Radiative Capture Cross Section

No data exist above 10 keV except for the α measurements of Diven and Hopkins (see Ref. 5) which extend to 1 MeV. Extrapolated to 20 MeV assuming a rise due to direct capture.

MT=251, 252, 253. μ_L , ξ , γ

Calculated from MF=3 and 4 data and input by Kinsey at BNL.

File 4. Neutron Angular Distributions

All neutron angular distributions isotropic in laboratory system except for the elastic (MT=2) which was taken from Version IV. The elastic and direct inelastic should be modified in the next update.

File 5. Neutron Energy Distributions

MT=16, 17. (n,2n), (n,3n) Energy Distributions

Represented by an evaporation spectrum with LF=9.

MT=18. (n,f) Neutron Energy Distributions

Represented by an energy-dependent Watt spectrum with an average energy at thermal of 2.073 MeV. This spectrum based on Grundl ratio data to ²³⁵U and ²³⁹Pu.

MT=91. Inelastic Continuum Energy Distributions

Represented by an evaporation spectrum with LF=9.

MT=455. Delayed Neutron Spectra

Evaluated in six time groups by Kaiser and Carpenter² at ANL-
Idaho.

File 8. Fission Product Yields and Decay Data

MT=454. Individual Fission Product Yields

Direct yields before neutron emission.

MT=459. Cumulative Yields

Cumulative yields along each isobaric chain after neutron emission taken from set 5D.3/78. Values recommended by CSEWG Yields Subcommittee (England, chairman).

Note: Both direct and cumulative yields are normalized by the same factors based on B. F. Rider evaluation. The isomeric state model, LA-6595-MS (ENDF-241), and delayed neutron emission branchings (Pn values) for 102 emitters, and pairing effects, LA-6430-MS (ENDF-240), have been incorporated.

Uncertainties are based on the total yield to each ZA. When there is an isomeric state, the independent nuclide yield to each state has a larger uncertainty than the total yield in state distributions. (Uncertainties average 50% but can be larger). Any yield with an uncertainty of 45-64% may be model estimate or a value assigned in the wings of the mass distribution. These small yields may be accurate only within a factor of two.

Data prepared for ENDF/B-V by T. R. England (Ref. LA-UR-78-687).

MT=457. Radioactive Decay Data

Evaluated by C. Reich (INEL).

Q (ALPHA) - 1974 Version of Wapstra-Bos-Gove mass tables.

Half-life - Average of values by Vaninbroukx²² and Jaffy et al.²³

Alpha Energies and Intensities - Are based mainly on the results of Ellis²⁴ with a few deletions based on level-scheme considerations. Energies and intensities of the two most prominent alpha groups are those recommended by Rytz.²⁵

Gamma-Ray Energies and Intensities - Based on results of Kroger and Reich.²⁶

Gamma-Ray Multipolarities - Taken from level scheme considerations
(see reference 26).

General Note. The decay data (MT=457) were translated into the ENDF/B-V format by Mann and Schenter at HEDL. Also, much of the above data provided by other laboratories were first input in the file by Bob Kinsey at BNL and then sent to LASL. His help was significant and is gratefully acknowledged in assembling this file.

REFERENCES

1. H. D. Lemmel, Proc. of a symposium on Neutron Standards and Applications held at NBS on March 28-31, 1977. See p. 170.
2. Kaiser and Carpenter, private communication to BNL (1978).
3. D. G. Madland and P. G. Young, LA-7200-PR (1978) p. 11 and p. 13.
4. G. W. Carlson and J. W. Behrens, Nucl. Sci. Eng. 66, 205 (1978).
5. D. I. Garber and R. R. Kinsey, BNL-325, Vol. 11 (1976).
6. J. W. Boldeman, J. Nucl. Ener. 25, 321 (1971), and Boldeman, Bertram, and Walsh, Nucl. Phys. A265, 337 (1976).
7. L. Reed, R. W. Hockenbury, and R. C. Block, report COO-3058-39, p. 9 (Sept. 1973).
8. D. S. Mather, Nuc. Phys. 66, 149 (1965).
9. G. N. Smirenkin, At. Ener. 4, 88 (1958).
10. N. N. Flerov, At. Ener. 10, 86 (1961).
11. A. N. Protopopov, At. Ener. 5, 71 (1958).
12. R. Sher, S. Fiarman, and C. Beck, private communication to BNL (1976).
13. W. P. Poenitz, J. F. Whalen, P. Guenther, and A. B. Smith, Nucl. Sci. Eng. 68, 358 (1978).
14. J. W. Meadows, Nucl. Sci. Eng. 54, 317 (1974).
15. W. P. Poenitz, ANL-NDM-36 (1978).
16. L. Stewart, D. Madland, and P. Young, Trans. Am. Nuc. Soc. 28, 721 (1978).
17. L. Weston et al, Nucl. Sci. Eng. 42, 143 (1970).
18. M. Cao et al., J. Nucl. Ener. 24, 111 (1970).
19. S. Nizamuddin and J. Blons, Nucl. Sci. Eng. 54, 116 (1974).

20. L. Weston et al., Nucl. Sci. Eng. 34, 1 (1968).
21. N. Pattenden et al, Nucl. Sci. Eng. 17, 404 (1963).
22. R. Vaninbroukx et al., Phys. Rev. C13, 315 (1976).
23. A. H. Jaffy et al., Phys. Rev. C9, 1991 (1974).
24. Y. A. Ellis, Nucl. Data Sheets B6, #3, 257 (1971).
25. A. Rytz, At. Data and Nucl. Data Tables 12, #5, 479 (1973).
26. L. A. Kroger and C. W. Reich, Nucl. Phys. A259, 29 (1976).

ENDF/B-V Summary Documentation
Isotope: 92-U-234 MATT = 1394

M. Divadeenam	(BNL)	Aug. '78
F.M. Mann & R.E. Schenter	(HEDL)	Apr. '78
C.R. Reich	(INEL)	Apr. '78
M.K. Drake & P.F. Nichols	(GGA)	Jan. '67

The present work supersedes the ENDF/B-IV evaluation, MAT = 1043 by Drake and Nichols. Neutron and photon production data are given between 10^{-5} ev and 20 MeV. The cross sections included are total, elastic, inelastic, (n,f), (n,2n), (n,3n), (n,n'γ), and (n,γ) and are described in HEDL-TME-77-54. The photon data include multiplicities and transition probabilities, photon production cross sections, and secondary energy spectra. File 2 has been evaluated for this version. Details will be published in a BNL report.

MF=1: General information.

MT=452

Nu based on Mather, et al., (ref. 9). Mather's data normalized to the ENDF/B-V Cf Nu. Least squares fit to a straight line.

MT=458

Energy from fission. Based on Sher (ref. 10).

MF=2: Resonance parameters.

MT=151

Resolved resonance parameters from ref. 7. Bound level parameters modified to fit BNL-325 Vol. I (ref. 11) thermal and resonance integral cross sections. Unresolved resonance parameters obtained by fitting averaged (n,f) data of James, et al., (ref. 7) and ENDF-IV capture cross sections from 1.5 keV to 100 keV. Code UR (ref. 12) was used for this purpose.

MF=3: Smooth cross sections.

MT=1

Total. sum of partial cross sections.

92-U-234
MAT 1394

MT=2

Elastic. Same as U-238 (ref. 1).

MT=4

Inelastic. From Parker (ref. 2).

MT=16

(n,2n). From Parker (ref. 2).

MT=17

(n,3n). From Parker (ref. 2).

MT=18

Fission above 100 keV based on Behrens, et al., (ref. 3) normalized to U-235 (ENDF/B-V).

MT=19

Same as MT=18, until (n,nf) threshold. Thereafter constant.

MT=20

Is (MT=18) - (MT=19) until (n,2nf) threshold. Constant thereafter.

MT=21

Is (MT=18) - (MT=19) - (MT=20).

MT=51 ... 56.91

From Parker (ref. 2).

MT=102

(n, γ) (ref. 5). Also MT-27 absorption.

MT=251, 252, 253

Calculated by Chad.

MF=4: Angular distributions.

MT=2

Diff. elastic (ref. 5). Same as thorium (ref. 6).

MT>2

Assumed isotropic.

MF=5: Energy distributions.

MT=16, 17, 18, 19, 20, 21, 91

From ref. 5.

MF=8, MT=457

Radioactive decay data. References: Q(alpha)-1974 version of Wapstra-Bos-Gove Mass Table; half-life - see R. Vaninbroukx, Euratom Report EUR-5194E (1974). Other - see Y.A. Ellis, Nuclear Data Sheets B 4, No. 6, 581 (1970) and Table of Isotopes, 7th ed., (preliminary data, priv. comm. from C.M. Lederer). Note: The L-X-ray data represent measured values. See C.E. Bemis, Jr., and L. Tubbs, ORNL-5297, 93 (Sept., 1977).

Note: The gamma-ray intensity normalization and its uncertainty have been derived from intensity-sum considerations. Using theoretical values for the internal-conversion coefficients.

REFERENCES

1. G.D. Joanou and C.A. Stevens, GA-6087.
2. K. Parker, AWRE-0-37/64 (1964).
3. J.W. Behrens, G.W. Carlson, and R.W. Bauer, Nuclear Cross Section and Technology, NBS 425 (1975) p. 591.
4. F.M. Mann and R.E. Schenter, Trans. Amer. Nucl. Soc. 23 (1976) 546, and to be published.
5. M.K. Drake and P.F. Nichols, GA-8135 (1967).
6. M.K. Drake and P.F. Nichols, GA-6404 (1966).
7. G.D. James, J.W. Dabbs, J.A. Harvey, N.W. Hill and R.H. Schindler, Phys. Rev. C15, 2083 (1977).
8. J.A. Harvey and D.J. Hughes, Phys. Rev. 109 (1958), 471.
9. D.S. Mather, P. Fieldhouse, and A. Moat, Nucl. Phys. 66 (1965), 149.
10. R. Sher, S. Fiarman, and C. Beck (private communication, 1976).
11. S.F. Mughabghab and D.I. Garber, BNL-325, Vol. I (Third edition) (1973).
12. UR: E. Pennington (private communication).

1h

Summary Documentation for ^{235}U .

(MAT=1395)

M. R. Bhat

1. Introduction

The present evaluation of ^{235}U for ENDF/B-V is based on the ENDF/B-IV evaluation by L. Stewart (LASL), H. Alter (A.I.) and R. Hunter (LASL) [1] except for changes and updates in the following sections discussed below. These changes represent the work of many people either as individuals or as a group such as The Normalization and Standards Subcommittee of CSEWG. Some of these contributions have been discussed in separate reports by the authors. These will be referred to here and their contents will not be discussed in detail.

2. File 1

(i) Nu-bar Total (MT=452)

These values were changed to reflect changes made in the $\bar{\nu}_{\text{prompt}}$ and $\bar{\nu}_{\text{delayed}}$.

(ii) Nu-bar Delayed (MT=455)

The delayed neutron yields were evaluated by Kaiser and Carpenter [2] where the details of the evaluation are discussed.

(iii) Nu-bar Prompt (MT=456)

The data sets [3-19] were used. They were first normalized to ^{252}Cf $\bar{\nu}_{\text{prompt}} = 3.757 \pm 0.015$ and $^{235}\text{U} \bar{\nu}_{\text{prompt}} (0.0253 \text{ eV}) = 2.420 \pm 0.012$ as recommended by The Normalization and Standards Subcommittee [20]. Data were fitted with straight lines in the energy region 0-2 MeV, 2-5.5 MeV, 6-20 MeV with a join from 5.5 to 6.0 MeV. A plot of the renormalized data indicates that there is a step in the $\bar{\nu}_{\text{p}}$ from 5.5 to 6 MeV, and this was included in the evaluation. The details of the evaluation and data plots are in Ref. 21.

(iv) Energy Released in Fission (MT=458)

The energy released in fission and its partition into the different modes of decay was evaluated by R. Sher et al., [22].

3. File 2

(i) The Resolved Resonance Region (MT=151) (1.0-82.0 eV).

The resolved resonance parameters are the same as those evaluated by Smith and Young [23] for ENDF/B-III.

(ii) The Unresolved Resonance Region (MT=151) (82.0-2.5E+04 eV)

Evaluation of the bin averaged fission and capture cross-sections is described in Ref. [21,23]. The fine structure in fission cross-section was a consensus structure arrived at by energy shifting the data of Blons [24], ORNL-RPI [25], Gwin [26] with respect to the Lemley [27] data. Similarly, the fine structure as well as the bin average of the capture cross-section were determined. Results of the analysis of Moore [28] were used and the unresolved resonance region parameters were extracted using the code UR by Pennington [29].

4. File 3

(i) The Thermal Energy Region (1.0E-05 - 1.0 eV)

The total scattering capture and fission cross-sections in this energy region were obtained by Leonard [30]. This evaluation was modified between 0.85 and 1 eV to join smoothly with the resolved resonance region at 1 eV. The 0.0253 eV values for capture and fission are $98.38 \pm 0.76b$ and $583.54 \pm 1.70b$ respectively.

(ii) Fission Cross-Section (25 keV-100 keV).

The structure in the fission cross-section as given in ENDF/B-IV and based on Gwin data was preserved by multiplying the ENDF/B-IV cross-section by 0.9781 to give the average cross-section evaluated in Ref. 23.

(iii) Fission Cross-Section (100 keV-20 MeV)

This evaluation is by Poenitz [31].

(iv) Capture Cross-Section (25 keV-20 MeV).

This was obtained by multiplying the evaluated ENDF/B-V fission cross-section by the capture-to-fission ratio of ENDF/B-IV.

5. File 4

The angular distributions are the same as in ENDF/B-IV [1].

6. File 5

(i) Fission Neutron Spectra

The energy dependent Watt spectrum representation is used for fission neutrons. The procedure used was to take the a and b parameters for an energy dependent Watt spectrum as given by Kujawski and Stewart for their Pu-239 evaluation (for the fission part of file 1399/5/19) calculate the mean energy \bar{E} and divide it by 1.04, the value obtained by Adams [32] for the $\bar{E}_{\text{Pu-239}} / \bar{E}_{\text{U-235}}$ to give \bar{E} for U-235 as a function of energy. From these values, and assuming $a=0.988$ MeV as given by Adams at low energies, b is calculated. These are assumed to be constant for $E_n = 1.0E^{-5}$ eV to 1.5×10^6 eV and a small energy dependence is built into a and b to give the correct \bar{E} . The pre-fission part of sections 5/20 and 5/21 are given as an evaporation spectrum with a temperature obtained from section 5/91, i.e., at a particular energy E_n one finds $(E_n - E_{\text{thresh.2nd}})$ chance fission or $(E_n - E_{\text{thresh 3rd}})$ chance fission and the corresponding temperature above the 5/91 threshold is given. Having fixed these parameters, the mean energy corresponding to section 5/18 could be calculated knowing σ_f Total, $\sigma_{nn'f}$, $\sigma_{n,2nf}$ and \bar{v}_p , and the energy dependent parameters a and b calculated.

(ii) Delayed Neutron Spectra

The evaluation is by Kaiser and Carpenter [2].

7. File 8

(i) Fission Product Yield Data (MT=454 and 459)

The fission product yield data were reviewed and recommended by the Fission Products Yields Subcommittee and the data files prepared by T.R. England [33].

(ii) Radioactive Decay Data (MT=457)

Radioactive decay data were evaluated by C.W. Reich. The Q (alpha)-values are from [34] and the half-life data are from Jaffey et al., [35],

File 8 (cont'd)

(ii) Radioactive Decay Data (MT=457) (cont'd)

and also Vaninbroukx [36]. Alpha energies and intensities are from Ref., [37,38], and the gamma-ray and L x-ray data are from Ref. [37].

8. File 13

(i) Gamma-ray Production Cross-Section from $E_n = 1.09 - 20$ MeV (MT=3)

This was re-evaluated to include the new data of Drake et al., [39,40]. These were compared with the earlier data of Nellis and Morgan [41], and Buchanan et al., [42] above $E_\gamma = 0.5$ MeV and are found to be in good agreement. The Drake data in Ref. [39] have a low-energy cut-off of $E_\gamma = 0.25$ MeV and for their 14.2 data [40] it is $E_\gamma = 0.3$ MeV. The low-energy part of the spectrum was obtained by a simple extrapolation of the data.

9. File 15

(i) Energy Distribution of the Gamma-rays $E_n = 1.09 - 20$ MeV (MT=3)

These are based on the Drake data [39,40].

10. Files 31 & 33

(i) Data Variance - Covariance Files (MT=452,18,102)

The evaluation of these files for \bar{v}_{Total} , σ_f and σ_{ny} is by R.W. Peelle [43].

References

1. L. Stewart, H. Alter and R. Hunter, ENDF-201 (1976).
2. R.E. Kaiser and S.G. Carpenter (ANL-West) Priv. Comm. (1978).
3. J.W. Meadows, WASH-1053, 9 (1964).
4. J.W. Meadows and J.F. Whalen, Jour. Nuc. Energy 21, 157 (1967).
5. D.W. Colvin and M.G. Sowerby '65 Salzburg Conf., 31 (1965).
6. H. Conde, Arkiv for Fysik, 29, 293 (1965).
7. B.C. Diven et al., Phys. Rev. 101, 1012 (1956).
8. J.W. Meadows and J.F. Whalen, Phys. Rev. 126, 197 (1962).
9. J.W. Boldeman et al., Nuc. Sci. and Eng. 63, 430 (1977).
10. M. Soleilhac, Priv. Comm. to L. Stewart (1976).

11. V.G. Nesterov, '70 Helsinki, CN-26/74 (1970).
12. J.C. Hopkins and B.C. Diven, Nuc. Phys. 48, 433 (1963).
13. D.S. Mather et al., Phys. Rev. B133, 1403 (1964).
14. L.I. Prokhorova et al., Sovt. Nuc. Phys. 7, 579, (1968).
15. A. Moat et al., Jour. Nuc. Energy 15, 102 (1961).
16. J. Frehaut, Priv. Comm. to L. Stewart (1976).
17. J. Frehaut et al., see Ref. 9.
18. A. De Volpi et al., '66 Paris Conf. Vol. I, p297 (1966).
19. D.W. Colvin and M.G. Sowerby '65 Salzburg Conf.
20. B.R. Leonard, Jr., Priv. Communication (1978).
21. M.R. Bhat, U-235 Evaluation for ENDF/B-V (ENDF-248) to be published.
22. R. Sher, S. Fiarman and C. Beck, Private Communication (1977).
23. M.R. Bhat, ANL-76-90 (ERDA-NDC-5/L) p307 (1976).
24. J. Blons, Nuc. Sci. and Eng. 51, 130 (1973).
25. G. de Saussure et al., ORNL-TM-1804 (1967).
26. R. Gwin et al., Nuc. Sci. and Eng., 59, 79 (1976).
27. J.R. Lemley et al., Nuc. Sci. and Eng. 43, 281 (1971).
28. M.S. Moore et al., Phys. Rev. C18, 1328 (1978)
29. E. Pennington, Private Communication (1973).
30. B.R. Leonard, Jr., et al., EPRI NP-167 (1976).
31. W.P. Poenitz, ANL/NDN-45 (1978) to be published.
32. J.M. Adams, AERE-R-8636 (1977).
33. T.R. England, Private Communication (1978).
34. 1974 Version of Wapstra-Bos-Gove Mass Tables.
35. A.H. Jaffey et al., Phys. Rev. C8, 1889 (1971).
36. R. Vaninbroukx, Euratom Report EUR-5194E (1974).
37. E. Vano et al., Nuc. Phys. A251, 225 (1975).
38. A. Artna-Cohen, Nuclear Data B6, 287 (1971).
39. D.M. Drake, Nuc. Sci. and Eng. 55, 427 (1974).
40. D.M. Drake, E.D. Arthur and M.G. Silbert, Nuc. Sci. and Eng. 65, 49 (1978).
41. D.O. Nellis and I.L. Morgan ORO-2791-17 (1966).
42. P.S. Buchanan, D.O. Nellis and W.E. Tucker, ORO-2791-32 (1971).
43. R.W. Peelle (Appendix B) of EPRI Proj 612 Report by E.T. Tomilinson et al.
EPRI NP-346, Project 612, ENDF-252 (1977).

ENDF/B-V Summary Documentation

Isotope: 92-U-236 MAT = 1396

M. Divadeenam	(BNL)	Aug. '78
F.M. Mann & R.E. Schenter	(HEDL)	Apr. '78
C.R. Reich	(INEL)	Apr. '78
J. McCrosson	(SRL)	Oct. '71

The present work supersedes the ENDF/B-IV evaluation, MAT = 1163 by McCrosson. Neutron and photon production data are given between 10^{-5} eV and 20 MeV. The cross sections included are total, elastic, inelastic, (n,f) , $(n,2n)$, $(n,3n)$, $(n,n'\gamma)$, and (n,γ) and are described in HEDL-TME-77-54. The photon data include multiplicities and transition probabilities, photon production cross sections, and secondary energy spectra.

File 2 has been evaluated for this version. Details will be given in a BNL report.

MF=1: General Information

MT=452

Nu. Conde and Holmberg $\bar{\nu}_p$ (ref. 3) normalized to the ENDF/B-V Cf $\bar{\nu}_p$. Least squares fit to a straight line.

MT=458

Energy from fission based on Sher (ref. 11).

MT=2: Resonance parameters.

MT=151

Resolved resonance parameters from refs. 2a to 2d. Bound level parameters modified to fit BNL-325 Vol. I (ref. 13) thermal and resonance integral cross sections. Unresolved resonance parameters obtained by fitting Carlson's average capture data (ref. 2a). Energy dependent unresolved parameters range from 4.11 keV to 100 keV. UR code (ref. 14) was used to obtain the parameters.

MF=3: Smooth cross sections.

MT=1

Total., taken from ref. 1 and 4.

MT=2

Elastic., ref. 1 and 4.

MT=4

Inelastic., ref. 1 and 4, Q-value, ref. 5.

MT=16

(n,2n) ., ref. 1 and 4, Q-value, ref. 6.

MT=17

(n,3n) ., ref. 1 and 4, Q-value, ref. 7.

MT=18

Fission, above 100 keV data of Behrens, et al., (ref. 8) was used, normalized to U-235 (n,f) of ENDF/B-V.

MT=19

Same as MT=18 below (n,nf) threshold, thereafter constant.

MT=20

Is difference of MT=18 and MT=19 until (n,2nf) threshold, thereafter a constant.

MT=21

Difference of MT=18 and MT=19 and 20.

MT=51...56.91

Ref. 1 and 4.

MT=102

(n, γ), ref. 1.

MT=251, 252, 253

Calculated by Chad.

MF=4: Angular distributions

MT=2

Diff. elastic same as for Th-232, ref. 10.

MT>2

Assumed isotropic.

MF=5

MF=5: Energy distributions.

MT=16

(n,2n) energy dist. described by Maxwellian.

MT=17

(n,3n) energy dist. described by Maxwellian.

MT=18, 19, 20

Neutron energy distribution given by simple fission spectrum plus Maxwellian.

MT=91

Evaporation temp. from Gilbert and Cameron (ref. 12).

MF=8: Radioactivity information.

MT=454

Fission yield data. Fission product yield data for phase one review for ENDF/B-V set 5C 3/9/77. Values were obtained from the recommendations of the yields subcommittee (T.R. England, chairman).

MF=8, MT=457

Radioactive decay data. References Q(alpha)-1974 version of Wapstra-Bos-Gove mass table; half-life - K.F. Flynn, et al., J. Inorg. Nucl. Chem., 34 1121 (1972). Other - see M.R. Schmorak, Nuclear Data Sheets B 4, no. 6, 623 (1970) and Table of Isotopes, 7th ed., (preliminary data, priv. comm., from C.M. Lederer). See also M.R. Schmorak. Nuclear Data Sheets 20, 192 (1977).

Note: The energies and intensities of the two highest-energy alpha groups are those recommended by A. Rytz, At. Data and Nucl. Data Tables 12, No. 5, 479 (1973).

Note: The gamma-ray intensity normalization has been derived from intensity-balance considerations at the ground state. While this gives agreement between the alpha and 49.3 keV gamma-ray intensities. The corresponding data for the 112 keV gamma are not consistent.

REFERENCES

1. M. Drake and P.F. Nichols, GA-8135 (1967).
2. A.D. Carlson et al., GA-9057 (1968).
- 2a. A.D. Carlson, S.J. Freisenhahn, W.M. Lopez and M.P. Fricke, Nucl., Phys. 141, 577 (1970).
- 2b. G. Carraro and A. Bruesgen, Nucl. Phys. A257, 333 (1976).
- 2c. L. Mewissen, F. Poortmans, G. Rohr, J. Theobald, H. Weigmann and G. Vanpreat, Neutron Cross Section Technology, Vol. I, 729, (1975).
- 2d. J.P. Theobald, J.A. Wartena, H. Weigman and F. Poortmans, Nucl. Phys., A181, 639 (1972).
3. H. Conde and M. Holmberg, Jour. Nucl. Energy 25, 331 (1971).
4. K. Parker, AWRE-0-30/64 (1964).
5. M. Lederer et al., Table of Isotopes, Wiley, 6th ed. (1968).
6. C. Maples et al., UCRL-16964 (1966): Nucl. Data Tables 2, 429, 612 (1966).
7. R. Howerton et al., UCRL-14000 (1964).
8. J.W. Behrens, G.W. Carlson, and R.W. Bauer, Nucl. Cross Section and Technology, NBS 425 (1975). p. 591.
9. F.M. Mann and R.E. Schenter, Trans. Amer. Nucl. Soc. 23 (1976) 546 and to be published.
10. M. Drake and P.F. Nichols, GA-6404 (1966).
11. R. Sher, S. Fiarman, and C. Beck (priv. comm. Oct., 1976).
12. A. Gilbert and A.G.W. Cameron, Can. J. Phys. 43 (1965) 1446.
13. S.F. Mughabghab and D.I. Garber, BNL-325, Vol. I, Third Edition (1973).
14. UR: E. Pennington (private communication), unpublished.

Summary Documentation for ENDF/B-V ^{238}U (MAT=1398)

E. M. Pennington, A. B. Smith and W. Poenitz

Argonne National Laboratory
Argonne Illinois 60439
June 4, 1979

General Comments

The evaluation of ^{238}U for ENDF/B-V is completely new, and involves collaboration of several evaluators. Most of the neutron cross sections above 45 keV were evaluated by W. Poenitz and A. Smith. The resolved resonance parameters and thermal cross sections were evaluated by G. de Saussure at ORNL. R. Howerton at LLNL produced the gamma production files. E. Pennington evaluated most of the remaining data and assembled the file. Ref. 1 describes most of the neutron cross section data above 45 keV and the gamma production files, while Refs. 2 and 3 present the resolved resonance and thermal evaluations. It is planned to prepare an addendum to Ref. 1 which will describe the data not already described in Refs. 1-3. Note also that some of the data given in Ref. 1 have since been modified as a result of the changes in the ^{235}U fission cross section, which is one of the standards, during the course of the evaluation.

File 1

MT=452. The total nu-bar was obtained by summing the prompt (MT=456) and delayed (MT=455) nu-bar values.

MT=455. The delayed nu-bar was evaluated for both ^{238}U and the other major fertile and fissile materials by Kaiser and Carpenter (Ref. 4). The low energy value of v_d is 0.0440.

MT=456. A least-squares fit of a fifth order polynomial was made to experimental data to determine nu-bar prompt, which is given in tabulated form. The data include those in the review article by Manero and Konshin (Ref. 5) with results of Soleilhac replaced by his own later reevaluation of his experiments (Ref. 6). Also later measurements by Nurpeisov et al were included (Ref. 7). All values measured relative to nu-bar of ^{252}Cf spontaneous fission were renormalized to the value of 3.757 for nu-bar prompt based on nu-bar total = 3.766 ± 0.02 recommended by the CSEWG Normalization and Standards Subcommittee.

MT=458. The components of the energy release in fission as determined by R. Sher et al (Ref. 8) were used.

File 2

MT=151. The resolved resonance evaluation was done by G. de Saussure (Ref. 2,3). The energy range is 1 eV to 4 keV, as in ENDF/B-IV, but the formalism is now MLBW rather than SLBW. This avoids the negative excursions in total and elastic scattering cross sections, which were obtained with previous versions of ^{238}U . New measurements, mostly from GEEL, JAERI, ORNL, BNL and RPI, were considered in the evaluation. Of importance for thermal reactor calculations is the fact that results from the recent ORNL, BNL and RPI experiments have led to considerably smaller values of r for the first three positive s-wave resonances than was the case for ENDF/B-IV.

The unresolved resonance range is 4-149 keV, rather than 4-45 keV, as in ENDF/B-IV, and parameters are given for $l = 0,1,2$. Competitive widths are included to represent inelastic scattering to the first level. In fitting the cross sections, the neutron and competitive widths were varied to fit the (n,γ) and first inelastic level cross sections using an unpublished ANL code UR. The data which were fit are described below under File 3.

File 3

Thermal Energies - The thermal cross sections were evaluated by G. de Saussure (Ref. 2). Capture and elastic scattering cross sections at 0.0253 eV are 2.7 and 8.9 barns, respectively, compared to 2.7 and 8.9519 barns in ENDF/B-IV.

Resolved Resonance Region - Smooth capture and elastic backgrounds are provided (Ref. 2) with p-wave background capture later modified as suggested by D. Olsen, ORNL, in a memo of August 13, 1978.

Unresolved Resonance and Higher Energy Regions - The (n,γ) cross section was evaluated above 20 keV by W. Poenitz and from 4-20 keV by E. Pennington. Fission cross sections above 300 keV were evaluated by W. Poenitz, including the contributions from first, second, third and fourth chance fission. Subthreshold fission was evaluated by E. Pennington. Elastic and total cross sections from 4-45 keV were evaluated by E. Pennington. All other cross sections above 45 keV were evaluated by A. Smith. More details are provided under each reaction type below. Most of the evaluation above 45 keV is described in detail in ANL/NDM-32 (Ref. 1).

MT=1. Above 45 keV the total cross section was obtained by evaluating data referenced in ANL/NDM-32. From 4-45 keV the total background was determined as the difference between the total cross section calculated from unresolved parameters with $a = 0.944$ (the resolved radius) and $a = 0.89$ (the unresolved radius). This agrees with the sparse data in that region (BNL-325, 3rd Edition, Vol. 2.) The major difference from ENDF/B-IV is the region 400-800 keV, where ENDF/B-V is a few percent lower.

MT=2. Elastic scattering cross sections and angular distributions were evaluated using data referenced in ANL/NDM-32. Coupled-channel optical

model calculations assisted in the analysis (Ref. 9). Below about 1 MeV, the elastic cross section was determined for consistency with the total and partial non-elastics. Above 1 MeV, the total and elastic cross sections determine the non-elastic. The angular distributions are entirely experimental below 1.8 MeV, and calculated at higher energies. At most energies the ENDF/B-V elastic cross section is smaller than in ENDF/B-IV.

MT=4,51-77,91. The inelastic scattering evaluation is a correlation of theory (Ref. 9) and experiment. Experimental data referenced in ANL/NDM-32 are considered. Levels at higher energies are composites of actual levels. The total inelastic cross section is generally much higher than in ENDF/B-IV, except near threshold and over a region below 1 MeV. The individual levels have tails extending to much higher energies than in ENDF/B-IV resulting in a much smaller continuum. Thus inelastic scattering at high incident energies leads to higher average final energies in ENDF/B-V than in ENDF/B-IV. This tends to counteract the effect on the flux spectrum of having higher total inelastic in ENDF/B-V than in ENDF/B-IV. In performing the inelastic evaluation one revision was made in the first draft (Ref. 10) to give improved agreement with calculations for ZPR-6-7. No changes outside the estimated uncertainties were made.

MT=16,17. The $(n,2n)$ and $(n,3n)$ cross sections were evaluated considering all available experimental data, as referenced in ANL/NDM-32. The ENDF/B-V $(n,2n)$ cross section is lower than ENDF/B-IV to about 12.5 MeV, and higher at higher energies. The $(n,3n)$ cross section is a little lower than that of ENDF/B-IV.

MT=18. As a first step, separate evaluations of the $^{238}\text{U}/^{235}\text{U}$ fission ratio and the ^{238}U fission cross sections measured relative to hydrogen scattering or absolutely were carried out. The $^{238}\text{U}/^{235}\text{U}$ set was converted to ^{238}U fission using the evaluated ^{235}U fission cross section for ENDF/B-V (Ref. 11). Note that the original ENDF/B-V ^{235}U fission cross section was revised at the October, 1978 CSEWG meeting so that this conversion had to be redone. A weighted average of the two sets was then carried out. Experimental data used were from the 1976 ANL Fission Cross Section Meeting (Ref. 12). Subthreshold fission was based on Ref. 13.

MT=19,20,21,38. The cross sections for first, second, third and fourth chance fission were derived by setting a constant cross section value from the fission cross section minimum prior to the onset of the next fission threshold and extending it to 20 MeV.

MT=102. As a first step, separate evaluations of the following four quantities were carried out: 1. $^{238}\text{U}(n,\gamma)$ measured absolutely and relative to hydrogen scattering, 2. $^{238}\text{U}(n,\gamma)/^{10}\text{B}(n,\alpha)$, 3. $^{238}\text{U}(n,\gamma)/^{235}\text{U}(n,F)$ and 4. $^{238}\text{U}(n,\gamma)/^{197}\text{Au}(n,\gamma)$. The ratios of 2-4. were multiplied by the prior evaluated standards for $^{10}\text{B}(n,\alpha)$, $^{235}\text{U}(n,F)$ and $^{197}\text{Au}(n,\gamma)$. The resulting four cross section sets were combined to provide the final evaluated $^{238}\text{U}(n,\gamma)$ cross section. Note that the change in ^{235}U fission made at the October, 1978 CSEWG meeting necessitated some of this work being redone. The above procedure was used by W. Poenitz in the

92-U-238
MAT 1398

range from 20 keV to 1.7 MeV. Poenitz also performed the evaluation above 1.7 MeV, where data are sketchy and uncertain. E. Pennington did the evaluation from 4-20 keV, where all of the data considered were measured relative to $^{10}\text{B}(\text{n},\alpha)$.

MT=251,252,253. The quantities mu-bar lab, χ_1 , and gamma were calculated from the elastic scattering Legendre coefficients in MF = 4, MT = 2 using an ANL code, MUXICA.

File 4

MT=2. The elastic angular distributions are expressed as f_χ coefficients in the center-of-mass system at 31 energies. They were obtained above 45 keV as described above under MF = 3, MT = 2. At lower energies ENDF/B-IV was used. The coefficients at 20 MeV were modified in order to avoid negative excursions caused by the restriction to $\text{NL} \leq 20$.

MT=16,17,18,19,20,21,38,91. Angular distributions for all of these reactions were taken as isotropic in the lab system.

MT=51-77. The angular distributions for the inelastic levels are presented as probabilities in the c-of-m system. They were calculated with the model described in Ref. 9. Comparisons with experiment are given in ANL/NDM-32. In ENDF/B-IV all but the four highest levels were assumed isotropic.

File 5

MT=16,17. The $(\text{n},2\text{n})$ and $(\text{n},3\text{n})$ secondary energy distributions are both LF = 1 laws calculated by A. Smith according to the methods of Ref. 14, plus a pre-compound distribution.

MT=18. The total fission spectrum is an energy-dependent Watt (LF = 11) spectrum with parameters chosen to give the same average energy as the combination of MT = 19,20,21 and 38.

MT=19. An energy-dependent Watt spectrum was determined for first chance fission using methods similar to those of Ref. 15. A Watt spectrum has more neutrons at intermediate energies, and fewer at low and high energies than a Maxwellian of the same average energy.

MT=20,21,38. For second-, third- and fourth- chance fission, a combination of a Watt spectrum and 1,2 or 3 LF = 9 Maxwellian laws for MT = 20,21,38, respectively, is used.

MT=91. An LF = 1 law for the inelastic continuum was determined by A. Smith.

MT=455. Delayed neutron spectra evaluated by Kaiser and Carpenter (Ref. 4) for the six delayed neutron groups are presented using LF = 5 laws in histogram form. Since the original evaluation had no neutrons below about 80 keV, a modification was made by joining the values for the first histogram linearly from 80 keV down to zero at zero energy with the accompanying renormalization.

File 8

MT=454 and 459. The fission product yield data are set 5D, which contains values recommended by the Yields Subcommittee with T. England of LASL as chairman. Direct yields before delayed neutron emission are given in MT = 454 while MT = 459 contains cumulative yields along each isobaric chain after delayed neutron emission. The data were prepared for the files by T. England, and inserted at BNL by R. Kinsey.

MT=457. The radioactive decay data were evaluated by C. Reich of INEL, translated into ENDF/B-V format by F. Mann and R. Schenter of HEDL, and inserted into the file by R. Kinsey.

File 12

MT=18 and 102. Multiplicities are given for fission and (n,γ) reactions from 10^{-5} eV to 20 MeV (Ref. 1).

File 13

MT=3. Photon production cross sections are given above the inelastic threshold under MT = 3 to represent photons from the first three inelastic levels and a continuum.

File 14

MT=3,18,102. Isotropic photon angular distributions are given.

File 15

MT=3,18,102. Continuous photon energy spectra are present.

File 31

MT=455. The delayed nu-bar error files are based on error estimates given in Ref. 4 and 16.

MT=456. The prompt nu-bar error files are based on data obtained in fitting the experimental nu-bar prompt.

File 33

In the thermal energy range up to 1 eV, File 33 was derived from information in Ref. 2. Above 4 keV, most of File 33 was based on data from ANL/NDM-32 (Ref. 1). It was decided in consultation with F. Perey (ORNL) that no error information would be given over the resolved resonance range from 1 eV to 4 keV. In this range the user should refer to Ref. 2 for error information.

For the Watt fission spectrum in MF = 5, MT = 18, it is estimated that $\Delta a/a = 0.015$ and $\Delta b/b = 0.07$.

References

1. W. Poenitz, E. Pennington, A. B. Smith and R. Howerton, "Evaluated Fast Neutron Cross Sections of Uranium-238," ANL/NDM-32 (October 1977).
2. G. de Saussure, D. K. Olsen, R. B. Perez and F. C. Difilippo, "Evaluation of the ^{238}U Neutron Cross Sections for Incident Neutron Energies up to 4 keV." ORNL/TM-6152 (ENDF-257) (January 1978).
3. G. de Saussure et al, Prog. in Nuclear Energy. Vol.3, p. 87 (1979).
4. R. Kaiser and S. Carpenter, ANL-West (private communication) (March 1978).
5. F. Manero and V. Konshin, "Status of the Energy Dependent $\bar{\nu}$ Values for the Heavy Isotopes ($Z > 90$ from Thermal to 15 MeV and of $\bar{\nu}$ Values for Spontaneous Fission," Atomic Energy Review Vol. 10, No. 4, p. 637 (December 1972).
6. M. Soleilhac, revised data received from NNCSC (October 1976).
7. B. Nurpeisov et al, "Dependence of $\bar{\nu}$ on Neutron Energies up to 5 MeV for ^{233}U , ^{238}U , and ^{239}Pu ." Soviet Atomic Energy translation, p. 807 (March 1976).
8. R. Sher et al, "Fission Energy Release for 16 Fissioning Nuclides," Summary of CSEWG Meeting, October 27-28, 1976.
9. P. Guenther, D. Havel and A. Smith, "Note on Neutron Scattering and the Optical Model Near $A = 208$," ANL/NDM-22 (September 1976).
10. E. Pennington, W. Poenitz and A. Smith, "Evaluation of ^{238}U for ENDF/B-V," TANS, Vol. 26, p. 591 (June 1977).
11. M. Bhat paper in Ref. 12. Data were later revised at the October, 1978 CSEWG Meeting.
12. W. Poenitz and A. B. Smith, Editors, Proceedings of the NEANDC/NEACRP Specialist's Meeting on Fast Neutron Fission Cross Sections of U-233, U-235, U-238 and Pu-239, June 28-30, 1976 at Argonne National Laboratory, ANL-76-90.
13. R. Slovacek et al, " ^{238}U (n, F) Measurements below 100 keV," Nucl. Sci. Eng. Vol. 62, No. 3, p. 455 (March 1977).
14. M. Caner, M. Segev and S. Yiftah, "Energy Spectra of Secondary Neutrons from the ^{238}U ($n, 2n$) and ($n, 3n$) Reactions." Nucl. Sci. Eng. Vol. 59, No. 4, p. 395 (April 1976).
15. E. Kujawski and L. Stewart, "The Prompt Neutron Fission Spectrum for ^{239}Pu " TANS, Vol. 24, p. 453 (November 1976).
16. S. A. Cox, "Delayed Neutron Data Review and Evaluation" ANL/NDM-5 (April 1974).

ENDF/B-V Summary Documentation
Isotope: 93-NP-237 MAT = 1337

F.M. Mann and R.E. Schenter	(HEDL)	Apr '78
R. Benjamin	(SRL)	Oct '75
C. R. Reich	(INEL)	Apr '78
J. R. Smith	(ANL)	June '73
W. E. Stein	(LASL)	June '73

The present work supersedes the ENDF/B-IV evaluation, MAT=1263 by Smith and Stein. Neutron and photon production data are given between 10^{-5} eV and 20 MeV. The cross sections included are total, elastic, inelastic, (n,f) (n,2n), (n,3n), (n,n'γ), and (n,γ) and are described in HEDL-TME-77-54 (ref. 23). The photon data include multiplicities and transition probabilities, photon production cross sections, and secondary energy spectra.

MF=1 MT=452

Based on ref. 1.

MT=458

Energy from fission based on Sher (ref. 22)

MF=2 MT=151

Resolved resonance parameters below 1 eV are unchanged from version III, including negative energy resonances fitted by Leonard and the .485 eV level from BNL 325. From 1 to 130 eV the resolved resonance parameters of Paya(2) are used, with the fission widths multiplied by 0.625 in keeping with the re-normalization recommended by Paya in a private communication. Unresolved parameters were fitted by J.R. Smith and M.K. Bhat to the Paya data from 130 eV to 5 kev, using the UR code developed by E. Pennington (ANL). The unresolved parameters are designed to yield histograms in the fission cross section with areas equal to those of the -class 2- resonance areas determined by Paya (renormalized by factor 0.625).

Cross Section Values at E=0.0253 eV are

Total	186.63 Barns
Scatter	17.51 Barns
Capture	169.10 Barns
Fission	16.63 Millibarns

MF=3 MT=1

Below 0.3 eV the total cross section is unchanged from version III. From 0.3 eV to 40 keV the resolved and unresolved parameters yield the total xsec, with a small correction for inelastic scattering beginning at 33.34 keV. From 40 keV to 1 MeV the total is the sum of the partials. Above 1 MeV, the total is also the sum of the partials, but all cross sections have been constrained to keep the total close to the recent measurements made at RPI on Pu-239 (3).

MT=2

A 10.5 barn potential scattering cross section is assumed. Above the resonance range the elastic xsec follows an extrapolation of the unresolved calculation to 1 MeV, above which it follows a curve based on cross sections of neighboring nuclei.

MT=4

The inelastic cross sections for ENDF/B-I were based on a calculation by D.T. Goldman(4). They have been progressively modified since. For version III the inelastic cross sections were reduced so the total cross section would be consistent with measurements on neighbouring nuclei above 1 MeV. For version IV the inelastic cross sections have been again adjusted to insure that the total inelastic was equal to the sum of its parts, and to accommodate reevaluated $(n, 2n)$, $(n, 3n)$ and capture cross sections in the constrained total cross section. For version V, the cross sections were smoothly continued above 1.0 MeV (Stewart and Young, LASL).

MT=16 MT=17

Both (n,2n) and (n,3n) cross sections are based on calculations made by S. Pearlstein (5). The (n,2n) cross section was normalized to the integral measurement of Paulson and Hennelly (ref. 6, to obtain cross section to short lived state) and of Myers et al., (ref. 7, to obtain ratio of short-lived to long-lived state).

This evaluation disagrees (factors of 3 low) with differential measurements of Lindeke et al. (ref. 8) and of Landrum et al. (ref. 9) as well as Hauser Feshbach calculations (ref. 10).

The (n,3n) cross section keeps the Pearlstein in shape and was renormalized to a maximum value of .203 barn to maintain the constraints on the total xsec.

MT=18 (Figure 93-237-1)

Below 0.3 eV the fission cross section is given by the same pointwise file that was used in version III. The fission cross section at 0.0253 eV is 16.63 mb. Above 10 keV the data is an average of experimental data (ref. 11 - 19).

MT=51...61.91

See comment under MT=4.

MT=102 (Figure 93-237-2)

Below 0.3 eV the capture cross section is given by the pointwise data in file 3, which is normalized to a value of 169.1 barns at 0.0253 eV. From 0.3 eV to 40 keV the capture is given by the resolved and unresolved resonance parameters. From 120 keV to 20 MeV the capture is from a smooth curve drawn through the measurements of Nagle et al. (20). Between 40 and 120 keV the capture is pointwise, taken from an unresolved calculation which had been extended to 120 keV using parameters adjusted to yield the evaluated capture cross section at that point. The Nagle measurements are appreciably lower than the Stupegia data on which previous ENDF/B files were based and tie in much more smoothly with the extrapolation of the unresolved calculation.

93-Np-237

MA' 1337

MF=4 MT=2

Angular distributions were supplied by H. Alter, then of AI, based on optical model calculations made on neighboring nuclei.

MF=4 MT>2

Assumed isotropic.

MF=5 MT=16

Nuclear temp calculated for Maxwell dist. (LF=9) calc. and θ of the temp distribution follows prescription used for the Pu240 file of ENDF/B-1.

MF=5 MT=18

Fission spectrum has Maxwellian density with the temp based on Terrells prescription (20).

MT=91

Inelastic secondaries based on D.T. Goldman data (4). Both discrete level and evaporation spectra are included.

MF=8 MT=16

Based on ENDF/B-V decay data of NP-237(S) and (L)

MT=454

Fission yield data. Fission product yield data for phase one review for ENDF/B-V set 5E 3/9/77. Values were obtained from the recommendations of the yields subcommittee (T.R. England, chairman).

MF=8 MT=457

Q(alpha)-1974 version of Wapstra-Bos-Gove mass table. Other - see Y.A. Ellis, Nuclear Data Sheets 6. No. 6, 539 (1971) and also Table of Isotopes, 7th ed. (preliminary data. priv. comm. from C.M. Lederer). The gamma-ray energy and relative intensity values are those of M. Skalsey and R.D. Connor, Can. J. Phys. 54, 1409 (1976).

93-Np-237
MAT 1337

Note: The data on the more prominent alpha groups are those recommended by A. Rytz, at. Data and Nucl. Data Tables 12, no. 5, 479 (1973).

Note: The K X-ray intensities represent measured values

MF=9 MT=16

Based on Meyers et al. (ref. 7). Hauser Feshbach calculations (ref. 10) give energy dependent ratios.

93-237-5

References

1. Keyworth and Vesser, LASL memo P-3-2080(U), 1976.
2. D. Paya, Thesis, University of Paris-South, Center D-orsay, 1972.
3. R.C. Block, private communication.
4. D.T. Goldman, Trans. Am. Nucl. Soc., Vol. 7, p. 84 (1964).
5. S. Pearlstein, Nucl. Sci. Engr., Vol. 23, p. 238 (1965).
6. C. K. Paulson and E. J. Hennelly, Nucl. Sci. Eng., 55, (1974) 24.
7. W.A. Myers, M. Linder, and R.S. Newbury, J. Inorg, Nucl. Chem., 37(1975) 637.
8. K. Lindeke, S. Specht, and H.-J. Born. Phys. Rev. C12 (1975) 1507.
9. J.H. Landrum, R.J. Nagle, and M. Linder, Phys. Rev. C8 (1973) 1938.
10. F.M. Mann, private communication (1977)
11. P.H. White, et al., Phys. and Chem. of Fission, p. 219, IAEA, Salzburg, (1965).
12. E.D. Klema, Phys. Rev. Vol. 72, p. 88 (1947).
13. W.E. Stein et al., conf-660303, p. 623. Washington 1966.
14. V.M. Pankratov. Sov. Journ. Atomic Energy, Vol. 14, p. 197 (1963).
15. P.H. White and G.P. Warner, J. Nucl. Energy, Vol. 21, p. 671 (1967)
16. W.K. Brown, D.R. Dixon, and D.M. Drake, Nucl. Phys. A156(1970)609, LA-4372(1970).
17. R.J. Jacoletti, W.K. Brown, and H.G. Olson, Nucl. Sci. and Eng., 48(1972)412.
18. K. Kobayaski, I. Kimura, H. Gotoh, and H. Yagi, EANDC(J)26L(1972)39.
19. S. Plattard, Y. Pranal, J. Blons, C. Mazur, KIEV conference (1975).
20. J.J. Nagle et al., Conf-710301, VI, p. 259, Knoxville (1971)
21. J. Terrell, Phys. Chem. of Fission., vol. 2, p. 3, IAEA, Vienna (1965).
22. R. Sher, S. Fiarman, and C. Beck (P.C. Oct. 1976).
23. F.M. Mann and R.E. Schenter, HEDL-TME-77-54 (1977).

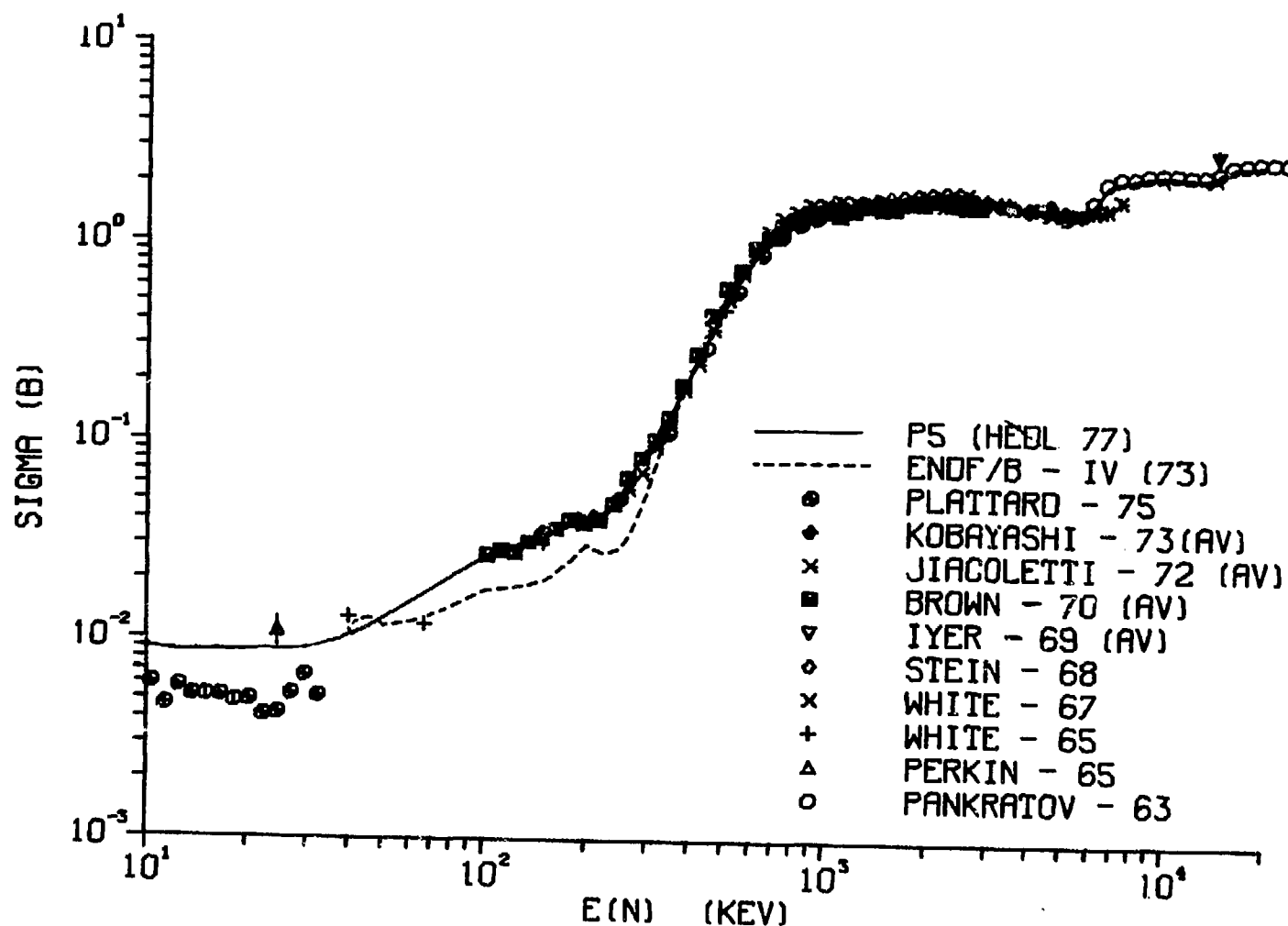


Figure 93-237-1
Np-237 (N, F)

93-237-7

93-NP-237
MAT 1337

93-Np-237
MAT 1337

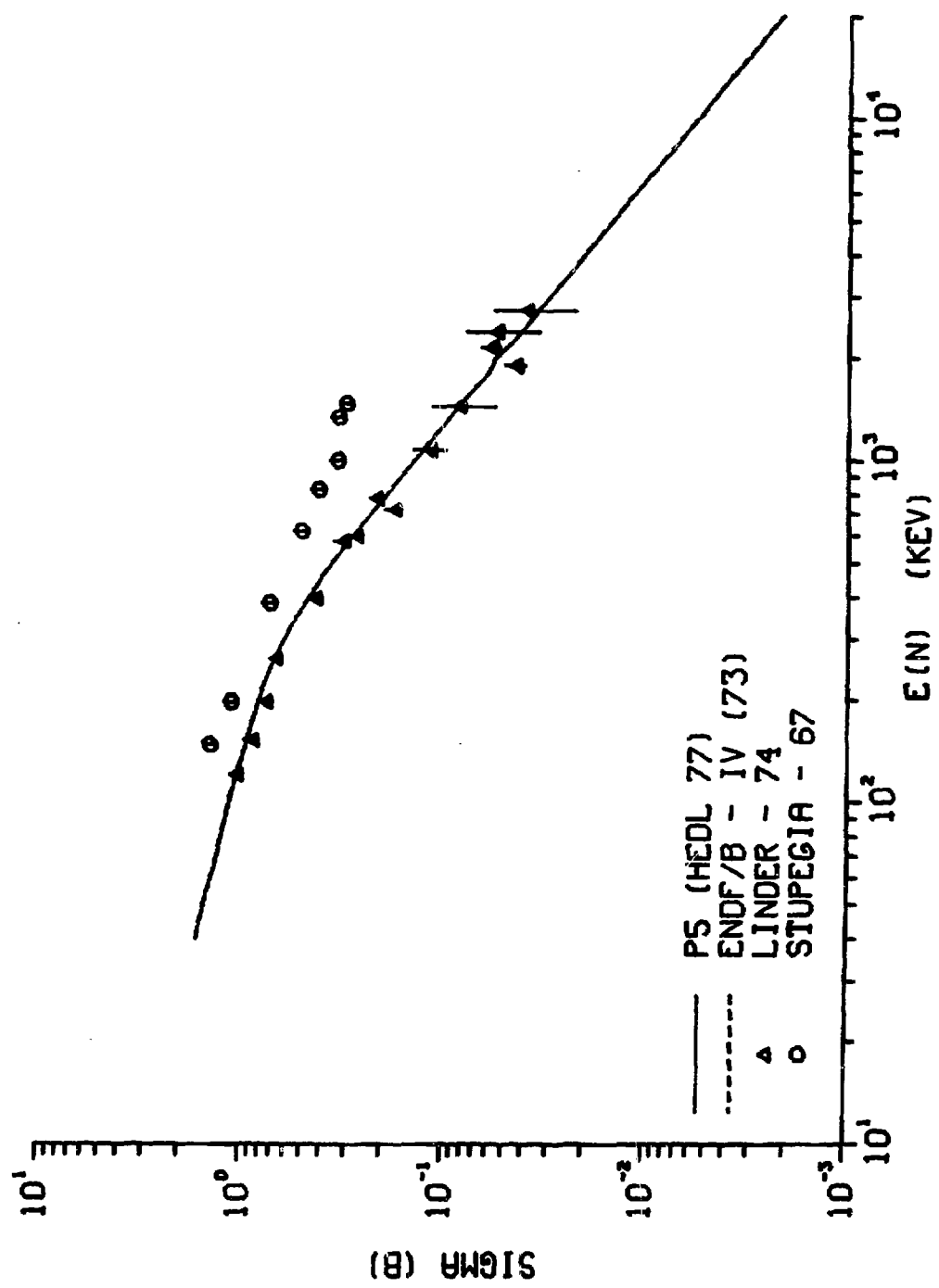


Figure 93-237-2
NP-37 (N, Gamma)

93-237-8

ENDF/B-V Summary Documentation

Isotope: 94-Pu-238 MAT = 1338

F.M. Mann and R.E. Schenter	(HEDL)	Apr '78
C.R. Reich	(INEL)	Apr '78
H. Alter and C. Dunford	(AI)	May '67

The present work supersedes the ENDF/B-IV evaluation, MAT = 1050 by Alter and Dunford. Neutron and photon production data are given between 10^{-5} eV and 20 MeV. The cross sections included are total, elastic, inelastic, (n,f), (n,2n), (n,3n), (n,n'γ), and (n,γ) and are described in HEDL-TME-77-54 (ref. 15). The photon data include multiplicities and transition probabilities, photon production cross sections, and secondary energy spectra.

MF=1 General Information.

MT=452

Nu. Thermal value based on Jaffey et al. (ref. 16) and Kroshkin et al. (ref. 17). Energy dependence from Howerton (ref. 1)

MT=458

Energy from fission based on Sher (ref. 8).

MF=2 Resonance parameters.

MF=151

Resolved parameters taken from Young et al. (ref. 2) unresolved parameters are from resolved region and optical model (unchanged from ENDF/B-1)

Thermal Cross Section

Total = 590 B (ref. 5 = 590)
Capture = 552.4 B
Fission = 17.0 B (ref. 7 = 16.6)

Resonance Integral (0.5 eV cutoff)

Capture = 276.3
Fission = 14.3

MF=3 Smooth cross section.

MT=L

Total from optical model.

94-Pu-238
MAT 1338
MT=2

Elastic from optical model.

MT=4

Inelastic scattering data results from the scattering to 15 levels plus continuum. Statistical compound nucleus model is used (ref. 15).

MT=16

$n, 2n$ based on statistical model calculations (ref. 15).

MT=17

$n, 3n$ based on statistical model calculations (ref. 15).

MT=18 (Figure 94-238-1)

Fission based on experiments of Ermagambetov (ref. 11), Fomushkin (ref. 12), Drake (ref. 13), and Silbert (ref. 14).

MT=51 . . . 65.91

Inelastic scattering data results from the scattering to 15 levels plus continuum. Statistical compound nucleus model is used (ref. 15).

MT=102

Capture from statistical model (ref. 16).

MT=251

MUBAR calculated from DOM angular distributions.

MT=252

XIBAR calculated from DOM angular distributions.

MT=253

Gamma calculated from DOM angular distributions.

MF=4 Angular distributions.

MT=2

Elastic scattering legendre coefficients for 15th order fit to calculated angular distributions (DOM) are provided between 10 keV and 11 MeV and 19th order between 12 and 15 MeV.

MT>2

Are assumed isotropic.

MF=5 Secondary energy distributions.

MT=16

$n, 2n$ Nuclear temperature with energy dependence as in reference 9.

MT=17

Same as MT=17.

MT=18

Fission Maxwellian with constant temperature from correlation of ref. 1.

MT=19, 20

Same as MT=18.

MT=91

(n,n) Temperature from Gilbert and Cameron (ref. 6).

MF=8 MT=457

Radioactive decay data. $Q(\alpha)$ -1974 version of Wapstra-Bos-Gove mass table. Spontaneous-fission branching ratio from data of J.D. Hastings and W.W. Strohm, J. Inorg. Nucl. Chem. 34, 25(1972). Other - see Table of Isotopes 7th ed. (preliminary data, priv. comm. from C.M. Lederer) and Y.A. Ellis, Nuclear Data Sheets B 4, No. 6, 635 (1970).

94-Pu-238
MAT 1338

Note: The intensity values of the K-X-rays and of the gamma rays below 852 keV (except those at 258 and 299 keV) are those of R. Gunnink, J.E. Evans and A.L. Prindle, UCRL-52139 (1976).

Note: The L-X-ray data represent measured values. See C.E. Bemis, Jr., and L. Tubbs, ORNL-5295, 93(Sept. 1977).

References

1. R.J. Howerton, Nucl. Sci. Eng. 62(1977)438.
2. T.E. Young, F.B. Simpson, J.P. Berreth, and M.S. Coops, Nucl. Sci. and Eng., 30(1967)355.
3. Stubbings, W., et al., UCRL, 33(1966).
5. Young, T., Wash 1068 (1966).
6. A. Gilbert and A.G.W. Cameron, Can. J. Phys. 43(1965)1446.
7. Hulet, E., et al., Phys. Rev. 107, 1294 (1957).
8. Hill, D., Wheeler, J., Phys. Rev. 89, 1102 (1953).
9. Parker, K., AWREO-79/63 (1964).
10. Barnard, E., et al., Nucl. Phys., 71, 228(1965).
11. S.B. Ermagambetov and G.N. Smirenkin, Sov. J. Atom, Energy 25 (1968) 364, JETP letters 9(1969)309, Sov. J. Atom, Energy 29(1970)1190.
12. E.F. Fomushkin and E.K. Gutnikova, Sov. J. Nucl. Phys., 10(1970)529.
13. D.M. Drake, C.D. Bowman, M.S. Coops, and R.W. Hoff LA-4420 (1970)101.
14. M.G. Silbert, A. Moat, and T.E. Young, Nucl. Sci. Eng. 52(1973)176.
15. F.M. Mann and R.E. Schenter, Trans. Amer. Nucl. Soc. 23(1976)546 and HEDL TME-77-54 (1977).
16. Jaffey et al., Nucl. Phys. A145(1970)1.
17. Kroshkin et al., Nucl. Phys. A145(1970)1.
18. R. Sher, S. Fiarman, and C. Beck (priv. comm., Oct. 1976).

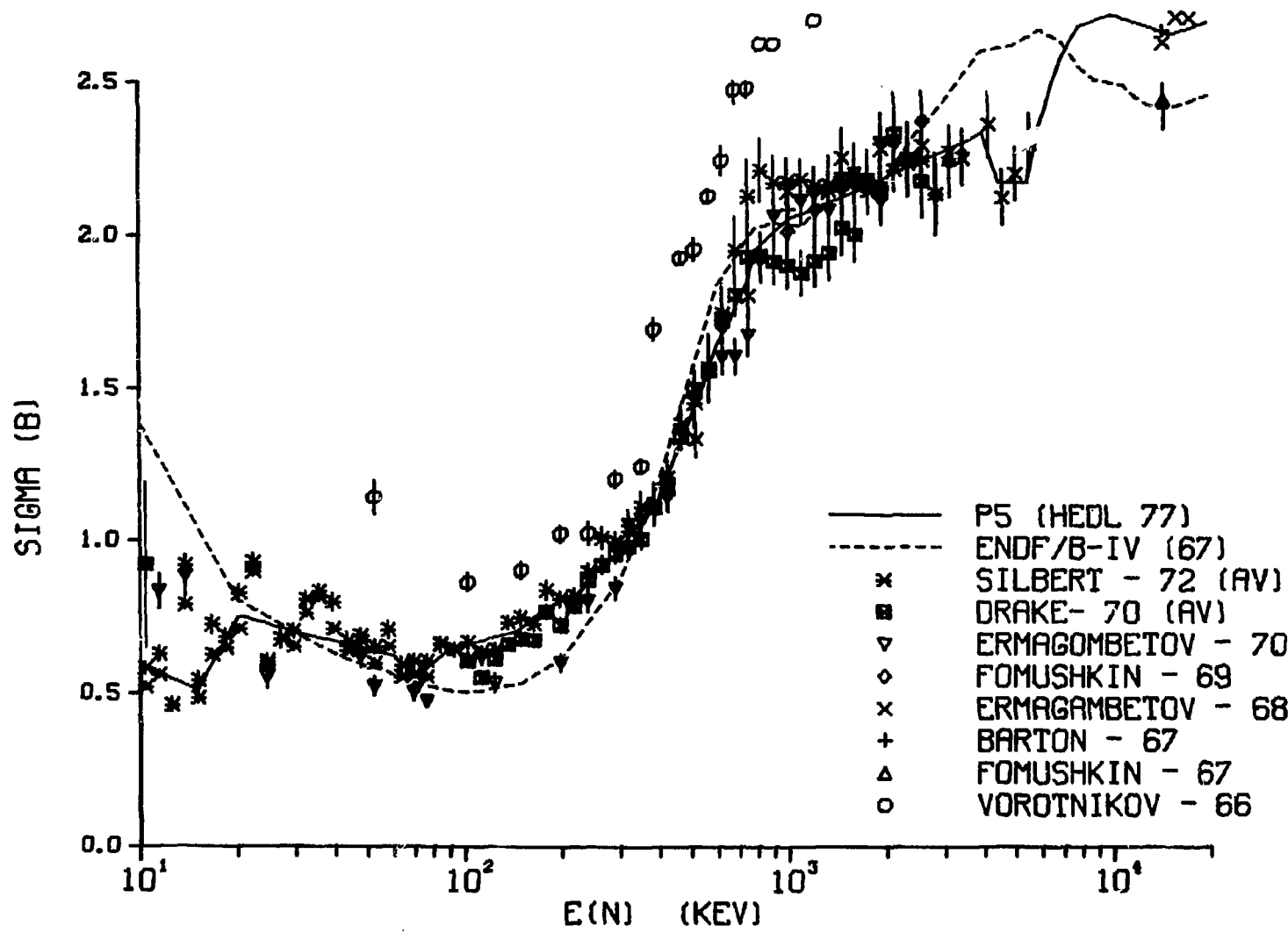


Figure 94-238-1
Pu-238 (N,F)

Eval-Oct78 E. Kujawski (GE-ARSD), L. Stewart (LASL)

94-Pu-239 for ENDF/B-V

Principal evaluators - E. Kujawski (GE-ARSD), L. Stewart (LASL), R. LaBauve (LASL). More details, although somewhat different than the final evaluation, are available in Ref. 1.

Contributing evaluators

Nu-bar - E. Kujawski, R. Howerton (LLL), L. Weston (ORNL), Thermal Task Force
Resolved Res. - Same as ENDF/B-IV
Unresolved Res. - E. Kujawski and E. Pennington (ANL)

Smooth data

Thermal Range - ENDF/B-IV (Ref. 2)
1 eV to 301 eV - ENDF/B-IV
25 keV to 200 keV - E. Kujawski
200 keV to 20 MeV - E. Kujawski, Big 3+2 Task Force
Inelastic Scattering - L. Stewart and R. Hunter (Ref. 3)
Sec. Neut. Dist. - E. Kujawski and L. Stewart
Gamma Prod. - R. Hunter and L. Stewart (Ref. 3)
Covariance File - Capture, Fission, and Nu-bar - E. Kujawski

Bases for evaluations

MF = 1

MT=452 (Nu-bar Total)
Consistent with MT=455 and 456

MT=455 (Delayed)
Delayed neutron yields (Ref. 4)

MT=456 (Prompt) (Ref. 5)
Least squares fits over a number of energy ranges up to 5.5 MeV to data since 1969. Thermal range decoupled from analysis - energy dependence based on Gwin. Normalized with respect to v_t (Cf-252) = 3.766.

MT=458 (Energy Release in Fission)
Evaluation based on work by R. Sher. Not consistent with MF = 5 and MF = 15.

MF = 2

Resolved res.

Primary data sources are Gwin for fission and capture and Derrien for total. Parameters (SLBW) generated by Smith, Kinsey and Garber. Energy range 1 eV to 301 eV - same as ENDF/B-IV.

94-Pu-239
MAT 1399

Unresolved res.

Primary data sources are latest ORELA data (1976) for normalization of capture and fission cross sections. Fine structure based on ENDF/B-IV. Energy dependent parameters obtained by fitting fission and capture data. Energy range - 301 eV to 25 keV. Interpolation should be based on cross sections. Data of ORELA renormalized to B-10(n, alpha) from ENDF/B-V (Ref. 6).

MF = 3

Smooth data

Thermal data

1 eV to 301 eV - Smooth contributions in the resolved range chosen to make combined resonance and smooth fission and capture cross sections consistent with Gwin measurements and total with Derrien. Same as ENDF/B-IV.

25 keV to 200 keV - Average values of fission based on latest ORELA measurements as renormalized to B-10(n, alpha) of ENDF/B-V evaluation. Capture obtained from alpha measurements of Gwin, Weston and Hopkins as evaluated for ENDF/B-IV. Total based on measurements of Smith and Heaton as evaluated for ENDF/B-IV. Inelastic data as evaluated for ENDF/B-IV.

200 keV to 20 MeV - Fission cross sections based on the Pu-239 to U-235 fission ratio measurements of 1) Carlson and Behrens (Ref. 7) 2) Meadows (Ref. 8). Between 12.0 and 20.0 MeV same data as ENDF/B-IV. First, second, third and fourth chance fissions included with MT=18 being the sum. Capture cross sections essentially based on alpha values of ENDF/B-IV.

MF = 4

Angular distributions

Data used from evaluations of Hunter. Primary sources are Coppola and Kamerdiener. Analysis by G. Foster (LASL).

MF = 5

MT=18,19,20,21, and 38

Energy distribution of prompt neutrons uses energy dependent watt spectrum. Up to 1.5 MeV based on data of Johansson (Ref. 9). Energy dependence above 1.5 MeV same as ENDF/B-IV which is based on data of Barnard and Zamyatnin. MT=18 spectrum has average energy consistent with spectra given in MT=19,20,21.

MT=455 Delayed Nu-bar Spectra (Ref. 5)

MF = 8

MT=454 and 459 Inserted into File at BNL by R. Kinsey 9/78

Fission product yield data for Phase I review set 5E, 7/78. Values obtained from the recommendations of the Yields Subcommittee, T.R. England (Chairman), D.M. Gilliam, Y. Harker, J.R. Liaw, W.J. Maeck, D.G. Madland, V. McLane May, P.L. Reeder, B.F. Rider, R.E. Schenter, B.I. Spinrad, J.P. Unik, A. Wahl, W. Walker, B.W. Wehring, and K. Wolfsberg.

Uncertainties are based on the total yield to each ZA. When there is an isomeric state, the independent nuclide yield to each state has a larger uncertainty than the total yield in state distributions (uncertainties average approximately 50 percent but can be larger). Any yield having a large uncertainty (45-64 percent) may be a model estimate or a value assigned to the yields on the wings or valley of the mass yield distribution. These small yields may only be accurate to within a factor of 2.

MT=454 contains direct yields before delayed neutron emission.

MT=459 contains cumulative yields along each isobaric chain after delayed neutron emission.

Direct and cumulative yields are normalized by the same factors based on B.F. Rider evaluation. The isomeric state model, LA-6595-MS (ENDF-241), and delayed neutron emission branchings (PN values) for 102 emitters, LA-UR-78-688, and pairing effects, LA-6430-MS (ENDF-240), have been incorporated.

Data prepared for files by T.R. England (LASL LTR. T-2-L-2891).

94-PU-239 INEL EVAL-Aug78 Reich
Data added to file by R. Kinsey at BNL 9/78
MF=8, MT=457 Radioactive Decay Data

References Q(alpha)-1974 version of WAPSTRA-BOS-GOVE Mass Table Other - Table of Isotopes, 7th ed. (Preliminary Data, Priv. Comm. from C.M. Lederer) and A. Artna-Cohen, Nuclear Data Sheets 6, No. 6, 577 (1977). See also M.R. Schmorak, Nucl. Data Sheets 21, 153 (1977).

Note The energies and intensities of the K-alpha X-rays and of the gamma rays above 38.0 keV are those measured by R. Gunnink, J.E. Evans and A.L. Prindle, UCRL-52139 (Oct., 1976).

Note The L-X-ray data represent measured values. See C.E. Bemis, Jr. and L. Tubbs, ORNL-5297, 93 (Sept., 1977).

Note The energies and intensities of the three most intense alpha groups are those recommended by A. Rytz, At. Data and Nucl. Data Tables 12, No. 5, 479 (1973).

Translated into ENDF/B-V format by Mann and Schenter (HEDL) 8/78

MF = 12-15

Gamma production

Data taken from Hunter and Stewart (Ref. 10). Cross sections based upon neutron files (MF=2,3) and calculated multiplicities. Data above 1.09 MeV based on Drake and Nellis.

MF = 33

Covariance file

- Fission data from 200 keV to 20 MeV (MT=18). Correlated to fission cross section of U-235. Normalization and statistical errors are included.
- Capture data (MT=102) correlated with Pu-239 fission data. Uncertainties in alpha are given.
- Total Nu-bar (MT=452) simplified representation of least square fit.

Principle References

1. Evaluation of Pu-239 Data for ENDF/B-V, GEFR-00247 (October 1977). Note that some of the presented data was preliminary in nature and therefore different from the final ENDF/B-V evaluation.
2. ENDF/B-IV.
3. R.E. Hunter, et al., LA-5172 (1973).
4. Data for Nu-Prompt.
D.S. Mather and P.F. Bampton, AWRE/0-86/70 (1970).
M.V. Savin, et al., in Proc. 2nd Intern. Conf. Nuclear Data for Reactors, (IAEA, 1970), p. 157.
Bolodin, et al., Atom. Energy 33, 901 (1972).
R.L. Walsh and J.W. Boldeman, Annals. Nucl. Sci. Eng. 1, 353 (1974).
R. Gwin, Private Communication.
5. R.E. Kaiser and S.G. Carpenter (ANL-West), Priv. Comm., Mar. 1978.
6. R. Gwin, et al., Nucl. Sci. Eng. 59, 79 (1976).
7. G.W. Carlson and J.W. Behrens, Nucl. Sci. Eng. 66, 205 (1978).
8. J.W. Meadows, Nucl. Sci. Eng. 68, 360 (1978).
9. P.I. Johansson, et al., Precision Measurements of Fission Neutron Spectra of U-235, U-238, Pu-239, presented at the Fifth Conference on Neutron Cross Sections and Technology (March 1975).
10. R.E. Hunter and L. Stewart, LA-4901 (1972).

94-Pu-240
MAT 1380

Summary Documentation

^{240}Pu

ENDF/B-V

Mat = 1380

L. W. Weston and R. Q. Wright

September 1, 1978

The present evaluation supersedes the ENDF/B-IV evaluation by E. Pennington and H. Hummel (1974). Changes from the earlier evaluation were in nubar, resonance parameters, fission cross sections, capture cross section, fission product yield data, radioactive decay data, and error files.

File 1, MT=452

Prompt nubar ratios to Cf of Frehaut¹ were used to derive nubar. Nubar prompt of Cf was assumed as 3.741. Delayed nubar was unchanged.

File 2, MT=151

Resolved resonance region extends from 10^{-5} eV to 3.91 keV. The resonance at 1.058 eV which dominates the thermal neutron energy region was made to agree with the Weigmann² and Caner and Yiftah³ evaluations. From 20 to 665 eV the resonance parameters are the weighted averages of those reported by Weigmann,⁴ Moxon,⁵ and Hockenbury.⁶ Resonance parameters above 665 eV are unchanged and were derived from Kolar and Bockhoff.⁷ Fission widths for the 20.46 and 38.32 eV resonances are from Weigmann² and the others from Migneco⁸ or Auchampaugh⁹ or the weighted average of the values. The parameters of the unresolved region from Frehaut¹ which agree with the data of Hockenbury⁶ and Weston¹⁰ on the average capture cross section.

File 3, MT=1 and 2

The scattering cross section was unchanged so that the changes in the total cross section reflect the changes in the fission and capture cross sections.

File 3, MT=18

No smooth fission cross section in the resonance region. From 40 keV to 1 MeV the fission cross section was derived from the ratio measurements of Behrens.¹¹ From 1 to 2.75 MeV is a compromise between the ratio measurements of Behrens,¹¹ Gilboy,¹² and Savin.¹³ Above 2.75 MeV the fission cross section was derived from the ratio measurements of Behrens.¹¹ The ENDF/B-V evaluation of the ^{235}U fission cross section was used to convert the ratio measurements to the fission cross section of ^{240}Pu .

File 3, MT=19

First chance fission was assumed constant above the threshold for second chance fission at 5.5 MeV.

File 3, MT=20

Second chance fission was derived by subtracting MT=19 from MT=18 from 6 to 13 MeV and was assumed constant above 13 MeV.

File 3, MT=21

Third chance fission was derived by subtracting MT=19 and 20 from MT=18.

File 3, MT=102

The average capture cross section in the resolved resonance region from 200 eV to 3.91 keV was forced to agree with Weston¹⁴ in decade

type intervals. There are no smooth capture cross sections in the unresolved resonance region. From 40 to 250 keV the capture cross section was based on Weston.¹⁰ The capture cross section blends back to ENDF/B-IV at 400 keV.

File 5, MT=455

Delayed neutron secondary energy distribution was Kaiser and Carpenter¹⁴ data transmitted by E. Pennington and inserted by R. Kinsey.

File 8, MT=454 and 459

MT=454 contains direct yields before delayed neutron emission. MT=459 contains cumulative fission product yields along each isobaric chain after delayed neutron emission. Values were obtained from the recommendations of the yields subcommittee, T. R. England (Chairman).

File 8, MT=457

Radioactive decay data evaluated by C. Reich, April 1978.

File 32, MT=151

Resonance parameter error file from 0.5 to 105 eV. Uncertainties were based on the differences in the measurements because quoted errors were not consistent.

File 33, MT=102

Broad group error file for the capture cross section. The file is subjective because of insufficient data for statistical analysis.

References

1. J. Frehaut et al., Proc. Second All-Union Conf. on Neutron Physics, Part 3, 153 (1974).
2. H. Weigmann and J. P. Theobald, J. Nucl. Energy 26, 643 (1972). See also reference 7.
3. M. Caner and S. Yiftah, IA-1243 (1972), Israel Atomic Energy Commission.
4. H. Weigmann, G. Rohr, and F. Poortmans, Proc. Conf. Resonance Parameters of Fertile Nuclei and ^{239}Pu , Saclay, 219 NEANDC(E) 163U (1974).
5. M. Moxon, Proc. Conf. Resonance Parameters of Fertile Nuclei and ^{239}Pu , Saclay, 219, NEANDC(E) 163U (1974).
6. R. W. Hockenbury, W. R. Moyer, and R. C. Block, Nucl. Sci. Eng. 49, 153 (1972).
7. W. Kolar and K. H. Bockhoff, J. Nucl. Energy 22, 299 (1968).
8. E. Migneco and J. P. Theobald, Nucl. Phys., A112, 603 (1968).
9. G. F. Auchampaugh and L. W. Weston, Phys. Rev. C12, 1850 (1975).
10. L. W. Weston and J. H. Todd, Nucl. Sci. Eng. 63, 143 (1977).
11. J. W. Behrens, J. C. Browne, and G. W. Carlson, UCID-17047, LLL (1976).
12. W. B. Gilboy and G. Knoll, KFK-450, Kernforschungszentrum (1966).
13. M. V. Savin et al., INDC(CCP)-8/U (1970).
14. R. E. Kaiser and S. G. Carpenter (ANL-West) private communication.

Summary Documentation

^{241}Pu

ENDF/B-V

Mat = 1381

L. W. Weston, R. Q. Wright, and R. J. Howerton

The present evaluation supersedes the ENDF/B-IV evaluation by H. Hummel and E. Pennington (1974). Changes from the earlier evaluation were in nubar, resonance parameters, fission cross section, capture cross section, gamma-ray production, (n,xn) reactions, fission product yield data, radioactive decay data, and error files.

File 1, MT=452, 455, and 456

Thermal, total nubar of 2.953 was used as recommended by CSEWG in 1978. Nubar prompt of CF assumed as 3.757. Nubar for ^{241}Pu kept constant to 0.47 MeV and based on the energy dependance measured by Frehaut¹ at higher energies. Delayed nubar unchanged from Kaiser and Carpenter² evaluation except at thermal.

File 2, MT=151

The resolved resonance region extends from 2.873 to 100 eV in the Adler-Adler formalism. The resonance parameters of Blons³ and Weston⁴ were given the most weight with some weight given to Moore,⁵ James,⁶ Simpson,⁷ and Carlson.⁸ Renormalizations were done for better agreement with Wagemans.⁹ The unresolved resonance parameters were adjusted to reflect the observed average structure in fission and capture.

94-Pu-241
MAT 1381

File 3, MT=1 and 2

At neutron energies above the unresolved resonance region (40.2 keV) the scattering cross section was not changed so that the total cross section reflects changes in the fission and capture cross section.

File 3, MT=18

The thermal region fission cross section was based on Wagemans³ and Weston.⁴ Above 40.2 keV the fission cross section was based on the ratio measurements of Behrens,¹⁰ Käppeler,¹¹ and Szabo¹² with the most weight given to the data of Behrens.¹⁰ The ENDF/B-V evaluation of the ²³⁵U fission cross section was used to convert the ratios to the fission cross section of ²⁴¹Pu.

File 3, MT=102

The capture cross section was based on the data of Weston.⁴ Only slight changes were made above 40.2 keV.

File 5, MT=16 and 17

The (n,2n) and (n,3n) cross sections were revised by R. J. Howerton.

File 5, MT=18

Fission neutron energy distribution given as a simple fission spectrum plus a Maxwellian (AWRE 0-101/64).

File 5, MT=91

Inelastic scattering evaluated by R. J. Howerton.

File 5, MT=455

Delayed neutron secondary energy distribution based on Kaiser and Carpenter² as evaluated by E. Pennington (1978).

File 8, MT=454 and 459

MT=454 contains direct yields before delayed neutron emission. MT=459 contains cumulative fission product yields along each isobaric chain after delayed neutron emission. Values were obtained from the recommendations of the yields subcommittee, T. R. England (Chairman).

File 8, MT=457

Radioactive decay data evaluated by C. Reich, April 1978.

File 12, MT=18

Fission gamma-ray spectrum is data of Peelle and Maienschein¹³ for ²³⁵U thermal fission spectrum.

File 12, MT=102

Capture gamma-ray spectrum is the ²³⁸U spectrum adjusted for multiplicity and energy conservation.

File 13, MT=3

Photon production cross sections evaluated by R. J. Howerton.

File 15, MT=3, 18, and 102

Energy distribution of photons evaluated by R. J. Howerton. For fission the data of Peelle and Maienschein¹³ for ²³⁵U was used with the evaluation method described by Perkins.¹⁴

File 33, MT=18 and 102

Broad group error files for the fission and capture cross sections. Evaluation of error files was subjective because of insufficient data for statistical analysis.

References

1. J. Frehaut et al., CEA-R-4626 (1974).
2. R. E. Kaiser and S. G. Carpenter (ANL-west) Private Communication (1977).
3. J. Blons, Nucl. Sci. Eng. 51, 130 (1973).
4. L. W. Weston and J. H. Todd, Nucl. Sci. Eng. 65, 454 (1978).
5. M. S. Moore et al., IDO-16976 (1964).
6. G. D. James, Helsinki Conf., Vol. 1, 267 (1970).
7. O. D. Simpson et al., Proc. Cross Sections and Tech. Conf., Washington, II, 910 (1966).
8. G. W. Carlson, J. W. Behrens, and J. B. Czirr, Nucl. Sci. Eng. 63, 149 (1977).
9. C. Wagemans and A. J. Deruytter, Proc. Conf. Nuclear Cross Sections and Tech., Washington, NBS-425, II, 603 (1975).
10. J. W. Behrens and G. W. Carlson, UCRL-51925 (1975).
11. F. Käppeler and E. Pfletschinger, Nucl. Sci. Eng. 52, 124 (1973).
12. I. Szabo et al., Symp. Neutron Standards, Argonne, 257 (1970).
13. R. W. Peelle and F. C. Maienschein, Nucl. Sci. Eng. 40, 485 (1970).
14. S. T. Perkins, R. C. Haight, and R. J. Howerton, Nucl. Sci. Eng. 57, 1 (1975).

SUMMARY DOCUMENTATION FOR ^{242}Pu

by

F. Mann and R. Schenter
Hanford Engineering and Development Laboratory
Richland, Washington

and

D. G. Madland and P. G. Young
Los Alamos Scientific Laboratory
Los Alamos, New Mexico

I. SUMMARY

A new evaluation of neutron-induced reactions on ^{242}Pu was performed for Version V of ENDF/B (MAT 1342). The analysis was divided between HEDL, where the resolved and unresolved resonance regions were evaluated, and LASL, where the data above a neutron energy of 10 keV were evaluated. These evaluations are documented in HEDL-TME-77-54 (Ma77B) and LASL-7533-MS (Ma78). Additionally, decay data were provided by C. Reich (INEL), thermal data by R. Benjamin (SRL), and gamma-ray production data by R. Howerton (LLL). The evaluation covers the energy range 10^{-5} eV to 20 MeV and includes covariance data at all energies.

II. ENDF/B-V FILES

File 1. General Information

MT=451. Descriptive data

MT=452. $\bar{\nu}$ Total

Sum of MT=456 and a delayed $\bar{\nu}$ of 0.015 from the measurement of Kr70 as compiled by Ma72.

MT=456. $\bar{\nu}$ Prompt

Based on a fit to ^{240}Pu experimental data by Fr74 using systematics to infer delta $\bar{\nu}$ to ^{242}Pu , and renormalized to ^{252}Cf thermal $\bar{\nu}$ of 3.757.

MT=458. Energy of Fission

Based on work of Sh76.

File 2. Resonance Parameters (E_n=0-10 keV)

MT=151. (a) Resolved Resonances

The resolved resonance region covers the energy range 0-986 eV. One bound level and 67 resolved resonances describe the cross section data from zero to 986 eV. Except for the bound and 2.68 eV levels, parameters are from BNL-325 (Mu76). Parameters for the bound and 2.68 eV levels have been modified to preserve the cross section values and shapes in the thermal region as described by Yo70 and Yo71, along with the higher resonance capture integral suggested by integral and production experiments (Bu57, Ha64, and Be75).

(b) Unresolved Resonances

The unresolved resonance region covers the energy range from 986 eV to 10 keV. Average parameters obtained by averaging the resolved resonance data were used for the L=0 resonances. The remaining data were obtained from MAT 1161, ENDF/B-IV.

File 3. Neutron Cross Sections

General

Evaluation from 0.01 - 20 MeV described in Ma78. Statistical compound nucleus and direct reaction theory calculations performed with LASL versions of COMNUC (Du70, 3-29-78 version) and JUKARL (Re71). All calculations used LASL preliminary global actinide optical potential (Ma77). Complete set of calculations performed but elastic and fission cross section evaluations differ slightly (less than 5%) from calculations because of influence of fission measurements. (n,f), (n,nf), and (n,2nf) cross sections calculated subject to constraint that their sum equals measured (Be78) total fission cross section within 5%. Discrete fission channels (up to 12) and deformed level density continuum fission channels used.

MT=1. Total Cross Section

Spherical optical model calculation with nuclear deformation effects accounted for by coupled-channel calculations of up to 5 states of ground state band.

MT=2. Elastic Cross Section

Difference between MT=1 and MT=4, 16, 17, 18, and 102. Agrees with model calculation to within few per cent.

MT=4. Inelastic Scattering Cross Section

Sum of MT=51-69 and MT=91.

MT=16, 17 (n,2n) and (n,3n) Cross Sections

Based on compound nucleus statistical model calculations.

MT=18. Fission Cross Sections

Below 100 keV based on experimental data of Au71. From 0.1 to 20 MeV based on experimental data of Be78 (see Figs. 1 and 2).

MT=51-54. Discrete Inelastic Cross Sections

Based on Hauser-Feshbach compound nucleus calculation and coupled-channel calculation of direct inelastic scattering for first 5 levels of ground state rotational band using deformation parameters of Be73.

MT=55-69. Discrete Inelastic Cross Sections

Based on Hauser-Feshbach compound nucleus calculation.

MT=102. Capture Cross Sections

Based on compound nucleus statistical calculation with gamma strength function adjusted to agree with Ho75 measurements $2\pi\Gamma_\gamma/D = 0.01045$, Mu73). Above 4 MeV, semi-direct contribution added from preequilibrium cascade calculation with gamma-ray emission probability, calculated at each stage (Ar78). See Fig. 3 for comparison with measurements.

File 4. Neutron Angular Distributions

MT=2. Elastic Scattering Angular Distributions

Shape elastic component based on deformed optical model calculation. Compound nucleus component assumed isotropic. All distributions given in form of Legendre coefficients.

MT=16, 17, 18. (n,2n), (n,3n), and (n,f) Angular Distributions

Given as Legendre coefficients and assumed isotropic in the laboratory system.

MT=51-54. Discrete Inelastic Angular Distributions (A)

Direct component taken from deformed optical model calculation, and compound nucleus component assumed isotropic. Given in form of Legendre coefficients.

MT=55-69. Discrete Inelastic Angular Distributions (B).

Legendre coefficient representation assumed isotropic in the center-of-mass system.

94-Pu-242
MAT 1342

MT=91. Continuum Inelastic Angular Distributions

Legendre coefficient representation assumed isotropic in the laboratory system.

File 5. Neutron Energy Distributions

MT=16, 17. (n,2n), (n,3n) Energy Distributions

Nuclear temperatures calculated from level density parameters used in model calculations (Gi65 and Co67).

MT=18. (n,f) Neutron Energy Distributions

Fission Maxwellian using energy-dependent temperatures from Terrell (Te65).

MT=91. Continuum Inelastic Neutron Energy Distributions

Nuclear temperatures calculated from level density parameters used in nuclear model calculations (Gi65 and Co67).

File 8. Fission-Product Yield and Nuclide Decay Data

MT=454. Fission Yield Data

Fission-product yields were obtained from the recommendations of the CSEWG Yields Subcommittee (T. R. England chairman).

MT=457. Decay Data

The Q (alpha) was obtained from the 1974 version of the Wapstra-Bos-Gove mass tables. Half-life values were taken from reference Va74, and other data were obtained from the Table of Isotopes (Le77) and Nuclear Data Sheets (E70). Note that the energies and intensities of the two highest energy alpha groups are those recommended by Rytz (Ry73).

All the decay data were translated into ENDF/B-V format by Mann & Schenter (HEDL, 6/76).

Files 12-15. Photon-Production Data

Files taken from the LLL evaluations of R. Howerton (Ho76). Files extended to the energy range 1.0^{-5} eV to 20 MeV and merged to this evaluation at BNL by R. Kinsey.

File 33. Neutron Cross Section Covariances (HEDL and LASL)

Approximate error files determined from estimated uncertainties in model calculations (MT=1, 2, 4, 16, 17, 102) and in experimental measurements (MT=18, 102).

REFERENCES

Ar78 E. D. Arthur, private communication (1978).
Au71 G. F. Auchampaugh, J. A. Farrell, and D. W. Bergen, Nucl. Phys. A171, 31 (1971).
Be73 C. E. Bemis et al., Phys. Rev. C8, 1466 (1973).
Be75 R. Benjamin et al., DP-1394 (1975).
Be78 J. W. Behrens et al., Nuc. Sci. Eng. 66, 433 (1978).
Bu57 J. Butler et al., Can. J. Phys. 35, 147 (1957).
Co67 J. L. Cook et al., Aust. J. Phys. 20, 477 (1967).
Du70 G. L. Dunford, AI-AEC-12931 (1970).
El70 Y. A. Ellis, Nucl. Data Sheets B4, #6, 683 (1970).
Fr74 J. Frehaut et al., CEA-R-4626 (1974).
Gi65 A. Gilbert and A. G. W. Cameron, Can. J. Phys. 43 1446 (1965).
Ha64 J. Halperin et al., ORNL-3679, 13 (1964).
Ho75 R. W. Hockenbury et al., NBS Special Publication 425, Vol. 2, p. 584, (1975).
Ho76 R. Howerton et al., UCRL-50400, Vol. 15, Part A (Methods, 1975) and Part B (Curves, 1976).
Kr70 M. S. Krick and A. E. Evans, Trans. Am. Nucl. Soc. 13, 746 (1970).
Le77 C. M. Lederer, Table of Isotopes, 7th Ed (preliminary data received in private communication, 1977).
Ma72 F. Manero and V. Konshin, At. En. Rev. 10, 637 (1972).
Ma77 D. Madland, LA-7066-PR, p. 12 (1977).
Ma78 D. G. Madland and P. G. Young, LA-7533-MS (1978).
Mu73 S. Mughabghab and D. Garber, BNL-325, 7th Ed., Vcl. 1 (1973).
Re71 H. Rebel and G. W. Schweimer, KFK-133 (1971).
Ry73 A. Rytz, At. Data and Nucl. Data Tables 12, #5, 479 (1973).
Sh76 R. Sher, S. Fiarman, and C. Beck, private communication (Oct. 1976).
Va74 R. Vaninbroukx, Euratom report EUR-5194E (1974).
Wi78 K. Wissak and F. Käppeler, Nucl. Sci. Eng. 66, 303 (1978).
Yo70 T. Young and S. Reeder, Nucl. Sci. Eng. 40, 389 (1970).
Yo71 T. Young et al., Nucl. Sci. Eng. 43, 341 (1971).

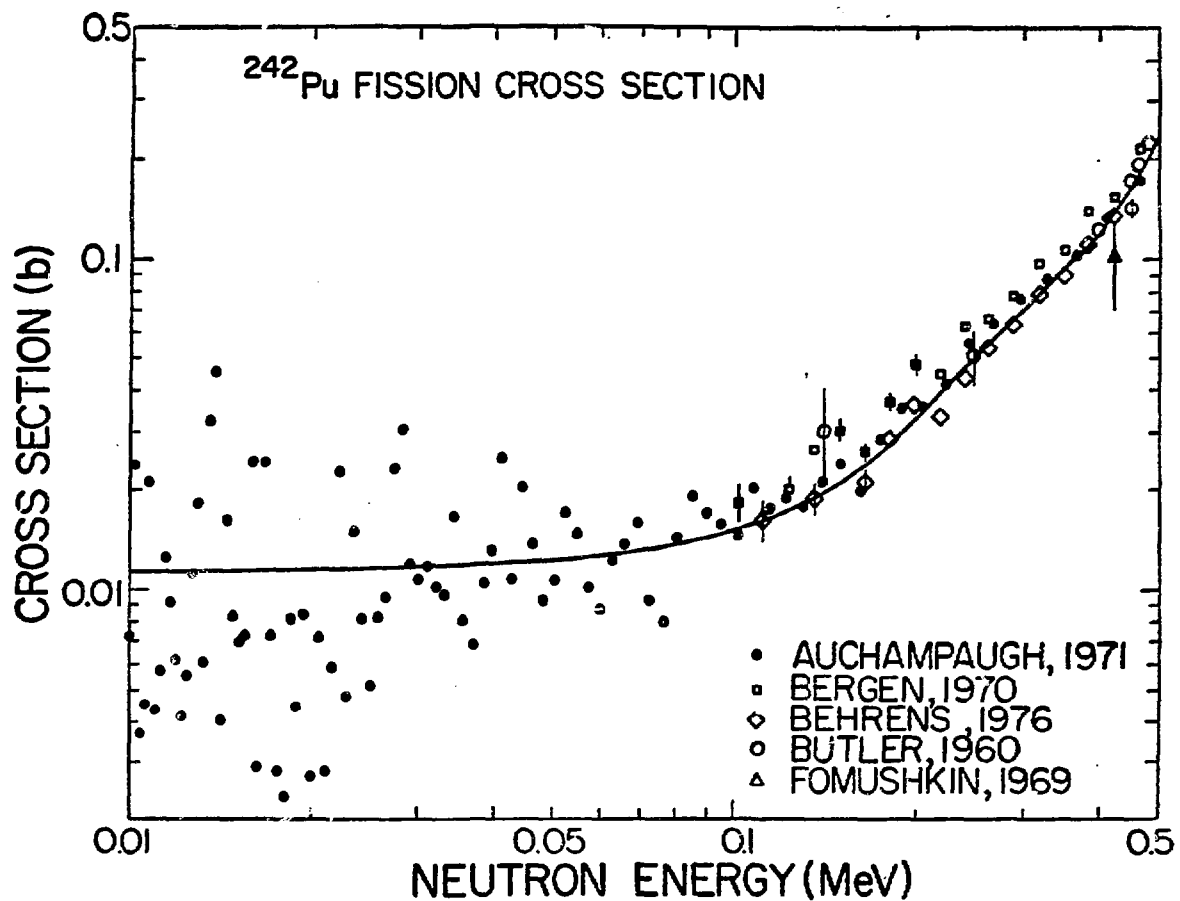


Fig. 1.

Experimental and evaluated cross sections for the $^{242}\text{Pu}(n,f)$ reaction from 10 keV to 0.5 MeV. The evaluated curve is based upon the Auchampaugh (Au71) and Behrens (Be76) ratio measurements relative to the $^{235}\text{U}(n,f)$ reaction. The values shown here were converted using a preliminary evaluation of the $^{235}\text{U}(n,f)$ cross section and will be adjusted by up to 4% in the final evaluation.

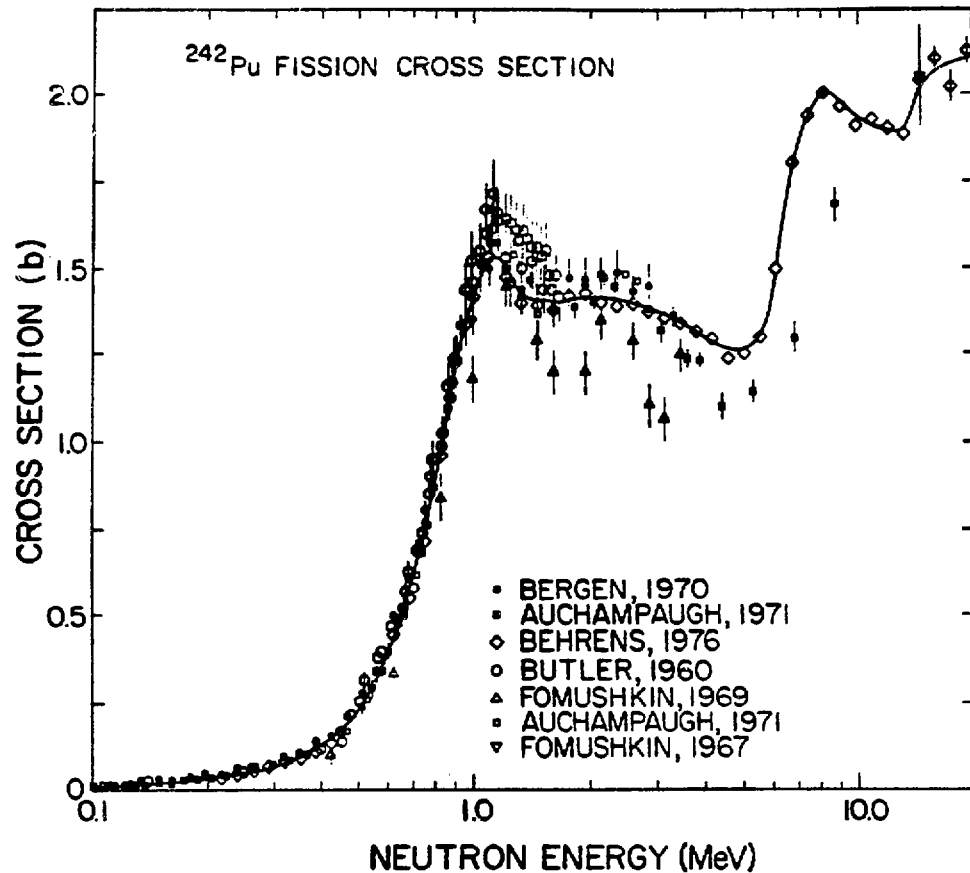


Fig. 2.

Experimental and evaluated cross sections for the $^{242}\text{Pu}(n,f)$ reaction from 0.1 to 20 MeV. See caption for Fig. 1.

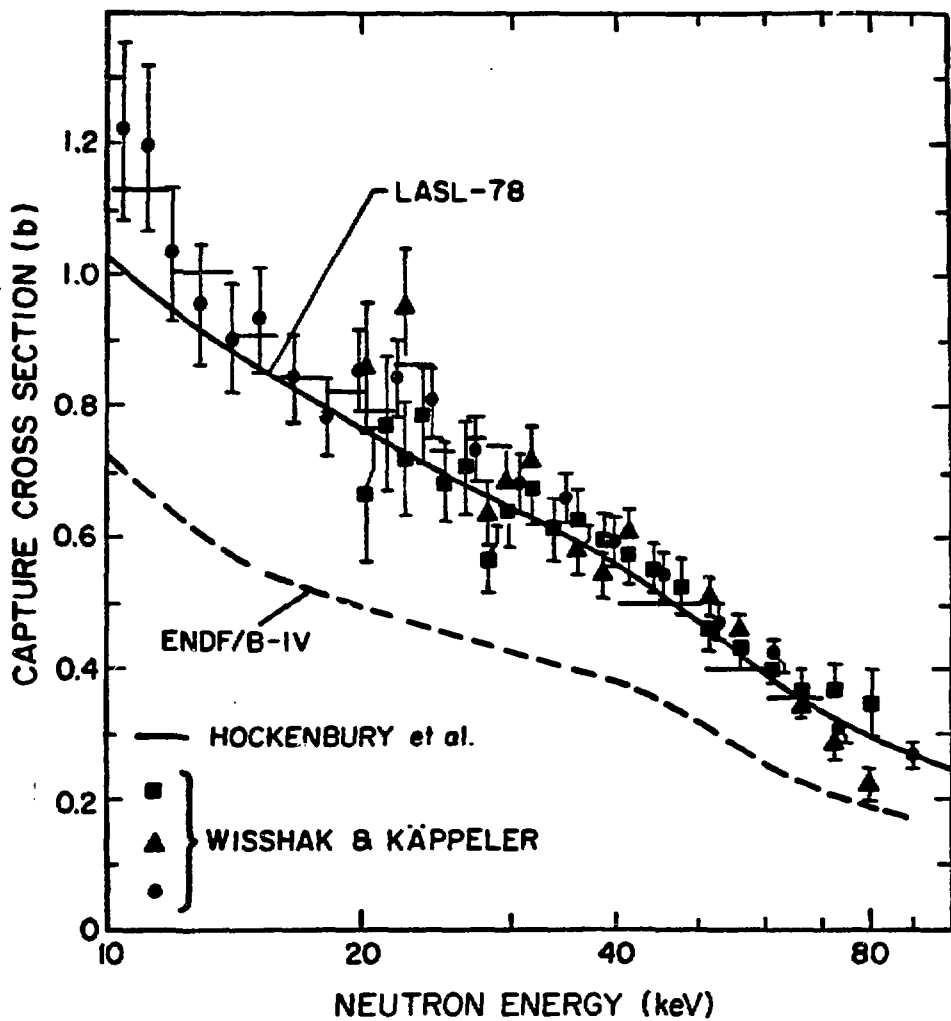


Fig. 3.

Experimental and evaluated cross section for the $^{242}\text{Pu}(n,\gamma)$ reaction between 10 and 100 keV. The experimental data are from Hockenbury (Ho75) and Wissak and Käppeler (Wi78).

ENDF/B-V Summary Documentation

Isotope: 95-Am-241 MAT = 1361

F.M. Mann and R.E. Schenter	(HEDL)	Apr '78
L. Weston	(ORNL)	Apr '78
C.R. Reich	(INEL)	Apr '78
R.J. Howerton	(LLL)	Apr '78

The present work supersedes the ENDF/B-IV evaluation, MAT = 1056 by Smith and Grimesey. Neutron and photon production data are given between 10^{-5} eV and 20 MeV. The cross sections included are total, elastic, inelastic, (n,f), (n,2n), (n,3n), (n,n'γ), and (n,γ) and are described in HEDL-TME-77-54 (ref. 3). The photon data include multiplicities and transition probabilities, photon production cross sections, and secondary energy spectra.

MF=1 General information.MT=452

Nu. A weighted average of the individual determinations of nu assigns most of the weight to the data of V.I. Lebedev et al., (ref. 1) using the value of nu for 235 of 2.43, nu=3.09 is obtained for the constant term. The slope is that of the universal curve of J.C. Hopkins and B.C. Diven (ref. 2) from ENDF/B-I.

MT=485

Energy from fission based on Sher (ref. 13).

MF=2 Resonance information.MT=151

Resolved resonance parameters (0-50 eV) from Ref. 10 and 11. Unresolved parameters obtained using methods from ref. 3 and data from ref. 10 and 11.

MF=3 Smooth cross section.

95-241
MAT 1361

MT=1

Total sum of partial cross sections

MT=2

Elastic. Result of optical model calculation (ref. 5)

MT=4

Inelastic result of statistical model calculations. 18 levels were included (ref. 3).

MT=16

n, 2n based on statistical model calculations (ref. 3)

MT=17

n, 3n based on statistical model calculations (ref. 3)

MT=18 (Figure 95-241-1 and -2)

Fission. Below 400 keV, result of statistical model calculation (ref. 3) guided by data of Bowman et al., (ref. 4) and Sphak et al., (ref. 5). Above 400 keV, average of data of Sphak et al., (ref. 5), Seeger et al., (ref. 6), Fomushkin et al., (ref. 7, 8), and Iver et al., (ref. 9).

MT=19

(n,f) same as MT=18 until (n,nf) threshold, constant thereafter.

MT=20

(n,nf) difference between MT=18 and 19.

MT=51...68.91

Result of statistical model calculations using 18 excited levels plus continuum (ref. 3).

MT=102 (Figure 95-241-3 and -4)

Capture statistical model calculation (ref. 3) based on data of Weston and Todd (ref. 10). In resolved resonance background of $20.5/\text{SQRT}(E)$ from ref. 10.

MF=4 Angular distributions.

MT=2

Evaluation based on optical model (ref. 3).

MT>2

Inelastic assumed isotropic.

MF=5 Energy distribution.

MT=16

Evaporation temp. from Gilbert and Cameron (ref. 12).

MT=17

Same reference as MT=16.

MT=18

Simple Maxwellian with energy dependent temperature.

MT=19

Same reference as MT=18.

MT=20

Same reference as MT=18.

MT=91

Same reference as MT=16.

MF=8 Radioactivity.

95-AM-241
MAT 1361

MT=102

(n,γ) decay chain from ENDF/B-V.

MF=8, MT=457

Radioactive decay data. Q(alpha)-1974 version of Wapstra-Bos-Gove mass table; half-life-weighted average of data of H. Ramthun and W. Muller, Int L. J. Appl. Rad. and Isotopes 26, 589 (1975) and of F.L. Oetting and S.R. Gunn, J. Inorg. Nucl. Chem. 29, 2659 (1967). Spontaneous-fission branching ratio derived from listed half-life and weighted average of S.-F. half-life values of R. Gold et al., Phys. Rev. C 1, 738 (1970) and of D. Galliker et al., Helv. Phys. Acta 43, 593 (1970. Other - see table of isotopes, 7th ed. (preliminary data, priv. comm. from C.M. Lederer) and Y.A. Ellis, Nuclear Data Sheets 6, No. 6, 621(1971).

Note: The K-X-ray intensities listed are measured values.

Note: Energies and intensities of the ground-state alpha and the two most intense alphas are taken from A. Rytz, At. Data and Nucl. Data Tables 12, No. 5, 479 (1973).

Note: The L-X-ray data are those of J.L. Campbell and L.A. McNelles, Nucl. Instrum. and Methods 117, 519 (1974).

Note: The gamma-ray intensities (except those of the 55- and 67-keV gammas) are those reported by R. Gunnink, J.E. Evans and A.L. Prindle, UCRL-52139 (Oct., 1976). Those of the 55- and 67-keV gammas are deducted from the internal-conversion coefficients and intensity-balance considerations.

MF=9 Cross section branching.

MT=102

(n,γ) from statistical model calculation (ref. 3 and 10).

95-Am-241
MAT 1361

MF=12, 13, 14, 15

Photon production. Files taken from the LLL evaluations of R. Howerton documented in UCRL 50400, Vol. 15, Part A (methods) Sept. '75 and Part B (curves) Apr. '76.

MF=32, 33 Error files.

MT=1, 2, 4, 16, 17, 18, 102, and 151

95-241-5

95-Am-241
MAT 1361

References

1. V.I. Lebedev et al., Atomnaya Energiya 52(1958)176.
2. J.C. Hopkins and B.C. Diven, Nucl. Phys. 48(1963)433.
3. F.M. Mann and R.E. Schenter, Trans. Amer. Nucl. Soc., 23(1976)546 and HEDL TME 77-54 (1977).
4. C.D. Bowman, and M.S. Coops, G.F. Auchampaugh, and S.C. Fultz, Phys. Rev. 137B(1965)326.
5. D.L. Sphak, Jv.B. Ostapenko, and G.N. Smirenkin, ZEP 9(1969)196.
6. P.A. Seeger, A. Hemmendinger, and B.C. Diven, Nucl. Phys. A96 (1967)605, LA-3586(1966).
7. E.F. Fomushkin et al., YF 5(1967)966.
8. V.F. Fomushkin and E.K. Gutnikova, Sov. J. Nucl. Phys. 10(1970)529.
9. R.H. Iyer and R. Sampathkumar, BARC 474(1970).
10. F.M. Mann and R.E. Schenter, Nucl. Sci. and Eng. 63(1977)252.

95-AR-241
MAT 1361

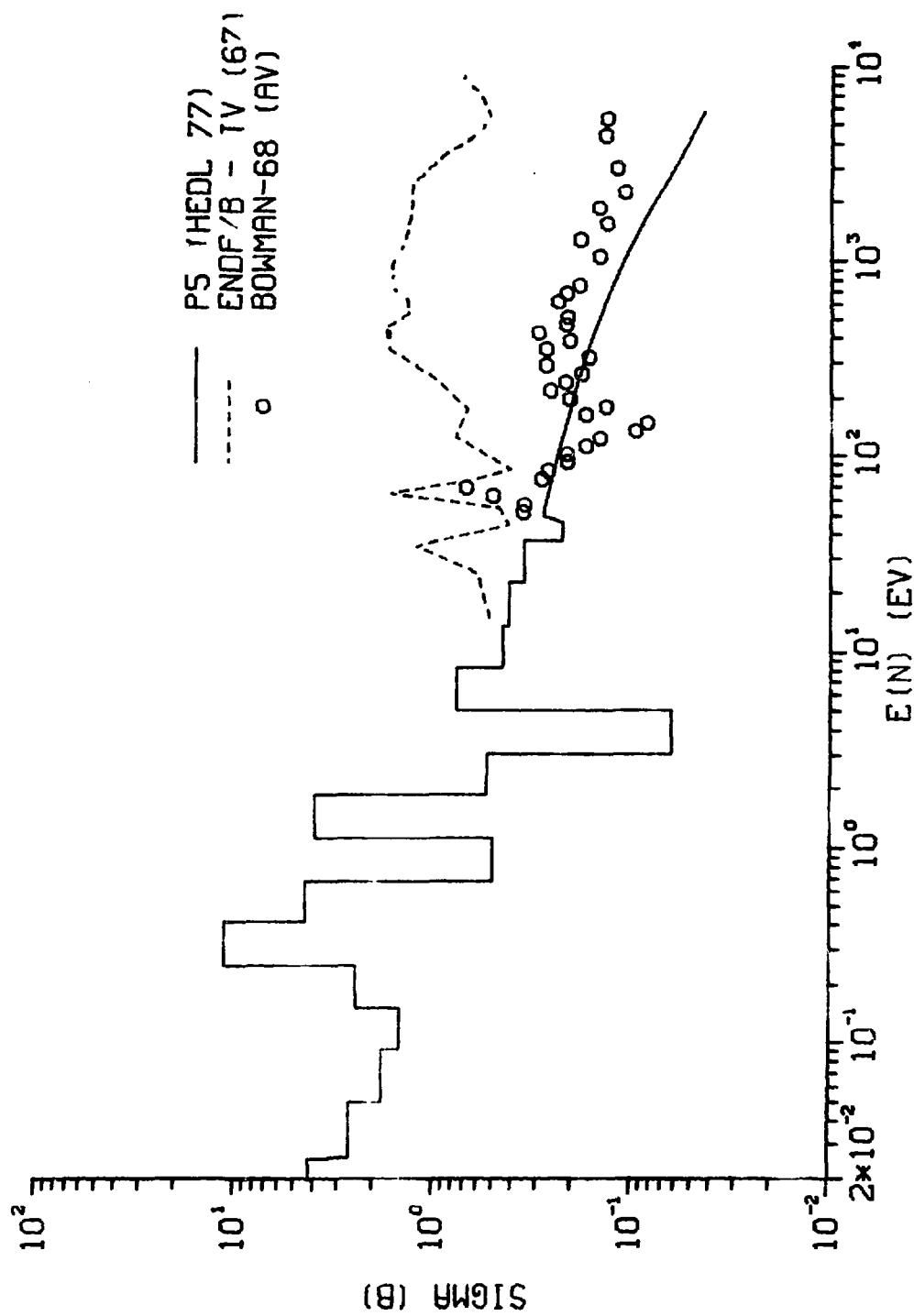


Figure 95-241-1
Am 241 (N,F)

95-241-7

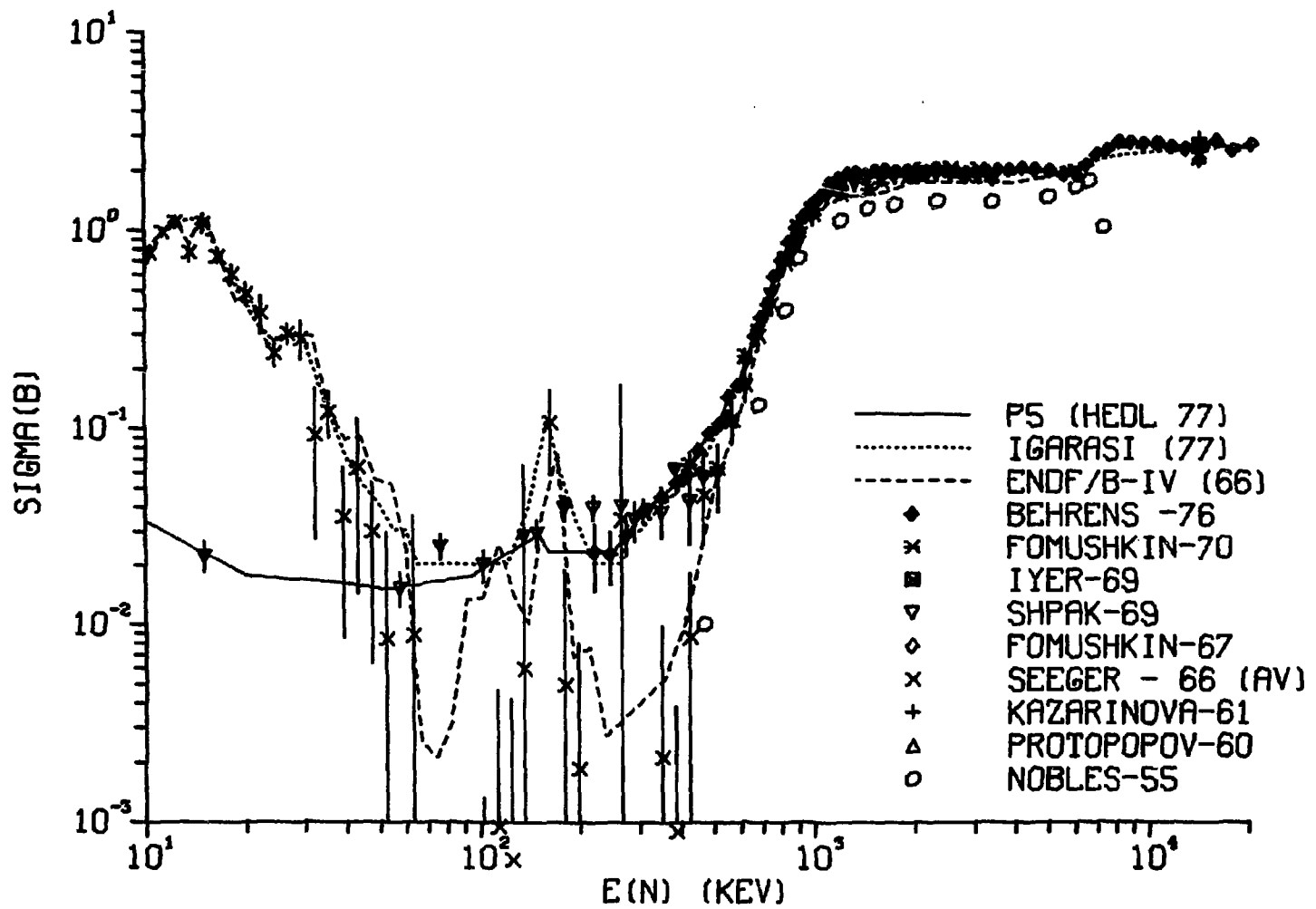


Figure 95-241-2
Am 241 (N,F)

95-Am-241
MAT 1361

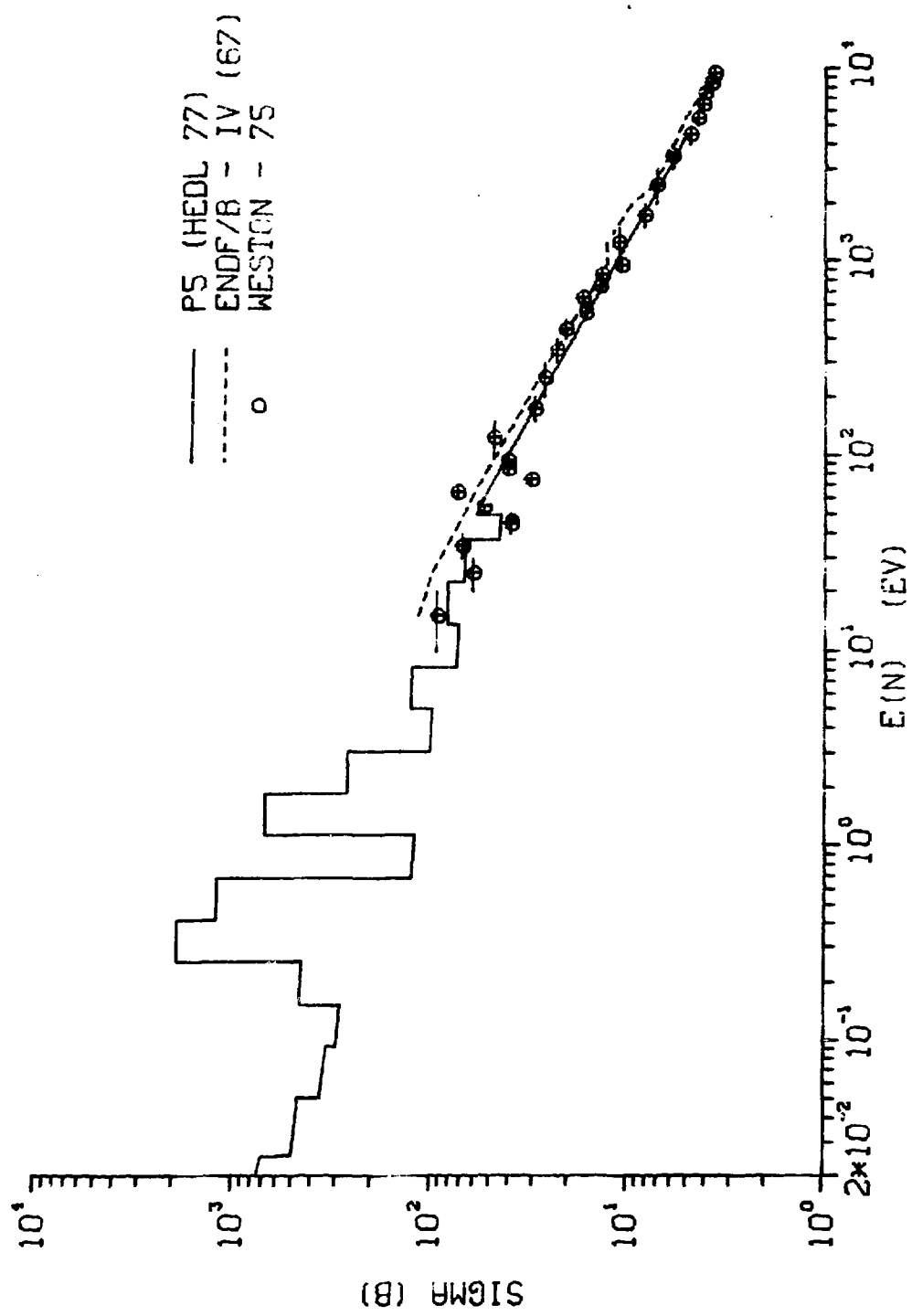


Figure 95-241-3

Am 241 (N,G)

95-241-9

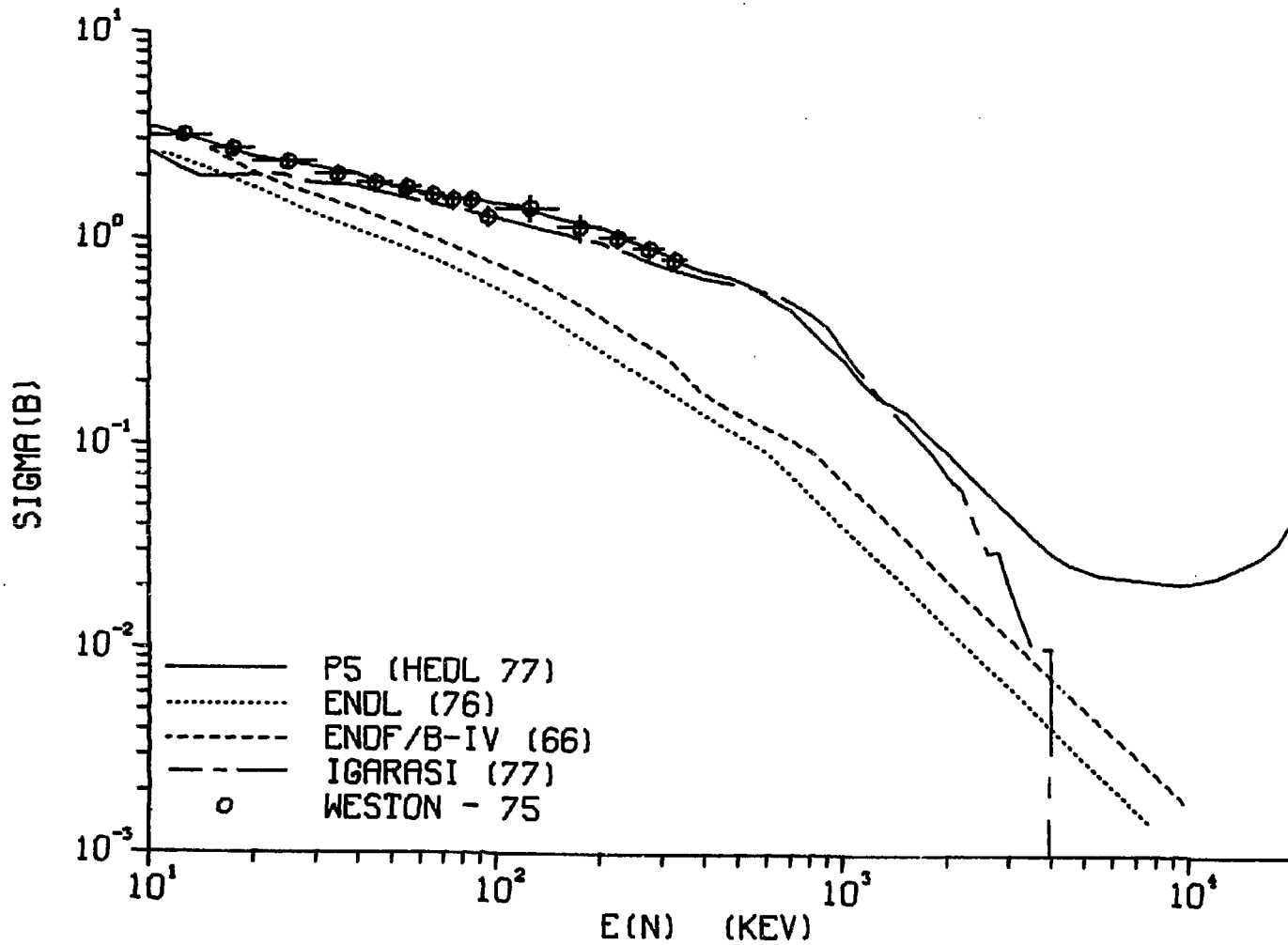


Figure 95-241-4
Am 241 (N,G)

ENDF/B-V Summary Documentation

Isotope: 95-Am-242* MAT = 1369

F.M. Mann and R.E. Schenter	(HEDL)	Apr. '78
R. Benjamin	(SRL)	Oct. '75
R.J. Howerton	(LLL)	Apr. '78
C.R. Reich	(INEL)	Apr. '78

This is the first evaluation for ENDF/B for this isotope. Neutron and photon production data are given between 10^{-5} eV and 20 MeV. The cross sections included are total, elastic, inelastic, (n,f) , $(n,2n)$, $(n,3n)$, $(n,4n)$, and (n,γ) and are described in HEDL-TME-77-54 (ref. 7). The photon data include multiplicities and transition probabilities, photon production cross sections, and secondary energy spectra.

MF=1 General information.

MT=452

NUBAR. Thermal value from measurements of Jaffey and Lerner (ref. 1).
Energy dependence based on work of Howerton (ref. 2).

MT=458

Energy of fission. Systematics of Sher (ref. 11).

MF=2 Resonance parameters (0 to 10 keV).

MT=151

Resolved resonances. Resonance parameters for six resolved resonances from work of Bowman et al., (ref. 5). Resolved region - 0 to 3.55 eV. Unresolved resonances average parameters from ref. 5. Unresolved resonance region - 3.55 eV to 10 keV.

95-Am-242m
MAT 1369

MF=3 Smooth cross sections (0 to 20 MeV)

MT=1

Total sum of partial cross sections.

MT=2

Elastic optical model calculations (ref. 7)

MT=4

Inelastic statistical model calculations to 13 excited levels plus continuum (ref. 7)

MT=16

$n, 2n$ based on statistical model calculations (ref. 7).

MT=17

$n, 3n$ based on statistical model calculations (ref. 7).

MT=18 (Figure 95-242*-1)

Fission statistical model calculation based on data of Bowman et al., (ref. 8) and Seeger et al., (ref. 9).

MT=19

Same as MT=18 until $i(n, nif)$ threshold, then constant.

MT=20

I_s (MT=18) - (MT=19).

MT=37

$n, 4n$ based on statistical model calculations (ref. 7).

MT=51....63.91

Statistical model calculations to 13 excited levels plus continuum (ref. 7).

MT=102

Capture statistical model calculation (ref. 7).

MT=251, 252, 253

Based on data in MF=4, MT=2.

MF=4 Angular distributions

MT=2

Based on optical model calculations (ref. 7).

MT>2

Assumed isotropic.

MF=5 Energy distributions.

MT=16

Based on parameters of Gilbert and Cameron (ref. 10).

MT=17

Same reference as MT=16.

MT=18

Fission. Simple fission Maxwellian with energy-dependent temperature.

MT=19, 20

Same as MT=18.

MT=37

Same reference as MT=16.

MT=91

Based on parameters of Gilbert and Cameron (ref. 10).

95-Am-242m
MAT 1369

MF=8, MT=457

Radioactive decay data. Q-values-1974 version of Wapstra-Bos-Gove mass table. Other - see Table of Isctopes, 7th ed. (preliminary data, priv. comm. from C. M. Lederer) and Y. A. Ellis, Nuclear Data Sheets B 4, No. 6, 683 (1970). Note: The energy and intensity data for the ground-state alpha and the two most intense alpha groups are the recommended value of A. Rytz, At. Data and Nucl. Data Tables 12, No. 5, 479 (1973).

MF=12, 13, 14, 15

Photon production. Files taken from the LLL evaluation of R. Howerton documented in UCRL 50400, Vol. 15, Part A (methods) Sept. 75 and Part B (curves) Apr. 76.

References

1. A.H. Jaffey and J.L. Lerner, Nucl. Phys. A145 (1970) 1.
2. R.J. Howerton, Nucl. Sci. Eng. 46 (1971) 42.
3. Y.A. Ellis, Nucl. Data Sheets, 4 (1970) 683.
4. A.H. Wapstra and N.B. Gove, Nucl. Data Tables 9 (1971) 267.
5. C.D. Bowman, G.F. Auchampaugh, S.C. Fultz, and R.W. Hoff, Phys. Rev. 166 (1968) 219.
6. S.T. Perkins, G.F. Auchampaugh, R.W. Hoff, and C.D. Bowman, Nucl. Sci. Eng. 32 (1968) 131.
7. F.M. Mann and R.E. Schenter, Trans. Amer. Nucl. Soc. 23 (1976) 546 and HEDL TME 77-54 (1977).
8. C.D. Bowman, G.F. Auchampaugh, S.C. Fultz, and R.W. Hoff, Phys. Rev. 166 (1968) 1219.
9. P.A. Seeger, A. Hemmendinger, and B.C. Diven, Nucl. Phys. A96 (1967) 605.
10. A. Gilbert and A.G.W. Cameron, Can. J. Phys. 43 (1965) 1446.
11. R. Sher, S. Fiarman, and C. Beck (priv. comm., Oct. 1976).

95-Am-242m
MAT 1369

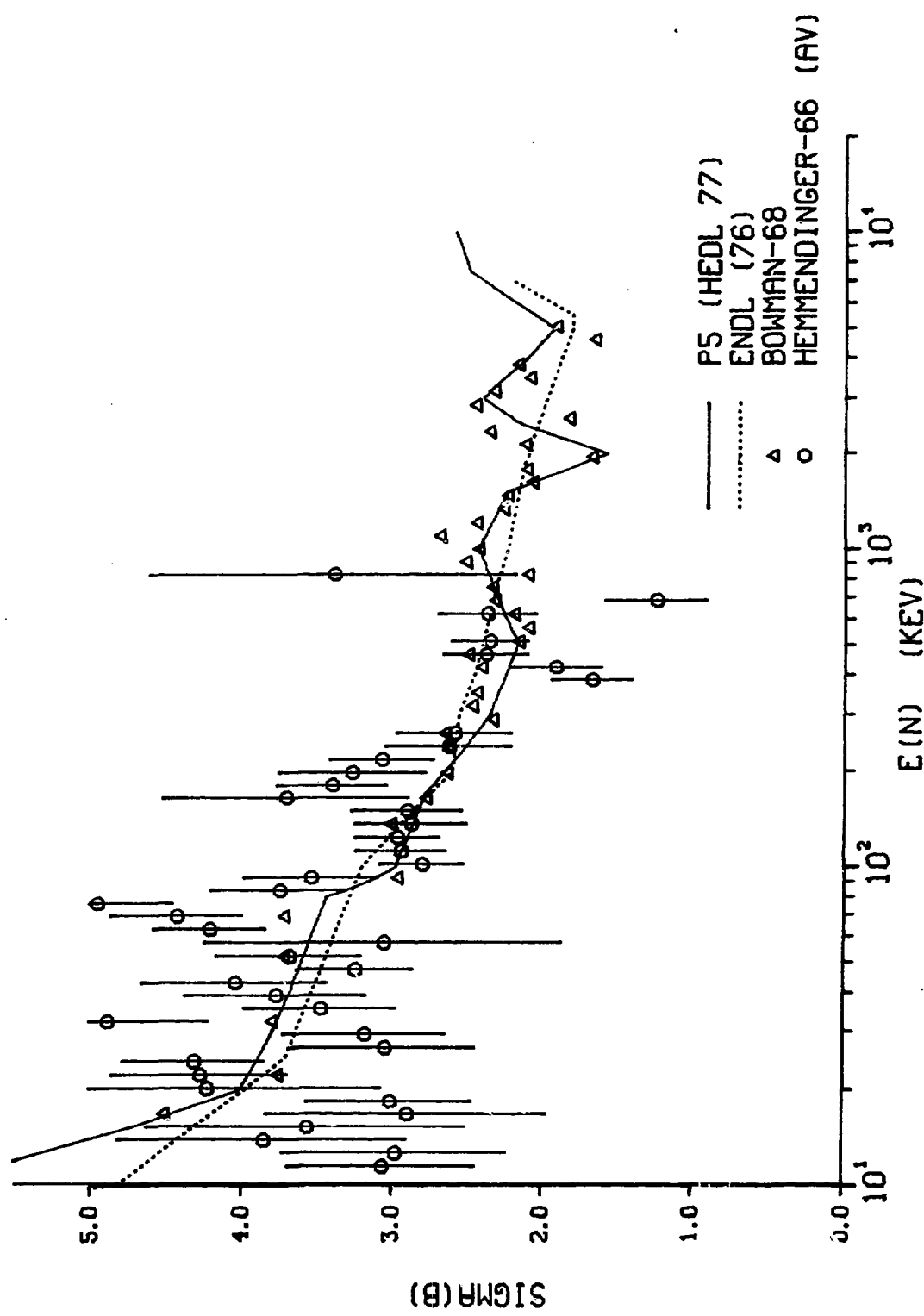


Figure 95-242*-1
Am 242* (N, F)

95-242m-6

ENDF/B-V Summary Documentation

Isotope: 95-Am-243 MAT = 1363

F.M. Mann and R.E. Schenter	(HEDL)	Apr '78
R. Benjamin	(SRL)	Oct '75
R.J. Howerton	(LLL)	Apr '78
C.R. Reich	(INEL)	Apr '78

The present work supersedes the ENDF/B-IV evaluation, MAT = 1057 by Smith and Grimesey. Neutron and photon production data are given between 10^{-5} eV and 20 MeV. The cross sections included are total, elastic, inelastic, (n, f) , $(n, 2n)$, $(n, 3n)$, $(n, 4n)$, and (n, γ) and are described in HEDL-TME-77-54 (Ref. 13). The photon data include multiplicities and transition probabilities, photon production cross sections, and secondary energy spectra.

MF=1 General information.

MT=452

NUBAR. Thermal value computed from semi-empirical work of Gordeeva and Smirenkin (ref. 1) as revised by Manero and Konshin (ref. 2). Energy dependence based on work of Howerton (ref. 3).

MT=458

Energy from fission based on Sher (ref. 12).

MF=2 Resonance parameters (0 to 10 keV).

MT=151

Resolved resonances 219 resolved resonances plus one bound level are included based upon the total cross section measurements of Simpson et al. (ref. 4) and the production results of Benjamin et al., (ref. 5). Resolved region - 0 to 250 eV.

95-Am-243
MAT 1363

Unresolved resonances average resonance parameters based on the measurements of Simpson et al., (ref. 4) were used. Unresolved region - 250 eV to 10 keV.

MF=3 Smooth cross sections (0 to 20 MeV)

MT=1

Total sum of partial cross sections.

MT=2

Elastic based upon optical model calculations (ref. 7).

MT=4

Inelastic based on statistical model calculations to 17 excited levels plus continuum (ref. 7).

MT=16

n, 2n based on statistical model calculation (ref. 7).

MT=17

n, 3n based on statistical model calculations (ref. 7).

MT=18 (Figure 95-243-1)

Fission based on data of Seeger et al., (ref. 8).

MT=19

Same as MT=18 until (n,nf) threshold, after which cross section constant.

MT=20

is (MT=18) - (MT=19).

MT=37

n, 4n based on statistical model calculations (ref. 7).

MT=51....67.91

Based on statistical model calculations to 17 excited levels plus continuum
95-243-2

(ref. 7).

95-Am-243
MAT 1363

MT=102

Capture based on statistical model calculations normalized to match file 2 at 10 keV (ref. 7).

MT=251, 252, 253

MU-BAR (L-system), XI, gamma calculated by Chad.

MF=4 Angular distributions.

MT=2

Elastic angular distributions supplied by H. Alter of AI, composed of a mixture of measured data for U235, U238, and Pu239, values of gamma slowing down parameter above 10 keV are suspect and are not to be used without study.

MT>2

Assumed isotropic.

MF=5 Energy distributions.

MT=16

Based on parameters of Gilbert and Cameron (ref. 9).

MT=17

Same as reference as MT=16.

MT=18

Fission spectrum has Maxwellian density with the temp based on Terrell's prescription (ref. 6); the thermal value of NU was used to determine the temperature.

MT=19, 20

Same as MT=18.

MT=37

Same reference as MT=16

95-243-3

95-Am-243
MAT 1363
MT=91

Same reference as MT=16.

MF=8 Radioactivity data.

MT=102

Used decay data of ENDF/B-V, MAT numbers = 7544 and 7554.

MF=8, MT=457

Radioactive decay data. Q(alpha)-1974 version of Wapstra-Bos-Gove mass table. Other - see table of isotopes, 7th ed. (preliminary data, priv. comm. from C.M. Lederer). See also Y.A. Ellis and A.H. Wapstra, Nuclear Data Sheets 8, 3, no. 2.1 (1969) and Y.A. Ellis, Ibid, 19, no. 1, 103 (1976). Spontaneous-fission branching ratio derived from listed half-life value and S.-F. half-life data of B.M. Aleksandrov et al., Sov. At. Energy 20, 352 (1966).

Note: The listed L-X-ray intensity is a measured value.

Note: The energies and intensities of the ground-state alpha and the two most intense alpha groups are the recommended values of A. Rytz, At. Data and Nucl. Data Tables 12, No. 5, 479 (1973).

MF=9, MT=102

Based on statistical model calculations (ref. 7)

MF=12, 13, 14, 15

Photon production. Files taken from the LLL evaluations of R. Howerton documented in UCRL 50400, Vol. 15, part A (methods) Sept. 75 and part B (curves) Apr. 76.

References

1. L. Gordeeva and G. Smirenkin, Sov. At. En. 14 (1963) 562.
2. F. Manero and V. Konshin, At. En. Rev. 10 (1972) 637.
3. R. Howerton, Nucl. Sci. Eng. 46 (1971) 42.
4. O. Simpson, F. Simpson, J. Harvey, G. Slaughter, R. Benjamin, and C. Ahlfeld, Nucl. Sci. Eng. 55 (1974) 273.
5. R. Benjamin, F. McCrosson, V. Vandervelde, and T. Gorrell, USERDA report DP-1394 (1976).
6. J. Terrell, Phys. and Chem. of Fission, Vol. 2, IAEA (1965).
7. F.M. Mann and R.E. Schenter, Trans, Am. Nuc. Soc. 23 (1976) 546 and HEDL TME-77-54 (1977).
8. P.A. Seeger LA-4420 (1970).
9. A. Gilbert and A.G.W. Cameron, Can. J. Phys. 43 (1965) 1446.
10. J.G. Cunningham, J. Inorg, Nucl. Chem. 4 (1957) 7.
11. R.R. Richard et al., Trans. Am. Nuc. Soc. 6 (1963) 2.
12. R. Sher, S. Fiarman, and C. Beck, priv. comm. (Oct. 1976).
13. F.M. Mann and R.E. Schenter, HEDL-TME-77-54 (1977).

95-243-6

95-Am-243
MAT 1363

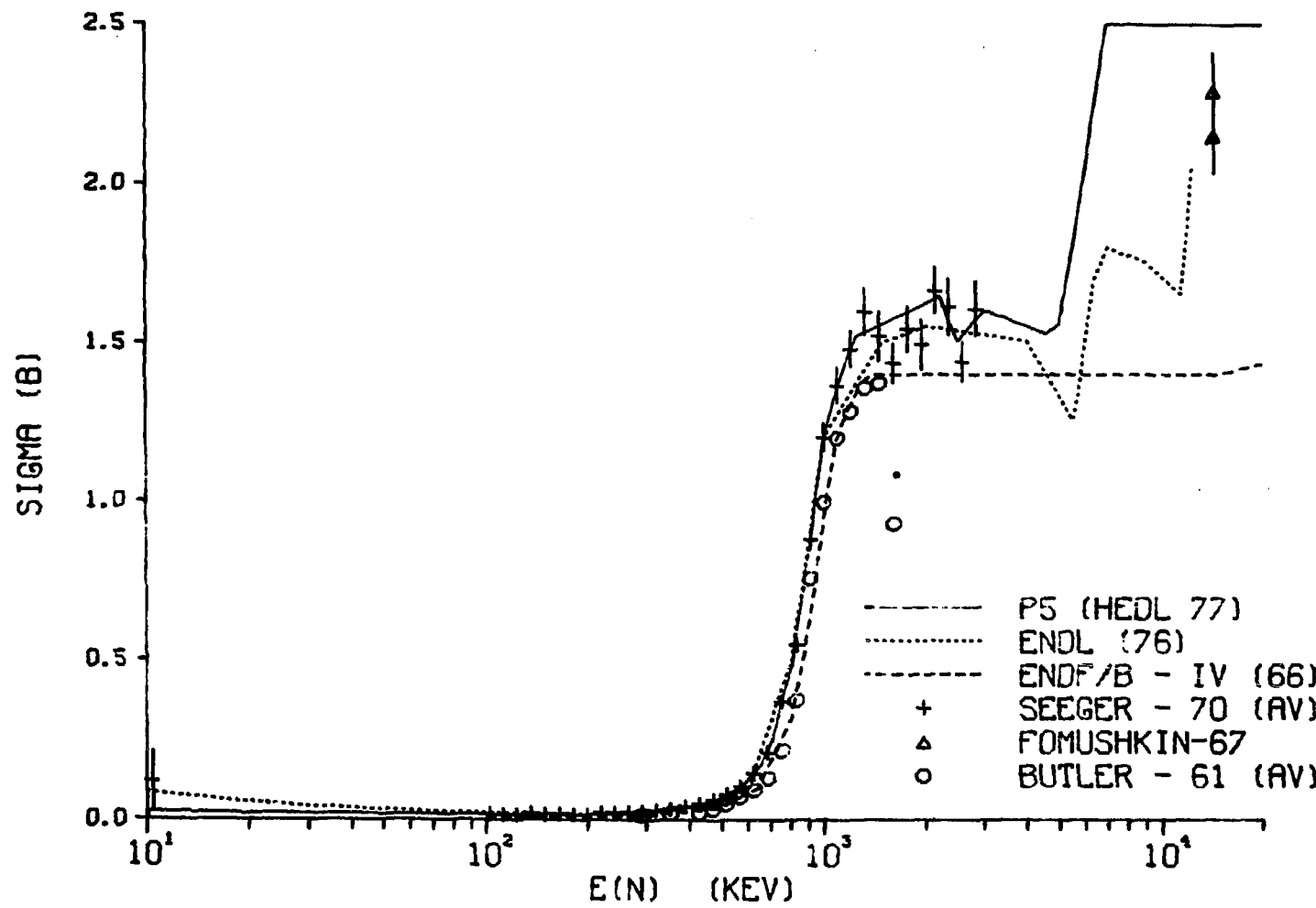


Figure 95-243-1
Am 243 (N,F)

ENDF/B-V Summary Documentation

Isotope: 96-Cm-243 MAT = 1343

F.M. Mann and R.E. Schenter	(HEDL)	Apr '78
R. Benjamin	(SRL)	Aug '75
R.J. Howerton	(LLL)	Apr '78
C.R. Reich	(INEL)	Apr '78

This is the first evaluation for ENDF/B for this isotope. Neutron and photon production data are given between 10^{-5} eV and 20 MeV. The cross sections included are total, elastic, inelastic, (n,f) , $(n,2n)$, $(n,3n)$, $(n,4n)$, and (n,γ) and are described in HEDL-TME-77-54 (ref. 6). The photon data include multiplicities and transition probabilities, photon production cross sections, and secondary energy spectra.

MF=1 General information.

MT=452

NUBAR. Thermal value from work of Jaffey and Lerner (ref. 1). Energy dependence based on work of Howerton (ref. 2).

MF=2 Resonance parameters (0 to 10 keV).

MT=151

Resolved resonances. 15 resolved resonances from work of Berreth et al., (ref. 4). One bound level added with average resonance parameters to fit thermal fission cross section of Hulet et al. (ref. 5). Resolved region: 0 to 27 eV. Unresolved resonances. Unresolved parameters are an average of the resolved parameters of Berreth et al., (ref. 4). Unresolved region: 27 eV to 10 keV.

MF=3 Smooth cross sections (0 to 20 MeV)

96-Cm-243
MAT 1343

MT=1

Total sum of partial cross sections.

MT=2

Elastic optical model calculation (ref. 6).

MT=4

Inelastic statistical model calculation to 15 excited levels and continuum (ref. 6).

MT=16

$n, 2n$ based on statistical model calculations (ref. 6).

MT=17

$n, 3n$ based on statistical model calculations (ref. 6).

MT=18 (Figure 96-243-1)

Fission cross sections are based on statistical model calculations (ref. 6).

The fission cross section agrees well with data of Fullwood et al. (ref. 7).

MT=19

(n, f) Same as MT=18 until (n, nf) threshold, constant thereafter.

MT=20

(n, nf) Difference between MT=18 and MT=20.

MT=37

$n, 4n$ Based on statistical model calculations (ref. 6).

MT=51 ... 65.91

Inelastic statistical model calculation to 15 excited levels and continuum (ref. 6).

MT=102

Capture statistical model calculations (ref. 6).

MT=251, 252, 253

Based upon MF=4, MT=2.

MF=4 Angular distributions.

MT=2

Based upon optical model (ref. 6).

MT>2 Assumed isotopic.

Assumed isotropic.

MF=5 Secondary neutron energy distributions.

MT=16

Based upon parameters of Gilbert and Cameron (ref. 8).

MT=17

Same reference as MT=16.

MT=18

Fission. Simple fission Maxwellian with energy-dependent temperature.

MT=19 and 20

Same as MT=18.

MT=37

Same reference as MT=16.

MT=91

Based upon parameters of Gilbert and Cameron (ref. 8).

MF=8, MT=457

Radioactive decay data. Q-values-1974 version of Wapstra-Bos-Gove mass table; half-life-derived from data of G.R. Choppin and S.G. Thompson, J. Inorg.

96-Cm-243

MAT 1343

Nucl. Chem. 7, 197 (1958). Their reported value has been corrected to the current value of the Cm-244 half-life. Other - see table of isotopes, 7th ed. (preliminary data, priv. comm. from C.M. Lederer). See also Y.A. Ellis, Nucl. Data Sheets 19, 103 (1976).

Note: The listed values of the gamma-ray energies are those as determined from the NP-239 decay. (See also, A. Artna-Cohen, Nuclear Data Sheets B 6, No. 6, 577 (1971) and M.J. Martin, ORNL-5114 (1976)). The gamma-ray multipolarities are those reported by G.T. Ewan et al., Phys. Rev. 116, 950 (1959). (See also M.J. Mart op. cit.).

Note: The energies and intensities of the ground-state alpha and the three most intense alpha groups are the recommended values of A. Rytz, At. Data and Nucl. Data tables 12, No. 5, 479, (1973).

Note: The Pu K-x-ray intensities are measured values.

MF=12, 13, 14, 15

Photon production. Files taken from the LLL evaluations of R. Howerton documented in UCRL 50400, vol. 15, Part A (methods) Sept. 75 and Part B (curves) Apr. '76.

References

1. A.H. Jaffey and J.L. Lerner, Nucl. Phys. A145 (1970)1.
2. R.J. Howerton, Nucl. Sci. Eng. 46(1971)42.
4. J.R. Berreth, F.B. Simpson, and B.C. Rusche, Nucl. Sci. Eng. 49(1972)145.
5. E.K. Hulet, R.W. Hoff, H.R. Bowman, and M.C. Michel, Phys. Rev. 107(1957)1294.
6. F.M. Mann and R.E. Schenter, Trans. Amer. Nucl. Soc. 23(1976)546 and HEDL TME 77-54 (1977).
7. R.R. Fullwood, D.R. Dixon, and R.W. Lougheed, LA-4420(1970)157.
8. A. Gilbert and A.G.W. Cameron, Can. J. Phys. 43(1965)1466.
9. R. Sher, S. Fiarman, and C. Beck (priv. comm., Oct. 1976).

96-243-6

96-CM-243
MAT 1343

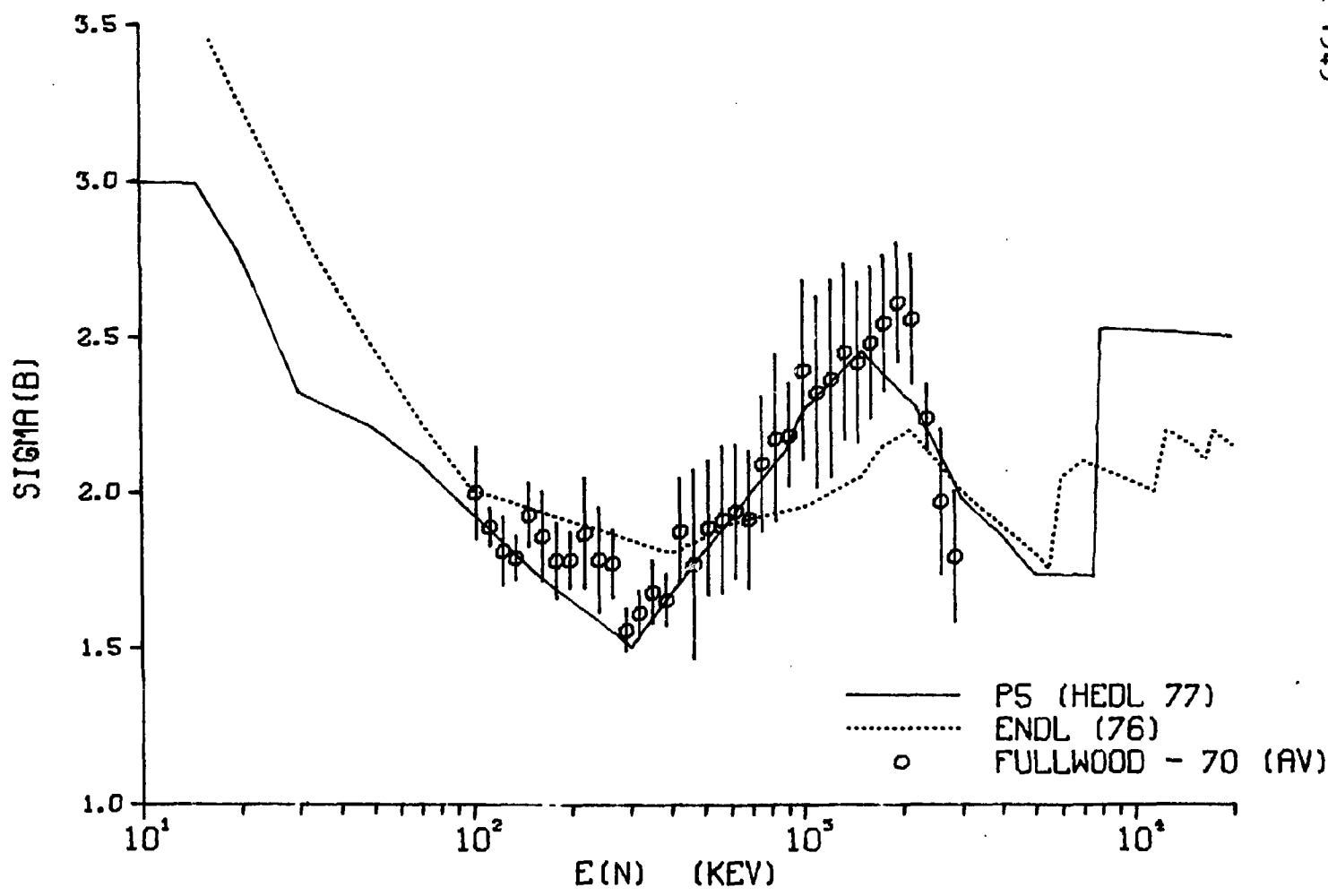


Figure 96-243-1
CM 243 (N,F)

Isotope: 96-Cm-244 MAT = 1344

F.M. Mann and R.E. Schenter	(HEDL)	Apr '78
R. Benjamin	(SRL)	July '75
R.J. Howerton	(LLL)	Apr '78
C.R. Reich	(INEL)	Apr '78
H. Alter and C. Dunford	(AI)	May '67

The present work supersedes the ENDF/B-IV evaluation, MAT = 1162 by Alter and Dunford. Neutron and photon production data are given between 10^{-5} eV and 20 MeV. The cross sections included are total, elastic, inelastic, (n, f) , $(n, 2n)$, $(n, 3n)$, $(n, n'\gamma)$, and (n, γ) and are described in HEDL-TME-77-54 (ref. 12). The photon data include multiplicities and transition probabilities, photon production cross sections, and secondary energy spectra.

MF=1 General information.

MT=452

NUBAR. Thermal value computed from semi-empirical work of Gordeeva and Smirenkin (ref. 1) as revised by Manero and Konshin (ref. 2). Energy dependence based on work of Howerton (ref. 3).

MT=458

Energy from fission based on Sher (ref. 17)

MF=2 Resonance parameters (0 eV to 10 keV)

MT=151

Resolved resonances parameters are included for 37 resolved resonances and one bound level based on ORELA, LASL, and MTR measurements (ref. 4-5) up to 520 eV. Parameters of the bound level and the first resonance were modified within reasonable experimental limits to provide agreement with integral data (refs. 7 + 8) and production studies (refs. 9 + 10). The potential scattering

96-CM-244

MAT 1344

cross section is 10.32 barns from optical model calculations. 2200 m/s cross sections from resonance parameters are capture - 10.4 B, fission - 0.60 B, elastic - 7.16 B, total - 18.13 B. This value differs from the total cross section determined by Berreth et al., (23 \pm 3 B). But Berreth's data was not corrected for small angle scattering, a correction which would reduce the measured 2200 m/s total cross section significantly. Resolved range: 0 to 525 eV.

Unresolved resonances parameters for s-wave resonances are averages from the resolved region, with the fission width from Moore's more extensive data for the fission resonances (ref. 5). For the p-wave resonances: D, GG, and GF are also based on the resolved region, while GNO is determined from the p-wave strength functions of Dunford and Alter (ref. 11). Unresolved range: 525 eV to 10 keV.

MF=3 Smooth cross sections (above 10 keV)

MT=1

Total cross section: fast region from an optical model calculation (ref. 12)

MT=2

Elastic scattering data obtained in procedure identical to MT=1.

MT=4

Inelastic scattering data results from the scattering to 3 levels plus continuum. Again an OM is used with a statistical compound nuclear model (ref. 12).

MT=16

n, 2n based on statistical model calculations (ref. 12)

MT=17

n, 3n based on statistical model calculations (ref. 12)

MT=18 (Figure 92-244-1)

Fission thermal region data calculated from resonance parameters. Fast region based on data of Moore (ref. 13) with higher energy evaluations based on statistical model calculations (ref. 12).

MT=19

(n,f) same as MT=18 until (n,nf) threshold, constant thereafter.

MT=20

(n,nf) difference of MT=18 and MT=19

MT= 51, 52, 53, 91

Inelastic scattering data results from the scattering to 3 levels plus continuum. Again an OM is used with a statistical compound nucleus model (ref. 12)

MT=102

Capture thermal data calculated from resonance parameters. Fast region data from a statistical model assuming dipole radiation.

MT=251

MUBAR. Calculated from DOM angular distributions.

MT=252

XIBAR. Calculated from DOM angular distributions.

MT=253

GAMMA. Calculated from DOM angular distributions.

MF=4 Angular distributions.

MT=2

Elastic scattering legendre coefficients for 15th order fit to calculated angular distributions (DOM) are provided between 10 keV and 11 MeV and 19th order between 12 and 15 MeV.

96-Cm-244
MAT 1344

MT=2

Assumed isotropic.

MF=5 Secondary energy distributions.

MT=16

$n, 2n$ Nuclear temperature with energy dependence as in reference 14.

MT=17

Same reference as MT=16

MT=18

Fission Maxwellian with constant temperature from correlation of Ref. 15.

MT=19 and 20

Same as MT=18

MT=91

Based on parameters of Gilbert and Cameron (ref. 16).

MF=8 MT=457

Radioactive decay data. $Q(\alpha)$ -1974 version of Wapstra-Bos-Gove mass table; half-life-weighted average of values reported by W.C. Bentley, J. Inorg, Nucl. Chem., 30, 2007 (1968) and W.J. Kerrigan and R.S. Dorsett, J. Inorg, Nucl. Chem., 34, 3603 (1972). Other - see M.R. Schmorak, Nuclear Data Sheets 17, No. 3, 402 (1976) and table of isotopes, 7th ed. (preliminary data, priv. comm. from C.M. Lederer). See also M.R. Schmorak, Nuclear Data Sheets 20, 218 (1977).

Note: The L-X-ray data represent measured values. See C.E. Bemis, Jr., and L. Tubbs, ORNL-5297, 93 (Sept., 1977).

Note: The intensities of the gamma rays above 153 keV are taken from NDS 20.218 (1977) (ref. above). The energy values are as measured from the NP-240M decay.

Note: The gamma-ray intensity normalization was derived from the listed information on the 42.8-keV gamma ray and the ground-state alpha branch.

Note: The energies and intensities of the two highest energy alpha groups are those recommended by A. Rytz, At. Data and Nucl. Data tables 12, No. 5, 479 (1973).

MF=12, 13, 14, 15

Photon production. Files taken from the LLL evaluations of R. Howerton documented in UCRL 50400, vol. 15, Part A (methods) Sept. '75 and Part B (curves) Apr '76.

References

1. L. Gordeeva and G. Smirenkin, Sov. At. En. 41 (1963) 562.
2. F. Manero and V. Konshin, At. En Rev. 10 (1972) 637.
3. R.J. Howerton, Nucl. Sci. Eng., 46 (1971) 42.
4. O. Simpson, F. Simpson, T. Young, J. Harvey, N. Hill, and R. Benjamin (private communication).
5. M. Moore and G. Keyworth, Phys. Rev. C3 (1971) 1656.
6. J. Berreth, F. Simpson, and B. Rusche, Nucl. Sci. Eng. 49 (1972) 145.
7. R. Benjamin, K. Macmundo and J. Spencer, Nucl. Sci. Eng., 47 (1972) 203.
8. M. Thompson, M. Hyder, and R. Reuland, J. Inorg. Nucl. Chem., 33 (1971) 1553.
9. R. Benjamin, V. Vandervelde, T. Gorrell and F. McCrosson, Proc. Conf. Nucl. Cross Sect. and Tech., Washington, D.C., March, 1975.
10. R. Benjamin, V. Vandervelde, T. Gorrell and F. McCrosson, USERDA report to be issued.
11. C. Dunford and H. Alter, USAEC report NAA-SR-12271 (1967).
12. F.M. Mann and R.E. Schenter, Trans. Amer. Nuc. Soc., 23 (1976) 546 and HEDL TME 77-54 (1977).
13. M.S. Moore and G.A. Keyworth, Phys. Rev. C3 (1971) 1656.
14. K. Parker, AWREO-79/63 (1964).
15. E. Barnard et al., Nucl. Phys. 71 (1965) 228.
16. A. Gilbert and A.G.W. Cameron, Can. J. Phys. 43 (1965) 1466.
17. R. Sher, S. Fiarman, and C. Beck (priv. comm., Oct. 1976).

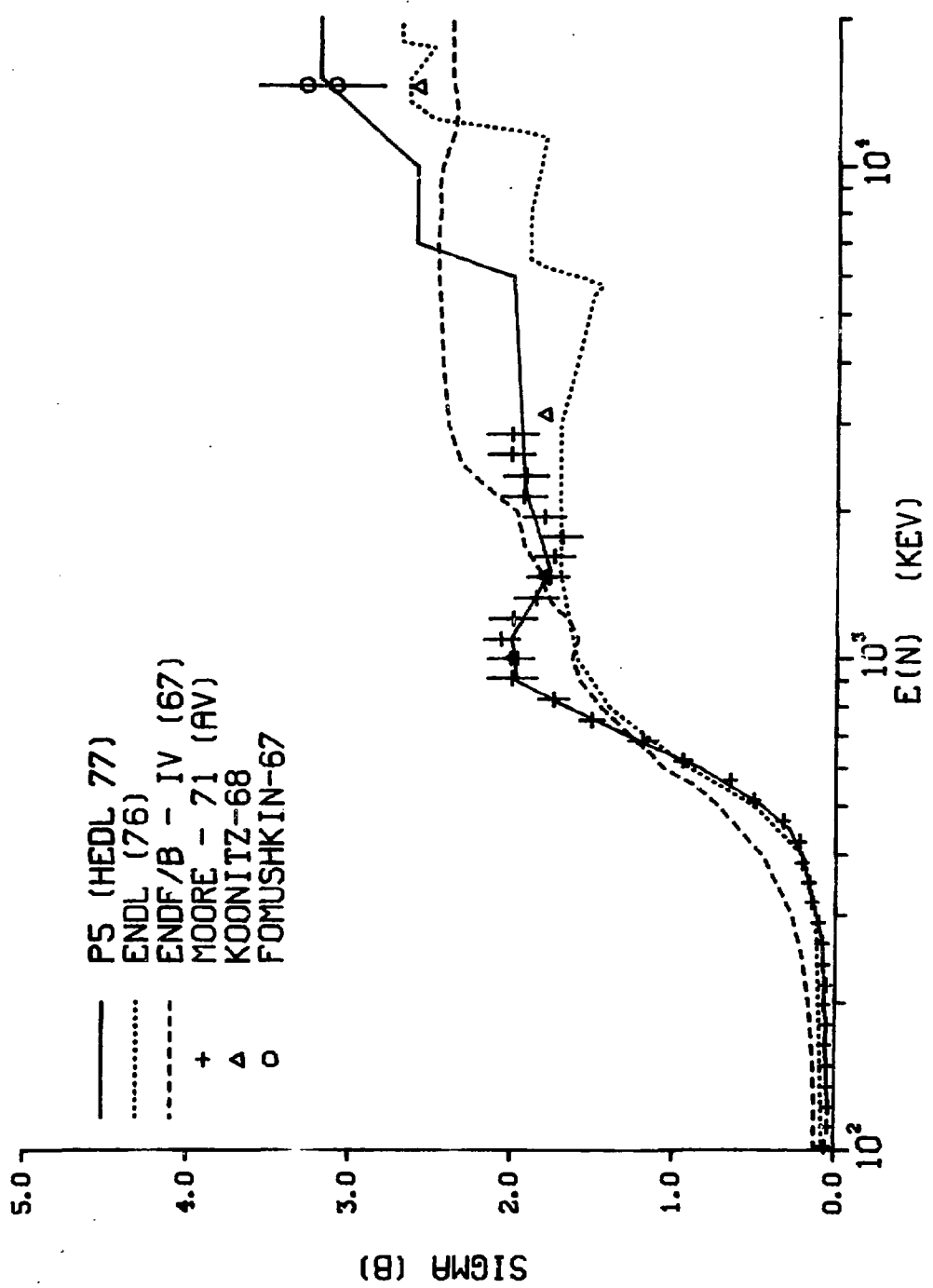


Figure 96-244-1
Cm 244 (N, F)

96-Cm-245
MAT 1345

SUMMARY DOCUMENTATION

^{245}Cm EVALUATION BELOW 10 keV

ENDF/B - V MOD II

MAT = 1345

R. W. Benjamin and R. J. Howerton

January 1979

96-245-1

96-Cm-245
MAT 1345

^{245}Cm Summary Documentation

This evaluation of ^{245}Cm supercedes the current ENDF/B-V evaluation (release date 1/79) below 10 keV. The major improvements are the inclusion of more recent results from the differential neutron fission measurements of Browne et al.¹ and Moore and Keyworth.² Cross sections included below 10 eV are total, elastic, capture and fission, and they are described entirely through the single-level Breit-Wigner resonance parameters. The only significant changes from ENDF/B-V are in Files 1, 2, and 3.

File 1 The Average Number of Neutrons per Fission

The average number of neutrons per fission \bar{v} is described by

$$\bar{v}(E) = 3.83 + 0.190 E \text{ (E in MeV)}$$

The thermal value is from the compilation of Manero and Konshin,³ who renormalized the work of Jaffey et al.⁴ The energy dependence is based upon the work of Howerton.⁵

File 2 Resonance Parameters

The region from 10^{-5} eV to 60 eV is described entirely with resonance parameters for 38 resolved s-wave resonances and one bound level. The parameters are a blend of analyzed results from the LINAC measurements of Browne et al.² and the nuclear detonation measurements of Moore and Keyworth.² Other, more limited, recent data⁶⁻⁸ have been examined, but References 1 and 2 provide a consistent data base below 60 eV and sufficient resonance information to obtain reasonable unresolved resonance parameters from 60 eV to 10 keV. The only notable difference in the resolved range is a very small resonance at 3.207 eV reported in Reference 6. This resonance adds little to the strength and is implicitly accounted for in the resonance analysis of Reference 1. The resolved resonance parameters are listed in Table 1 with

uncertainties derived from Reference 1 and recommended by M. S. Moore.⁹ Associated with these resonance parameters is a potential (hard sphere) scattering cross section of 10.1 b from optical model calculations at 10 keV.

Unresolved resonance parameters for s- and p-wave neutrons have been determined from average parameters in the resolved region combined with a p-wave strength function $S_1 = 2.00 \times 10^{-4}$ obtained through extrapolation of Lynn's work.¹⁰ The unresolved resonance parameters are summarized in Table 2. Upon expansion with the single-level Breit-Wigner formalism, these unresolved parameters provide a reasonable match below 10 keV to the recent fission measurements of Nakagome and Block.¹¹

These resolved and unresolved resonance data combined with the ENDF/B-V evaluation of Howerton above 10 keV yield the thermal cross sections and infinitely dilute resonance integrals listed in Table 3 where they are compared with the best integral data.^{12,13} The evaluation represents the best current description of the ²⁴⁵Cm cross sections below 10 keV.

File 3 Smooth Cross Sections

There are no File 3 data below 10 keV.

File 4 Angular Distributions

The elastic angular distribution is from Howerton's LLL evaluation⁴ and is identical with the current ENDF/B-V.

File 5 Secondary Neutron Energy Distributions

The fission neutron energy spectrum is a simple fission Maxwellian with an energy-dependent temperature.

96-Cm-245
MAT 1345

References

1. J. C. Browne, R. W. Benjamin, and D. G. Karraker, Nuclear Science and Engineering 65, 166 (1978).
2. M. S. Moore and G. A. Keyworth, Physical Review C3, 1656 (1971).
3. F. Manero and V. A. Konshin, Atomic Energy Review 10, 637 (1972).
4. A. H. Jaffey and J. L. Lerner, Nuclear Physics A145, 1 (1970).
5. R. J. Howerton, Nuclear Science and Engineering 62, 438 (1977).
6. T. S. Belanova, Yu. S. Zamyatnin, A. G. Koiesov, V. M. Lebedev, and V. A. Poruchikov, Atomnaya Energiya 42, 52 (1977). [See also the Kiev Conference Proceedings, 1977].
7. S. M. Kalebin, "Total Neutron Cross Section Measurements on the Transactinium Isotopes $^{241,243}\text{Am}$, $^{244,245,246,248}\text{Cm}$," Transactinium Isotope Nuclear Data TND, International Atomic Energy Agency IAEA-186, Vol. II, p 121 (1976).
8. J. R. Berreth, F. B. Simpson, and B. C. Rusche, Nuclear Science and Engineering 49, 145 (1972).
9. M. S. Moore, private communication.
10. J. E. Lynn, The Theory of Neutron Resonance Reactions, Clarendon Press, Oxford, 1968, p 290.
11. Y. Nakagome and R. C. Block, private communication (to be published).
12. S. F. Mughabghab and D. I. Garber, "Neutron Cross Sections," Vol. 1, "Resonance Parameters", BNL 525, Third ed. Brookhaven National Laboratory (1973).
13. R. W. Benjamin, K. W. MacMurdo, and J. D. Spencer, Nuclear Science and Engineering 47, 203 (1972).

TABLE 1

RESOLVED RESONANCE PARAMETERS* FOR ^{245}Cm - 10^{-5} to 61.5 eV

E_0 eV	ΔE_0 eV	$2g\Gamma_n^0$ meV	$\Delta 2g\Gamma_n^0$ meV	Γ_f meV	$\Delta \Gamma_f$ meV
-0.1	-	0.144	0.004 ^a	300	50
0.85	0.03	0.102	0.009	800	50
1.98	0.03	0.24	0.03	175	25
2.45	0.05	0.11	0.017	300	50
4.68	0.05	2.10	0.02	325	30
5.75	0.10	0.11	0.03	300	100
7.53	0.05	1.91	0.12	300	30
8.65	0.15	0.53	0.10	500	100
9.15	0.15	0.39	0.10	200	50
10.15	0.10	0.40	0.05	200	50
11.34	0.10	0.88	0.12	150	25
13.75	0.10	0.34	0.10	170	30
16.0	0.1	0.66	0.20	400	100
21.4	0.1	3.41	1.0	490	100
24.8	0.1	4.05	1.2	225	50
25.8	0.1	0.04	0.01	550	165
26.8	0.1	0.77	0.2	130	39
27.6	0.1	0.73	0.2	200	50
29.4	0.1	3.58	1.0	350	100
31.7	0.1	0.50	0.05	690	200
33.0	0.1	0.37	0.04	4	2
34.6	0.1	0.23	0.02	60	20
35.3	0.1	7.58	0.80	4195	1200
36.3	0.1	1.54	0.15	190	60
39.5	0.1	0.653	0.07	102	30
40.4	0.1	4.48	0.45	585	170
42.5	0.1	6.37	0.54	10	4
43.1	0.1	1.73	0.17	537	160
44.6	0.1	2.61	0.26	694	210
45.8	0.1	0.59	0.10	900	270
47.5	0.1	3.56	0.36	280	80
49.2	0.1	5.04	0.50	1399	420
50.5	0.1	1.79	0.18	751	225
51.6	0.1	0.625	0.08	207	60
53.6	0.1	12.35	1.24	896	270
54.6	0.1	0.33	0.05	1057	325
56.3	0.1	1.40	0.14	505	150
58.5	0.1	13.85	1.39	393	120
60.0	0.1	0.610	0.08	518	150

* A value of $\Gamma_f = 40$ meV was used for all resonances except for the bound level at -0.1 eV where 50 eV was used. The uncertainty attributed to these values should be $\pm 20\%$.

^a For this (bound) level, $2g\Gamma_n^0$ is listed.

TABLE 2

UNRESOLVED RESONANCE PARAMETERS FOR ^{245}Cm - 61.5 eV to 10 keV

ℓ	J	\bar{D} eV	$S_\ell \times 10^4$	$\bar{\Gamma}_n^\sigma$ meV	$\bar{\Gamma}_\gamma$ meV	$\bar{\Gamma}_f$ meV
0	3	2.57	1.17	0.30	40	519
0	4	2.00	1.17	0.23	40	519
1	2	3.59	2.00	0.70	40	519
1	3	2.57	2.00	0.51	40	519
1	4	2.00	2.00	0.40	40	519
1	5	1.63	2.00	0.33	40	519

TABLE 3

THERMAL CROSS SECTIONS AND RESONANCE INTEGRALS FOR ^{245}Cm

	Thermal (2200 m/s) Cross Sections (b)		Resonance Integrals (b - eV)	
	σ_{nf}^{2200}	$\sigma_{n\gamma}^{2200}$	I_{nf}	$I_{n\gamma}$
			$(>0.625 \text{ eV})$	
Calculated (this work)	2210	341	821.4	107.5
Measured	2145 ± 58^1	345 ± 20^{12}	772 ± 40^{13}	101 ± 8^{12}

SUMMARY DOCUMENTATION

^{246}Cm EVALUATION

ENDF/B - V

MAT = 1346

R.W. Benjamin and R.J. Howerton

October, 1978

This evaluation of ^{246}Cm combines the evaluation of Benjamin, McCrosson, and Gettys¹ (SRL) from 10^{-5} eV to 10 MeV with parts of the ENDL evaluation of Howerton² (LLL) for neutron cross sections from 10 MeV to 20 MeV and photon production over the entire energy range. The evaluations were merged at BNL by R.R. Kinsey. The cross sections were adjusted near 10 MeV to provide a smooth curve between the two evaluations. The cross sections included are total, elastic, inelastic, $(n,2n)$, $(n,3n)$, fission, $(n,4n)$, (n,n') and (n,γ) .

File 1

The average number of neutron per fission \bar{v} is described by

$$\bar{v}(E) = 3.48 + 0.196E \text{ (E in MeV)}$$

The thermal value is based upon the compilation of Manero and Konshin³, and the energy dependence upon the work of Howerton⁴.

File 2

The region from 10^{-5} eV to 385 eV is described entirely with parameters for 10 s-wave resolved resonances below 385 eV based on references 5, 6, and 7. The parameters of the first resonance were modified within the experimental uncertainties to give reasonable agreement with the integral data and production studies. A potential (hard sphere) scattering cross section of 10.466b associated with these parameters was obtained from spherical optical model calculations. Expansion of the resonance parameters yields 2200 m/s (0.0253 eV) cross section values of

$$\sigma_{nT} = 11.04b, \sigma_{nn} = 9.68b, \sigma_{nf} = 0.06b, \text{ and } \sigma_{n\gamma} = 1.30 b.$$

96-Cm-246
MAT 1346

The region from 385 eV to 10 keV is described by s- and p-wave unresolved resonances. The $\ell = 0$ (s-wave) resonance parameters were derived from the PHYSICS-8 results⁷. The $\ell = 1$ (p-wave) parameters were selected such that the capture cross section from the combination of $\ell = 0$ and $\ell = 1$ parameters joins smoothly to the results of model calculations at 10 keV.

File 3

Below 10 MeV

Cross sections between 10 keV and 10 MeV were computed with nuclear model codes; only the fission cross sections have been measured⁷. The optical model calculations are described in detail in reference 1, as well as the variation of the fission parameters to give good agreement with the fast fission cross section data of Moore and Keyworth⁷.

Level energies for the first three inelastic levels were taken from the compilation of Lederer et al⁸. The remaining inelastic levels were inferred from similar, neighboring, even-even nuclei. Level schemes for the odd-mass curium isotopes needed for (n,2n) calculations were obtained from the work of Braid et al⁹. Cross Sections were determined for the excitation of discrete inelastic levels for incident neutron energies from 0.03 to 3.0 MeV. Between 0.5 and 3.0 MeV, the remaining (n,n') cross section was treated as a continuum of levels; above 3.0 MeV, the (n,n') reaction was treated wholly as a continuum.

At 10 MeV

The total, fission, inelastic continuum, and n, γ cross sections were smoothly joined at 10 MeV by R. Kinsey.

Above 10 MeV

MT=16 The n,2n cross section was done by R. Kinsey. A general n,2n cross section shape was used, adjusted to Howerton's 14 MeV value.

MT=17 The n,3n cross section was obtained entirely from nuclear systematics. The threshold is at 12.02 MeV and the excitation function rises in the usual sigmoid shape to a plateau of 900 mb, then falls due to the

MT=17 (cont.)

onset of the $n,2nf$ reaction at about 17.5 MeV and the $n,4n$ reaction at about 18.8 MeV, to a value of 250 mb at 20.0 MeV.

MT=18 The fission cross section was evaluated by Howerton for $E_n \geq 13.0$ MeV and is based entirely on systematics.

MT=37 The $n,4n$ cross section thresholds at 18.84 MeV, rising from threshold to a value of 0.3 barns at 20.0 MeV.

File 4

Elastic scattering angular distributions are from the LL evaluations.

Angular distributions for n,n' level reactions are assumed isotropic in the center of mass system. Angular distributions for other neutron producing reactions are assumed to be isotropic in the laboratory system.

File 5

Secondary neutron energy distributions for the inelastic-continuum and the $(n,2n)$ reactions are assumed to be evaporation spectra. They are described by Maxwellian distribution with energy dependent temperatures consistent with the work of Drake and Nichols¹⁰.

Energy distributions for secondary neutrons from the $n,3n$ and $n,4n$ are presented in tabular form and were done by Howerton. Fission neutron energy distributions are described by a simple Maxwellian fission spectrum with energy dependent temperature.

File 8

The decay data included are from C. Reich (INEL). The α -particle Q values are from the unpublished 1974 Wapstra-Bos-Gove mass Tables and the alpha particle data are those recommended by Rytz¹¹. Remaining data are from references 12 and 13.

File 12-15

The photon production data are as described below except that the

96-Cm-246
MAT 1346

File 12-15 (cont.)

calculations using the NXGAMEL code used an evaluation that was done by SRL below 10 MeV and LLL above 10 MeV. In the current evaluation the n,2n cross section (R. Kinsey) and the energy distributions for the n,2n and inelastic continuum (SRL) replaced the data used in the calculation. As a result the photon production cross sections and spectrum will not conserve energy when used with the neutron interaction data of this evaluation.

MF=12, MT=18
MF=14, MT=18
MF=15, MT=18

The cross section for photon production from fission is entered as a multiplicity applied to the fission cross section. The photon energy from fission of 6.2 MeV. This value is divided by the average energy in the photon spectrum, using the measured fission photon spectrum for U²³⁵. Photons from fission are assumed to be isotropic.

MF=12, MT=102
MF=14, MT=102
MF=15, MT=102

Photon production from the neutron capture reaction is handled by using multiplicities and normalized spectra. The photon multiplicities for these reactions are derived by dividing the average photon energy into the total available energy. The spectrum of secondary photons is assumed to be the same as that for the measured U²³⁸ photon spectrum. Photons from neutron capture are assumed to be isotropic.

MF=13, MT=3
MF=14, MT=3
MF=15, MT=3

For energies below 43 keV, photon production is assumed to originate only from capture and fission processes. From 43 KeV to 20 MeV (in the absence of measurements) the photon production cross sections

96-Cm-246
MAT 1346

MF=13, MT=3

MF=14, MT=3

MF=15, MT=3 (cont.)

and spectra are calculated with the NXGAMEL code. This code is based on systematics described by Perkins, Haight, and Howerton in Nucl. Sci. Eng. 57, 1 (1975). A summary of this method of calculating photon production data is discussed in UCRL-50400, Vol. 15, Part A, pp. 38 to 41. Photons are assumed to be emitted isotropically.

96-Cm-246

MAT 1346

REFERENCES

1. R.W. Benjamin, F.J. McCrosson, and W.E. Gettys, "Evaluation of Neutron Cross Sections for ^{244}Cm , ^{246}Cm , and ^{248}Cm ," ERDA Report DP-1447 (1977).
2. R.J. Howerton and M.H. MacGregor, "An Integrated System for Production of Neutronics and Photonics Calculational Constants, Vol. 15, Part D, Rev. 1, "Descriptions of Individual Evaluation for Z 0-98," UCRL 50400, Vol 15, Part D, Rev. 1 (1978).
3. F. Manero and V.A. Konshin, Atomic Energy Review 10, 637 (1972).
4. R.J. Howerton, Nucl. Sci. Eng. 46, 42 (1971).
5. J.R. Berreth, F.B. Simpson, and B.C. Rusche, Nucl. Sci. Eng. 49, 145 (1972).
6. R.W. Benjamin, C.E. Ahlfeld, J.A. Harvey, and N.W. Hill, Nucl. Sci. Eng. 55, 440 (1974).
7. M.S. Moore and G.A. Keyworth, Phys. Rev. C3, 1656 (1971).
8. C.M. Lederer, J.M. Hollander, and I. Perlman, Tables of the Isotopes, Sixth Edition, John Wiley, New York (1968).
9. T.H. Braid, R.R. Chasman, J.R. Erskine, and A.M. Friedman, Phys. Rev. 4C, 247 (1971).
10. M.K. Drake and P.F. Nichols, "Neutron Cross Sections for ^{234}U and ^{236}U ," USAEC Report GA-8135 (1967).
11. A. Rytz, At. Data and Nuclear Data Tables 12, 479 (1973).
12. M.R. Schmorak, Nucl. Data Sheets, 17, 410 (1971).
13. C.M. Lederer, Tables of the Isotopes, 7th Edition, (to be published).

* U.S. GOVERNMENT PRINTING OFFICE: 1980-614-090/39